CRANFIELD UNIVERSITY

MASA LAW

The Development and Modelling of a Novel Clamp-on Ultrasonic-Thermal and Ultrasonic Multiple Reflection Flowmeter for Liquid Applications

(Volume 1)

DEPARTMENT OF FLUID ENGINEERING & INSTRUMENTATION

Ph.D. THESIS

CRANFIELD UNIVERSITY

DEPARTMENT OF FLUID ENGINEERING AND INSTRUMENTATION

Ph.D. THESIS (TOTAL TECHNOLOGY)

Academic Year 1993-94

MASA LAW

The Development and Modelling of a Novel Clamp-on Ultrasonic-Thermal and Ultrasonic Multiple Reflection Flowmeter for Liquid Applications

(Volume 1)

Supervisors: Professor M. L. Sanderson
Dr. A. R. Guilbert
G. Ward

February 1994

DEDICATION

TO MY PARENTS

ABSTRACT

The development of a novel combined "ultrasonic/thermal" with "ultrasonic multiple reflections" clamp-on meter for measuring a wide flowrate range of clean liquids in small diameter pipes is presented. Current existing flowmeters based on ultrasound cannot measure very low flowrates for single phase liquids. The ultrasonic/thermal technique can measure single phase flows in the range 0 to 0.6 m s^{-1} in pipes with diameters as small as 15 mm. It can also detect and measure reverse flows. The minimum flowrate for the ultrasonic multiple reflection technique is about 0.55 m s^{-1}, and theoretically, the measurement accuracy increases with increased flow velocity.

The ultrasonic/thermal technique is based on a heating element and transducer pair(s) which can be clamped to the outside of a pipe. With the heaters switched on, the changes in the temperature of the pipe and the liquid inside it result in changes in transit time. The flowrate can be therefore estimated by either the transit time difference across the pipe at the two symmetric locations with respect to the heater centre, or at one location with a heater off/on comparison. The latter approach was felt to be the promising for low flowrate measurements and therefore selected for the numerical and the experimental investigations. The multiple reflection technique was developed based on the conventional transit time flowmeter. This technique extended the measuring range of the flowmeter and provided cross calibration for the ultrasonic/thermal technique. A computer model was developed for the ultrasonic multiple reflection technique. However, there was insufficient experimental data to confirm the computer prediction.

Results from computational fluid dynamics (CFD) analysis of the meter are presented. For vertical pipes an axisymmetric model was used, but the presence of buoyancy forces required the use of a 3-D model for horizontal pipes. Temperature and velocity distributions and ultrasonic transit times have been computed and are presented.

In order to overcome the problem of mode conversion and refraction at the pipe wall/transducer mounting interface, novel transducers and mounting blocks are presented. A prototype heater and ultrasonic transducer system together with electronics for signal generation and transit time measurement have been designed and constructed. A hydraulic system has also been designed and constructed for testing the developed clamp-

on flowmeter. Experimental results from this apparatus are presented and compared with the CFD predictions, and a technique for compensating for variations in inlet temperature is described. The full scale difference between the computed values and experimental results of the meter for low flowrate measurement was about 3.5%.

ACKNOWLEDGEMENT

The support and assistance of various members of staff and fellow students of the Department of Fluid Engineering & Instrumentation is gratefully acknowledged, and in particular, the following:

I wish to express my gratitude to my supervisors, Prof. M.L. Sanderson, Dr. A. Guilbert and Mr. G. Ward for their valuable advice and guidance throughout the period of this research.

Special thanks to Mr. D. Macleod for his expertise and guidance with the electronics work. Thanks also due to Dr. J. Hemp and Dr. G. Oddie for their valuable discussions.

Appreciation is sent to the Science and Engineering Research Council and Severn Trent Water Limited (Birmingham, U. K.) who, between them sponsored this research.

Finally, I must acknowledge the support given to me by my parents, my brother and his family over the years in matters both spiritual and physical.

CONTENTS

LIST OF FIGURES

LIST OF TABLES

NOTATION

TERMS

PDE - Partial Differential Equation

IAD - Implicit Alternating-Direction

Roman

A - heating area, m^2

A_m - cross section area of metal wire, m^2

C_L - speed of sound in water at 10 ^0C, m s^{-1}

$C_L(T)$ - speed of sound in water at T ^0C, m s^{-1}

C_s - speed of sound in transducer shoes at 10 ^0C, m s^{-1}

C_T - speed of sound in transducer at 10 ^0C, m s^{-1}

C_W - speed of sound in pipe wall at 10 ^0C, m s^{-1}

C_p - specific heat capacity of water at constant pressure, W m^{-3} $^0C^{-1}$

d - copper pipe wall thickness, m

δd - increase of copper pipe wall thickness, m

d_s - transducer shoe thickness, m

D - copper pipe outer diameter, m

D_T - transducer diameter, m

E - energy loss due to radiation , W m^{-2} s^{-1}

err (%) - percentage error of reference flowmeter, %

f - operating frequency of transducers

g - gravity, m s^{-2}

I - electrical current(DC), A

k_M - flow velocity coefficient for multiple reflection technique,

K_L - thermal conductivity of water, J s^{-1} m^{-1} K^{-1}

K_M - thermal conductivity of constantan wire

K_W - thermal conductivity of copper pipe wall, J s^{-1} m^{-1} K^{-1}

l - length of test section, m

l_1, l_2 - sections of the test pipe, m

L - length of sound beam in water, m

L_m - length of metal wire of the heater, m

L_S - length of sound beam in transducer shoes, m

L_W - length of sound beam in pipe wall, m

N - number of ultrasonic beam reflections,

N_{Re} - Reynolds number

p_S - pressure,

P - heater power input, Watt

P_I - heat power transferate from the heater to the liquid, Watt

q_H - heat flux, W m^{-2}

q_{Ref} - reference heat flux, W m^{-2}

Q - flowrate, ml s^{-1}

$\overline{Q}$ - average flowrate, ml s^{-1}

Q_{Ref} - reference flowrate, ml s^{-1}

r - copper pipe outer radius, m

r_i - position i at copper pipe radius, m

Δr - mesh size, m

R - resistance of metal wire at reference temperature, Ω

R_T - resistance of metal wire at T ^{0}C, Ω

Δt - transit time difference, s

Δt_0 - transit time (heater off), s

Δt_1 - transit time (heater on), s

Δt_{AB} - transit time difference for one reflection, s

Δt_M - transit time difference for multiple reflection technique, s

Δt_{Exp} - transit time delay due to pipe expansion, s

t_{12}, t_{21} - time of flight of ultrasound beam, s

t_d - transit time across the pipe for transducer positioned down stream, s

t_N - transit time of N reflections, s

t_p - time delay of measurement system in multiple reflection technique, s

t_s - steady state heating time, s

t_u - transit time across the pipe for transducer positioned upstream, s

T^* - dimensionless temperature

T_d - down stream temperature, °C

T_L - liquid temperature, °C

T_u - up stream temperature, °C

T_{Ref} - reference temperature, 10 °C

T_w - pipe wall temperature, °C

T_{ij} - temperature at position (i,j) of the mesh, °C

ΔT - liquid temperature difference (T_l - T_{Ref}), °C

ΔT_W - pipe wall temperature difference (T_W - T_{Ref}), °C

V - flow velocity, m s^{-1}

V_A - applied voltage to the heater, volts

V(r) - point flow velocity at pipe radius, m s^{-1}

V_c - corrected flow velocity, m s^{-1}

V_m - mean flow velocity, m s^{-1}

V_r - flow velocity in radial direction, m s^{-1}

V_x - flow velocity in axial direction, m s^{-1}

V_ϕ - flow velocity in circumferential direction, m s^{-1}

x - distance along the pipe axial direction, m

Δx - mesh size in axial direction, m

X - separation distance between the heater and the transducer, m

X_{def} - deflection distance of sound beam in water, m

X_L - travelling distance of sound beam in water, m

X_N - separation distance between the two angled

transducers for N reflections, m

X_s - travelling distance of sound beam in transducer shoe, m

X_w - travelling distance of sound beam in pipe wall, m

δX - deflection of sound beam due to flow, m

α_L - thermal diffusivity of water,

α_W - thermal diffusivity of pipe wall,

β_L - velocity of sound temperature coefficient

β_m - temperature coefficient of electrical resistivity of heater wire

$\beta_{L.E}$ - thermal expansion coefficient of liquid

β_W - temperature coefficient of sound speed in pipe wall

$\beta_{W.E}$ - thermal expansion coefficient of pipe wall

ϕ_d - angle of divergent ultrasonic beam spreading

ϕ_i - angle of ultrasound beam at interfaces, i = T (transducer), W (pipe wall), S (transducer shoes), L (water).

τ_0 - delay in measurement system for heater off, s

τ_1 - delay in measurement system for heater on, s

τ_M - delay in multiple reflection technique, s

τ_T - delay in transducers and electronics, s

ρ - density of water, kg m^{-3}

ρ_m - resistivity of metal wire of the heater, Ω m

ρ_W - density of pipe wall, kg m^{-3}

μ - kinematic viscosity of water, m^2 s^{-1}

ν - dynamic viscosity of water, kg m^{-1} s^{-1}

δ_s - Stefan constant,

1. INTRODUCTION AND LITERATURE REVIEW

1.1. Introduction

This research work presents the development of a clamp-on flowmeter which can be used as a calibrator for the flowmeters currently used by water industry.

The principle design requirement put forward are listed below:

fluid:	clean water
flowrate range:	1.0 - 5600 ml s^{-1}
pipe material:	copper
pipe diameter:	15 - 40 mm
accuracy:	error < 2.0% at high flowrate
	error < 5.0% at low flowrate

For the form of the flowmeter, the main requirements are:

clamp-on meter
portable

The flowmeter was designed and constructed based on above requirements together with the consideration of capability to extend its application to other measurement areas.

Ultrasonics is currently the technique commonly available for clamp-on flow measurement. Existing clamp-on flowmeters based on ultrasound use time-of-flight, Doppler, or cross-correlation techniques all of which have some drawback - especially for small pipes and low flowrates. Time-of-flight methods are unable to measure very low flowrates because of the very small time differences [Pedersen and Lynnworth, 1973]. Doppler meters generally require scatterers in the flow. These are not always present and may not be moving at the same speed as the liquid to be measured [Chappell, 1978]. Cross-correlation meters cannot measure very low flowrates as the delay time becomes too large and the correlation between the signals may drop. They

also require disturbances in the flow to alter the ultrasonic signal [Karras, Tornberg, and Harkonen, 1985]. Experimental measurements taken within the department reveal that for a 15 mm pipe current commercially available clamp-on ultrasonic flowmeters give typical errors of ± 22% [Guilbert and Law, 1990]. The meter presented in this thesis addresses these problems, being able to measure low flowrates in small diameter pipe without the need for scatterers or other disturbances and with considerably better accuracy, the full scale difference between the computed values and the experiment results being ± 3.5%.

In the next Section, a review of the currently available commercial flowmeters is given.

1.2 Literature Review

1.2.1. General Review of Flowmeters

In this Section, a brief review of the most common flowmeter type is given. The aim is to select suitable techniques for use in designing a flowmeter which meets the requirements listed in Section 1.1.

Table 1.2.1 lists the main types of flowmeters [Baker, 1989], which are commercially available. For convenience they are subdivided into three groups: momentum, volume and mass meters.

The momentum flowmeters measure flowrates by sensing the momentum change of the flow passed through the flowmeter. The differential pressure devices are simple to construct, but these meters must be installed in the flow stream (intrusive), and hence are not suitable for a clamp-on flowmeter.

In the volumetric flowmeter group, the positive displacement, the turbine and the oscillatory meters can only sense the flow if the meters are installed in the flow stream, therefore these techniques cannot be applied to clamp-on flow measurement. The principle of electromagnetic flowmeters is that when a fluid flows through a non-

magnetic tube in a transverse magnetic field, voltage and current are generated in the fluid due to the motion. If the voltage is measured between two electrodes in the pipe wall it will provide an indication of the volumetric flowrate in the pipe. Electromagnetic flowmeters can be used as clamp-on device but are only applicable to electrically conducting liquid flows through a non-magnetic pipe. Ultrasonic flowmeters fall into three categories or models of operation: ultrasonic transit time, ultrasonic cross correlation and ultrasonic doppler flowmeter (see Section 1.2.2.3 for detail of these flowmeters). With the capability of penetrating through materials, ultrasonics has the potential for designing clamp-on flowmeters.

In the mass flowmeter group, apart from the thermal mass flowmeter, the other mass flowmeters listed in Table 1.2.1 can only be used in an intrusive manner, i.e. the flowmeter needs to be installed inside the pipe. Thermal flowmeters can be used as clamp-on devices. If a heat source is applied to the pipe wall, heat is transferred to the fluid passing through a tube so that the temperature rises. This rise is proportional to the mass flow rate for a particular fluid and is measured by two thermocouples. The temperature rise, assuming that all this heat is transferred, is also proportional to the heat capacity of the fluid [Komiya, Higuchi and Ohtani, 1988]. The device is likely to be affected by heat transfer rate, and this will be affected, in turn, by the nature of the fluid plus the condition of the pipe. If the device operates in the laminar regime, then turbulence effects will not be present [Bobrovnikov and Novozhilov, 1989]. The thermal flowmeter is suitable for measuring slow flowrates in very small diameter pipes and can measure flowrates from outside of the pipe. Effects such as the condition of the pipe (roughness, thickness), flow profile sensitivity and space sensitivity can be reduced by monitoring the temperature changes in cross section of the pipe (which includes the pipe wall and the liquid flow inside the pipe) instead of only the pipe wall temperature. A combination of thermal and ultrasonic techniques was considered as suitable for this application.

In addition to the common type flowmeters listed in Table 1.2.1 clamp-on optical instruments exist. The basic principle of these techniques is to shine incident light onto or through the surface of the object to be investigated. The most advantage of the optical methods is the freedom from electromagnetic interference. The optical

instruments are in general expensive and may be particularly useful in areas of high hazard.

In the next section, a review of the ultrasonic measurement techniques and clamp-on ultrasonic flowmeters is given.

1.2.2. Review of Ultrasonic Flow Measurement Techniques

1.2.2.1. Fundamentals of Ultrasound

Ultrasound travels with the speed of sound relative to the medium. In liquids and gases it exists as a compressive wave in which there are regions of high and low pressure as shown in Fig 1.2.1. The wave length, and frequency of ultrasound are related by [Nelkon and Parker, 1977]

$$\lambda = \frac{C_L}{f}$$

where λ is the wave length, C_L is the velocity of sound in liquid, f is the frequency.

Ultrasound in a solid, as shown in Fig 1.2.2, may be transmitted either as a longitudinal wave in which the motion of the particles is in the same direction as the propagation of the sound beam, or as a transverse wave in which the motion of the particles is orthogonal to the direction of propagation of the sound beam. The velocity of the transverse wave is lower than that of the longitudinal wave. In a liquid, only longitudinal wave can propagate [Sanderson, 1990].

When an ultrasonic beam is incident on the interface between two materials (solid and liquid or, liquid and solid), the incident wave undergoes reflection and refraction as shown in Fig 1.2.3 [Sanderson, 1990]. The incident transverse wave 1 gives rise to the

two reflected waves 3 and 4. The wave 3 is a transverse wave and the wave 4 is a longitudinal wave. In the liquid only the longitudinal wave can propagate. At the second interface the longitudinal wave in the liquid gives rise to both longitudinal and transverse waves in the solid. The relationships of the angles between the beams and normal to the boundary surfaces are given by Snell's Law which states that [Nelkon and Parker, 1977]

$$\frac{C_W}{\sin\phi_W} = \frac{C_L}{\sin\phi_L}$$

or $$\phi_L = \sin^{-1}(\frac{C_L}{C_W}\sin\phi_W)$$

where ϕ_W, ϕ_L are the angles between the beam and the normal to the interface and C_W and C_L are the sound speeds in the solid and liquid respectively.

In next two sections, the application of ultrasound to non invasive flow measurement will be discussed.

1.2.2.2. Introduction to clamp-on flow measurements

Clamp-on or non-intrusive measurements implies that the probe or sensing means is either radiations (including heat, light, electromagnetic, radio waves or nucleonic radiations) or sound, all of which have been used. Developments have accelerated rapidly with the introduction of microchips and computers. Ultrasound seems to have the best potential for improvements in non-invasive measurement science.

Clamp-on ultrasonic flowmeters promise very attractive advantages by being non-invasive, they do not upset what one is measuring, and sensitivity is not limited by

friction and inertia effects. Although flowmeters are not necessarily inexpensive to purchase, their installed cost is low, because the instruments can be readily attached to the outside of existing pipes. The economic advantage over conventional flowmeters increases with pipe size.

Recent accounts of ultrasonic flowmeters, usually concentrate on either transit time or Doppler type. Although these are the most common types in use today, a few other types exist. Fig 1.2.4 shows the range of use of ultrasonics in flow measurements [Lynnworth, 1981].

Time of flight flowmeters use the transit time difference between ultrasonic beams transmitted upstream and downstream in the flowing medium, which is proportional to flow velocity.

Doppler type flowmeters use the frequency shift of ultrasound scattered from particles or air bubbles in the flow.

Correlation flowmeters use the ultrasound as the mechanism for detecting disturbances in the flow in the form of a second phase or eddies in the field.

Beam shifting in which the direction of an ultrasonic beam is modified by the flow of the fluid can be used as a measurement technique. The degree of beam shift can be used by setting two receivers side by side on the wall of the flowmeter and measuring the relative intensity of their received signals.

In vortex shedding detection the ultrasound from a transmitter is modulated by the vortices shed from the bluff body. a receiver detects this amplitude modulation and extracts the frequency of the modulation.

Open channel flow measurement using ultrasonics is a commonly used technique. These devices depend for their operation on the measurement of the transit time through the air path. Such devices usually incorporate a linearization routine for the particular notch

or weir being employed in order to be able to compute flow from height. Compensation for air temperature is also required.

Prior to any great detail about the development and construction of the proposed flowmeter, a review of previous research work in non-invasive ultrasonic and non-invasive thermal flow measurement techniques was undertaken. The Fluidex, Comspendex, Inspec, Chemical Engineering Abstracts and DELFT HYDRO on-line databases were used as an initial basis for a search through the literature on non-invasive ultrasonic and thermal flowmeters dating back to 1928.

1.2.2.3. Review of non-invasive ultrasonic flowmeters

A vast number of schemes were found in the scientific literature and in patents whereby ultrasonics was employed to measure flowrates.

a. Ultrasonic flowmeters before 1960

The earliest reference to the use of sound to measure fluid flow in pipe appears to be a German patent [Rutten, 1928]. This scheme necessitated the transducers being in the fluid. Three transducers were used, the central one was the driver, and the two receivers were located equidistantly on opposite sides of the driver on a line parallel to the fluid flow. The difference in travel time to the two receivers was then a measure of fluid flow.

The next proposal is found in a U. S. patent [Gray, 1945]. This is an apparatus for measuring airspeed and requires two sound receivers, one located upwind and one downwind of a centrally interposed sound transmitter. The principle of the technique is similar to that of the conventional transit time flowmeter. It would appear that the sound velocity in the medium, or specifically, changes in sound velocity, do not affect the accuracy of the meter indication, also, the indiction should be linear.

[Sproule, 1949] presents a British patent entitled "Improvements in and relating to electric oscillator generators". Either temperature, pressure, distance sound velocity, or liquid flow may supposedly be measured by his technique. Essentially he employs two distinct sound paths with four transducers located in the liquid, one transmitter and receiver pair transmits in the direction of flow and the other pair transmits against the flow. The carrier frequency is modulated, and after transmission through the fluid the modulation is fed back to the modulator. The frequency of the modulation will adjust itself until the fed-back modulation is in phase with the output of the modulator. The difference frequency between the two modulation frequencies is thus an indication of flow independent of properties of the fluid such as temperature and pressure. It is stated in the patent that with one set of transducers the temperature of a liquid may be determined, with no excess pressure and no flow, even through the walls of a container or pipe. It is not readily apparent that the multiple echoes between transducers even without walls, and the multiple echoes within the walls if the transducers are located outside a pipe, are not a complicating factor affection the phase of the received signal in this modulated continuous-wave system. It would appear that, with the transducers in direct contact with the liquid, this is a promising scheme.

A flowmeter with two transducers and an interchange of functions between transmitting and receiving was reported [Hess, Swengel, and Waldorf, 1950]. The sound elements were located inside and diagonally across a rectangular pipe. The fluid velocity is expressed as a function of velocity of sound, the frequency and projection of transducer spacing on the axis of flow, and the phase difference between the signals received alternately on each crystal. In 1954, the authors improved this scheme, showing that it is possible to eliminate the sound velocity dependent of the flow [Swengel, Hess and Waldorf, 1954].

In 1952, a U.S. patent [Kalmus, 1952] presented an apparatus for measuring flow from outside of plastic tubes. The main feature of this invention would seem to be improved switch for interchanging the functions of the two transducers. In this scheme, the transducers were fixed on a line parallel to the axis of the tubing on the outside wall. The attenuation of sound in the plastic tube was sufficiently high to minimize acoustic

energy leakage via the wall. In this scheme, the flow indication is dependent on the sound velocity in the fluid.

A current meter for water application was reported [Stull, 1955]. Two transducers with a separation were used, their axes lining up in the direction of flow by means of a streamlined mount. An interchange of functions (difference in wave length) was used for estimating flow but the flow indication was obviously still dependent on sound speed.

A commercial Fischer and Porter-Maxson flowmeter was described in [Kritz, 1955]. The principle appears to be similar to that of 4-crystal scheme in [Sproule, 1949], the difference being the degree of modulation. The Kritz flowmeter allows a frequency to be developed by turning the transmitter off during the time sound is impinging on the respective receiving crystals. The frequency difference between the two sets of transducers is then directly related to flow, and independent of found speed. It is not apparent how this scheme eliminates the difficulties attendant with multiple reflections between crystals, much less how it could be adapted to transmission through pipe walls.

In 1957, the feasibility of using wholly external ultrasonics to measure fluid flow within thick wall metal pipe was reported in [Grosso, and Spurlock, 1957]. The scheme was developed for large diameter pipes (11.19 inches). It might be possible that this method may be readily adopted to other pipe dimensions but limited amount of theoretical and experimental work were not enough to confirm this.

b. Non-invasive ultrasonic flowmeters reported in the 60s

Most of the methods discussed so far have been based on measuring effect of the flow on velocity of sound. A new clamp-on ultrasonic flowmeter which operates on the principle of beam deflection using an amplitude sensing system for flowrate measurement was reported in [Dalke and Welkowitz, 1960], this idea was first patented in USA [Petermann, 1957]. With this type of design, the flowmeter suitable for measuring all type of liquids and independent on speed of sound. However, Phase-shift

decreases with decreases in flowrates.This puts a lower limit to the flowmeter.This flowmeter was suitable only for higher flowrate measurement.

In 1962, the phase-comparison version of clamp-on ultrasonic flowmeter was presented in [Fischbacher, 1962]. For this technique, maximum accuracy of detection the phase difference should be as large as possible but not exceed 360^0. This puts an limit to the performance of flowmeters operated at high and low flowrates measurements. The author stated that, the flowmeter was suitable for measuring flowrates at about 200 $inch^3$ s^{-1} in a two inch inner diameter pipe. Little experimental detail was reported in this paper.

c. Non-invasive ultrasonic flowmeters reported in the 70s

Cross-correlation flowmeter

In 1970s, more papers relating to clamp-on ultrasonic flowmeters were published. [Coulthard, 1973] presented an ultrasonic cross-correlation flowmeter for measuring flows of liquids and gases. The measurement accuracy is in principle independent of the velocity of sound in the fluid and there is no restriction to the flow. The technique is advanced in the sense that the processing signal units combines the amplitude modulation with the phase-modulation. The amplitude modulation technique may be used when the acoustic standing waves do not exist or do not cause phase differences between the two received signals, phase-modulation technique would be employed other wise. With this design, the flowmeter was stated to be suitable for all types of fluids.

In [Bazerghi and Serdula, 1977] a scheme for a clamp-on ultrasonic cross-correlation flowmeter is proposed. The basic approach involves monitoring random variation in some properties of the flowstream. For single phase flow measurements, the meter is suitable only for measuring turbulent flow. The calibration results shower that the meter has an absolute error of about 3.0%

Transit time and Doppler ultrasonic flowmeters

A non-invasive transit time (phase comparison) flowmeter for measuring liquids is presented in [Pedersen and Lynnworth, 1973]. In this flowmeter, the choice of obliquely incident shear waves, instead of obliquely incident longitudinal waves, typically doubles the solid/liquid energy transmission and doubles the refracted angle in the liquid.Two pairs of ultrasonic transducers were used and the electronic measuring system employed two different frequencies (each near 1 MHz). These frequencies were transmitted continuously, one upstream and the other downstream, over a common path. The frequencies were servoed such that the phase in each direction in maintained constant. By means of subtracting the two voltages corresponding to the two frequency deviations, an output signal was produced which was proportional only to fluid velocity and was independent of variation in sound speed. The flowmeter was designed for large diameter pipe (300 mm) and higher flowrate (greater than 0.2 m^3 s^{-1}).

A vessel diameter independent volume flow measurement using ultrasound is presented in [Drost, 1978]. the principle is much the same as the transit time (phase shift) flowmeters. In this flowmeter, a rectangular beam of ultrasound, uniform in intensity across its surface was used to produce the desired volumetric output. This design could eliminated the flow profile effects. No experimental results concerning the measurement range were presented but the theory shows that this flowmeter is suitable for measuring higher flowrates.

An ultrasonic transit time difference current flowmeter is proposed in [Audunson and McClimans, 1975], which is useful for measurements of velocity fluctuations in a strongly stratified estuary. A comparison of velocity spectra above and below the density jump shows the utility of the meter in evaluating the energetics of the entrainment progress. The meter shows great promises for water quality investigations.

[Chappell, 1978] proposed an ultrasonic flowmeter,which measures two-phase flow with Doppler effect ultrasonic techniques. This ultrasonic flowmeter utilizes the Doppler principle for velocity measurements in lines of various materials and sizes in which the flowing liquid contains suspended solids or small entrained bubbles of air or gas. A single sensing transducer, containing two crystals, one is a transmitter and the other is a receiver, is held on to the pipe for transmitting and receiving signals. The test results

for water based liquids, with sufficient suspended solids or bubbles of air or gas were presented, the meter is capable of measurement to within 2% error or better. This flowmeter is not suitable for single phase flow measurements.

d. Non-invasive ultrasonic flowmeters reported in the 80s

In the early 1970s, clamp-on ultrasonic flowmeters completed their 'introductory' period. Since then, the clamp-on ultrasonic flowmeter has been continually developed and widely used in industry in 1980s and 1990s. With the advent of the microprocessor, it was then possible for ultrasonic flowmeter suitable for industrial applications to be designed and constructed. Various developments of the ultrasonic flowmeters were reported in 1980s

Cross-correlation flowmeter

A few scheme using the cross-correlation technique were found in 1980s. An accurate microprocessor-based peak-seeking correlator possessing good resolution, a large range, and fast response is described in [Leitner, 1980]. It consists of two separate correlators operating in parallel. The first microprocessor correlator evaluates the cross-correlation function at a number of equally spaced points over the range of delay of interest and finds the approximate position of the main correlation peak. The resolution of this correlator is poor, and its response is slow. It therefore directs the two-point difference correlator to the approximate peak position by controlling the clock rate of the delay lines. The latter correlator has good resolution and can lock onto, and track the correlation peak. It was established by the experimental results that, the correlator can locate a correlation peak with an accuracy of ± 0.2%. The reproducibility was checked at a number of time delays and a reproducibility of better than ± 0.1% was achieved at all delay settings.

[Sheen and Raptis, 1983] proposed a technique applied to flow velocity measurement in a coal/liquid slurry. The active acoustic cross-correlation system, consists of two pairs of transducers, a signal demodulation system, and a cross-correlator. The demodulation system uses a balanced mixer followed by a low-pass filter. The mixer

mainly multiplies the driving and received signals and the filter cuts off the carrier frequency. Demodulated signals are then fed into a cross-correlator, to calculate the cross-correlation function. By permitting variation of transducer separation together with demodulated the signals (by the demodulation system), the accuracy of the cross-correlation technique is increased. The cross-correlation technique can measure particle velocity within 5% error.

A modified cross-correlation flowmeter for measuring velocity of water is presented in [Tahkola and Karras, 1984]. The ultrasonic cross-correlation flow measurement system, consists of an adjustable signal generator, two pairs of wideband ultrasonic transducers with a centre frequency of 2 MHz, a phase demodulation unit, a correlator and a recorder. The coherence of the signals depends on the turbulence intensity and on the flow model stability. So in practice the flowmeter is not suitable for measuring flow velocity in transit region and laminar flows.

Another ultrasonic cross-correlation coal-slurry flowmeter for high temperature application is presented by [Sheen, Bobis, Raptis and Turgeon, 1987]. This flowmeter uses the combined technique presented in [Sheen and Raptis, 1983] and [Tahkola and Karras, 1984]. The cross-correlation flowmeter uses two sets of ultrasonic transducers. To isolate the transducers from the hot surface of the pipe, the flowmeter includes transducer standoffs. The transducers fixed onto the standoffs are clamped directly onto the pipe, separated by a distance. In each set, one transducer is excited by a continuous wave and transmits ultrasonic waves through the pipe wall and the flow medium. In the presence of flow disturbances or inhomogeneities, the interrogating ultrasonic wave is modulated before being received by the other transducers across the pipe. The flow modulation can consist of amplitude and phase modulations. A demodulator is needed to extract the modulation signals that are used for cross-correlation.

The ultrasonic inferential mass flowmeter for solids carried by the pulp suspension measurements is given in [Karras, Tornberg, and Harkonen, 1985]. The developed meter combines the cross-correlation ultrasonic flowmeter and the ultrasonic densitometer based on the attenuation of the transmitted beam. The transit time of the flow between the beams is determined by the cross-correlation of the intensity modulation of the

reflected amplitudes. The attenuation of the transmitted intensity can be measured as a ratio of the consecutive amplitudes and its logarithm is found to be linearly proportional to the consistency.

The cross-correlation flowmeter described in [Keech and Coulthard, 1985] is based upon a microprocessor-controlled multichannel correlation signal processor. In its present form it is a general purpose instrument intended for use in many different applications. Cross-correlation theory normally assumes that the processed data is statistically stationary, i.e., the statistical properties of the signal do not vary with time. However, when the velocity is changing, the data is non-stationary so that the basic cross-correlation principle is inapplicable. Another problem is that when the signal spectrum is not very wide, for example at low velocities, the time taken for a correlation peak to emerge can be too long particularly if the instrument forms part of a control feedback loop. There is no advantage in increasing the sampling rate but each of these problems can be largely overcome by the multichannel principle which allows increased data acquisition by using additional data sensing transducers detecting statistically independent data of the same event. The additional data is combined internally. The experimental results showed that when this technique is applied to single phase flow measurement, the meter is flow profile sensitive and with increased errors at low velocity, correspond to a gradual decrease in the correlation coefficient as the mean flow velocity decreases. This puts limit on the flowmeter accuracy at low flowrate measurements.

Transit time and Doppler ultrasonic flowmeters

A few ultrasonic transit time flowmeters (time of flight, phase shift) for clean fluid application were reported in 1980s. A multichannel ultrasonic flowmeter which can overcome the hydromechanical errors which are due to the different between the measured velocity and the mean flow velocity is given in [Antonov,Borisevich, and et al., 1980]. The theory for this flowmeter was considered by the author in 1976 and subsequently developed. Having many acoustic channels (the transducer pairs located in a plane that intersects the pipe at certain angle), the ultrasonic flowmeter, in principle, measures the averaged local flow velocity along each acoustic channel and

sums them according to the pipe section of the flow transducer. This design and operating principle avoid the need to take weighting factor into account. The accuracy of the flowmeter is increased by this design but accuracy of 0.5% could be obtained for an ultrasonic transit time flowmeter is rather high to be believed. This flowmeter is suitable for higher flow ranges.

[Baird, 1983] proposes an improved type of noninvasive ultrasonic phase-shift flowmeter which was claimed to be operated with virtually all liquids regardless of their amount of suspended solids. The Doppler-Type Flowmeter, was selected as the initial approach for design purposes. The first improvement was to eliminate the requirement for suspended solids or bubbles as reflectors. This was accomplished by using the normal turbulence of flow as a sound reflector and by measuring the phase shift of ultrasonic sound waves reflected from the turbulence of flow. The discontinuities formed by small masses of swirling liquid cause local pressure gradients which present a higher impedance to the ultrasonic wave, causing refraction. To reduce the effects of varying amounts of solids, a second transducer was mounted 180^0 apart and used as a receiver. The Noninvasive Ultrasonic Phase-shift flowmeter, as developed, appears to provide accuracies within a 1% - 2% range or better for liquids bearing less than 2% of suspended solids. For clean liquids, flow turbulence provides energy for reliable operation.

A Transit time ultrasonic flowmeter for pressurized water power plant applications is presented in [Ikenaga, Matsumoto, Takahashi and et al., 1983]. The ultrasonic flowmeter utilizes the principle that the propagation velocity of ultrasound varies depending on the flow velocity of the medium through which the ultrasound travels. The ultrasonic flowmeter directly measures the transit times of the upstream and downstream ultrasonic pulses and the transit time difference between them. Successive switchings of the two pairs of transducers (fitted at the end of the guide rods which keep the transducers away from the fluid heat) between upstream and downstream and averaging the transit time differences over a number of switchings, which can cancel out the imbalance effect, if any, due to the differences of the lengths and temperature distributions among the four guide rods. The author emphasized the importance of sound velocity compensation for this meter and claimed that, there is a built-in

compensation for the ultrasound velocity dependency on the water temperature without knowledge of the temperature and pressure but the author did not record in the paper how this compensation procedure was actually achieved. An accuracy of about ± 0.6%, stated by the author was rather high to be believed. This flowmeter is only applicable to higher flowrate measurements.

The flowmeter presented in [Kelley, and Bau, 1985] is essentially a transit time measurement device measuring flowrate in thermal convection loops. The instrument typically transmits pulses upstream, and then downstream and the difference in the measured transmission time is used to calculated the flowrate. The ultrasonic flowmeter is a viable solution only flowrate measurement in cases involving average velocities above 3.0 cm s^{-1} and moderate heating conditions.

A self calibrating clamp-on transit time ultrasonic flowmeter is presented in [Sanderson and Torley, 1985]. The paper describes a new clamp-on ultrasonic flowmeter system which provides self calibration in terms of pipe size and liquid being monitored. The microprocessor based flowmeter employs two additional ultrasonic transducers to measure the pipe wall thickness and the velocity of sound in the liquid. The measurements from these transducers are used to place the conventional transducers at optimum separation and to calibrate the flow measurement under operating conditions. The test results shows that, the accuracy of the meter is high (error is always less than 2.0%). Again as with other transit time flowmeters, this flowmeter cannot measure small flowrates.

e. Non-invasive ultrasonic flowmeters reported in the 90s

Cross-correlation flowmeter

Various developments of clamp-on ultrasonic flowmeters were reported in early 1990s. [Byrne, Coulthard and Yong Yan, 1990] describes a clamp-on flowmeter which is suitable for solid-liquid mixture measurement applications. The instruments combines the conventional cross-correlation ultrasonic technique with the gamma ray attenuation techniques to enable the flowmeter to make simultaneous measurement of instantaneous

fluid density and flow velocity, the product of the two being taken as the mass flow rate. Flow velocity is measured by cross-correlation and density by gamma ray attenuation or by a measure of capacitance/charge. This flowmeter is not suitable for single phase measurement applications.

Transit time and Doppler ultrasonic flowmeters

A noninvasive flowmeter for medical application is proposed in [Dymling, Persson and Hertz, 1991]. The method utilize a nondirectional continuous wave Doppler flowmeter. The instrumentation consists of an oscillator to produce a sinusoidal waveform which is amplified and used to drive the transmitting transducer, a pair of ultrasonic transducers for transmitting and receiving ultrasonic signals, and a pre-amplifier for amplifying the received low level signals. The mixer makes a frequency transformation with an amount determined by the reference signal coming from the oscillator. In this way it is possible to eliminate the constant frequency term so that the Doppler difference signal is found at the output of the mixer, i.e., the Doppler shift is obtained. After further amplification in a low-frequency amplifier, the output signal from the mixer is analyzed by an analyzer which can rapidly measure the spectral distribution of a low-frequency signal. Finally the analyzer is connected to a computer which can access the Doppler spectrum in the analyzer. This flowmeter can measure flow speed of as low as 1mm s^{-1}, but is suitable only for measuring flow with scatters.

[Szebeszczyk and Pietraszek, 1991] proposed a clamp-on transit time ultrasonic flowmeter for homogeneous liquid applications. The sing-around method of transit time measurement has been applied. Control functions, data processing, results presentation and communication with the external devices are performed by a single chip microprocessor. The calibration results proved that, the error of the flowmeter is about than 1%. this flowmeter is suitable for water measurement, but it cannot measure very low flowrates.

Conclusions

Various developments of the non-invasive ultrasonic flowmeters have been reviewed. The review considered the historical background and present developed clamp-on ultrasonic flowmeters. A fair number of clamp-on ultrasonic flowmeters were reported in the literature but none seems applicable to the flowrate specification of this work: measurement of single phase liquid with slow flowrate in small diameter pipe (see Section 1.1 for detail).

In the next section review of the thermal measurement technique will be given.

1.2.3. Review of thermal flow measurement techniques

1.2.3.1. Fundamentals of thermal flow measurements

For the thermal mass flow measurement techniques, heat is supplied to the fluid passing through a tube so that the temperature rises. This temperature rise is inversely proportional to the mass flowrate for a particular fluid and is measured by, for example, thermocouples [Baker, 1989] and [Harrison, 1981] or by some other means [Hummel, Ohlmer and Chenneaux, 1991]. The temperature rise, assuming that all this heat is transferred, is also inversely proportional to the specific heat capacity of the fluid. The specific heat capacity of the liquid varies with temperature changing but by a very small amount [Kaye and Laby, 1973].

The thermal mass flow measurement technique is dependent on the heat transfer rate and this will be affected in turn by the nature of the fluid plus the condition of the pipe [Bobrovnikov and Novozhilov, 1979]. Heat transfer in laminar flow is different from that in turbulent flow. If the device operates in the laminar flow region, turbulence effects will not present. [Hemp, 1993] discussed a technique for calculating velocity profile effects for laminar flow in thermal flowmeters.

In application, the thermal mass flowmeter which is based directly on the output of the temperature sensors [Baker, 1989] and is suitable for low flowrate measurements in small diameter tubes. For this type of design, the temperature difference between the

sensors is too small at very low flowrates and is also insignificant at high flowrates, this put limit on the flowmeter. The measurement range can be extended by combining the thermal technique with some other technique such as ultrasonic [Guilbert, Law and Sanderson,· 1993] or temperature correlation [Hummel, Ohlmer and Chenneenx, 1991]. Section 1.2.3.2 describes various techniques which have applied the heat transfer principle to flow measurement.

In the mathematical aspect of the thermal mass flowmeter, a basic energy equation which can be used to estimate the average temperature rise for a flowrate Q passed through a heater of a power P is given by [Nelkon and Parker, 1977] and [Baker, 1989],

$$P = QC_p\Delta T \tag{1.3.4}$$

where ΔT is the average temperature rise in the fluid and C_p is the heat capacity per unit volume of the fluid at constant pressure.

Although Equation (1.3.4) is simple to compute, the changes of fluid properties (such as density and viscosity) with temperature, flow profile and the efficiency of heat transfer from the heater (through the pipe wall) to the fluid are not included. The equations governing fluid motion and energy transfer in laminar pipe flow with heat source clamped on the outside of the pipe wall can be found in [Geankoplis, 1978]. These equations include the variation of fluid properties with temperature and pressure changes. The equation governing heat transfer in the pipe wall is purely heat conduction [Irons,1987]. Refer to chapter 3 for detail of these equations.

Heat transfer in turbulent flow is expected to be different from that in laminar flow due to the turbulence of the fluid motion which results in an improved heat transfer rate. Equations governing heat transfer are therefore required to predict temperature distribution for turbulent flow. It is not intended to present here a great detail of numerical techniques for turbulent flow heat transfer. The governing equations together

with suggested computation techniques for simulation can be found in [Yan and Lin, 1991].

If the thermal technique is combined with an ultrasonic technique [Guilbert, Law and Sanderson, 1993] then estimation of speed of sound and hence the transit time for ultrasound across the pipe is required. Once the temperature of the fluid is accurately known, the speed of sound can be estimated. For water, the temperature coefficient close to standard temperature pressure is of the order of about 0.2% per degree [Homans, 1982], i.e.

$$C_L(T) = C_L + 0.002C_L(T - T_{Ref}) \qquad (1.3.5)$$

It should be noticed that the relationship between the sound speed and liquid temperature is not perfectly linear, and Equation (1.3.5) should be used only for estimation. More accurate reference relating to sound speed changes with temperature can be found in standard physical tables, such as [Kaye and Laby, 1973].

In the next section, a review of thermal flowmeters is presented.

1.2.3.2. Review of the non-invasive thermal flowmeters

A non-invasive gas flow monitoring technique applicable to metal pipe with low thermal conductivity and high electrical resistivity is reported in [Harrison, 1981]. The rate of flow of gas can be measured by heating a short length of the pipe externally (the operational temperature range of a pipe in this system is typically between 70^{0}C and 200^{0}C and detecting the resulting temperature change by measuring the change in the pipe's electrical resistance between two externally applied electrodes. For a constant heater power the temperature of the pipe and hence the resistance, decreases with increasing flowrate. This flowmeter is not suitable for water measurement applications as tap water is an electrically conducting fluid. Added to that, to maintain the pipe wall temperature range from 70^{0}C to 200^{0}C for the pipe size and flowrate defined in Section

1.2 would require a very high heater power input and multi-phase flow would created due to the boiling point of water being 100°C.

The heat flowmeter presented in [Kuchnir, Gonezy and Tague, 1985] is not suitable for clamp-on measurement applications. However, the paper contains some material which is relevant for temperature measurement. This heat flowmeter is a device based on the thermal conductivity measuring technique. It consists of a thermally conducting body between two thermometers, with provisions for thermal connections and calibration. Instead of the traditional methods for measuring enthalpy change [Schwab, Greiner and Winter, 1990], this meter measures the thermal conductance of the thermometers. The advantages of this technique are higher sensitivity, better accuracy, shorter waiting times and a dependence on only electrical measuring equipment. The higher sensitivity results from the use of resistance thermometers (platinum, carbon or germanium), while the better accuracy comes from the direct comparison with electrically generated heat, which can be accurately measured. The shorter waiting times are a result of the technique depending only on the temperature of the cold liquid reservoir, not on the steadiness of the object being tested.

A thermal gas flowmeter is described in [Komiya, Higuchi and Ohtani, 1988]. The operating principle of this method is based on the heat transfer between the tube and the flowing fluid within the tube, and the measured quantity is the temperature difference of two points along the pipe wall. The temperature differences between the points on the pipe are the outputs for predicting flowrates. The flowrate decreases, the temperature difference between the two sensors also decreases, this puts a lower bound on the range of measurement. Furthermore, for relatively high flowrate, the temperature rise is insignificant and hence the magnitude of temperature difference is also too small to be measured accurately. This type of technique is therefore not suitable for very low or relatively high flowrate measurement applications. The author tested the flowmeter for several gases but did not specify the suitable application range and the accuracy of this flowmeter.

An integrated sensor for non-invasive monitoring of flow in low thermally conducting pipes is given in [Oudheusden and Bruijn, et al., 1989]. Flow detection is based on the

measurement of a temperature difference of an integrated circuit chip, which is heated with respect to the flow. The device is direction sensitive and has a zero output in the absence of flow. The sensor is small (4 x 4 x 0.3 mm); simple to construct, and easy to assemble (bonded onto the pipe by adhesive). The sensors contain resistors for heating and at least one transistor for the measurement of the chip temperature. The on-chip temperature difference is measured either by means of a differential transistor pair, or by using an integrated thermopile. The device is not intended for accurate flow rate measurements, but for indicative results, such as the presence of flow and its direction. Good results have been obtained for pipe materials with low thermal conductivity such as PVC and perspex. In the case of highly-conductive metals, such as aluminium, brass and copper, the method is not effective.

The basic principle of the pipe flow enthalpy difference meter presented in [Schwab, Greiner and Winter, 1990] is similar to the thermal mass flowmeter presented in [Baker, 1989]. The intensity of the output signals is increased by using a thermopile (composed of 40 Cu/CuNi thermocouples connected in series and the output is the sum of thermocouples readings). This design resolved the difficulty of measuring small temperature outputs. The calibration results shows that, this flowmeter could detect a temperature difference of 1 K with an accuracy of ± 1%. However, the flowmeter needed to be installed in the flowstream for measurement application

A flow velocity measurement system based on temperature noise correlation is given in [Hummel, Ohlmer and Chenneaux, 1991]. The TK instrument comprises essentially four parts, the sensor or TK-probe, the electronic signal conditioner, a signal correlator and a personal computer (PC) for the data handling and for the system control via an IEEE-Bus. The principle of this flowmeter is similar to the ultrasonic cross correlation technique except that the signals from the temperature sensors are used for cross correlating. The advantage of using the signal from the temperature sensor is that, temperature differences as low as 0.01 K still provide useful signals. This flowmeter is able only to measure thermally hydraulic fluids flows. The method is suitable for velocity in the range of about 0.01 to 10 m s^{-1}. The typical error is in the order of a few percent of reading. For optimal conditions, the error can be better than 1%.

1.2.4. Conclusion

Various developments of the non-invasive ultrasonic and thermal flowmeters have been reviewed. The review considered the historical background and present developed clamp-on flowmeters. A fair number of clamp-on ultrasonic flowmeters and thermal flowmeters were reported in the literature but none seems applicable to the flowrate specification of this work: measurement of single phase liquid with flowrate range as low as 0.5 mm s^{-1} to as high as 3.8 m s^{-1} in a 15 mm diameter pipe. A new flowmeter which combines the ultrasonic/thermal technique with ultrasonic multiple reflection is proposed for this application. The ultrasonic/thermal technique was considered for low flowrate measurement and the ultrasonic multiple reflection (time-of-flight) technique was proposed for higher flowrate measurement applications. Over a defined flowrate range both can operate.

In the next section, concept of the proposed flowmeter will be given.

1.3. The Proposed Flowmeter

1.3.1. System Configurations

The proposed flowmeter is essentially a combined ultrasonic transit time flowmeter with thermal measurement device, its configuration is shown in Fig 1.3.1. For low flowrate measurement, the ultrasonic/thermal technique is used. The ultrasonic multiple reflection technique is designed for higher flowrate measurement. Over a limited range of flow, both these techniques are employed which enable the flowmeter to perform cross checks.

There are several components required in the ultrasonic/thermal technique. A heat supply unit, a clamp-on heater with an automatic switch and an adjustable DC power supply, are needed to create a temperature difference in the flowing fluid. A signal generator is needed to generate sine wave signals. Direct beam transducers are essential for transmitting and receiving ultrasonic signals. Time measurement units are required

to measure the transit time for ultrasound to travel across the pipe. a data acquisition system is necessary to compute and output measurement results

The elements required for the ultrasonic multiple reflection techniques are: a signal generator, a pair of angled beam transducers to transmit and receive ultrasound signals, a multiplexer to alternate the function of the transducer pair (i.e. transmitter to receiver, and vice versa), and time measurement units. Elements such as the signal generator, electronics and computation system could be shared between the two techniques.

In both techniques, the transit time from the transmitter to the receiver is measured, and used for estimating the flowrates.

1.3.2. Basic Theory of the ultrasonic/thermal Technique

The proposed ultrasonic/thermal meter is based on a heater which is clamped onto the outside of the pipe. Ultrasonic transmit-receive transducer pairs are also clamped onto the pipe a short distance from the heater. With the heater switched on, heat propagates both upstream and downstream in the pipe and the liquid by conduction. When the liquid is flowing, heat convection by the flow results in a change in the heat distribution within the meter area. This change results in a variation in the speed of sound which is detected by the transmit-receive transducer pairs which send and detect ultrasonic bursts whose propagation time is measured.

Two transducer configurations (two transducer pair configurations and a single transducer pair configuration) have been proposed which results in different modes of operation and performances. One configuration uses two pairs of ultrasonic transducers - one pair upstream and the other downstream - and the other has a single pair of transducers mounted downstream of the heater.

In the two transducer pair configuration (Fig 1.3.2a) the asymmetry due to flow between the heat distribution upstream and downstream of the heater is determined by measuring the difference in ultrasonic transit times between the transducer pairs. Reverse flows are

automatically detected and measured by this form of the meter as the transducer pair downstream of the heater will always measure a shorter transit time than pair upstream. (Speed of sound increasing with temperature). If the flow reverses, the transducer pair measuring the shorter transit time will change. As the flowrate decreases, the difference in transit time will also decrease. This puts a lower bound on the range of this configuration of the meter.

The single transducer pair configuration overcomes the problem of low flow inaccuracy. However, it is unable to measure reverse flows. In this form the meter has a single pair of transducers mounted downstream of the heater (Fig 1.3.2b). As with the two pair configuration, these transducers determine ultrasonic transit time which is related to average temperature across the measurement path. The transit time is measured with the heater switched on and off periodically. The difference in transit times is then used to determine flowrate. When the heater is off the transit time gives a measure of the temperature of the fluid entering the meter and so can be used to compensate for inlet temperature variations. Because the difference in transit times is greater at lower flowrates, this configuration becomes more accurate as the flowrate decreases and so has a lower minimum flowrate. However, the transit time needs to be measured at steady state (after transients due to switching the heater on or off have decayed). This reduces the response time of the meter - especially at low flowrates when the heat is not convected away as quickly. Nevertheless, this configuration was felt to be the more promising and was selected for the numerical and experimental investigations.

The basic equations for single transducer pair configuration can be outlined as follows:

When the heater is on, the transit time for an ultrasound beam to travel across the pipe diameter (Referring to Fig 1.3.3. for definition of coordinate system and dimensions) is given by

$$\Delta t_1 = \int_0^d \frac{dr}{C_W(t)} + \int_d^{D-2d} \frac{dr}{C_L(t)} + \int_{D-2d}^{D} \frac{dr}{C_W(t)} \qquad (1.3.1)$$

where Δt_1 is the transit time for ultrasound to travel across the pipe, $C_W(t)$ and $C_L(t)$ are speed of sound in copper pipe wall and liquid respectively which are temperature and position dependent (i.e. dependent on both the heater power and the coordinates (x, r, ϕ) of the pipe).

When the heater is off, the transit time for an ultrasound beam to travel across the pipe diameter is equal to

$$\Delta t_0 = \frac{2d}{C_W} + \frac{D - 2d}{C_L} \qquad (1.3.2)$$

where Δt_0 is the transit time for ultrasound to travel across the pipe, C_W and C_L are speed of sound in copper pipe wall and liquid respectively at a reference temperature.

For a given heater power, the transit time for ultrasound across the pipe diameter is a function of flowrate only, and hence the flowrate Q can be estimated by the transit time difference between the heater off and on, which is defined as

$$\Delta t = \Delta t_0 - \Delta t_1$$

i.e. $$Q = F(\Delta t) \qquad (1.3.3)$$

1.3.3. Basic Theory of the ultrasonic multiple Reflection Technique

As flowrate increases, the temperature rise in the liquid decreases, which results in an insignificant change in the transit time difference. An alternative approach was therefore required for measuring higher flowrates. This was based on a pair of angled beam transducer clamped onto the outside of the pipe (Fig 1.3.2c). In this technique, the transit time difference between ultrasonic beams transmitted upstream and downstream in the flowing medium is proportional to flow velocity, and is therefore used to predict flow velocity.

The ultrasonic transit time method consists basically of sending two ultrasonic pulses at an angle across the pipe, one in the direction of flow and the other in opposite direction. The pulses emitted in the direction of the flow will travel the distance between the two transducers in a shorter time than the pulses travelling against the flow.

If the fluid in Fig 1.3.4 is moving with velocity V at a angle ϕ_L to the ultrasound beam in a fluid for which the velocity of sound beam is C_L, then the transit time for ultrasound beams to travel from transducer 1 to transducer 2, and from transducer 2 to transducer 1 respectively are

$$t_{12} = \frac{N(D - 2d)}{\sin\phi_L(C + V\cos\phi_L)} + \tau_d \qquad (1.3.6a)$$

$$t_{21} = \frac{N(D - 2d)}{\sin\phi_L(C - V\cos\phi_L)} + \tau_d \qquad (1.3.6b)$$

where t_{12} is the transit time from transducer 1 to transducer 2, t_{21} is the transit time from transducer 2 to transducer 1. (D-2d) is the inner diameter of the pipe, N is number of reflections and τ_d is the delay time of the transducers and electronics.

The transit time difference, Δt_{AB} , is obtained by subtracting t_{12} from t_{21},

$$\Delta t_{AB} = t_{21} - t_{12} = \frac{2N(D - 2d)\cot\phi_L}{C^2 - V^2\cos^2\phi_L} V \qquad (1.3.7a)$$

since in general, $C^2 \gg V^2\cos^2\phi_L$, Equation (1.3.7a) can be simplified to

$$\Delta t_{AB} = t_{21} - t_{12} = \frac{2N(D - 2d)\cot\phi_L}{C^2} V \qquad (1.3.7b)$$

The difference in transit time of the two ultrasonic signals Δt_{AB} is a measure of the flowrate.

1.4. Thesis Layout

Following the introduction into the field of non-invasive measurement technologies given in Chapter 1, in Chapter 2, management aspects of the project are given.

Chapter 3 describes the mathematical modelling and integration of the mathematical model into computer models for the heat transfer from the heater clamped outside the pipe to the fluid flow inside the pipe, and hence speed of sound in the pipe wall and the fluid could be predicted, which are essential for designing the ultrasonic/thermal flowmeter.

In Chapter 4, theoretical aspects of the flowmeter are examined in detail. Component requirements of the flowmeter and the operating principle are given in Chapter 5. Chapter 6 presents the design, construction and preliminary tests of the developed flowmeter. In Chapter 7, the design and construction of a refined hydraulic test facility with a computer data acquisition system for calibration of the proposed clamp-on flowmeter is described in detail. In Chapter 8, various experiments for testing the performance of the proposed flowmeter are presented. The experimental results are discussed and analyzed in Chapter 9. Finally, the conclusions drawn from this work together with the suggestions for further research are stated in Chapter 10.

2. MANAGEMENT ASPECTS

2.1. Introduction

In this Chapter, the management of the research work for developing a clamp-on flowmeter is considered together with the benefit analysis. In the first section, the planning and controlling of the major activities that make up the technical content are discussed. The target is to break the overall task down into a series of steps, taking care to consolidate each step before progressing to the next. In the second section, the problems associated with invasive domestic flowmetering and the benefits of the clamp-on flowmetering are given. The installation costs analysis for the domestic flowmeter is discussed. The calculation was based on the realistic values reported in the National metering trials report conducted by various Water Service plc's and Companies involved.

2.2. Applying the Principle of Project management for Planning the Research

2.2.1. Management of the Research Work

It has been proved in the past that, whatever the end product, the method of successfully completing a project (or research work) can be best achieved by good management. An innovation case study given in [Bradnam, 1992] is an example showing that project management is the most effective way to execute a complex multi-discipline task.

The characteristics, advantages and phases of the project management system could be found in [Ritchie, 1992]. One of the important characteristics of a project is that generally, it goes through a series of phases. Sometime the phases are carried out sequently, but very often they overlap to a large extent. The phases that are usually included are: conceptual study; feasibility study; planning; basic design; detailed design;

procurement and commission. The advantage of breaking the overall task down into a number of phases is to study each in depth before progressing to the next.

The phases for the Ph.D. research work are illustrated in Fig. 2.2.1. The Conceptual study would be a study to examine the basic ideas of the flowmeter to be developed. The advantages that would be gained by proceeding with the research work and to give a very general indication of the cost and the overall economics of the venture were carried out by members of the client organisation (Severn Trent water company) and members of the department (Dept. of Fluid Engineering & Instrumentations, Cranfield University). The contents of the Feasibility study would include an exact description of the flowmeter including: size; flowmeter type; technologies to be used; equipment that needed to be purchased and personnel required to perform part of the work (such as electronic expertise and laboratory assistance). Again, the estimated running costs were considered by a different group of people. During the Planning phase a list of activities of the research work were outlined and they will be asked to prequalify for the work. There are two important factors that have been considered in the planning of this research work: personnel to provide assistance on part of the work and resources available (such as equipment, space and services). Whilst the project planning is being carried out the basic design documents can be prepared. This defines in sufficient detail the actual scope of the work which was chosen during the feasibility study. Sufficient technical information is generated so that more accurate assessment of the schedule can be made and the quality of the flowmeter can be defined. By this time, a very clear idea of the flowmeter (its size, flowmeter type, quality and work schedule) can be defined. In the engineering and procurement phase the detailed drawings are prepared, materials and equipments are specified and purchased. The Construction phase is to construct the clamp-on flowmeter in accordance with the design documents. The final phase of the research work is the Commissioning phase, where the developed flowmeter is thoroughly tested and brought to full working order.

In the next section, the principle of project control and its application to the research work will be discussed.

2.2.2. Project Control

The project control is to ensuring that meticulous attention is paid to essential activities of the research work. It should be noted that there are five elements of this research work that need to be controlled: Scope; quality; schedule; personnel and resource; and costs. The project control should be executed in parallel with each phase of the Ph.D. which was discussed in section 2.2.1.

Controlling the scope of the research work is to define exactly the final form of the flowmeter this is to ensured that, start designing and constructing the flowmeter for which the basic concept is firm. work breakdown structure have been adopted for defining scope of the Ph.D. work (see section 2.2.3 for detail). When, and only when the scope is fully defined should a plan be prepared. Once the plan has been agreed, the detailed planning can start. A master project schedule can be prepared to accomplish the objective laid down in the plan. This is a schedule for the whole job from basic engineering to completion showing only the major activities. Quality assurance/Quality control is vitally important because delays can be caused by poor quality engineering. A comprehensive quality assurance procedure has been prepared to advice all the people involved in the work of the level of quality that must be maintained. Attention was also paid to purchase suitable materials and equipment for constructing and testing of the flowmeter. In personnel control, it is vital that, the personnel involved in the work are fully motivated and productive. The people involved in this research work are the author, the supervisors, electronic experts, laboratory assistants and the client who provide financial support for this work. An effective way for the members in the team to communicate is to use the one leader task force given in [Ritchie, 1992]. Meeting have been organized quarterly, at which all senior members of the team including the client are present. From the meeting the personnel involved received up to date information and also the schedule for the next phase of work.

In the next section, use of the work breakdown structures for defining the scope of the Ph.D. thesis will be discussed.

2.2.3 Work BreakDown Structures

A work breakdown structure is a formal and systematic way of defining the scope of a project (or research work). Of equal importance, the process helps to identify missing scope items and areas of ignorance.

The work breakdown structure is developed by exploding the research work into its component parts and services required. The packages of work so formed must be clearly distinguishable from all other work packages. Each package is further subdivided into lower level elements of work representing units of work at a level where the work is to be performed. This process of breaking down the work is continued until the research project is fully defined in terms of "WHAT" is to be done to complete the Ph.D. A work breakdown structure for the Ph.D. is illustrated in Fig. 2.2.2 to Fig. 2.2.6. This work breakdown structure divides the work of the Ph.D. research into manageable units for which individual responsibility can be assigned and work schedule together with the resources required for completing a particular unit of the work can be planned.

2.3. Cost And Benefit Analysis

2.3.1. Introduction

In order to achieve a sensible cost for widespread metering of water in the future (from 1 April 2000), it would be necessary to select flowmeters which are inexpensive, accurate, and have low installation and maintenance costs. Flowmeters which possess less problems and whose repair cost is low could reduces maintenance cost. The intrusive domestic flowmeters currently used by the water companies are inexpensive to purchase but possess problems and the repair cost is high. The unit cost for clamp-on flowmeter is higher than that of the domestic flowmeter but installation and maintenance cost are low, which would maintain the cost advantage in the long term plan. Clamp-on flowmeters might be a sensible choice for use as a calibrator for calibrating installed domestic flowmeters and can also be installed in properties for metering water.

In this section, the problems associated with the intrusive domestic flowmeters will be examined in detail. The intention is to show the benefits of the clamp-on flowmeter and that the use of the clamp-on flowmeter type would maintain the cost advantage in the long term plan. The cost analysis for the domestic flowmeter is also discussed.

The facts and values used in this work are the results of metering trials which were conducted by the Water service plc's companies, the Water Research Centre and Department of Environment for a widely different range of customers from Northumbria to the Isle of Wight. Fig. 2.3.1 shows the locations and Table 2.3.1 listed number of properties.

In the next section, the problem associated with the domestic flowmeter will be given.

2.3.2. Problem with the Domestic Flowmeters and Advantages of Clamp-on Flowmeters

To understand the benefits which could be gained by using the clamp-on flowmeter in water industry, one must first understand the problems associated with the domestic flowmeters. There are two approaches which were adopted for domestic flowmeter installation, internal metering (domestic flowmeter is installed inside of the property) and external metering (domestic flowmeter is located immediately outside of the property boundary, which in most case has been in the public footpath). Typical practical problems experienced were: customers complaints; electrical earthing; leakage; and most serious of all is the poor performance of the metering equipment.

Most of the complaints where internal meters were installed stem from accidental damage to a customers property (eg. rectifying damage to carpet, wallpaper and paint work; removing dirty marks and stains). Most of the complaints about external installation were that customers complained about the inconvenience of having their garden, pathway or drive dug up and about the mismatch of the final resurfaced appearance. Where compensation has been agreeded, it has generally been paid by the water company involved.

Another problem was the affect the installation of an external meter (which has a predominance of plastic components) or the replacement of a metal service pipe with a plastic one might have on the effectiveness of the electrical earth of property. As can be seen in later section, the cost for solving the electrical earthing problem would be about £5.70 per property.

The problems caused by the poor performance of the metering equipment are of more significance and are harder to resolve. The most common problems encountered are summarised as follows: meters have been found to leak from the joints; meters reported by customers as jammed or failing to record; condensation on the meter display/body; broken seals; and reported problem concerned with meter box mainly difficulty in removing the box lids (which tend to fit very tightly and the disintegration of insulating material), quality control during box assembly and the durability of box components. The main problems found with the metering equipment at each trial site and the repair expenses are presented in Table 2.3.2 and Table 2.3.3. As can be seen from the values recorded in these Tables, installation and maintenance cost for the domestic flowmeters are high. Most of the problems identified for domestic flowmeters would not occur with clamp-on flowmeter installations.

Meter accuracy checks are high for domestic flowmeters, due to the labour required to remove and install flowmeters into the pipeline. However, the cost of confidence checks on the accuracy of the domestic flowmeter could be reduced by the use of a clamp-on flowmeter as a calibrator for calibrating the domestic flowmeter. Accuracy checks could be done without the need to remove the flowmeter.

In next Section the cost analysis for domestic flowmeter installation will be given.

2.3.3 Domestic Flowmeter Installation Cost Analysis

In this Section, the cost analysis for domestic flowmeter installation will be discussed. The calculation is based on the realistic values reported in the watering meter trials

(referring to Fig. 2.3.1 for trial site locations and Table 2.3.1 for information about the trail sites properties).

The main types of expenditure involved in the installation of a straight forward or standard meter installation are identified as: basic installation cost; leakage repair; electrical earthing; survey costs; management and supervision costs; and outreader system installation costs.

A complete cost analysis should also included the long term maintenance costs. As the values for long term maintenance costs are not available, a full costs and benefits analysis is not possible. According to the results shown in section 2.3.2, a number of problems were identified and the costs in correcting these problems were significant. This strongly suggests that the maintenance costs for the domestic flowmeter are high.

A detailed costs estimation for a standard domestic flowmeter installation is presented below:

Meter Installation Costs Estimation

a. Basic Installation Costs

The basic installation costs include the material costs, installation costs and permanent reinstatement cost. Material costs involving the cost of the meter, its fittings, and the meter box for external installations. Costs average at £61.83 per property. Installation costs including the hiring of plant and labour. Costs average at £88.86 per property. Permanent reinstatement cost involving the labour and materials used in restoring a property after installation. Costs average at £10.16 per property. Hence, the average cost for a basic installation is £157.80 per property excluding survey and management costs.

b. Leakage Repair Costs

The average costs for repairing a leak was £55.50 per property, where a leak was found.

c. Electrical Earthing Costs

Electrical earthing costs including the cost of materials and labour for restoring the electrical earthing problem which resulting from installation of the external domestic flowmeter. Material for electrical earthing costs average at £5.70 per property.

d. Survey Costs

Survey costs involving the identifying of the position of external/internal stopcock, location of service pipe and configuration, and the most suitable location for the meter. Survey costs average at £22.81 per property.

e. Management Costs

Management and supervision dealing with procedures for access, communication between the customers and the company, the requirements for meter installations, and computer systems and data input/output requirements. Management costs average at £33.12 per property.

f. Outreader Costs

Outreader costs involving the technology for installing of remote electronic display or outreaders. The cost could be ranged from £39.64 to £164.05 per property. For this calculation, the minimum cost was used. Costs average at £39.64 per property.

<u>Total Cost</u>

The averaged total cost for domestic flowmeter installation is £254.74 per property.

2.4. Conclusions

The principles of project management have been applied for planning the Ph.D. research work. The phase by phase planning enable one to divide the whole task down into manageable steps, so that the working schedule, the resources and work force required for each phase of the research work could be easily identified and controlled.

To point out the benefits of the developed clamp-on flowmeter for water industry application, the problems exist with the current domestic flowmeter were examined and clamp-on flowmeter could overcome most of these problems. The results show that the unit costs of the domestic flowmeter, although lower than that of the clamp-on flowmeter, possess problems with poor meter equipment performance, installation, together with a great likelihood of compensation claims. Any difficulties with meter maintenance, such as would occur with leakage, defective or noisy meters, or condensation are harder to resolve. Electrical earthing is potentially difficult where external meters are installed. Its not as yet possible to draw any conclusions about the long term maintenance costs of the domestic flowmeters. The results obtained from the trails strongly suggest that, the maintenance cost for these flowmeters would be high.

The unit cost of the clamp-on flowmeter is higher than that of the domestic flowmeters. However, there is a substantial installation cost saving and a great opportunity for long term maintenance saving, which would maintain the cost advantage.

3. MATHEMATICAL MODELLING OF THE HEAT TRANSFER IN PIPE FLOW

3.1 Physical Model

In this section, the derivation of a set of second order partial differential equations governing the relationship between time, temperature, velocity and position of the coupled heat transfer for the given physical model is considered. This mathematical model would predict the temperature profile and hence speed of sound in the pipe and the liquid, which is essential for modelling the ultrasonic/thermal flowmeter.

The geometry under consideration is illustrated in Fig 3.1.1. Fluid with uniform temperature enters a copper pipe with circular cross section. The flow is assumed to be fully developed (laminar or turbulent). An electric heater (about 1/10 of the test section length) is clamped on to the pipe. The power of the heat flux generation is determined by a DC input to this heater.

Flow enters the test section and is heated by a constant heat flux (the heater) applied to the pipe wall. By considering the energy balance of the system described in Fig 3.1.1, one may assume that part of the heat generated will be stored in the pipe wall by virtue of the wall heat capacity and the remainder will be transferred from pipe wall to the fluid. The temperature in the section is a function of input power Q, flow speed V, time t, dimensions of the pipe and position,

i.e., $T(Q, t, V, r, \phi, x)$.

3.2 Derivation of the Mathematical Model

Derivation of the mathematical model was started by considering in detail the energy transfer inside a differential volume $rdxdrd\phi$ in cylindrical co-ordinates. The model

is derived as follows: firstly, write an energy balance equation for an element of size $rdxdrd\phi$

which is stationary then apply the law of conservation of energy, which is really the first law of thermodynamics. For the energy in this volume at any time, the law of conservation of energy states that:

(Rate of energy accumulation) (3.2.1)

= (Rate of energy in) - (Rate of energy out) + (Rate of external work)

Fig 3.2.1 shows the heat flows in and out of an element of volume $rdxdrd\phi$.

Derivation of the differential equation governing energy transfer is best done by considering the heat flowing in and out and the energy stored in each of the radial, circumferential and axial directions for the element.

The heat flowing into the element in the radial direction is

$$\partial T_r = -K_L dxrd\phi \frac{\partial T}{\partial r}\Big|_r + \rho C_p V_r T dxrd\phi\Big|_r \qquad (3.2.2)$$

and out

$$\partial T_{(r+dr)} = -K_L dxrd\phi \frac{\partial T}{\partial r}\Big|_{r+dr} + \rho C_p V_r T dxrd\phi\Big|_{r+dr} \qquad (3.2.3)$$

where K_L is the thermal conductivity, ρ is the density and C_p is the specific heat capacity of water.

The first term in the right hand side of the above equations represents the heat transfer due to the temperature gradient. The second term is the heat transported by the fluid flow with velocity V_r.

Taking Taylor expansions for (3.2.3), with second and higher order terms being ignored, one obtains

$$\partial T_{(r+dr)} = - K_L dx r d\phi \frac{\partial T}{\partial r} + \frac{\partial}{\partial r}(- K_L dx r d\phi \frac{\partial T}{\partial r}) dr +$$

$$\rho C_p V_r T dx r d\phi + \frac{\partial}{\partial r}(\rho C_p V_r T dx r d\phi) dr \qquad (3.2.4)$$

The net heat stored is therefore

$$\partial T_r - \partial T_{(r+dr)} = \frac{\partial}{\partial r}[(K_L dx r d\phi \frac{\partial T}{\partial r}) dr] - \frac{\partial}{\partial r}[(\rho C_p V_r T dx r d\phi) dr] \qquad (3.2.5)$$

In a similar manner, the net heat flowing in, flowing out and stored in the element in the circumferential direction are

$$\partial T_\phi = -K_L dr dx \frac{1}{r} \frac{\partial T}{\partial \phi}|_\phi + \rho C_p V_\phi T dr dx|_\phi \qquad (3.2.6)$$

$$\partial T_{\phi+d\phi} = -K_L dr dx \frac{1}{r} \frac{\partial T}{\partial \phi}|_{\phi+d\phi} + \rho C_p V_\phi T dr dx|_{\phi+d\phi} \qquad (3.2.7)$$

$$\partial T_{\phi} - \partial T_{\phi+d\phi} = \frac{\partial}{\partial \phi}[(K_L dr dx \frac{1}{r}\frac{\partial T}{\partial \phi})rd\phi] - \frac{\partial}{\partial \phi}[(\rho C_p V_{\phi} T dr dx)rd\phi] \tag{3.2.8}$$

respectively.

Finally, the net heat flows in the axial direction are

$$\partial T_x = -K_L rd\phi dr \frac{\partial T}{\partial x}|_x + \rho C_p V_x T rd\phi dr|_x \tag{3.2.9}$$

$$\partial T_{x+dx} = - K_L rd\phi dr \frac{\partial T}{\partial x}|_{x+dx} + \rho C_p V_x T rd\phi dr|_{x+dx} \tag{3.2.10}$$

$$\partial T_x - \partial T_{x+dx} = \frac{\partial}{\partial x}[(K_L rd\phi dr \frac{\partial T}{\partial x})dx] - \frac{\partial}{\partial x}[(\rho C_p V_x T rd\phi dr)dx] \tag{3.2.11}$$

The rate of change of energy with time is

$$rd\phi dr dx \rho C_p \frac{\partial T}{\partial t} \tag{3.2.12a}$$

Applying the law of conservation of energy (3.2.1), the energy balance for the element leads to

$$rd\phi\,drdx\rho C_p\frac{\partial T}{\partial t} = [\frac{\partial}{\partial r}(K_L dx rd\phi\frac{\partial T}{\partial r})dr - \frac{\partial}{\partial r}(\rho C_p V_r T dx rd\phi)dr] +$$

$$[\frac{\partial}{\partial \phi}(K_L drdx\frac{1}{r}\frac{\partial T}{\partial \phi})rd\phi - \frac{\partial}{\partial \phi}(\rho C_p V_\phi T drdx)rd\phi] +$$

$$[\frac{\partial}{\partial x}(K_L rd\phi dr\frac{\partial T}{\partial x})dx - \frac{\partial}{\partial x}(\rho C_p V_x T rd\phi dr)dx]$$

(3.2.12b)

Dividing the Equation (3.2.12b) through by $rd\phi\,drdx$, with the assumptions that the variation of K_L, C_p, and ρ with temperature can be ignored and that the substance is homogeneous, the differential equation for laminar flow is

$$\rho C_p(\frac{\partial T}{\partial t} + V_r\frac{\partial T}{\partial r} + \frac{V_\phi}{r}\frac{\partial T}{\partial \phi} + V_x\frac{\partial T}{\partial x}) = K_L(\frac{\partial^2 T}{\partial r^2} + \frac{1}{r}\frac{\partial T}{\partial r} + \frac{1}{r^2}\frac{\partial^2 T}{\partial \phi^2} + \frac{\partial^2 T}{\partial x^2})$$

(3.2.13)

Further restricting the problem to 2-D heat transfer $(\frac{\partial T}{\partial \phi} = 0)$ and hydrodynamically fully developed flow ($V_r = 0$), the mathematical model governing time-temperature-position relation for the heat conduction and convection in the fluid region is given by

$$\frac{\partial T}{\partial t} = \alpha_L(\frac{\partial^2 T}{\partial r^2} + \frac{1}{r}\frac{\partial T}{\partial r} + \frac{\partial^2 T}{\partial x^2}) - V_x\frac{\partial T}{\partial x} \qquad (3.2.14)$$

where α_L is the diffusivity of water and $\alpha_L = \frac{K_L}{\rho C_p}$.

In the pipe wall, heat transfer occurs purely by conduction. The heat transfer equation for this solid region can be derived directly from Equation (3.2.14) by replacing the convection term in Equation (3.2.14) by zero. The heat conduction equation for the wall is then given by

$$\frac{\partial T}{\partial t} = \alpha_w\left(\frac{\partial^2 T}{\partial r^2} + \frac{1}{r}\frac{\partial T}{\partial r} + \frac{\partial^2 T}{\partial x^2}\right) \qquad (3.2.15)$$

where $\alpha_w = \frac{K_w}{\rho_w C_w}$.

If the physical properties of the fluid were to vary with temperature, and the pressure gradients were to be taken into account, the equations should include the continuity, the momentum and the energy formulations. At steady state, the equations in vector form are

$$\nabla \cdot \underline{V} = 0 \qquad (3.2.16)$$

$$\rho(\underline{V}\cdot\nabla)\underline{V} = -\nabla p + \mu\nabla^2\underline{V} + \rho\underline{g}\beta T \qquad (3.2.17)$$

$$\rho C_p \underline{V}\cdot\nabla T = K_L\nabla^2 T \qquad (3.2.18)$$

The governing equations for heat transfer in pipe flow at high Reynolds number (turbulent flow) are complex, and will not be discussed here. Refer to [Yan and Lin, 1990] for details of these equations.

3.3. Numerical Approach

The temperature profile for the fluid and the pipe wall regions at any given time could be found by solving the coupled heat transfer differential Equations (3.2.16) to (3.2.18) numerically with the boundary conditions specified in Fig 3.3.1. Two different numerical approaches were used for the computation: finite difference approach and finite element approach. A recommended finite difference numerical technique [Peaceman, 1955] for solving the energy equation is described in Appendix A.1 to A.3. Several fluid dynamic packages for solving these type of equations exist. [FIDAP, 1991] was considered as one suitable package and it was available in DFEI (Dept. of Fluid Engineering & Instrumentation, Cranfield University).

3.3.1 Finite Difference Approach

Detail of the finite difference approach for solving this type of heat transfer equations is given in Appendix A.1 to A.4.

The developed finite difference method for solving the energy equation worked but had limitations. The software did not include the continuity equation and momentum equation, also the changing of the physical properties of the fluid with temperature was not accounted for. Extending the software to 2-D turbulent, 3-D laminar and turbulent models would require further modifications. Added to the above problems, the computer resources at Cranfield University were not adequate for the required computations.

An alternative approach to the problem was therefore considered, which used a commercial finite element package (FIDAP). This will be discussed in the next Section.

3.3.2. Finite Element Approach

3.3.2.1. FIDAP (finite element package for fluid dynamics)

A finite element package (FIDAP), specially designed for solving fluid dynamics problems was installed in the Department. Although considerable time and effort was required to master the package, it was considered worthwhile since the package was very flexible, and most important of all, allowed one to include changes in the physical properties with temperature. Furthermore, little effort was required to convert the 2-D laminar flow heat transfer model to 2-D turbulent, and 3-D heat transfer models. With the aid of super computer resource in Manchester, the package has been used successfully for solving the specified coupled heat transfer equations.

The FIDAP User's Manuals contain more detail on the package. The work presented here concentrated mainly on developing appropriate models using the package.

3.3.2.2 Problem Description

The physical model is the same as the one described in Section 3.1 and is shown in Fig 3.1.1. The test section has open ends and is heated round the pipe circumference by a constant heat flux q_H (clamped heater) sited at the midpoint of the pipe section. Fully developed laminar (or turbulent) flow enters from the left, passes through the heated section and exits to the right.

The operating conditions and dimensions for the problem under consideration were

pipe material	copper	
pipe length	500	mm
pipe diameter	15	mm
pipe wall thickness	0.75	mm
heater length	40	mm
heater power	40-100	watts

fluid	water

The properties of clean water and copper pipe were taken at a reference temperature of 10 °C and are as follows [Kaye and Laby, 1973]:

For water:

viscosity	1.3037E-3	Ns m^{-2}
density	999.7	kg m^{-3}
specific heat	4191.9	J kg^{-1} $°C^{-1}$
thermal conductivity	0.561	W m^{-1} $°C^{-1}$
volume expansion coefficient	2.1E-4	

For copper pipe:

density	8933	kg m^{-3}
specific heat	377	J kg^{-1} $°C^{-1}$
heat conductivity	403	W m^{-1} $°C^{-1}$

The heat transfer equations at steady state are given by Equations (3.2.16), (3.2.17) and (3.2.18), which were discussed in Section 3.2.2.1.

3.3.2.3. Dimensionless Parameters

FIDAP can handle both dimensional and dimensionless parameters. To eliminate the large difference in orders of magnitude between the terms in the equation which could slow down and even prohibit the convergence of the solution, dimensionless parameters were introduced.

The procedure to obtain the dimensionless parameters based on the known values such as velocity V_x, reference temperature T_{Ref}, reference heat flux q_{Ref} and the radius of the pipe r can be summarized as follows:

a. Define a reference velocity

$$U = \frac{\alpha_L}{r}\sqrt{RaPr}$$

b. Define the following dimensionless variables:

$$u^* = \frac{V_x}{U}$$

$$T^* = \frac{K_L(T - T_{Ref})}{q_{Ref}\, r}$$

$$X^* = \frac{l}{r}$$

$$p_S^* = \frac{p_S V_x}{\mu U}$$

The continuity, momentum and energy equation can then be written, dropping asterisks, as

$$\nabla \cdot u = 0 \qquad (3.3.1)$$

$$\sqrt{Ra/Pr}\ (u\cdot\nabla)\underline{u} = -\nabla p + \nabla^2\underline{u} + \sqrt{Ra/Pr}\ T\hat{\underline{g}} \qquad (3.3.2)$$

$$\sqrt{RaPr}\ \underline{u}\cdot\nabla T = \nabla^2 T \qquad (3.3.3)$$

Where $\hat{\underline{g}}$ is the unit vector in the direction of gravity.

The resulting dimensionless parameters are the Rayleigh number

$$Ra = \frac{\rho\beta g(q_{Ref})r^4}{\mu\alpha_L K_L}$$

and the Prandtl number

$$Pr = \frac{\nu}{\alpha_L} = \frac{C_p\mu}{K_L}$$

The dimensionless heat flux can be written in terms of a reference heat flux

$$q^* = \frac{q_H}{q_{Ref}}$$

where the reference heat flux can be obtained from the problem constraints

$$q_{Ref} = \frac{IV_A}{A}$$

Using the above dimensionless parameters in the analysis allowed the replacement of the physical properties required by FIDAP (compare (3.2.17) and (3.2.18) with equations (3.3.2) and (3.3.3)) with the following parametric values or unity:

$$\rho = \sqrt{Ra/Pr}$$

$$C_p = Pr$$

$$\mu = 1$$

$$g = 1$$

$$\beta = 1$$

$$K_L = 1$$

or for variable viscosity model,

$$\rho = 1$$

$$C_p = \sqrt{RaPr}$$

$$\mu = \frac{1}{\sqrt{Ra/Pr}}$$

$$\beta = 1$$

$$g = 1$$

$$K_L = 1$$

3.3.2.4. Boundary Conditions for Vertical Pipe Orientation

The dimensionless boundary conditions for this problem become (see Fig 3.3.2 for notations):

$u_r = 0$ $\qquad 0 < r < 1$ $\qquad x = 0$

$u_r = u_x = 0$	$0 < x < l/r$	$r_i = (r-d)/r$
$q = 0$	$0 < x < l_1/r$	$r_i = 1$
$q = 0$	$l_2/r < x < l/r$	$r_i = 1$
$q = 1$	$l_1/r < x < l_2/r$	$r_i = 1$

The first equation specifies that the incoming velocity is parallel to the x axis. The second equation is the non-slip condition around the inner surface of the pipe. The third and the fourth equations specifies a zero heat flux in the defined regions on the pipe circumference. the last equation specifies a non-dimensional heat flux of unity along the heated section.

3.3.2.5. FIDAP interface input file development

The input file to interface with the package consisted of two parts. The first part generated the mesh upon which the solution would be found and could be done using a menu system or manually. The second part defined the equations to be solved and the method to be used, and could be generated in a similar manner.

The mesh generation was based on the development at a logical space upon which dimensions could be laid and links made to produce the actual physical model. The setup of the logical planes for the 2-D and 3-D problems are shown respectively in Fig 3.3.3 and Fig 3.3.4. Three techniques could be used for generating mesh for the 3-D pipe [FIDAP, 1991]: Circular mesh, Triangular mesh and Wedge elements. The circular mesh enables direct trace of the co-ordinates across the pipe diameter, hence it has been selected for this work. The commands input to Fimesh (the mesh generator) and the commands input to Fiprep (the solution definer) are listed in Appendix A.4.

In the mesh generating process, attention must be paid to estimation of the mesh size to ensure that the mesh near the pipe wall is fine enough to resolve the boundary layer. An estimation of the boundary layer thickness is given by [FIDAP, 1991]:

$$\frac{\delta}{l} \approx \frac{1}{Ra^{0.25}}$$

3.3.2.6. Solution Procedure and Results

The input files for FIDAP listed in Appendix A.4 can be used for obtaining all the results required for this work. The changes to the basic files which were considered were

a. velocity of flow
b. flow patterns (laminar or turbulent flow regions)
c. heat flux (different power input)
d. pipe size (different diameter)
e. pipe orientation (angle vs gravity)

The FIDAP input files were specially designed so that minimum change was needed for different applications. The changes from a to e (above) were easily obtained by changing values of the constants declared under the Parameter heading, a section of the FINNP files.

Although in the present study particular attention was paid to application of heat transfer to ultrasonic measurement, it is useful at this stage to look at some theoretical results (temperature distribution) obtained from FIDAP. To test the interface software, a series of flowrates were used and the heat distributions were examined. The parameters used for this test are the same as those used for the experiments which were listed in Section 3.3.2.2. Heater power input was 40 watts. The FIDAP input file for these computation is listed in Appendix A.4.1. Results for steady state temperature

distributions in forced convection for a vertical pipe orientation in the laminar flow range (1 to 20 ml s^{-1}) will be presented.

Fig 3.3.5 shows a typical velocity profile of the flow, which is parabolic. The colour plots given in Fig 3.3.6a to Fig 3.3.6d show the temperature distribution (in °C) of the pipe wall and liquid for four different flowrates. As can be seen from the pictures, heat is transferred from the pipe wall to the fluid. When the flowrate is low (Fig 3.3.6a), the smaller quantity of water results in a significant rise in temperature across the pipe diameter. As the flowrate increases (Figs 3.3.6b to 3.3.6d), heat was swept down stream by the flow, leading to an insignificant rise in temperature at the pipe centre.

Fig 3.3.7a and Fig 3.3.7b show the temperature profiles in radial direction of the pipe at heater centre and 165 mm from the heater centre (down stream). The zero of the x axis is the outside of the copper tube. As can be seen in Fig 3.3.7a, at heater centre, the pipe wall temperature is high but the bulk liquid temperature is low, as it needs time for the heat to diffuse from the pipe wall into the liquid. At 165 mm away from the heater centre (Fig 3.3.7b), the pipe wall temperature decreases and liquid temperature increases, due to the heat transferred from the wall to the liquid.

The average temperature rise along the pipe axial direction (from inlet to outlet) is shown in Fig 3.3.8 (assuming the centre of the heater was clamped on at x = 250 mm). The temperature was low at the inlet, and increased gradually towards the heater, the maximum temperature of the pipe wall and the liquid were to be expected at a region (down stream side) near the position where the heater was clamped. Beyond this region, on the down stream side, the temperature of the pipe wall decreases as the distance from the heater increases, which is due to heat being transferred from the wall to the flowing liquid (within a certain distance from the heater centre). The temperature at the pipe wall for one particular location is always higher compared with the bulk water temperature. This is because copper is a better heat conductor than water, so heat was conducted along the pipe faster than it diffused into the water).

Fig 3.3.9 shows a typical temperature profile for the horizontal pipe orientation computed using FIDAP input file shown in Appendix A.4.3. As could be seen, at the

same axial position of the pipe, the temperature is higher at top region of the horizontal pipe, which is due to the buoyancy effect. Even with a coarse mesh, the computation shows sensible results.

These results obtained from FIDAP showed encouraging signs but still needed to be confirmed by data either from literature or experiment. Due to the pipe dimensions used together with the specified heating condition, no comparable data could be found for this purpose. An experimental rig was therefore constructed on which measurements could be taken. This rig is described in Chapter 7. The measured data from the experiments will be compared with computer simulations using FIDAP (see section 9.2).

4. THEORETICAL MODELLING OF THE FLOWMETER

4.1. Introduction

In this chapter, the feasibility of using the ultrasonic/thermal technique for measuring low flowrates of a single phase liquid (water) together with the multiple reflections of an ultrasonic beam to estimate high flowrates in a small diameter pipe is theoretically examined.

The specification for the flowmeter was, firstly, that it could be used as a clamp-on device, secondly, that it would measure flowrate from 1 ml s^{-1} to 550 ml s^{-1}. In a defined region of flow, both the ultrasonic/thermal and multiple reflection were to be usable to enable cross-calibration.

The theoretical aspect of the ultrasonic/thermal technique and the multiple reflection technique are discussed in detail in Sections 4.2 and 4.4 respectively.

4.2. Ultrasonic/Thermal Technique For Low Flowrate Measurement

4.2.1. Application of heat transfer to ultrasonic measurement

In this Section, the application of heat transfer to ultrasonic measurement is considered. A mathematical formulation for the ultrasonic/thermal technique was developed based on the property that the speed of ultrasound in media is temperature dependent. Modelling of the technique is best considered by referring to Fig 4.2.1 (results obtained using FIDAP simulations, with heater power equal to 40 watts and flowrate equal to 2.21 ml s^{-1}), the graph for bulk water temperature (average across the pipe radius) along the pipe axis was computed from inlet (x = 0 mm) to outlet (x = 500 mm) of the test section (assuming the heater was clamped on at x = 250 mm).

With no flow, the heat transfer would be symmetric with respect to the centre of the heater but in the presence of flow, heat is transported downstream by the flowing fluid (see Fig 4.2.1), leading to a temperature difference between the upstream and downstream with respect to the heater. If ultrasound is transmitted across the pipe, the change in temperature will lead to a change in the speed of ultrasound. The flowrate can be therefore estimated by either the transit time difference across the pipe at the two symmetric locations with respect to the heater centre, or at one location with a heater off/on comparison. The latter approach was selected for the experimental work described in Chapter 8. In this method, only one pair of transducers was required which was clamped on to the pipe downstream to the heater. The steady state transit time difference at heater off/on was used to estimate the flowrates.

Mathematically, the speed of ultrasound in water at temperature T could be represented by [Homans, 1982]

$$C_L(T) = C_L + \beta_L C_L(T - T_{ref}) \qquad (4.2.1a)$$

Similarly, the speed of ultrasound in copper pipe at temperature T is given by

$$C_W(T) = C_W + \beta_W C_W(T - T_{ref}) \qquad (4.2.1b)$$

where $C_L(T)$ and $C_W(T)$ are the speed of sound in water and pipe wall at T °C, β_L and β_W are the temperature coefficient of speed of sound in water and pipe wall, C_L and C_W are the speed of sound in water and pipe wall at a reference temperature (10 °C), and T_{Ref} is the reference temperature (10 °C).

The transit time across the vertical pipe at upstream location can be represented mathematically by

$$t_u = \frac{2}{C_L}\int_0^{r-d} \frac{dr}{1 + \beta_L[T_u(r) - T_{ref}]}$$

$$+ \frac{2}{C_W}\int_{r-d}^{r} \frac{dr}{1 + \beta_W[T_u(r) - T_{ref}]} \qquad (4.2.2a)$$

where the first integral is the transit time for ultrasound to travel across the bulk water of the pipe, and the second integral is the transit time for ultrasound to travel across the copper pipe wall. A discrete approximation of Equation (4.2.2a) gives

$$t_u = 2\sum_{i=1}^{i=n_l} \frac{(\Delta r)_i}{C_L[1 + \beta_L((T_u)_i - T_{ref})]}$$

$$+ 2\sum_{i=n_l}^{i=n} \frac{(\Delta r)_i}{C_W[1 + \beta_W((T_u)_i - T_{ref})]} \qquad (4.2.2b)$$

Similarly, the transit time across the vertical pipe at downstream location is given by

$$t_d = \frac{2}{C_L}\int_0^{r-d} \frac{dr}{1 + \beta_L[T_d(r) - T_{ref}]}$$

$$+ \frac{2}{C_W}\int_{r-d}^{r} \frac{dr}{1 + \beta_W[T_d(r) - T_{ref}]} \qquad (4.2.3a)$$

and a discrete approximation of Equation (4.2.3a) is

$$t_d = 2\sum_{i=1}^{i=n_l} \frac{(\Delta r)_i}{C_L[1 + \beta_L((T_d)_i - T_{ref})]}$$

$$+ 2\sum_{i=n_l}^{i=n} \frac{(\Delta r)_i}{C_W[1 + \beta_W((T_d)_i - T_{ref})]} \qquad (4.2.3b)$$

where t_u and t_d are the transit times for ultrasound across the pipe diameter at upstream and downstream locations. C_L and C_W are the speed of ultrasound in water and copper pipe taken at the reference temperature T_{ref} (10 °C). The upstream and downstream temperatures are denoted respectively by T_u and T_d. Δr is the mesh size, i is the index to indicate the position of Δr in the finite mesh shown in Fig 4.2.2, and i = n_l is the interface between the pipe and water.

If the expansion of the pipe due to the increase in temperature is ignored (see Section 4.3.2 for detailed analysis) then the transit time difference between upstream and downstream paths is given by

$$\Delta t = t_u - t_d \qquad (4.2.4)$$

i.e., the transit time difference after rearrangement of the terms can be written as follows:

$$\Delta t = \frac{2}{C_L}\sum_{i=1}^{n_l} (\Delta r)_i \frac{\beta_L[(T_d)_i - (T_u)_i]}{[1 + \beta_L((T_u)_i - T_{ref})][1 + \beta_L((T_d)_i - T_{ref})]} +$$

$$\frac{2}{C_W}\sum_{i=N_l}^{n} (\Delta r)_i \frac{\beta_W[(T_d)_i - (T_u)_i]}{[1 + \beta_W((T_u)_i - T_{ref})][1 + \beta_W((T_d)_i - T_{ref})]} \qquad (4.2.5)$$

For the case of no flow, the upstream temperature T_u is equal to the downstream temperature T_d, hence $\Delta t = 0$. When the flow speed is not equal to zero,

$T_u \neq T_d$, *hence* $\Delta t \neq 0$.

Equation (4.2.5) is still valid if only one pair of transducer is clamped on downstream of the heater, with the heater off/on comparison. In this case, T_u is equal to the inlet water stream temperature with the heater off which would be a constant, and T_d is the down stream water temperature with the heater on which varies with flowrate.

The upstream temperature $(T_u)_i$ and downstream temperature $(T_d)_i$ for different flowrates could be obtained by using FIDAP computer simulations.

4.2.2. Modelling the Flowmeter Using the FIDAP

The important parameters which were required in the design of the flowmeter and could be modelled are listed below:

a. Heater power input P for different flowrate regions
b. distance X from heater (where to clamp the transducers)
c. transducer orientation (with respect to vertical) in horizontal pipe measurement
d. generation of the flowmeter calibration curve.

4.2.2.1 Heater power determinations

As can be seen from Chapter 3, the links between the power input, transit time and flowrate are complex. To decide on an optimum value for the power input P, one can either solve the partial differential equations (numerically) as described in Chapter 3, or investigate experimentally.

Using FIDAP to obtain a model for the link between heater power input with transit time (or flowrate) was not difficult, once correct models had been established. The work involved providing different powers P and flowrates in the FIDAP input file whose design has been discussed in Chapter 3 and listed in appendix A.4. Δt (transit time difference) could then be computed using Equation (4.2.5). The selection of the power input P was then reduced by deciding what magnitude of Δt would be suitable for the application.

Using the theoretical model to obtain values for P would have been ideal but due to the limitations on computer resources together with limitation on time, it was not possible to obtain power input P theoretically.

Instead of obtaining P theoretically, experiments were carried out to investigate suitable values (see Section 8.5.1 for details). The conclusions drawn from the tests were:

a. It is not possible to use one fixed power input for flowrates from 1 to 80 ml s^{-1}.

   High power input gives $\Delta t \geq 10(-3)\ \mu s$ but results in the temperature of the heater being too high at low flowrates. Low power input results in transit time difference which are too small to be measured accurately at high flowrates.

b. The flow range was therefore divided into three ranges:

1	to	20 ml s^{-1}	
10	to	40 ml s^{-1}	
30	to	80 ml s^{-1}	

c. The optimum power inputs P for each range of flow was experimentally investigated (Section 8.5.1) and are listed below

for	1	to	20 ml s^{-1}	P = 40 watts
for	10	to	40 ml s^{-1}	P = 100 watts

for 30 to 80 ml s^{-1} P = 200 watts

4.2.2.2 Separation Distance between the heater and transducers

The other important parameter required from the theoretical model was the separation distance between the transducers and the heater. To examine this value, the transit time difference at heater off/on states for ultrasound to travel across the pipe along the pipe axial direction were computed using FIDAP. The range of flowrates selected was within 1 to 20 ml s^{-1}, with the power input P equal to 40 watts. Plots of the results are shown in Fig 4.2.3 (assuming the heater was clamped on at x = 250 mm).

From the plots one could see that, at the down stream side, the transit time difference decreases as the separation distance (measured from the heater centre) increases. To obtain the maximum transit time difference and hence the maximum measurement accuracy, the transducer would be clamped on as close to the heater as possible, but this requires high accuracy of the transducer clamping-on position, as the gradients of the curves (transit time difference vs separation) are high near the heater.

Clamping the transducers at a location along the pipe where the variation of the transit time difference is minimal results in the flowmeter being less dependent on spacing. A distance of 150 to 200 mm was therefore recommended to separate the transducer pair from the heater (i.e. x = 400mm to 450mm in Fig 4.2.3). In this work, a distance of 165 mm from the heater was used for clamping the transducer pair.

4.2.2.3 Orientation of transducers

The orientation of the clamped-on ultrasonic transducers is not important in vertical pipe orientation as the heat transfer in a vertical pipe is symmetrical above the pipe mid-line. In the case of horizontal pipe or other pipe orientations, however, transit time difference varied for different transducer orientations (see Fig 4.2.4). The FIDAP interface input file for the 3-D pipe flow computation can be found in Appendix A.4.3.

The experimental results show that, when the transducer pair was clamped at angle 0^0 with respect to the vertical, the transit time difference was a maximum (Section 8.7.1). The transducer pair was therefore clamped in a vertical orientation for the horizontal pipe experiments and at the same spacing as in the vertical orientation.

4.2.2.4 Generating a Calibration Curve for the Flowmeter Using FIDAP

The work of this Section is to generate calibration curves for the ultrasonic/thermal flowmeter. The FIDAP interface input file for this computation could be found in Appendix A.4.1. The data for the computation are listed below

pipe material	copper
pipe o.d.	15 mm
pipe thickness	0.75 mm
test pipe length	500 mm
heater length	40 mm
heater power input	40 watts

These data were chosen purposely so that they could be compared directly with the experimental data presented in Section 8.6.1. The comparison result will be discussed in Section 9.1.

The physical data (such as density, thermal conductivity, special heat capacity, viscosity and speed of sound) for water and copper required for the computation could be found in [Kaye and Laby, 1973]. Ten different flowrates (see Table 4.2.5) were selected within 1 to 20 ml s^{-1} for the FIDAP computation.

Fig 4.2.5 shows a typical calibration curve for the flowmeter which was generated using FIDAP. In this graph, the transducers were assumed to be sited at a distance of 165 mm from the heater (measured from the heater to the centre of the transducers). See Section 9.1 for comparison of computation results with experimental data.

In the next Section, the errors associated with the flowmeter (ultrasonic/thermal technique) are examined theoretically and compensation methods are discussed.

4.3 Error Analysis for Ultrasonic/Thermal Technique

4.3.1 Source of errors

In the assessment of errors it is convenient to consider individually each of the parameters in the mathematical equations which represent the performance of the proposed meter.

The transit time difference for ultrasound travelling the pipe diameter at heater off/on states is given by

$$\Delta t = \Delta t_0 - \Delta t_1 + \Delta t_{Exp} =$$

$$[\frac{2d}{C_W} + \frac{D - 2d}{C_L} + \tau_0] - [\frac{2d}{C_W(1 + \beta_W \Delta T_W)} + \frac{D - 2d}{C_L(1 + \beta_L \Delta T_L)} + \tau_1] + \Delta t_{Exp}$$

(4.3.1a)

where Δt_0 and Δt_1 are transit time across the pipe diameter with heater off and on respectively, and Δt_{Exp} is the delay due to pipe expansion increasing the propagation time, τ_0 and τ_1 are delays in the measurement system with heater off and on respectively, ΔT_W and ΔT_L are the average temperature changes in pipe wall and water respectively.

The quantity Δt_0 (transit time measured at heater off) is given by

$$\Delta t_0 = \frac{2d}{C_W} + \frac{D - 2d}{C_L} + \tau_0$$

rearranging the above equation, one obtains

$$\frac{D - 2d}{C_L} = \Delta t_0 - \frac{2d}{C_W} - \tau_0 \qquad (4.3.1b)$$

Eliminating the term (D - 2d)/C_L, by substituting Equation (4.3.1b) in Equation (4.3.1a), gives

$$\Delta t = \Delta t_0 - [\frac{2d}{C_W(1 + \beta_W \Delta T_W)} + \frac{\Delta t_0 - \frac{2d}{C_W} - \tau_0}{1 + \beta_L \Delta T_L} + \tau_1] + \Delta t_{Exp} \qquad (4.3.1c)$$

If the same measurement system with the same settings were used, then

$$\tau_0 = \tau_1 \qquad (4.3.2)$$

This allows elimination of τ_0 and τ_1 from Equation (4.3.1a).

Inspection of Equation (4.3.1c) shows that, error can arise in three ways:

a. inaccuracy of the instruments for transit time measurements leads to inaccuracy in Δt_0 (instrumentation error),

b. expansion of the pipe wall (d) with changing temperature increases the propagation time.

c. inaccuracy of ΔT_W and ΔT_L caused by: inaccuracy of the heater power supply measurement; inaccuracy of the heater and transducer separation distance measurement; heat losses due to radiation and convection; and imperfect thermal contact between the heater and pipe.

Assessment of these theoretical errors and possible compensation approaches are discussed in detail in the next Section. The instrumentation errors due to instruments will be discussed in Section 8.4.

4.3.2 Error Assessment and Proposed Compensation Methods

The error associated with the timer/counter was considered as significant (see Section 8.4). A highly accurate timer/counter would therefore be required.

The other parameter which is likely to contribute error to the transit time measurement is the pipe expansion due to temperature change. The variation of pipe wall thickness with temperature is given by

$$\frac{\delta d}{d} = \beta_{We}(T_w - T_{Ref}) \qquad (4.3.5)$$

where δd is the expansion of the pipe wall at temperature T_w, β_{We} is the thermal expansion coefficient of copper.

Putting typical values into Equation (4.3.5), one can determine δd and $\delta(D - 2d)$, and hence their effect on Δt . The maximum temperature difference of the pipe wall where the transducers are located is about 10 ^{0}C, therefore taking (T_W - T_{Ref}) equal to 10 ^{0}C, β_{We} equal to 16.7E-6 per ^{0}C [Kaye and Laby, 1973], and pipe wall thickness equal to 7.5E-4 m, and substituting these values into Equation (4.3.5), then

$$\delta d = 7.5E\text{-}4 \times 16.7E\text{-}6 \times 10 = 1.25E\text{-}7 \text{ m}$$

The pipe wall thickness is therefore increased by 1.25E-7 m. The expansion of pipe wall with temperature results in the increase of the inner diameter of the pipe. For the given temperature, length of the inner circle of the pipe is increased by

$$\delta L = \pi(D - 2d) \times 16.7E\text{-}6 \times 10$$

and hence the inner diameter is increased by

$$\delta L/\pi = (D - 2d) \times 16.7E\text{-}6 \times 10 = 0.0135 \times 16.7E\text{-}5 = 2.25E\text{-}6 \text{ m}$$

The delay due to pipe expansion, Δt_{Exp} can be estimated as follows, refer to [Kaye and Laby, 1973] for values of the constants:

$$\Delta t_{Exp} = \frac{2\delta d}{C_W(T)} + \frac{\delta(D - 2d)}{C_L(T)} = \frac{2.5E-7}{4759} + \frac{2.25E-6}{1509} = 1.54E\text{-}9 \text{ s} = 1.54 \text{ ns}$$

where $C_W(T)$ and $C_L(T)$ are speed of sound at T ^{0}C in pipe wall and liquid respectively. δd and $\delta(D - 2d)$ are the changes of pipe wall and inner diameter with temperature respectively.

For a transit time difference of 0.030 μs, the maximum percentage error caused by the pipe expansion is about 5.1%, which is decreased with increased flowrate. The above calculation shows that the error caused by the variation in pipe size with temperature is significant.

Compensation for the pipe expansion effect can be achieved by monitoring the pipe wall temperature using temperature sensors mounted on the pipe wall. With the known temperature, the variation in pipe diameter with temperature and hence Δt_{Exp} can be estimated.

The multimeters used for measuring heater power supply were commercially available products. Although the parameters such as voltage and current were under strict control they could only be accurate to ± 0.01 V and ± 0.01 A (according to manufacturer's documentation). The maximum error for this application is about 0.6% (see Section 8.4.2 for detail).

In the measurement of separation distance between the heater and the transducers, an reading error of about ± 0.5 mm will be considered. To examine how this error would affect the transit time difference, value computed using FIDAP with a flowrate equal to 10 ml s^{-1} and a distance of 165 mm between the heater and transducers, a heater power equal to 40 Watts was used. The estimated error for vertical pipe flow was ± 8.0E-7 μs, for a transit time difference of 0.015 μs, the maximum percentage error is ± 5.3E-3 %, which is small and can be ignored. For a horizontal pipe, the error due to the separation distance was investigated experimentally (refer to Section 8.7.2 for experimental details). The experimental results shows that for a separation distance of 100 mm, the transit time difference is about 0.01 μs. Therefore, for an error of 0.5mm, the error in transit time difference is about ± 5.0E-5 μs, i.e. with a transit time difference of 0.02 μs (minimum transit time difference), then the percentage error is about ± 0.25%.

To examine radiation heat losses, a simple calculation of the radiation heat transfer due to temperature gradient between the pipe and the surrounding air was considered. The mathematical expression for this heat loss due to radiation is given by [Peters, 1984]:

$$E = \delta_s(T_1^4 - T_2^4) \qquad (4.3.6)$$

where E is the heat loss due to radiation (W m^{-2}), T_1 and T_2 are temperature of the pipe and the surrounding air respectively (K), and δ_s is Stefan constant [Kaye and Laby, 1973]

$$\delta_s = 5.67E\text{-}8 \text{ (W m}^{-2} \text{ K}^{-4})$$

If T_1 equals to 293 K and T_2 equals to 283 K, with a 15 mm diameter copper pipe and length of the test section equal to 0.05 m, the maximum heat loss due to radiation would be

$$E = 5.7E\text{-}8 \times (293^4 - 283^4) \times \pi \times 0.015 \times 0.05 \approx 0.128 \text{ W}$$

Hence the energy loss due to radiation is about 0.128 Watts. For a heater power input of 40 Watts, the percentage error is about 0.32%.

The convection heat loss from the pipe to surrounding air was examined experimentally. The experimental results showed that the transit time difference measured for the insulated pipe and uninsulated pipe were not significantly different.

In this section, theoretical errors of the ultrasonic thermal flowmeter have been discussed:

a. the error due to pipe expansion with temperature might reach to about 5.1% at the
low flow rate (with a temperature difference of 10 ^{0}C). At high flow rate, the temperature difference decreases, and hence the error decreases (see Section 9.2.

for further discussion). Compensation for this could be achieved by using a temperature sensor to monitor pipe wall temperature.

b. the error due to inaccurate measurement of the heater and transducer separation was insignificant for both vertical pipe measurement (± 2.6E-3 %) and horizontal pipe measurement (± 0.25%).

c. the errors due to heat loss through radiation was about 0.32%, which is small and can be ignored.

In the next section, the theoretical aspects of the ultrasonic multiple reflection technique will be discussed.

4.4. Multiple Reflection Ultrasonic Technique for High Flowrate Measurement

4.4.1. Mathematical Analysis

The principle of multiple reflection ultrasonic flow measurement is best described by referring to Fig 4.4.1. For simplicity, time of flight for one crossing of the liquid region (beam AB) is analyzed. The time of flight of ultrasound in the direction of flow (from A to B) is given by

$$t_{12} = \frac{L}{C_L + V\cos\phi'_L} + \tau_M \qquad (4.4.1.1)$$

and against the direction of flow (from B to A) is given by

$$t_{21} = \frac{L}{C_L - V\cos\phi'_L} + \tau_M \qquad (4.4.1.2)$$

where τ_M is the time taken for sound travel in block materials including pipe wall, and wedge and delays in the electronics and transducers.

The transit time difference Δt_{AB}, is then given by

$$\Delta t_{AB} = t_{12} - t_{21} = \frac{2LV\cos\phi'_L}{C_L^2 - V^2\cos^2\phi'_L} \qquad (4.4.1.3a)$$

In this thesis, the maximum water flow velocity in the pipe to be considered is 4.0 m s^{-1} which is very small compared with the speed of sound in water (about 1500 m s^{-1}), i.e. $V^2 << C_L^2$, therefore $V^2\cos^2\phi'_L$ can be ignored with no significant change to the transit time Δt_{AB}. Equation (4.4.1.3a) becomes

$$\Delta t_{AB} = t_{12} - t_{21} = \frac{2LV\cos\phi'_L}{C_L^2} \qquad (4.4.1.3b)$$

If the flow is steady, single phase without impurities, and the pipe material is homogeneous and the inner surface of the pipe is smooth, then the transit time for N crossings in the liquid can be derived directly from Equation (4.4.1.3b), which is modified to give

$$\Delta t_M = \frac{2NL\cos\phi'_L}{C_L^2}V \qquad (4.4.1.4)$$

where N is the number of the ultrasound beam crossings.

Thus, by using multiple reflections instead of a single transit of the pipe, it is possible to increase the transit time difference to values which are suitable for the measurement of slow flows in small pipe sizes. The feasibility of the method together with the maximum number of reflections obtained is investigated experimentally in Section 6.5.

Equation (4.4.1.4) shows that, the velocity of flow is related to Δt_M through N, L, ϕ'_L and C_L. In the case of clamp-on ultrasonic flowmeters neither L nor ϕ'_L are directly measurable, but it is possible to express L and ϕ'_L in terms of the values such as the inner diameter of the pipe, the angle of the transducers ϕ_T, and the speed of sound in the liquid. Focusing on the sound beam length L shown in Fig 4.4.2, it is clear that

$$L = \frac{D - 2d}{\sin\phi'_L}$$

or expressed in terms of ϕ_L

$$L = \frac{D - 2d}{\cos\phi_L} \qquad (4.4.1.5)$$

ϕ_L is related to the transducer's angle ϕ_T by Snell's Law, which states that

$$\frac{C_T}{\sin\phi_T} = \frac{C_L}{\sin\phi_L} \qquad (4.4.1.6a)$$

Expressing ϕ_L in terms of the information provided by the transducer specification (the transducer angle) and the speed of sound in pipe wall and liquid, one obtains, (see Fig 4.4.1),

$$\sin\phi_L = \frac{C_L}{C_T}\sin\phi_T \qquad (4.4.1.6b)$$

Substituting values of L and $\cos\phi_L'$ (since $\cos\phi_L' = \sin\phi_L$) into Equation (4.4.1.4), and expressing $\cos\phi_L$ in terms of $\sin\phi_L$ by using

$$\sqrt{\cos^2\phi_L} = \sqrt{1 - \sin^2\phi_L}$$

then the transit time difference Δt_M can be written as

$$\Delta t_M = \frac{2N(D - 2d)\sin\phi_T}{C_L C_T \sqrt{1 - (\frac{C_L}{C_T}\sin\phi_T)^2}} V \qquad (4.4.1.7)$$

In next section, formulation for the separation distance for the transmitter and receiver will be discussed.

4.4.2 Transducer Spacing Determination

Knowing exactly where to place the transducer is very important in transit time ultrasonic flowmeters. This section presents a development of mathematical expressions to calculate the separation between the transmitter and the receiver for multiple reflections of ultrasonic beams.

Wave propagation in media is a very complicated 3-D problem. To simplify the problem, only a single beam (assumed to be a beam from centre of the transducer and propagating in a direction normal to the transducer's surface) is considered. Fig 4.4.2 shows the path of an ultrasound beam transmitted from the transmitter and received by the receiver after the beam has travelled through the transducer shoes, pipe wall and been reflected N times through the liquid.

There are a variety of possible sound beam paths, Fig 4.4.3 shows a few possible paths created by reflection at the pipe wall and the interface between the pipe wall and the liquid. W_1 and W_2 are two examples of beams propagated through the pipe wall. Examples of sound beams propagated in the liquid are denoted by M_1, M_2 and M_3. The beams propagating through the pipe wall and liquid were detected by an ultrasonic receiver located at a distance from the transmitter. The sound beams may arrive at the receiver at different times but it is also possible that two or more beams may arrive at the receiver at the same time.

The location of the receiving transducer should be investigated so that the required ultrasonic beam arrives at the centre of the receiver after N crossings. The two parameters specifying the characteristic of this beam are the separation between the transmitter and the receiver (distance x_N measured from centre of the transmitter to centre of the receiver) and the transit time for the transmitted signal from the firing transducer to arrive at the receiver, t_N.

From the geometry of the diagram given in Fig 4.4.2, the distance X_N and time t_N could be deduced and are given by Equations 4.4.2.1 and 4.4.2.2 respectively

$$X_N = 2(X_S + X_W) + NX_L \qquad (4.4.2.1)$$

where X_S, X_W and X_L are distances in shoes, pipe wall and water respectively, and X_N is the distance between the two angled transducers (see Fig 4.4.2).

$$t_N = 2(t_S + t_W) + Nt_L + \tau_T \qquad (4.4.2.2)$$

where t_S, t_W and t_L are ultrasonic transit times in shoes, pipe wall and water respectively, τ_T is the delay time in the electronics and transducers, and t_N is the ultrasonic transit time for N crossings.

The values in the right hand side of Equation (4.4.2.1) can be expressed in terms of the known or measurable parameters such as transducer angle, wedge thickness and pipe diameter. Values for each parameter are now considered in turn. The distance X_s (in the wedge) can be deduced by referring to Fig 4.4.2. From the geometry, the angle ϕ_s is given by

$$Tan\phi_s = \frac{X_s}{d_s} \quad \Rightarrow \quad X_s = \frac{\sin\phi_s}{\cos\phi_s} d_s \qquad (4.4.2.3)$$

Expressing ϕ_s in term of the known angle ϕ_T (angle of the transducers) and the speed of sound, C_T, using Snell's law

$$\frac{C_T}{\sin\phi_T} = \frac{C_s}{\sin\phi_s} = \frac{C_W}{\sin\phi_W} = \frac{C_L}{\sin\phi_L}$$

$$\frac{C_T}{\sin\phi_T} = \frac{C_s}{\sin\phi_s} \quad \Rightarrow \quad \sin\phi_s = \frac{C_s}{C_T}\sin\phi_T$$

Substituting the value for $\sin\phi_s$ into Equation (4.4.2.3) gives,

$$X_s = \frac{\frac{C_s}{C_T}\sin\phi_T}{\sqrt{1 - (\frac{C_s}{C_T}\sin\phi_T)^2}}\, d_s \qquad (4.4.2.4)$$

d_s is the thickness of the wedge and is known. ϕ_T is the angle of the transducer and its value is also available. C_T and C_s are the speeds of sound and are known, and hence X_s can be calculated.

X_W , the distance travelled by the sound beam in one traverse of the pipe wall is found by the similar procedure and its mathematical formula is given by

$$X_W = \frac{\frac{C_W}{C_T}\sin\phi_T}{\sqrt{1 - (\frac{C_W}{C_T}\sin\phi_T)^2}}\, d \qquad (4.4.2.5)$$

An expression for the distance X_L in the liquid region is derived in exactly the same manner. The distance X_L is represented by

$$X_L = \frac{\frac{C_L}{C_T}\sin\phi_T}{\sqrt{1 - (\frac{C_L}{C_T}\sin\phi_T)^2}} (D - 2d) \qquad (4.4.2.6)$$

The time t_N in Equation (4.4.2.2) is the total time needed for the sound beam to travel from the transmitter to the receiver. t_S, t_W, t_L can be written as follows:

$$t_S = \frac{L_S}{C_S} \qquad (4.4.2.7a)$$

$$t_W = \frac{L_W}{C_W} \qquad (4.4.2.7b)$$

$$t_L = \frac{L}{C_L + V\sin\phi_L} \qquad (4.4.2.7c)$$

The indirectly measurable lengths (L_S, L_W and L) in above Equations can be expressed in term of the known values such as the magnitude of the beam angle between the two media and the medium thicknesses, i.e.

$$L_S = \frac{d_S}{\cos\phi_S}$$

$$L_W = \frac{d}{\cos\phi_W}$$

$$L = \frac{D - 2d}{\cos\phi_L}$$

Substituting the values for the lengths (L_s, L_w and L) into Equations (4.4.2.7a) to (4.4.2.7c), then

$$t_S = \frac{d_s}{C_S\cos\phi_S}$$

$$t_W = \frac{d_W}{C_W\cos\phi_W}$$

$$t_L = \frac{D - 2d}{(C_L + V\sin\phi_L)\cos\phi_L}$$

τ_T is the delay time of the electronics and the transducers and its value can be predetermined.

A FORTRAN program was written to compute X_N and t_N for 1 to 8 reflections. The program assumed a 15 mm diameter copper pipe with a pipe wall thickness of 0.75 mm, and the fluid was water. The results are listed in Table 4.4.1.

Experiments were carried out to investigate the existence of the ultrasound beams predicted by the computer model. The results are presented in Section 6.5.

In the next Section, the error associated with the flowmeter (ultrasonic multiple reflection technique) are examined theoretically and compensation methods are discussed.

4.5. Error Analysis

4.5.1 Source of Errors

In this Section, an attempt is made to examine all the factors that influence the prediction of the flowrate and to propose methods of compensation for those that are significant. The errors can be classified into two groups, the first group is inaccuracy in the parameters presented in Equation (4.4.1.7) and the variation of these parameters with temperature. The second group are effects due to flow such as Reynolds number and beam shift effects.

Analysis of the source of error is started by examining the parameters of the mathematical expression for flowrate. Rewriting Equation (4.4.1.7) in terms of flowrate, one obtains

$$Q = \frac{\pi(D - 2d)C_L C_T \Delta t_M \sqrt{1 - (\frac{C_L}{C_T}\sin\phi_T)^2}}{8N \sin\phi_T} \qquad (4.5.1.1)$$

Inspection of Equation (4.5.1.1) shows clearly that designing an accurate flowmeter relies upon accurately knowing the values of (D - 2d), the transducer angle, ϕ_T , speeds of sound C_L, C_T and being able to measure Δt_M accurately.

The parameters that can change with temperature are speed of sound in liquid (C_L), speed of sound in transducer material (C_T) and pipe wall thickness (d).

It can be seen directly that a percentage error in (D - 2d) reflects directly as the same percentage error in Q. The problem of measuring (D - 2d) accurately is particularly difficult. Pipe manufacturers tolerances would appear to range up to ± 3% for pipe wall thickness [Spendel, 1987], this presents a severe problem in small diameter pipes.

In formulating the expression governing the flowrate, it has been assumed that the velocity is uniform throughout the pipe. In reality this is not the case and account must be taken of the velocity profile. Another effect to be considered is the beam shift due to flow. This is important for making a decision on where to clamp the ultrasonic receiver.

In next Section, proposed methods of compensation for these errors are discussed.

4.5.2 Error Assessment and Proposed Compensation Methods

4.5.2.1 Changes in C_T and C_L

C_T should not present a severe problem since the transducers material and its characteristics would be well known and understood.

Equation (4.5.1.1) gives variation in flowrate Q with C_L. The difficulty in measuring C_L in a clamp on system is due to the fact that both the path length L and angle ϕ_L are not directly measurable, added to that, monitoring of temperature of flowing fluid by using temperature sensor is not possible in a clamp-on meter. For clamp on techniques, the compensation for changes in C_L means the ability to measure C_L and to trace it should it change from outside of the pipeline. In [Spendel, 1987], the author discussed a method for C_L compensation. The mathematical formula is obtained by considering the wavefront transmitted in both flow directions and establishing an expression for C_L based on the geometry of the sound paths. However, the accurate estimate of C_L is dependent on the accurate estimate of too many parameters for this equation to be used for compensation.

The compensation approach for C_L adopted in this work is simpler due to the availability of the two direct angle transducers. If one considers the transit time for ultrasound across the pipe diameter, Δt_0 ,

$$\Delta t_0 = \frac{D - 2d}{C_L} + \frac{2d}{C_W} + \tau_0$$

where τ_0 is the delay time in electronic instruments and transducers, and C_w is the speed of sound in the pipe wall. Rearranging the above Equation for C_L, one gets

$$C_L = \frac{D - 2d}{\Delta t_0 - \frac{2d}{C_W} - \tau_0} \qquad (4.5.2.1)$$

C_L is thus a function of (D - 2d), Δt_0 , 2d and C_W.

Δt_0 would be of order of the transit time across the pipe and this value is quite large (9.3 μs), hence can be accurately measured. The maximum error associated with the electronics is about ± 2.0E-3 μs (see Section 4.3.3), i.e. the percentage error is 0.02%, which is insignificant. τ_0 is the delay time in the transducer pair and the associated electronics and can be pre-determined accurately.

C_W varies with temperature. A simple calculation below will show the effective change of C_W (speed of sound in the pipe wall) with temperature on the transit time. At a temperature of 20 ^{0}C, C_W is equal to 4750 m s^{-1} [Kaye and Laby, 1973], with a copper pipe wall thickness (d) of 0.00075 m, the transit time across the pipe wall thickness 2d is 0.0015/4750, which is 3.15E-7 seconds. At temperature of 30 ^{0}C, the transit time is 0.0015/4845, or 3.09E-7 seconds. Hence at a temperature difference of 10 ^{0}C, the difference in transit time would be 5.4E-9 second. The percentage error due to change in C_W with temperature would be 0.0058%, which is insignificant and can be ignored.

From Equation (4.5.2.1), the main source of error for estimating C_L is due to (D - 2d) which cannot be accurately measured, its value relies upon the pipe manufacturer's tolerance which is ± 3%, hence the inaccuracy in (D - 2d) results in a ± 3% inaccuracy in estimating C_L.

To examine how this would affect flowrate measurement, substitute the following values into Equation (4.5.1.1.):

D	=	0.015 m
d	=	0.00075 m
C_L	=	1500 m s^{-1} and C_L change by 3% (1500 ± 45)
C_W	=	4750 m s^{-1}

Δt_M = 9.6E-06 S

ϕ_T = 70^0

N = 1

The results showed that a ± 3.0% error in C_L due to change in (D - 2d) resulted in a ± 0.69% error in flowrate Q.

One possible compensation method for (D - 2d) is to include ultrasonic transducers for measuring the thickness of the pipe wall.

4.5.2.2 Changes in Pipe Wall Thickness and Diameter

Variation of the pipe wall thickness and hence diameter of the pipe wall with temperature in the multiple reflection technique is similar to that in the ultrasonic/thermal technique, which has been discussed in Section 4.3.2.

4.5.2.3 Reynolds Number and Beam Shift Effects

The compensation for Reynolds number effects is important for a transit time ultrasonic flowmeter. If one examines the expression for Δt_M obtained by assuming the velocity is uniform through the pipes, Δt_M is given by

$$\Delta t_M = \frac{2(D - 2d)\cot\phi_L'}{C_L^2} V \qquad (4.5.2.2)$$

In reality, the velocity distribution in the pipe is dependent upon the Reynolds number. Generalizing Equation (4.5.2.2) to include these effects, one gets

$$\Delta t_M = \frac{2(D - 2d)\cot\phi_L'}{C_L^2} \frac{\int_0^{\frac{D-2d}{2}} V(r)\, dr}{\frac{D - 2d}{2}} \qquad (4.5.2.3)$$

$$= \frac{4\cot\phi_L'}{C_L^2} \int_0^{\frac{D-2d}{2}} V(r)dr$$

where (D - 2d)/2 is the radius of the pipe. Clearly V(r) varies across the pipe diameter and V(r) is dependent upon the Reynolds number N_{Re}, which is given by

$$N_{Re} = \frac{\rho V(D - 2d)}{\mu}$$

where ρ is density of fluid, V is mean velocity of fluid, μ is kinematic viscosity of fluid, and (D -2d) is the inner diameter of the pipe.

The velocity profile effects can be compensated by multiplying the estimated velocity by a predetermined (precalibrated) correction factor $K_{Re,}$ i.e.

$$V_C = K_{Re}\, V_E$$

where V_E is the estimated velocity measured by the proposed flowmeter, V_C is the corrected velocity.

Practically, the correction factor K_{Re} can be obtained experimentally by test of the clamp-on flowmeter for a range of flowrates. V_C was measured by the installed positive displacement reference flowmeters and/or by the scale-stopwatch method. The correction factor K_{Re} for a given flowrate is given by

$$K_{Re} = \frac{V_C}{V_E}$$

Since V_C/V_E is a slowly varying function of fluid velocity (N_{Re}), it is not necessary to calibrate values at close intervals.

Another parameter needed to be considered is the beam shift effect. Considerable beam shift could result in loss of signal. Formulation of the beam shift due to flow is best done by referring to Fig 4.5.1. Assuming flow speed V deflected the ultrasound beam by amount δx and the beam deflection is linear with the flow speed, then

$$\delta X = \frac{D - 2d}{C_L \cos\phi_L} V \qquad (4.5.2.4)$$

To assess the values for δx, put few typical values into Equation (4.5.2.4), if

$D - 2d = 0.0135$ m

$C_L = 1500$ m s^{-1}

$V = 4.0$ m s^{-1}

$\phi_L = 20^0$

then $\delta X = 0.038$ mm

For the pipe size (15 mm) and flow range considered in the multiple reflection technique (flow velocity of 0.5 m s^{-1} to 3.8 m s^{-1}), the magnitude of δX in the above example appears to be small and can be ignored.

4.6. Conclusion

In this Chapter, theoretical aspects of both the ultrasonic/thermal and the multiple reflection technique were discussed. Mathematical analysis for both methods were examined in detail. Sources of error which were likely to affect the performance of the flowmeter were discussed. Suggested compensation methods for errors which affect the flowmeter were given.

5. PRINCIPLES AND REQUIREMENTS OF THE PROPOSED FLOWMETER

5.1. Introduction

The theoretical work in Chapters 3 & 4 showed that it should be possible to estimate flowrate in a small bored pipe using a combination of ultrasonic/thermal and multiple reflection techniques. The advantages of combining the two techniques are that it enables the flowmeter to measure a large range of flowrates and also to cross calibrate over a defined flowrate range where both can operate.

In this Chapter, the general operating principles and basic design concepts of the proposed flowmeter will be given. The suitability of the proposed flowmeter for the application requested by a water company (Severn Trent, Birmingham) will also be discussed.

5.2. Operating Principles of the Flowmeter

The ultrasonic/thermal technique and the multiple reflection technique are independent, however, the parameter which one has to measure in both techniques is the transit time of the transducers.

5.2.1. Ultrasonic/Thermal Technique

In the ultrasonic/thermal technique, according to the chosen flow range, a defined DC power (current & voltage) is supplied to the clamped heater(s), creating a temperature difference in the flowing fluid and hence changing the speed of sound. The heating time of the heater is controlled by an automatic switch.

To measure steady state transit time, time (t_s) needed for the temperature of the pipe wall and the liquid to reach equilibrium must be pre-determined. t_s varies according to flowrate and power input. If the flowrate is low and/or power supply is high, then it takes longer for the temperature to become steady and vice versa.

The proposed measurement procedure is outlined as follows:

a. decide heater power input

b. start to log data (continuously at certain frequency)

c. switch on the heater at time t_1

d. switch off the heater at time t_2

e. stop logging.

f. compute the transit time difference.

Fig 5.2.1 shows one example of this type transit time measurement. With a heater power of P watts, the transit time was measured continuously (say at 10 Hz) for 6 min (t_2), and the output data (transit time) were recorded and stored. The heater was switched on at 2 mins (t_1), the water temperature increased and therefore the transit time decreased. The transit time reached steady state after 4 min (t_s).

The transit time at heater off, Δt_0 , is obtained by averaging the data from 1 to 2 mins, and the transit time at heater on, Δt_1 , is obtained by averaging the data from 5 to 6 mins (the error was reduced by averaging the data). The transit time difference is given by

$$\Delta t = \Delta t_0 - \Delta t_1$$

If more readings are required for data analysis (i.e. averaging), procedures c. and d. (above) could be repeated, see the dashed curve in Fig 5.2.1.

Transit time difference Δt is a function of heater power input (P) and flowrate (Q), i.e.

$$\Delta t = F(P,Q)$$

and with a fixed heater power input (P),

$$\Delta t = F(Q)$$

5.2.2. Multiple Reflection Technique

In the multiple reflection technique, transit time with the flow direction (Δt_{12}) and transit time against the flow direction (Δt_{21}) are measured and stored. The transit time difference is given by

$$\Delta t_M = \Delta t_{12} - \Delta t_{21}$$

and flow velocity (V) is given by

$$V = k_M \Delta t_M$$

where k_M is a coefficient, i.e. flow velocity is proportional to the transit time difference Δt_M .

5.3. Design Concept of the proposed Flowmeter

5.3.1. General Requirements

The design of the proposed flowmeter was governed by the need to turn the theories given in Chapters 3 & 4 into a practical measurement tool. It was therefore necessary to undertake the following:

a. examination of the elements and instrumentation required, and
b. determination of how to fit the parts together to produce the proposed flowmeter.

The requirements of the flowmeter (by the Severn Trent water company, Birmingham) are given below:

a. an ultrasonic based clamp-on flowmeter,
b. could be used as a portable clamp-on flowmeter,
c. highly accurate (within 2.0% for high flowrates and better than 5.0% for low flowrates),
d. capable of measuring a large range of flowrates (from 0.5 ml s^{-1} to 550 ml s^{-1}),
e. capable of measuring flowrate for different pipe diameters (15 mm to 40 mm).

The work in Sections 4.2 and 4.4 shows that the ultrasonic/thermal technique is suitable for flowrates ranged from 0 to 80 ml s^{-1} and the ultrasonic multiple reflection technique is applicable only for flowrates higher than 60 ml s^{-1}. To enable the flowmeter to measure the whole flow range defined by (c) above, the proposed flowmeter was to use two independent ultrasonic techniques: ultrasonic/thermal and multiple reflection techniques. As both methods are ultrasonic based, most controlling electronics and instruments could be shared, but some instruments to be used in the proposed flowmeter would be only applicable to one technique and not the other.

The main elements of the proposed flowmeter could be grouped into three areas:

a. thermal instrumentation
b. ultrasonic instrumentation
c. electronics/signal processing.

In the subsequent sections, the components needed for designing the proposed flowmeter will be examined.

5.3.2. The thermal instrumentation

The thermal instrumentation would comprise a heater, a DC power supply (rectifier or batteries) and an automatic timing control switch.

In the ultrasonic/thermal technique, a heater which could be wrapped round the pipe to supply heat evenly to the pipe circumference was essential. Since the meter was considered to be used as a portable device, a heater with a smaller size would be an advantage.

To supply a direct current to the clamped heater, a DC power supply was also needed, which could be provided by two sources: a rectifier or a battery. Although various AC/DC rectifiers were commercially available, a battery with suitable capacity could be used for designing a clamp-on portable flowmeter.

To control the states (on/off) and heating timing of the heater, an automatic switch was to be used to turn the heater on/off at specified times.

5.3.3. The Ultrasonic Instrumentation

To detect ultrasonic transit time, the following devices were needed:

a. two pairs of ultrasonic transducers to transmit and receive signals,

b. a device to clamp the transducers onto the pipe,

c. a signal generator

d. controlling electronics to measure the transit time.

This section concentrates on the selection of the ultrasonic transducers for the ultrasonic/thermal and multiple reflection measurement applications.

Selection of Transducers

For the ultrasonic/thermal technique, since one is interested in measuring the transit time across the pipe diameter, it was sensible to choose direct beam transducers (i.e. transducers which could transmit and receive ultrasonic signals across the pipe diameter at a 90^0 angle to the pipe axis).

To eliminate (or reduce) the beam spreading effect, transducers of high frequency are an advantage. However, absorption of ultrasound in the liquid increases with the square of operating frequency, and so thus puts an upper limit on frequency (see Section 6.2.2 for reasons and explanation in detail). Transducers with a frequency of about 1 MHz were considered.

Because measurement was to be carried out in a confined place, transducers with a small diameter were preferred. Unless curved transducers (see right hand side of Fig 6.2.2) of the same shape and diameter of the pipe were to be used, contacting the transducers on sized and shaped shoes would increase the contact area between transducers and pipe and therefore result in better signals. Transducers with a diameter of 10 mm were considered for the application.

The ultrasonic devices required for the multiple reflection technique were chiefly a pair of angled beam transducers. As mentioned above, transducers with small diameter and high frequency would be preferred. The angle of the transducers (and hence the ultrasound beam) also needed to be taken into consideration. Equation (4.4.1.7) links the transit time difference with the transducer angle and it can be seen that transducers with a larger angle would be an advantage (see Section 6.2.2 for detail). Transducers with a beam angle of 70^0 were selected.

Clamping the Transducers onto the Pipe

For the ultrasonic/thermal technique, clamping the transducers onto the pipe required (see Fig 5.3.1):

a. a pair of sized and shaped shoes, which allowed the transducers to be clamped onto the pipe with ease as well as allowing them to be diametrically opposite each other.
b. a plate fitted with screws, which would hold the two transducers firmly on to the shoes (and hence the pipe).

To improve the received ultrasonic signals, ultrasonic gel was to be used to fill the air gaps between the surfaces of the pipe wall and transducer shoes and the surfaces of the shoes and transducers.

For the multiple reflection technique, the two transducers would not be diametrically opposite but separated by a certain axial distance (see right hand side of Fig 5.3.3). One possible design was to fix the transducers to two plates first, and then clamp the two plates (which would be fitted with screws) onto the pipe. The role of the two plates would be to fix the transmitter but allow the receiver to move only along the pipe in the axial direction. A rule could then be used to measure the distance between the transmitter and the receiver (see Fig 6.2.3 for the elements).

5.3.4. Electronics/Signal Processing

In order to use the clamp-on devices described above for flowrate measurement, electronic/signal processing would be required for sending ultrasound bursts and processing the transmitted and received signals. The following electronic/signal processing instruments would be required:

a. a signal generator to send out signals,
b. electronics to process the ultrasonic signals and hence to measure the ultrasonic transit time,
c. processing of the results

To send out signals to the ultrasonic transmitter, a signal generator would be required. Electronics would be required for processing the ultrasonic signals and measuring the ultrasound transit time as shown in Fig 5.3.2 (see Appendix B.4 for electronics design). This system could be used for both ultrasonic/thermal and multiple reflection techniques. A PC with installed software was considered for measurement data treatment.

5.4. Conclusion

In this chapter, the operating principles and the general requirements of the clamp-on flowmeter have been given. The procedure and principle of flowrate measurement have been discussed.

A photo of the proposed design is given in Fig 5.3.3. With the combination of the two ultrasonic techniques, the flowmeter would be capable of measuring a large range of flowrates (say from 0.5 to 550 ml s^{-1}).

Selection of the instruments and materials for construction of the proposed flowmeter is given in Chapter 6.

6. PRELIMINARY SYSTEM DESIGN AND EXPERIMENTS

6.1. Introduction

To experimentally check the theory and lay a basic foundation for the proposed flowmeter, a preliminary test system was first designed and constructed. A photo of the whole system is shown in Fig 6.1.1. The results in the preliminary test facility lacked refinement in controlling, measuring and data handling. However, results from the rig showed sufficient promise for further investigation.

The design of the flowrig was kept as simple as possible. Instrumentation for the measurements composed of a signal generator, an oscilloscope, a DC power supply and a thermocouple for temperature measurement (see Fig 6.1.2). The main attention of this Chapter was paid to the design of the components for the test section shown in Fig 6.1.3, notably the design of the heater, the ultrasonic devices for the ultrasonic measurement applications (a pair of direct beam ultrasonic transducers, a pair of angled beam transducers and transducer clamps).

Operation of the test facility is best understood by reference to Fig 6.1.4. Water was supplied to the system by the connected tap. The gravity tank was located at a fixed height and always maintained at constant head to provide a steady flow. The pipes used to construct the rig (except the test Section) were glass tubes. The pipe used for the test section was a 500 x 15 x 0.75 mm copper pipe. Flow passed through the heated section of the pipe and was heated by the mounted heater. The transit time across the pipe (at heater off/on stages) was measured by the two clamped transducers, and its reading was obtained from the oscilloscope. The water flow then passed a mixer, the average temperature of the flow was then measured by a temperature sensor. The reference flowrate was measured by the scale - stopwatch method.

Experiments for the ultrasonic/thermal and the multiple reflection technique were performed on the preliminary test facility, and are discussed in Sections 6.4 and 6.5. Results are then compared with the theoretical predictions.

6.2. Design of the Heater and the Ultrasonic Devices

6.2.1. Design & Construction of the Heater

The role of the heater is to supply heat to the fluid. The design considerations were, most importantly, that (i) the maximum amount of heat be transferred to the fluid, (ii) small size and (iii) the ability to be clamped and reclamped onto the pipe.

Figs 6.2.1a, 6.2.1b, 6.2.1c and 6.2.1d show the basic design of the heater. This consists of:

a. two heating elements (wire coils held by a support sheet), which are fixed to
b. two semicircular support frames, and
c. two fitted screws to clamp b. (above) onto the pipe.

Wire with a small diameter was required for constructing the heating elements. The small cross sectional area of the wire together with its high thermal conductivity resulted in fast heat transfer within the heating elements, hence to the pipe wall then the liquid. Other physical properties of the wire such as high melting point and resistance constant with temperature were also important.

The support sheet should be a good electrically and thermally insulating material and capable of withstanding high operating temperatures. These three properties are essential to prevent the leakage of heat from the back of the heater and short circuiting and melting of the support sheet which could result in the burning of the heater coil. For construction, it should be easily shaped and have excellent bonding strength to metal.

The supporting frame is shaped in form of semicircles, which allow the shaped heating elements to be fixed onto and wrapped round the pipe circumference.

The fitted screws hold the two halves of the heater onto the pipe and force the heating elements to contact the pipe wall tightly.

Fig 6.2.2 (left hand side of the photo) shows the size and appearance of the designed heater.

6.2.2 Design of the Two Ultrasonic Devices

The main elements required for the ultrasonic measurements were direct beam transducers for the ultrasonic/thermal technique and angled beam transducers for the multiple reflection technique.

In selecting transducers for the multiple reflection measurements, the angle of the transducers and hence the ultrasonic beam needed to be taken into consideration. Equation (4.4.1.7) links the transit time difference with the transducer angle and it can be seen that transducers with large angle would be an advantage. In both ultrasonic/thermal and multiple reflection techniques, the measurement needed to be undertaken in a confined space, for this reason, transducers with small diameters were chosen.

Spread of ultrasound beam is related to operation frequency of the transducers by the following approximate expression [Hemp, 1988]:

$$\phi_d = \frac{C_L}{fD_T} \qquad (6.2.2.1)$$

where ϕ_d is the angle of divergency, C_L is speed of sound in water, f is the operating frequency and D_T is transducer diameter.

According to Equation (6.2.2.1), transducers with a high frequency give small angles of divergence. Hence, to eliminate the beam spreading effect, transducers of high frequency were chosen. For a 1 MHz transducer with disc diameter of 10 mm and C_L

equal to 1500 m s^{-1} (speed of sound in water), then the angle of divergent is about 0.15 radian (8.6°). Transducers with operating frequency of 1 MHz (or higher) and disc diameter of 10 mm suited the specified experimental requirements.

The transducers selected for the ultrasonic/thermal experiment were therefore:

Frequency	1 MHz
Disc Diameter	10 mm

For the multiple reflection techniques, transducers used were

Frequency	2 MHz
Disc Diameter	10 mm
Beam angle	70°

Both selected transducer specifications could be met by commercially available products, therefore design and fabrication of transducers could be avoided.

To clamp the transducers onto the pipe, brass shoes and perspex plates fitted with screws were used. The role of the shaped brass shoes was to increase the contacting area between the transducers and the pipe circumference and hence obtain better signals. The two plates with fitted screws were used to hold two transducers on to the pipe in a confined space. The two transducers contact the pipe firmly by the force of the tightened screws.

The selected transducers together with various components designed for the clamp-on ultrasonic device are shown in Fig 6.2.2 and Fig 6.2.3. Fig 6.2.4 is a picture of the clamp-on transducers assembled onto the pipe.

In the next Section, selection of products and materials for construction of the elements shown in the Fig 6.2.4 is examined.

6.3 Selection of Materials

Before attempting to construct the proposed flowmeter, the availability of the product and materials was investigated. The first target was to look for commercial products which suited the experiment requirement with minimum or no modification. If such products could not be found then the alternative was to construct the element from commercially available materials. Fortunately, few essential components required for the experiment were commercially available. The direct beam transducers and the angle beam transducers required very little work to turn them into clamp on devices. The next essential element required for the experiment was a heater. Due to its size and shape together with high power requirements, no such product could be found among the commercial products. Design and construction of the heater from scratch was needed.

In this section, effort will be paid mainly to the selection of materials for constructing the heating element. The components needed for the prototype heater are: resistance metal wire; wire support (thermal & electrical insulating material); electrical insulating material; and heater frame.

6.3.1. Selection of Resistance Wire

The only purpose of the heater was to supply the maximum amount of heat to the flowing fluid. Selection of resistance wire with physical properties to satisfy the above purpose is best started by considering basic electrical equations. The resistance, power and the change of resistance with temperature are given respectively by following Equations:

$$R = \rho_m \frac{L_m}{A_m} \tag{6.3.1}$$

$$P = I^2R = \frac{V_A^2}{R} \tag{6.3.2}$$

$$R_T = R[1 + \beta_m(T - T_{Ref})] \qquad (6.3.3)$$

(Where ρ_m is the resistivity of the wire, A_m is the wire cross sectional area, L_m is the wire length, V_A is the applied voltage, I is the current, R_T and R are resistances measured at temperatures T and T_{Ref} respectively, and β_m is the temperature coefficient of the wire electrical resistivity).

Equation (6.3.2) shows that the power of the heater (P) is proportional to the resistance of the wire (R), given a fixed current (I). In this case, metal wire with high resistance is preferred. However, with the same length and cross section area, if the resistance of the wire was too high, a DC power supply with a high voltage and low current outputs would be required (DC power supplies with an output voltage equal to or lower than 24 volts are common commercially available products). A DC rectifier or a battery with a maximum output voltage of 12V and a maximum output current of 10A were recommended for this application.

From Equation (6.3.1), it can be seen that with a fixed length L_m, metal wire with large resistivity gives a high resistance value. Increase of the resistance can also be achieved by choosing a wire with a small diameter.

From the application (maximized heat transfer) and construction (easily fitted and shaped) points of view, a metal wire with small diameter and relatively high resistance was chosen.

Another physical property that needed to be considered was the operating temperature limit. Since the operating temperature of the wire was to be high, selecting a wire with a high melting point was essential.

The variation of resistance of metal wire with temperature is governed by Equation (6.3.3). To keep the resistance of the wire constant (or minimally varying) with

changing temperature, wire with a zero or small temperature coefficient, β_m , was required.

Another factor which required consideration was the thermal conductivity of the wire (K_M). Wire with a high thermal conductivity was preferred since it would conduct heat fast within the coil and hence transfer it quickly to the pipe and then the fluid.

From the theoretical equations and the practical application requirements, the basic criteria for selecting the resistance wire for the heater were: commercially available materials; relatively high resistivity; resistance constant with changing temperature; high operating temperature limit; high thermal conductivity; and easily shaped and machined.

Table 6.3.1 lists the likely candidates for the wire identified by the search and shows the significant parameters for each.

Some of the metal wires given in Table 6.3.1 satisfy the requirements listed above except that the change of resistance with temperature is too significant for this application. The metal wires whose resistances are nearly constant with temperature are Aluchlom O^R, Constantan R.A. and Manganin R.A.

Although the temperature coefficient β_m of Manganin R.A. is low (0.01E-3 k^{-1}), its maximum operating temperature is low (300 °C) compared with Constantan R.A. (900 ^{0}C) and Aluchrom O^R (1250 °C).

Aluchrom O^R, has a high resistivity (135 -145 $\mu\Omega cm$) but its thermal conductivity is low (12.5 W $m^{-1}k^{-1}$) compared with the thermal conductivity of Constantan R.A. (19.5 W $m^{-1}k^{-1}$).

The temperature coefficient β_m of Constantan R.A. is low (0.02E-3 k^{-1}), and its maximum operating temperature is high (900 °C). Although the thermal conductivity of Constantan is rather low compared with some of the wires listed in the Table, it was considered to be good enough for this application. Constantan R.A. was therefore selected.

6.3.2. Selection of Wire Support Material

The next item to be considered was the wire support, which would hold the shaped metal coil. To meet the design and be suitable for the specified applications, the physical properties required for this material were:

a. electrically insulating (this property was essential),
b. thermally insulating (to prevent heat transfer to the back of the heater and away from the pipe), and
c. high operating temperature limit, (this was very important due to one side of this material being directly in contact with the heating coil. The temperature of the coil was high, especially when flow rate was low or at zero flow. Deforming of the wire support could result in short circuiting hence burning out of the heater).

In order for the support sheet to be easily shaped in the form of a semicircle and capable of bonding to the metal coil, the material used needed to be mechanically flexible, elastic and adhesive. Several electrical insulating grease and tapes were considered. The materials listed in Table 6.3.2 were all identified as suitable for the application, but from construction point of view, silicon rubber seemed to be a better choice due to its excellent bonding strength to metal which allowed one face of the heating coil to be fixed onto it.

6.3.3. Selection of Electrically Insulating Layer

To prevent short circuiting, an electrically insulating material was required to prevent the metal wire from direct contact with the copper pipe. Furthermore, this material had to allow the maximum amount of heat to be transferred from the heating coil to the pipe wall and hence the fluid. Materials with high thermal conductivity and negligible thickness would maximize the heat transfer rate. Since one face of this insulating layer would be directly in contact with the resistance wire, the maximum operating temperature of the material must be taken into account. Refer to Table 6.3.3 for listing of materials which were identified as possible solutions.

Although "Heat Sink compound paste" would not be as convenient and easy to use as the tapes, its thermal conductivity was high (almost triple the thermal conductivity of other materials listed in Table 6.3.3), which was very important from the heat transfer point of view. Mixing and painting of the paste onto either the pipe or the heater was also not difficult. It was therefore selected for this project.

6.3.4. Selection of Frame Material

The last item to be considered was material for the heater frame construction. This would hold the heating element and enable it to wrap around the pipe. The requirements for this material were mainly that it be electrically insulating, light in weight and easily machined.

A variety of non-metallic materials suited the requirements. Selection of this material was simply a matter of preference. Perspex was chosen for this work due to its availability, lightness and ease of machining. The transducer clamps were also made from this type of material.

All the required materials were commercially available. Construction of the proposed flowmeter was based on the design given in Section 5.3. A picture of the clamp-on flowmeter assembled onto the pipe is shown in Fig 6.2.5.

To study the feasibility of the proposed flowmeter, several transit time measurement experiments will be discussed in Section 6.4.

6.4 Ultrasonic/Thermal Transit Time Measurement (Preliminary Experiments)

6.4.1 Experimental Specification

Based on the analysis in Section 4.2 and the original specification for the final meter, the following experimental values were used:

Pipe:	15 mm (od) copper pipe
Fluid:	water
Heater Power Input:	80 watts
Transducer Frequency:	1 MHz
Distance X:	43 mm
Flow Rate Range:	1 ml $s^{-1} \leq Q \leq 8$ ml s^{-1}

The length of the copper pipe used for the experiments was limited by space consideration therefore the transducers were located at the nearest position to the heater which was 43 mm (measured from centre of the heater to centre of the transducers). Only very low flowrates were tested, as for higher flowrates, the transit time difference across the pipe diameter was small and could not be read accurately from the oscilloscope.

6.4.2 Experiment 1: Convection Investigation

Initially, the thermocouple for measuring the temperature was placed 20 mm from the centre of the heater, but fluctuating reading from the sensor output device suggested that convective mixing occurred close to the heater. A simple experiment was therefore performed to investigate the convection effect.

The set up of the experiment is shown in Fig 6.4.1. A 100 mm long, 15 mm diameter copper pipe with a clamped heater was fitted on to the flow rig. Transparent tubes (glass tube) were used for construction of the remainder of the pipe line so that the flow pattern of an injected dye stream could be observed. Dye was injected in to the flowing fluid at an upstream location using an injection cylinder. The flow patterns both upstream and downstream were observed, with the help of a slide projector modified to provide a sheet of white light.

A heater power of 80 watts and a flowrate of 3.38 ml s^{-1} were used for the test. Flow patterns of an injected dye stream were observed at heater off and on states. When the heater was off, the injected dye flowed downstream without being disturbed (Fig 6.4.2a). When the heater was on, convective mixing occurred near the heater region, this effect is shown in Fig 6.4.2b.

Since the average temperature across the pipe diameter was of interest in determining transit time, the convection effect was considered unlikely to affect the result of the overall ultrasonic measurements. No further attempt was therefore made to investigate the characteristics of the convection effect, although its appearance confirmed the need for separate numerical models for horizontal and vertical flows.

6.4.3. Experiment 2: Ultrasonic/Thermal Transit Time Measurements

6.4.3.1 Experiment Set Up

The set up of the experiment is shown in Fig 6.1.4. The experiment specification is as given in Section 6.4.1. The parameter to be investigated was ultrasonic transit time under steady state conditions.

6.4.3.2 Transit Time Measurements

In the experiments, the flowrate was controlled by the fitted needle valve located at the inlet and measured using a scale-stopwatch system. Water passed through the copper

pipe section where the heater was clamped, and its temperature increased when the heater was switched on. The pair of ultrasonic transducers was clamped downstream of the heater, transmitting and receiving ultrasonic signals. The transit times with the heater on and off were measured via the connected oscilloscope. The typical transit time decrease of the received signals from the measurements with the heater off and heater on under steady state conditions are given in Fig 6.4.4a and Fig 6.4.4b respectively.

From the signals shown in the Figures, one could see that, when the heater was off the transit time was higher compared with that when the heater was on. This effect was expected because when the heater was off, the temperature of the liquid was low and hence the speed of sound was lower, resulting in a longer transit time and vice versa.

The difference in transit time with heater on and off is given by

$$\Delta t = \Delta t_0 - \Delta t_1$$

where Δt_0 and Δt_1 represent the transit times with the heater off and on respectively. The transit time measurements were performed for eight different flowrates selected within the flow range from 1.0 ml s^{-1} to 8.0 ml s^{-1}. Table 6.4.1 shows the results of these measurements, which will be compared with the theoretical values in the next Section.

6.4.3.3. Comparison of Experiment Data with Computed Values

The experimental results obtained from the last Section were compared with values computed using the mathematical models derived in Chapter 4. Fig 6.4.4a compares the experimental data with the results obtained from the numerical simulation using FIDAP (see Table 6.4.4a for numerical values).

Fig 6.4.4a shows the plot of transit time for the ultrasonic beam travelling across the pipe diameter against flowrate with the heater on. The experimental data points in the plots were defined by

$$\Delta t_1 - \tau_T$$

where Δt_1 was the measured transit time, and τ_T was the delay time of transducers and electronic instruments which was predetermined. The theoretical values were obtained by the FIDAP simulation with the same inputs as those used in the experiments in Section 6.4.3.2.

The temperature in the numerical prediction is higher than that of the experiments which results in a higher speed of sound hence a shorter time for ultrasound to travel across the pipe in the numerical computation data. This was expected as the heat losses in the experiments were ignored in the calculation. The two sets of data were not far apart and followed the same trend with a constant offset of about 1.4%.

Although the two sets of data seem very close, the comparison was based on the assumptions: a vertical pipe model was used to compute results to predict the readings from horizontal pipe experiments; the theoretical model did not include heat transfer to the electrical insulating layer (i.e. it was assumed that the resistance wire was directly in contact with the copper pipe wall, and heat loss to the silicon rubber support sheet and perspex frame at the back of the heater were ignored); and the thickness of the pipe was over estimated in the theoretical model (the thickness of the pipe used for the experiment was 0.71 mm. In the computation, the pipe thickness was 0.75 mm).

The confidence in the preliminary test facility was not high, the main drawbacks of the flowrig and the instruments are listed below:

a. Small physical size of the rig: the limited height of gravity tank resulting in limited water supply of the rig which made it not possible to measure higher flowrates; and the limited test pipe length which affected the flow profile in the pipe.

b. The simple instruments used did not meet the requirement of the experiment especially in the control and data acquisition sense. The main drawbacks were: the transit time was measured by an oscilloscope this could not recording data continuously at high frequency; no reference flowrate meter was installed to carry out reference flowrate measurement continuously at high frequency; and it was not possible to get very accurate readings from the oscilloscope (reading accurate only to ± 0.1 μs). With these instruments, an error of ± 0.005 μs could result in a percentage error of up to 13% (see Fig 6.4.4b). More accurate instruments would be required for further experiments.

Even with the above limitations, the preliminary experiment produced very encouraging results but confidence in the test facility was low. A modified flow rig together with electronics and an advanced computer based control and data acquisition system for the experiments was therefore required for more precise tests. This rig will be discussed in Chapter 7.

In the next section, preliminary experiments for multiple reflection technique will be described.

6.5. Ultrasonic Multiple Reflections Preliminary Experiments

6.5.1 Experimental Specification

The pipe and fluid used in this experiment were the same as in Section 6.4.1. The transmitter was clamped on to the pipe at a fixed location. The positions along the pipe where the receiver should be clamped were theoretically investigated in Section 4.3.2. The separation distance between the transmitter and the receiver for 1, 3 and 5 reflections are listed in Table 6.5.1. Transit times were measured for the receiver

clamped at specified locations along the pipe. The following experimental values were used:

Pipe:	15 mm (od) copper pipe
Transducer Frequency:	2 MHz
Transducer Angle:	70°
Fluid Under Test:	Water

6.5.2 Experimental Set Up and Multiple Beams Existence Investigation

The set up of the experiment is shown in Fig 6.5.1. The flowrate was controlled by a needle valve fitted at the inlet and measured by a scale-stopwatch system. A pair of angled ultrasonic transducers were clamped onto the copper pipe to transmit and receive ultrasonic signals. The transmitter and the receiver were separated by a distance X_N (see Table 6.5.1), which was measured using a rule. The transit times were measured via an oscilloscope. The parameter to be measured was the transit time for signal transmitted from the transmitter (with reflections) to the receiver.

The preliminary experiments to investigate the existence of the multiple beams predicted by the computer model were performed using 15 mm diameter copper pipe. Accurate measurement of the separation distance X_N (between the transmitter and receiver) was important in this test, and the accuracy was about ± 0.5 mm. The transducer signal, controls and result handling were almost identical to the experiment presented in Section 6.4. Received signals for an empty pipe and a full one with low flowrate (0.7 ml s^{-1}) were observed for the receiver located at

X_N = 4.92 mm, 11.62 mm, 18.25 mm

respectively. Table 6.5.1 lists results of the experiments for 1, 3 and 5 reflections.

Figs 6.5.2a, 6.5.3a and 6.5.4a are plots of the received signals for the empty pipe, Figs 6.5.2b, 6.5.3b and 6.5.4b are plots of the received signals for a full pipe with a flowrate equal to 0.7 ml s^{-1}.

According to a prediction by the computer model, at X_N equal to 4.92 mm, and t_N equal to 17.75 μs, a signal for one crossing should be received, this prediction was confirmed by the experimental results which is shown in Fig 6.5.2b.

In Fig 6.5.3b, two signals arrived at the receiver, the right hand side signal is the signal for three reflections which was predicted by the computer model (see Table 6.5.1 for numerical values).

According to a prediction by the computer model, at X_N equal to 18.25 mm, and t_N equal to 55.30 μs a signal for five reflections should be received, this prediction was also confirmed by the experimental results which is shown in Fig 6.5.4b (see Table 6.5.1).

6.5.3. Comparing Experimental Data with Theoretical Values

The experimental results from the section confirms the theory of existence of ultrasonic multiple beams, which was discussed in Section 4.3.2. From the percentage error (Table 6.5.1), one could see that the two sets of data are very close, the maximum percentage error was about 2.3%.

The draw back of the test rig together with instruments used for the experiment was mentioned in Section 6.4. In addition, due to the limitations of the flow rig, tests conducted at high flow rates were not possible.

6.6. Conclusion

In this Chapter, the design of various elements for the clamp-on flowmeter were given. Suitable commercially available products and materials from several companies were searched and selected for construction of the heater and the clamp-on transducers.

A simple experimental system was setup to test the designed clamp-on flowmeter. Even with some drawbacks of the test facility, the preliminary experiments showed encouraging results.

In Chapter 7, the design and constructing of the refined flow rig together with advanced electronic control and data acquisition will be discussed.

7. DESIGN AND CONSTRUCTION OF THE EXPERIMENTAL SYSTEM

7.1 Introduction

The work presented in Chapter 4 and the preliminary experiments (Chapter 6) led to a model for the prediction of flowrate. The purpose of this chapter is to present the design and construction of a refined system for further experimental work.

The experimental results obtained from the preliminary experiment agreed with the theoretical values within the tolerances of the system. Due to a lack of refinement of the preliminary rig and data collection method, the results were not sufficiently accurate to determine the validity of the proposed flowmeter. It was therefore necessary to construct a refined test rig together with a data acquisition system and an accurate timing measurement electronic control system for subsequent experiments.

These experiments were to have two objectives. Firstly, it was intended to measure temperature distribution in a confined space in the pipe wall, secondly, to analyze more accurately the flowrate measurement technique using the ultrasonic/thermal method.

7.2. Experiment Specification for the Ultrasonic/Thermal Technique

There is no restriction on choosing the pipe size. The only reason a 15 mm diameter copper pipe was chosen because it is one of those used for class C/D flowmeters. Water was used as the fluid for the test since the flowmeter was designed for a water company (Severn Trent).

As heat transfer in vertical and horizontal pipe orientations was likely to be different (see Section 6.4.2), both horizontal and vertical pipes needed to be tested.

The selected flow range was based on, firstly, the Class D flowmeter specification, and secondly the maximum limit of the ultrasonic/thermal technique. 0.5 ml s^{-1} was the

minimum flowrate, and 80 ml s^{-1} was chosen as the maximum flowrate for ultrasonic/thermal technique, because if the flowrate is higher than 80 ml s^{-1}, the temperature increase in the fluid is insignificant leading to a transit time difference which is too small to be measured accurately (see Section 8.5.1 for experimental results).

The specification for the experimental rig was therefore as follows:

Pipe size:	15 mm diameter
Pipe material:	Copper
Pipe orientation:	Horizontal & Vertical
Fluid:	Water
Flowrate Range:	0.5 ml s^{-1} to 80 ml s^{-1}
Heated Section:	40 mm
Heater power:	40 w (0.5 ml s^{-1} < flowrate < 20 ml s^{-1})
	100 w (20 ml s^{-1} < flowrate < 40 ml s^{-1})
	200 w (40 ml s^{-1} < flowrate < 80 ml s^{-1})

Parameters to be measured were pipe wall temperature and transit time at steady state.

In the next section, the detailed design and construction of a refined hydraulic system for testing the proposed flowmeter will be discussed.

7.3 Design and Construction of the Hydraulic System

The test facility was designed and assembled in order to enable the measurements modelled in the previous Chapters to be tested experimentally. The main considerations for designing the hydraulic system were:

a. able to provide constant flowrate ranging from 0.5 ml s^{-1} to 350 ml s^{-1},
b. able to provide flowrates ranging from 1 ml s^{-1} to 80 ml s^{-1} with constant inlet flow temperature,

c. temperature sensor(s) for checking the temperature of the fluid,

d. reference flowmeters for measuring reference flowrates,

e. A scale-stopwatch system for conventional flowrate measurement,

f. Both the horizontal and vertical pipe orientations.

7.3.1. Design, Construction and Operation of the Rig

Diagrams depicting the design of the hydraulic system are shown in Fig 7.3.1a (horizontal pipe orientation) and Fig 7.3.1b (vertical pipe orientation). Fig 7.3.2 is a photo showing the rig.

Explanation of the operation of the test rig is best referred to Fig 7.3.1a (horizontal pipe orientation) or Fig 7.3.1b (vertical pipe orientation). The driving force for the water flow in the hydraulic system could be either gravity or a pump. The gravity tank was situated at about four meters from the ground which was high enough to provide a required maximum flow of 80 ml s^{-1}. The water in the gravity tank was always maintained at a fixed head level (by using an overflow path), which ensured a constant hydraulic pressure, and hence a stable flow into the pipe line. There was also a large tank below the gravity tank, which held a larger quantity of water (1000 l) and was connected to a pump of capacity 2.8 l s^{-1}. Both tanks were filled by a water supply from a main tap.

The reason for employing the gravity feed instead of the pump was to maintain the temperature of the inlet fluid. The variation of the fluid temperature on using the pump is shown in Fig 7.3.3. As can be seen, the temperature increases slightly. However, the gravity tank could not supply a very large flowrate due to its limited height. A dual system was therefore constructed.

For low flowrate measurement, water was drawn out from the gravity tank. For large flowrates, water was continually pumped into the pipe line from (and recycled into) the large tank. The inlet water supply from the main tap was not sufficient if a high flowrate was required, recycling the water into the large tank was therefore needed and

this could save water. Periodically, both tanks were drained, cleaned and refilled in order to provide a sufficiently clean water supply for the measurements.

At the outlet, a section of vertical pipe was fitted to the pipe line, which ensured the pipe line was always fully filled with fluid by preventing it from draining below the level of the top of the vertical pipe section.

The pipe line and the flow loop were designed in such a way (see Fig 7.3.1a) that, on leaving the gravity tank, water passed through a 40 mm diameter copper pipe. Valves were fitted at the inlet. When the pump was operated, valve 1 needed to be shut to stop water being pumped up to the gravity tank. Valves 2 and 2' were shut whenever the gravity tank was to be operated, this ensured that water all passed to the pipe line instead of flowing into the large tank. The connection between the pipe line and the test section was a flexible plastic tube. At the two ends of the test section, replaceable contractors were fitted to allow pipes of different diameters to be inserted easily. Details of the test section are given in Section 7.6.

Flow to be measured first passed through the reference flowmeter(s), then through the meter under test. The fluid then went either down to the fitted drain or returned to the large tank.

A small sized tank and a vessel were located at the outlet to allow the conventional scale-stopwatch method of flowrate measurement. This was vital not only for calibration of the reference flowmeters, but also to measure reference flowrates directly.

7.3.2. Components for Measuring Reference Values

The components installed in the pipe line to allow certain reference values to be measured are the reference flowmeters and reference temperature sensor.

To measure reference flowrates, two flowmeters were connected to the pipeline: one Foxboro 3/4 inch turbine flowmeter, and one D class positive displacement (SOCAM)

flowmeter. Both the meters could be bypassed individually. With this design, the two reference meters could be operated at the same time or individually if preferred (see Section 7.5.1).

A temperature sensor was fitted down-stream of the reference meters for measurement of the averaged inlet fluid temperature. The temperature sensor was a Pt100 model (Platinum resistance P.T.F.E. insulated probe, with a diameter of 3 mm). The accuracy of this type of temperature sensor was high (accurate to ± 0.1 ^{0}C). With the provided analog input/output, the sensor could be connected to an analog data acquisition system and hence the data could be viewed and/or logged into a computer for future reference (see Section 7.5.2).

In the next section, the instruments, data acquisition system and associated electronics selected for the application will be discussed. The means to apply the various parts to the measurement of temperature, flowrate and transit time, and to logging of data are presented.

7.4. Instrumentation, Associated Electronics and Applications

7.4.1. Selection and Usage of Instrumentation and Associated Electronics

To make the control and communication between the instruments possible, various commercially available hardware and software were selected. A PC with a 80 MB hard disk was used for installing various software and hardware so that the connected instruments could be controlled via the computer and the output data could be logged into a computer and viewed on the monitor screen.

Fig 7.4.1 is a photo showing all the instruments used for the experiment. Selection of the instruments was based on suitability to the specified application, availability and economical consideration. Fortunately, a few instruments (signal generator, timer-counter and DC power suppliers) were available from the department (DFEI), and met the requirements of the experiments. The Wavetek gate mode controller and the

controlling electronics were specially designed and prepared by an electronics expert [Macleod, 1992].

A brief outline of the usage of each individual instrument and reasons for selection are summarized as follows:

A signal generator was used to generate waveforms for the connected ultrasonic transmitter. The gate mode controller was designed to be used in conjunction with the signal generator to produce between 1 to 99 complete output cycles at a set repetition rate.

The oscilloscope was used for checking the transmitted and received signals of the connected ultrasonic transducers. With the signal shown on the oscilloscope screen, setting of threshold values for the ultrasonic timing interface instrument became easy. The timer-counter measured the time between start pulse and end pulse to a resolution of 2 ns. The timer-counter was compatible with the IEEE-488 bus, which allowed the timer-counter to be controlled via the computer.

The IEEE-488 bus was selected because it was compatible with the timer-counter and Workbench software. Its role was as the communication medium between the timer-counter and PC. Controlling commands, and measured results were transferred to and from the PC via the IEEE-488 bus.

The data acquisition board was used to accept signals from and send signals to the sensors and the instruments connected to it. Both the analog input and digital I/O channels were available. For this reason, the Mini-16 data acquisition board was selected for both the temperature measurement and heater switch control applications. The temperature sensors were connected to the analog channels and the heater switch was controlled by the digital I/O channel.

Workbench (interface software) was selected because, firstly, it was compatible with the IEEE-488 interface card and the data acquisition board, secondly, the package provided a large number of functions, and it was very easy to use due to the availability of icons.

Finally, it allowed the data to be logged onto a floppy diskette for future analysis and to be displayed on the computer screen graphically or numerically for inspection during the experiments.

The main purposes of the PC were to install the selected software and hardware so that the instruments connected to it could be controlled via the keyboard and the experimental results could be saved and viewed on monitor screen during the experiments. A 80 MB hard disc was enough for installing IEEE-488 bus, data acquisition board and WorkBench files, and also for logging experimental data. With a operation frequency of 20 KHz, a PC 386SX was considered fast enough to meet the experimental requirements.

The ultrasonic timing interface was used with the timer-counter to measure the transit times of ultrasonic sine wave bursts sent across a pipe. The three roles of this instrument are: amplifying the signals from the transducer; zero crossing detection; and comparing the zero crossing results with a preset counter value and outputting the data to the timer-counter (see Fig 7.4.2b). Refer to Appendix B.1 to B.4 for the associated electronic circuit design and detail description.

7.4.2. Operation of the Instruments

A connection diagram for instruments of the prototype ultrasonic/thermal flowmeter is given in Fig 7.4.2a. Description of operating these instruments is best done by reference to an example of the signal input and output in a diagram shown in Fig 7.4.2b. The Wavetek was used in conjunction with the Wavetek gate mode controller to generate a sine wave burst which after transmission across the pipe produced a signal (a). When this signal was input to the ultrasonic timing interface electronics, it was amplified (b) and processed (c) (The step by step performance of the ultrasonic timing interface electronics for the signal is shown in Appendix B.4). The processing for the transmitted signal was exactly the same as the received signal. Output signals from ultrasonic timing interface electronics were fed to the timer-counter for measuring transit time

across the pipe diameter. The measured transit times from the timer-counter were then transferred to the computer for logging or for inspection via interface IEEE-488 bus.

7.4.3. Application of the Instruments to Measurements

The application of the instruments to the specified experimental work can best be demonstrated by reference to the following examples:

a. temperature measurement
b. flowrate measurement
c. heater switch control
d. transit time measurement

In order to use the data acquisition system in controlling, measuring and logging, the sensors or instruments needed to be connected to the IEEE-488 bus and/or the data acquisition card. Transfer of information was controlled by requests/commands selected in a Workbench input file, which was created by using the icons provided or external functions.

Temperature measurement

A Workbench input layout for using the data acquisition system for measuring temperature is shown in Fig 7.4.3. The temperature sensors were connected to one analog input channel of the data acquisition board. Selection of specified channels, sensor types and data collecting frequency was done via the analog input icon (A1:1). Due to the availability of the icons provided by the interface software, selecting the required items (tasks) could simply be done by double clicking on the relevant icons, then selecting the required items from menu listings. The calculators were used to average the input data over a period of time (1.0 second). The experimental data were logged on to a floppy diskette by the log icon (Lo1). The results could be displayed graphically by using the chart icon and numerically by using the meter icon.

Flowrate measurement

There were two ways to measure reference flowrate using the instruments and data acquisition system: using the timer-counter and IEEE-488 bus or data acquisition board. The Workbench input layouts for the two methods are given in Fig 7.4.4 and Fig 7.4.5 respectively.

To use the timer-counter and IEEE-488 bus for flowrate measurement, the reference flow meter was connected to either channel A or B of the pre-set (voltage, data collecting mode) timer-counter. The timer-counter communicated with the data acquisition system via the IEEE-488 card. Requests/commands (set via the IE1 icon) were sent from the PC to the timer-counter, and data (frequency) were transferred from the timer-counter to the PC. The calculator (CA1) was used for converting the frequency of the flowmeter to flowrates. Data were logged onto a floppy diskette by the log icon (Lo1). The measurement results were displayed graphically by the chart and numerically by the meter.

A Workbench input layout for flowrate measurement using the data acquisition board is shown in Fig 7.4.5, the reference flowmeter was connected to one of the analog input channels of the data acquisition board. Selection of channel and frequency was via the analog input icon (A1:4). Calculator (CA1) was used to detect zero crossing of the signals. Pulse rate was computed by another calculator (CA2). To convert the pulse rate to flowrate, calculator (CA3) was used. Numeric data at specified frequency were logged on floppy diskettes by the log icon (Lo1). The results were shown on the terminal screen by the chart (graphically) and the meter (numerically).

Heater switch control

To use the data acquisition system to control the heater, the heater relay switch was connected to a digital I/O channel of the data acquisition board. A Workbench input layout is shown in Fig 7.4.6 (the two icons at the top of the fig). The pulse timing (high/low) were set via the pulse icon (PL1). With this setting, when the digital input

signal went high the heater was switched on, and when it went low the heater was switched off.

Transit time measurement

A workbench input layout for using the instruments and the data acquisition system to measure transit time of the transducers is shown in Fig 7.4.6. The two icon at the top are for controlling the states (on/off) of the heater. To measure the transit time, the transducers were connected to the signal generator and the associated electronics, which was connected to the timer-counter. The timer-counter communicated with the PC via the IEEE-488 bus. Sending of requests/commands and data to and from PC to the timer-counter, was controlled by the IEEE-488 icon (IE1). The experimental data were logged to diskettes for further analysis by the log icon (Lo1). The results were displayed graphically by a chart and numerically by a meter.

Calibration of the hydraulic system and the installed components using the instruments and data acquisition system provided is discussed in the following Sections.

7.5 Calibration of the Flowrig and the Test Facility

Prior to any experiments, a full calibration of the system was necessary. This included calibrations of:

a. the flowrig.
b. the temperature sensors.
c. the reference flowmeters.

7.5.1 The flowrig

When the rig was first constructed, time was spent on modification to best suit the system for the measurement requirement. The problems associated with the pipe line

were mainly water leakage, maintaining constant head for the gravity tank, and fitting bypass paths for the flowmeters.

Leakage in the pipe line would result in inaccurate flowrate measurement. As the rig was fitted with several parallel flow paths, leakage occurring in these connections could affect the measurement seriously. To ensure no leakage in the pipe line, all the connections and the fitted valves were carefully checked. A few valves were replaced. Periodical checking for pipe line leakage was carried out throughout the experimental work.

In order to get a steady flow, maintaining a constant head in the gravity tank during the experiments was essential. To ensure this, an overflow path was used. The sloshing of water in the tank created by direct feeding water from the main tap supply was eliminated by fitting a vessel with a large opening inside the gravity tank (Fig 7.3.1a and Fig 7.3.1b). With this design, instead of feeding water directly into the gravity tank, the inlet water first filled the vessel, from which it then overflowed into the gravity tank smoothly.

An alteration of the hydraulic system was to put bypass paths on the two installed reference flowmeters (in the initial design, the two reference flowmeters were connected in series). As the SOCAM flowmeter was installed with a rotating disc on it (see Section 7.5.3.1), high flowrates could result in damage to the rotating disc installed on the meter. A bypass path was therefore needed to protect the flowmeter when the rig was operated at high flowrates.

7.5.2 Calibration of the Temperature Sensors

The temperature measurement system includes:

a. temperature sensors
b. a data acquisition board

c. interface software.

The type of temperature sensors considered for the experiment were platinum resistance insulated probes (Pt100) and insulated T type thermocouples.

The temperature measurement system was calibrated by comparing its reading with a conventional mercury thermometer. The temperature sensors together with the conventional mercury thermometer were inserted in a vessel filled with water. A large vessel containing a large amount of water was used to ensure the temperature of the liquid was constant or had a minimum change during the measurement. Water of different temperatures were tested.

The sensors were connected to the channels of the date acquisition board which was connected to the computer and controlled via interface software (Workbench). Apart from the mercury thermometer's readings, the readings of other temperature sensors were obtained by using the data acquisition board, interface software (Workbench) and the computer.

The WorkBench input layout for the calibration of the temperature sensors is shown in Fig 7.5.1. Six temperature sensors (three platinum resistance P.T.F.E. insulated probes, three T type thermocouple) were connected to the six channels of the data acquisition board, and the sampling frequency was set at 20 Hz. The calculators were used for averaging the temperature readings (20) for every second.

Comparing the temperature reading of the mercury thermometer (minimum scale: 0.2 °C) and the data obtained for the sensors showed that the T type thermocouple overmeasured temperature by 1.25 °C. Although the difference was large, the offset was nearly constant for different test temperatures. The Pt100 probes were more accurate, the offset was only about 0.5 °C and again the offset was constant with different test temperatures. The constant offset could be compensated easily by using a calculator icon in WorkBench.

Although the Pt100 temperature sensor was accurate, its temperature output was the averaged temperature over the whole length of the probe. This was not suitable for measuring temperature in a confined space of the pipe wall. T type thermocouples were therefore chosen to measure the pipe wall temperature.

7.5.3 Calibration of the Reference Flowmeters

Both reference flowmeters for the experiments had been precalibrated by DFEI. Further calibrations were carried out when the meters were installed in the pipe line of the rig. Detail of the calibration is discussed in the next two Sections.

7.5.3.1 Calibration of the SOCAM flowmeter

The precalibrated SOCAM (positive displacement) flowmeter was specially modified for this research project. A frequency counter was installed with the SOCAM flowmeter which enabled the meter to be interfaced with the timer-counter. The frequency counter was a disc with holes and LED pick-up installed in the SOCAM flowmeter. When flow was present, the disc rotated. Frequency was defined by the number of the turns of the rotating disc and indicated by the LED signals. The output frequency of the rotating disc was directly proportional to the flowrate. An IEEE-488 card (communication medium between the timer-counter and PC), a PC and Workbench (software package) were used as the controlling and collecting data media.

To measure flowrate, the SOCAM was connected to a channel of the timer-counter. A WorkBench input layout for the flowrate measurement is shown in Fig 7.5.2. The timer-counter communicated with the data acquisition system via the IEEE-488 card. The calculator icon was used for converting the frequency of the flowmeter to flowrate. Data were logged onto a floppy diskette by the log icon (Lo1). The measurement results were displayed graphically by a chart and numerically by a meter. Single readings were collected at 0.5 second intervals, and 50 readings were collected for each flowrate. The averaged result for comparison was defined by:

$$\bar{Q} = \frac{1}{50} \sum_{i=1}^{50} Q_i$$

where Q_i was the ith output flowrate reading of the SOCAM reference flowmeter, and $\bar{Q}$ was the averaged flowrate.

The SOCAM was then calibrated using the conventional method of a scale-stopwatch system. The flowrate range considered for SOCAM flowmeter calibration is the same flow range as for the ultrasonic/thermal technique:

1 ml s^{-1} to 80 ml s^{-1}.

The result of the comparison is shown in Fig 7.5.3a. This can be seen in greater detail in the percentage error plot (Fig 7.5.3b), the percentage error was defined by

$$err(\%) = \frac{Q_{SOCAM} - Q_{Ref}}{Q_{Ref}} \times 100$$

where Q_{Ref} is the flowrate measured by the scale-stopwatch system. As can be seen, the maximum error was about 3.5% and the percentage error is higher at low flowrates.

As the SOCAM is a positive displacement meter, fractional rotation do not give a linear relationship between frequency and flowrate. At the higher flowrate, the optical encoder provided a lager number of rotations for each frequency reading whereas lower flowrates the optical encoder rotated fewer times. This gave larger error at these flowrates. The non-linearity of the reference SOCAM flowmeter was not taken into account in the ultrasonic/thermal flowmeter calibration which results in a larger difference between the computer simulation and the experiment result at lower flowrates (see section 9.2).

Fig 7.5.3b shows results of this calibration with an earlier calibration curve for the SOCAM meter on a different rig [Hampton, 1991], one could see that the two calibrations are close.

The following factors were identified as likely to provide inaccuracy in the scale-stopwatch measurement system:

a. Timing inaccuracy due to the stop watch readings. The maximum error was estimated to be within ± 0.3 second, and the minimum measuring time was 100 s, therefore the maximum error should be ± 0.3%.

b. Inaccuracy of the weight due to scale readings. The minimum reading of the scale was 0.1 g, the minimum weight of water was about 2000 g, leads to a maximum error of ± 0.05%, which is insignificant and can be ignored.

7.5.3.2 Calibration of the Turbine Flowmeter

The turbine flowmeter was used to measure the flowrates from 50 ml s^{-1} to 800 ml s^{-1} (maximum flowrate of the rig). As the flowrate increased, the scale-stopwatch method became difficult to implement. Instead of using the scale-stopwatch, the precalibrated data of the turbine flowmeter vs Hardall 5259 P.D. meter [Sweetland, 1989] were used as reference values.

The turbine reference flowmeter was connected to channel A of the timer-counter. The WorkBench input layout and the data collecting method used have been described in Section 7.5.3.1. Plots of the calibration results and the pre-calibration data [Sweetland, 1989] are given in Fig 7.5.4a. Fig 7.5.4b is the percentage error plot of the Turbine meter pre-calibration results.

7.6 Assembling the Test Section

The assembled test Section of the ultrasonic/thermal flowmeter is displayed in Fig 7.6.1. The test section comprises essentially a heater, a pair of direct beam transducers, and temperature sensors. Since the proposed flowmeter was designed as a clamp on measurement device, all the components were assembled onto the pipe in a clamp-on manner.

The heater is held tightly round the pipe circumference by the two support screws. Unclamping or reclamping of the heater was simply a matter of adjusting the fitted screws.

The two shaped brass wedges were used to improve the signal sent between the transmitter and the receiver. A pair of 1 MHz transducer were pressed firmly onto the wedges and clamped onto the pipe by the shaped perspex plates fitted with screws. To ensure no air gap between the pipe and the wedges, the wedges and the transducers, ultrasonic gel was used to fill the gaps created by the imperfect match between the transducer shoes circumference and the transducer surface. Similar to the clamp-on heater, unclamping or reclamping of the transducer pair was achieved by adjusting the fitted screws.

7.7 Conclusion

In this Chapter, design and construction of a refined test facility (hydraulic system and advanced electronics and computer controls) were discussed. Selection together with the usage for each selected instrument was summarized. An example showing the operation of the instruments was given. Application of the instruments for various measurements (temperature, flowrate, heater control and transit time) were discussed. The required components (temperature sensor, reference flow meters) which were needed as reference elements for the experiments were improved and calibrated. Clamping of the prototype flowmeter on to the test pipe was also discussed.

In the next Chapter, detail of testing the designed flowmeter will be given.

8. TEST OF THE PROPOSED FLOWMETER

8.1 Introduction

The work of previous chapters led to a model for prediction of flowrate using the combined thermal ultrasonic techniques. The purpose of this Chapter is to check the theory experimentally and to form a foundation for development of a commercial ultrasonic flowmeter.

Details of the experimental procedures, application of the instruments and computer data acquisition system for the specified experimental work will be discussed.

Tests of the ultrasonic/thermal flowmeter were conducted for both vertical and horizontal pipe orientations. The experiments to be considered are: heater input power determination; preliminary experiments; transducer spacing investigations; transducer clamp-on angle investigations; transit time measurement for different flow regions and repeatability check for the flowmeter.

For all the experiments listed above, the parameters to be measured are:

a. reference flowrate (obtained by using the reference flowmeter and/or the scale-stopwatch system),
b. power input (recording voltage and current of heater power supply),
c. temperature (to ensure inflow temperature is constant during the experiments),
d. transit time (heater off/on).

The test facilities, such as the flowrig, reference flowmeters and the temperature sensors, were monitored frequently to ensure that no problem was encountered which might effect the experiment results.

8.2 Experimental Specification

Basing on the analysis in Section 4.2 and the original specification for the proposed ultrasonic/thermal flowmeter, the experimental conditions were as following:

Fluid:	Water
Flowrate Range:	1 - 80 ml s^{-1}
Pipe Material:	Copper
Pipe Dimensions:	OD = 15.0 mm, ID = 13.5 mm
Pipe Orientations:	
Vertical pipe	with upwards flow
Horizontal pipe	heater upstream
Power Input:	40 - 200 Watts

8.3 Experimental Procedure

In this section, an overview of the experimental procedure and a step by step guide to the transit time measurement is given. Although a large number of experiments were needed, the procedure to carry out each experiment was almost identical. The work involved could be summarized as follows:

a. Ensure the temperature of the fluid flow in the pipe line was steady before starting the experiments. This was essential since the measurement data was based on the fluid temperature changes. Use of a temperature sensor would have been an ideal solution to check the fluid temperature but this required inserting the sensor into the pipe, which was not possible for the clamp on flowmeter. Checking the temperature was therefore done by inspecting the processed ultrasonic signals, a steady signal indicated that the temperature of the flowing fluid was constant. Fig 8.3.1 shows an example of such signal.

b. Wait until the electronic instruments were electrically at steady state. This was required only when the instruments were first turned on. In this thesis, all the

experimental data were collected after the instruments were turned on for not less than 1 hour). Fig 8.3.1 gives an example showing when both the electronic instruments and the temperature of the fluid had reached a steady state.

c. Check the transmitted and received ultrasonic signals on the oscilloscope and set a suitable threshold trigger value for zero crossing measurement of the ultrasonic timing interface before carrying out the experiments. This ensured clear signals and steady readings from the timer-counter. Fig 8.3.2 shows an example of the ultrasonic signals with the threshold setting values. Setting of the threshold values was done by tuning CH2 of the ultrasonic timing interface electronics (see Section 7.4 for detail) until a signal similar to one in Fig 8.3.2 was obtained.

d. Measure the reference flowrate. To obtain the reference flowrate, the pre-calibrated flowmeters (the SOCAM for flow range 0 to 40 ml s^{-1} and the Turbine for 40 - 80 ml s^{-1}) together with the conventional scale-stopwatch method were used. The measurement of reference flowrates was discussed in Section 7.4.2.2. The Workbench setup layouts shown in Fig 7.4.4 or Fig 7.4.5 were used for this application.

e. Adjust the input DC power supply to the desired values according to the flowrate ranges defined in Section 4.2, i.e.

P = 40 Watts	(1 - 20 ml s^{-1})
P = 100 Watts	(10 - 40 ml s^{-1})
P = 200 Watts	(30 - 80 ml s^{-1})

f. Acquire and log transit times and experimental data. Once procedures a. to e. were completed, transit time measurement could proceed using a pre-defined Workbench file (see Fig 8.3.3). The transit times were logged on to a floppy diskette for further analysis. The information obtained from the experiment was displayed on the monitor screen for inspection during the experiment.

g. Control the heater off/on timing. Due to the need for the maximum data collecting frequency, the automatic heater control switch was not used in the experiments as it

slowed down the Workbench. The heater off/on time was controlled manually. During one particular experiment, the only instrument needing control was the heater off/on timing. The time needed for the transit time to reach steady state for different flowrate ranges was investigated experimentally (see Section 8.5.1). Fig 8.3.4 shows a heater off/on time chart obtained from the experiments.

Fig 8.3.5 shows an example of the processed result for the transit time obtained by using the experimental procedure listed in a. to g. above. Data were logged onto a floppy diskette and displayed on the terminal screen continually for 10 minutes. The heater off/on timing for the experiments was as follows:

$t_1 = 0 - 60$ s (heater off)
$t_2 = 60 - 180$ s (heater on)
$t_3 = 180 - 360$ s (heater off)
$t_4 = 360 - 480$ s (heater on)
$t_5 = 480 - 600$ s (heater off)

If batteries are used as the power supply source then frequent checking of the voltage and current is essential. This ensures the power input to the heater is constant throughout the measurement.

8.4 Method for Experimental Data Analysis

8.4.1. Mathematical Treatment for the Experimental Data

From the graphical representation of the experimental data shown in Fig 8.3.5, one can see that in order to use the experimental data for comparing or for plotting graphs (transit time vs flowrate), some mathematical manipulation of the data was required. This included:

a. filtering out the readings which were out of range,
b. selecting and averaging the data measured in a time interval of heater off state,

c. selecting and averaging the data measured in a time interval of heater on state,

d. computing the transit time difference as the difference of the values obtained from b. and c.,

e. calculating the average value of reference flowrate.

A computer program was written (in FORTRAN 77) to implement the mathematics listed in a. to e. above. The computation procedure was applied to all the data obtained from the experiments.

8.4.2. Experimental System Error Analysis

The possible error associated with the instruments used for measuring experimental data are investigated in this Section. The sources of error are: accuracy of the timer-counter; time delay due to the associated electronics and the transducers; and accuracy of the multimeters.

For a single mode setting, the timer-counter was capable of measuring transit time accurate to ± 2.0E-3 μs. To reduce the error, about 1000 readings were used for averaging. The error associated with the transit time difference Δt is therefore reduced to about ± 6.5E-5 μs. As the minimum transit time difference of the experimental data was about 0.015 μs, the maximum percentage error would be ± 0.45%.

As the transit time difference was calculated from the difference between two measurements with the same settings, the time delay associated with the electronics and transducers was cancelled out. Throughout a completed set of experiments, the setting of the electronics and the instruments (signal generator, interface electronics and timer-counter) remained unchanged. For this reason, one could assume that the delay caused by the electronics and instruments could be cancelled in the mathematical calculation of transit time difference.

The multimeters used for measuring heater power supply were commercially available products. Although the voltage and current were controlled they could only be accurate to ± 0.01 V and ± 0.01 A, according to manufacturer's documentation.

The two examples below will illustrate the effect of the accuracy of the heater power input measurement on the transit time measurement. With accuracy of ± 0.01 V and ± 0.01 A, for a heater power input of 100.0 Watts (say a voltage of 10.00 V and a current of 10.00 A), the error being about ± 0.2 Watts. For a heater power equal to 100 Watts, the percentage error is about ± 0.2%. Similarly, for a heater power input of 40 Watts (say a voltage of 8.00 V and a current of 5.00 A), then the error of the heater power is about ± 0.13 Watts, the percentage error is about ± 0.33%.

In this Section, the errors associated with the instruments for measuring transit time difference were investigated. A list of the magnitude of the estimated errors were

Timer Counter:	± 0.45%
Heater power:	± 0.2% - 0.33%

hence the maximum percentage error is about ± 0.78%.

Various measurements on the experimental rig are discussed in the subsequent sections. The experimental procedure and the data analysis for all the experiments were identical to that presented in Section 8.3 and Section 8.4.

8.5 Preliminary Experiments

The aim of the preliminary experiments were to perform initial checks on the performance of the clamp-on flowmeter and, more importantly, to gain some idea as to whether the measurement techniques discussed in the previous chapters were feasible in practice.

8.5.1. Heater Power Determinations

The purpose of this experiment was to experimentally investigate suitable values for the heater power. The procedure involved in this experiment is outlined below:

a. apply different powers to the heater (from low to high)
b. test for range of flowrates
c. record the magnitude of Δt at each power and flowrate.

For this application, the accuracy required was ± 2%, Δt equal to 0.01 μs will require an instrument accuracy of 2.0E-4 μs which is what the instruments can provided. The minimum value chosen for Δt is about 0.01 μs. The conclusions drawn from the tests were:

a. It is not possible to use one fixed power input for flowrates from 1 to 80 ml s^{-1}. High power input gives $\Delta t \geq 0.01\ \mu s$ but results in the temperature of the heater being too high at low flowrates. Low power input results in transit time differences which are too small to be measured accurately at high flowrates.

b. The flow range was therefore divided into three subranges:

1	to	20 ml s^{-1}
10	to	40 ml s^{-1}
30	to	80 ml s^{-1}

c. The optimum power inputs P for each subrange of flow were experimentally investigated and are listed below

for	1	to	20 ml s^{-1}	P = 40 Watts

for	10	to	40 ml s^{-1}	P = 100 Watts
for	30	to	80 ml s^{-1}	P = 200 Watts

8.5.2. Preliminary Experiments for Transit Time Measurements

As the heat transfer in vertical and horizontal pipe orientations was expected to be different, preliminary experiments for both vertical and horizontal pipes were performed for a range of flows.

The specifications for the vertical pipe preliminary experiments were as follows:

flow range:	1 ml s^{-1} to 20 ml s^{-1}
power input:	40 Watts
distance:	x = 165 mm

where x was measured from the heater to the centre of the transducers.

Seven different flowrates (see Table 8.5.1a) were selected for testing. Parameters measured for each flowrate were transit time at heater off/on states. Transit time difference and inverse of transit time difference vs flowrate are shown respectively in Fig 8.5.1a and Fig 8.5.1b (see Table 8.5.1a and Table 8.5.1b for numeric values).

In the horizontal pipe preliminary experiments, the flowrate range was extended to 80 ml s^{-1} which was the maximum value specified for the proposed ultrasonic/thermal flowmeter. The power input was increased to 200 Watts to allow more heat to diffuse into the fast moving fluid, so that the transit time difference at high flowrates would increase and could be measured accurately. The experimental specification was

flow range:	10 ml s^{-1} to 80 ml s^{-1}
power input:	200 Watts
distance:	x = 165 mm

where x was measured from the heater to the centre of the transducers.

Eight different flowrates were selected for the experiments (see Table 8.5.2a). Transit time for each flowrate were measured at heater off/on states. Transit time difference and inverse of transit time difference vs flowrate are shown respectively in Fig 8.5.2a and Fig 8.5.2b (see Table 8.5.2a and Table 8.5.2b for numeric values).

The results from both the preliminary experiments showed that transit time difference decreased with increased flowrate as expected (see Chapter 9).

From the experimental results of this section, one could see that the refined rig and its associated instruments (see Chapter 7) could provide measurements over a wide range of flowrates, could control the instruments by computer and could log experimental data automatically, this overcame the drawbacks of the preliminary rig described in Chapter 6.

Further experiments were still needed for accurate evaluation of transit time measurement and measurement repeatability. Subsequent experiments were designed to test these factors and various other aspects of the proposed flowmeter.

8.6. Vertical Pipe Transit Time Measurements

8.6.1 Transit Time Measurement for Flow Range 1 ml s^{-1} to 20 ml s-1

Experiments were undertaken to investigate two aspects of the flowmeter:

a. the variation of transit times with flow rates,
b. the best separation distance between the heater and the transducer.

To form a comparison, all the experiments were carried out at the same power input and using the same heater. Transit times for a range of flows were measured with transducers fixed at different distances, x_i (measured from the heater to the centre of the

transducer), along the pipe.

The specifications for the experiment were:

Flowrate Range:	1 to 20 ml s^{-1}
Power Input:	40 Watts
Distance:	x_1 = 50 mm (Experiment 1),
	x_2 = 100 mm (Experiment 2),
	x_3 = 165 mm (Experiment 3).

Three different experiments were considered. In Experiment 1, the transducers were clamped at a distance of 50 mm from the heater. Six different flowrates were selected for testing, and transit time at heater off/on states were measured for each flowrate. Experiment 2 and Experiment 3 were similar to Experiment 1, except that the transducers were fixed at 100 mm and 165 mm from the heater respectively (see Table 8.6.3a for selected flowrates).

Figs 8.6.1a to 8.6.1f show the examples of the transit time trace obtained at heater Off/On states in Experiment 3.

Explanation of the heater Off/On timing is best made by examining one of the Transit time trace graphs. Take Fig 8.6.1c as an example. In this measurement, the heater was off for 2 minutes, then was on for 3 minutes which enabled the temperature of the pipe wall and the fluid inside the pipe completely to reach steady state. To repeat the measurement, the heater was off for 4 minutes which enabled the heater as well as the pipe wall to reach the inlet fluid temperature. Then the heater was on for 3 minutes. The total time for the experiment was 12 minutes.

Experiment data were logged at a frequency of 10 Hz. Higher frequencies can be set via the Log icon if more data are required for averaging.

Fig 8.6.2a and Fig 8.6.2b show the typical calibration curves for the flowmeter with the transducers fixed at a distance of 165 mm from the heater (combined results from

Experiment 3 in this section and the vertical pipe preliminary experiment described in Section 8.5).

To compare the transit time difference measured at different heater power and transducer separation, the results obtained for the three above experiments were all plotted. The transit time differences and inverse of transit time difference against flowrate are shown in Fig 8.6.3a and Fig 8.6.3b respectively (see Table 8.6.3a and Table 8.6.3b for numeric values).

Fig 8.6.3b shows that the transit time differences for a given flowrate measured at different distances (x) along the pipe are different. Transit time difference was slightly higher when the distance (x) decreased. This was expected since the maximum temperature gradient between the pipe wall and the liquid was near the clamp-on heater centre, leading to the maximum heat transfer and hence a higher temperature. The results from this experiments agreed with the numerical computation results (see Section 4.2 for detail).

In the next Section, transit time measurement for higher flowrates is considered.

8.6.2 Transit Time Difference Measurements for Flow Range 10 to 40 ml s^{-1}

The aim of these experiments was to measure transit time difference for flowrates from 10 to 40 ml s^{-1}. To increase the transit time difference, a higher power was supplied to the heater (about 2.5 times higher compared with the experiments in Section 8.6.1). The heater power was 100 Watts. Below is a list of experimental specification:

Flowrate Range:	10 to 40 ml s^{-1}
Power Input:	100 Watts
Distance x:	165 mm

Six different flowrates (see Table 8.6.4a) were taken within the above flowrate range. Transit times at heater off/on states were measured for each flowrate.

Fig 8.6.4a and Fig 8.6.4b are plots of transit time difference and inverse of transit time difference against flowrates respectively. In Fig 8.6.4b, the slope of the curve $(1/\Delta t \ vs \ Q)$ shows an increase at about Q = 25 ml s^{-1}, which indicates higher heater transfer rates beyond this flow region (see Chapter 9 for explanation).

The results obtained from this Section will be compared with the numerical simulation values (see Chapter 9). The experiments in this section have successfully demonstrated the principle of the flowmeter at higher flowrates in a vertical pipe.

The next experiment was designed to check the repeatability of the flowmeter.

8.6.3 Repeatability of the Flowmeter

Repeatability of measurement is a critical factor for flowmeters. For this proposed flowmeter, factors which could affect repeatability were

a. the transducers being unclamped and reclamped,
b. the heater being unclamped and reclamped,
c. different heater with the same power input being used.

Experiments were designed and carried out to check the effect of unclamping and reclamping of the transducer pair on the transit time measurement, with the same power input, distance x and flowrate specified in Section 8.6.2.

In these experiments, the transducers were unclamped, and the ultrasonic transducer's shoes were removed from the pipe. After the ultrasonic gel had been replaced, the shoes were fixed back at the same location, then the transducers were reclamped on to the pipe. The procedure was repeated between each experimental run.

Transit times were measured and compared with the results obtained in Section 8.6.2. Fig 8.6.5a and Fig 8.6.5b are the plots of the transit time difference and the inverse of

transit time difference against flowrate for the two experiments (refer to Table 8.6.5a and 8.6.5b for numeric values).

The experimental data were treated by non-linear regression using a graphic package [GPAD, Version 1], the deviation of the two sets of experiments ranged from 0 to 8% (see Fig 8.6.5c). Various repeatability checks for the flowmeter will be discussed further in Section 8.7.7.

8.6.4. Heater Power Rating

Experiments were undertaken to investigate scaling with respect to heater power input, this was to check whether it is necessary to recalibrate the meter for operating at different heater powers. The experimental arrangement was

Flowrate Range:	1 to 20 ml s^{-1}
Heater Power Input:	30, 40, 50, 60, 70 Watts
Distance x:	165 mm

Four different flowrates within 1 to 20 ml s^{-1} (see Table 8.6.6) were used for testing. For each flowrate, the transit time was measured at heater off/on states.

Fig 8.6.6a (see Table 8.6.6 for numeric values) shows the plots of transit time difference vs heater input powers for different flowrates. Fig 8.6.6b shows plots of transit time difference vs flowrate for given heater input power. From the scaled results shown in Fig 8.6.6c, it is possible to scale the transit time difference with respect to the heater power (see Section 9.1 for discussion).

Up to this stage, the flowmeter had shown strong promise for vertical pipe flow measurements. The calibration curves obtained from the vertical pipe were not expected to be applicable to the horizontal pipe orientation due to different heat transfer patterns in the two pipe orientations. In the following section, experimental results obtained from the flowmeter in a horizontal pipe orientation are presented.

8.7 Horizontal pipe transit time measurements

The heat transfer in a horizontal pipe is more complex compared with the axi-symmetric heat transfer in the case of a vertical pipe. For this reason, one should expect more complexity in the ultrasonic timing measurements. More experiments were required to cover all the possible effects. Apart from the similar experiments discussed in the vertical pipe measurements, the effects of transducer spacing and transducer angle with respect to the vertical and heater also needed to be considered. The experiments for horizontal pipe to be carried out are listed below:

a. effect of different transducer angle orientation on the transit time difference measurement
b. effect of different transducer heater separation on the transit time difference measurement
c. transit time difference measurement for flowrates from 1 to 40 ml s^{-1} at different heater powers
d. repeatability of the clamp-on flowmeter.

8.7.1 Effect of Transducer Angle

This experiment was to investigate the effect of the angle of the transducer (with respect to the vertical) on the transit time difference measurement.

With a fixed flowrate and heater power input, transit times were measured at various transducers angles (see Fig 4.2.4). The specification is summarized as follows:

Flowrate:	20 ml s^{-1}
Power Input:	100 Watts
Distance x:	165 mm
Transducer Angles:	90°, 45°, and 0° vs vertical

In this experiment, transit times at heater off/on states were measured respectively for transducers clamped at angles shown in Fig 4.2.4.

For any given flowrate, the angle of the transducer with respect to vertical was the only parameter which would affect the transit time difference value in this experiment. For this reason, experiments for one flowrate were sufficient.

The experiments showed that, when the angle of the transducers was at 0° (i.e. when they were vertical), the transit time difference was maximum, this was expected due to the buoyancy effect. The transit time difference was slightly lower when the angle of the transducer was at 45°. The minimum transit time difference was found at 90° (i.e. when they were horizontal), which was about 1/3 of the value measured at 0°.

After deciding the angle of the transducers (i.e. 0°) with respect to vertical, the next variable needing investigation was the distance between the heater and transducers. The experiments in next section were designed to find out the best location along the pipe to clamp the transducers.

8.7.2 Transducer Spacing

The purpose of this Section was to check experimentally where the transducers should be clamped along the pipe so that the transit time difference would be maximized.

The specification for the experiments is listed as follows:

Flowrate Range:	10 to 40 ml s^{-1}
Power Input:	100 Watts
Distance x:	50 - 350 mm

Four different flowrates (see Table 8.7.2) were selected within 10 to 40 ml s^{-1} for testing. For each flowrate, the transit time was measured at heater off/on states, with the transducers clamped at various locations along the pipe (x varying from 50 to 350

mm, with a step of 50 mm). Fig 8.7.2 shows the plots of transit time difference against distance x for various flowrates (see Table 8.7.2 for numeric values), with the same heater power input.

From the graph it is clear that, with a fixed power input to the heater, the value of transit time difference depends on distance x, and for different flowrates the characteristics are not identical. The distance x to clamp the transducers which gives maximum transit time difference was not the same for different flowrates, therefore to find a point on the pipe which would give the maximum transit time difference for all flowrates in a defined flow range was impossible. Based on Fig 8.7.2, the following criteria may be used to determine the distance between the transducers and heater:

a. avoid clamping the transducers at a distance which gives the minimum transit time difference for any flowrate within the flow range (from the graph, x less than 150 mm should be avoided).

b. within the flow range, choose a distance x, at which the maximum transit time difference for the largest flowrate occurs (in the graph shown in Fig 8.7.2, this point is at x equal to 200 mm), because this is where the transit time difference is the smallest and hence the hardest to measure.

Since the magnitude of the transit time for a range of flowrates was considered, using method b. (above) to determine the distance x was sensible. From Fig 8.7.2, x = 200 mm is probably the best choice. At this distance, a maximum peak of transit time difference occurred for both the highest and lowest flowrates.

A distance within the range of 160 to 200 mm appeared to satisfy both criteria moderately. For all the experiments described in the following sections, the transducers were clamped in a vertical direction and at a distance x = 165 mm from the heater. This distance allowed direct comparison with the vertical pipe experiments.

In the next Section, transit time measurement for the flowrate range 1 to 20 ml s^{-1} will be considered.

8.7.3 Transit Time Measurements for Flow Range 1 to 20 ml s^{-1} high heater power input)

The aims of the two separate experiments in this section were firstly to test the proposed flowmeter on a horizontal pipe orientation and secondly to carry out another repeatability check on unclamping and reclamping the transducers at low flowrate. The specification for the experiments was:

Flowrate Range:	1 to 20 ml s^{-1}
Heater Power Input:	100 Watts
Distance x:	165 mm

In the first experiment, seven different flowrates were selected (see Table 8.7.3a, Experiment 1). For each flowrate, transit times at heater off/on states were measured.

In the second experiment, the experimental specification was exactly the same as that used for the first experiments. Seven different flowrates (see Table 8.7.3a, Experiment 2) were selected within 1 to 20 ml s^{-1} for the measurements. For each chosen flowrate, transit time at heater off/on states were measured. After the completion of a measurement, the transducer pair was unclamped and the transducer shoes were removed from the pipe and cleaned. New ultrasonic gel was applied, the transducer shoes were relocated back on the pipe in their original positions and the transducer pair was then reclamped on to the pipe for next measurement.

For comparison, the results obtained from the two set of experiments were plotted. Fig 8.7.3a and Fig 8.7.3b show the transit time difference and inverse of transit time difference against flowrate respectively. After the experimental data were treated by non-linear regression using a graphic package [GPAD, Version 1], the deviation of the two sets of experiments was ranged from 0 to 10% (see Fig 8.7.3c).

In the next Section, transit time measurement results for the flow range 1 to 20 ml s^{-1} with a lower heater power input will be presented. The value of the heater power input

was purposely selected, so that the result obtained could be compared with the data previously obtained from the vertical pipe measurements.

8.7.4. Transit Time Measurements for Flow Range 1 to 20 ml s^{-1}

(Low Heater Power Input)

This experiment was designed for the horizontal pipe transit time measurement at low flowrate. The values for the test were selected so that the results obtained could be compared with the data previously obtained from the vertical pipe measurements. The experimental arrangements were:

Flowrate Range:	1 to 20 ml s^{-1}
Heater Power Input:	40 Watts
Distance x:	165 mm

In this experiment, seven different flowrates (see Table 8.7.4a) were selected for the measurement. Transit times at heater off/on states were measured for each flowrate.

The calibration curves (transit time difference and inverse of transit time difference against flowrate) obtained from the experiments are shown in Fig 8.7.4a and Fig 8.7.4b respectively.

8.7.5 Transit Time Measurements for Flow Range 10 to 40 ml s^{-1}

In the following experiments, transit times at heater off/on states were measured for a range of flowrates. The specification for the experiments was:

Flowrate Range:	10 to 40 ml s^{-1}
Power Input:	100 Watts
Distance x:	165 mm

The parameters were purposely chosen, so that the result could be compared with the data obtained from the vertical pipe experiments described in Section 8.6.3.

Six different flowrates (see Table 8.7.5a) were selected within 10 to 40 ml s^{-1}. For each flowrate transit times were measured at heater off/on states.

Fig 8.7.5a and Fig 8.7.5b show the graphs for transit time difference and inverse of transit time difference vs flowrate respectively. As in the case of the vertical pipes, the slope of the curves changes at higher flowrate (refer to the discussion in Section 9.3).

The experiments described in the following Section are to measure transit time for the same flow range but with the higher heater power input. The aim was to investigate the relation between the heater input power and transit time difference.

8.7.6 Transit Time Measurements for Flow Range 10 to 40 ml s^{-1} (High Heater Power Input)

This experiment is almost identical to the one in Section 8.7.5, except that the power input to the heater was 200 Watts. With the same flowrate, it was expected that the transit time difference could increase with increased heater power input. Fig 8.7.6a demonstrates the combined plot of results obtained from experiments in Section 8.7.5 and this Section (see Table 8.7.6a. It is clear that the transit time difference was increasing with the increased heater power supply, but not linearly (refer to Section 9.4 for scaling of heater power input discussion).

Next Section concentrates on measurement repeatability of the proposed flowmeter. Experimental work on the factors such as unclamping and reclamping the transducers, unclamping and reclamping the heater, and using different heaters will be discussed.

8.7.7 Repeatability of the Flowmeter

Two experiments were performed to check the repeatability of the flowmeter. The experimental arrangement was:

Flowrate Range:	10 to 40 ml s^{-1}
Heater Power Input:	200 Watts
Distance x:	165 mm

The first experiment was to check the effect of transducer clamping. For each selected flowrate (see Table 8.7.7a, Experiment 1 for flowrate values), transit times were measured at heater off/on states. After each measurement was completed, the transducer pair was unclamped and the transducer shoes were removed from the pipe. New ultrasonic gel was applied to both the transducers and the transducer shoes. The transducer shoes were then located back on the pipe in their original locations and the transducer pair was reclamped onto the pipe for next measurement.

The second experiment was to investigate the effects of the heater on measurement repeatability. The experiment not only tested the effect of unclamping and reclamping the heater, but also checked the effect of using different heaters. In this experiment, a different heater from that used in the last two experiments but constructed in the same way as previously with the same power input was used. The heater was unclamped then reclamped onto the pipe after the completion of each measurement. For each selected flowrate (see Table 8.7.7a, Experiment 2), transit times were measured at heater off/on states.

To compare the results, the measurement values from experiments described in Section 8.7.6 and the two set of experiments in this Section were plotted. Fig 8.7.7a and Fig 8.7.7b show the plots of transit time difference and inverse of the transit time difference against flowrate for these experiments (see Table 8.7.7a and Table 8.7.7b for numeric values).

After the experimental data were treated by non-linear regression [GPAD, Version 1], deviations between the three sets of experiments were estimated. The deviation between Experiment 1 (solid line) and Experiment 2 (dashed line) was ranged from about 0 to

11%. The deviation between Experiment 1 and Experiment 3 (dotted line) was ranged from 0 to 15%, which was slightly higher because the heaters used in this project were hand made, and hence the two heaters might be slightly different (i.e. wire separation, electrical insulating layer thickness, and thermal insulating layer thickness).

8.7.8. Heater Power Rating

Experiments were undertaken to investigate scaling with respect to heater power input. The experimental arrangement was

Flowrate Range:	5 to 22 ml s^{-1}
Heater Power Input:	30, 40, 50, 60, 70 Watts
Distance x:	165 mm

Four different flowrates within 5 to 22 ml s^{-1} (see Table 8.7.8) were selected for testing. For each flowrate, the transit time was measured at heater off/on states, the heater input power varied from 30 to 70 Watts, with a step of 10 Watts.

Fig 8.7.8a (see Table 8.7.8 for numeric values) shows the plot of transit time difference vs heater input power for different flowrates. Fig 8.7.8b shows plots of transit time difference vs flowrates for given heater input power. As could be seen, the transit time difference did not change linearly with heater input power increase. See Section 9.4. for discussion.

8.8. Conclusions

In this Chapter, details of the experimental procedure and mathematical analysis of the experimental data were discussed. The proposed flowmeter has been experimentally tested on both vertical and horizontal pipe orientations. A Large number of experiments were designed and performed to test many aspects of the proposed flowmeter. The experiments included: calibration of the meter on both vertical and horizontal pipe

orientation; calibration of the flowmeter for flow range 1 to 80 ml s^{-1}; calibration of the flowmeter for different power inputs (40 to 200 Watts); tests of the repeatability of the flowmeter (unclamping and reclamping the transducers, unclamping and reclamping the heater, and using different heaters); and variation in heater power rating of the flowmeter.

The results from the experiments indicate strongly that the prototype flowmeter ultrasonic/thermal flowmeter could be used for low flowrate measurement applications: the measuring flowrate range could be as low as 0.5 ml s^{-1}, and as high as 80 ml s^{-1}; the measurement repeatability in case of unclamping and reclamping the transducers was ranged from 0 to 10%; the measurement repeatability in case of unclamping and reclamping the heater as well as using different heaters with the same power input ranged from 0 to 15%. Better results could be obtained if high precision transducer clamps and heaters were used for the experiments.

In the next Chapter, further detailed analysis of the experimental results and comparison of experimental data with computer simulation data will be considered.

9. COMPARISON AND ANALYSIS OF EXPERIMENTAL DATA

9.1. Introduction

The results obtained from the experimental work in Chapter 8 show that it is feasible to use the proposed clamp-on flowmeter to measure a range of flowrates. Successful application of the flowmeter for measuring flowrates ranging from 0.5 ml s^{-1} to 80 ml s^{-1} has been demonstrated in the various experiments of the previous Chapter.

The work of this Chapter is to compare the experimental results with computer simulation results, analyze the experimental data, and discuss the option of power rating.

9.2. Comparison of Experimental Data with Computer Simulation Results

As only limited computer simulation results were available, only the vertical pipe experimental results for flowrates ranged from 1 to 20 ml s^{-1} with a heater power of 40 Watts were selected for comparison with the computed simulation results. The two sets of data used for the comparison were experimental results obtained from the experiments described in Section 8.5.2 (experiment 1) and Section 8.6.1 (experiment 3).

The theoretical values were computed using FIDAP. Appendix A.4.1 gives an interface input file for these computation. The parameters such as pipe diameter, heater power input and heater dimensions, separation distance between the heater and transducers were identical to specification of the experiments, which are listed below:

fluid	water	
pipe length	500	mm
pipe diameter	15	mm
pipe wall thickness	0.75	mm
heater length	40	mm

heater power	40	Watts
heater-transducer separation (X)	165	mm

The properties of clean water and copper pipe were taken at a reference temperature of 10 °C and are as follows [Kaye and Laby, 1973]:

For water:

viscosity	1.3037E-3	Ns m^{-2}
density	999.7	kg m^{-3}
specific heat	4191.9	J kg^{-1} $°C^{-1}$
thermal conductivity	0.561	W m^{-1} $°C^{-1}$
volume expansion coefficient	2.1E-4	

For copper pipe:

density	8933	kg m^{-3}
specific heat	377	J kg^{-1} $°C^{-1}$
heat conductivity	403	W m^{-1} $°C^{-1}$

The above dimensional parameters were non-dimensionalised by the procedure given in Section 3.3.2.3. To form a comparison, the flowrates selected for the computation were equal to the flowrates used for the experiments.

The results of the comparison are shown in Fig 9.2.1a (inverse of transit time difference vs flowrate), in the graph, the solid curve gives the computation results and the points represented by the triangles and circles are the experimental data for the two set of experiments respectively. As can be seen from the graphs (refer to Table 9.2.1a for numeric values), the experimental data were close to the computer prediction at higher flowrates.

The comparison results is shown in greater detail in the percentage error plots given in Fig 9.2.1b (graph for computed values and experiment 2 data set, refer to Table 9.2.1b

for numeric values). The percentage difference between the computed values and the experiment data, err (%), is defined by

$$err(\%) = \frac{\frac{1}{\Delta t} - \frac{1}{\Delta t_{comp}}}{\frac{1}{\Delta t}} \times 100$$

From the plot, it can been seen that when flowrate is low the experimental data is less close to the computed values compared with higher flowrates. One of the important factors that can be used to explain the difference between the computed values and experimental data at low flowrate was that the computer model did not include the effect of thermal expansion of the pipe. As the analysis result shown in Section 4.3.2, the percentage error due to thermal expansion of the pipe wall at low flowrates could be as high as 5.1% and would decrease with increased flowrates. If the thermal expansion of the pipe wall was included in the computed data, the magnitude of transit time difference would decreases, giving a larger $1/\Delta t$, resulting in a smaller difference between the computed values and experimental data at low flowrates.

Another factor which could contribute the higher $1/\Delta t$ at low flowrates was the heat loss due to radiation. From Fig 3.3.7a one can see that when the flowrates decreases, the pipe wall temperature near the heater increases, resulting in a larger quantity of heat loss by radiation and hence a lower transit time difference (higher $1/\Delta t$), the estimated error due to radiation heat loss was about 0.32% (see Section 4.3.2 for detail).

Besides, the experimental data used for averaging were not steady state data (see Fig 9.2.2). If the heater on/off timing for the low flowrate experiment had been extended

to the stage at which steady state conditions were reached, the magnitude of Δt would increase, resulting in a smaller $1/\Delta t$, then the difference between the computed values and experimental data would be reduced (see Fig 9.2.1a).

The full scale difference between the computed values and experimental data is shown in Fig 9.2.3. The full scale difference, err_f (%), is defined by

$$err_f(\%) = \frac{\frac{1}{\Delta t} - \frac{1}{\Delta t_{comp}}}{(\frac{1}{\Delta t})_{Max}} \times 100$$

where $(\frac{1}{\Delta t})_{Max}$ is the maximum of $1/\Delta t$. The full scale difference between the computed values and experimental data for flowrate ranged from 1 to 20 ml s^{-1} was about -2.0% to 4.0%.

In this Section, comparison of the experimental data with computer simulation results for vertical pipe for flowrates in the range 1 to 20 ml s^{-1} (laminar flow) have been discussed. In the next Section, analysis of experimental results will be given.

9.3. Discussion of Experimental Results

In this section, results obtained from the experiments will be discussed. As different phenomena occurred in horizontal and vertical pipe orientations, each case is to be considered separately. The experimental data analysis work includes

a. analysis of vertical pipe experimental data,

b. analysis of horizontal pipe experimental data,

c. comparison of the vertical and horizontal pipe orientation experimental data.

9.3.1. Discussion of Vertical Pipe Experimental Results

The data sets used for analysis were the results of the experiment given section 8.5.2 and experiment 3 in Section 8.6.1 (transit time measurement for flowrates ranged from 1 to 20 ml s^{-1}), and experimental data in Section 8.6.2 (transit time measurement for flowrate ranged from 10 to 40 ml s^{-1}).

Fig 9.3.1a shows the plot of transit time difference against flowrate for flowrates ranging from 1 to 20 ml s^{-1} (refer to Tables 9.3.1a for numeric values). As can be seen, the transit time difference decreases as flowrate increases, this effect is expected since the temperature difference for low flowrates is high so the speed of sound is high, which results in a larger difference in transit time difference and vice versa.

Fig 9.3.1b shows a plot of the inverse of transit time difference against flowrate (see Table 9.3.1b for numeric values), one can observe that for higher flowrates the gradient of $1/\Delta t$ against flowrate curve decreases. This drop in gradient begins well below any possible onset of turbulence (even allowing for the reduced viscosity caused by heating the liquid) and appears to be due to the thermal gradient across the pipe in the heater region. From [Baker, 1989] for an ideal thermal flowmeter the flowrate Q is related to the power input P and the temperature rise ΔT_L (which is directly related to Δt) by

$$\frac{1}{\Delta T_L} = \frac{C_P}{P_I} Q \qquad (9.3.1)$$

where ΔT_L is the average temperature rise in the liquid flow, C_p is the specific heat at constant pressure, P_I is the effective heat power transferred from the heater to liquid and Q is the flowrate. Furthermore, the rate of transfer of thermal energy into the liquid is proportional to the radial temperature gradient. Fig 3.3.7a and 3.3.7b show a series of temperature profiles across the pipe for various flowrates at the heater midpoint and a distance X = 165 mm from the heater in the down stream direction respectively. These were computed using FIDAP. As can be seen from the graphs, the temperature gradient increases with flowrate. Thus effective heat power transferred from the heater to the liquid (rather than lost by other means) increases. Referring to Equation (9.3.1) it can be seen that this reduces the gradient of the $1/\Delta T_L$ (and hence $1/\Delta t$) against flowrate curve. From the Fig 3.3.7a and Fig 3.3.7b the effect can be seen to diminish at higher flowrates.

Fig 9.3.2 shows the inverse time difference against flowrate plot for a higher flowrate range. From the plot, one can observe that a different phenomenon occurs at higher flowrates. The gradient of the curve increases significantly at a flowrate of about 20 ml s^{-1}. As the flowrate increases a different effect is believed to become dominant. The flow will start to become turbulent (20 ml s^{-1} correspond to a Reynolds number of approximately 1700 - 2000) and there will then be a transitional range of flows during which there is increasing mixing due to turbulence. This will improve the distribution of temperature across the liquid in the pipe so that the liquid will become more efficient at carrying the thermal energy again improving the heat transfer per unit liquid flowrate. Finally, when the flow is fully turbulent no further improvement in turbulent mixing occurs with increasing flowrate and so the slope of the curve in Fig 9.3.2 becomes constant as the efficiency of the system ceases to improve.

In this section, vertical pipe orientation experimental data have been analyzed for both high and low flow ranges (1 - 20 ml s^{-1} and 10 - 40 ml s^{-1}). In next Section, experimental results for horizontal pipe orientation will be examined.

9.3.2. Horizontal Pipe Experimental Results Discussion

The two sets of data used for analysis are experimental results described in Section 8.7.4 (transit times measurement for flowrates ranging from 1 to 20 ml s^{-1}) and Section 8.7.5 (transit times measurement for flowrate ranged from 10 to 40 ml s^{-1}).

Fig 9.3.3a shows the plot for transit time difference against flowrate for flowrates ranging from 1 to 20 ml s^{-1} (refer to Table 9.3.3 for numeric values). From the curve, one can see that the transit time difference decreases with increasing flowrates as explained in Section 9.3.1.

Fig 9.3.3b shows the plot for inverse of transit time difference against flowrate for flowrates ranging from 1 to 20 ml s^{-1} for horizontal and vertical pipe orientations (the triangles and the squares represent the results for horizontal and vertical pipe data respectively). In the vertical pipe case, the gradient of the curve of the inverse of transit time difference against flowrate appears to decrease with increased flowrates (see Section 9.3.1).

The transit time difference for horizontal pipe is higher (smaller $1/\Delta t$) compared with the vertical pipe data measured at the same flowrate. It is believed that in the case of a horizontal pipe a different phenomenon causes efficiency to be improved at low flows. Visualisation using a dye stream (see Section 6.4.2 for experimental detail) has shown that, even for very low flowrates, the flow regime is not laminar. The density changes induced in the liquid by the heater result in thermal convection of the liquid which causes a considerable amount of mixing. The temperature distribution is therefore expected to be much more even across the pipe. The liquid in the centre of the pipe will still be flowing faster than that at the edges and so will be more efficient at carrying the heat. Thus the meter will have a higher Δt (lower $1/\Delta t$) than the equivalent vertical pipe.

The experimental results for horizontal pipes and vertical pipes at higher flowrates with a heater power of 100W are shown graphically in Fig 9.3.4. Again, the triangles and the squares represent the results for horizontal and vertical pipe data respectively.

As the flowrate increases turbulent mixing will occur in the horizontal pipe in the same way as in the vertical pipe and will become more significant. Finally the turbulence levels will saturate preventing any further improvement in efficiency and the gradient of the Δt against flowrate curve will return to a steeper value which would be expected to be similar to the final gradient of the curve for the vertical meter.

9.4. Heater Power Scaling

In this section, scaling with respect to heater power will be examined. Fig 9.4.1 shows the experimental results for heater powers equal to 40 Watts and 100 Watts. The points represented by triangles and stars are the scaled values for vertical and horizontal pipe, which were obtained by dividing the transit time difference measured at heater power equal to 100 Watts by a factor of 2.5. From the graphs, one can observe that it might be possible to scale with respect to heater input power for vertical pipe measurements. For horizontal pipe results, the failure of the scaling with respect to heater power is believed to be due to greater convection mixing caused by high power inputs. This results in a much improved heat transfer within the liquid, leading to an increased Δt and hence a decreased $1/\Delta t$. The absence of such a significant variation in the case of vertical pipe orientation measurement serves to confirm this theory.

To confirm the above theory, additional data for transit time difference measured at different power inputs were analyzed and presented in the following graphs.

Fig 9.4.2a shows the vertical pipe experimental results (refer to Table 9.4.2a for numeric values) for heater power of 60 Watts and 40 Watts. The diamonds represent

the scaled value (60 W scaled to 40 W, i.e. times divided by 1.5) of the experimental data with 60 Watts heater power input. The scaled points overlap with the experimental data measured at 40 Watts (the difference ranged from 0% to 5.8%, and the averaged difference was about 2.0%). The transit time difference therefore seems to be linearly dependent on heater power input. The results strongly suggests that it might be possible to scale with respect to heater power for vertical pipe orientation transit time measurements.

To confirm the above hypothesis, experimental results measured at 70, 60 and 40 Watts were used for scaling. The scaled results presented in Fig 9.4.2b (see Table 9.4.2b for numeric values) are the results for measurements carried out at three different heater powers (70, 60 and 40 Watts), the diamonds and solid squares represent the values for 70 W scaled to 60 W, and 70 W scaled to 40 W respectively. The scaled values overlapped with the experimental results measured at equivalent heater powers (the difference ranged from 0% to 4.4%, and the averaged difference was about 2.0%). This confirmed that it might be possible to scale with respect to heater power for vertical pipe orientation transit time measurements and the convective effect presented in the horizontal pipe seems absent in the vertical pipe.

The effect of convective mixing presented in horizontal pipe measurement could be seen clearly in Fig 9.4.3. The solid squares represent the scaled value of the experimental data with 70 Watts heater power input (divided by 1.4). The diamonds represent the scaled value of the experimental data with 70 Watts heater power input (divided by 1.167). The scaled values for the transit time difference are higher than the experimental results obtained with 50 and 60 Watt respectively due to improved heat transfer by greater convective mixing at higher heater power input, as confirmed by the experimental results presented in Fig 9.4.1.

9.5. Discussion

In this section, comparison of vertical pipe orientation experimental data with FIDAP simulation results for flows ranging from 1 to 20 ml s^{-1} have been presented. The

maximum difference between the computer prediction and experimental results was about 2.5% for higher flowrates, the maximum difference is slightly larger (10.0%) at lower flowrates due to the reasons given in Section 9.2. The full scale difference of the flowmeter was about -2% to 4%.

The phenomena for both vertical and horizontal experimental results were discussed in detail. The transit time difference for vertical pipe is lower (higher $1/\Delta t$) compared with that for horizontal pipe data measured at the same flowrates. This is due to convective effect mixing present in the horizontal pipe orientation measurements.

The convective effect mixing presents in the horizontal pipe orientation measurement data which results in the failure in scaling with respect to heater power. For vertical pipe measurements, the results confirmed that, no convection mixing occurs and scaling with respect to heater power was therefore possible.

10. CONCLUSION AND PROPOSALS FOR FURTHER WORK

10.1. Introduction

In this Chapter, a summary of both the technical and managerial aspects of the work described in the thesis is given together with the main conclusions. This is followed by a section in which possible future development and testing of the clamp-on flowmeter are discussed.

10.2. Conclusions on technical aspects of the flowmeter

A clamp-on ultrasonic flowmeter has been developed, which could measure a wide range of flowrates in small diameter pipes. The literature review conducted in Chapter 1 showed that, although the development of a fair number of clamp-on ultrasonic flowmeters have been reported, none of these seems applicable to the specification of this work: clamp-on measurement of single phase liquid with flowrates ranged from 0.5 ml s^{-1} to 5.6 x 10^3 ml s^{-1} in a 15 mm diameter pipe. The accuracy requirement was better than 5% at low flowrates and within 2% for high flowrates.

The flowmeter developed in this work uses a combined ultrasonic/thermal technique for low flowrate measurement and a multiple reflection transit-time ultrasonic technique for higher flowrate measurement. A cross check between the two techniques is possible for a defined range of flowrates.

To study the feasibility of the proposed measurement techniques and to obtain various important parameters for designing the flowmeter, mathematical and computer models for heat transfer and variation of speed of sound with temperature were developed based on a physical model of the flowmeter. Because heat transfer in a vertical and a horizontal pipe are different, two separate models were developed. The equations governing heat transfer in the physical models were derived. The fluid motion equations and the coupled heat transfer equations obtained were too complex and impossible to solve analytically. A finite difference numerical approach together with finite element

computer software (FIDAP) was therefore used to solve the mathematical equations. The mathematical predictions shown that the ultrasonic/thermal technique could be used for low flowrate measurement and the multiple reflection technique for higher flowrate measurement.

Theoretical aspects of both the ultrasonic/thermal and the multiple reflection technique has been discussed in detail. Mathematical analysis was used to determine the important parameters for designing the flowmeter (such as the heater power, heater-transducer separation, heater On/Off timing and dimensions for clamping of the transducer pairs) and the sources of error which were likely to affect the performance of the flowmeter. The results from both theory and the experiments show that: the optimum heater power in the low flowrate range was 40 Watts and in the higher flowrate range was 100 Watts; the heating timing depended on flowrates, a longer heating time was required for low flowrate measurement and vice versa; and the optimum place for clamping of the transducers was within 150 to 200 mm measured from the centre of the heater.

The source of errors identified as significant were expansion of pipe wall due to temperature rise, inaccuracy of the instruments for transit time measurement and variation of the temperature of the incoming flows. The error due to thermal expansion of the pipe could be as high as 5%. The suggested compensation method for pipe wall expansion was to monitor the pipe wall temperature using temperature sensors. To reduced the errors caused by the measurement instruments a large set of data was used for averaging. The incoming flow temperature variation compensation could be achieved by using another pair of direct angled beam transducers to monitor the upstream transit time changes. The errors caused by inaccuracy of the power supply, heat loss due to radiation and beam shift due to flow were also analyzed. The results were shown, effects to be small and could be ignored.

Prior to the design and construct of the flowmeter, the required components for the clamp-on flowmeter were examined. The essential elements for the flowmeter are, a heater, a pair of clamp-on direct angled beam transducers, a pair of clamp-on angled beam transducers, DC power supply, ultrasonic time measurement electronics and a data

acquisition unit. The operating procedure and principle of flowrate measurement using the proposed instruments were discussed.

The design and construction of various elements for the clamp-on flowmeter were given. Suitable commercially available products and materials from several companies were searched for and identified for construction of the heater and the clamp-on transducers. Constantant wire and various electrically insulating materials were identified as suitable for construction of the heating element. Perspex was used for construction of heater and transducer clamps due to its electrically insulating property and lightness in weight. High frequency transducers were selected to eliminate the effect of spread of ultrasound. A simple experimental system was set up to test the performance of the proposed flowmeter. The experiment results agreed with the mathematical predictions. Even with the limitations of the test facility, the preliminary experiments showed encouraging results.

The detail design and construction of a refined test facility (hydraulic system and advanced electronics and computer controls) for precise testing of the flowmeter were discussed. This flowrig could provide a large range of flowrates and the gravity tank ensured constant inflow fluid temperature. The flowrig was installed with reference flowmeters and temperature sensors for reference flowrate and in coming flow temperature measurements. The selection and usage of each instrument was summarized. Application of the instruments for various measurements (temperature, flowrate, heater control and transit time) were discussed. The required components (temperature sensor, reference flow meters, and conventional scale-stopwatch system) which were needed as reference elements for the experiments were refined and calibrated.

The proposed flowmeter was experimentally tested on both the vertical and horizontal pipe orientations. Experiments were designed and performed to test many aspects of the proposed ultrasonic/thermal flowmeter. The experiments included: calibration of the meter on both vertical and horizontal pipe orientation; calibration of the flowmeter for the flow range 0.5 to 80 ml s^{-1}; calibration of the flowmeter for different power inputs (40 to 200 watts); tests of the repeatability of the flowmeter for unclamping and

reclamping the transducers, unclamping and reclamping the heater and using different heaters; and heater power rating analysis for the flowmeter.

The results from the experiments indicated strongly that the ultrasonic/thermal technique could be used for low flowrate measurement applications and that: the measured flowrate range could be as low as 0.5 ml s^{-1}, and as high as 80 ml s^{-1}; the measurement repeatability when unclamping and reclamping the transducers and the heaters was about 2.5%; the measurement repeatability when using a different heater with the same power input was approximate 5.6%. With the optimum calibration conditions, better result could be obtained.

Comparison of vertical pipe orientation experimental data with FIDAP simulation results for the flow range 1 to 20 ml s^{-1} were presented. The full scale difference between the computed data and experimental results of the flowmeter was in the range -2.0% to +4.0%.

The phenomena behind both the vertical and horizontal experimental results were discussed in detail. It was confirmed by the experimental results that convective mixing present in horizontal pipe orientation measurements results in a higher heat transfer rate for higher heater power and hence failure in scaling with respect to heater power. For vertical pipe measurements, the results confirmed that, as no convection mixing occurs across the pipe, scaling with respect to heater power was therefore possible.

10.3. Conclusion on The Management of The Research

In Chapter 2 management of the author's work for developing the flowmeter is considered. This starts with a study of the planning of the Ph.D. using the guide lines from the project management, project control and work breakdown structures. Its has been revealed how the original plan for the Ph.D. altered as the work proceeded because of new information obtained from both the theoretical and experimental work. The second part on the work on management of the Ph.D. was a benefit analysis. This was to investigate the benefits that could be gained by the water company by using the

clamp-on flowmeter as a calibrator for calibrating domestic flowmeters and the benefit of installing the clamp-on flowmeter in properties instead of the domestic intrusive flowmeters. The analysis showed that using the clamp-on flowmeter instead of the intrusive domestic flowmeter would save installation and maintenance costs.

10.4.Proposals for Further Research

In this Section, proposals for further research on the proposed clamp-on flowmeter are given.

Computation work for horizontal pipe orientation

Although the mathematical and computer models have been developed for both horizontal and vertical pipe orientations (Appendix A4), due to limitations on computer facilities, computational data were only obtained for the vertical orientation. These agreed well with the experimental results. Computational work is therefore needed to obtain numerical data for the horizontal pipe orientation, which can then be compared with the horizontal pipe experimental results. The 3-D numerical model given in Appendix A4 has been tested for a coarse mesh and show to work successfully (see Fig 3.3.4 and Fig 3.3.9). This file could be used for obtaining the horizontal pipe data.

Experimental work for multiple reflection technique

The proposed flowmeter is a combination of an ultrasonic/thermal technique and an ultrasonic multiple reflection technique. Although a large number of experimental measurements of the ultrasonic/thermal technique were carried out, only limited tests were carried out on the ultrasonic multiple reflection technique which is applicable for flow velocities ≥ 0.55 m s^{-1}, and for pipe diameters ≥ 15 mm. Further tests are required to confirm the multiple reflection theory described in Section 4.4.

Extending the results of this thesis

The experiment procedure described in chapter 8 could be applied directly to obtain results for further experimental work. The recommended tests are: Test of the flowmeter on pipes with different diameters. The purpose of these experiments is to obtain the upper limit of the flowmeter; Test of the flowmeter on pipes of different materials. Theoretically, the flowmeter should work on metal pipe of high thermal conductivity. Experiments have been performed successfully for copper pipe. Testing of the flowmeter on other metal pipes is needed to confirm this theory; Test of the flowmeter with different heat source (microwave) on non-metallic pipes. The heat source used so far was based on the electrical heating of resistance wire clamped outside the pipe wall. This method could not be applied to non-metallic pipes due to their low thermal conductivity. A microwave heat source is recommended as suitable in this application; Test of the flowmeter with different fluids. In principle,The flowmeter should be able to measure flow of any type of single phase fluid with relatively high thermal diffusivity. The flowmeter has been tested successfully for clean water. More Experiments are needed to shown the wide application possibilities of the flowmeter.

CRANFIELD UNIVERSITY

MASA LAW

The Development and Modelling of a Novel Clamp-on Ultrasonic-Thermal and Ultrasonic Multiple Reflection Flowmeter for Liquid Applications

(Volume 2)

DEPARTMENT OF FLUID ENGINEERING & INSTRUMENTATION

Ph.D. THESIS

CRANFIELD UNIVERSITY

DEPARTMENT OF FLUID ENGINEERING AND INSTRUMENTATION

Ph.D. THESIS (TOTAL TECHNOLOGY)

Academic Year 1993-94

MASA LAW

The Development and Modelling of a Novel Clamp-on Ultrasonic-Thermal and Ultrasonic Multiple Reflection Flowmeter for Liquid Applications

(Volume 2)

Supervisors: Professor M. L. Sanderson
Dr. A. R. Guilbert
G. Ward

February 1994

FIGURES

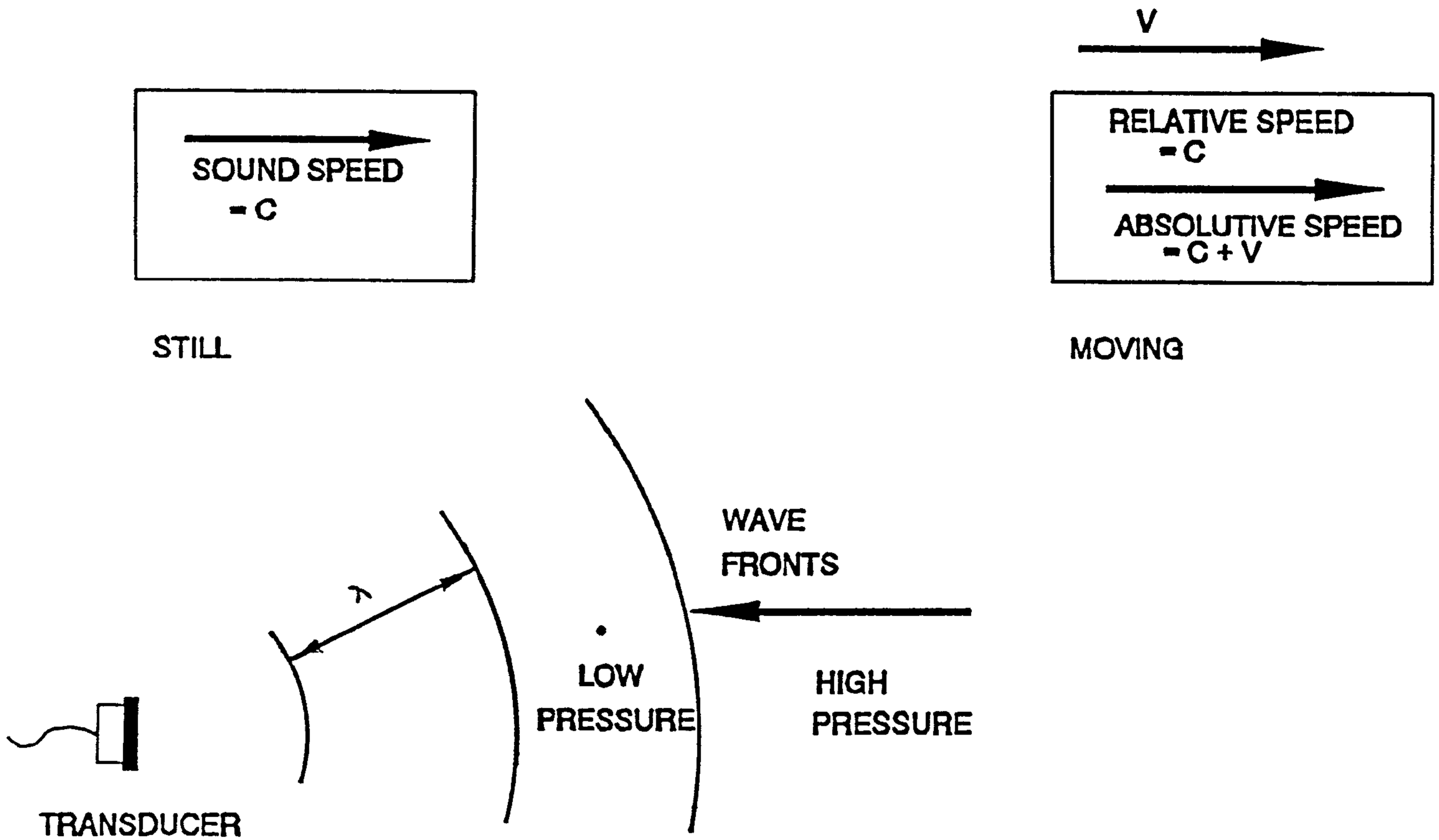

Fig. 1.2.1. Ultrasonic Waves

Fig. 1.2.2. Longitudinal and Transverse (Shear) Waves in a Solid

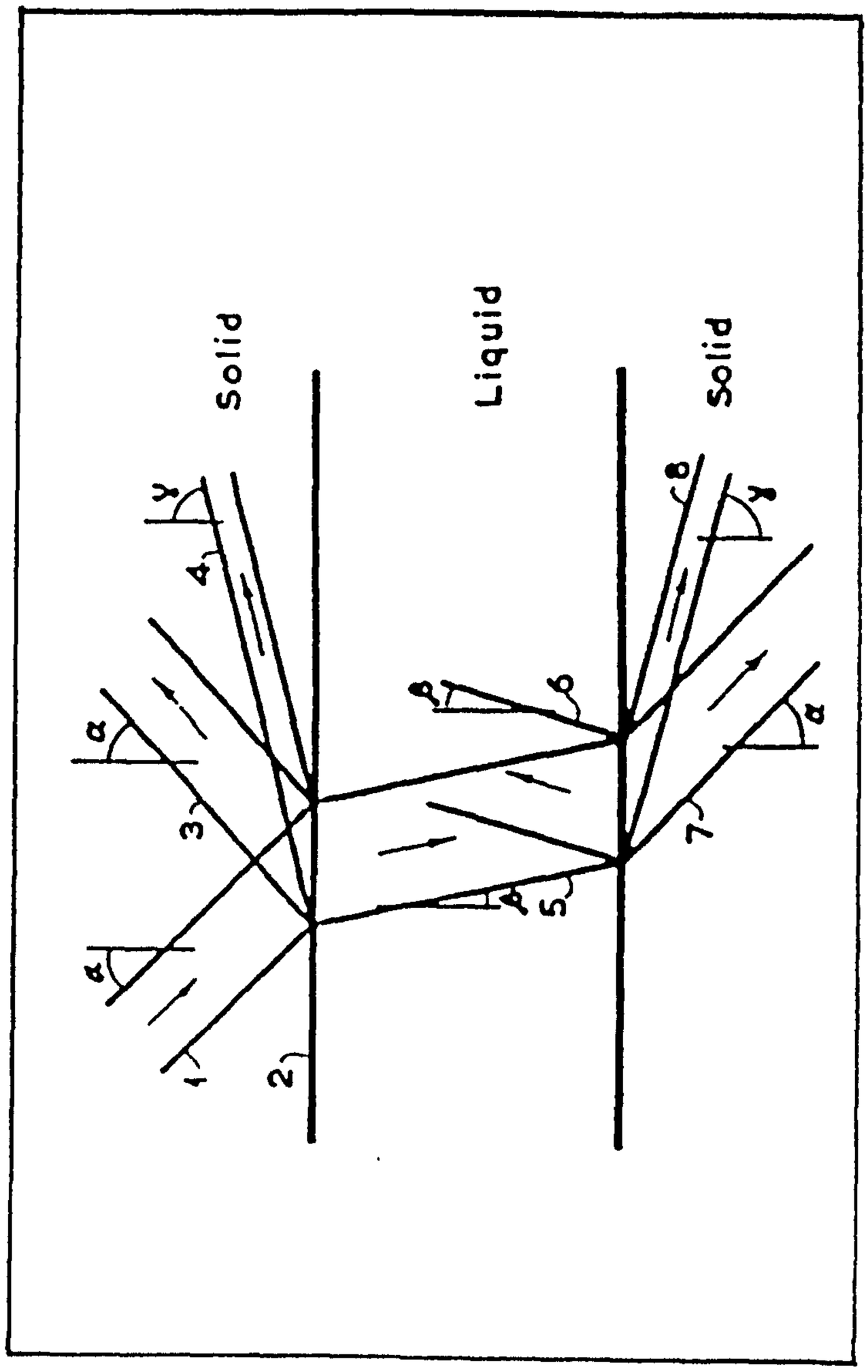

Fig. 1.2.3. The Behaviour of Ultrasonic Waves at an Interface

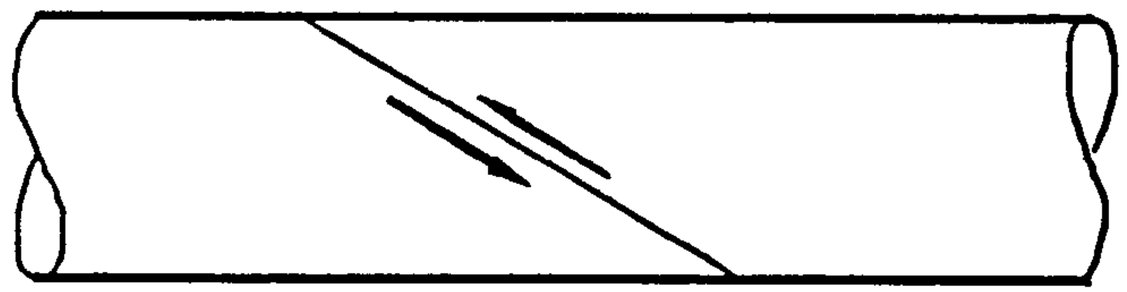

Time of Flight

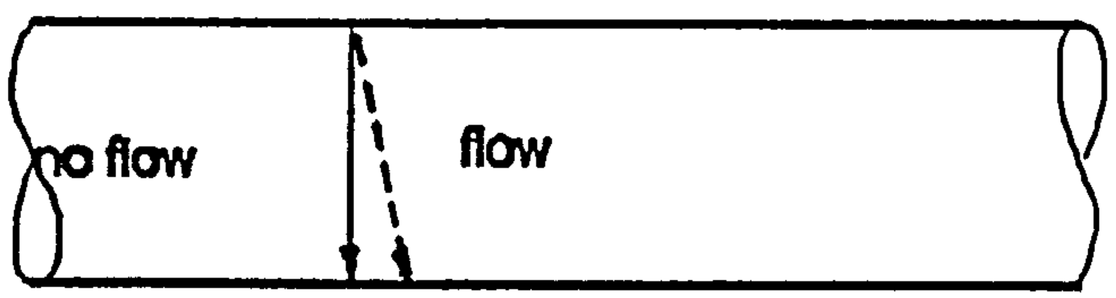

Beam Shifting

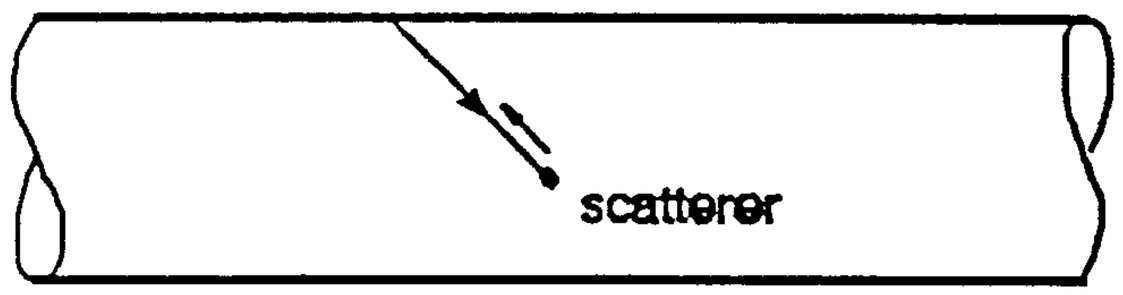

Doppler

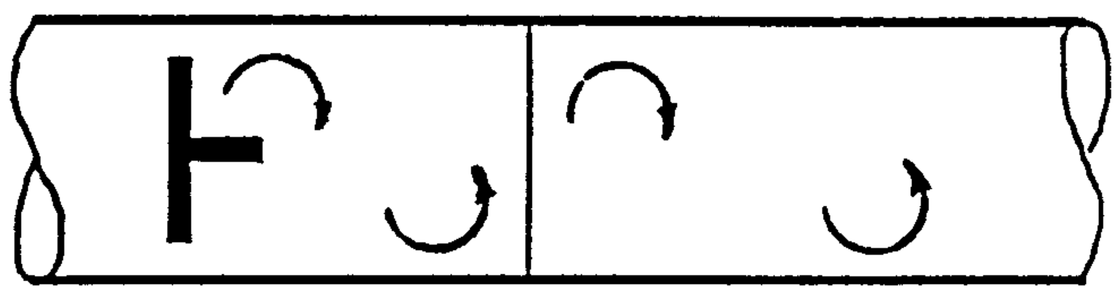

Vortex Shedding Detection

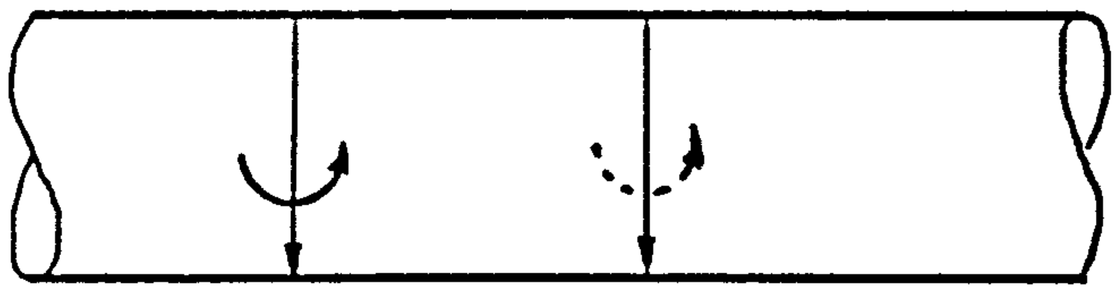

Correlation

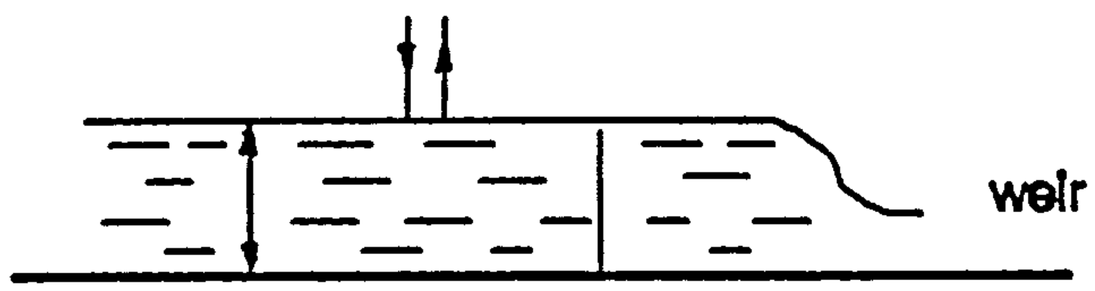

Height Measurement

Fig. 1.2.4. Flow Measurement Using ultrasonic Techniques

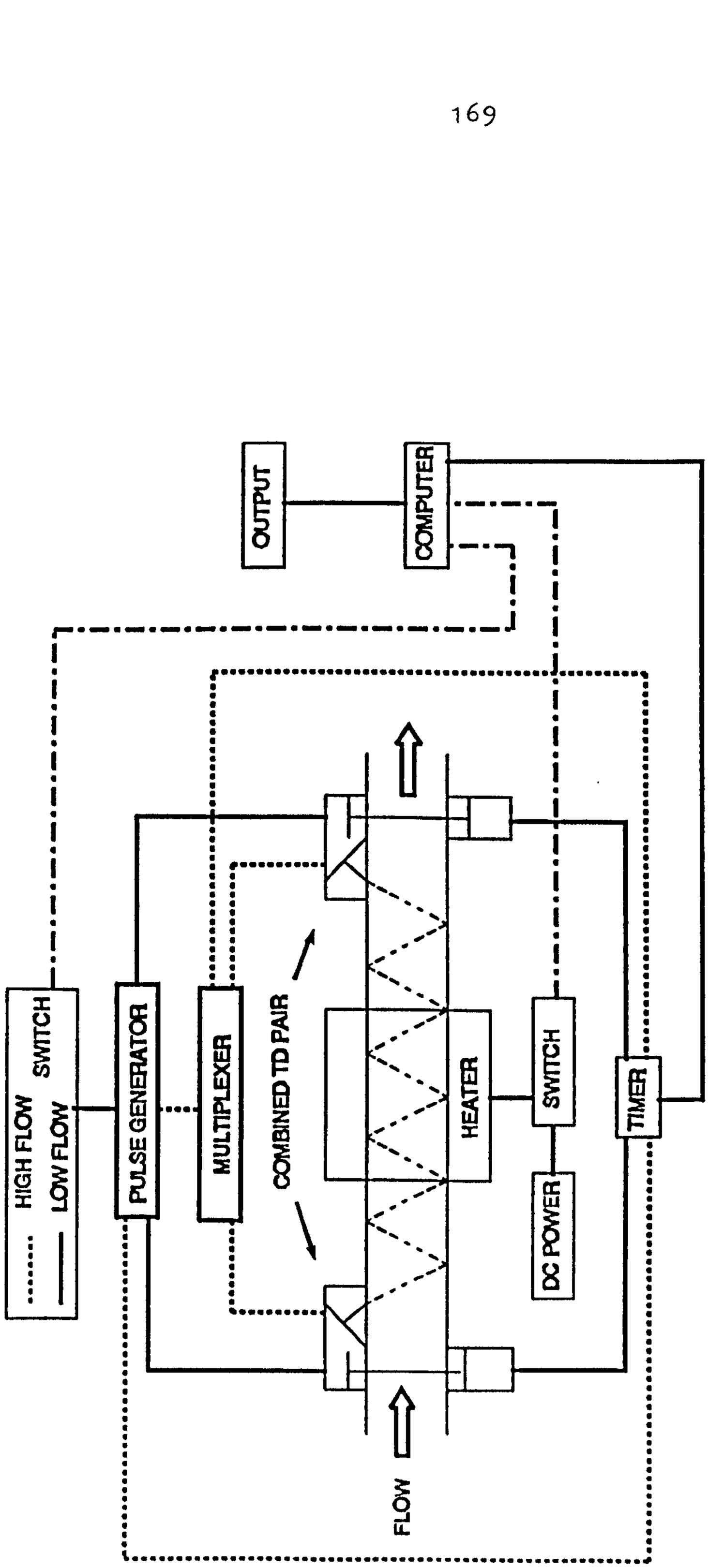

Fig. 1.3.1. Proposed clamp-on Ultrasonic Flowmeter for Small Diameter Pipe

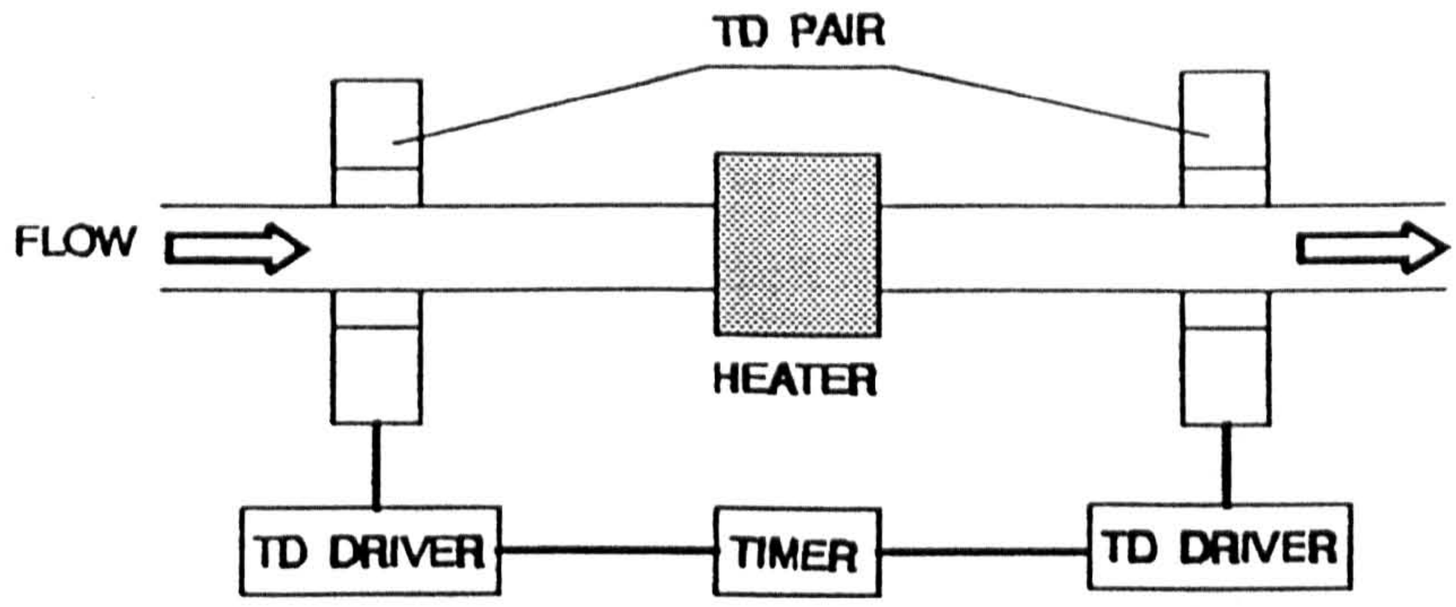

Fig. 1.3.2a. Two Transducer Pair Configuration

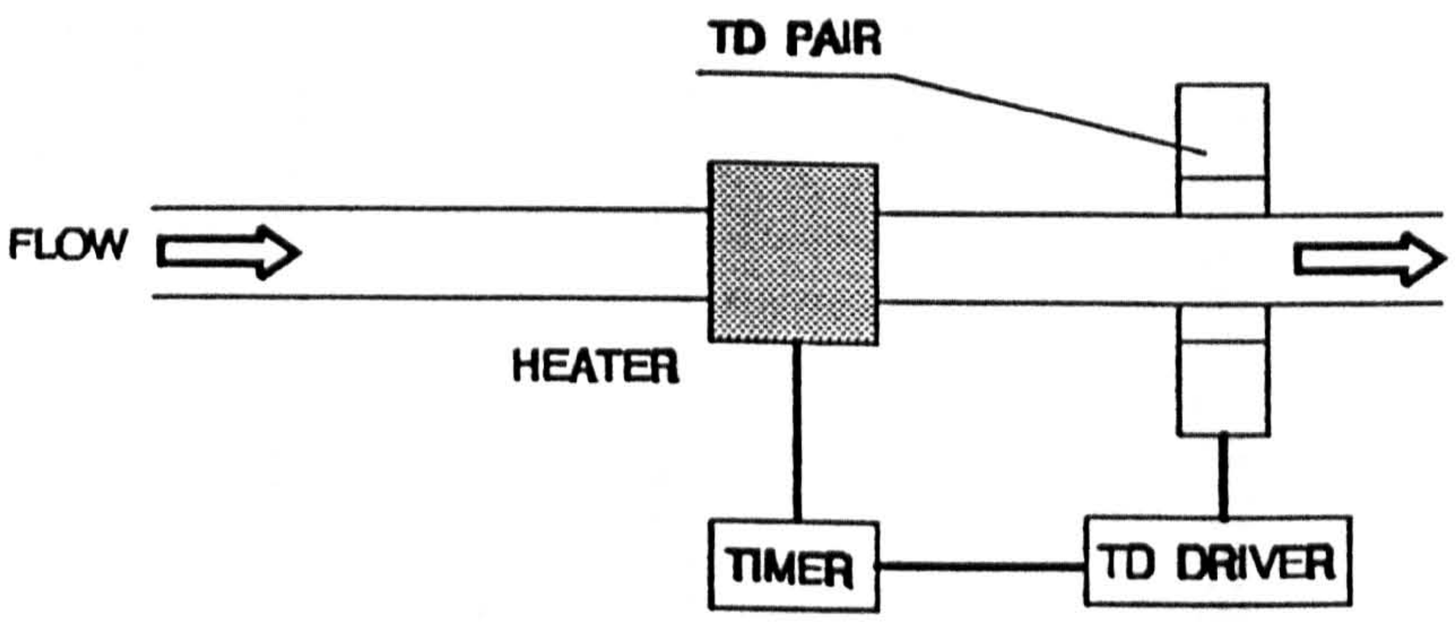

Fig. 1.3.2b. One Transducer Pair Configuration

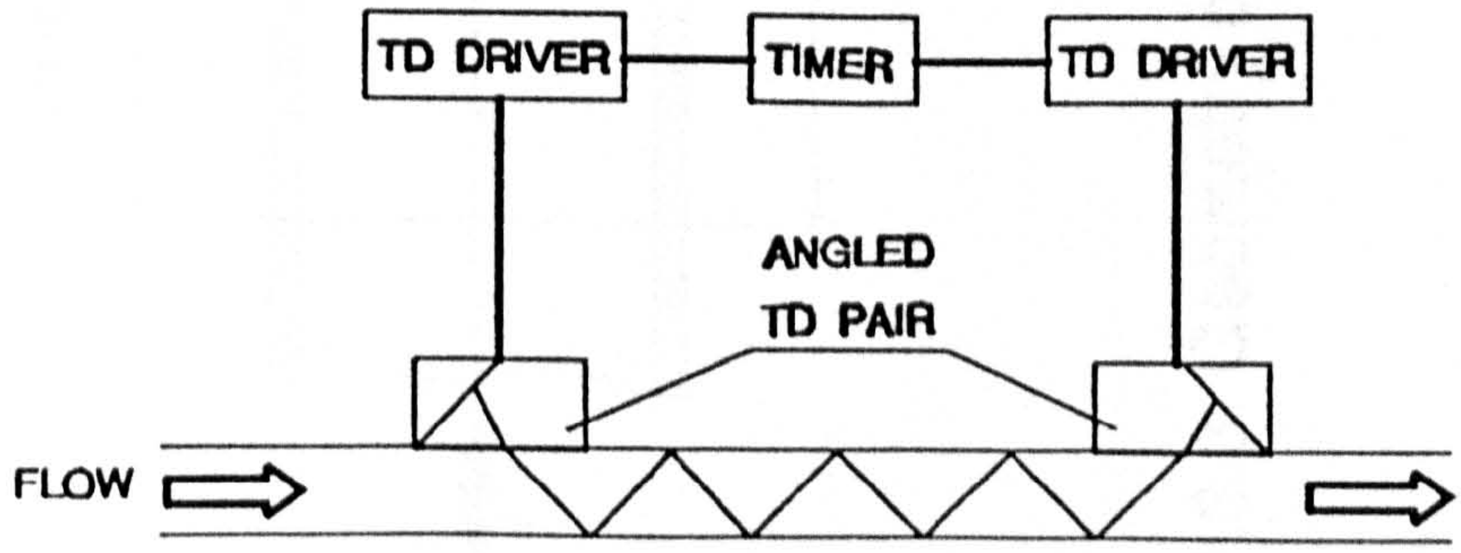

Fig. 1.3.2c. Angled Transducer Pair Configuration

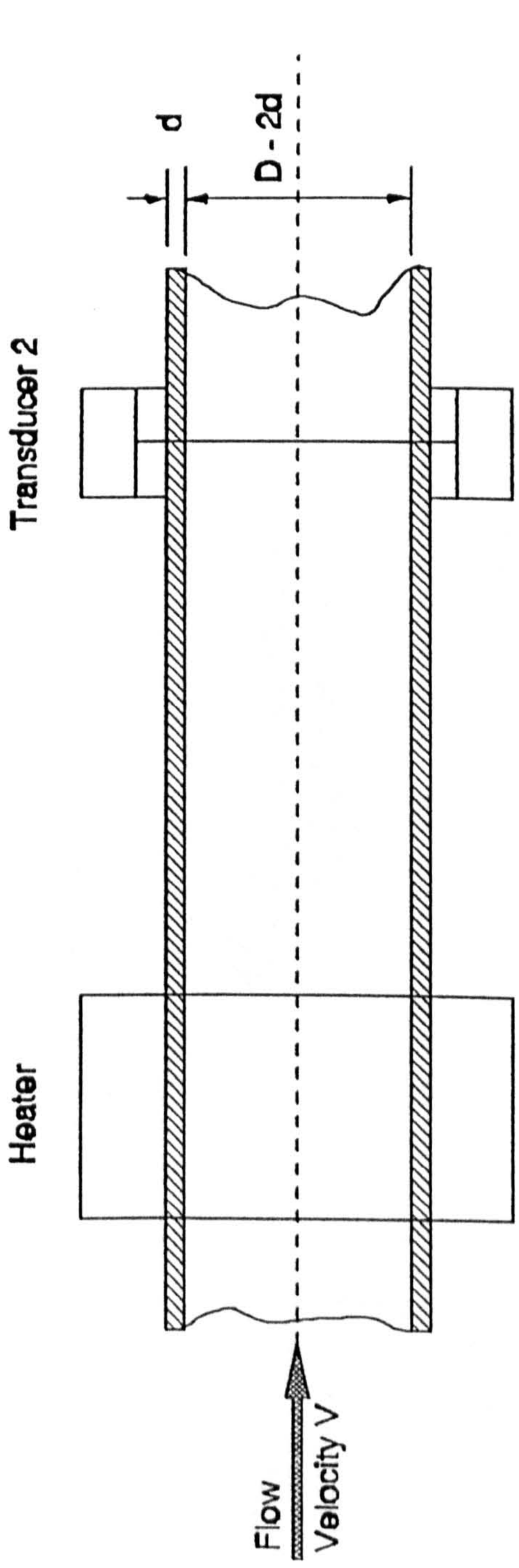

Fig. 1.3.3. Geometry of Ultrasonic Beam Travelling Across Pipe Diameter

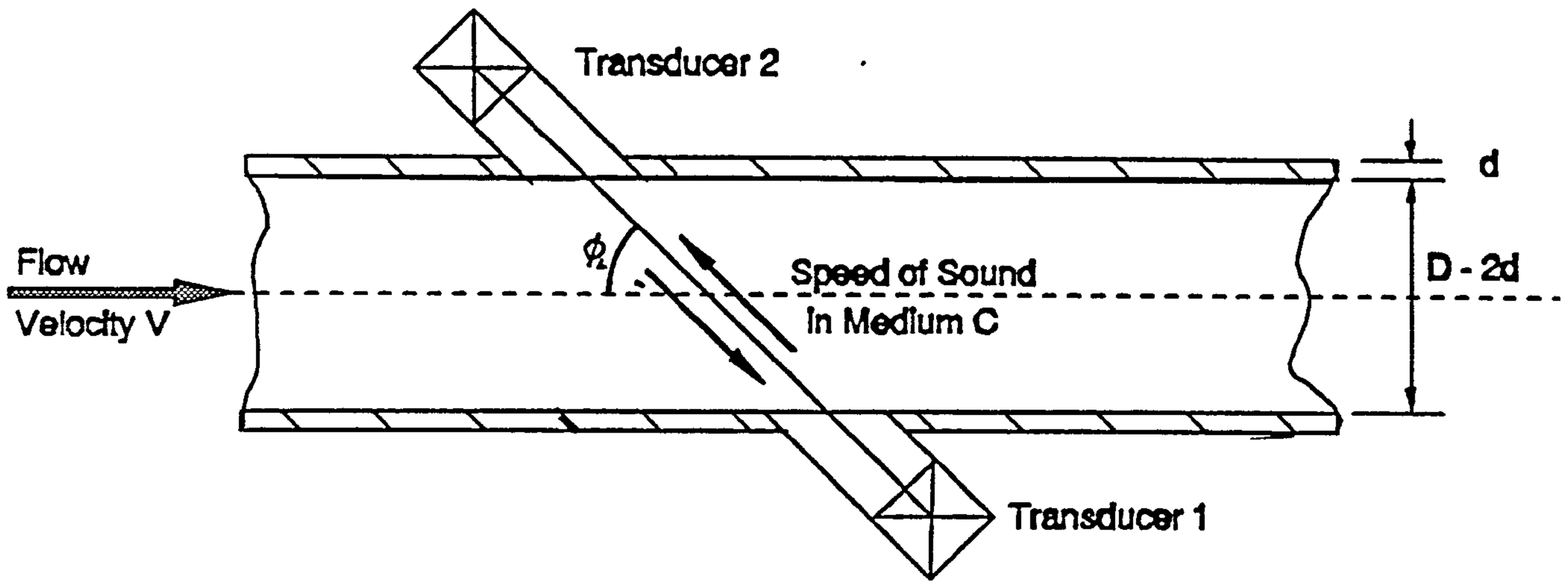

Fig. 1.3.4. Transit Time Ultrasonic Flowmeter

Fig. 2.2.1. Phases of the Research Work

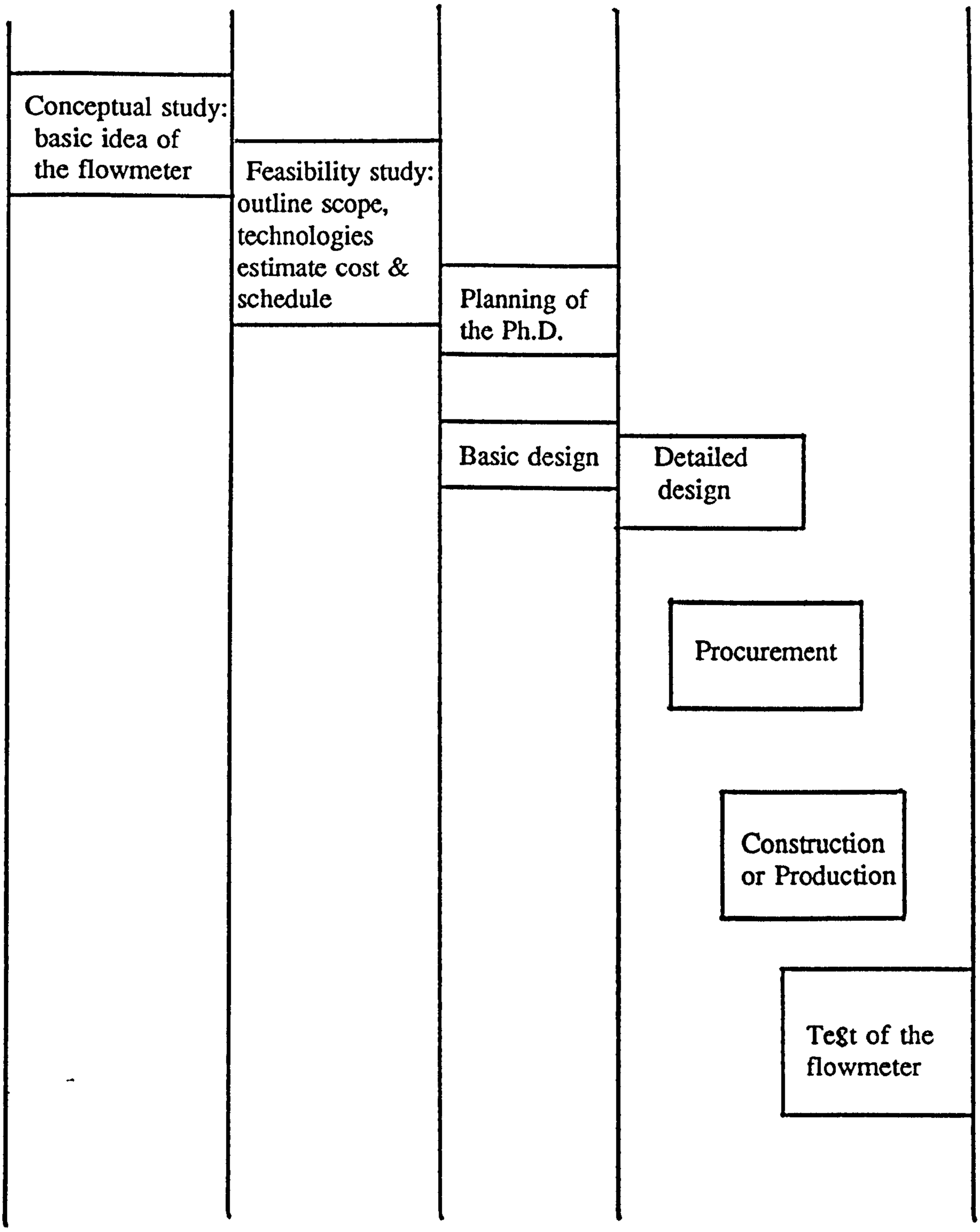

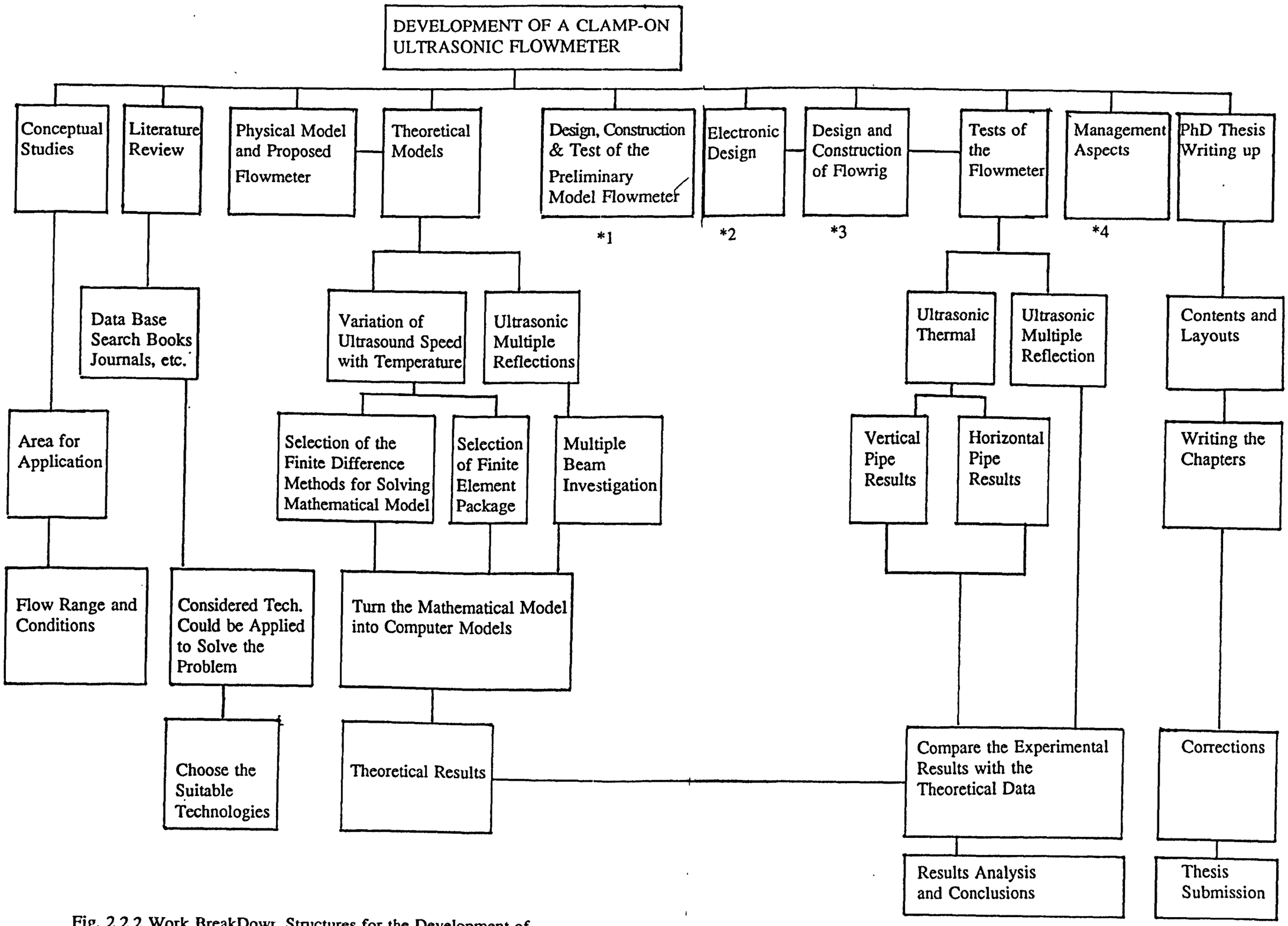

Fig. 2.2.2 Work BreakDowı Structures for the Development of A Clamp-on Flowmeter

Fig. 2.2.3 Design, Construction and Test of the Preliminary Model Flowmeter

*1

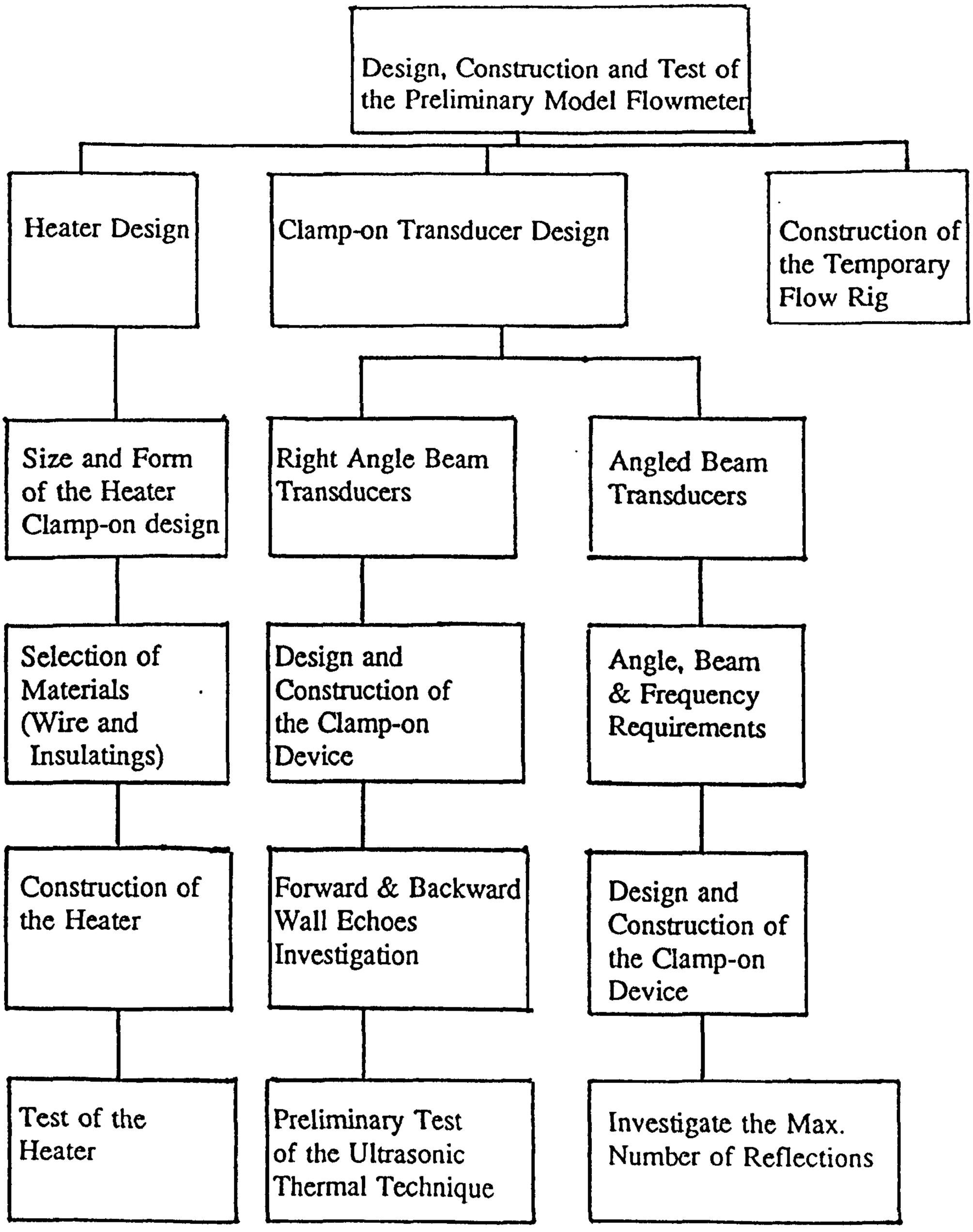

Fig. 2.2.4 Electronic Design and Construction

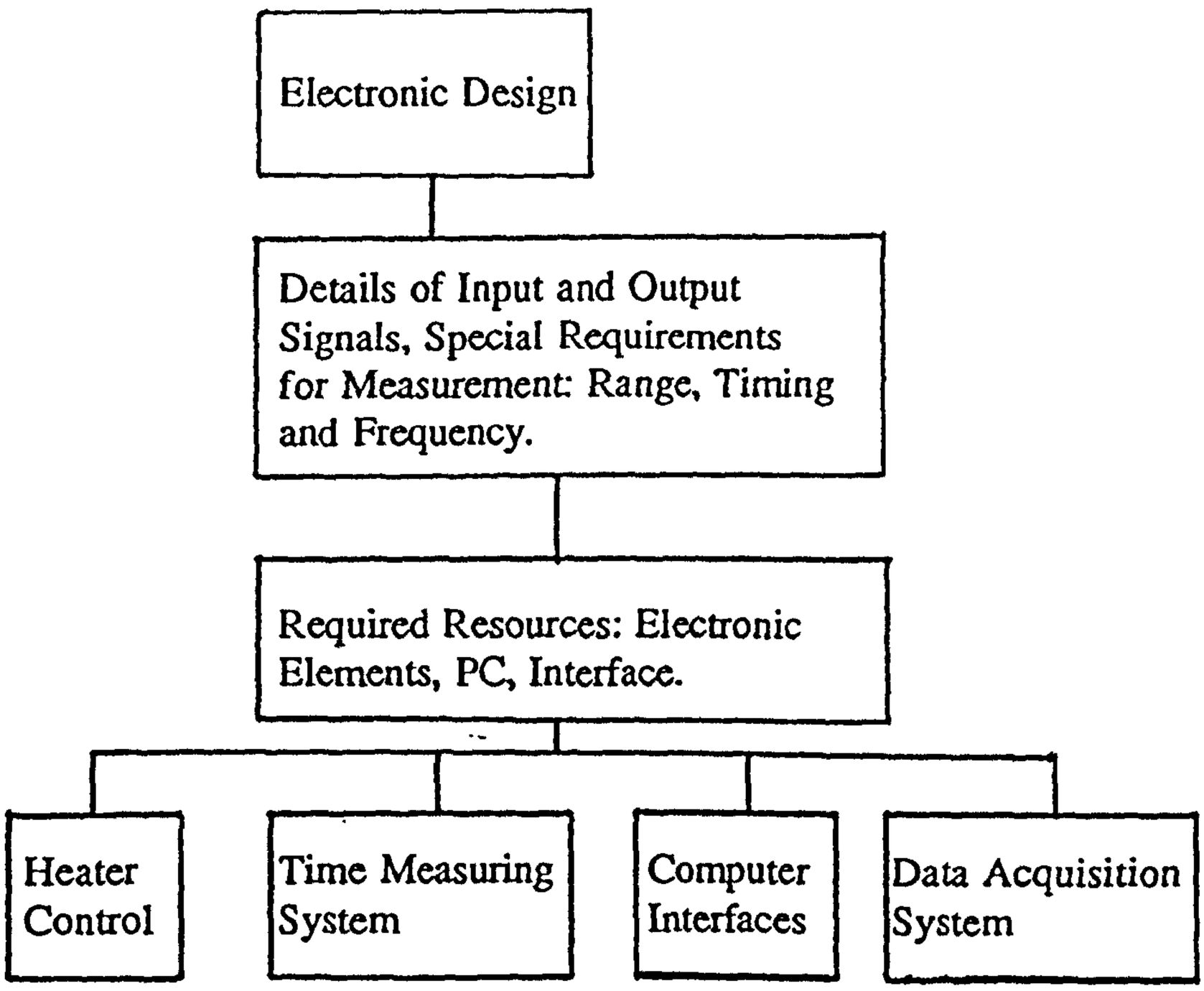

Fig. 2.2.5 Design and Construction of A Refined Test Facility

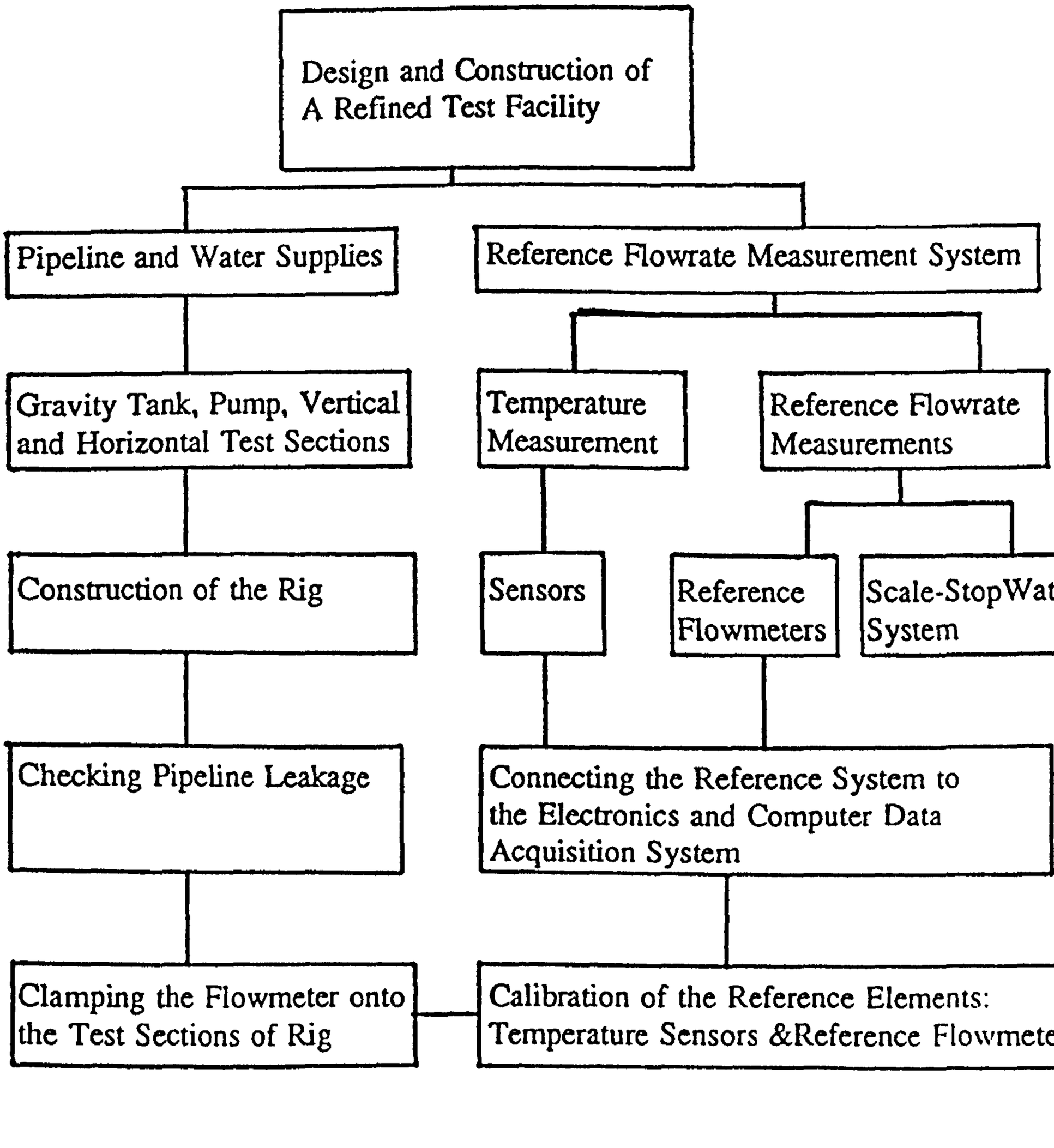

Fig. 2.2.6. Management Aspect

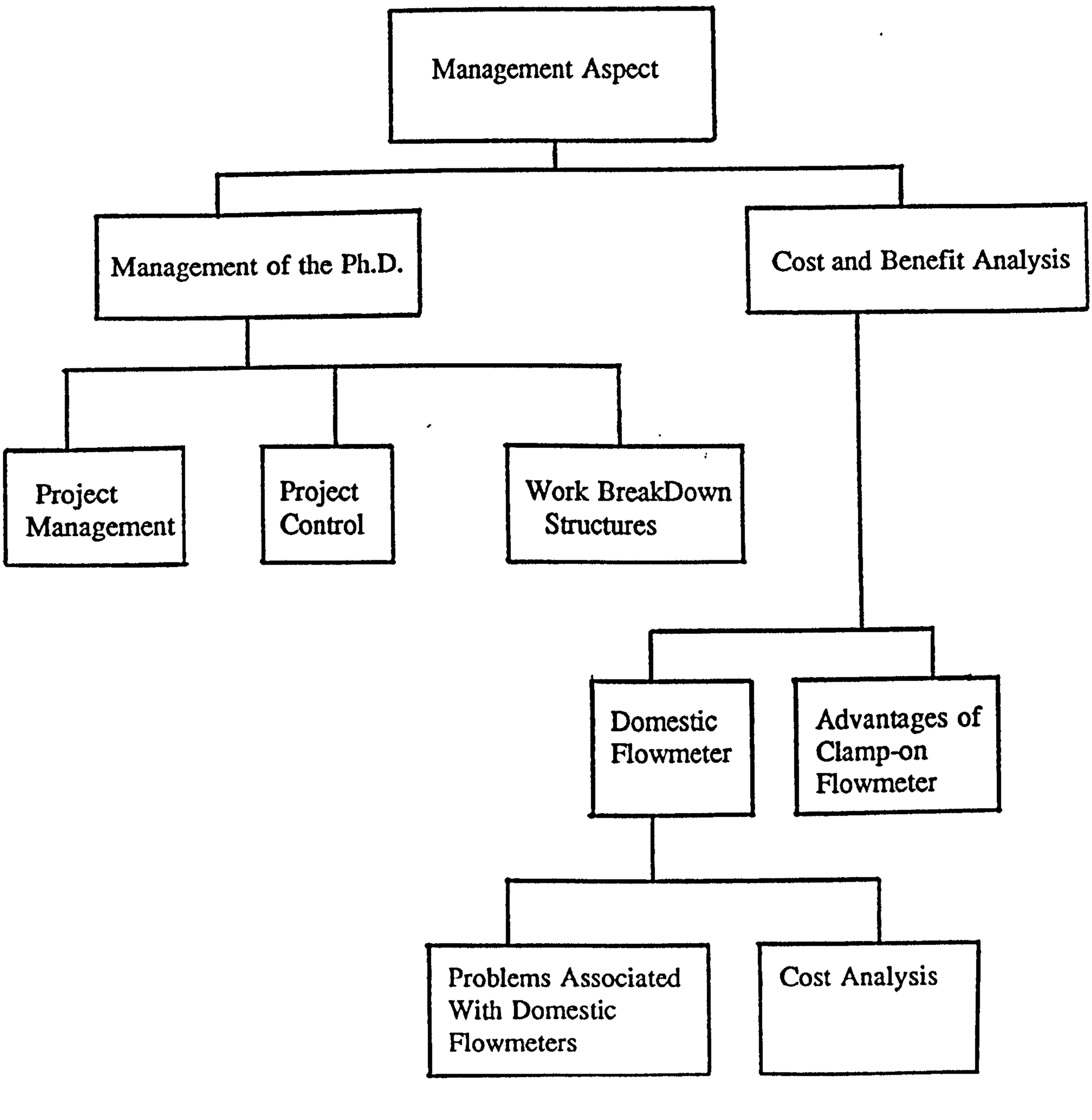

Fig. 2.3.1 Map of Metering Trail Sites

Large Scale Trial Site:

1. Isle of Wight - Southern Water

Small Scale Trial Sites:

2. Hotwells - Bristol Waterworks Company
3. Marlbrook - East Worcestershire Waterwork
4. Brookmans Park - Lee Valley Water Compa
5. Camberley - Mid Southern Water Company
6. Hutton Rudby - Northumbrian Water
7. Chorleywood - Rickmansworth Water Com
8. Chandlers Ford - Southern Water
9. Haling Park - Thames Water
10. Broadstone - Wessex Water
11. Turlin Moor - Wessex Water
12. South Normanton - Yorkshire Water

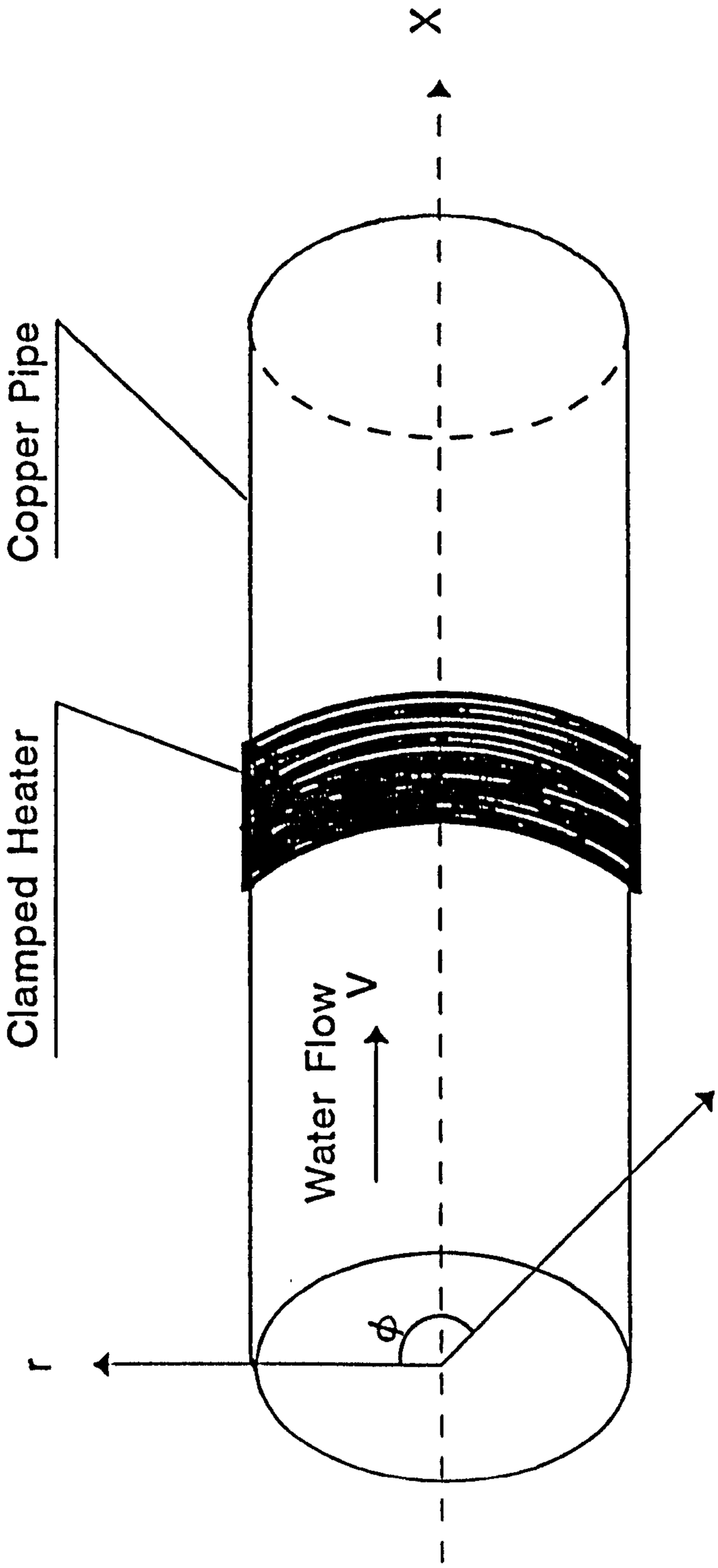

Fig 3.1.1. Physical Model of Heat Transfer in Pipe Flow

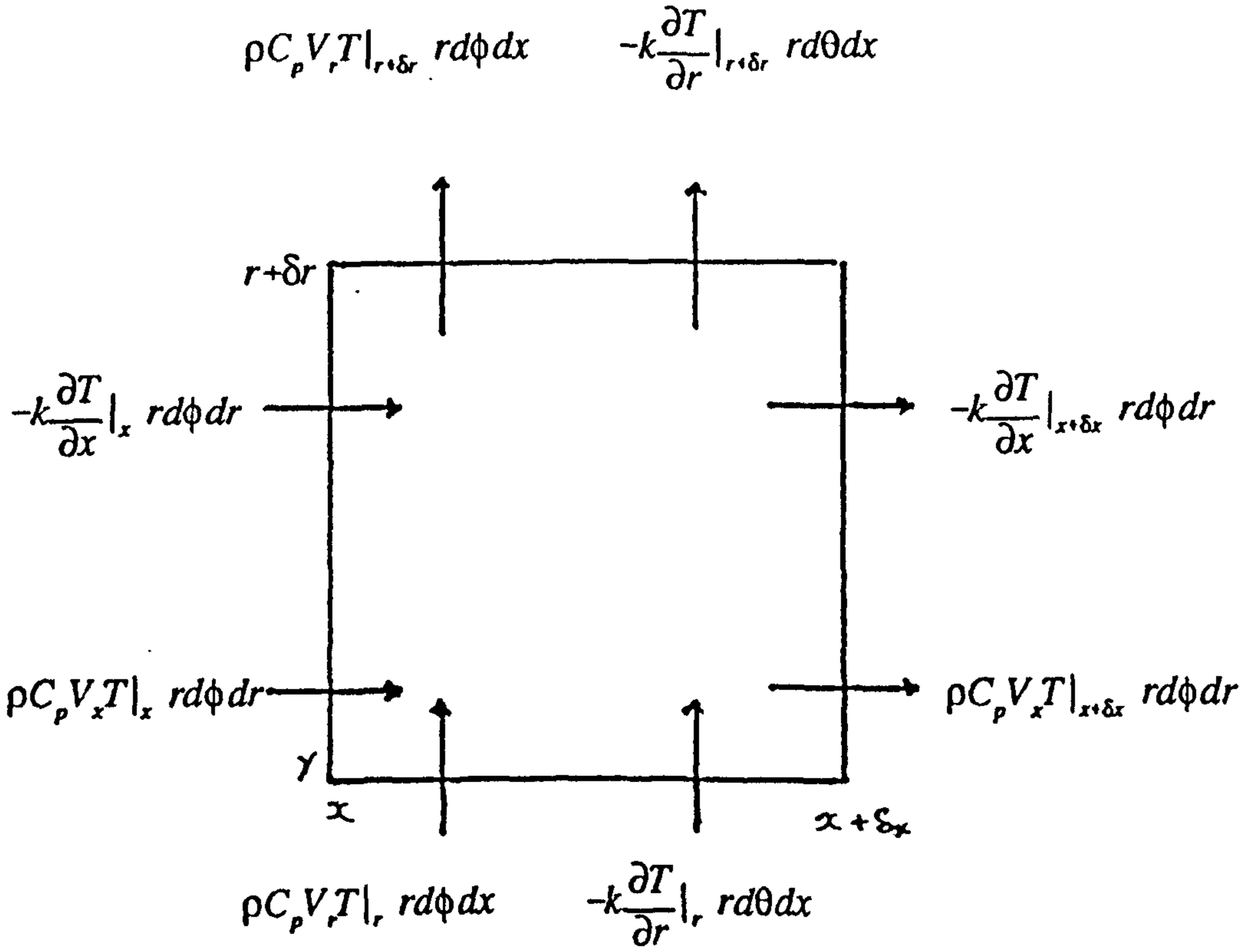

Fig 3.2.1 Heat Flow In/Out of an Element

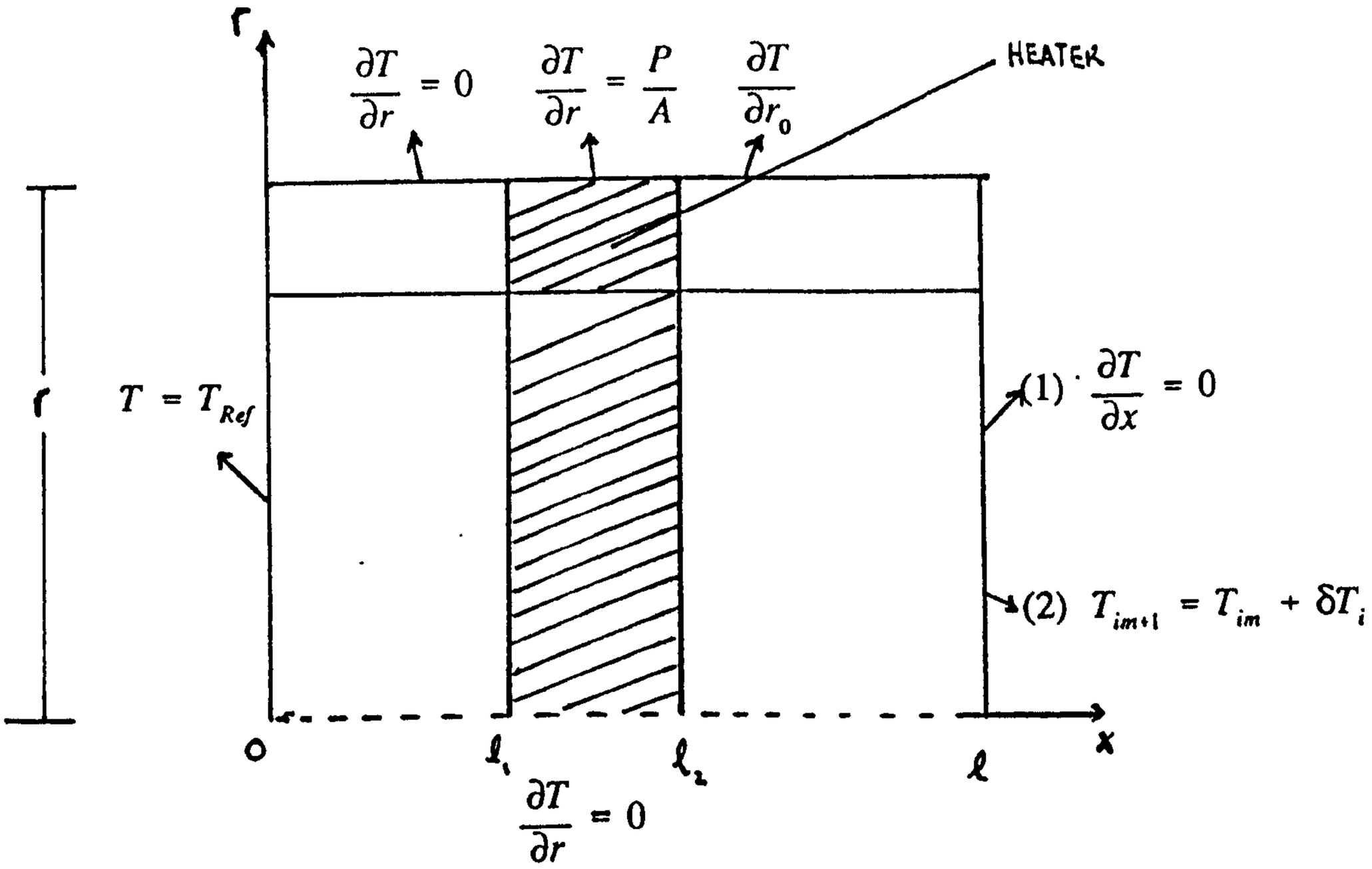

Fig 3.3.1 Boundary Conditions

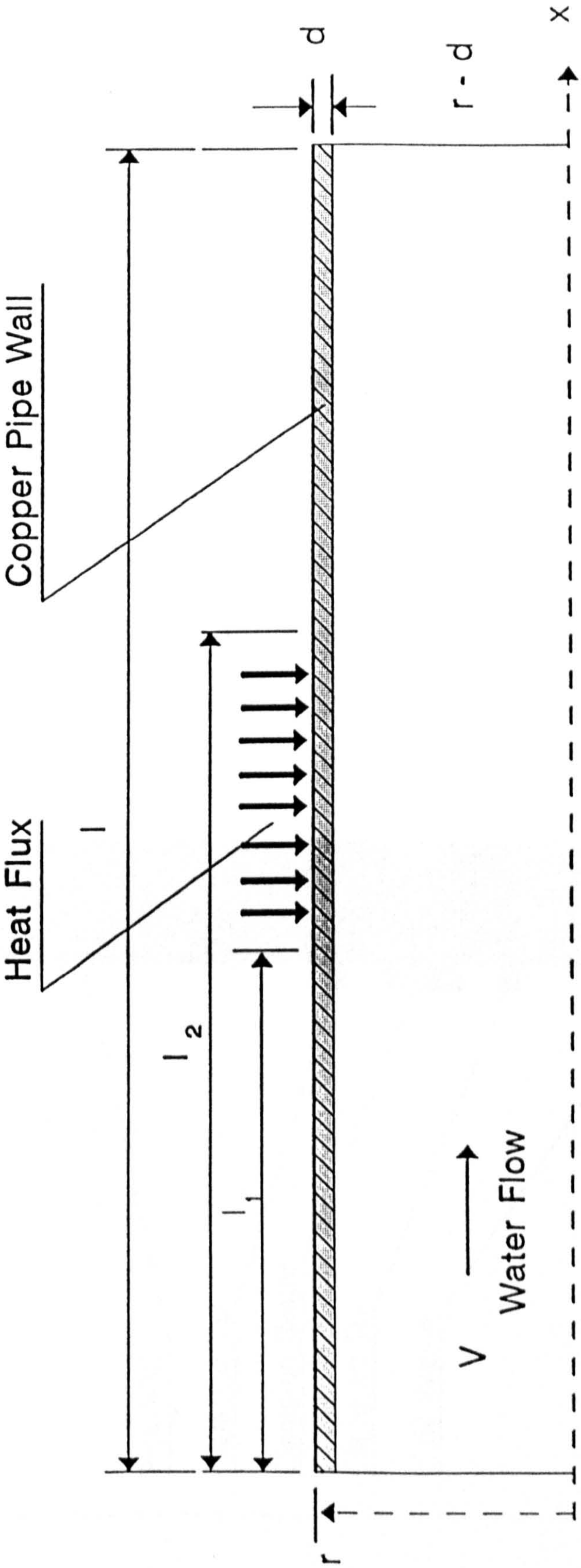

Fig 3.3.2. Two Dimensional Heat Transfer Geometry

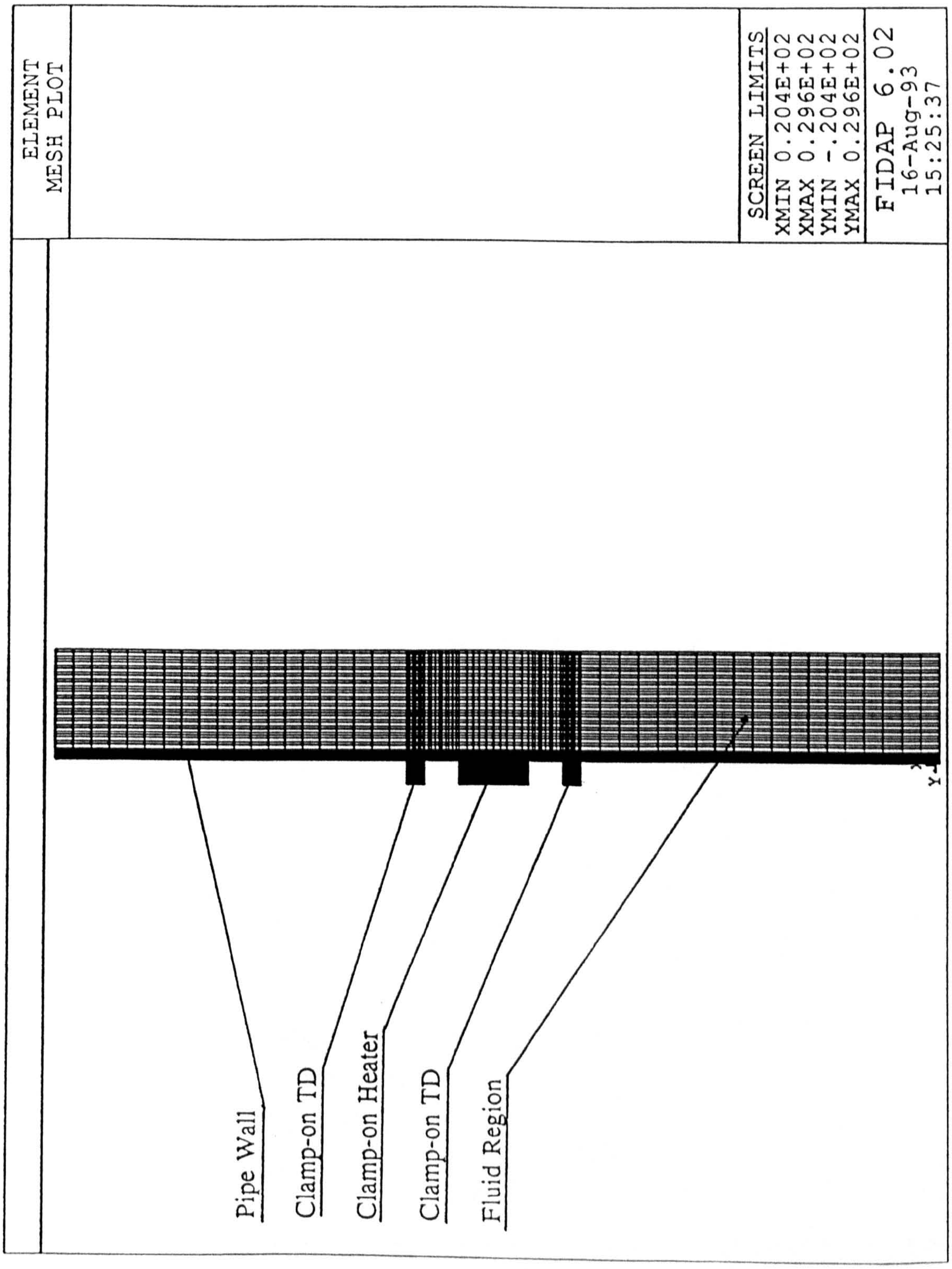

Fig. 3.3.3. 2-D Mesh

Fig. 3.3.4. 3-D Mesh

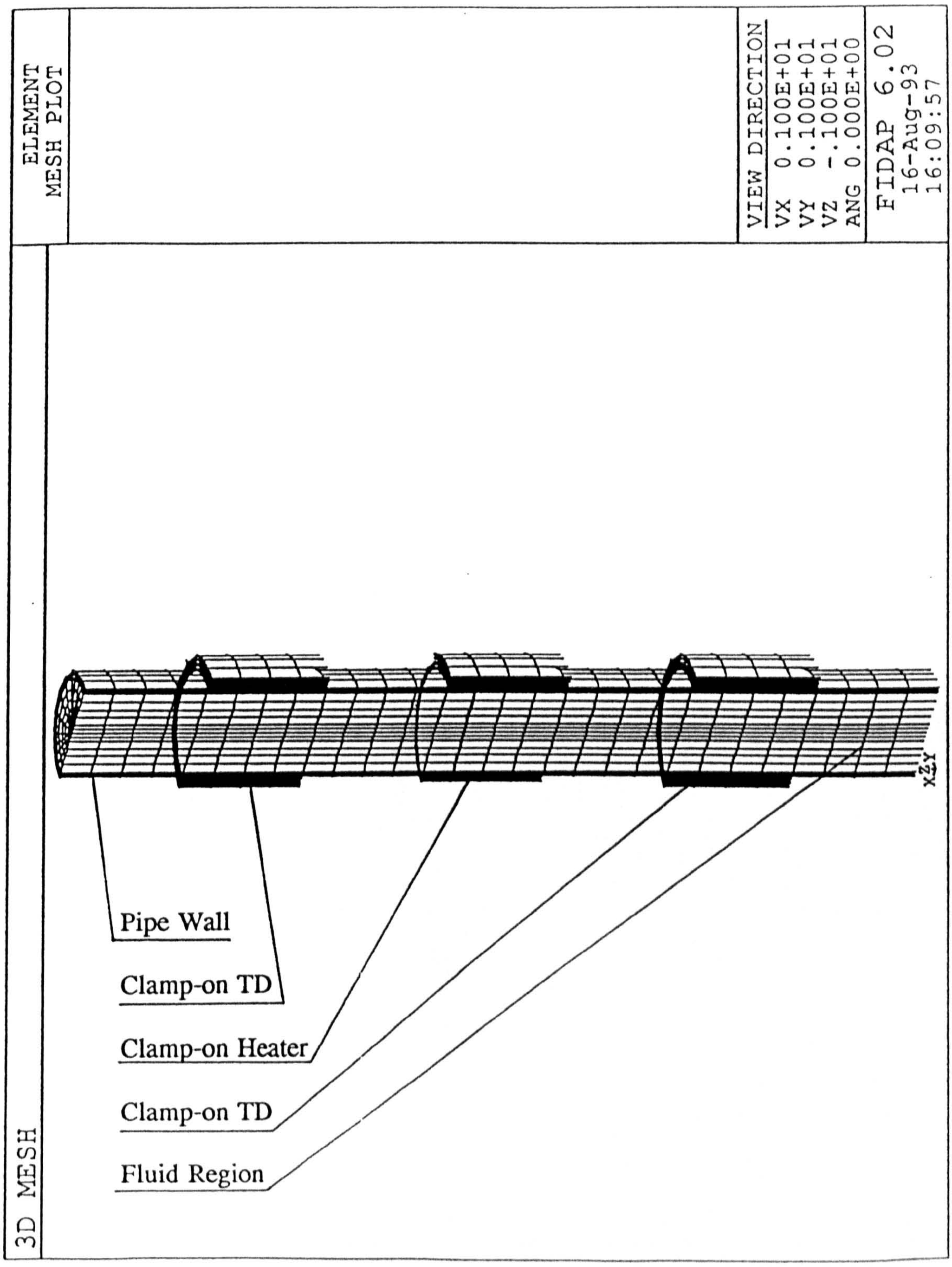

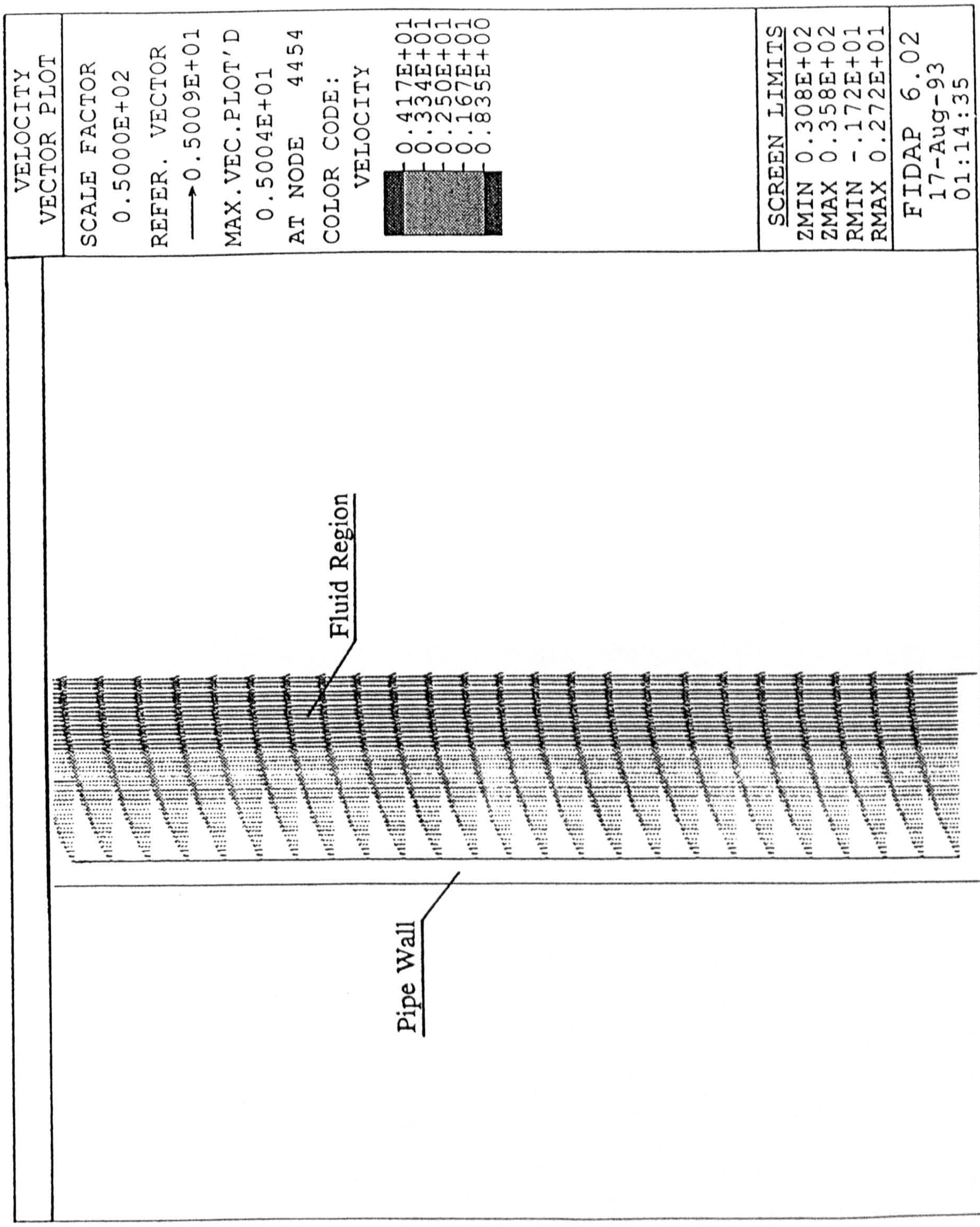

Fig. 3.3.5. Laminar Flow Velocity Profile

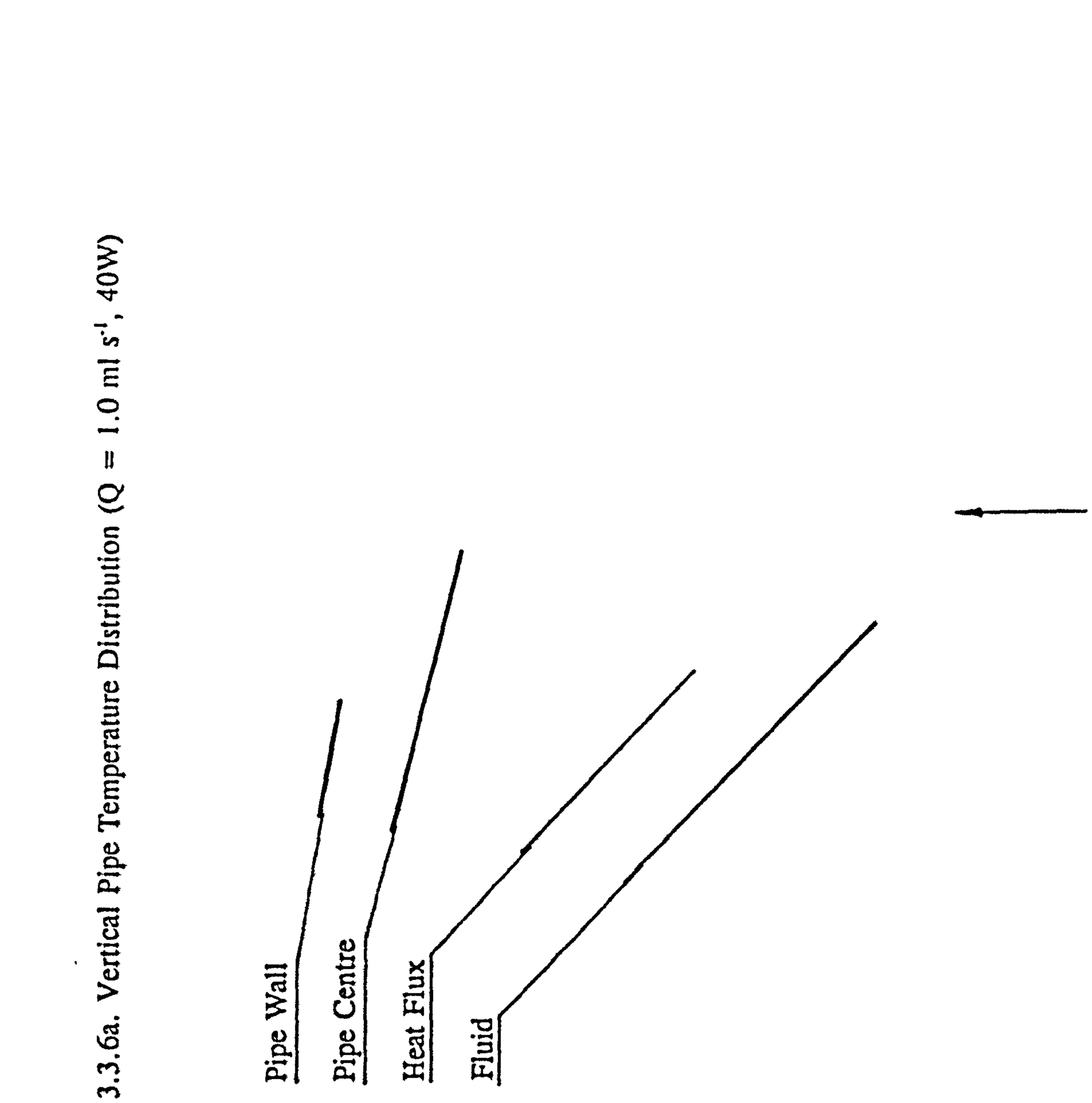

Fig. 3.3.6a. Vertical Pipe Temperature Distribution (Q = 1.0 ml s^{-1}, 40W)

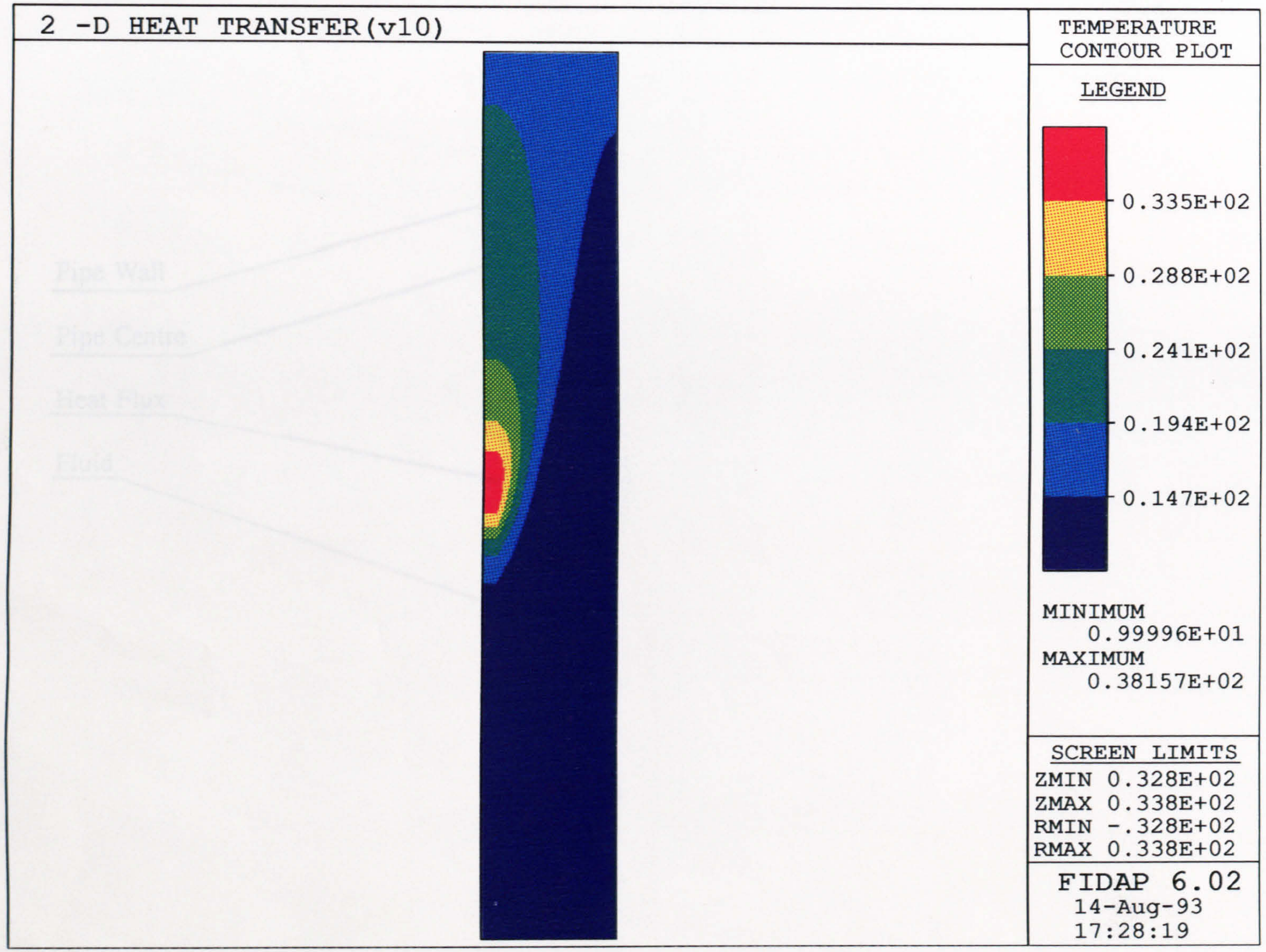
2 -D HEAT TRANSFER(v10)
TEMPERATURE
CONTOUR PLOT
LEGEND
0.335E+02
0.288E+02
0.241E+02
0.194E+02
0.147E+02
MINIMUM
0.99996E+01
MAXIMUM
0.38157E+02
SCREEN LIMITS
ZMIN 0.328E+02
ZMAX 0.338E+02
RMIN -.328E+02
RMAX 0.338E+02
FIDAP 6.02
14-Aug-93
17:28:19

Fig. 3.3.6a. Vertical Pipe Temperature Distribution (Q = 1.0 ml s^{-1}, 40W)

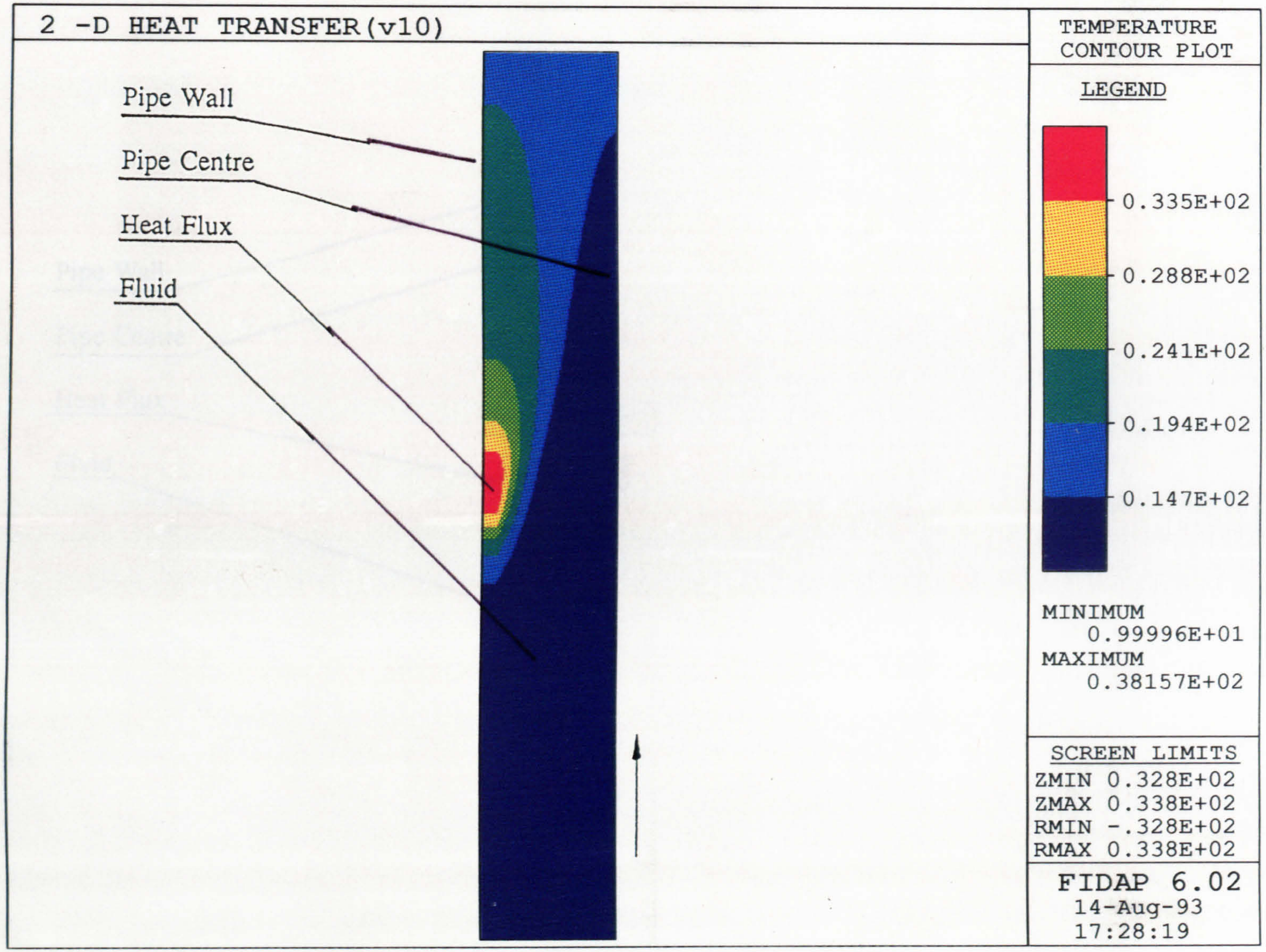

Fig. 3.3.6b. Vertical Pipe Temperature Distribution (Q = 4.84 ml s^{-1}, 40W)

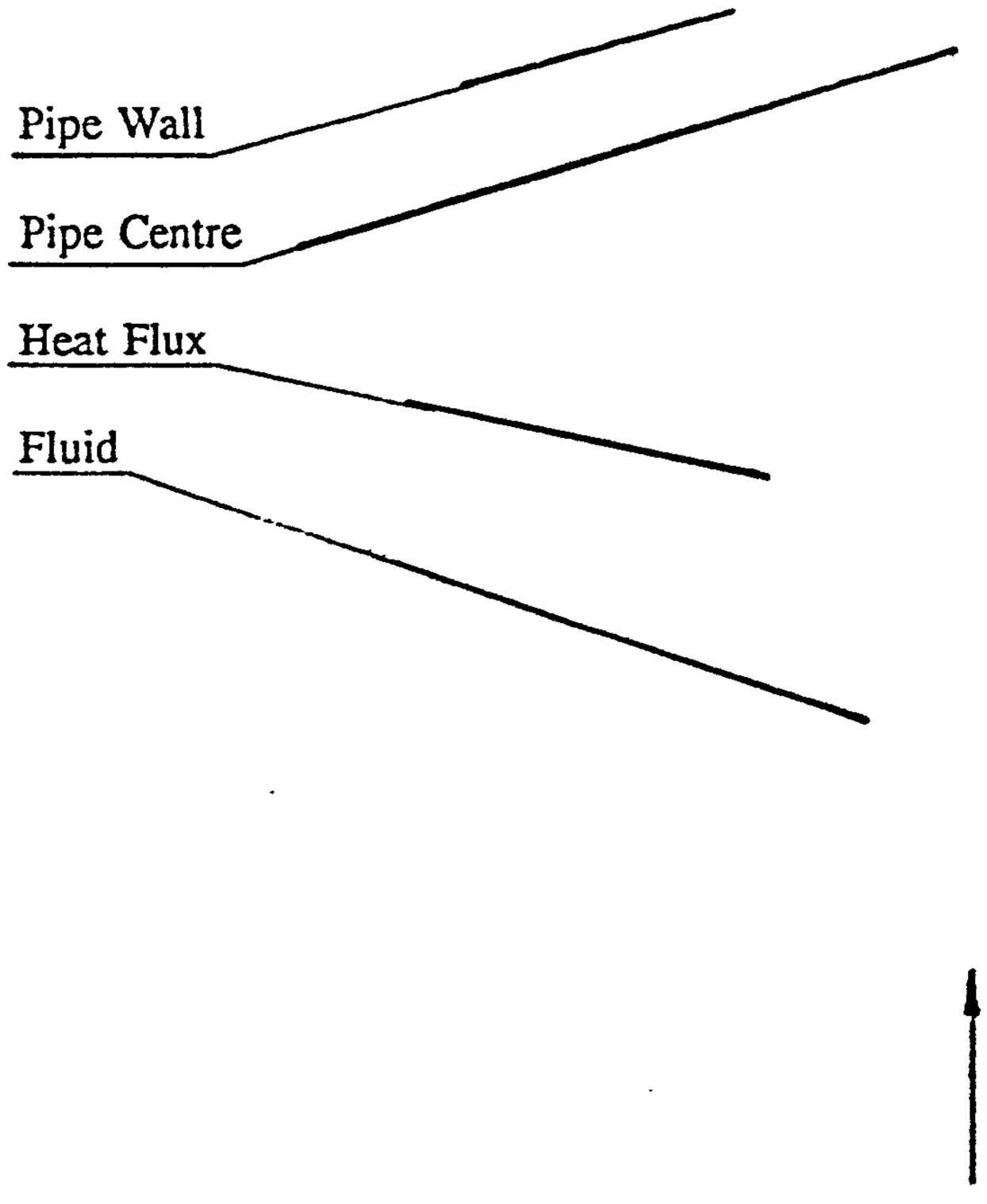

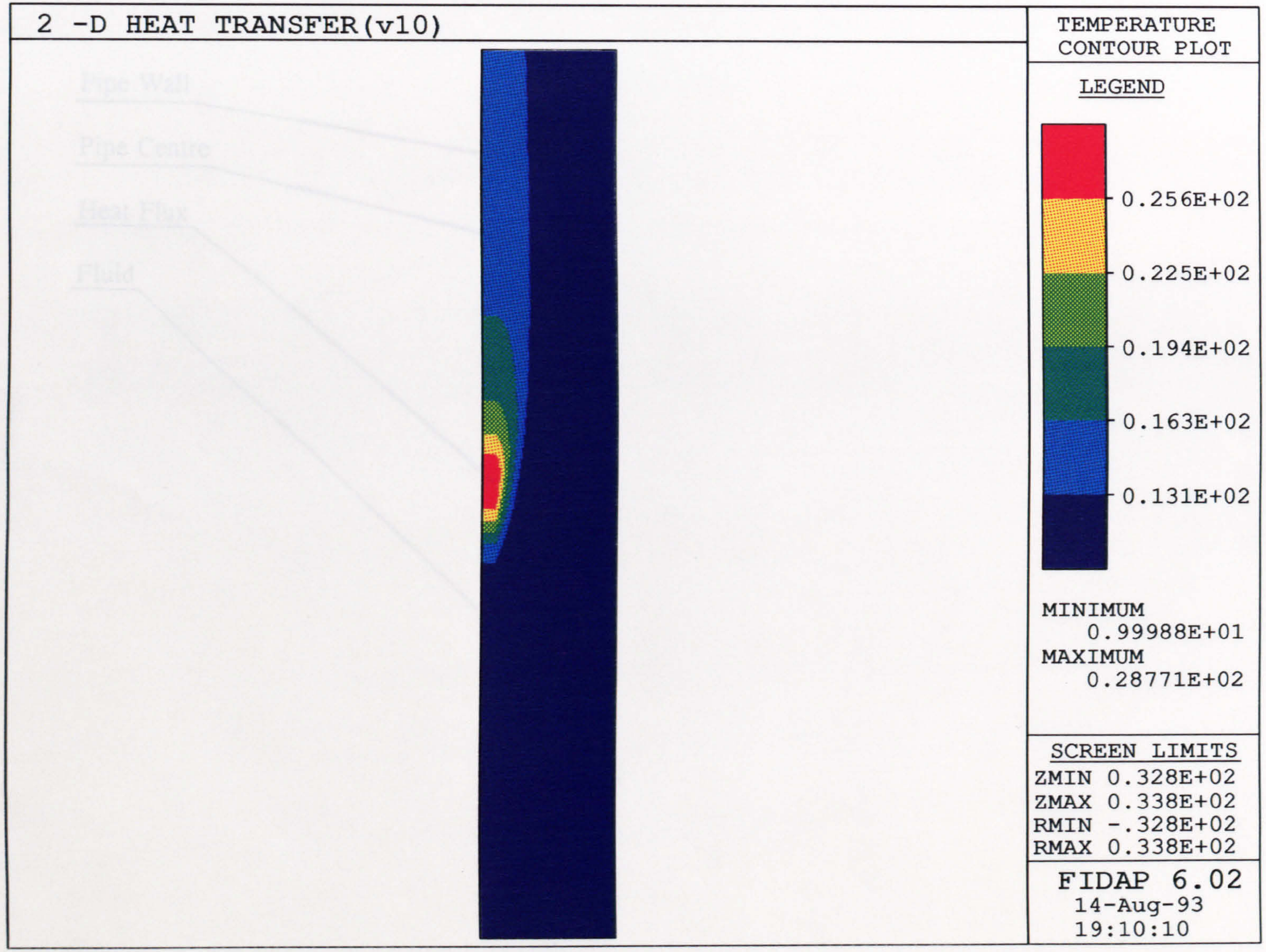
2 -D HEAT TRANSFER(v10)
TEMPERATURE
CONTOUR PLOT
LEGEND
0.256E+02
0.225E+02
0.194E+02
0.163E+02
0.131E+02
MINIMUM
0.99988E+01
MAXIMUM
0.28771E+02
SCREEN LIMITS
ZMIN 0.328E+02
ZMAX 0.338E+02
RMIN -.328E+02
RMAX 0.338E+02
FIDAP 6.02
14-Aug-93
19:10:10

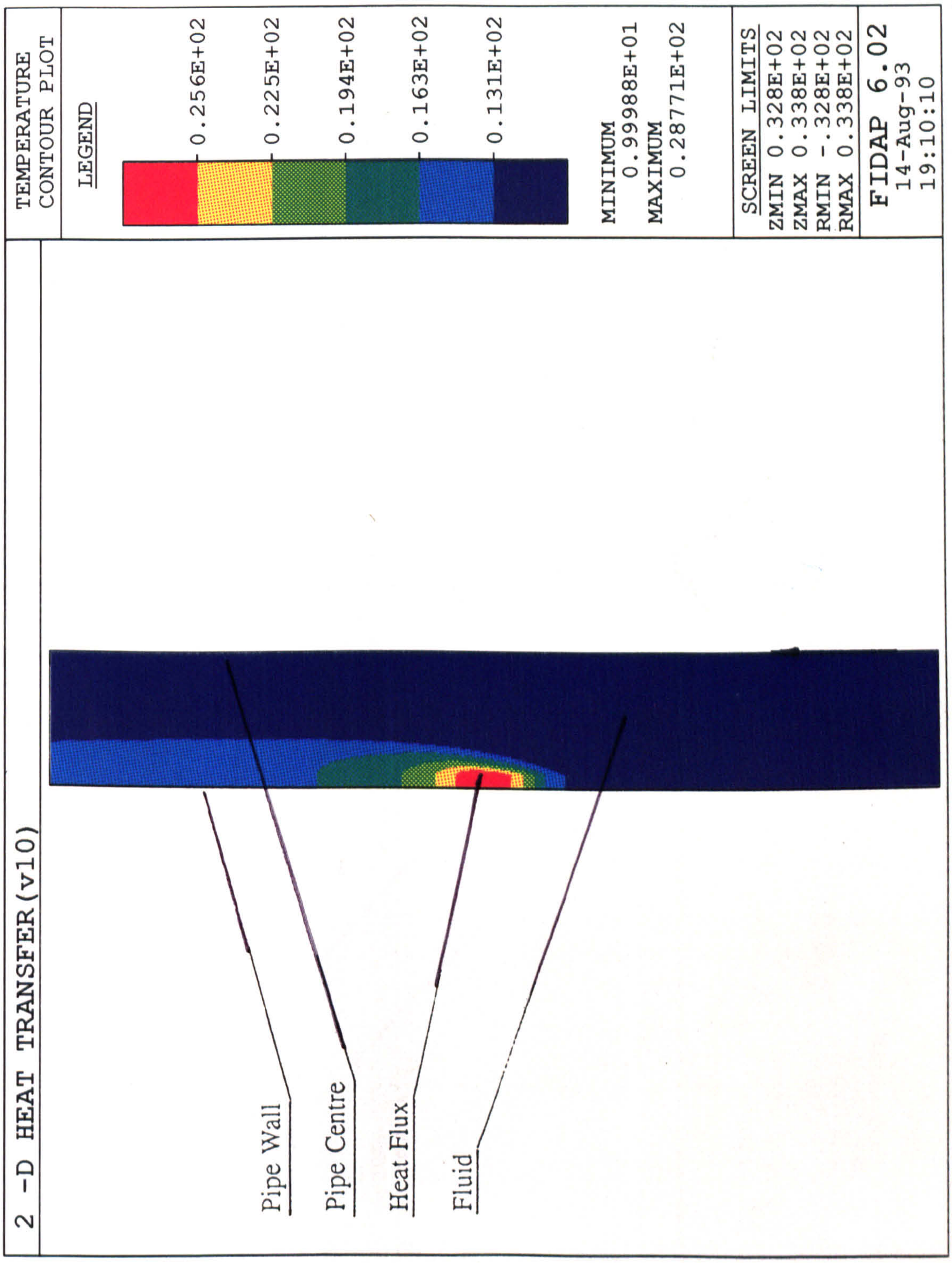

Fig. 3.3.6b. Vertical Pipe Temperature Distribution (Q = 4.84 ml s^{-1}, 40W)

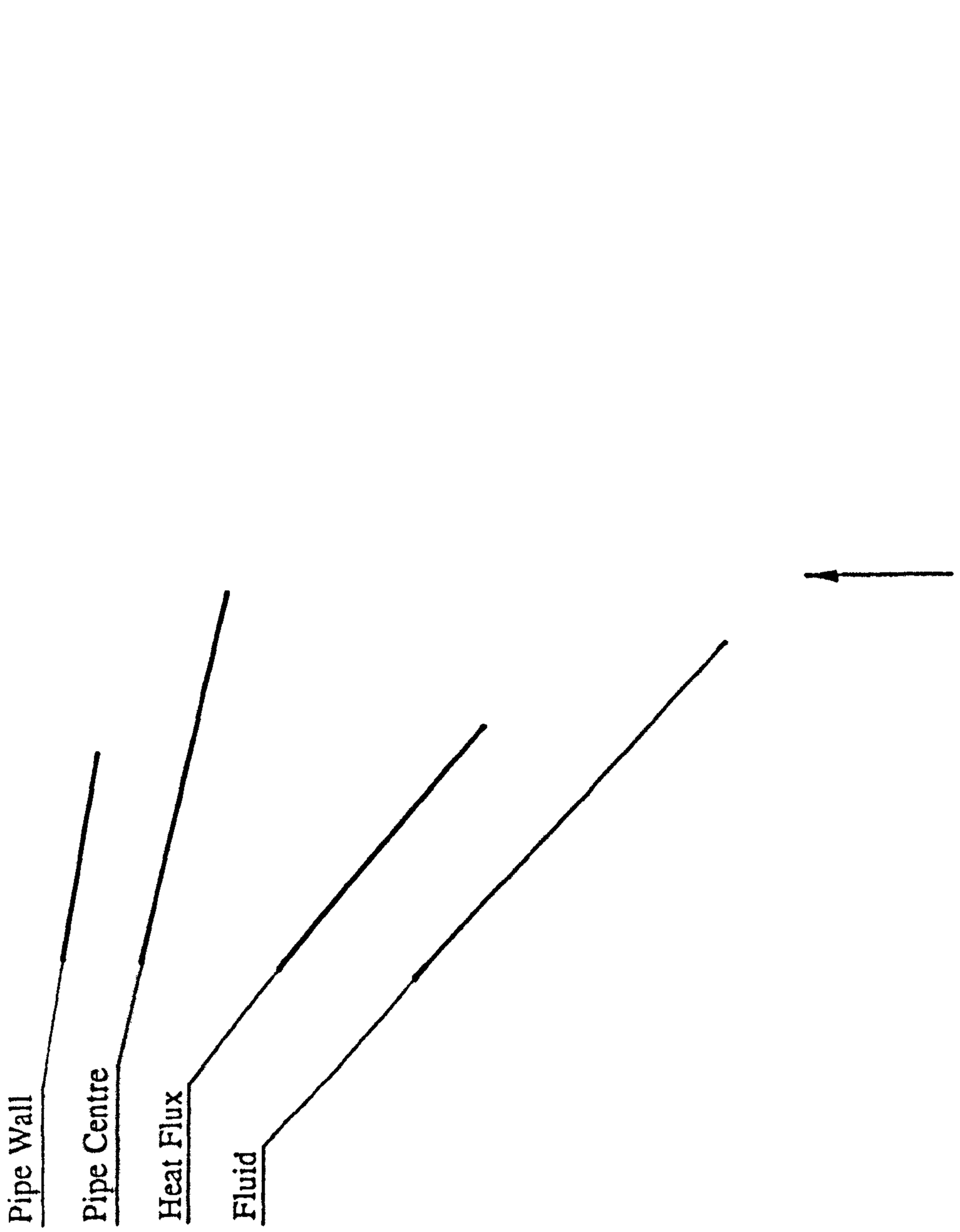

Fig. 3.3.6c. Vertical Pipe Temperature Distribution (Q = 13.29 ml s^{-1}, 40W)

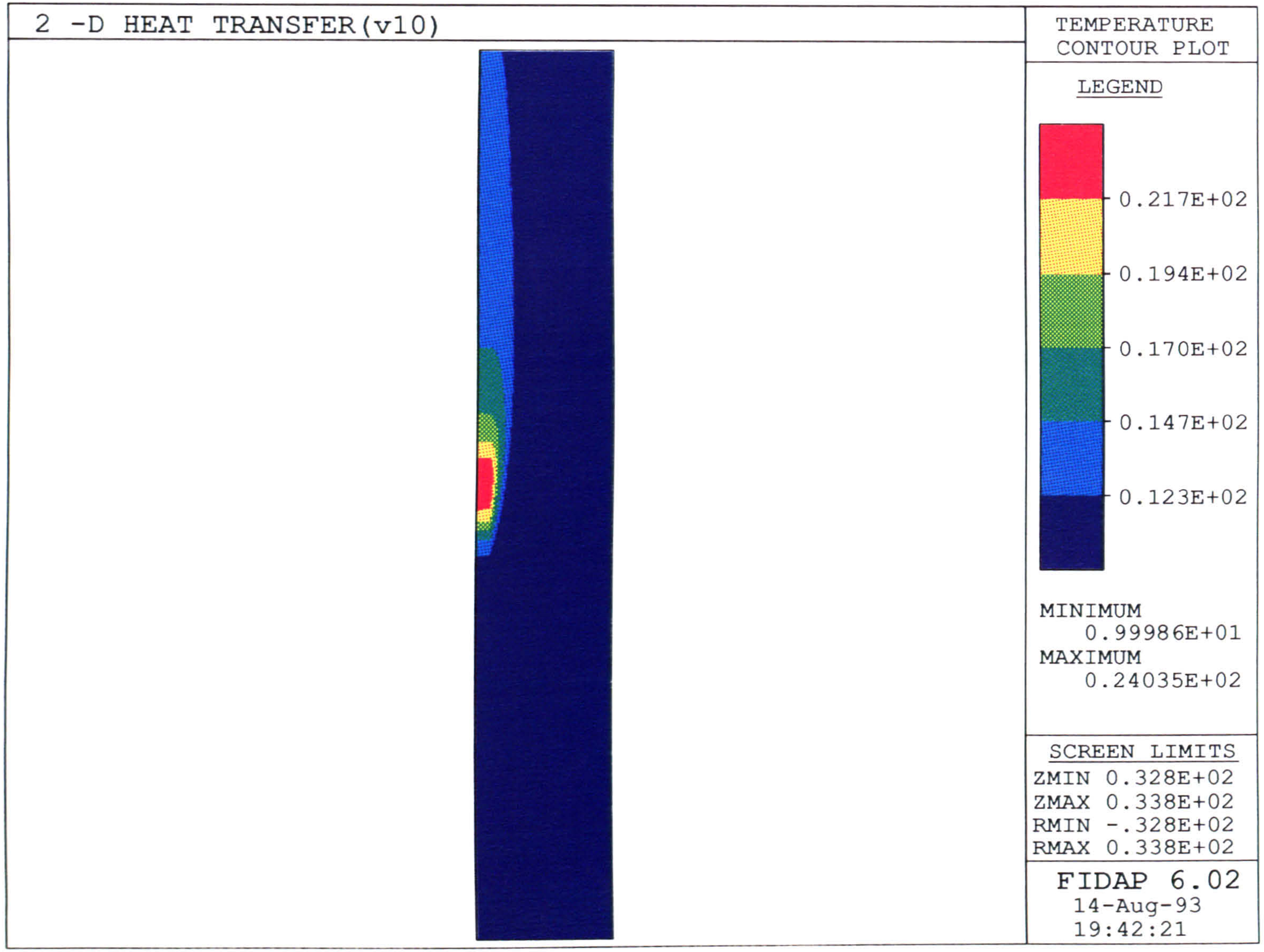
2 -D HEAT TRANSFER(v10)
TEMPERATURE
CONTOUR PLOT
LEGEND
0.217E+02
0.194E+02
0.170E+02
0.147E+02
0.123E+02
MINIMUM
0.99986E+01
MAXIMUM
0.24035E+02
SCREEN LIMITS
ZMIN 0.328E+02
ZMAX 0.338E+02
RMIN -.328E+02
RMAX 0.338E+02
FIDAP 6.02
14-Aug-93
19:42:21

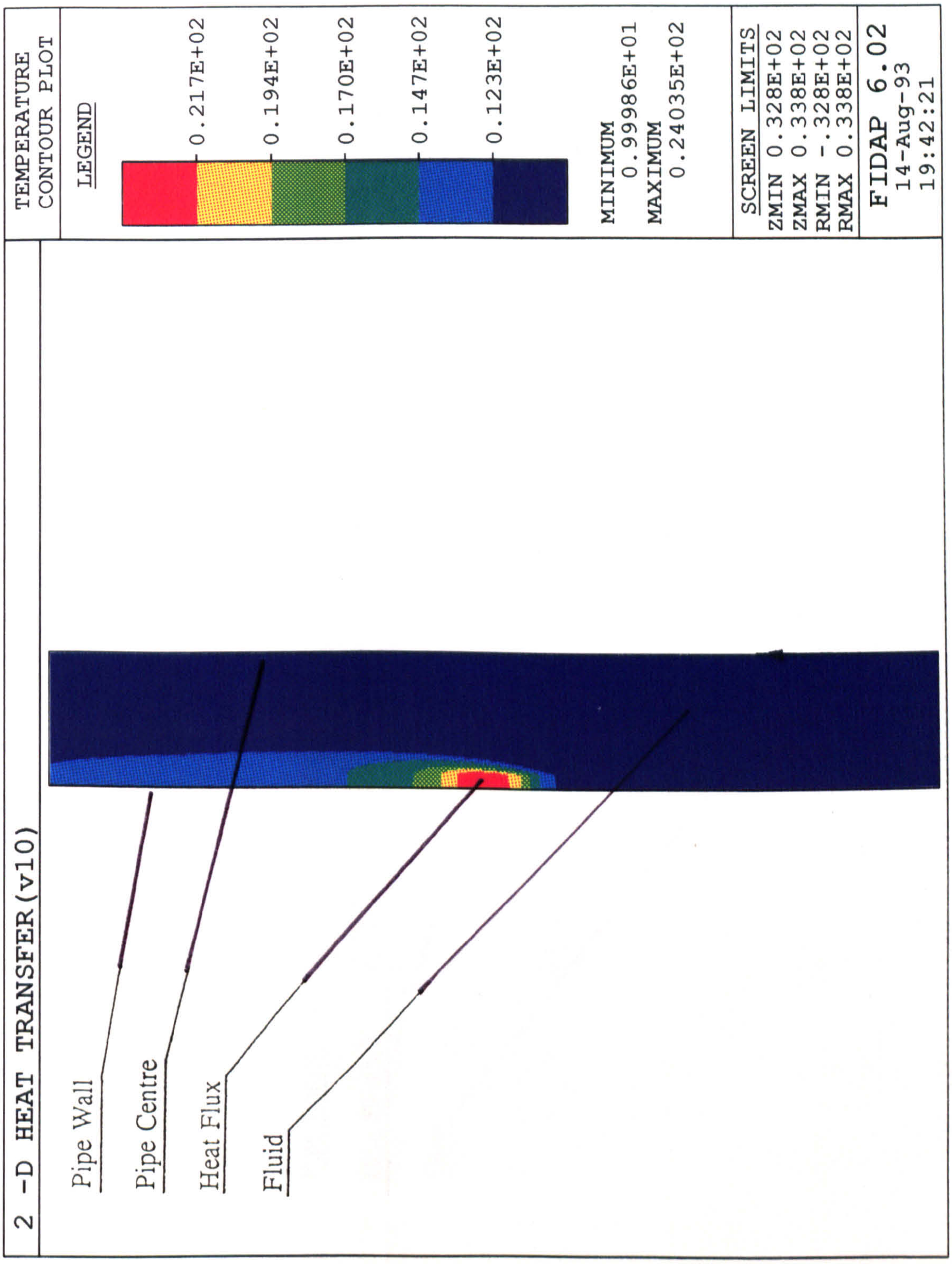

Fig. 3.3.6c. Vertical Pipe Temperature Distribution (Q = 13.29 ml s^{-1}, 40W)

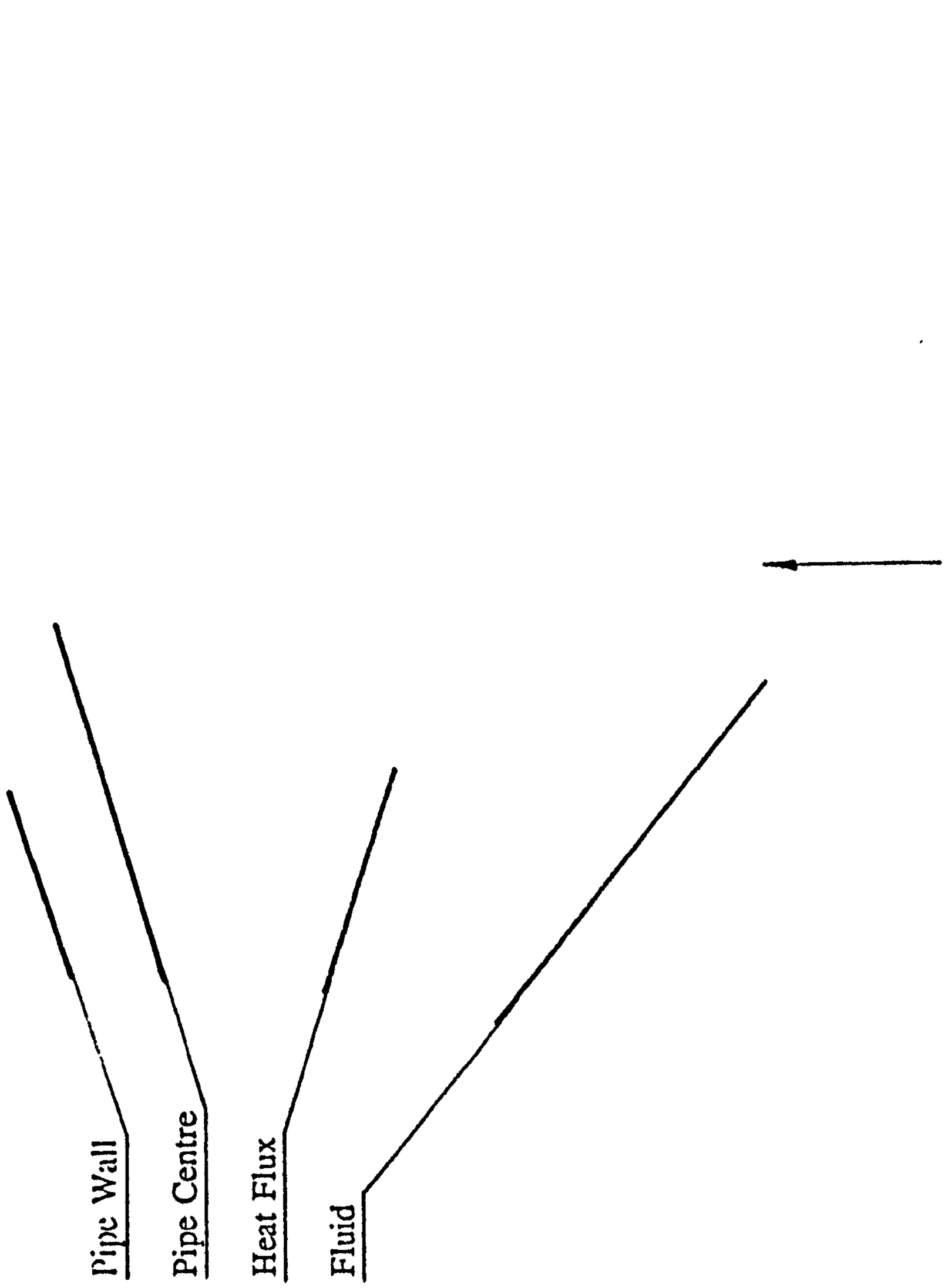

Fig. 3.3.6d. Vertical Pipe Temperature Distribution (Q = 17.63 ml s^{-1}, 40W)

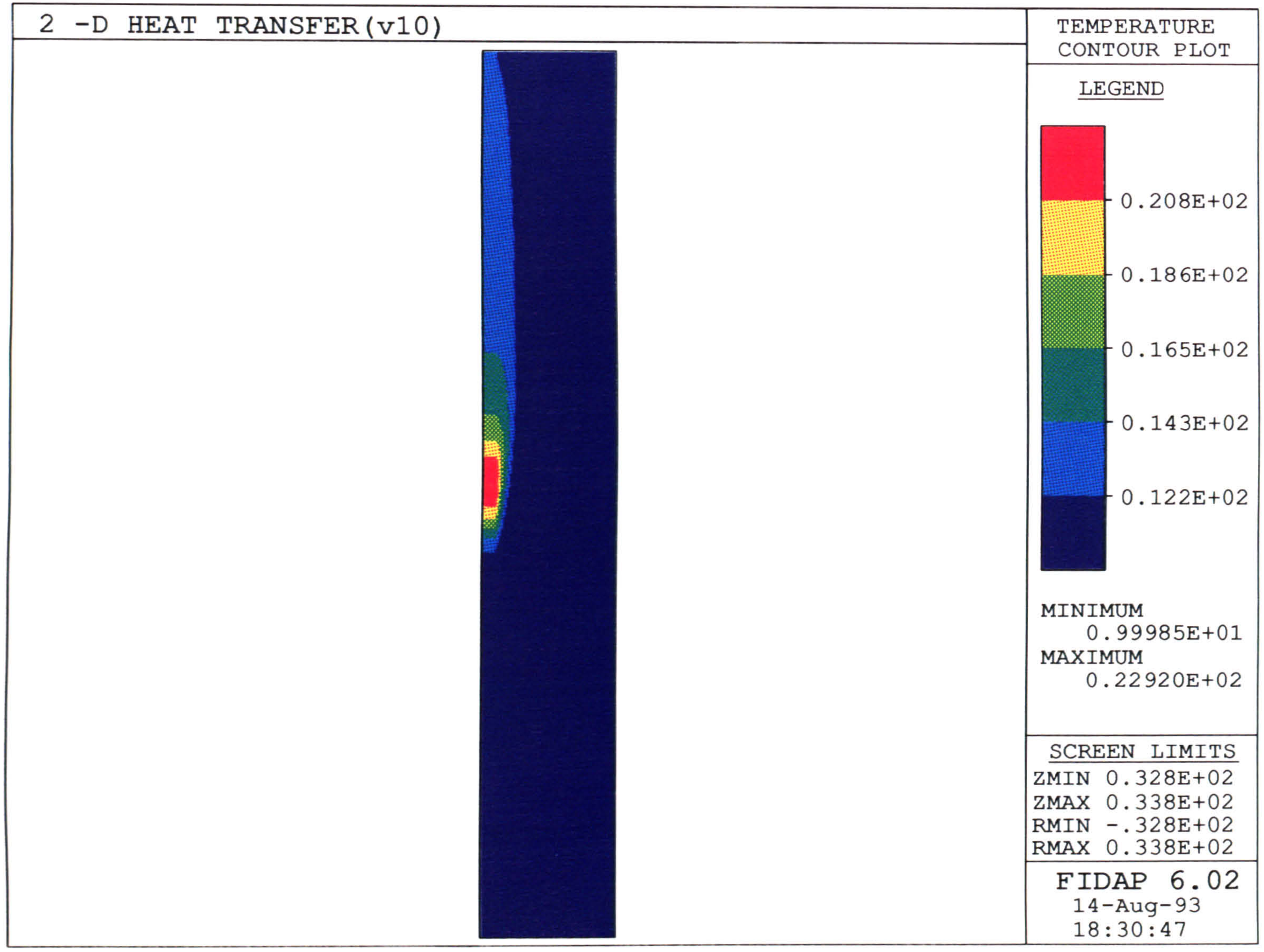
2 -D HEAT TRANSFER(v10)
TEMPERATURE
CONTOUR PLOT
LEGEND
0.208E+02
0.186E+02
0.165E+02
0.143E+02
0.122E+02
MINIMUM
0.99985E+01
MAXIMUM
0.22920E+02
SCREEN LIMITS
ZMIN 0.328E+02
ZMAX 0.338E+02
RMIN -.328E+02
RMAX 0.338E+02
FIDAP 6.02
14-Aug-93
18:30:47

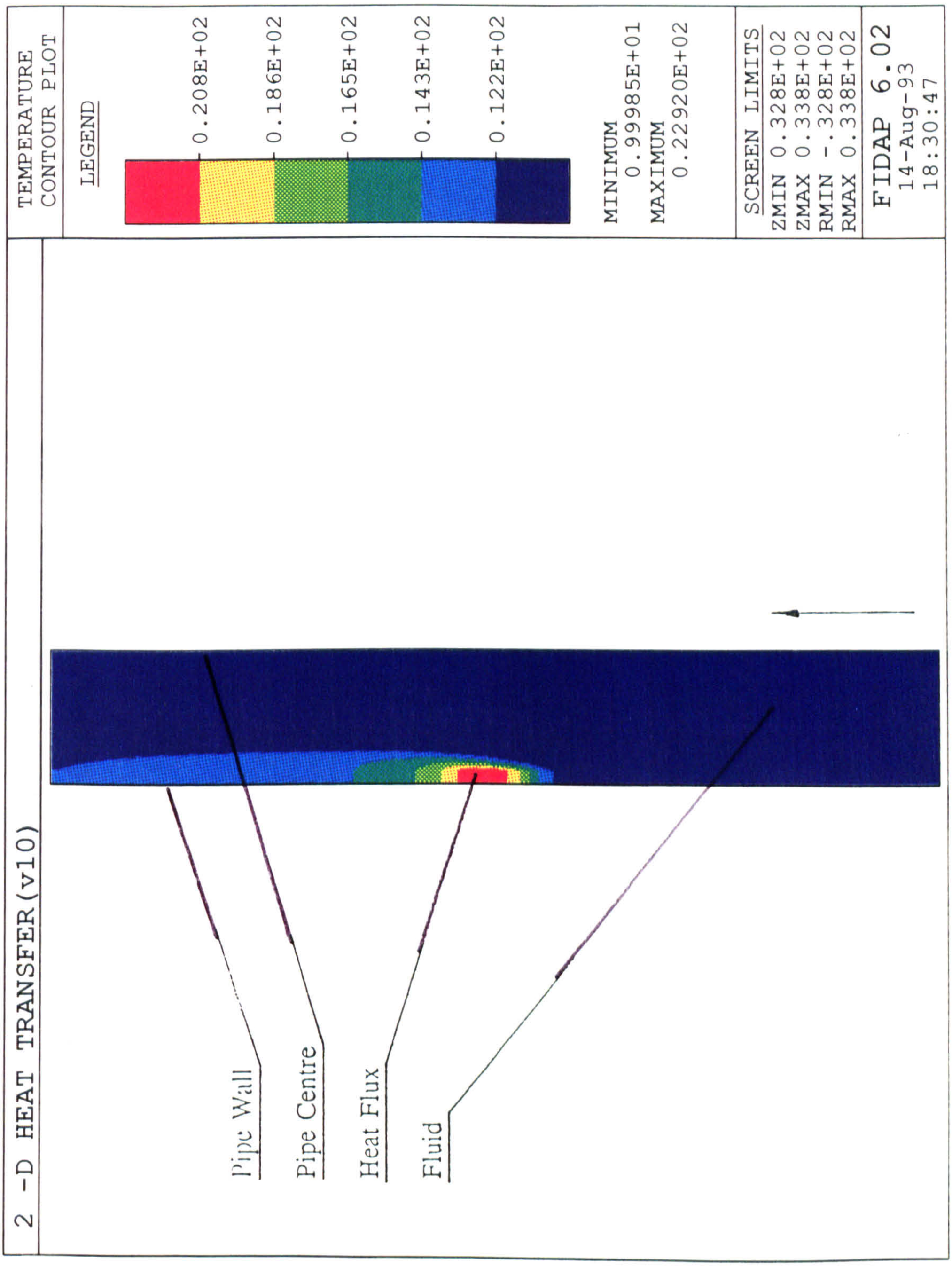

Fig. 3.3.6d. Vertical Pipe Temperature Distribution (Q = 17.63 ml s^{-1}, 40W)

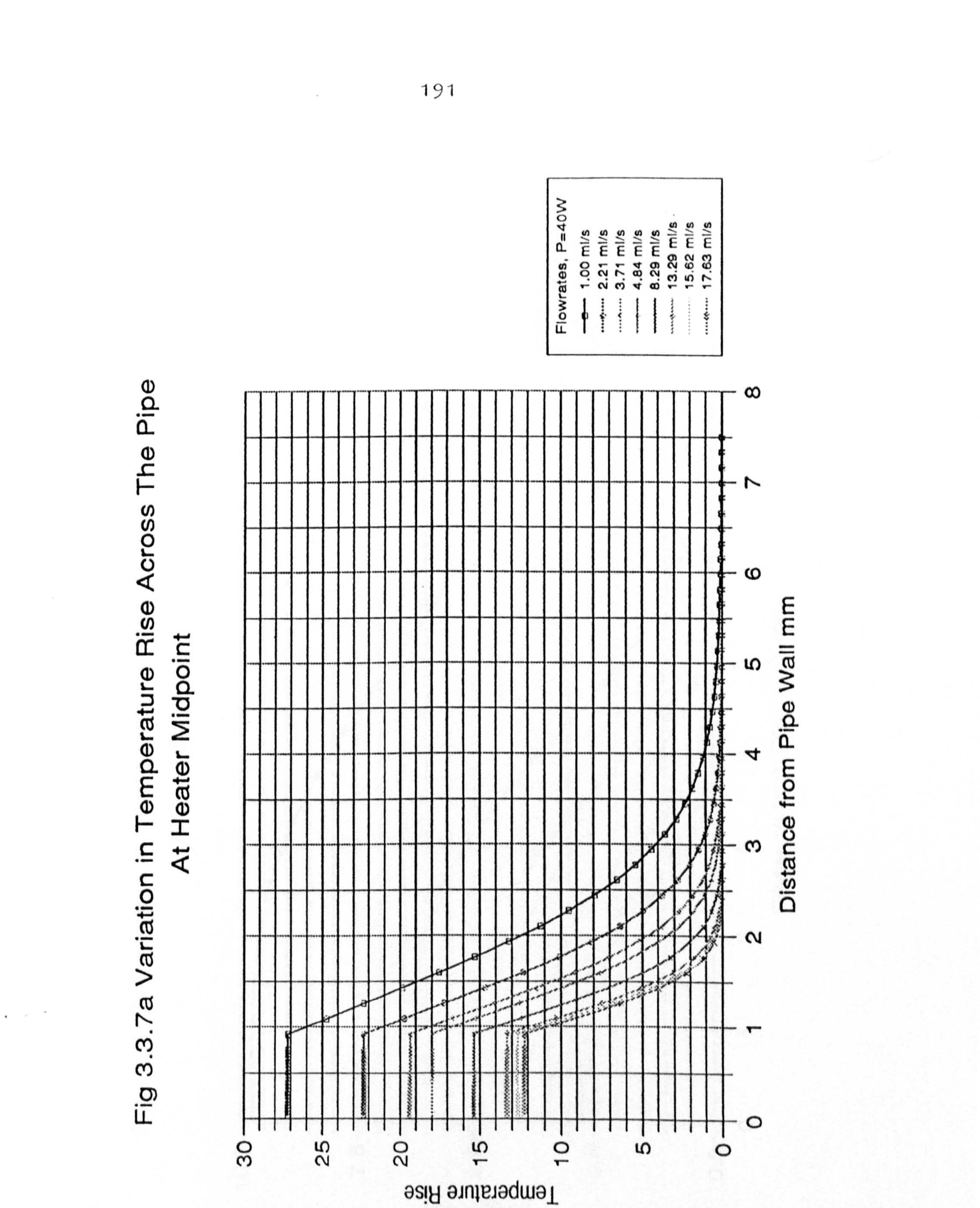

Fig 3.3.7a Variation in Temperature Rise Across The Pipe
At Heater Midpoint

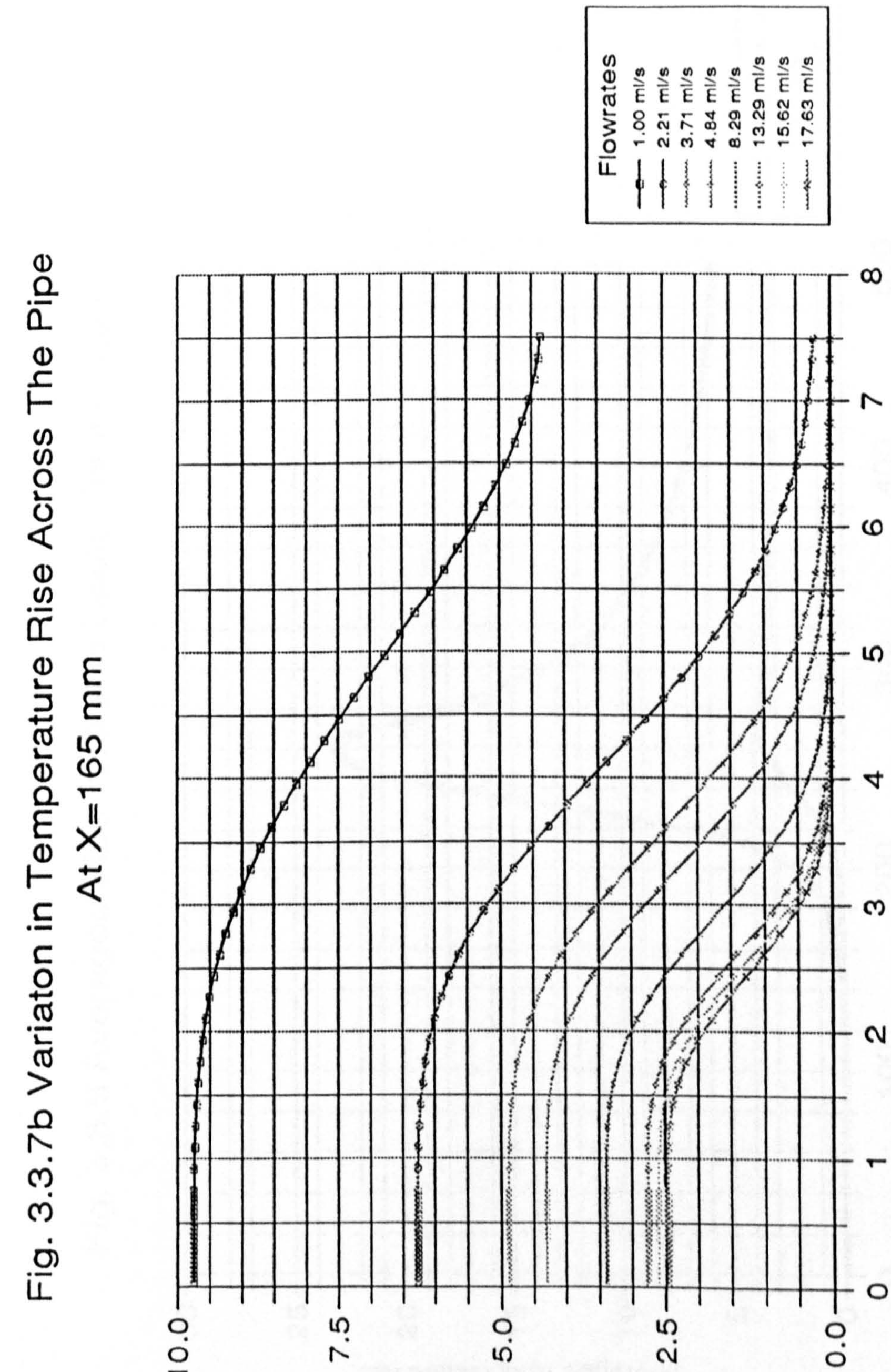

Fig. 3.3.7b Variaton in Temperature Rise Across The Pipe
At X=165 mm

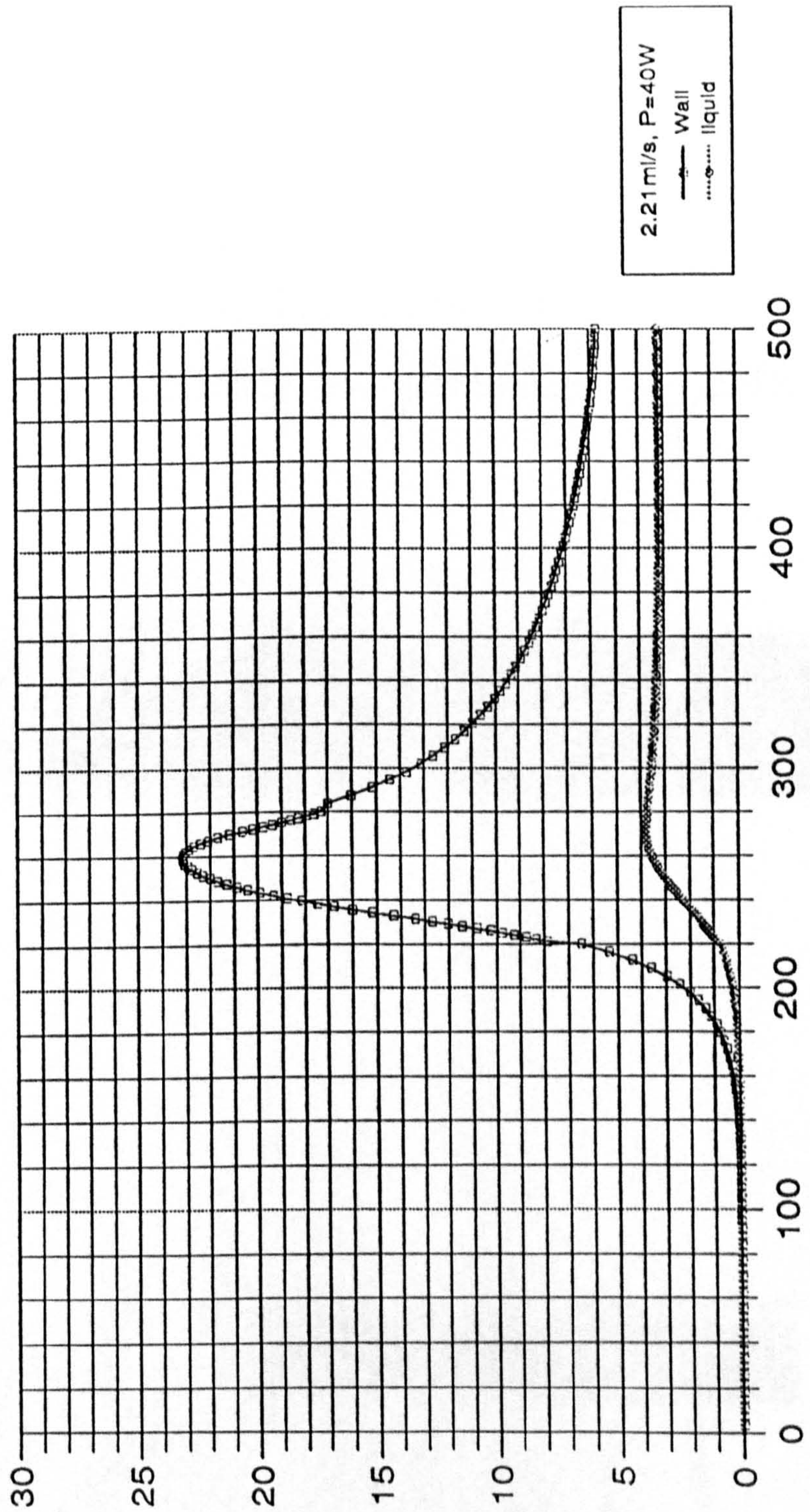

Fig. 3.3.8 Averaged Pipe Wall and Liquid Temperature

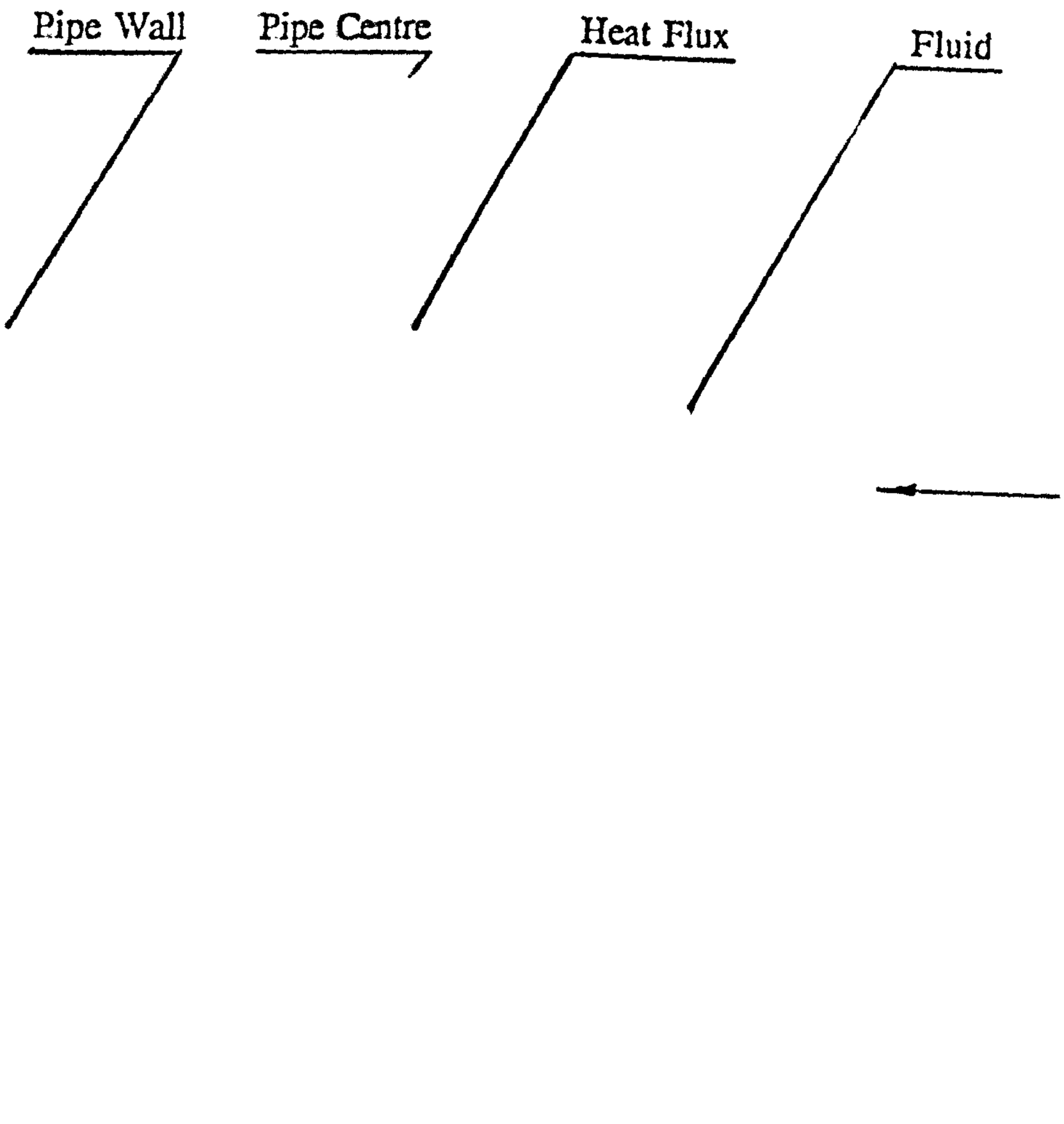

Fig. 3.3.9. Horizontal Pipe Temperature Distribution

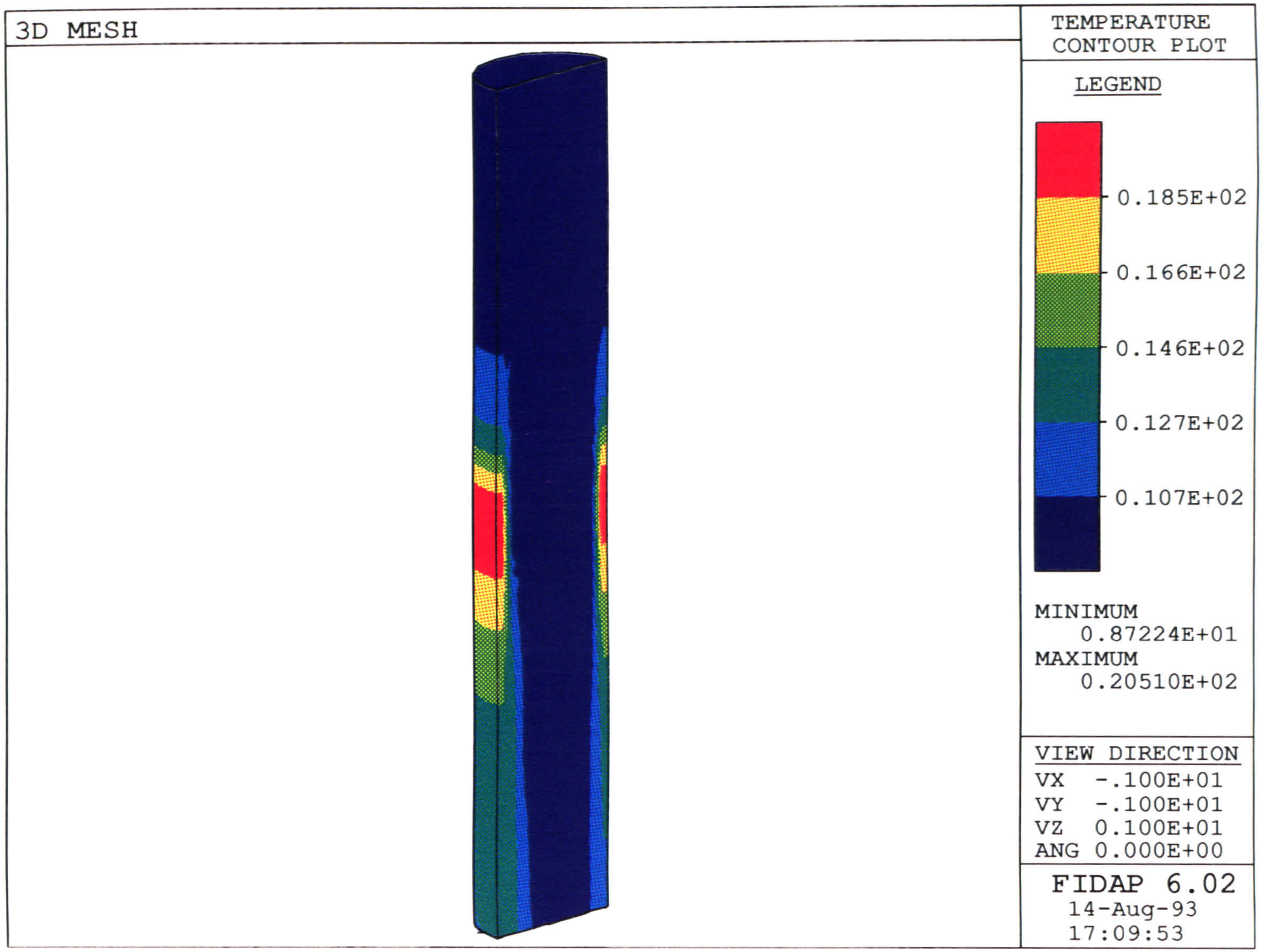
3D MESH
TEMPERATURE
CONTOUR PLOT
LEGEND
0.185E+02
0.166E+02
0.146E+02
0.127E+02
0.107E+02
MINIMUM
0.87224E+01
MAXIMUM
0.20510E+02
VIEW DIRECTION
VX -.100E+01
VY -.100E+01
VZ 0.100E+01
ANG 0.000E+00
FIDAP 6.02
14-Aug-93
17:09:53

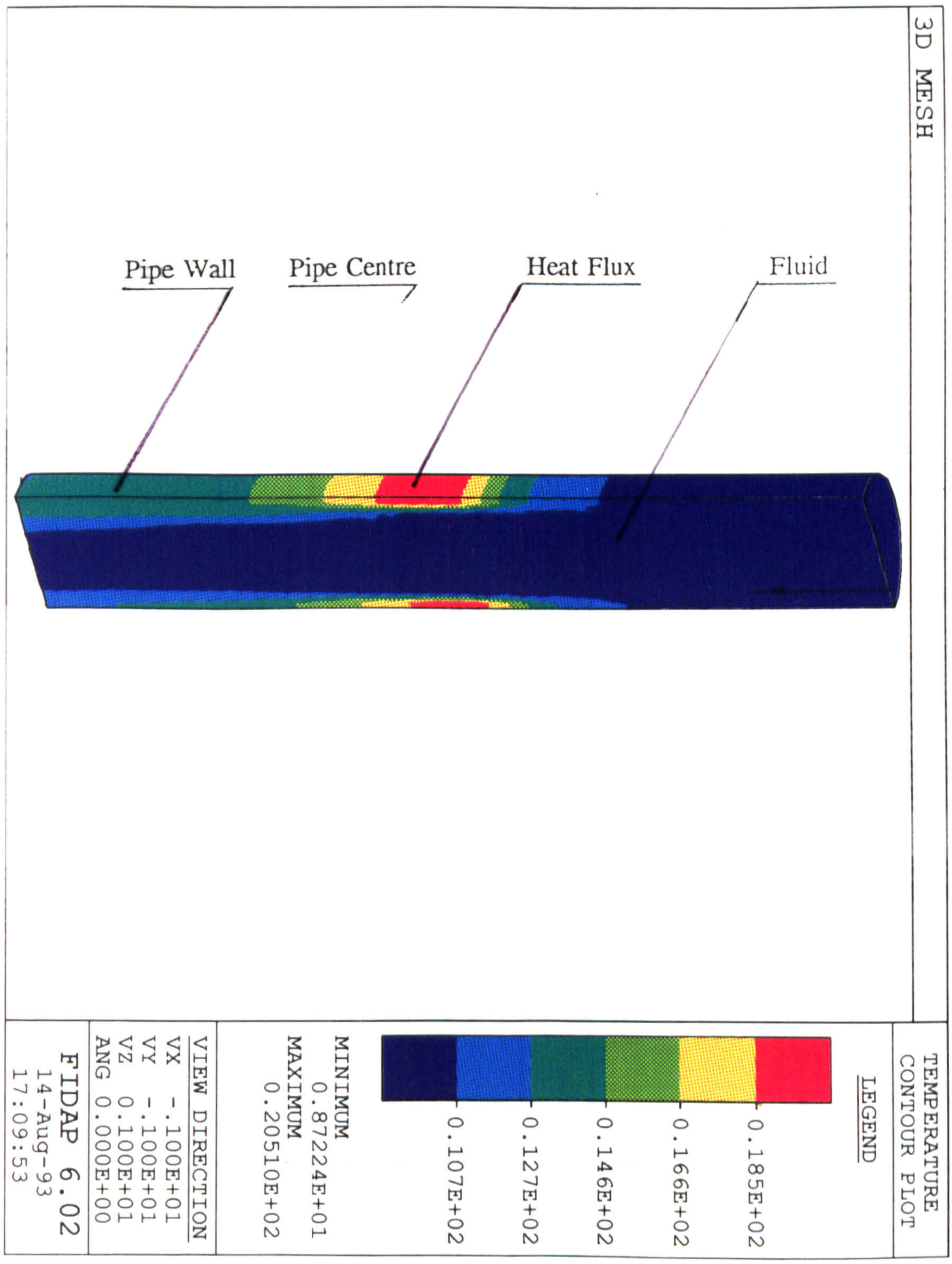

Fig. 3.3.9. Horizontal Pipe Temperature Distribution

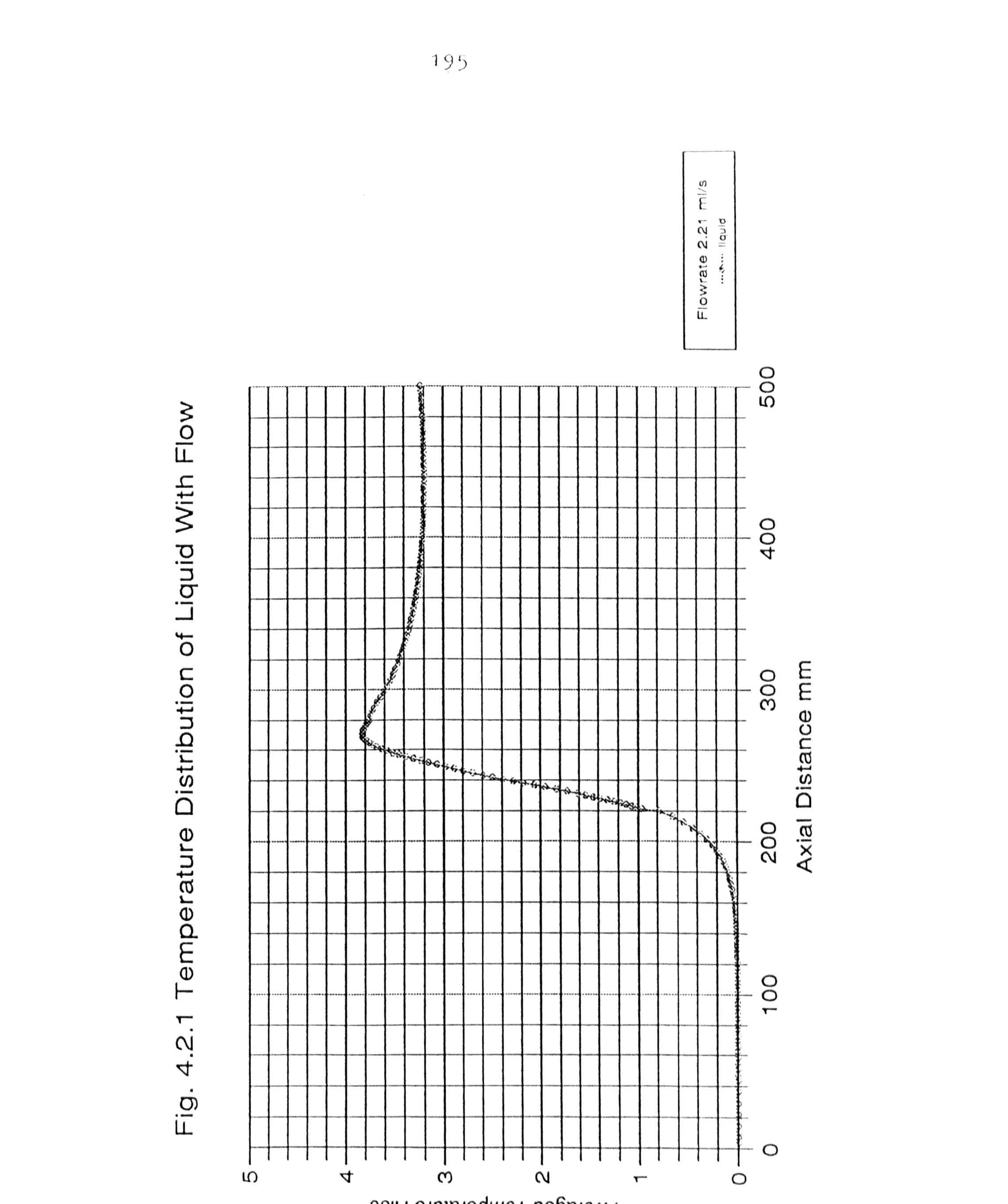

Fig. 4.2.1 Temperature Distribution of Liquid With Flow

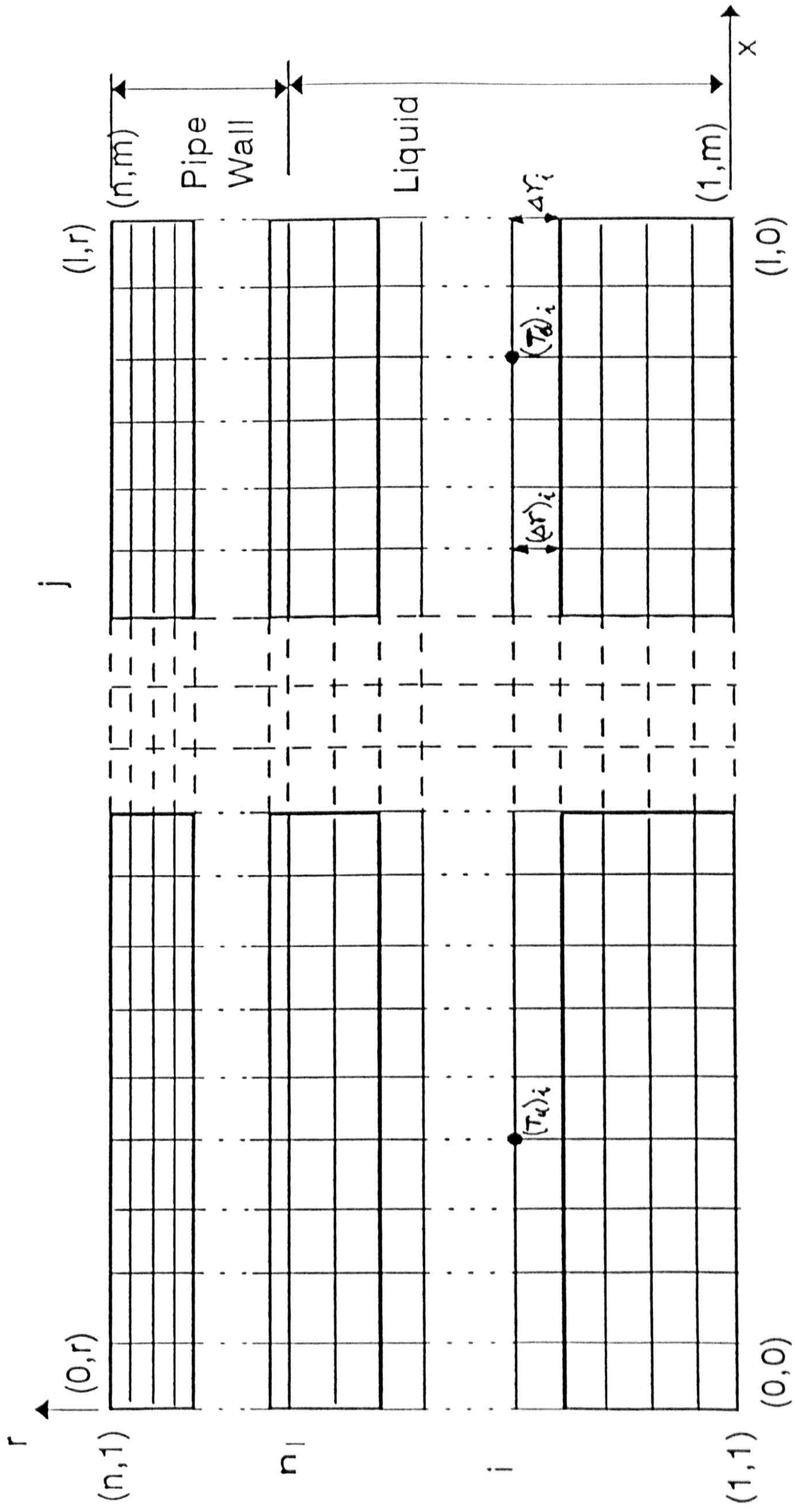

Fig 4.2.2. Reference Mesh for Notations

Fig. 4.2.3 Effect of Heater - Transducers Separation on the Flowmeter

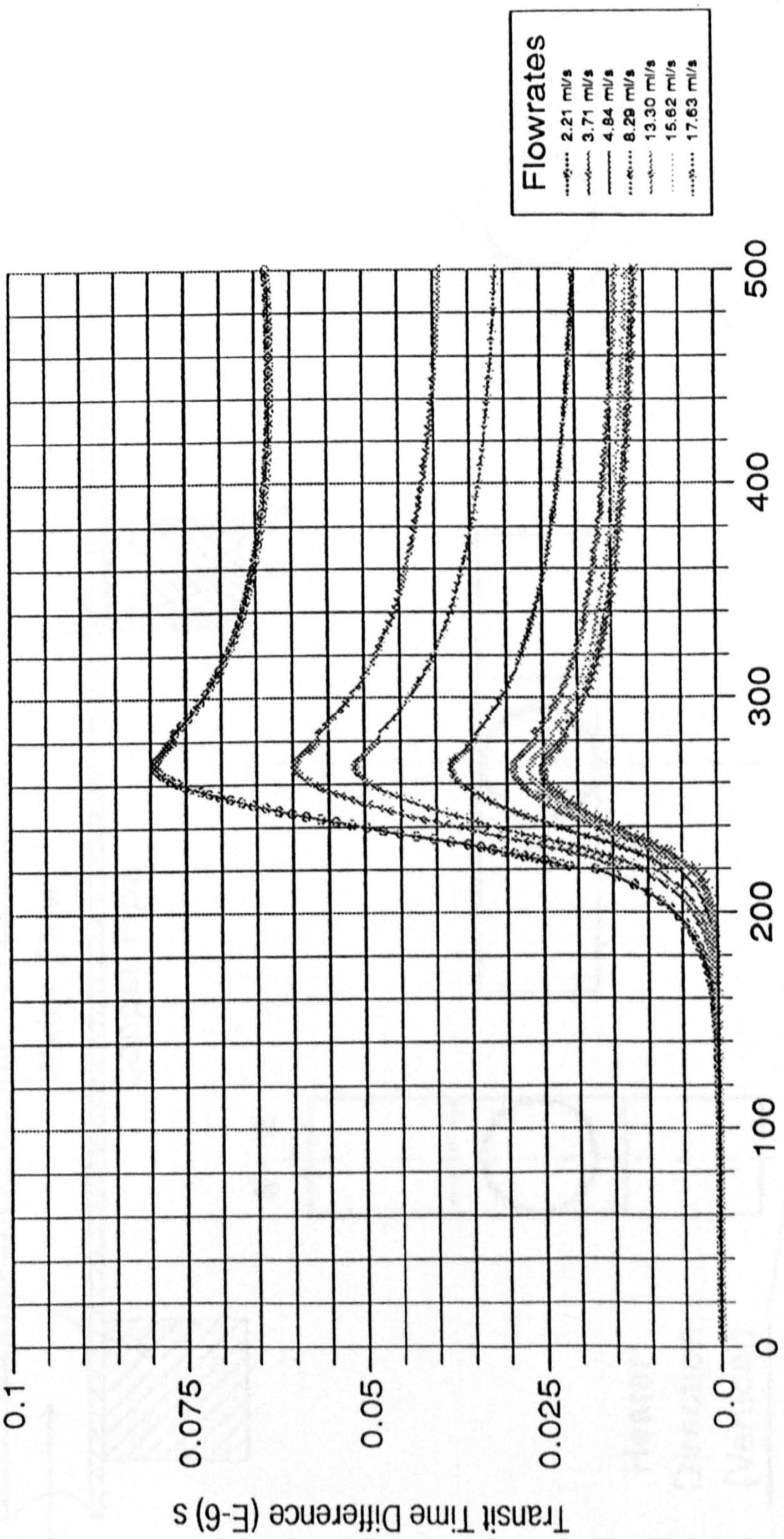

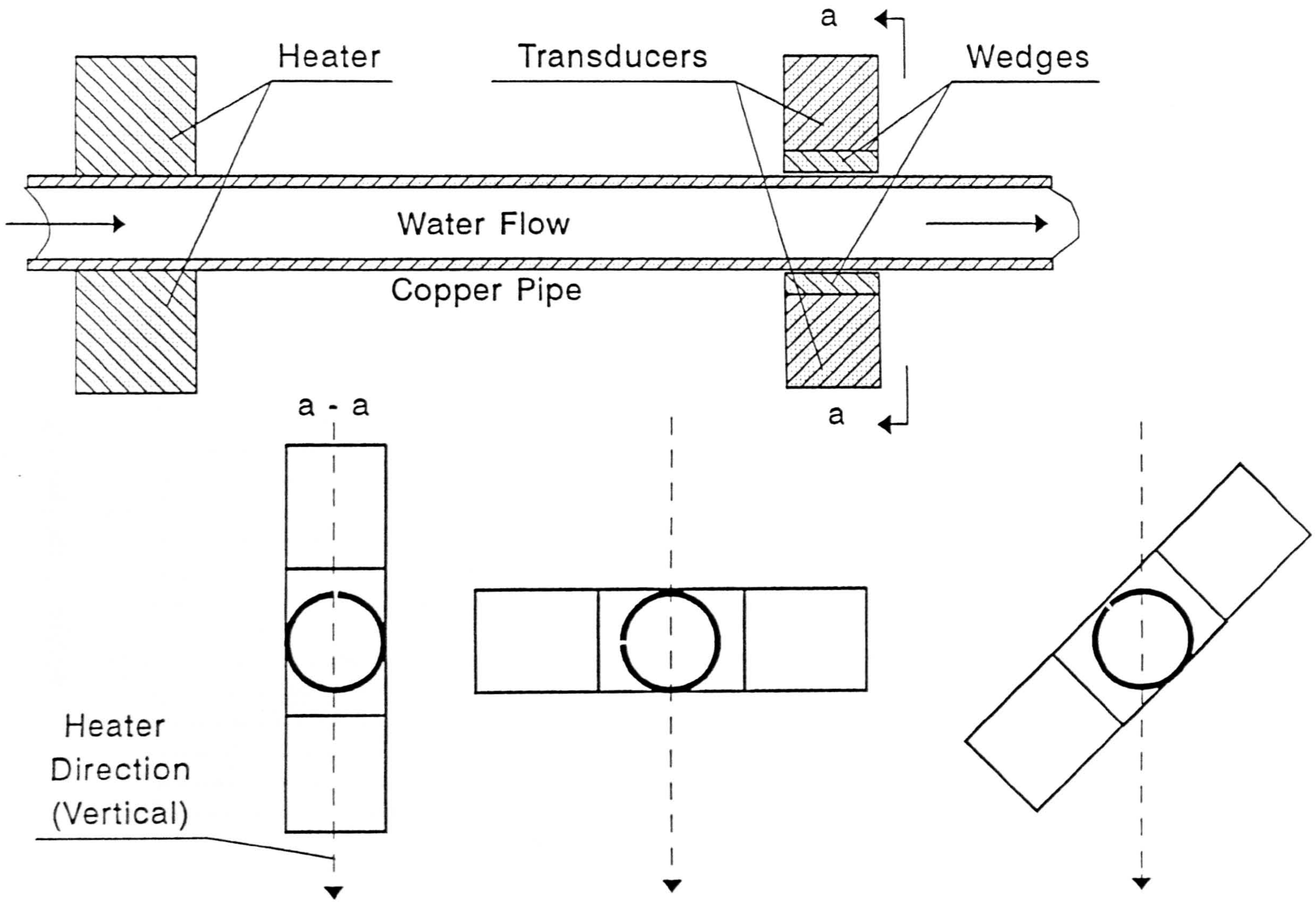

Fig 4.2.4. Transducer Clamp-on Angles

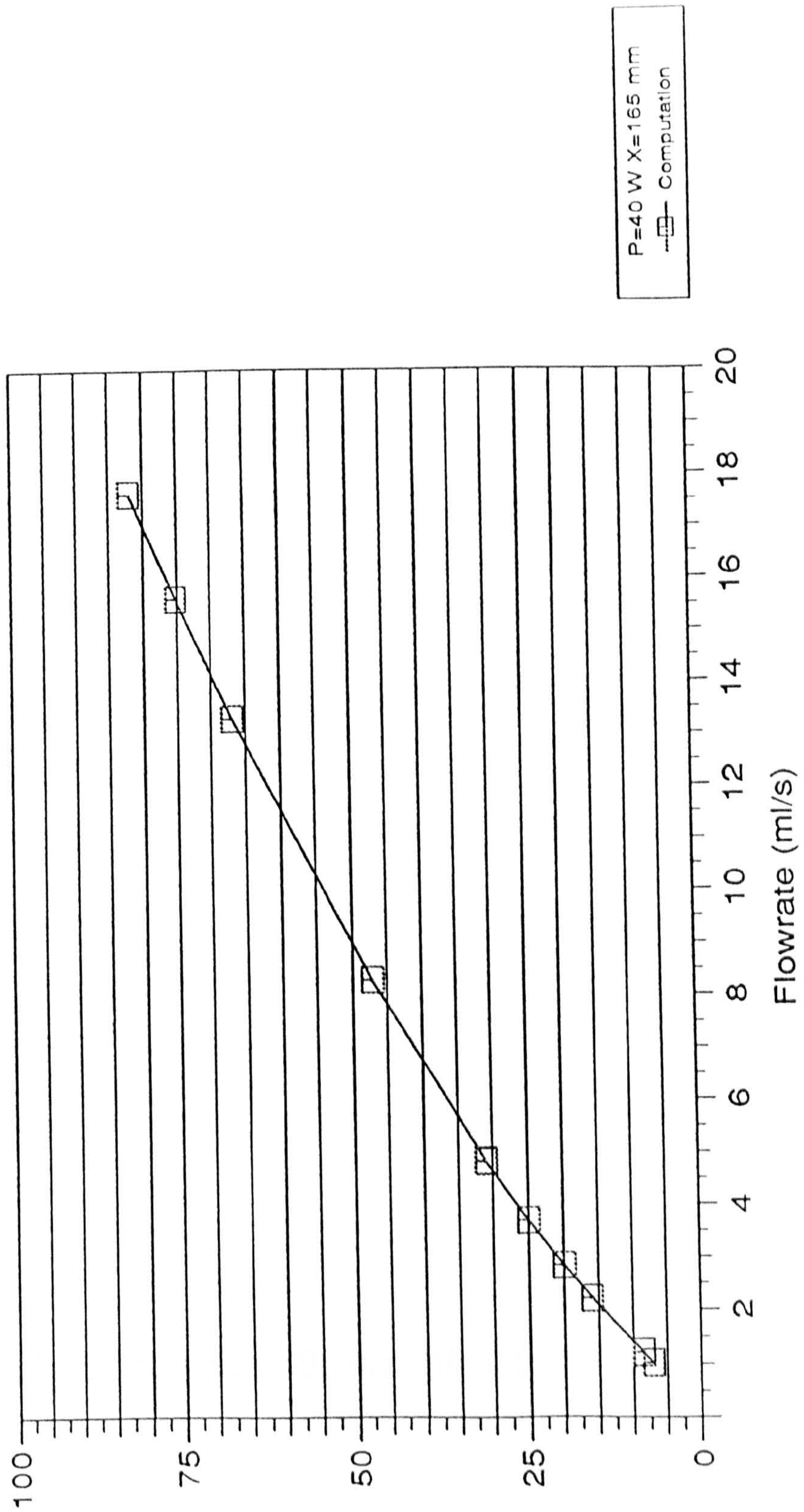

Fig. 4.2.5 Typical Calibration Curve for Vertical Pipe Orientation

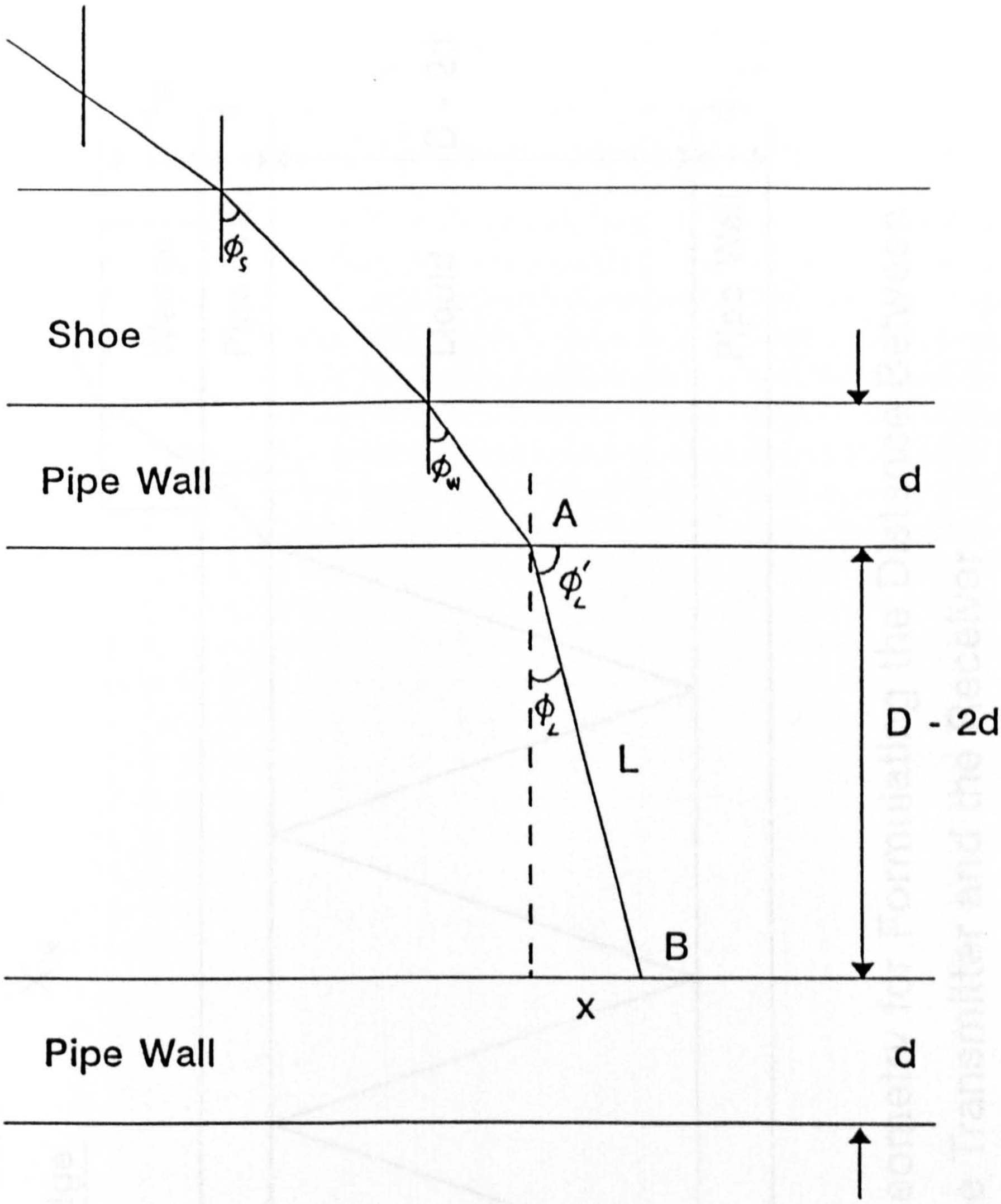

Fig 4.4.1. Ultrasonic Beam at Interfaces

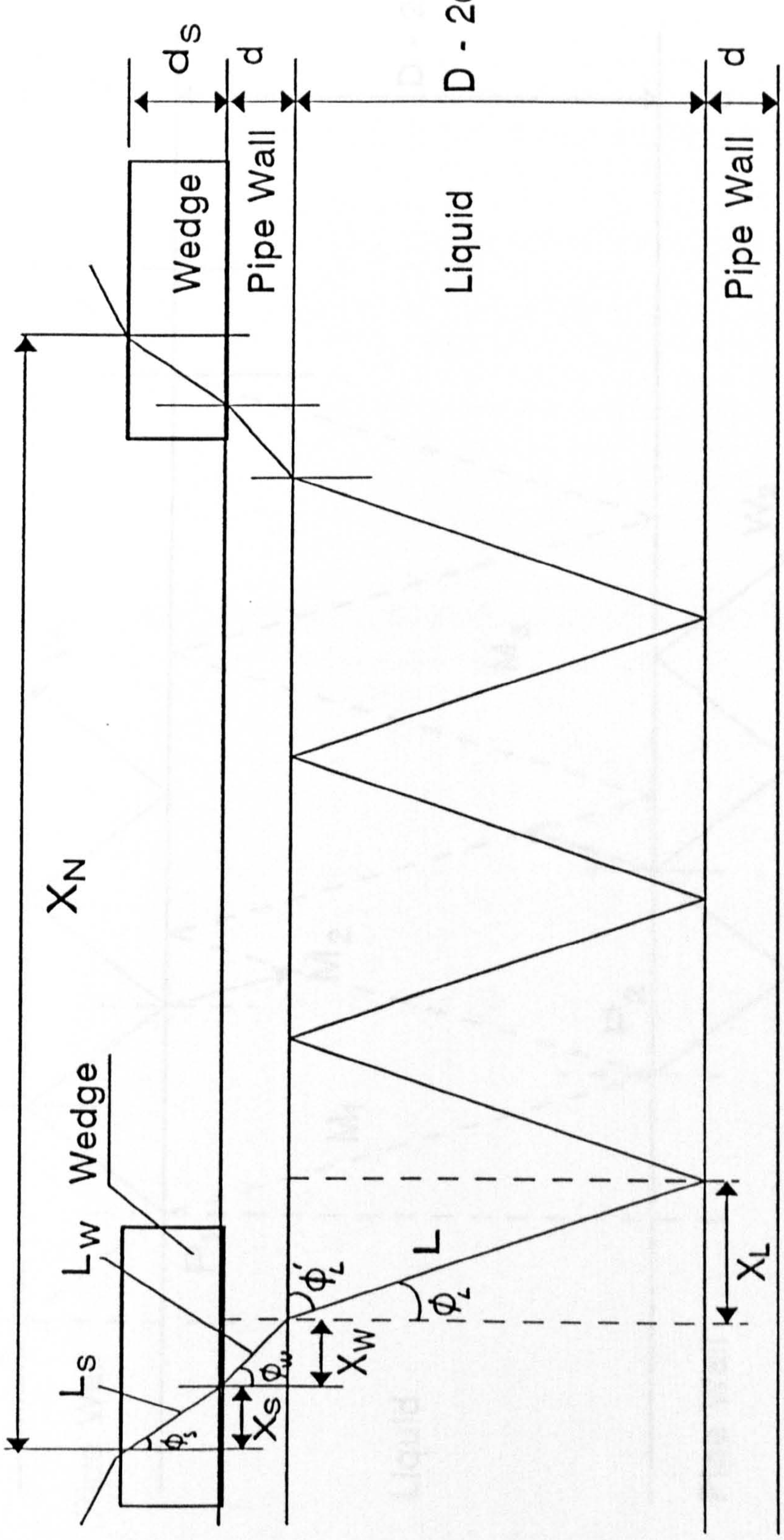

Fig 4.4.2. Geometry for Formulating the Distance Between the Transmitter and the Receiver

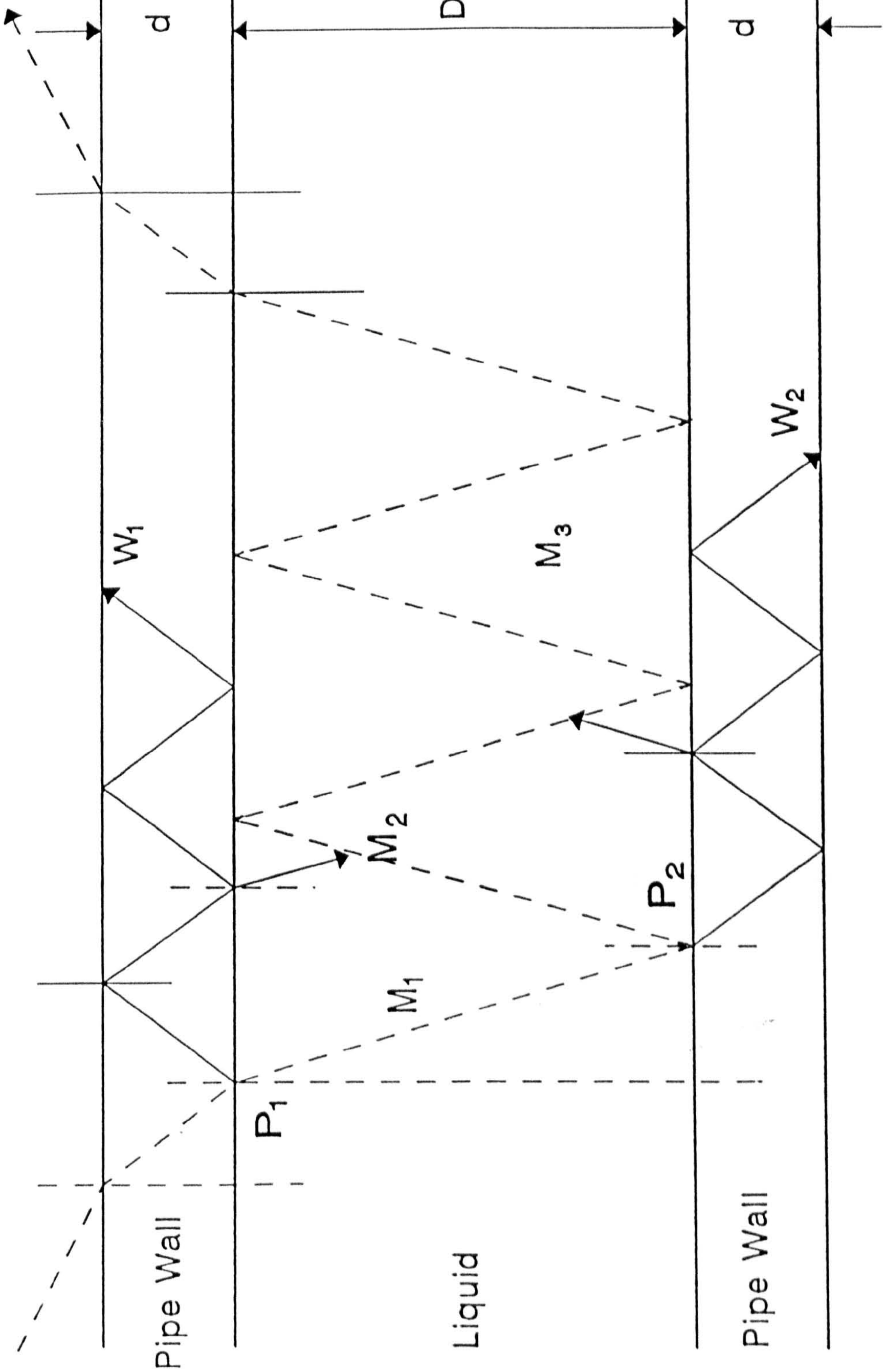

Fig 4.4.3. Propagation of Ultrasonic Beams

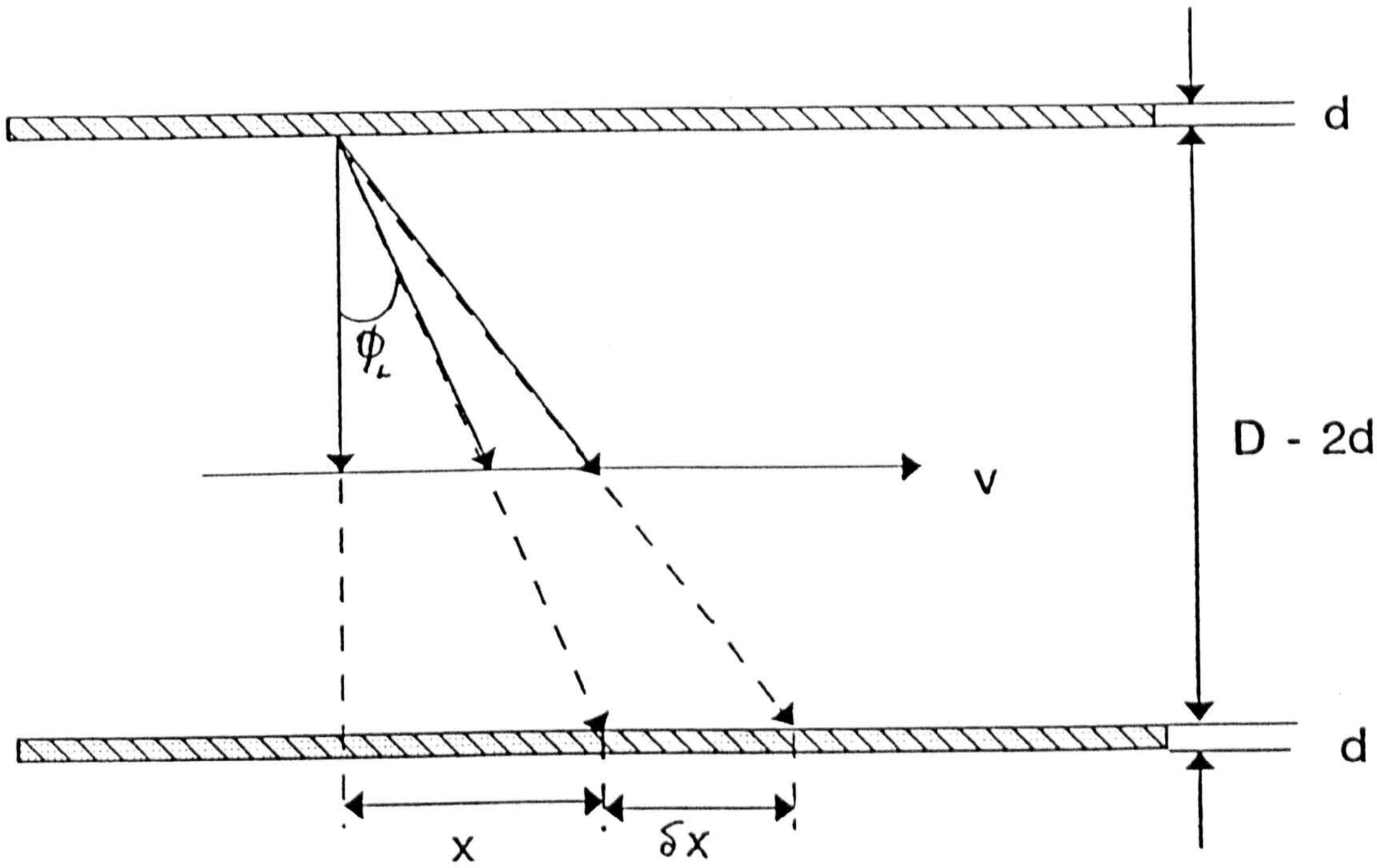

Fig 4.5.1. Geometry of Beam Shift Due to Flow

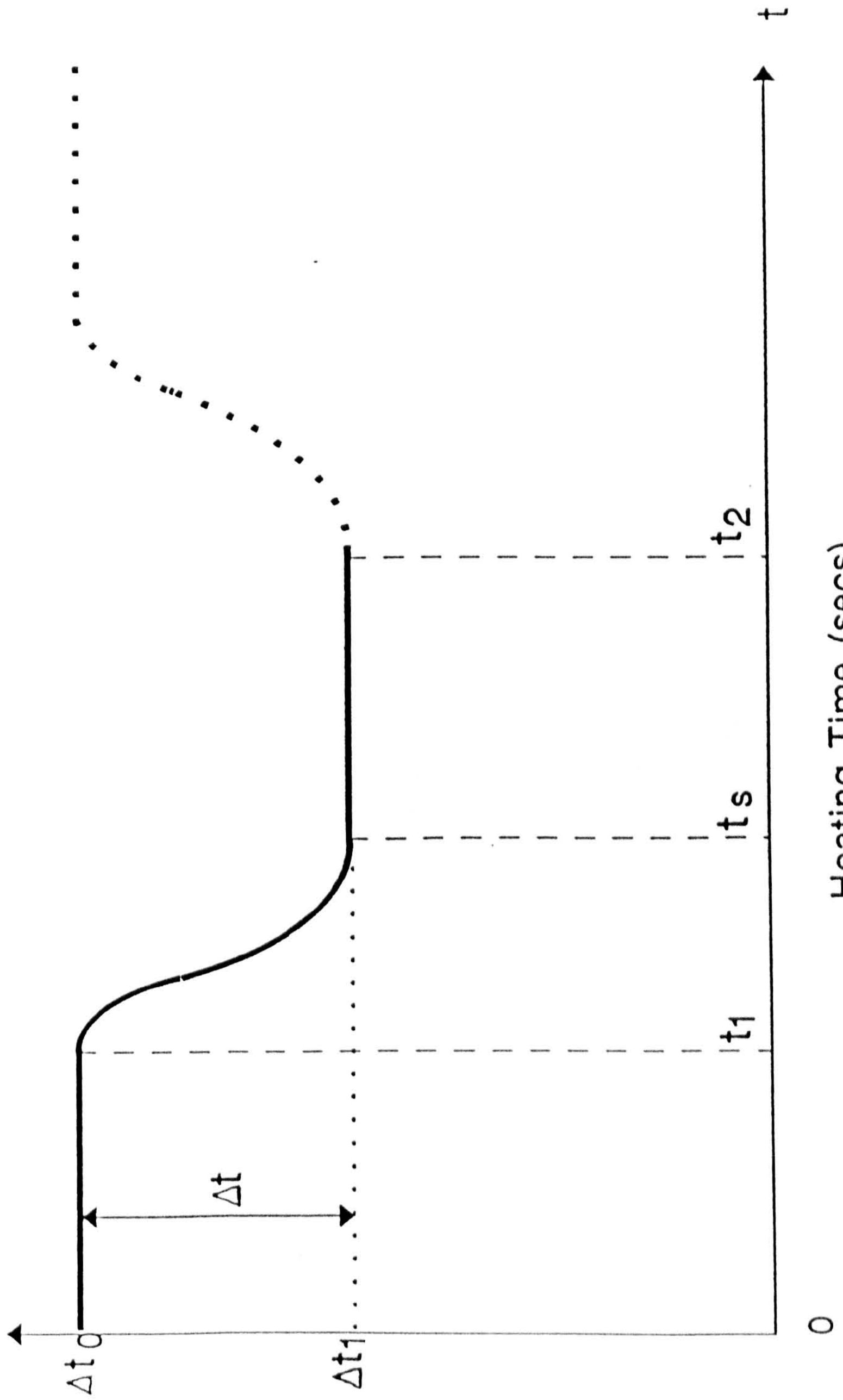

Fig 5.2.1. Principle of Transit Time Measurement

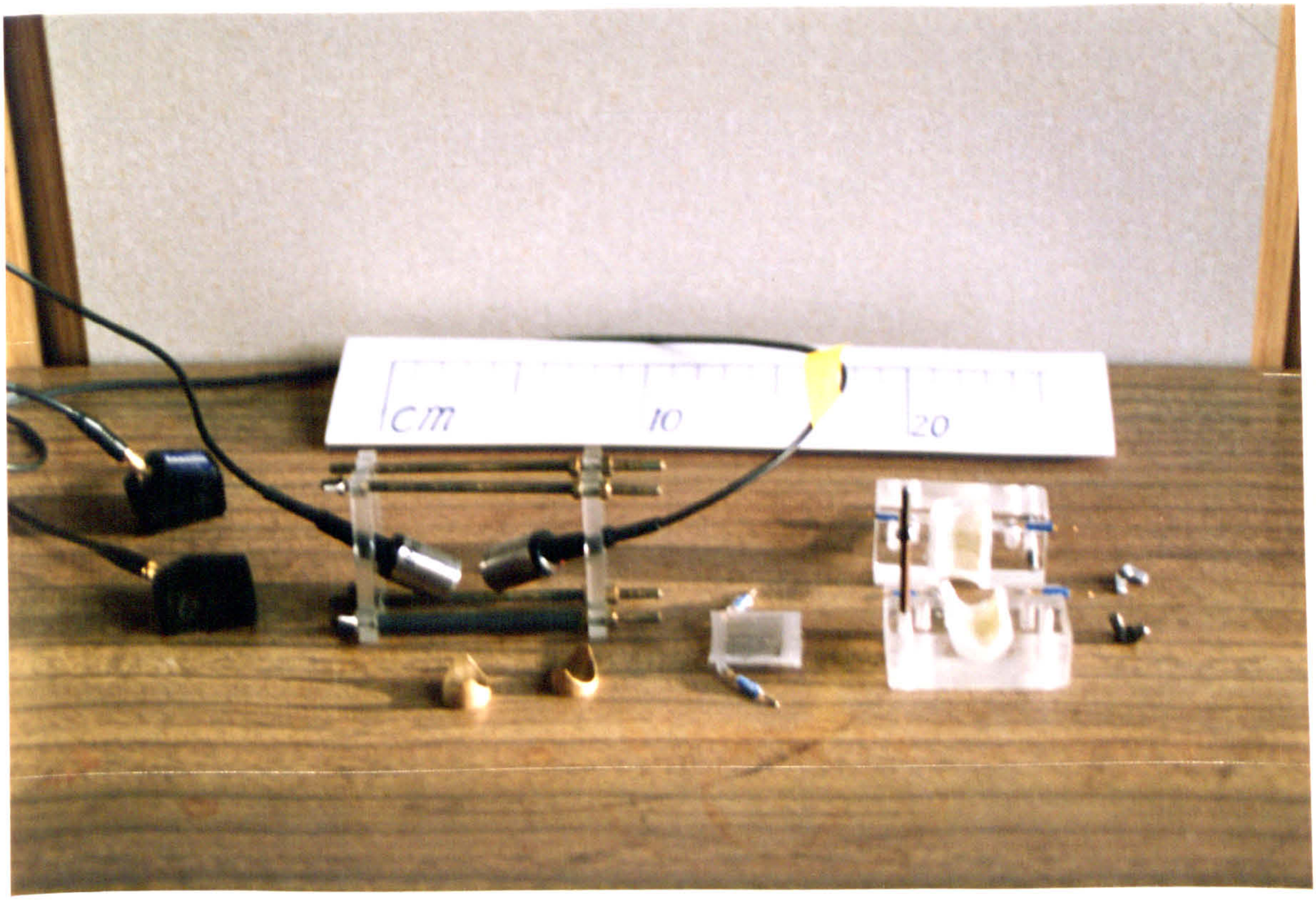

Fig. 5.3.1. Transducer Shoes and Clamps

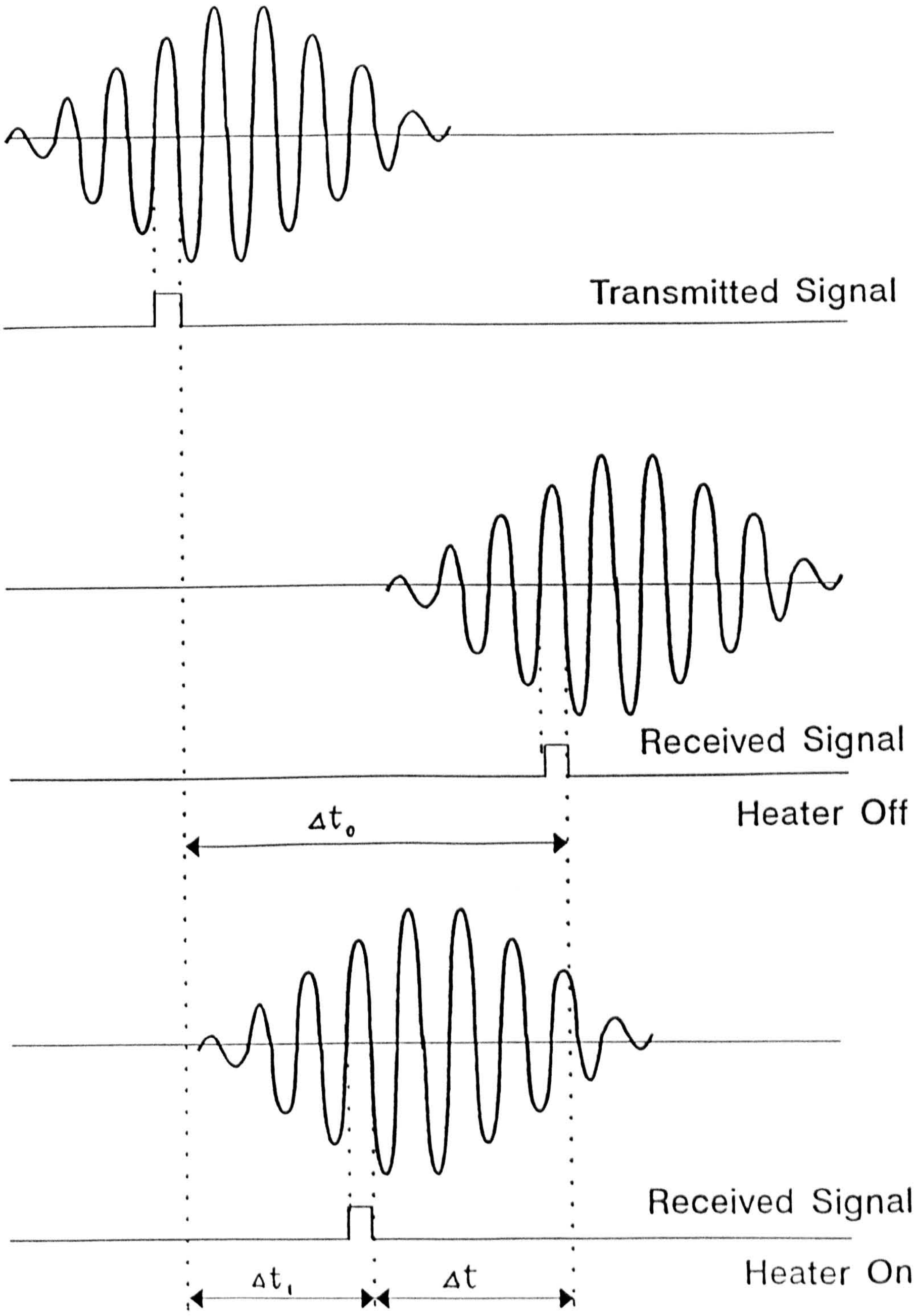

Fig 5.3.2. Signal Processing for Transit Measurement

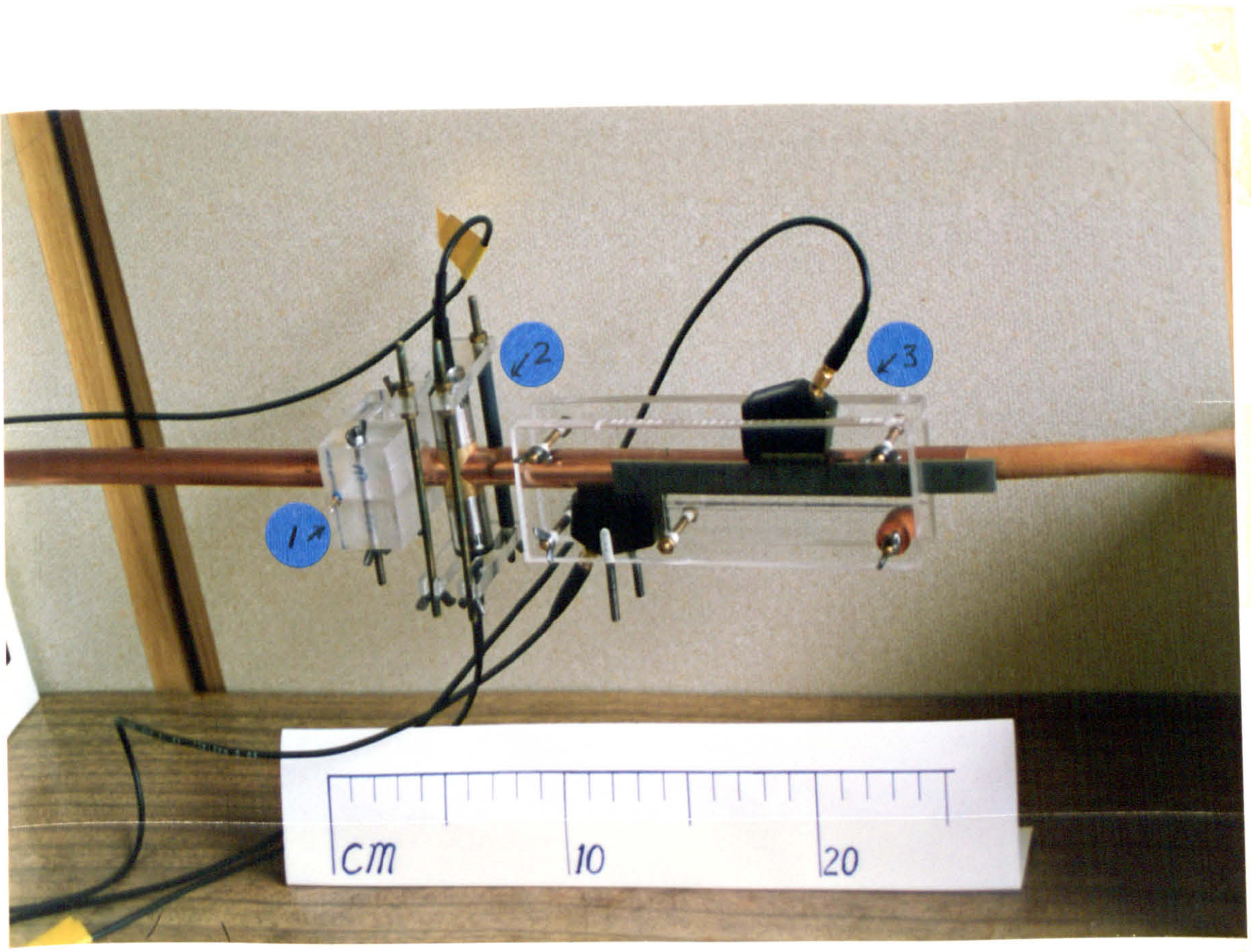

Fig. 5.3.3. Elements of the Proposed Flowmeter

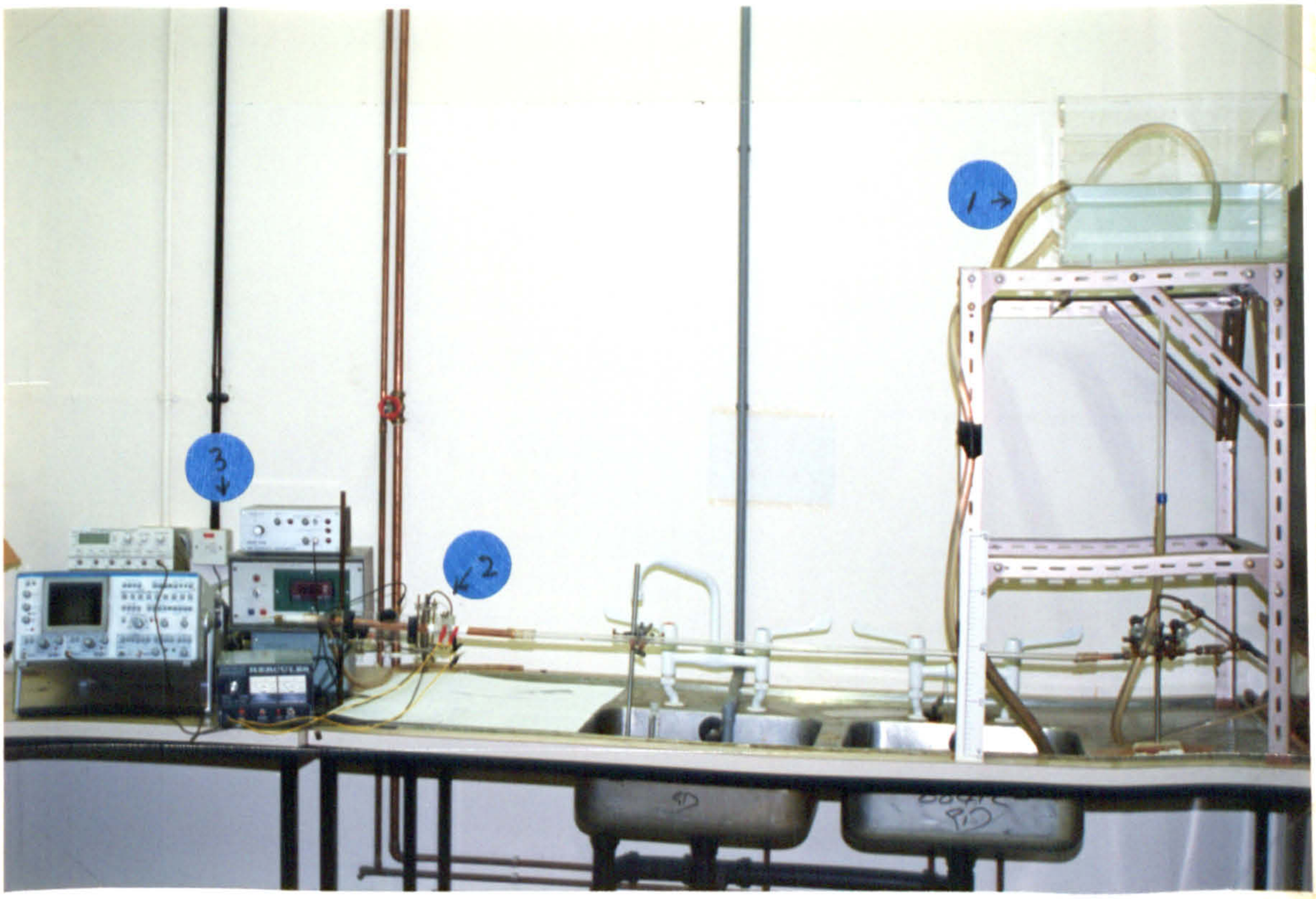

Fig. 6.1.1. The Preliminary Experimental System

1. Oscilloscope
2. Signal Generator
3. Spike Generator
4. Temperature Indicator
5. DC Power Supply
6. Test Section

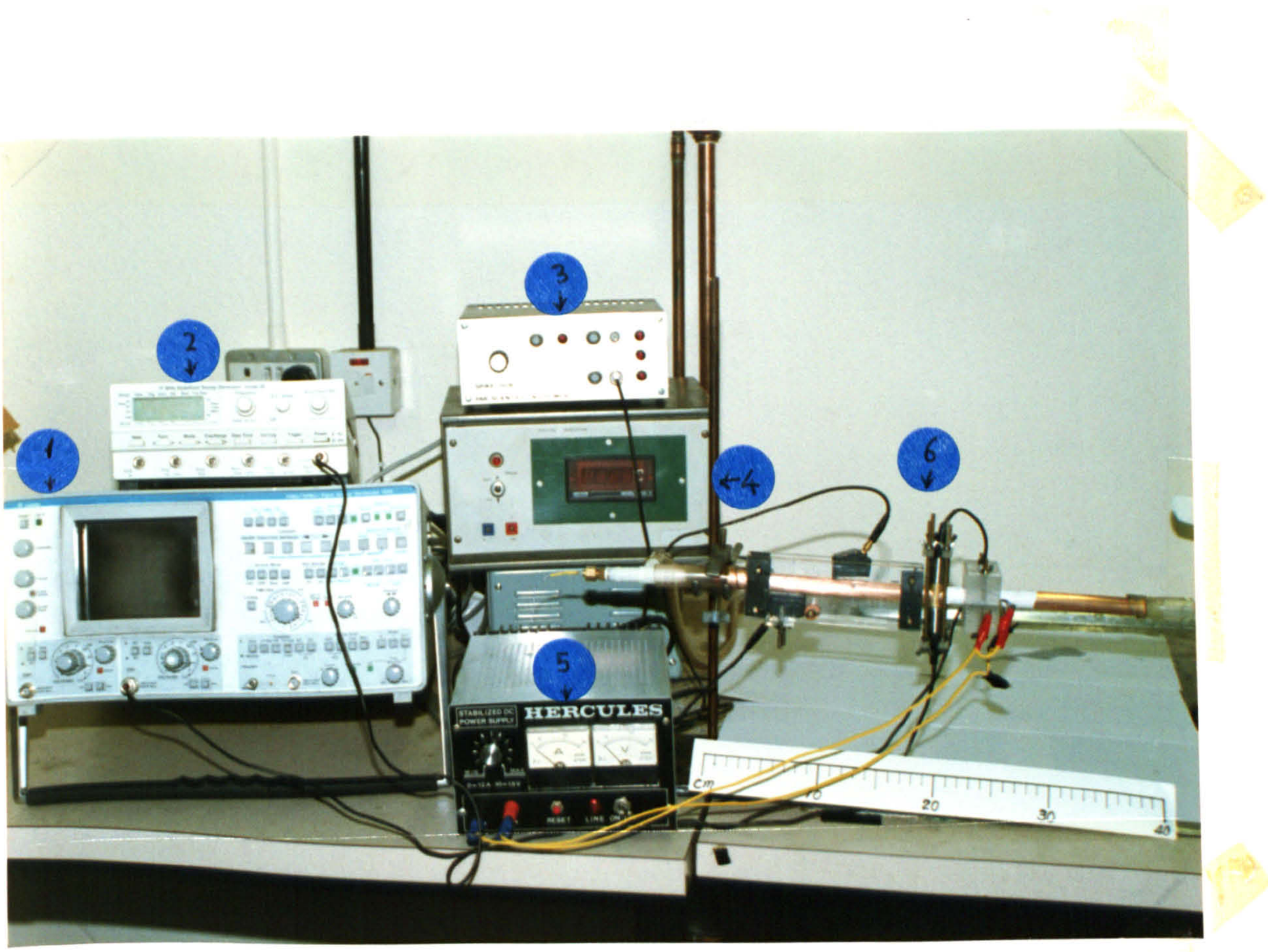

Fig. 6.1.2. Instrumentation for the Preliminary Experiments

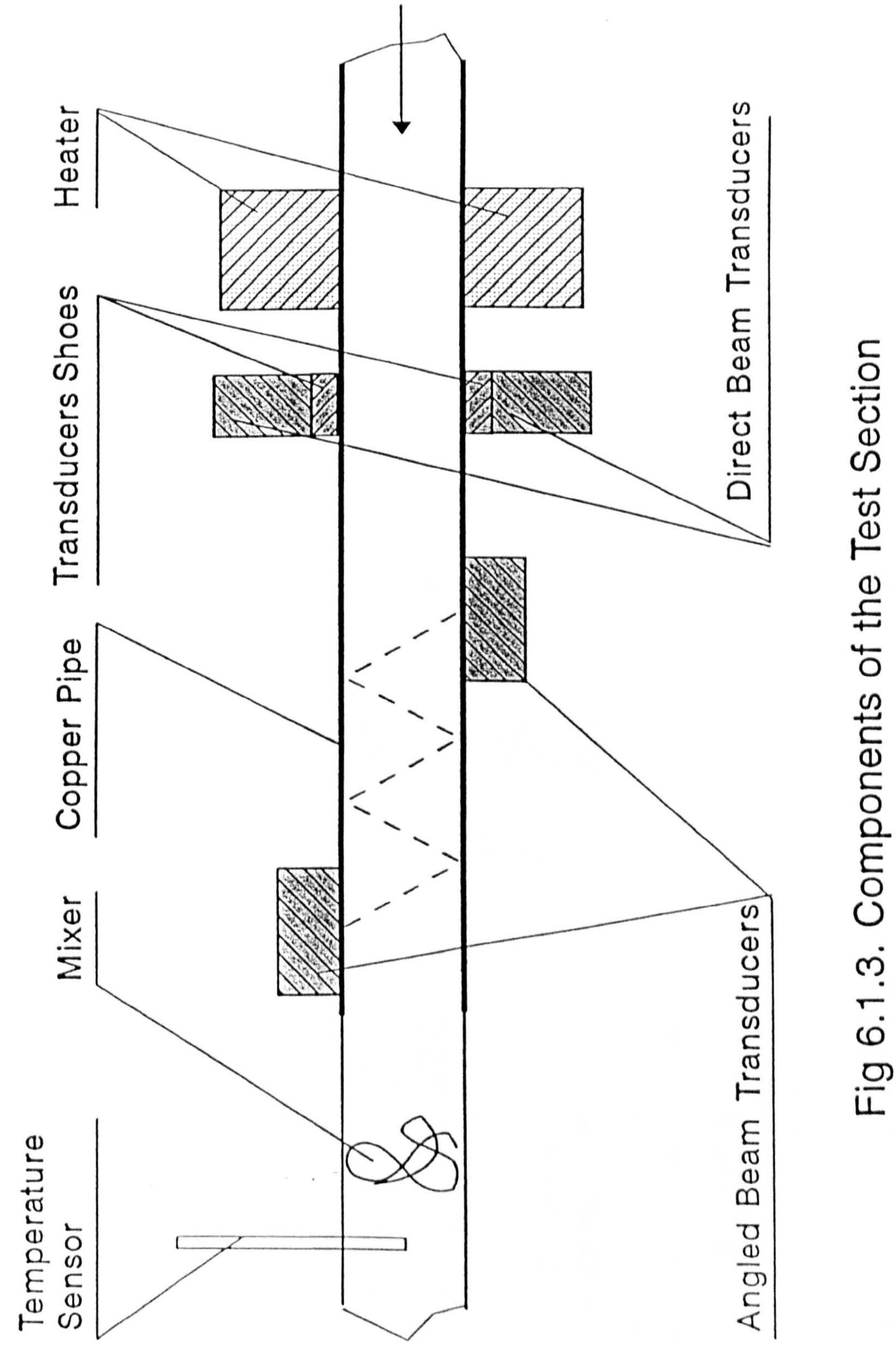

Fig 6.1.3. Components of the Test Section

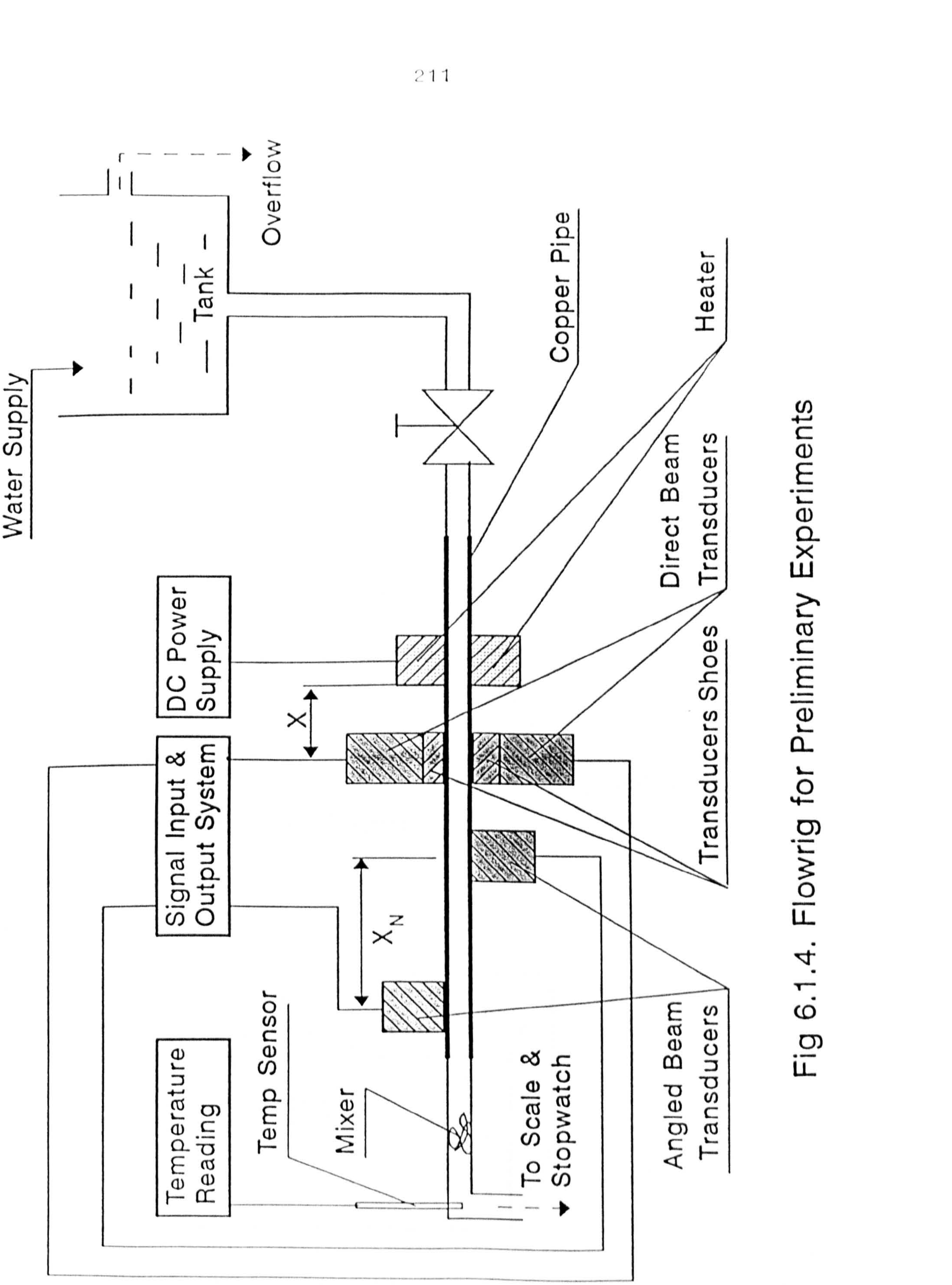

Fig 6.1.4. Flowrig for Preliminary Experiments

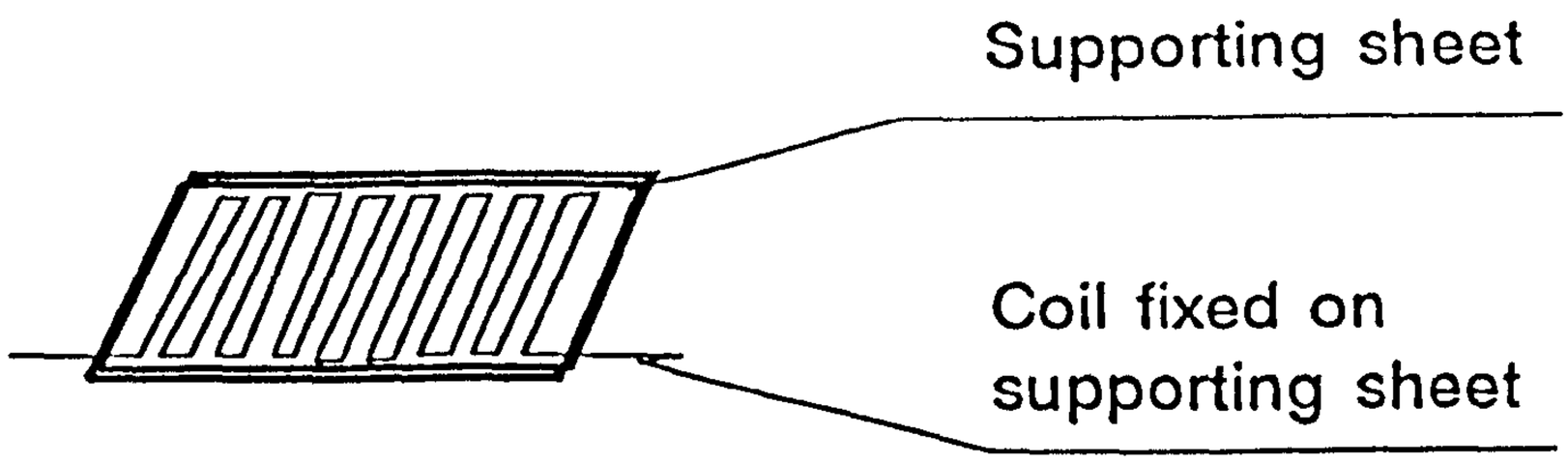

Fig 6.2.1a. Heating Element

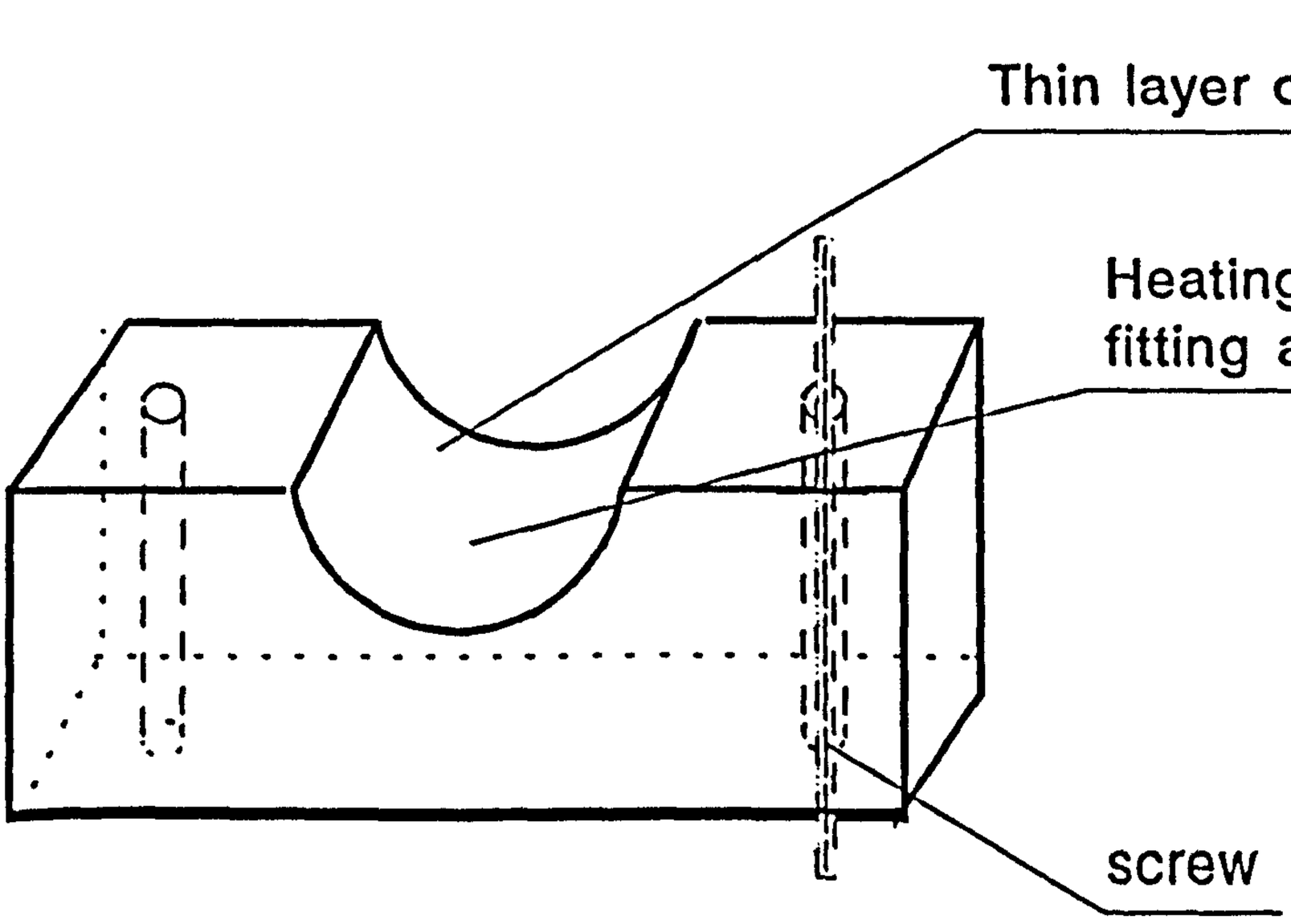

Fig 6.2.1b. Heater Frame

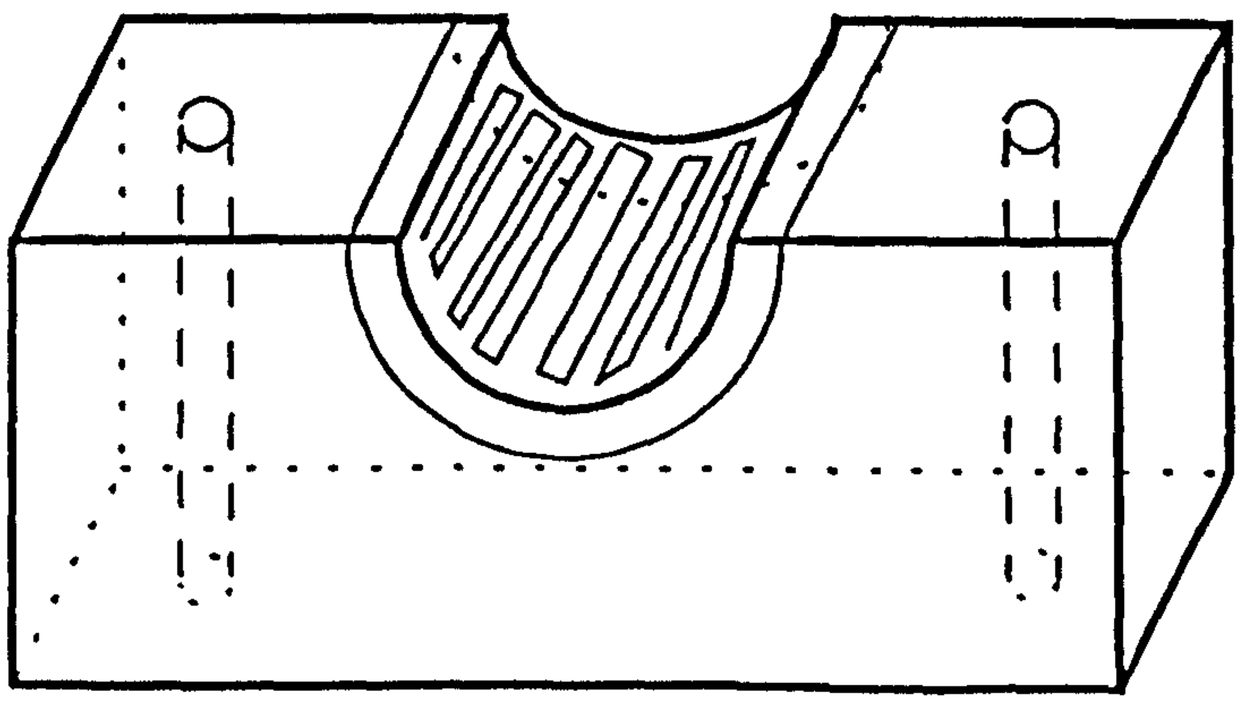

Fig 6.2.1c. Half of the Heater

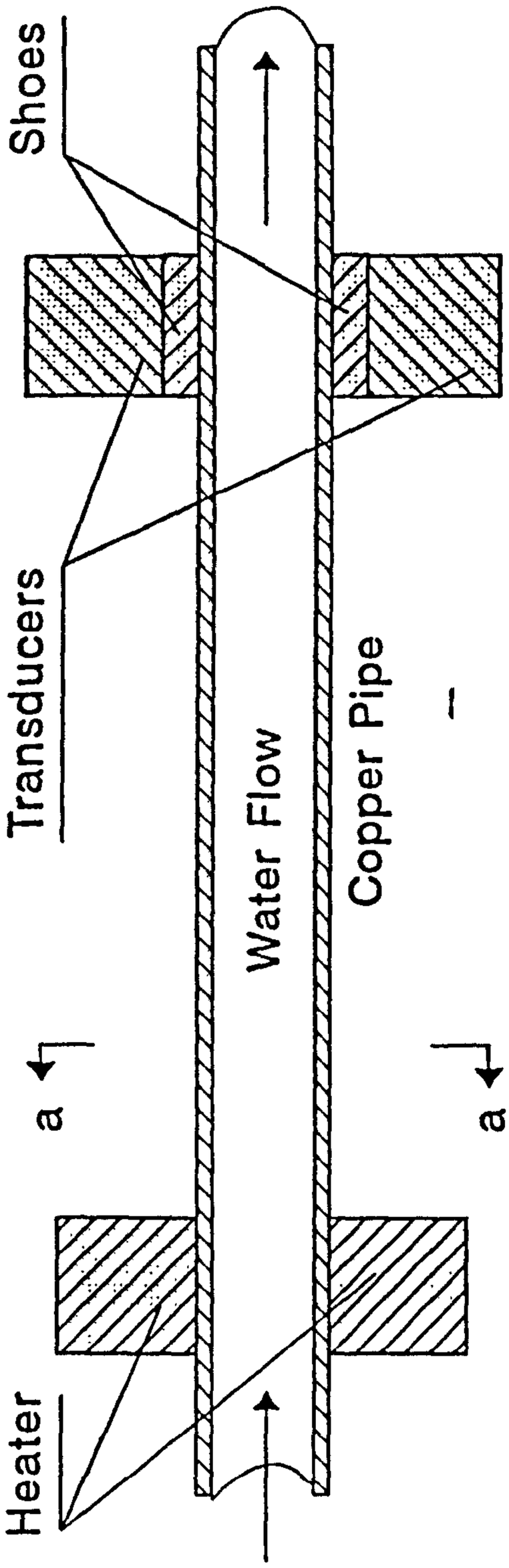

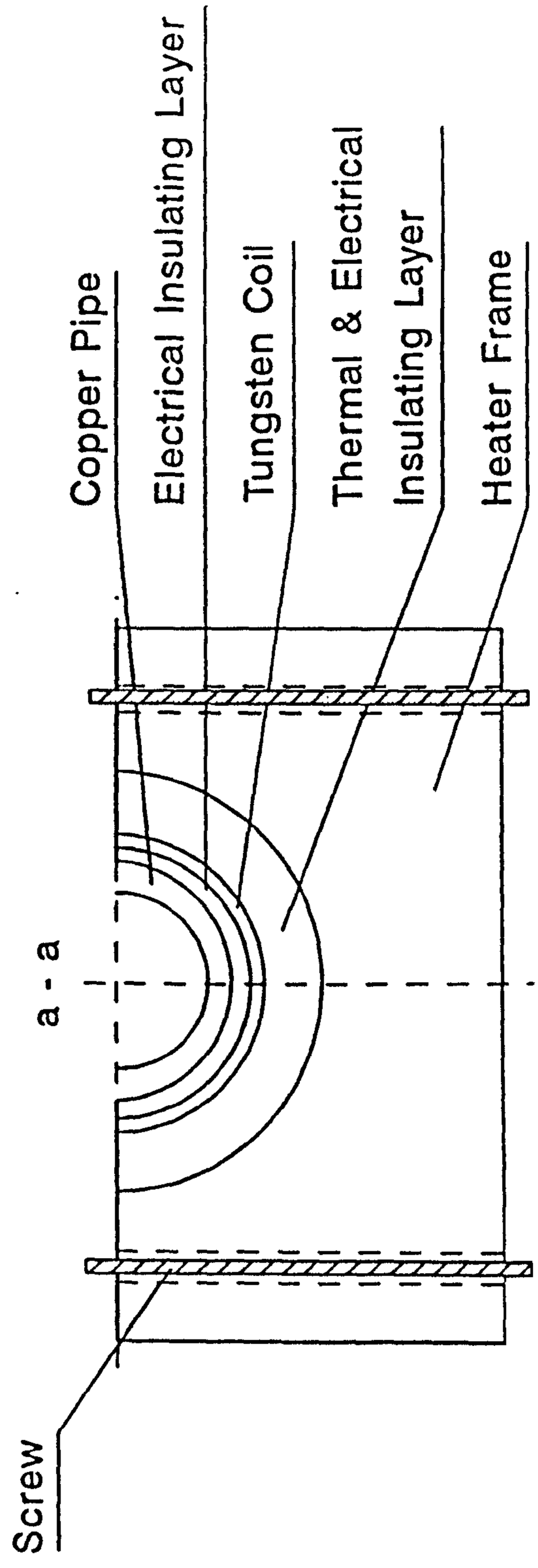

Fig 6.2.1d. Cross-Section View of the Clamp-on Heater

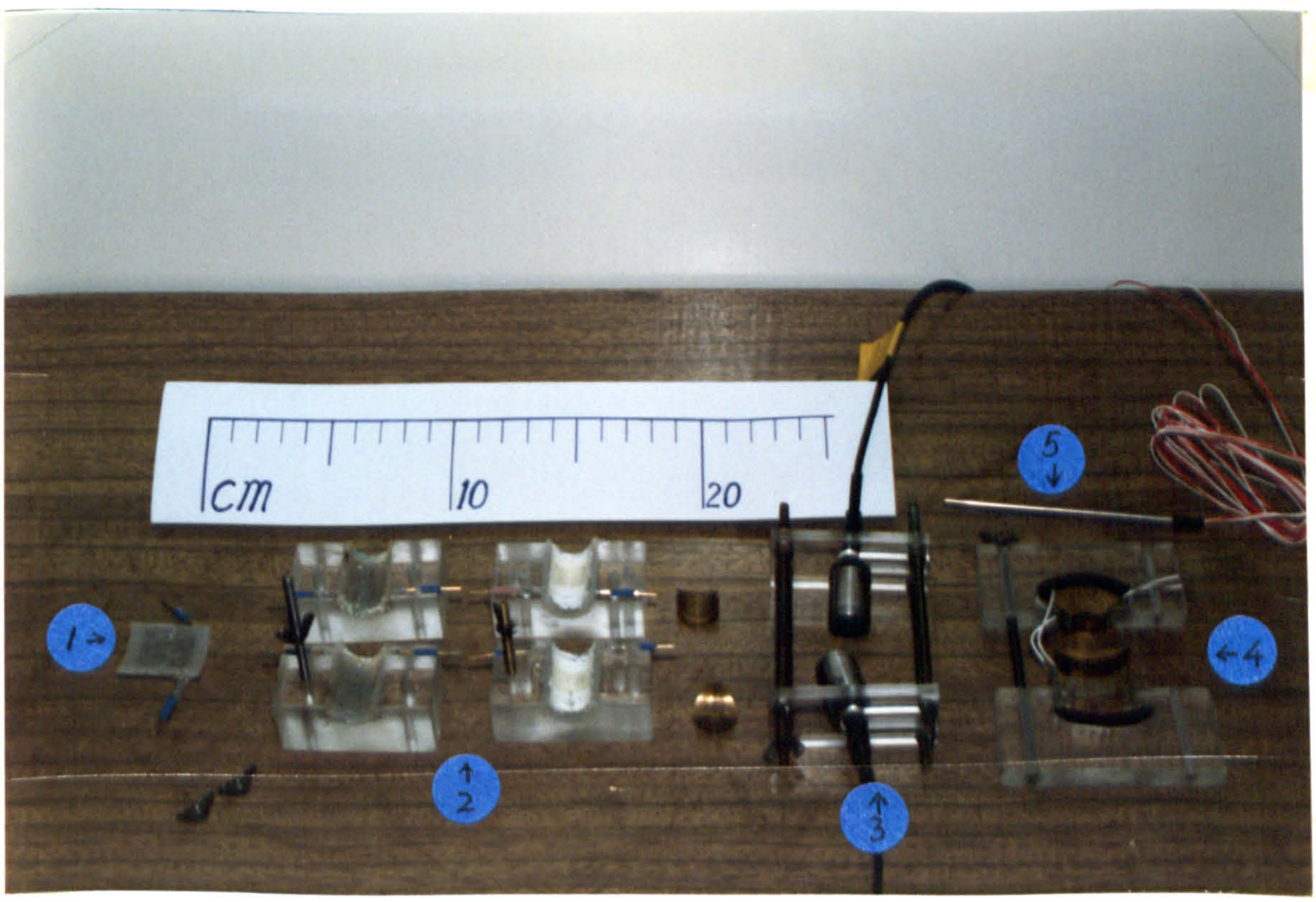

Fig. 6.2.2. Elements of the Ultrasonic/Thermal Flowmeter

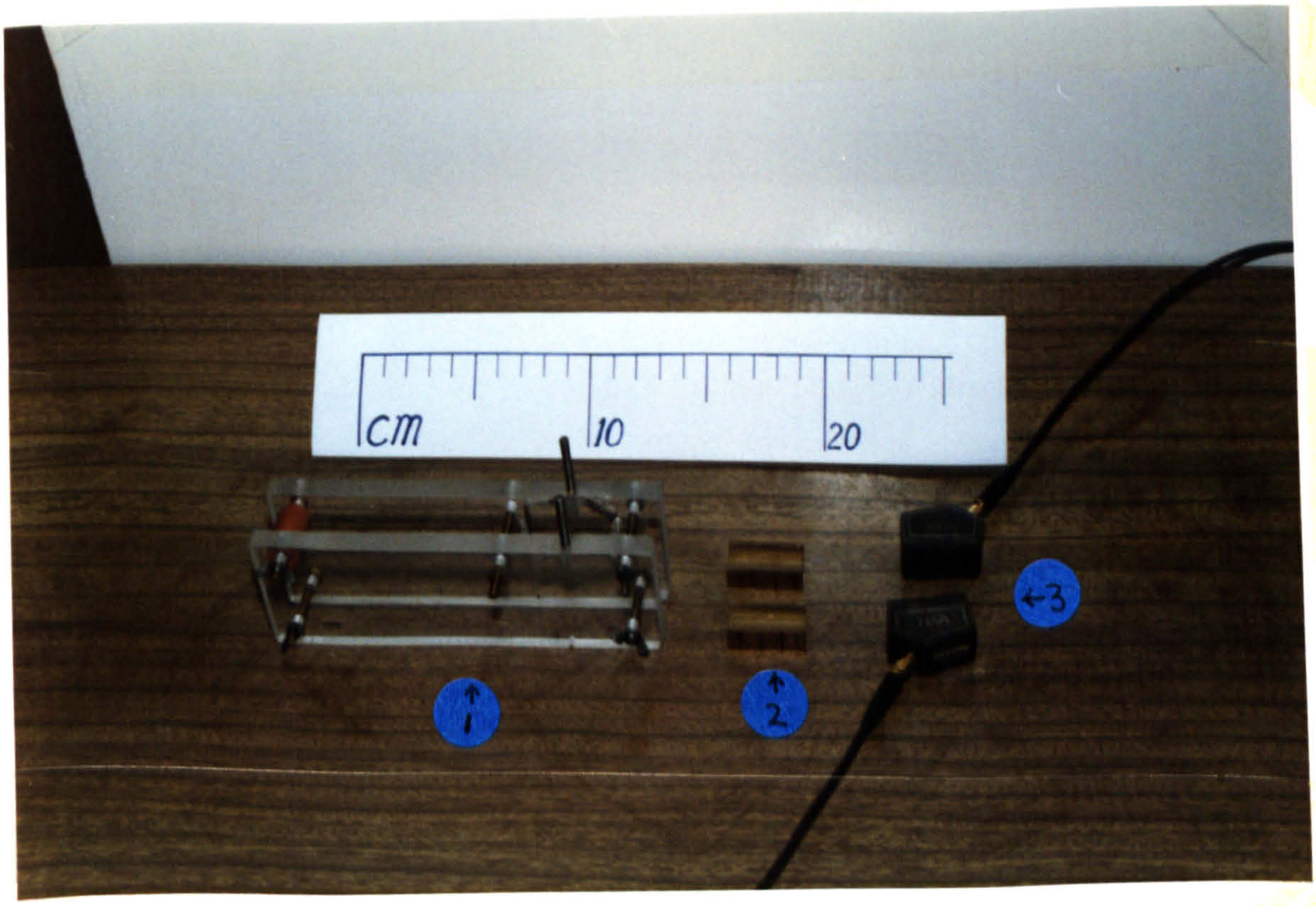

Fig. 6.2.3. Elements of the Ultrasonic Multiple Reflection Flowmeter

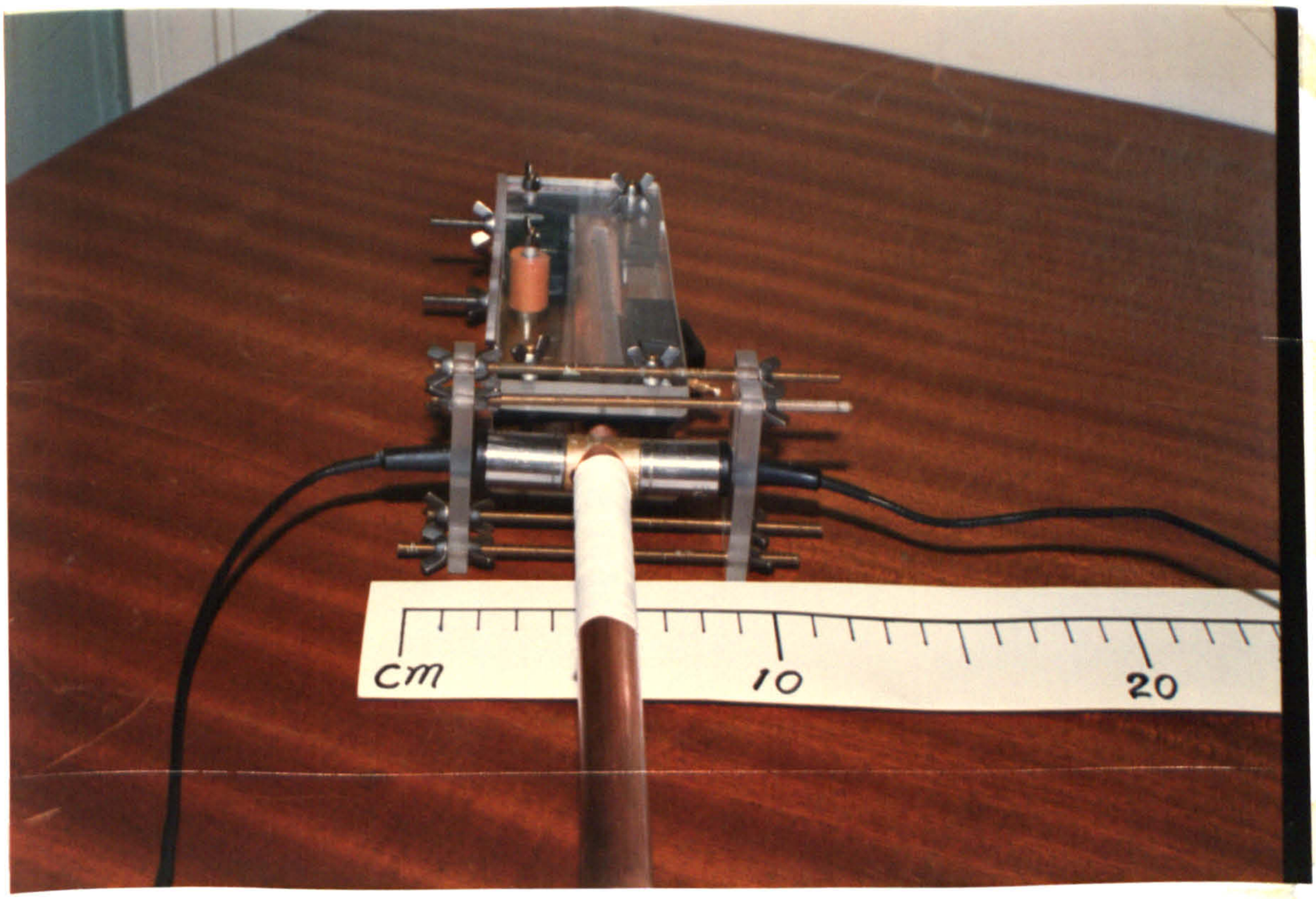

Fig. 6.2.4. Assembly of the Clamp-on Transducers

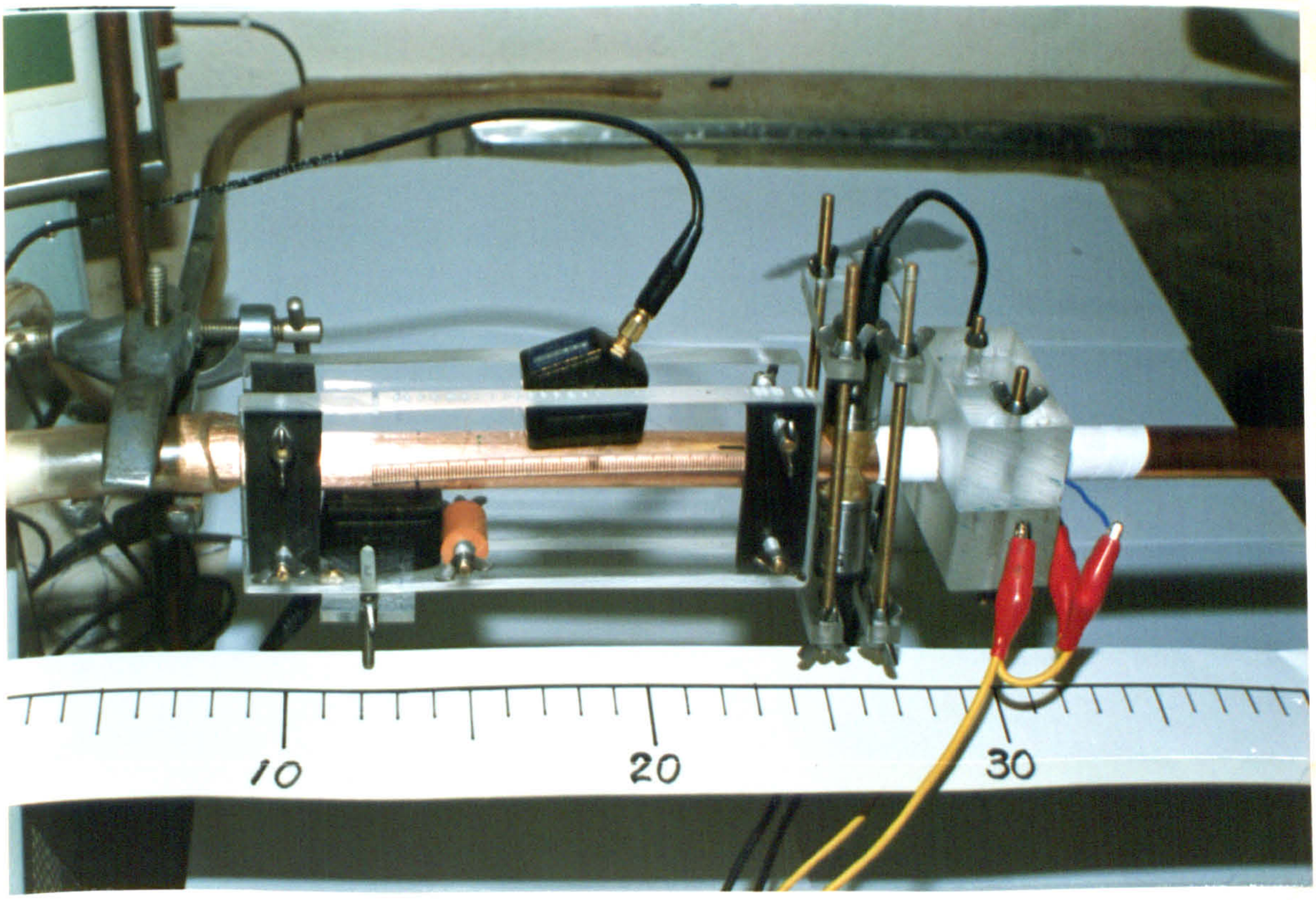

Fig. 6.2.5. Assembly of the Test Section

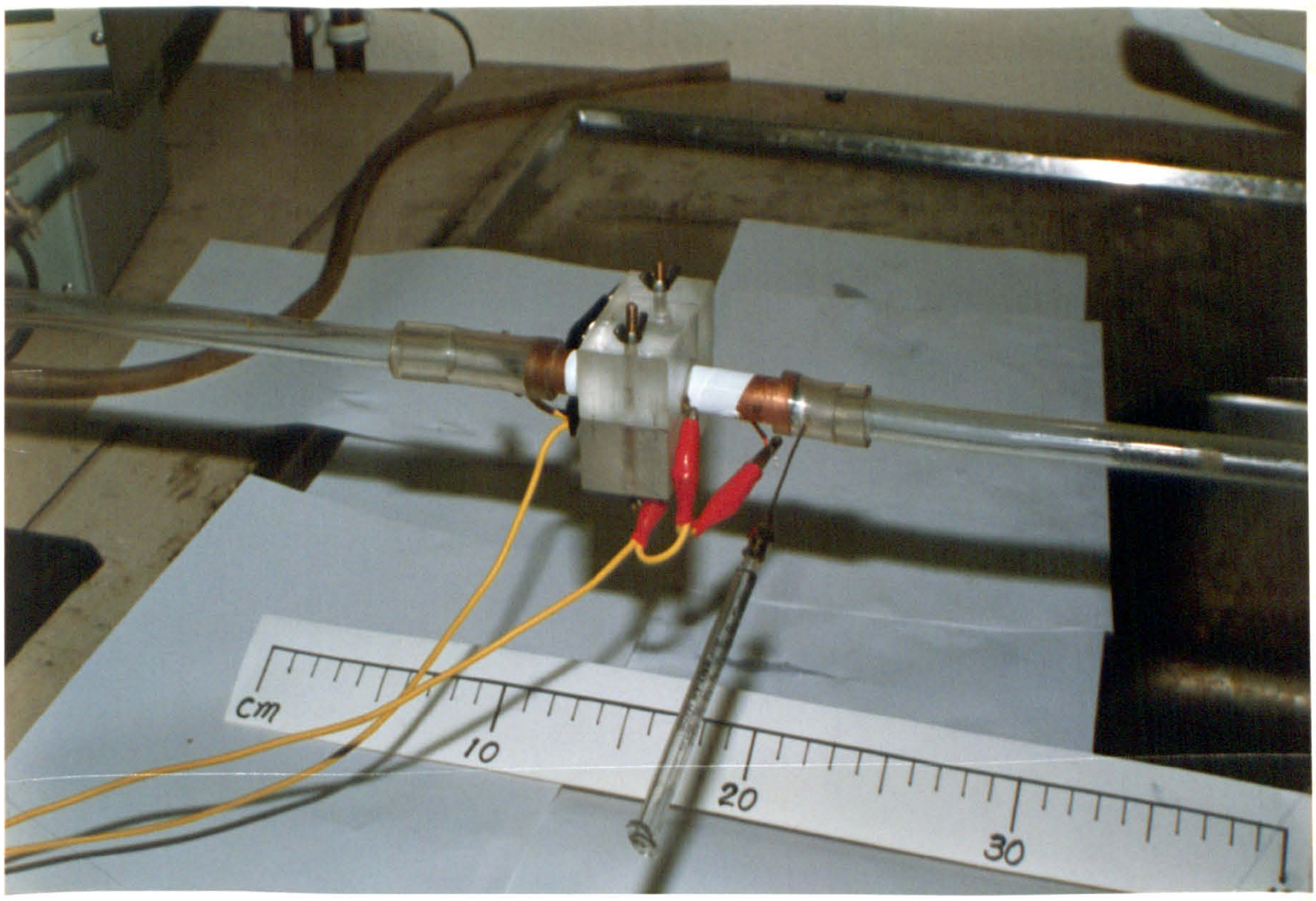

Fig. 6.4.1. Convection Experiment Setup

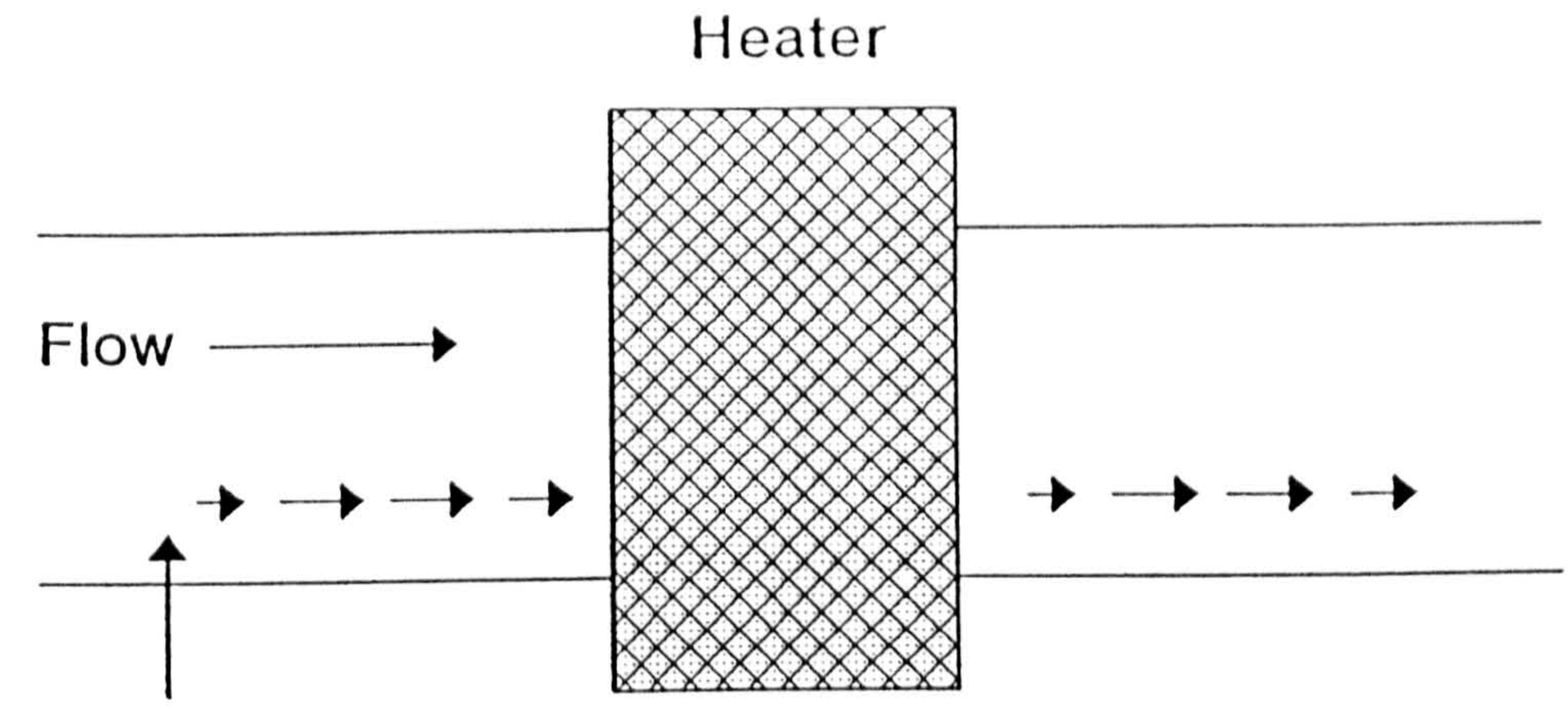

Fig 6.4.2a. Dye Stream Flow Pattern
With Heater Off

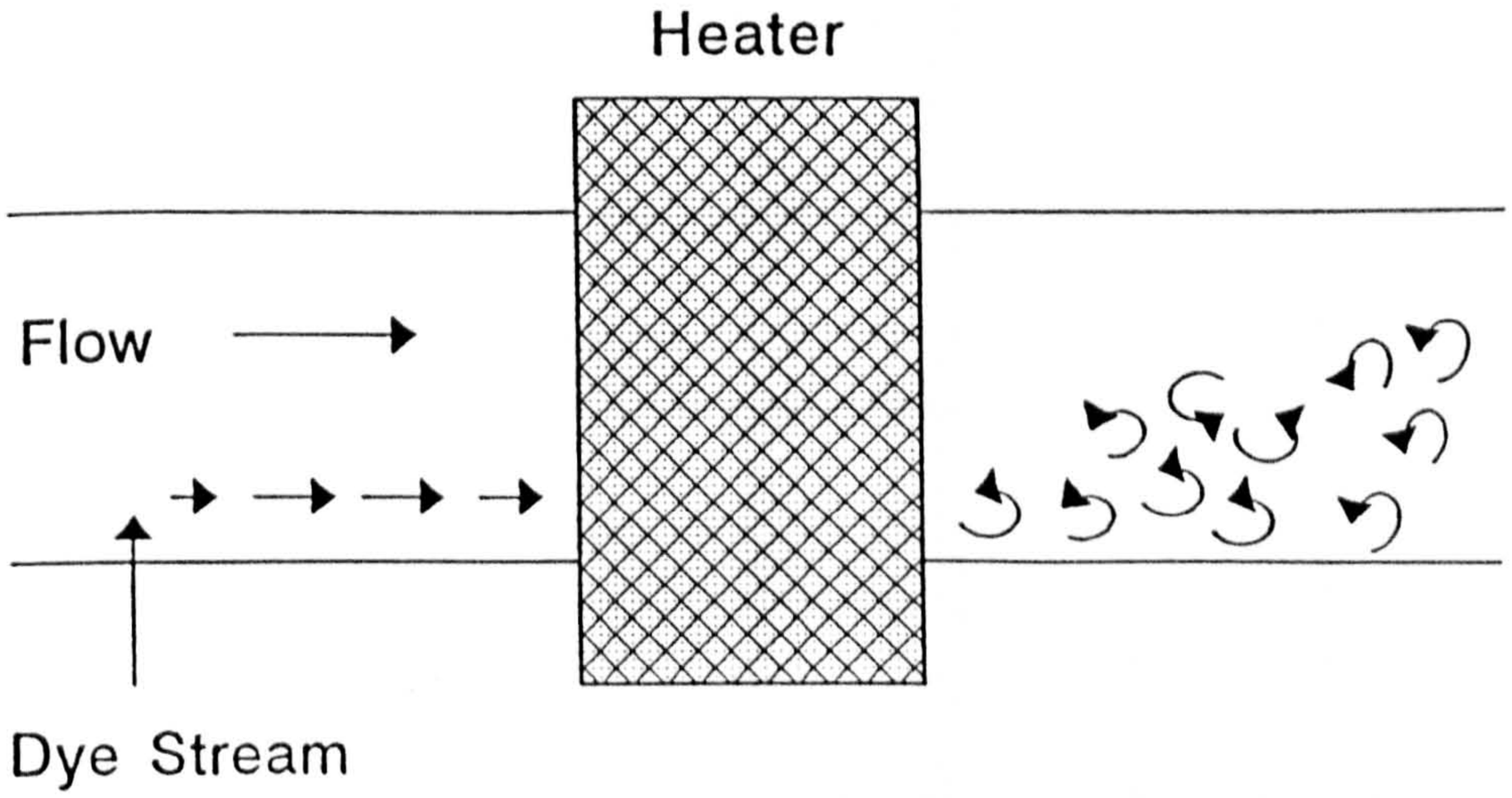

Fig 6.4.2b. Dye Stream Flow Pattern
With Heater On

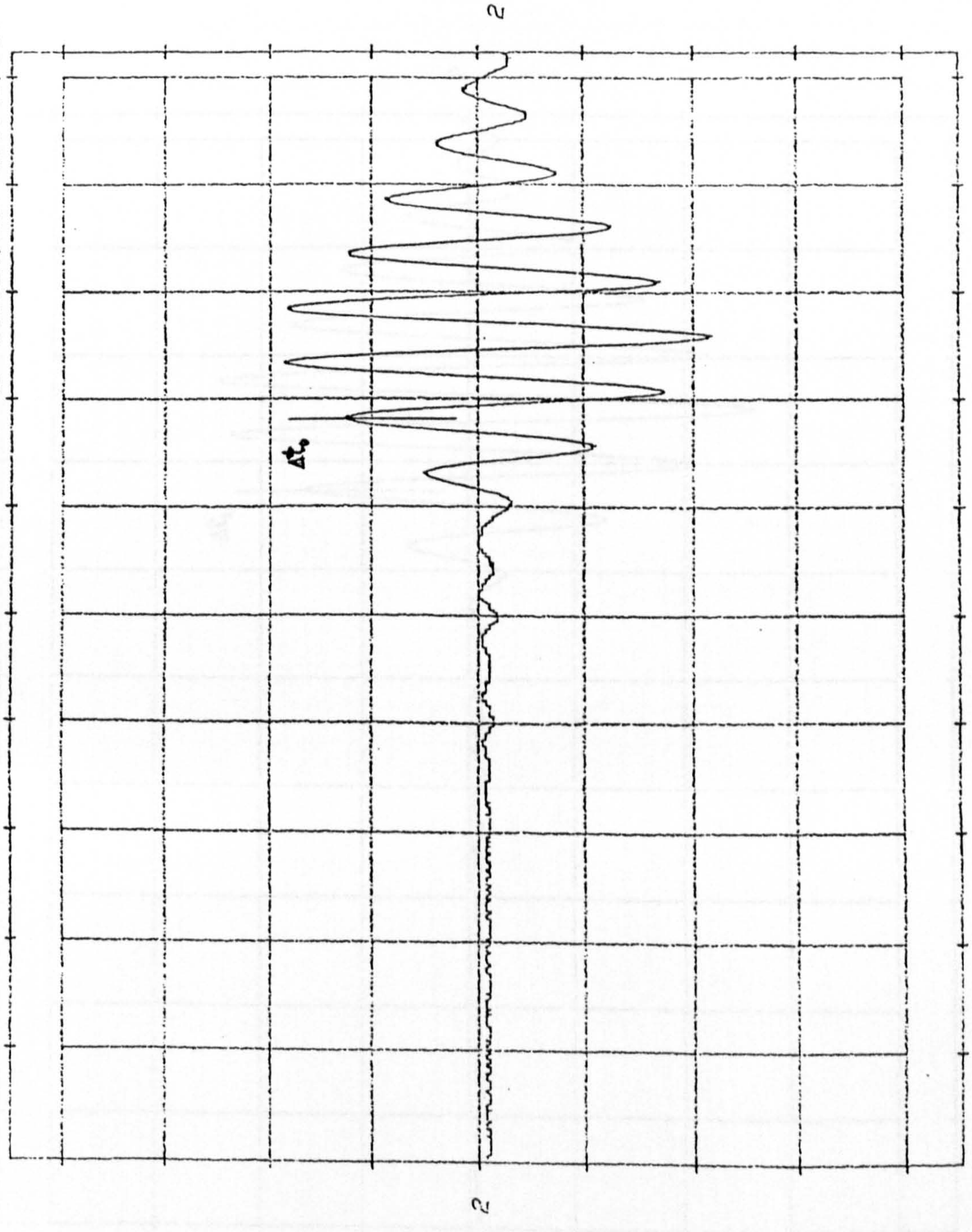

Fig. 6.4.3a. Typical Transit Time Trace (heater off, V = 0.79 cm s^{-1})

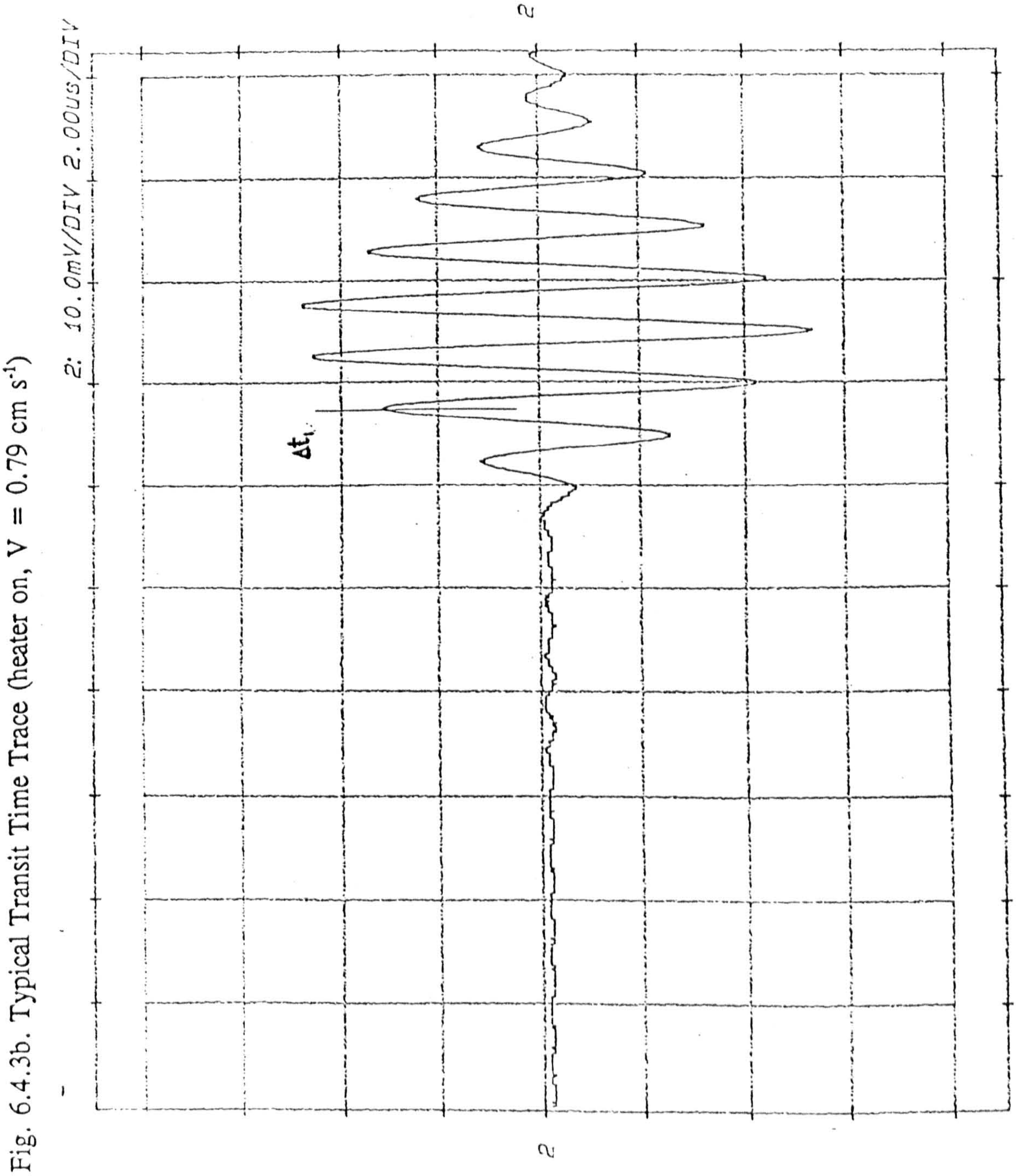

Fig. 6.4.3b. Typical Transit Time Trace (heater on, V = 0.79 cm s^{-1})

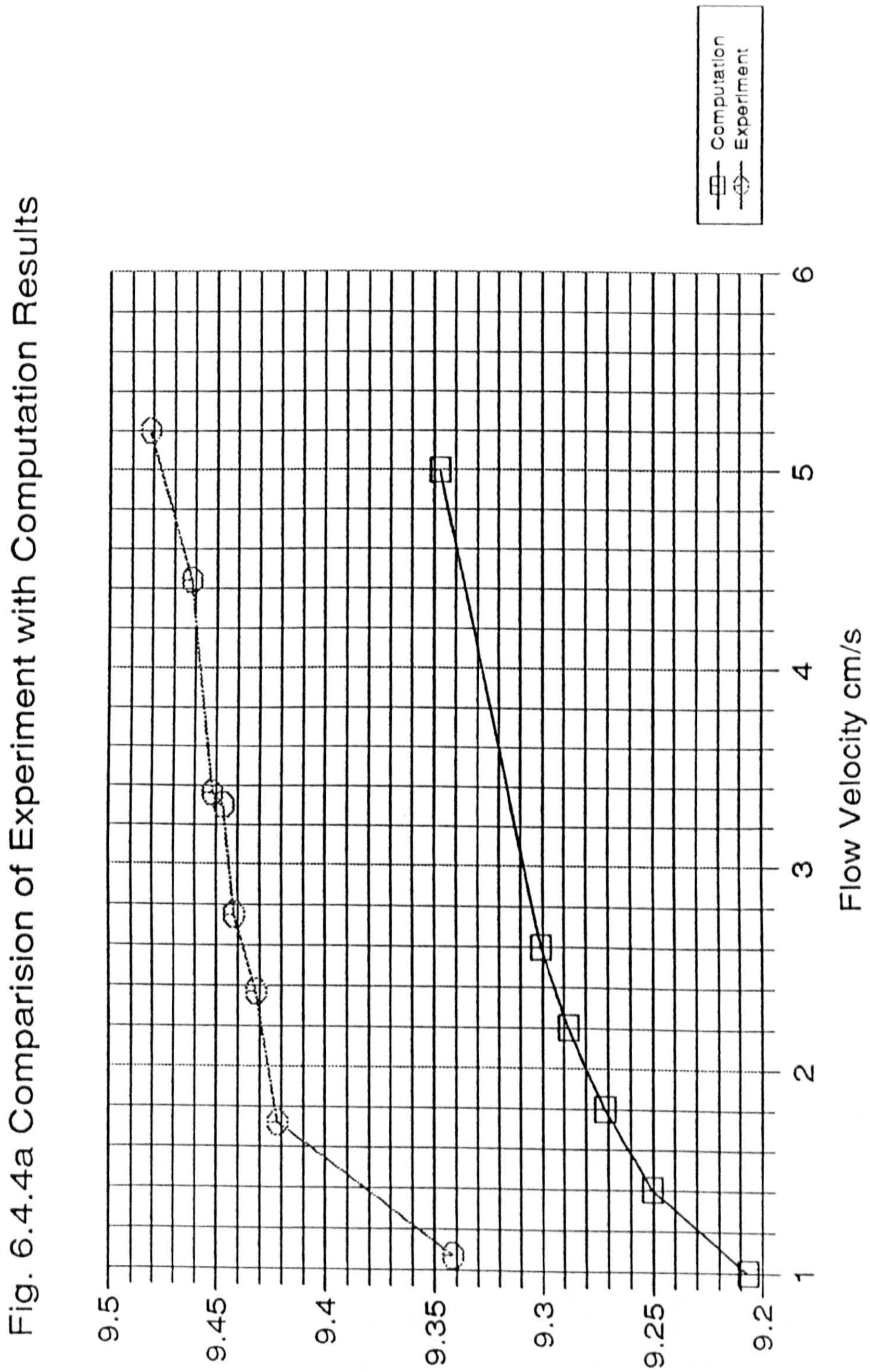

Fig. 6.4.4a Comparision of Experiment with Computation Results

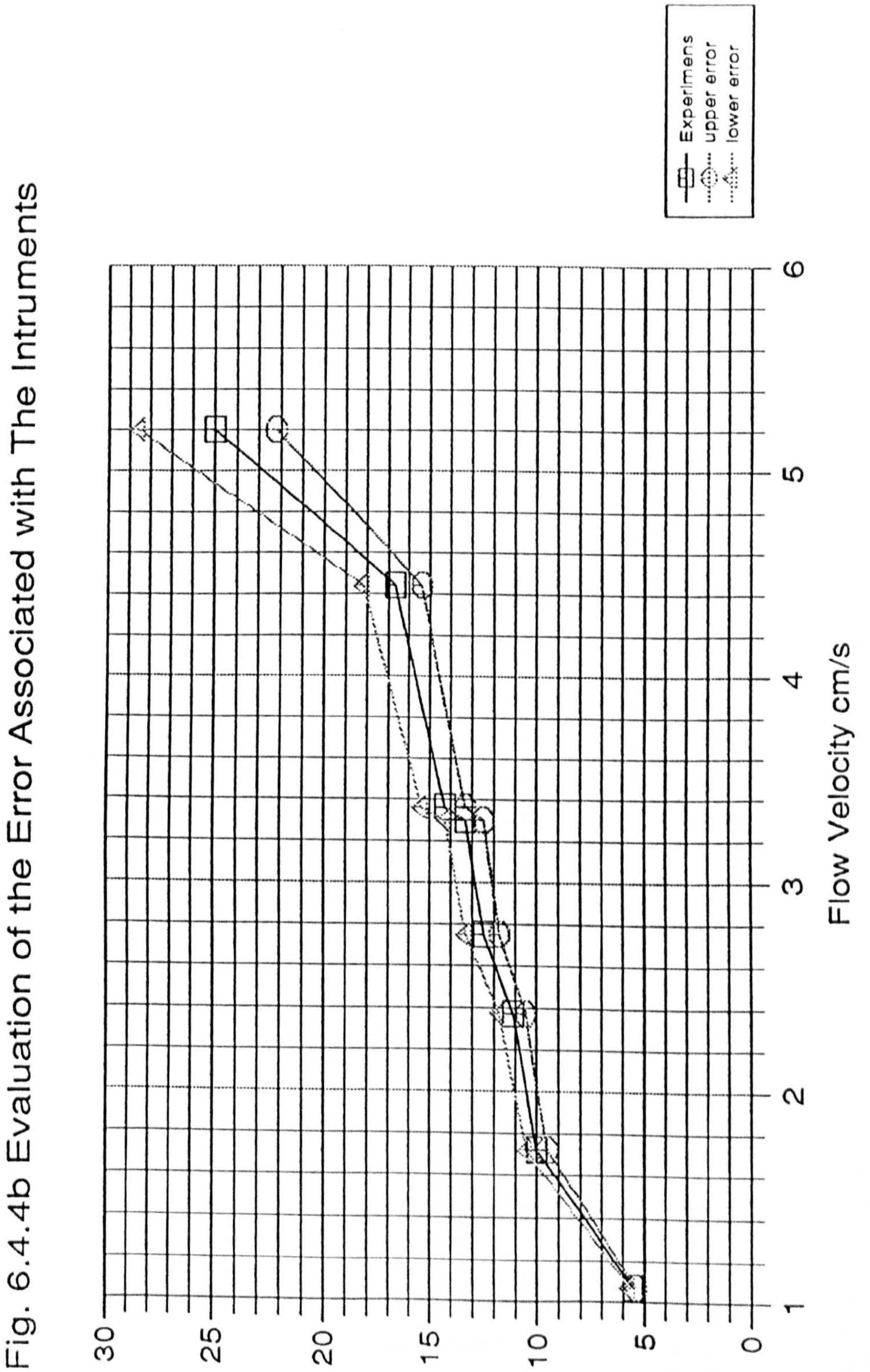

Fig. 6.4.4b Evaluation of the Error Associated with The Intrum

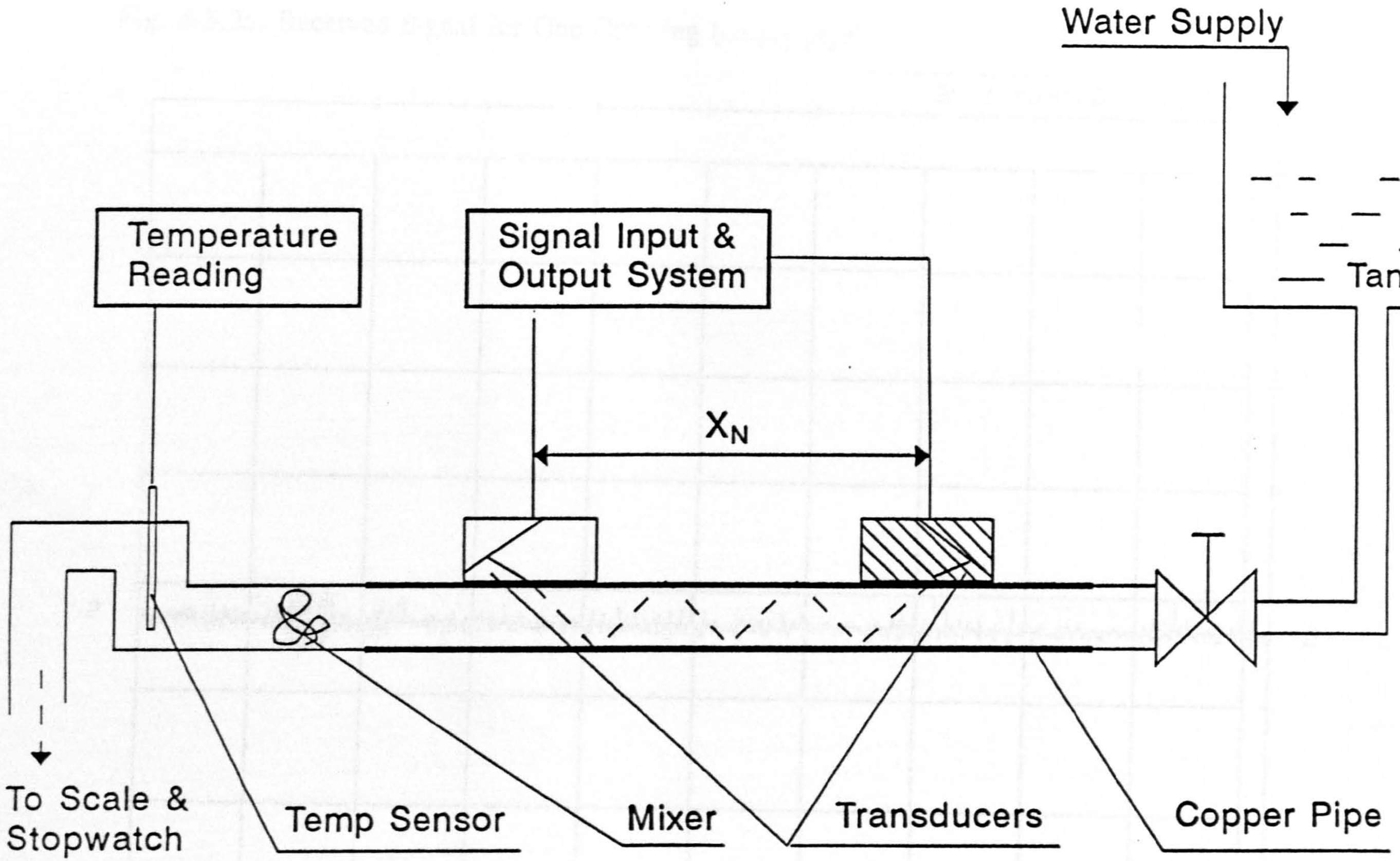

Fig 6.5.1. Setup for Preliminary Multiple-Reflection Experiments

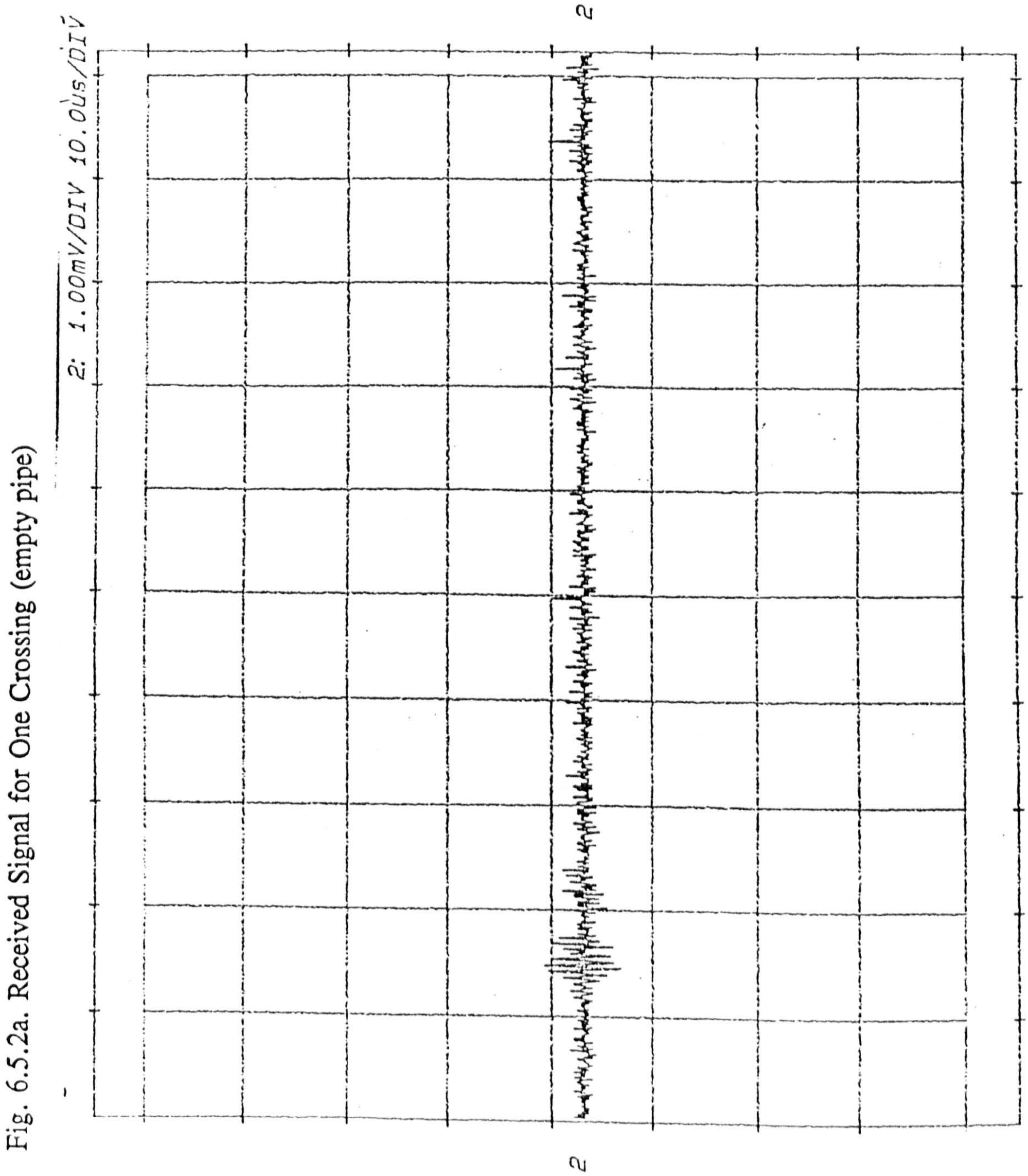

Fig. 6.5.2a. Received Signal for One Crossing (empty pipe)

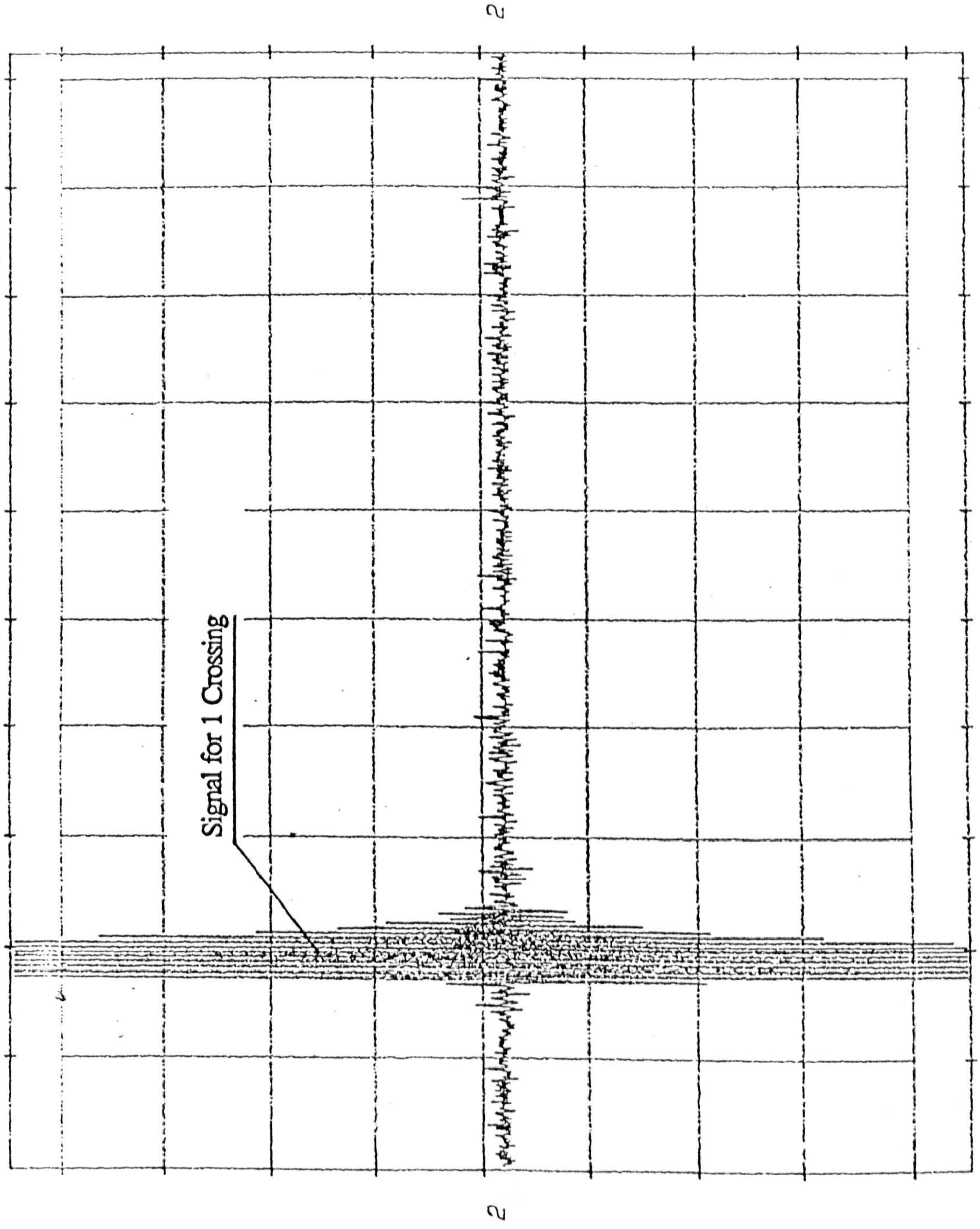

Fig. 6.5.2b. Received Signal for One Crossing (full pipe, Q = 2.7 ml s^{-1})

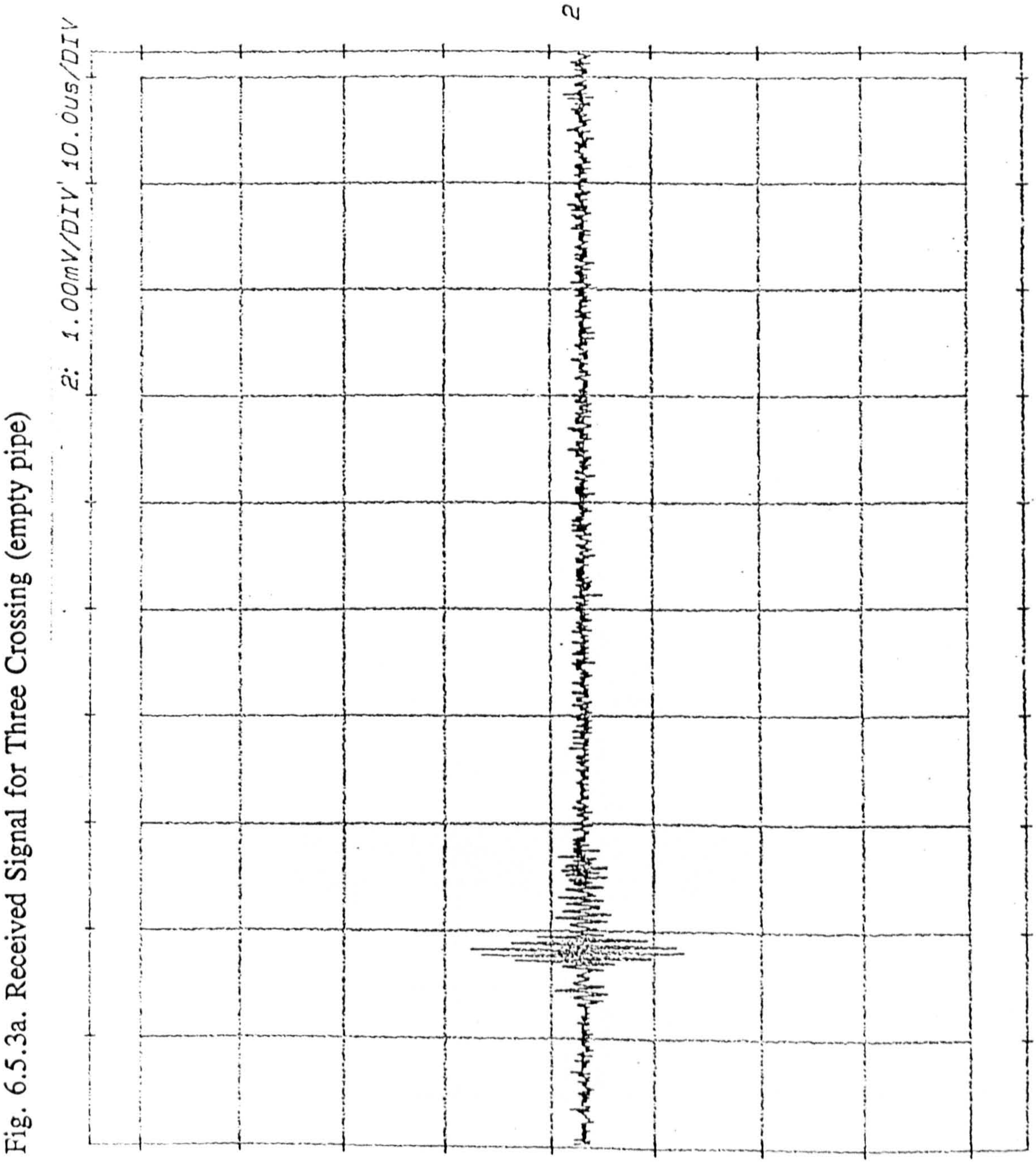

Fig. 6.5.3a. Received Signal for Three Crossing (empty pipe)

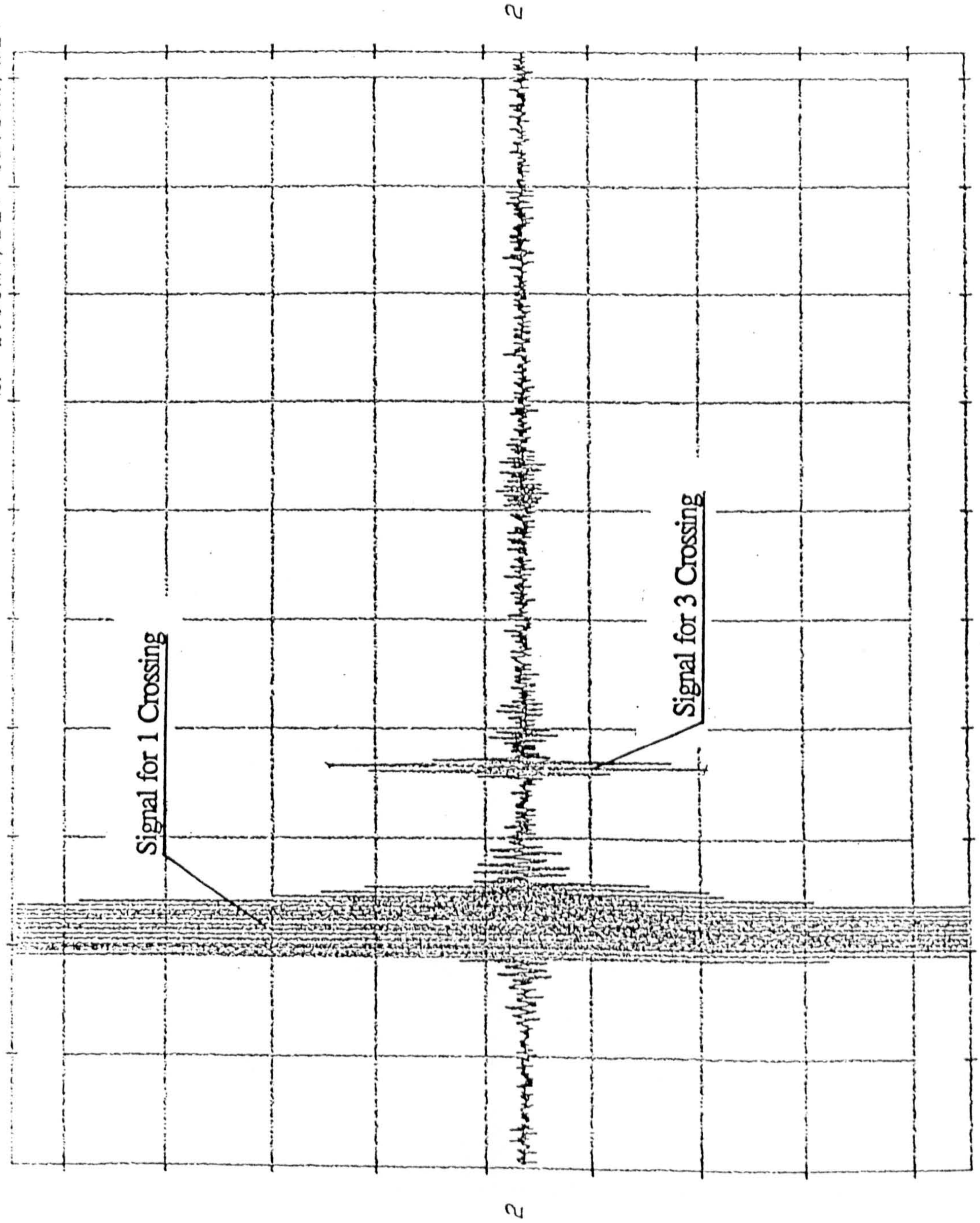

Fig. 6.5.3b. Received Signal for Three Crossing (full pipe, Q = 2.7 ml s^{-1})

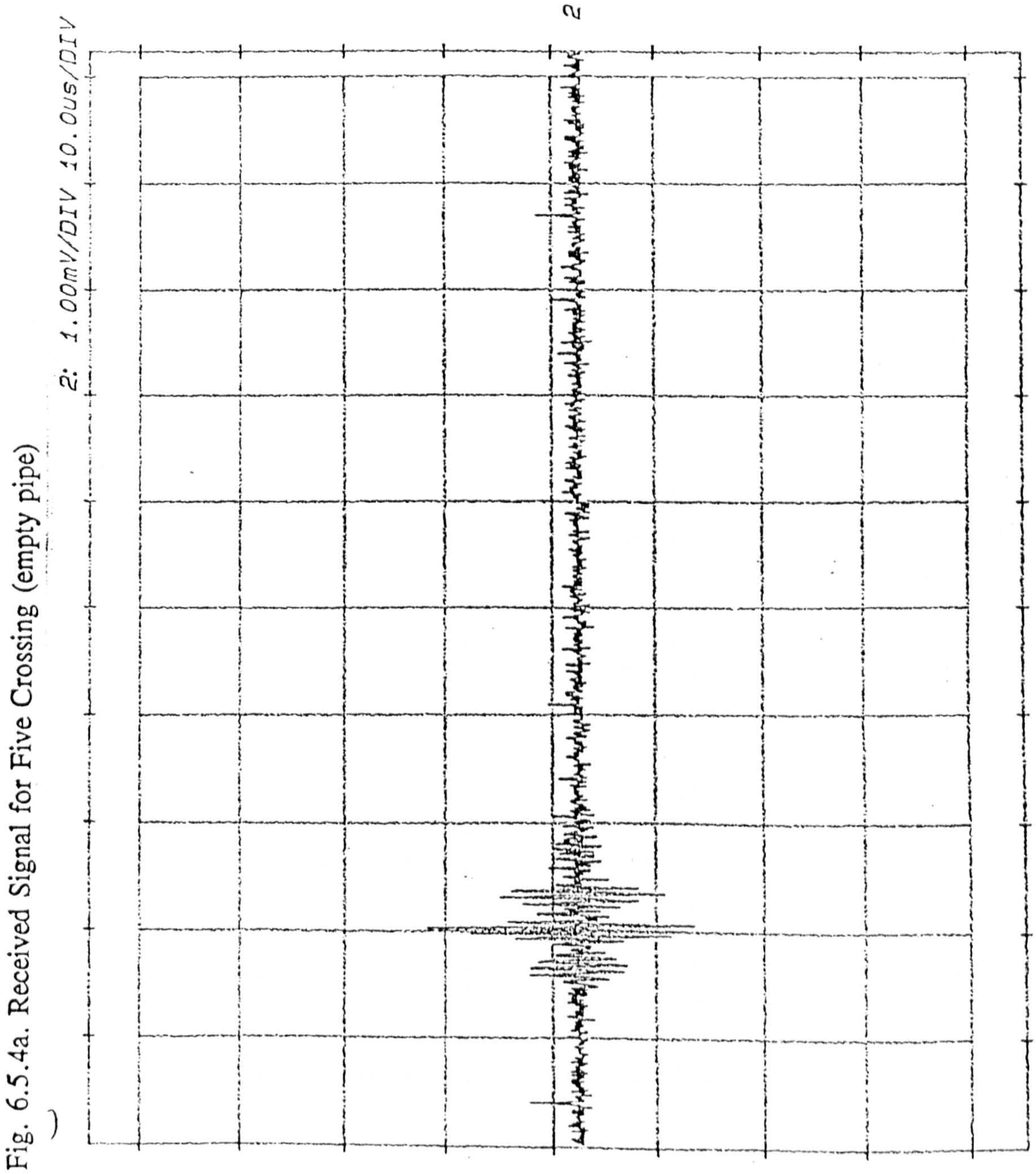

Fig. 6.5.4a. Received Signal for Five Crossing (empty pipe)

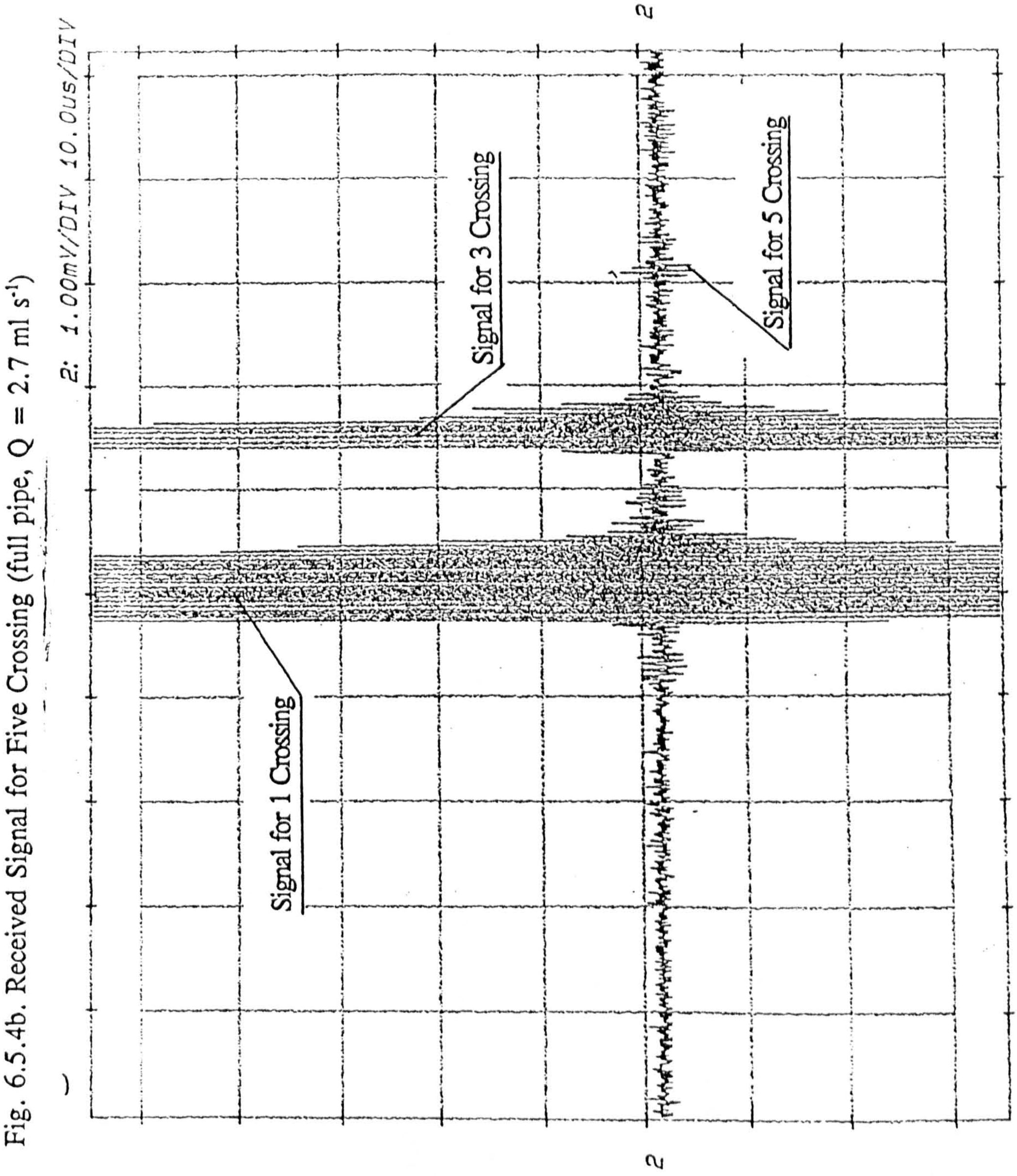

Fig. 6.5.4b. Received Signal for Five Crossing (full pipe, Q = 2.7 ml s^{-1})

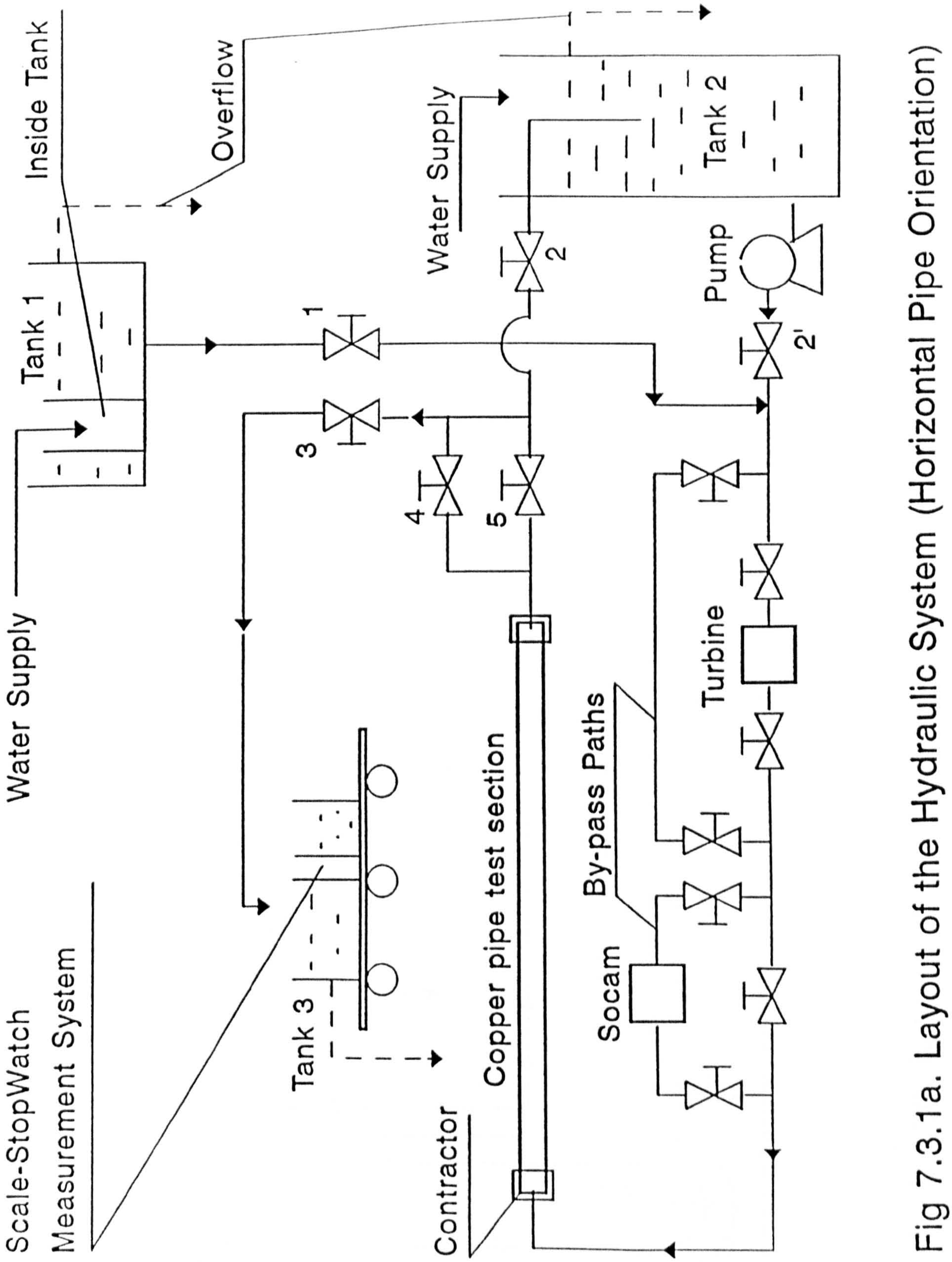

Fig 7.3.1a. Layout of the Hydraulic System (Horizontal Pipe Orientation)

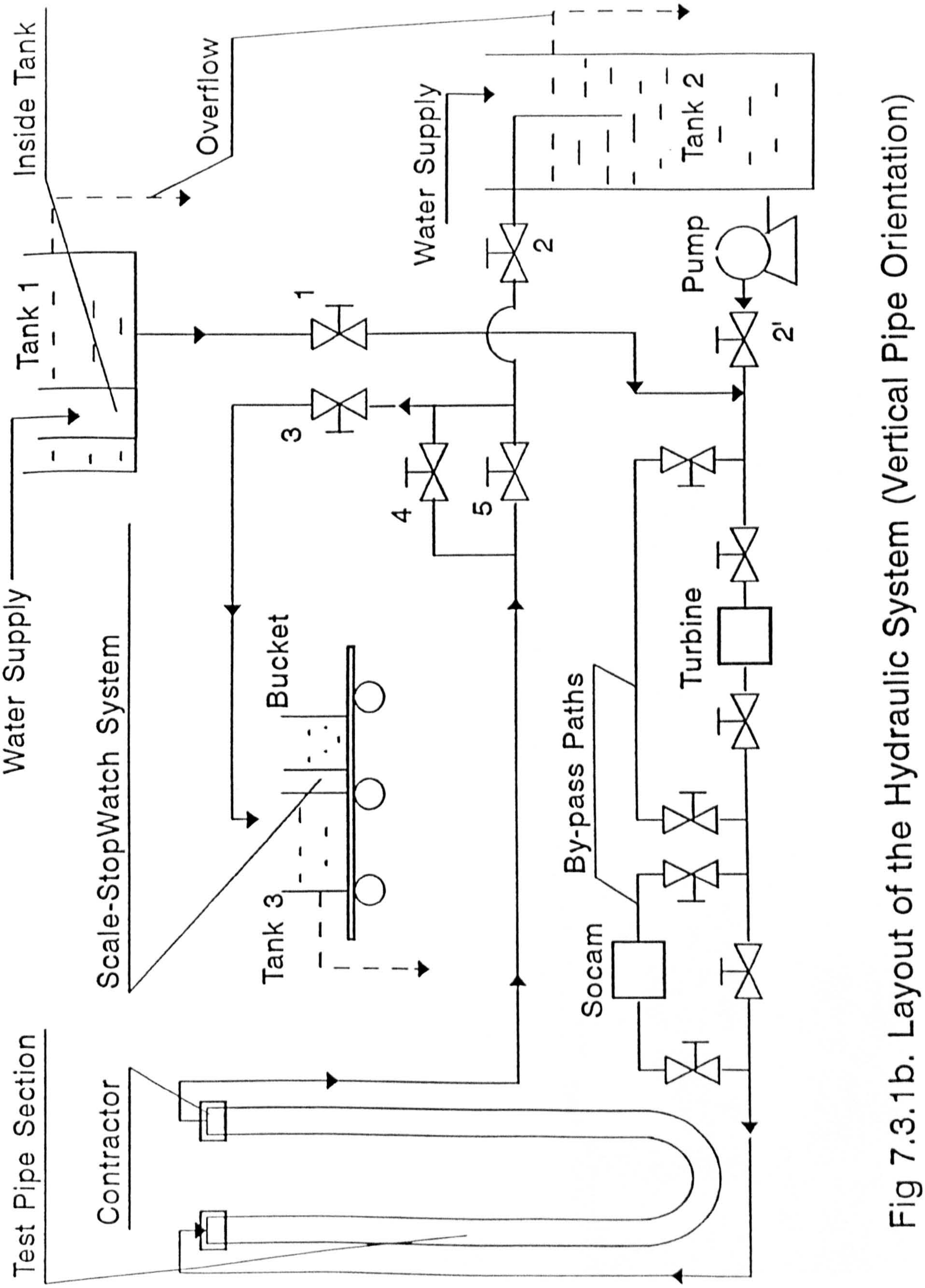

Fig 7.3.1b. Layout of the Hydraulic System (Vertical Pipe Orientation)

1. Gravity Tank
2. High Flowrate Tank
3. Scale and Stopwatch System
4. Reference Flow Meters
5. DC Power Supply
6. Horizontal Test Section
7. Vertical Test Section

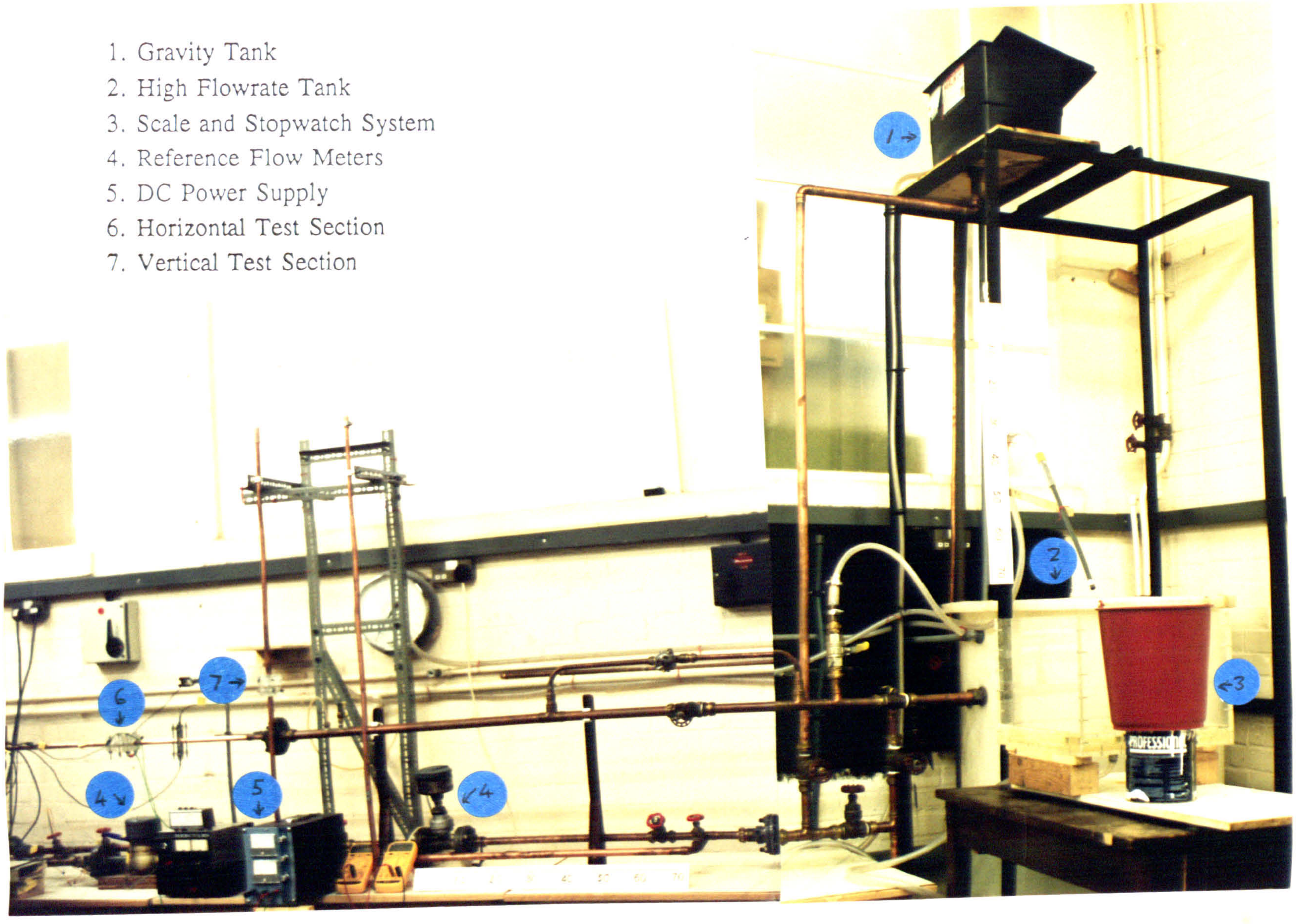

Fig. 7.3.2. The Hydraulic System

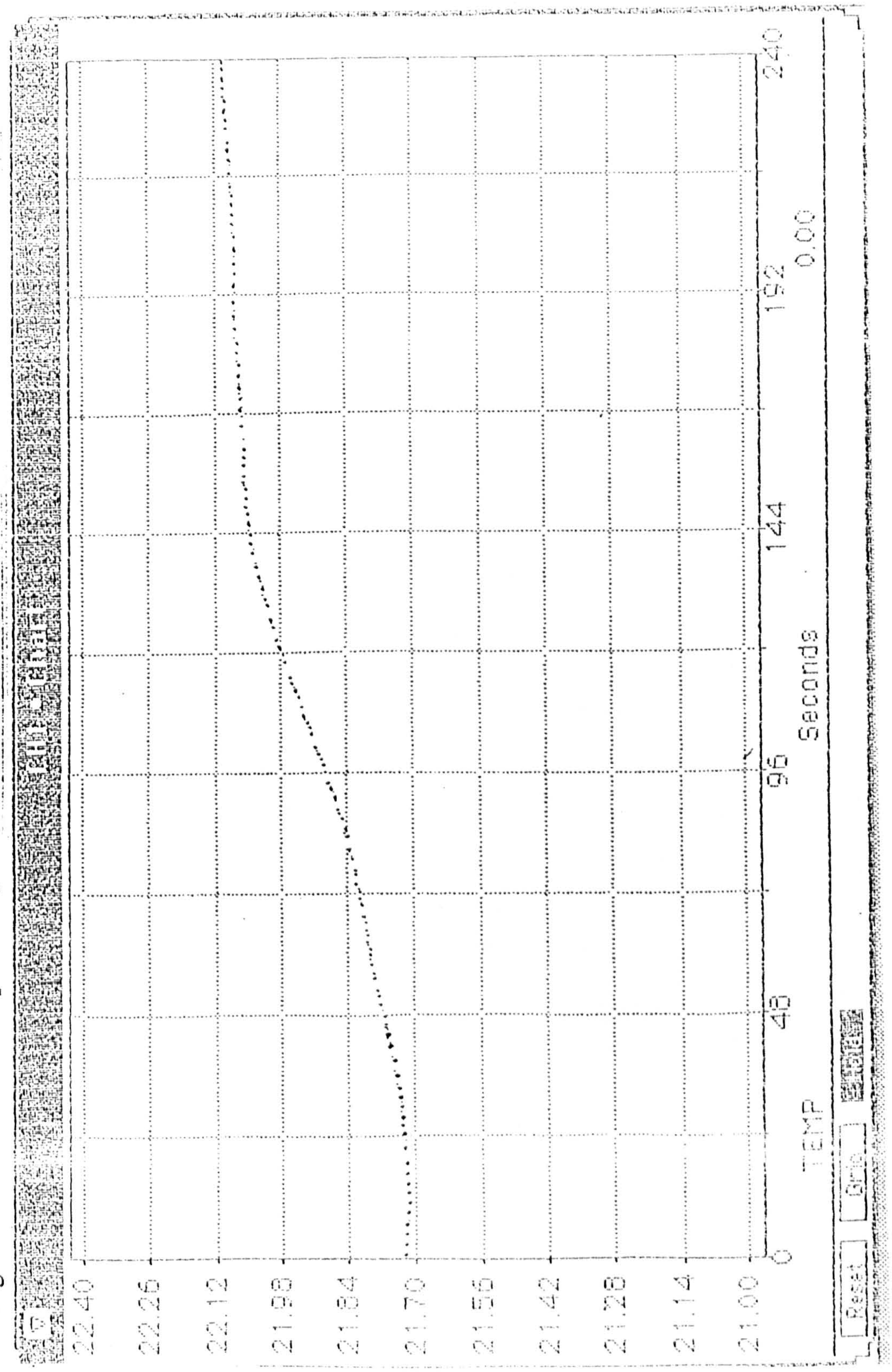

Fig. 7.3.3. Variation of Liquid Temperature When Operating the Pump

1. PC
2. Instruments Power Supply
3. Wavetec and Wavetec Gate Mode Controller
4. Ultrasonic Timing Interface
5. Timer/Counter
6. Oscilloscope

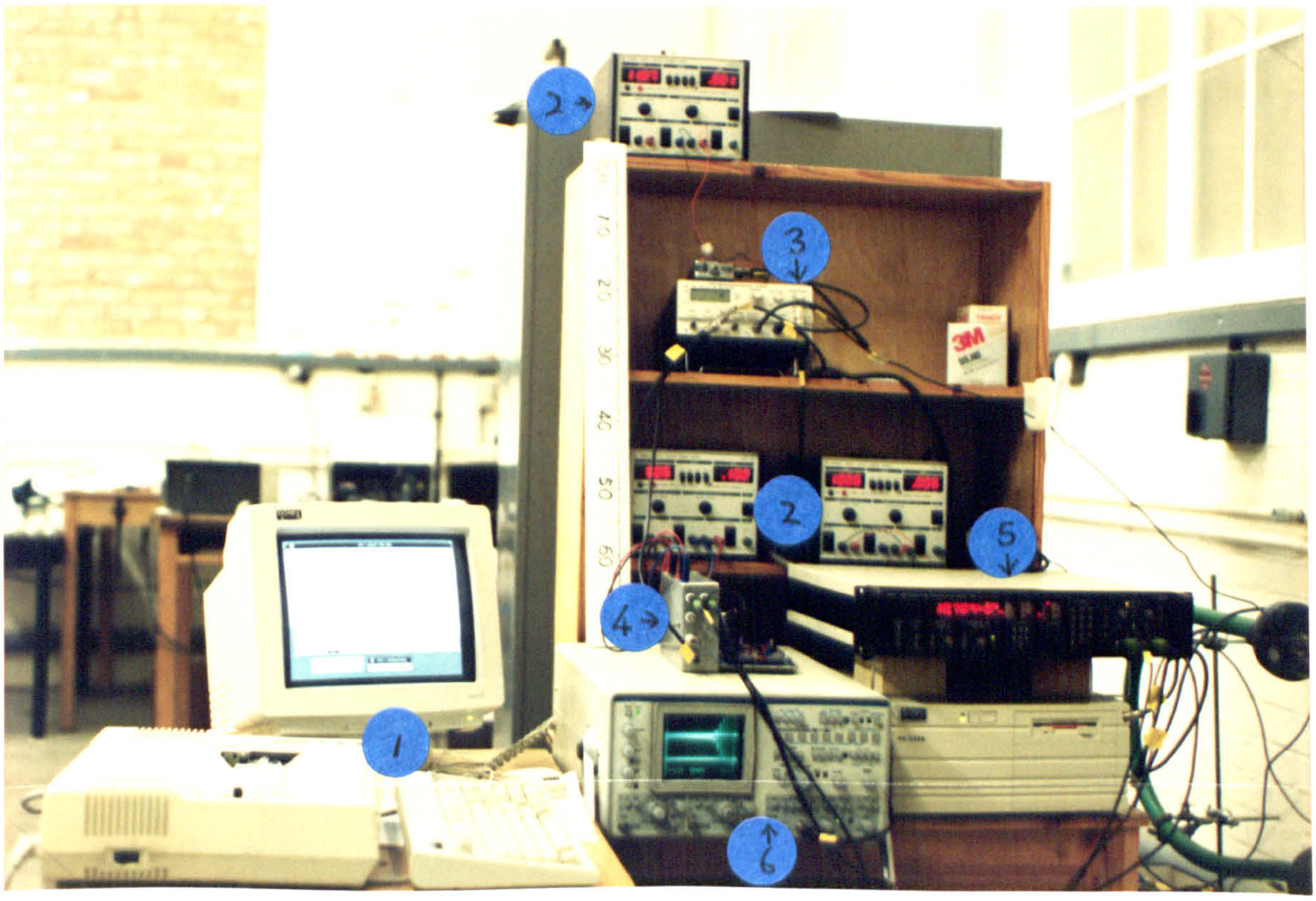

Fig. 7.4.1. Instruments Selected for the Experimental Work

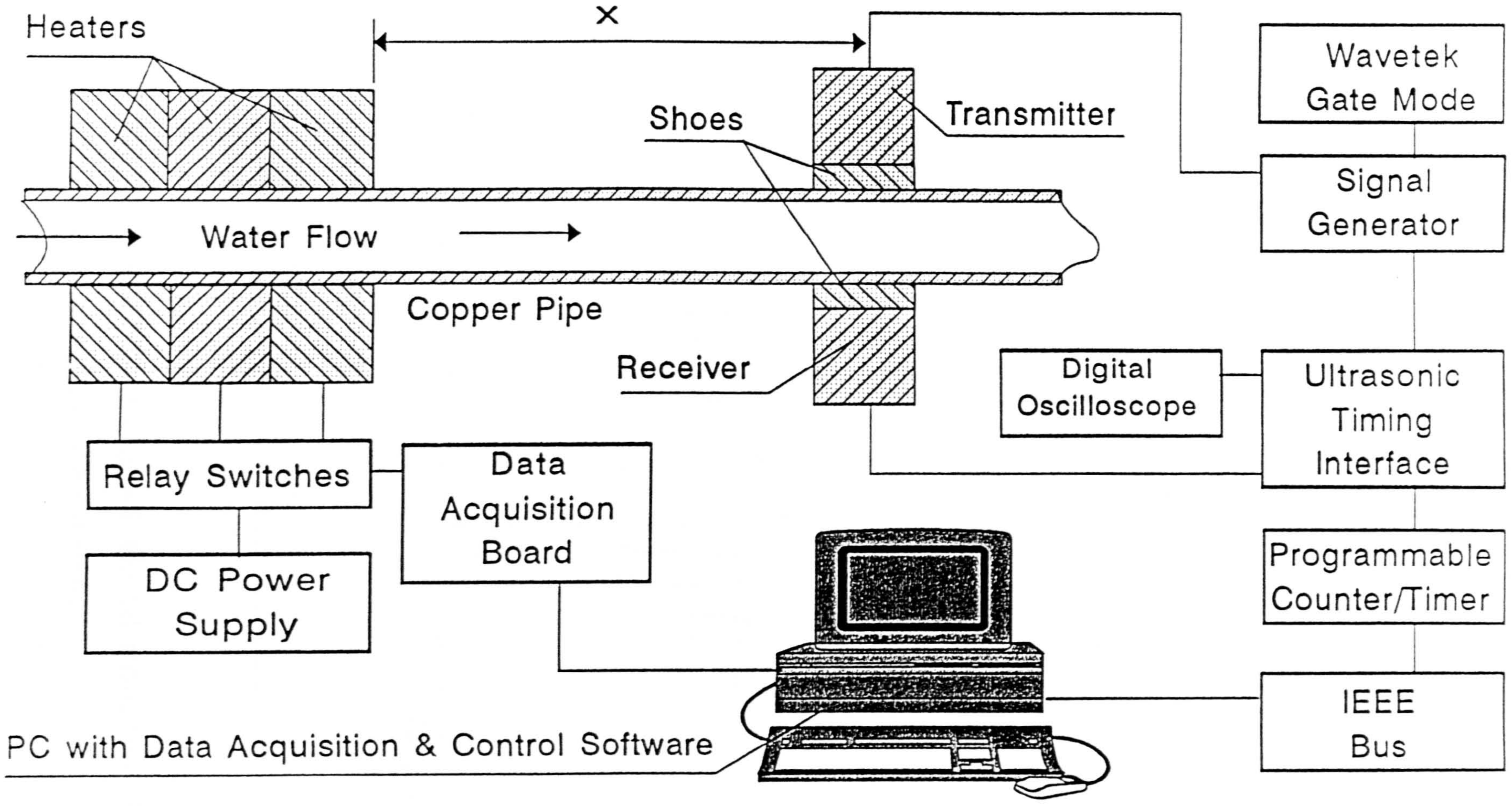

Fig 7.4.2a. Connection Diagram for the Ultrasonic/Thermal Prototype Flowmeter

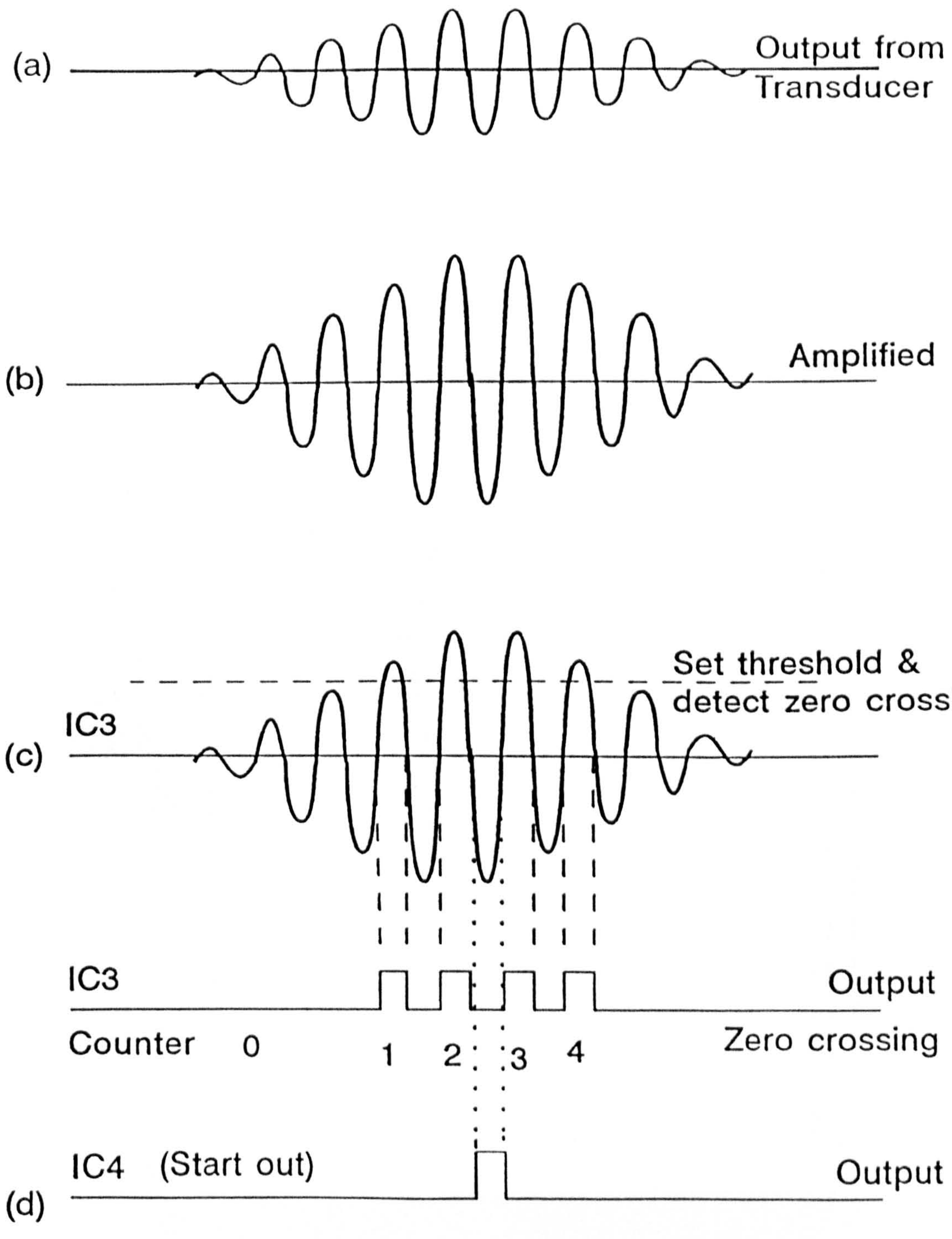

Fig. 7.4.2b. Processed and Output signal from the Ultrasonic Timing Interface Electronics

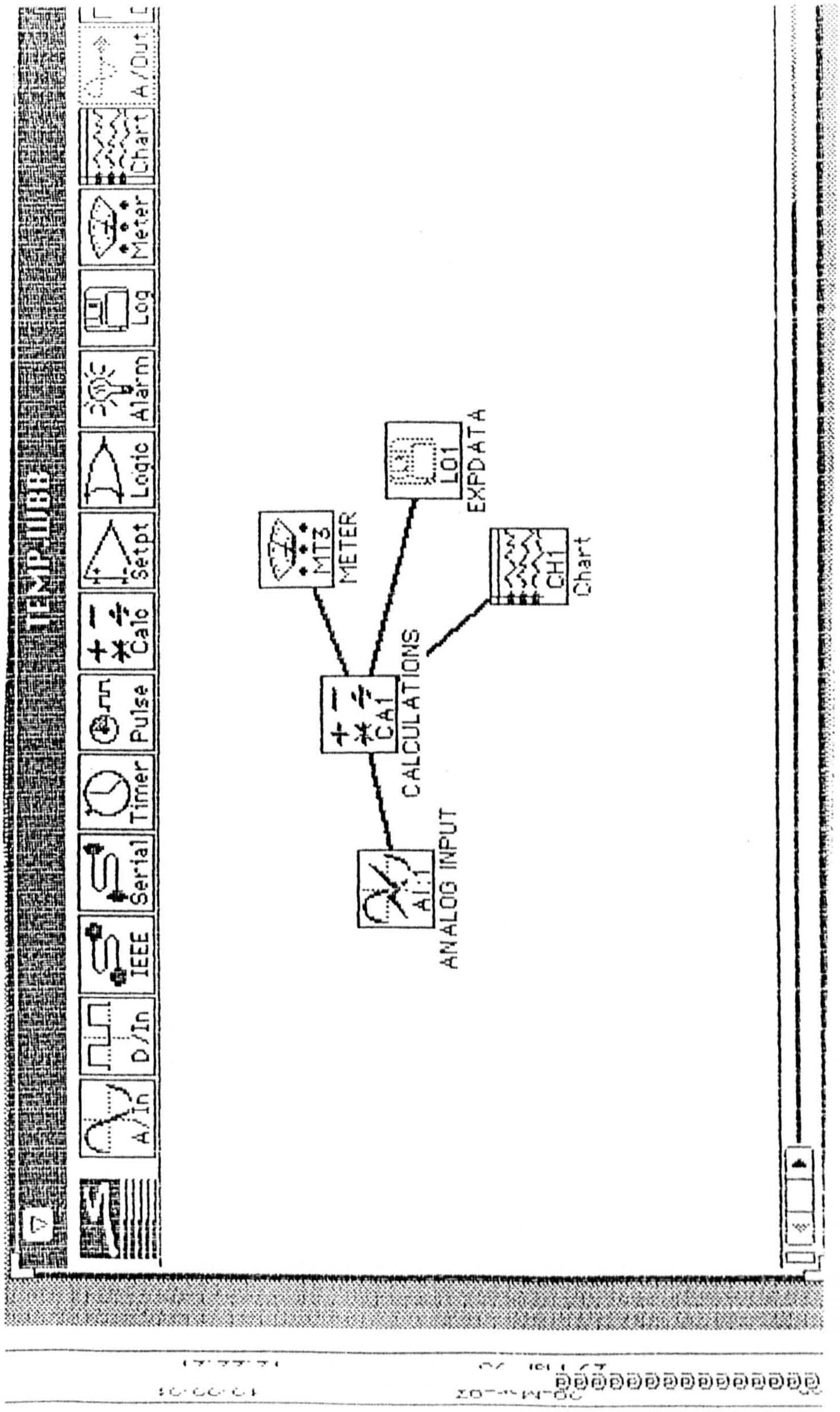

Fig. 7.4.3. Workbench Input Layout for Inflow Temperature Measurement

Fig. 7.4.4. Workbench Input Layout for Flowrate Measurement (IEEE)

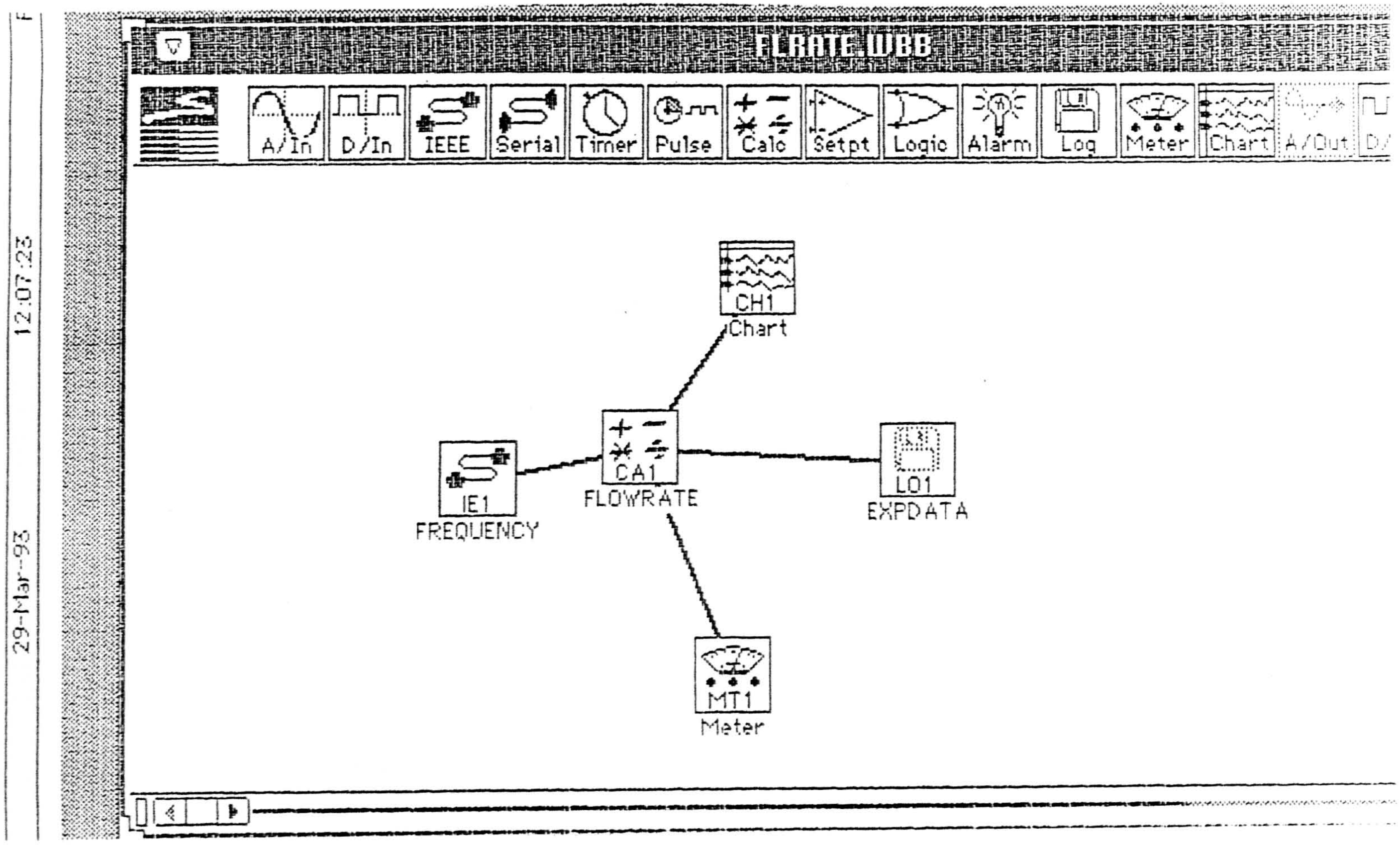

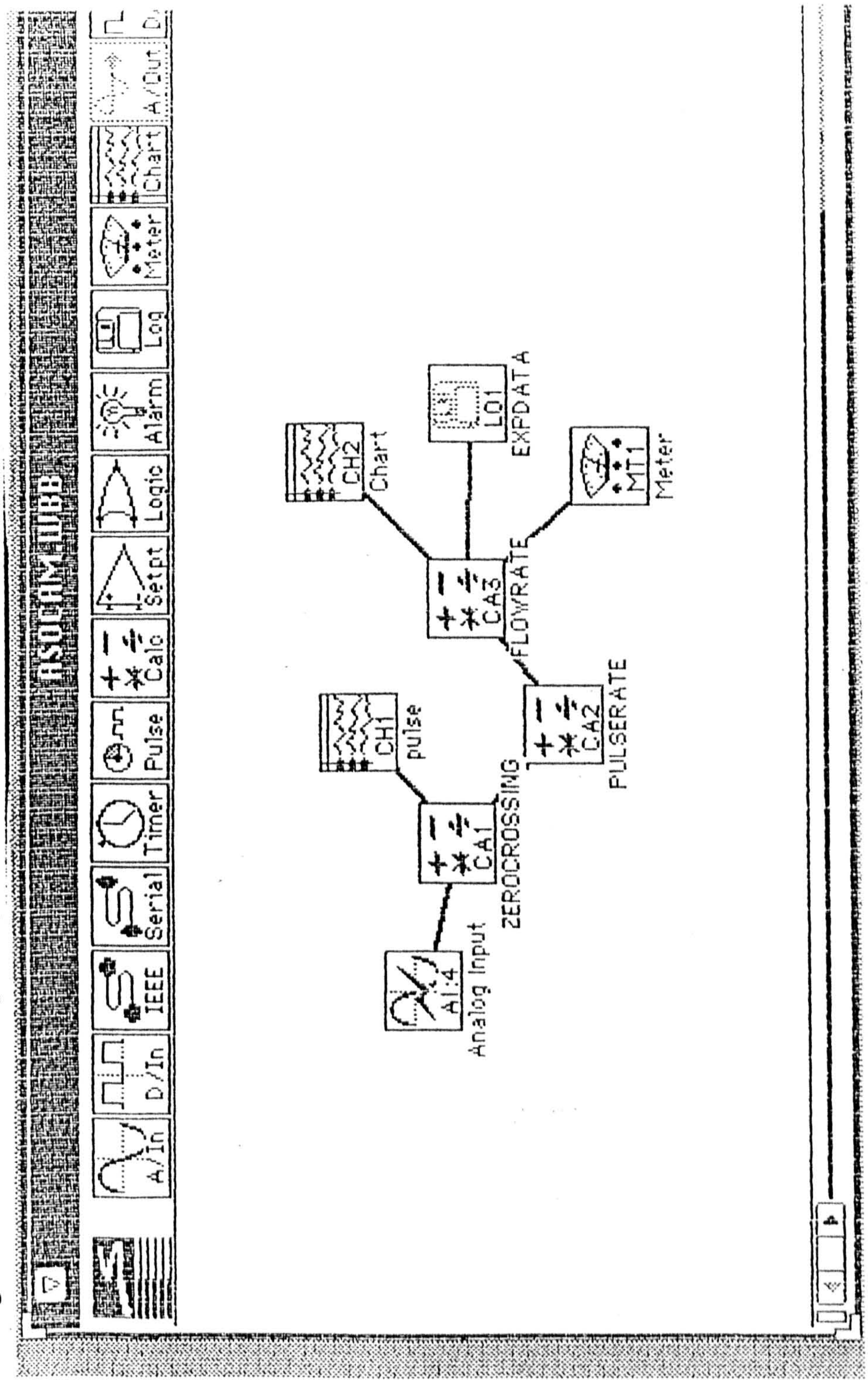

Fig. 7.4.5. Workbench Input Layout for Flowrate Measurement

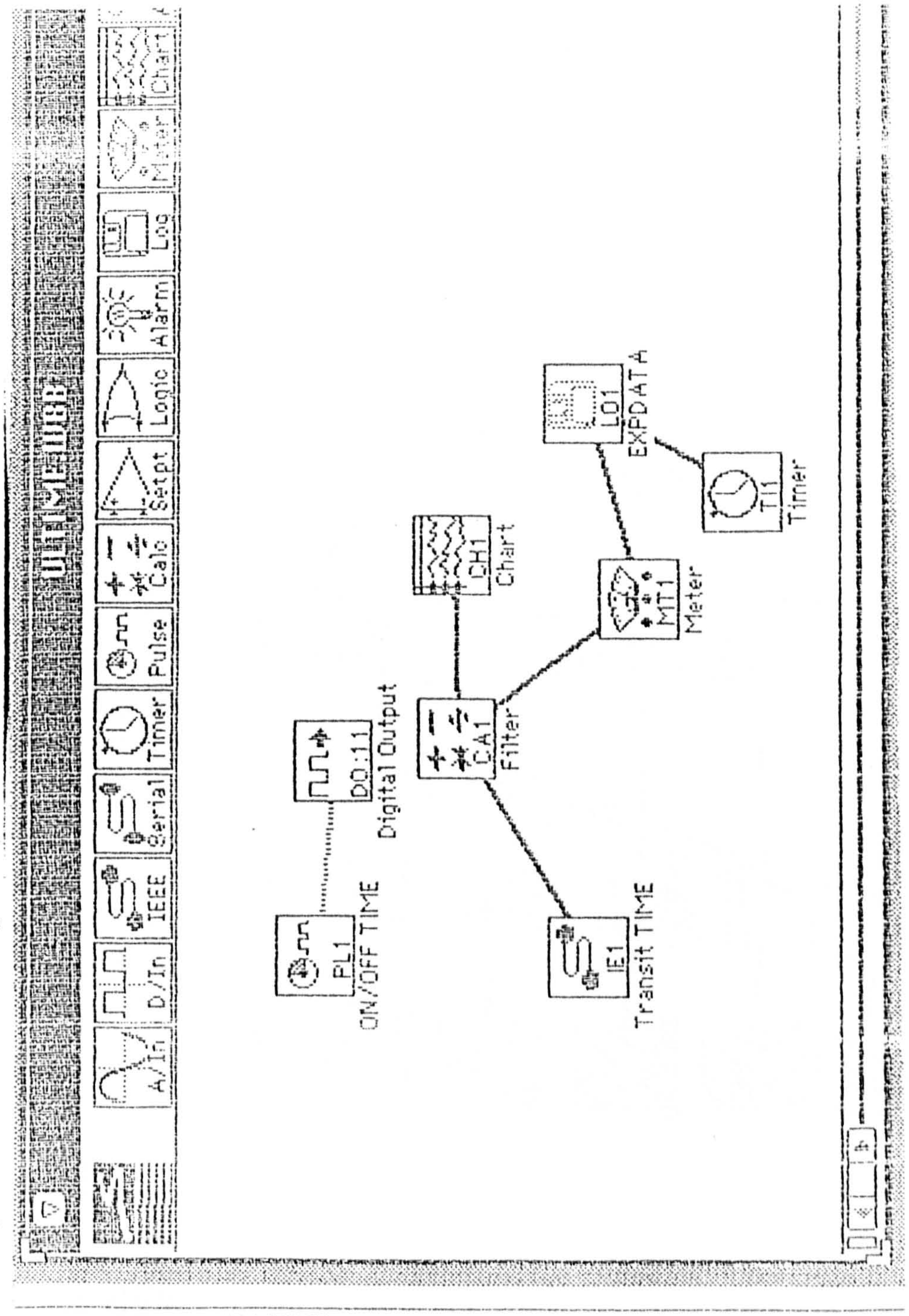

Fig. 7.4.6. Workbench Input Layout for Transit Time Measurement

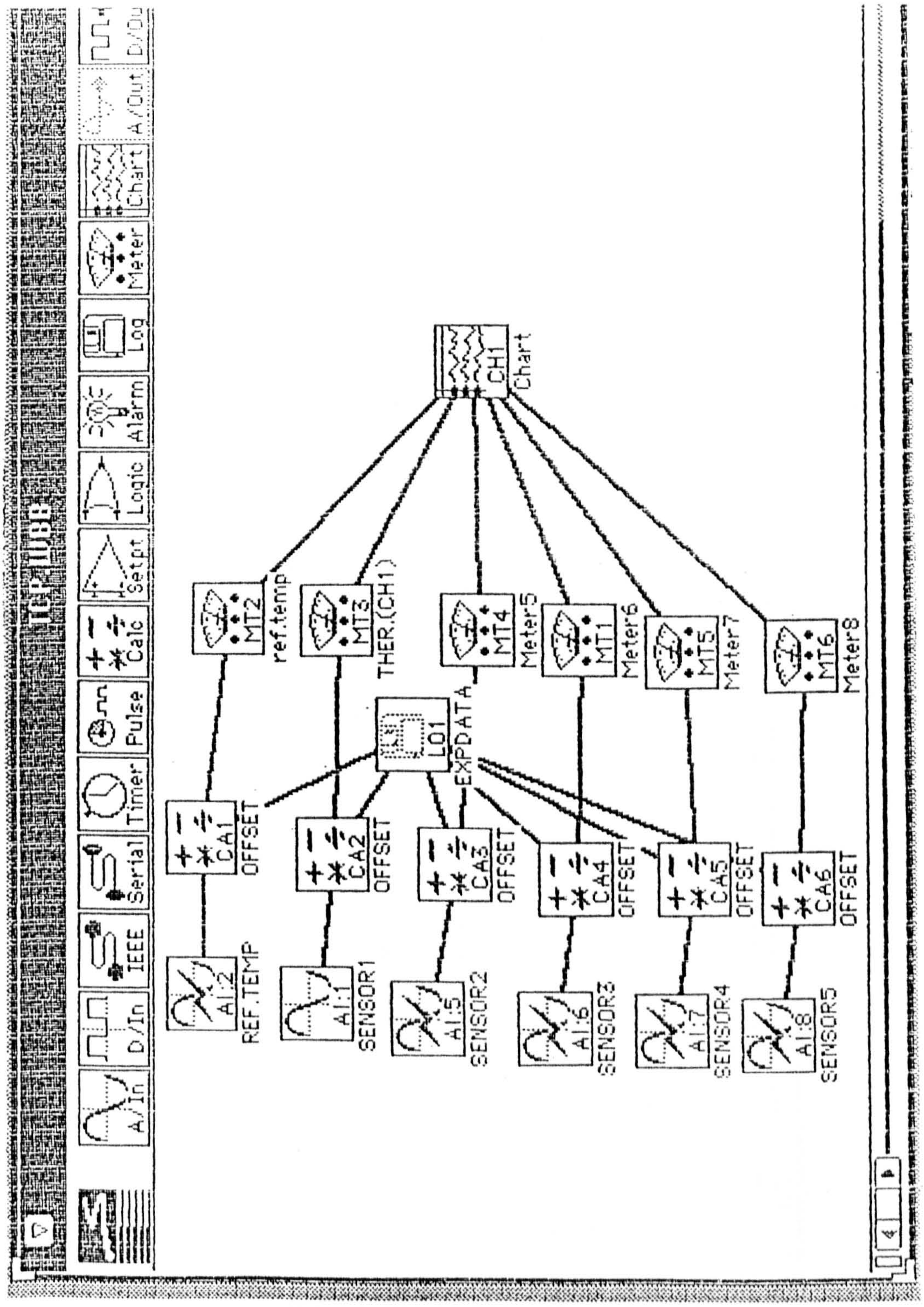

Fig. 7.5.1. Workbench Input Layout for Calibration of Temperature Sensors

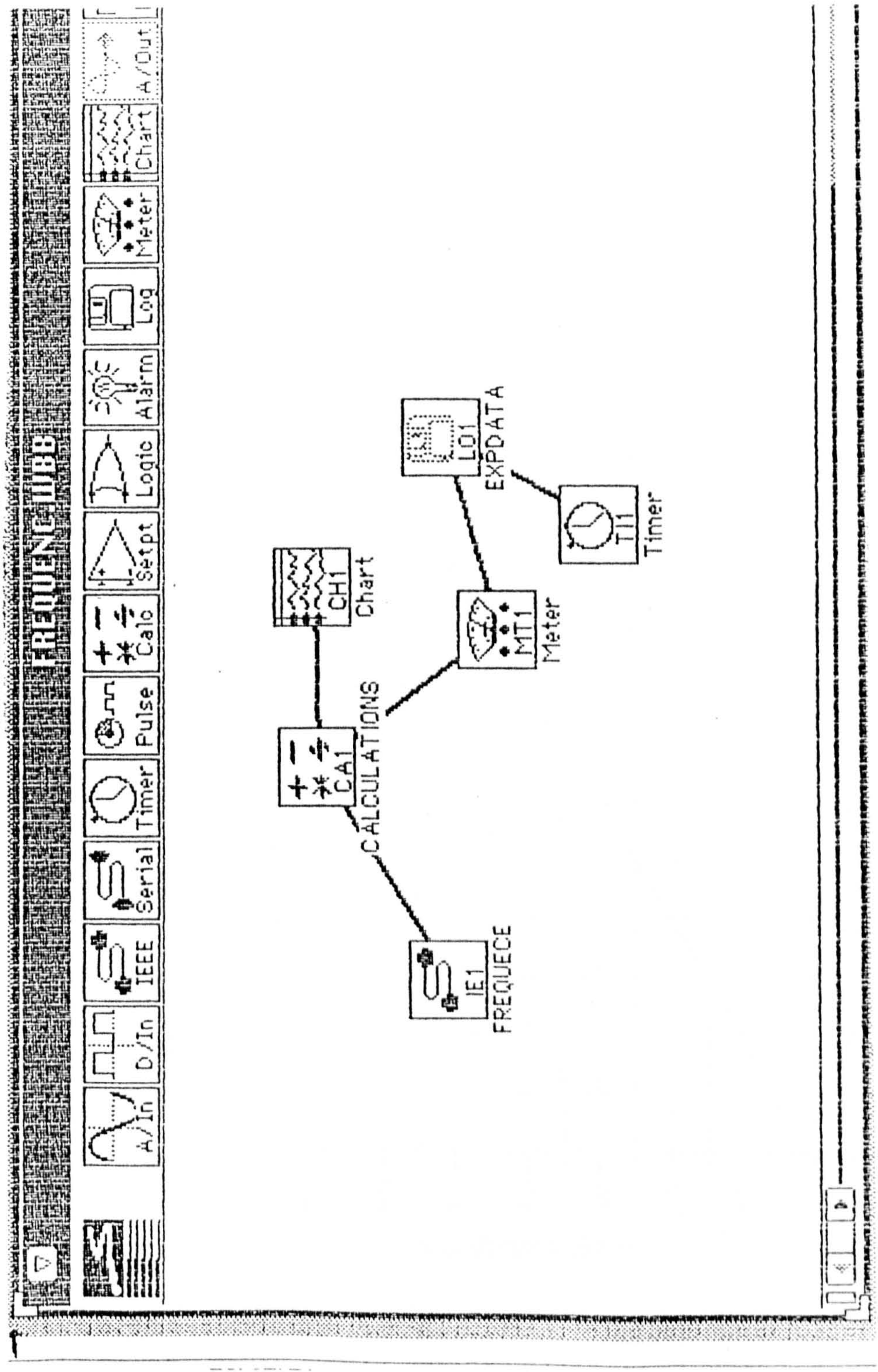

Fig. 7.5.2. Workbench Input Layout for Flowrate Measurement

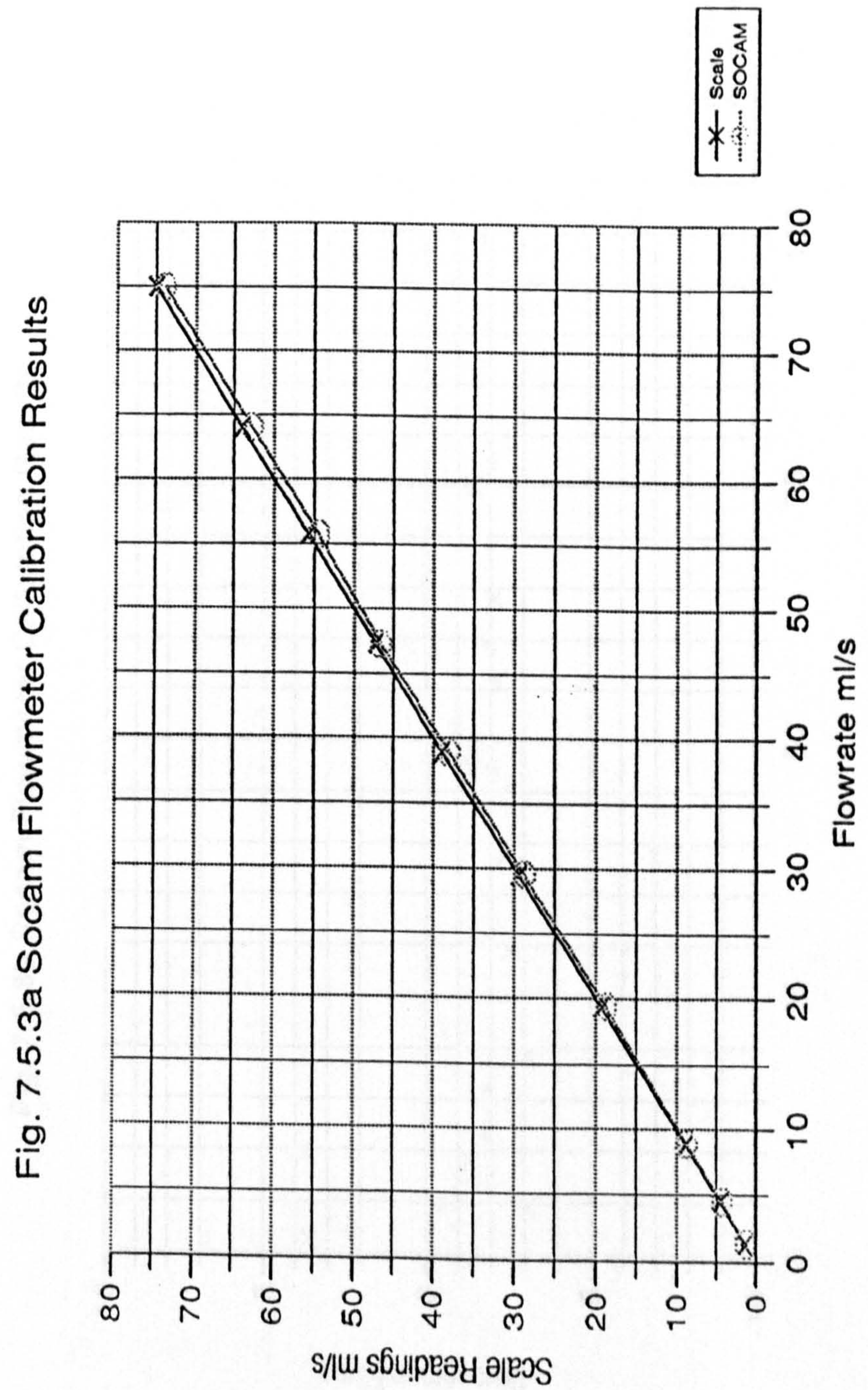

Fig. 7.5.3a Socam Flowmeter Calibration Results

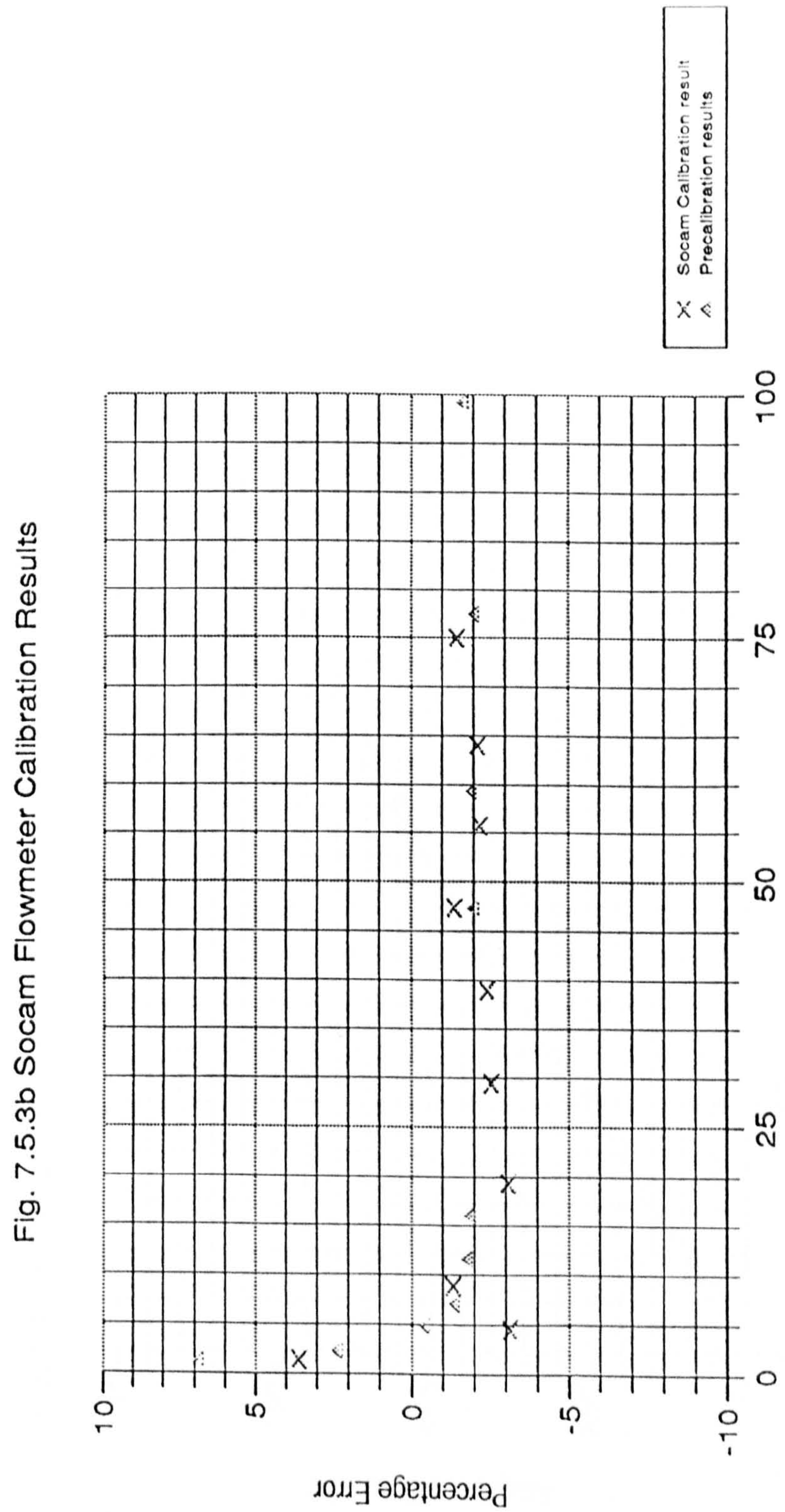

Fig. 7.5.3b Socam Flowmeter Calibration Results

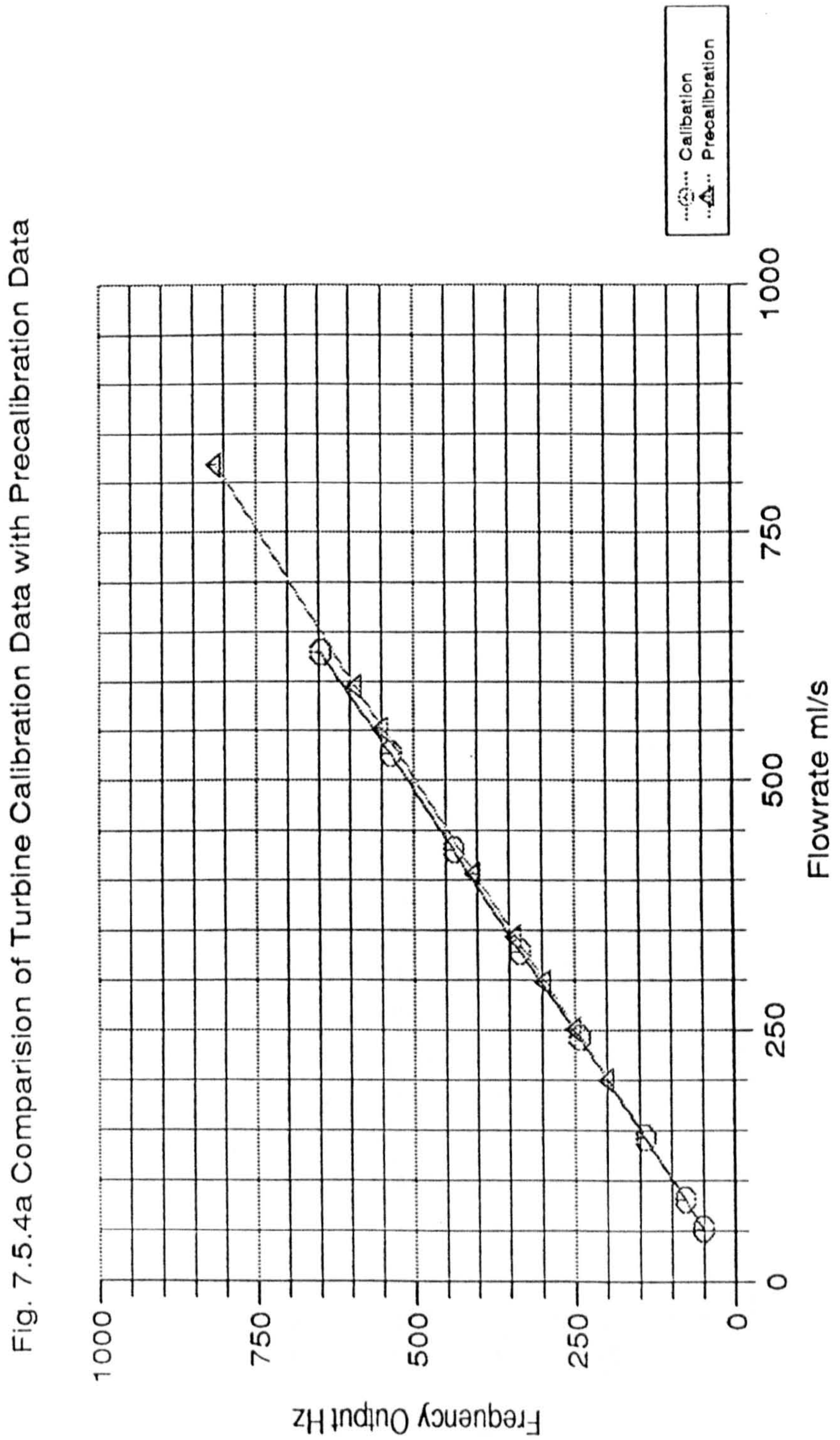
Fig. 7.5.4a Comparision of Turbine Calibration Data with Precalibration Data
Calibation
Precalibration
1000
750
500
250
0
Frequency Output Hz
Flowrate ml/s

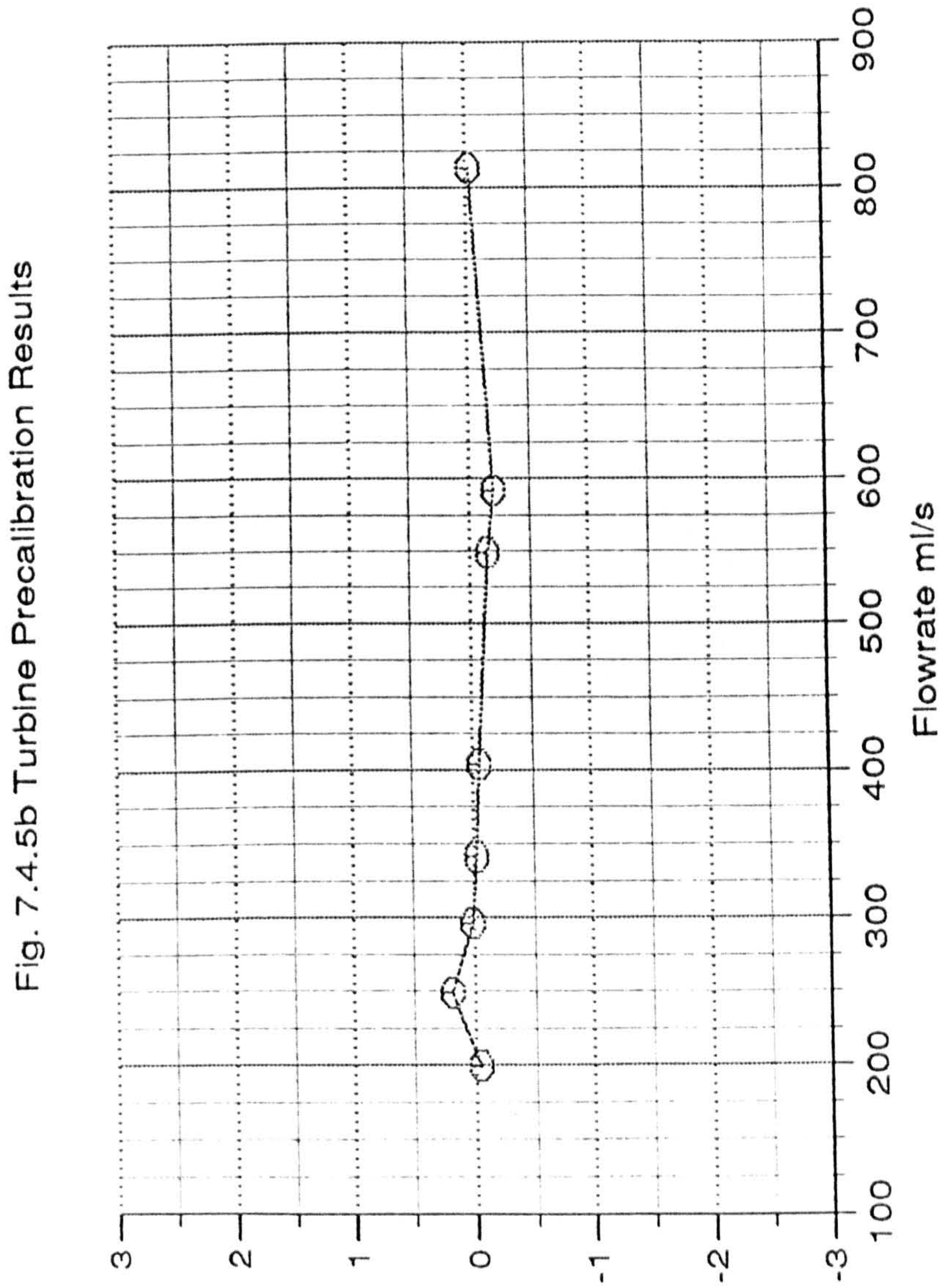

Fig. 7.4.5b Turbine Precalibration Results

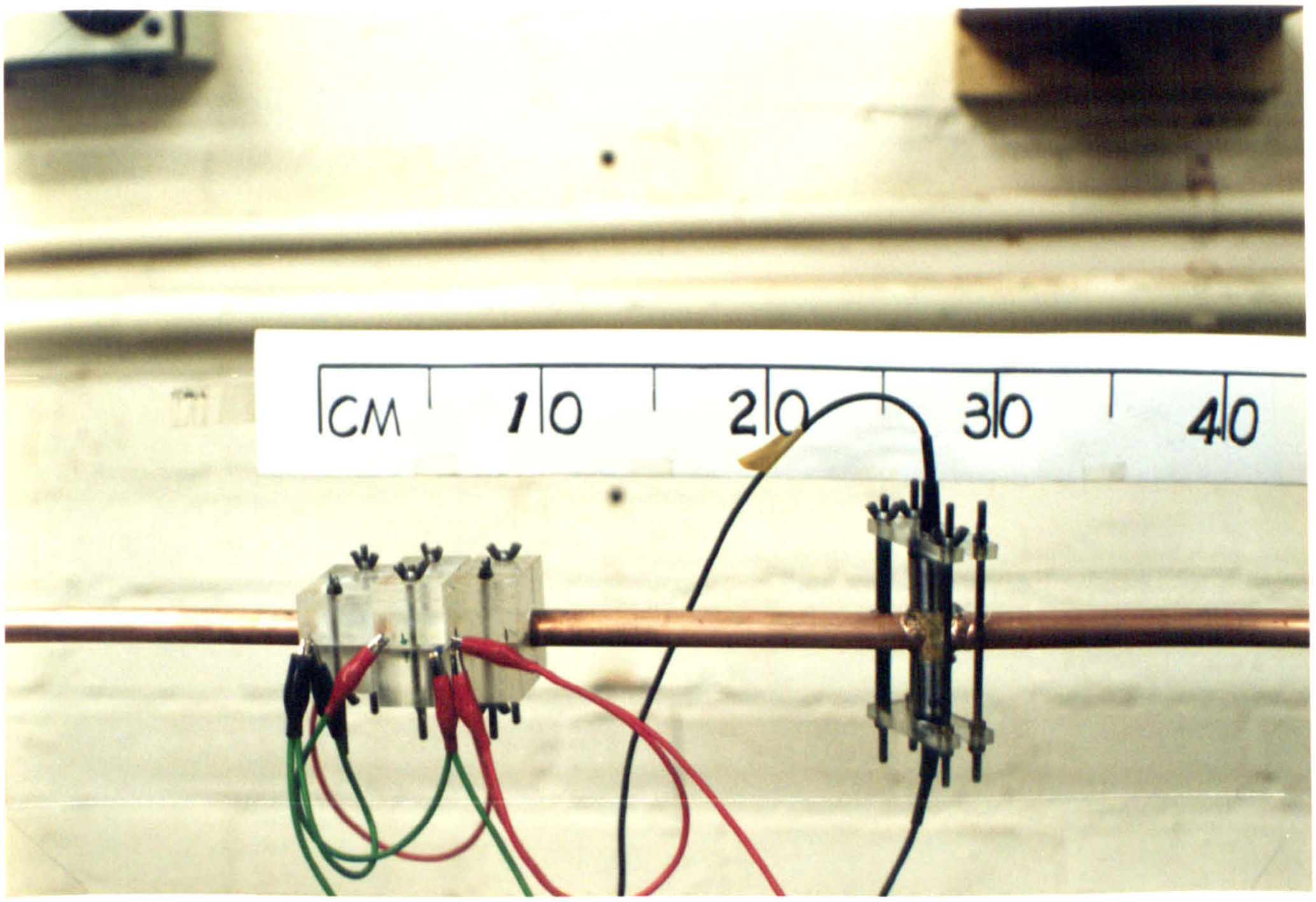

Fig. 7.6.1. View of the Test Section for the Ultrasonic/Thermal Technique

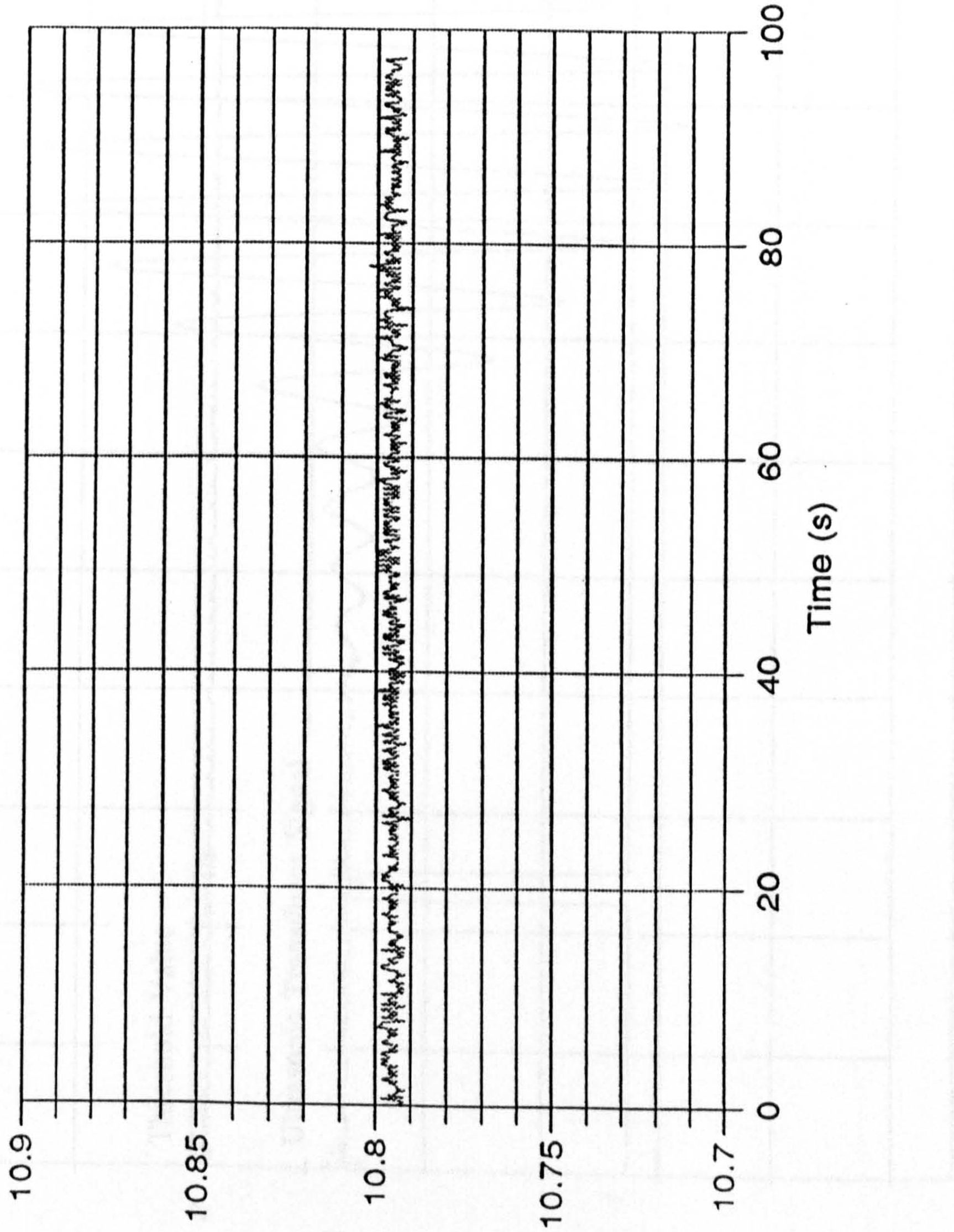
Fig. 8.3.1 Trace of Steady State Signal
Transit Time (E-6)s
10.9
10.85
10.8
10.75
10.7
0
20
40
60
80
100
Time (s)

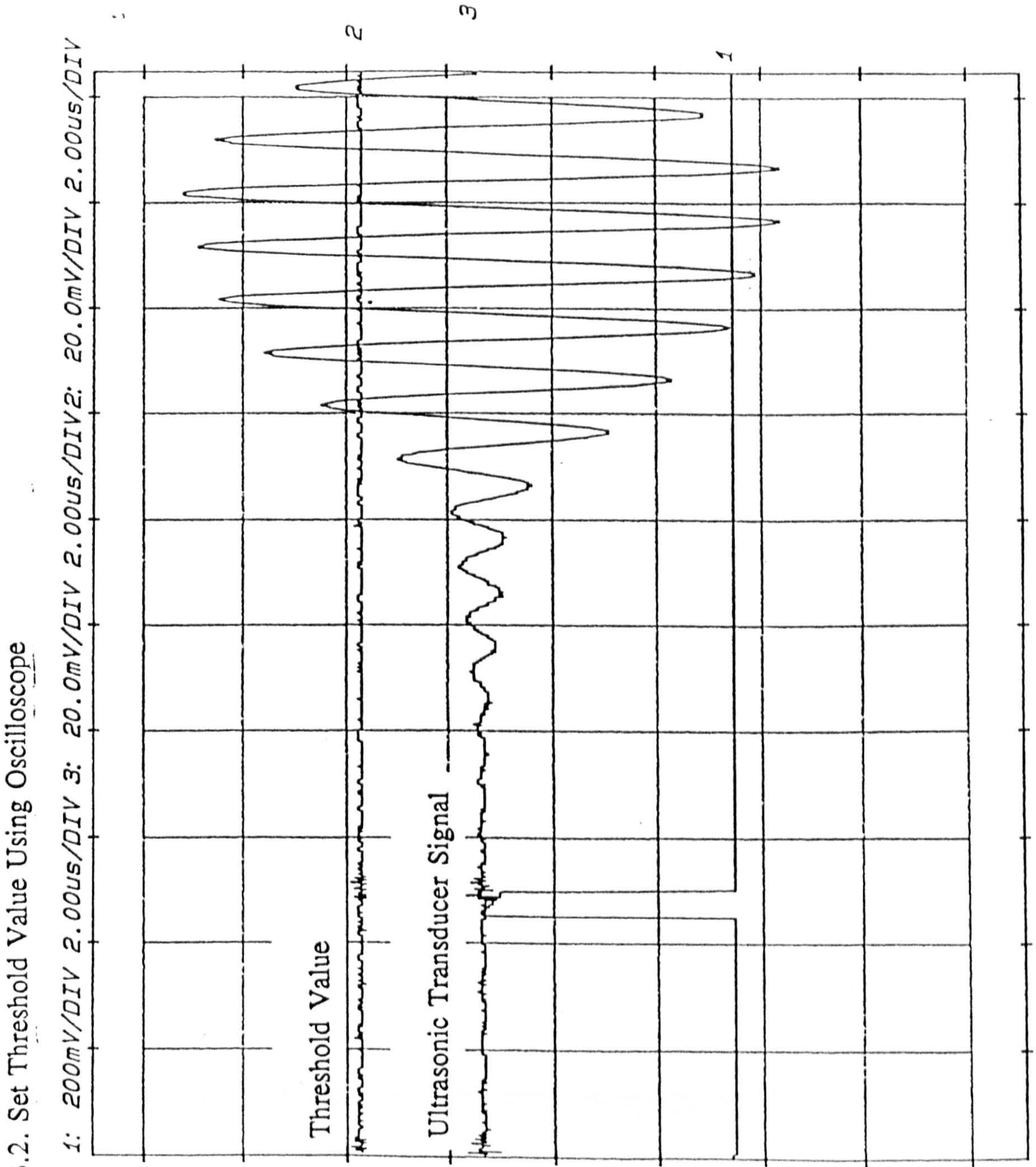

Fig. 8.3.2. Set Threshold Value Using Oscilloscope

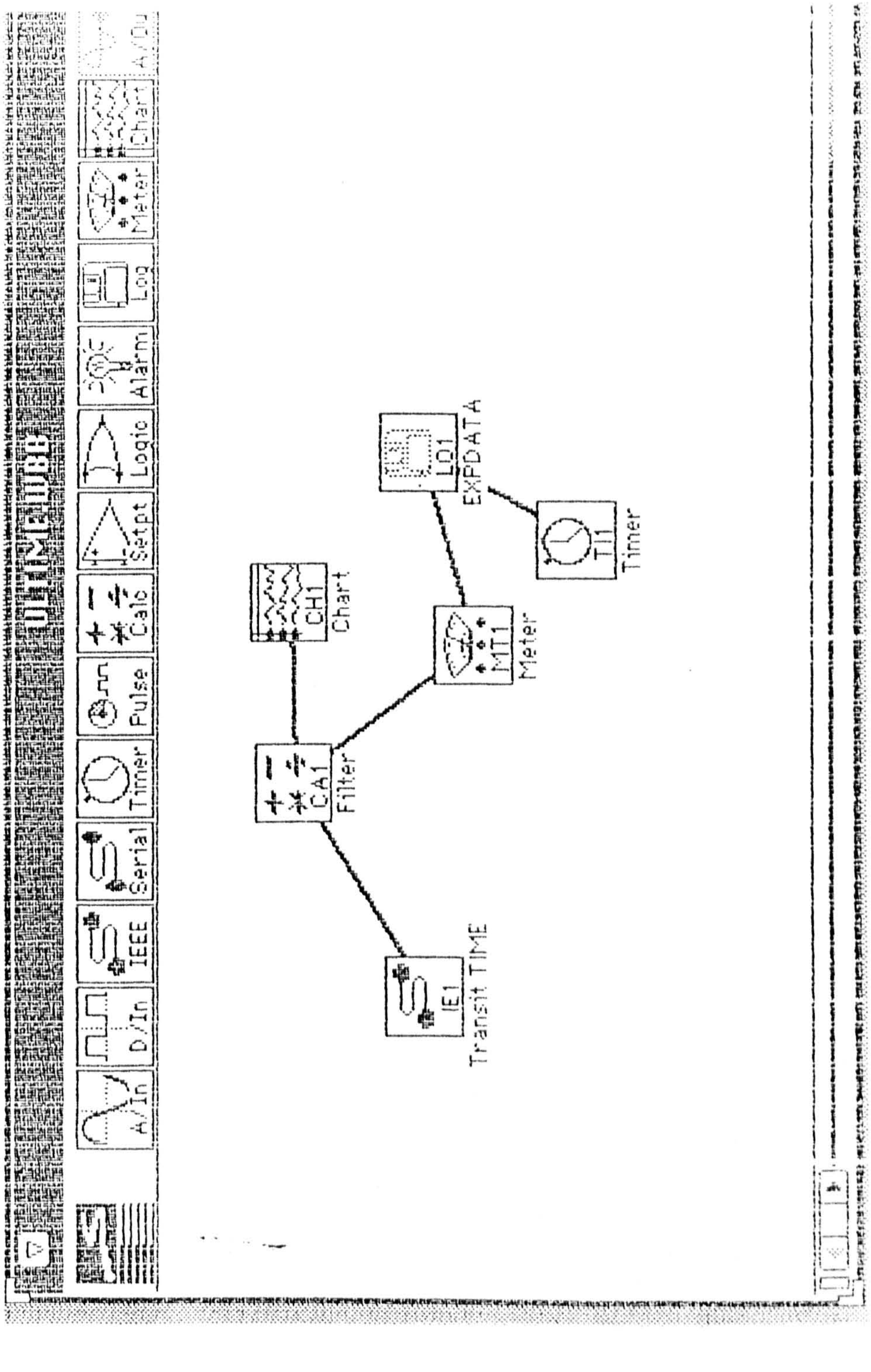

Fig. 8.3.3. Workbench Input Layout for Transit Time Measurement

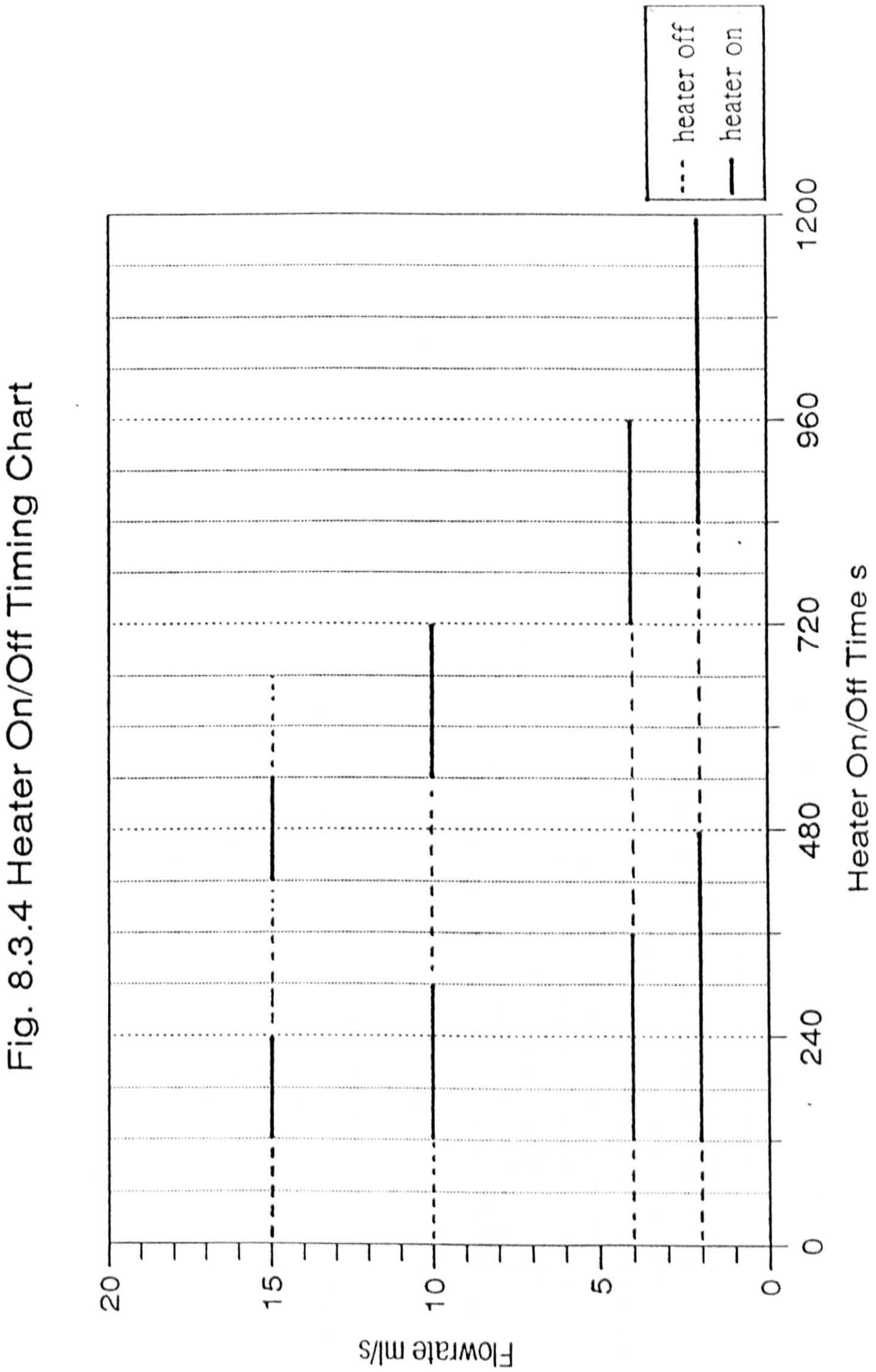

Fig. 8.3.4 Heater On/Off Timing Chart

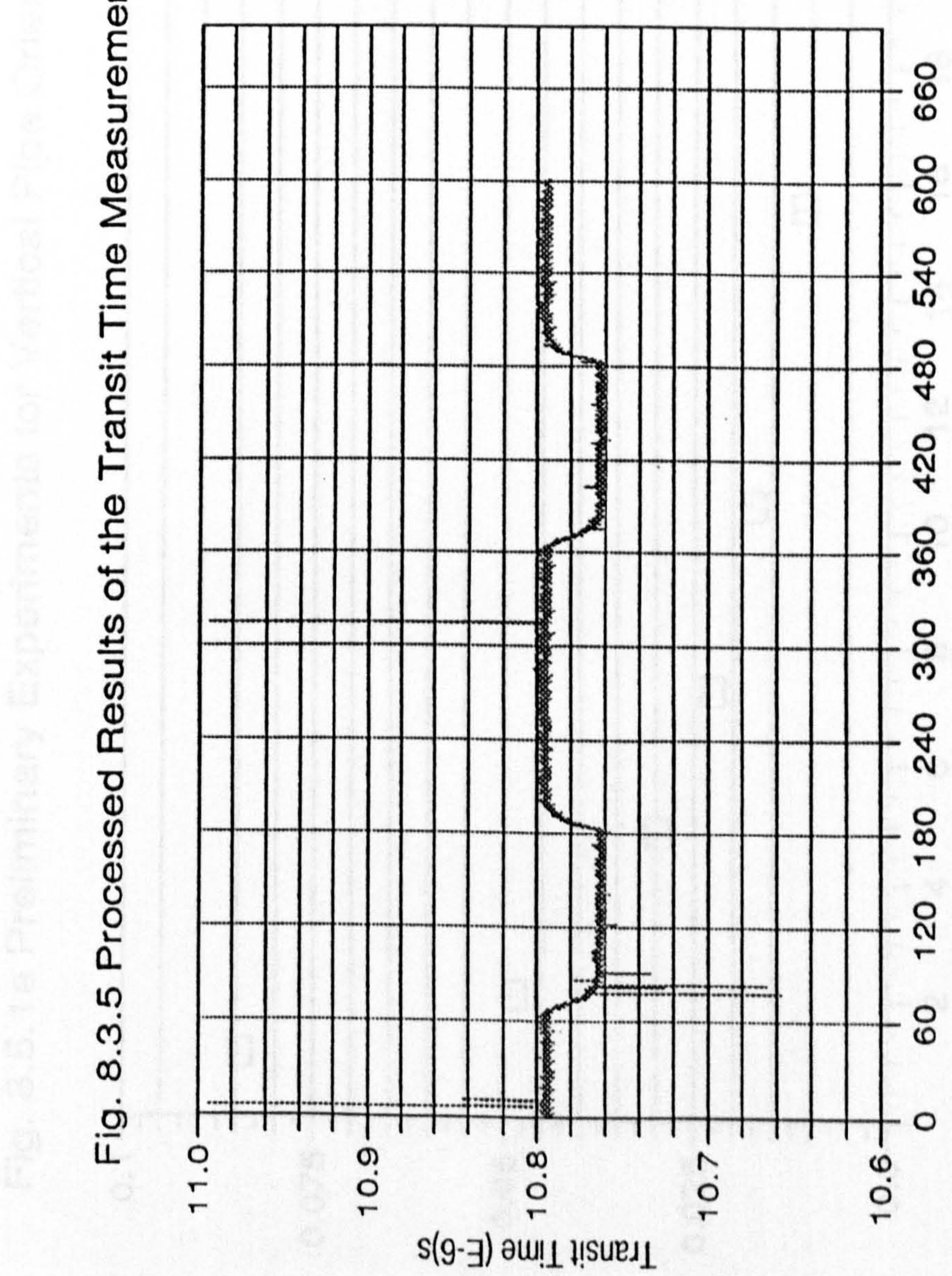

Fig. 8.3.5 Processed Results of the Transit Time Measurement

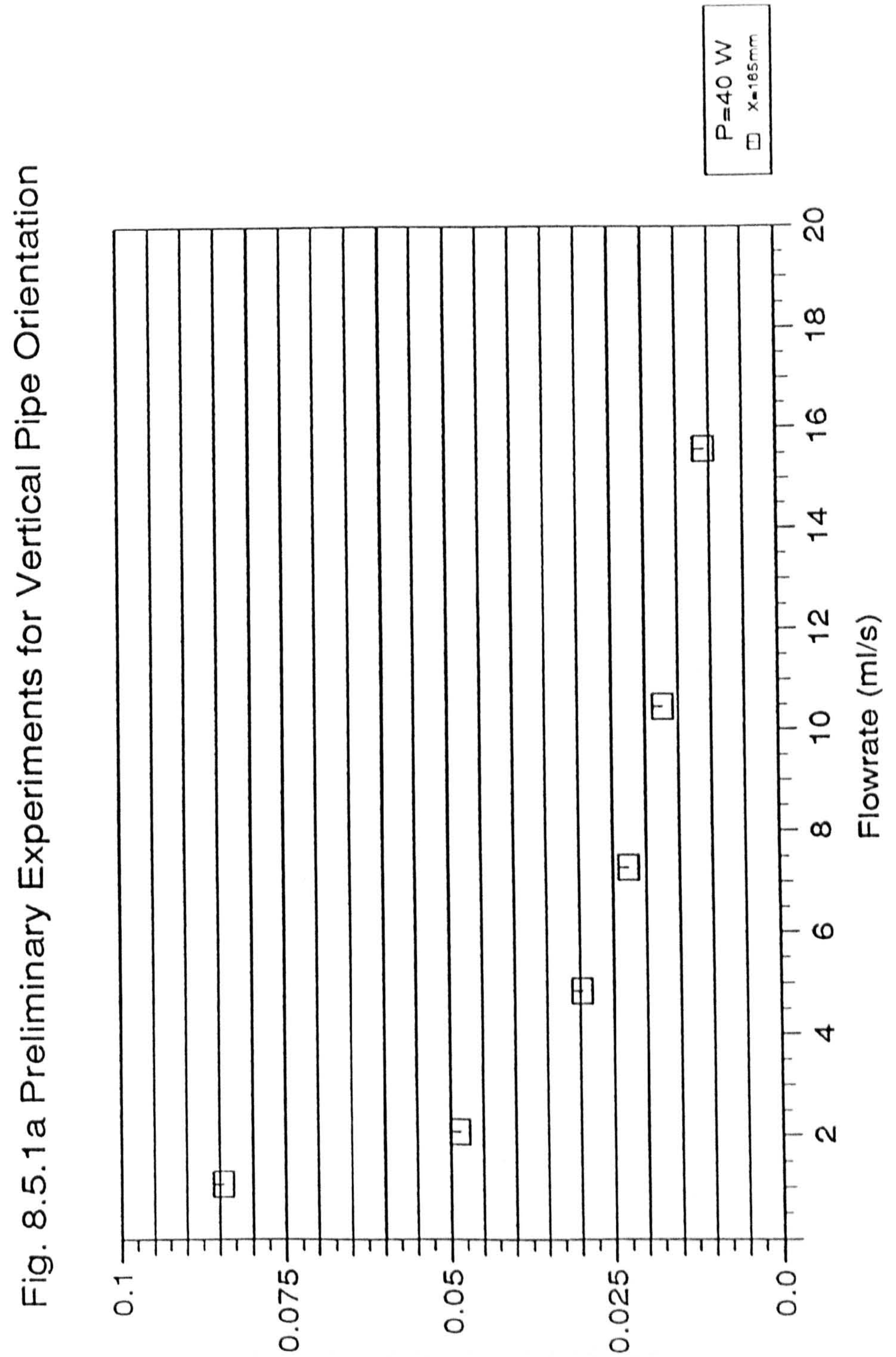

Fig. 8.5.1a Preliminary Experiments for Vertical Pipe Orientation

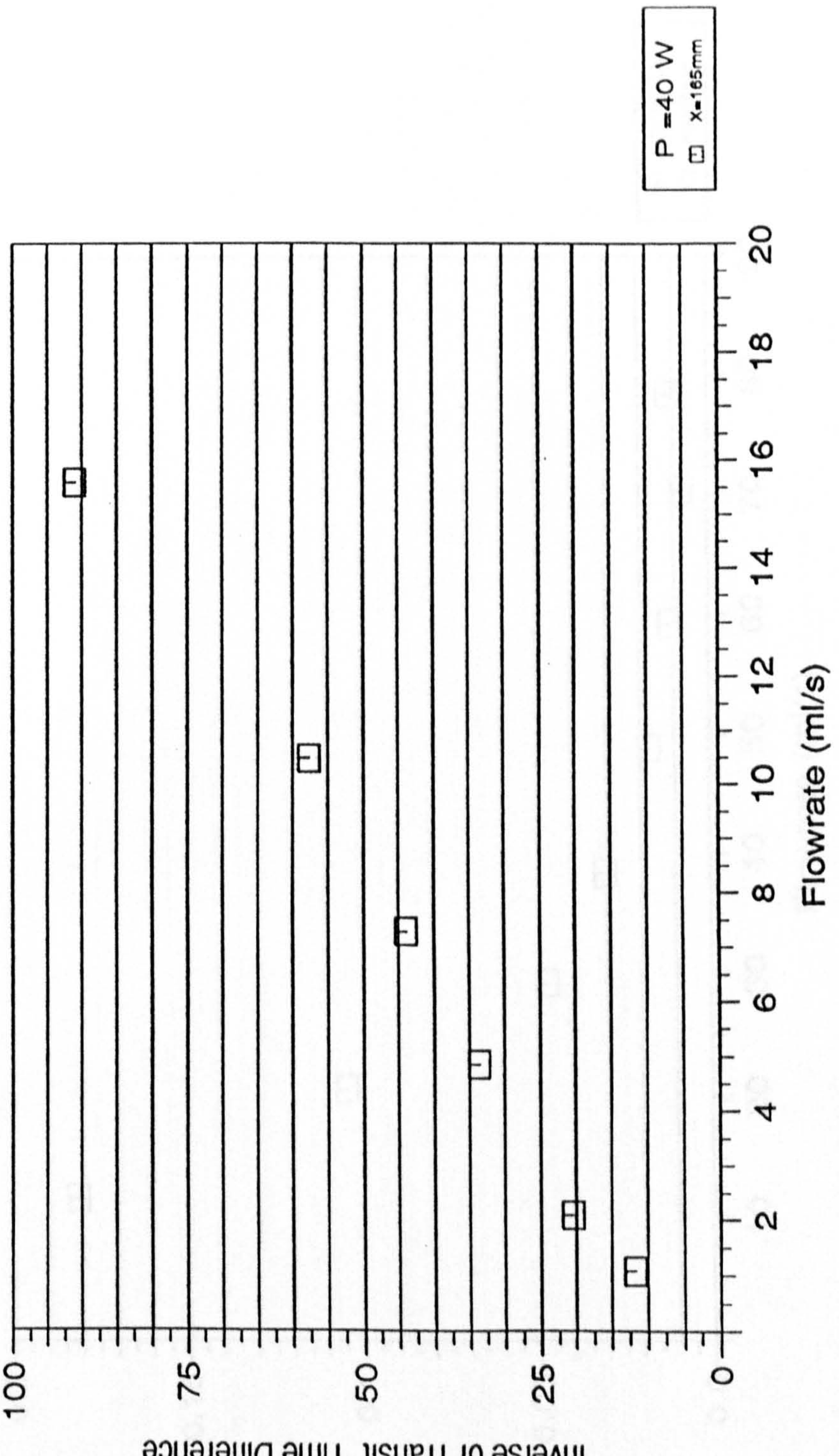

Fig. 8.5.1b Preliminary Experiments for Vertical Pipe Orientation

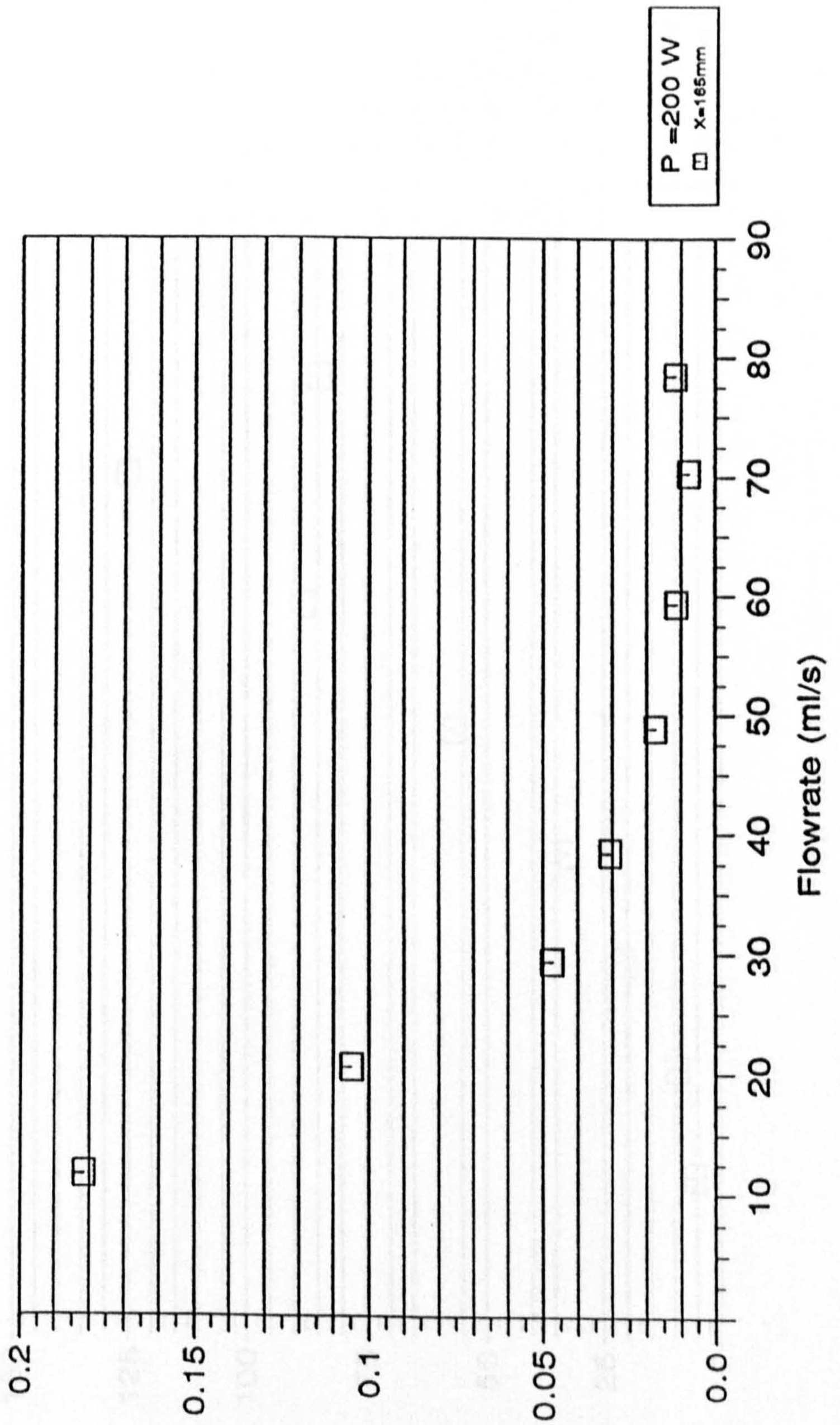

Fig. 8.5.2a Preliminary Experiments for Horizontal Pipe Orietation

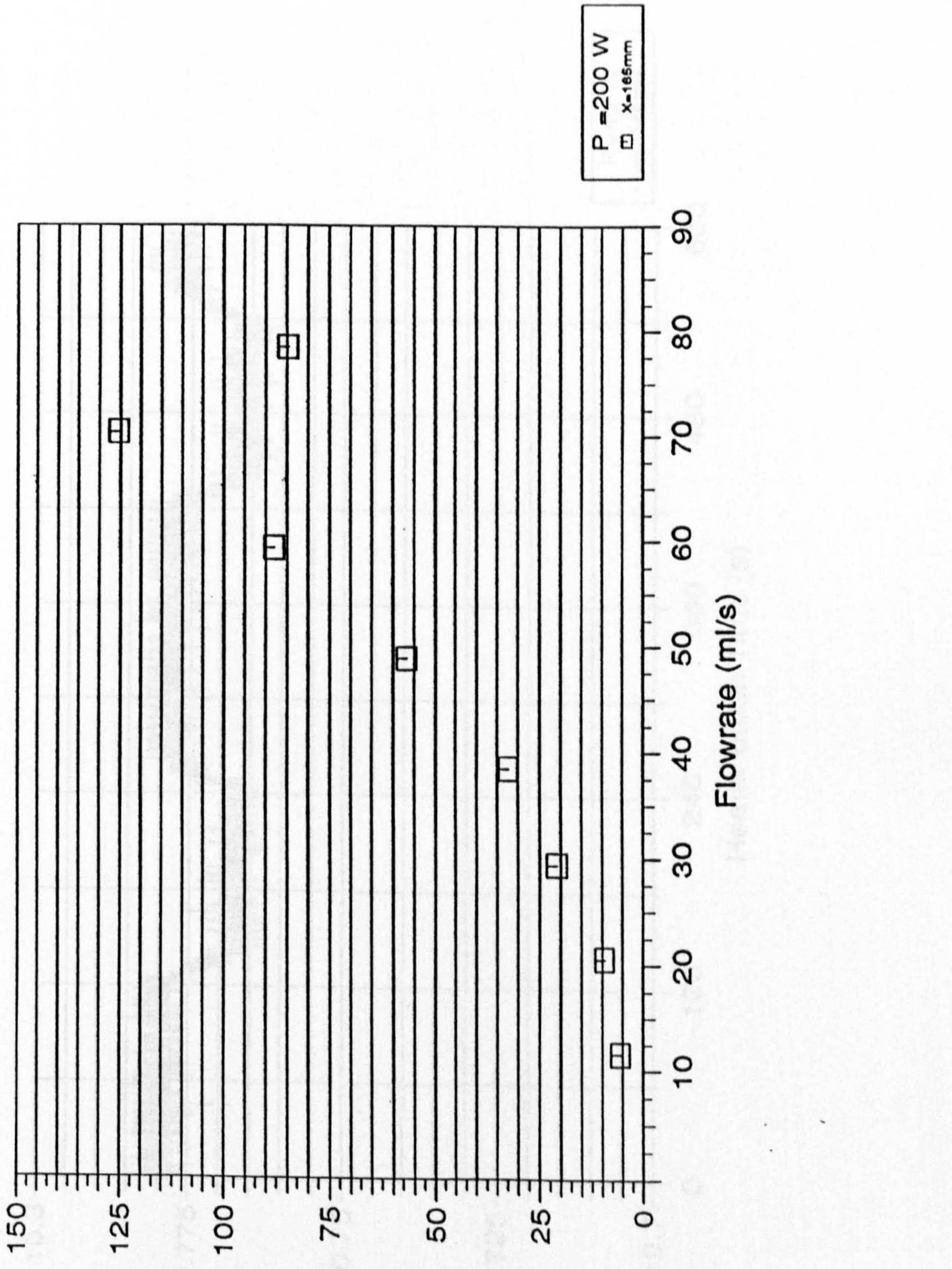

Fig. 8.5.2b Preliminary Experiments for Horizontal Pipe Orientation

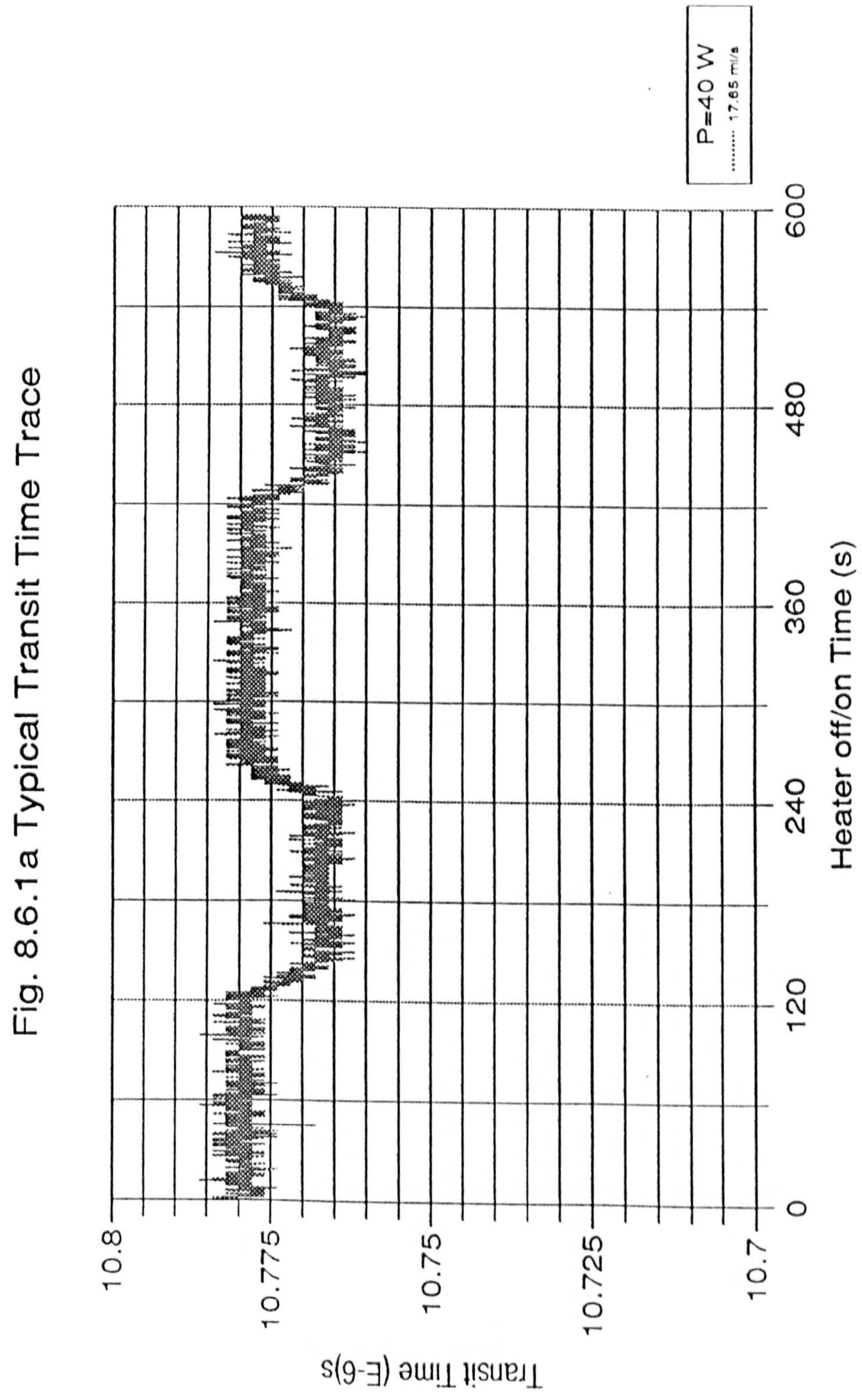

Fig. 8.6.1a Typical Tra

Fig.8.6.1b Typical Transit Time Trace

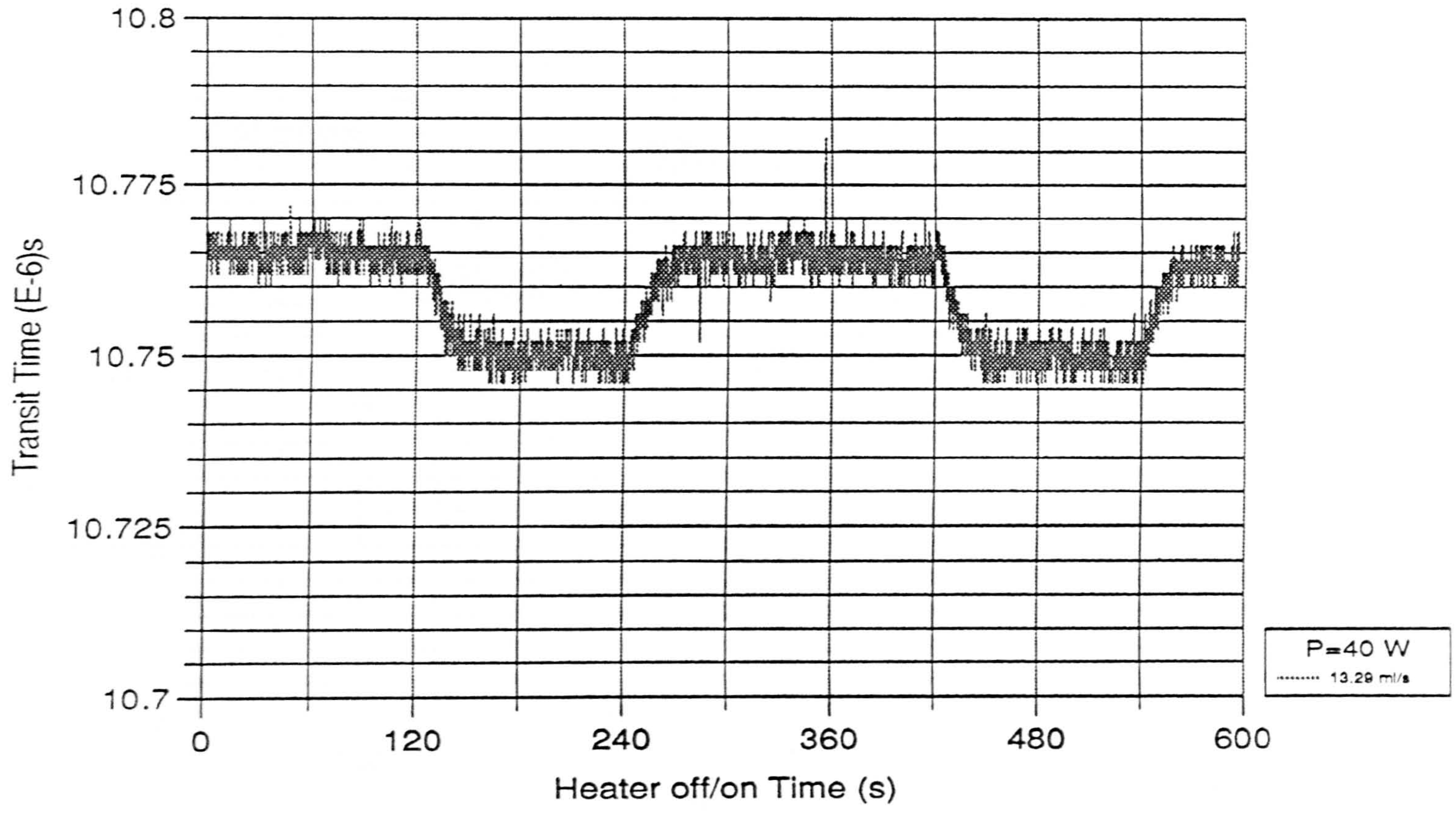

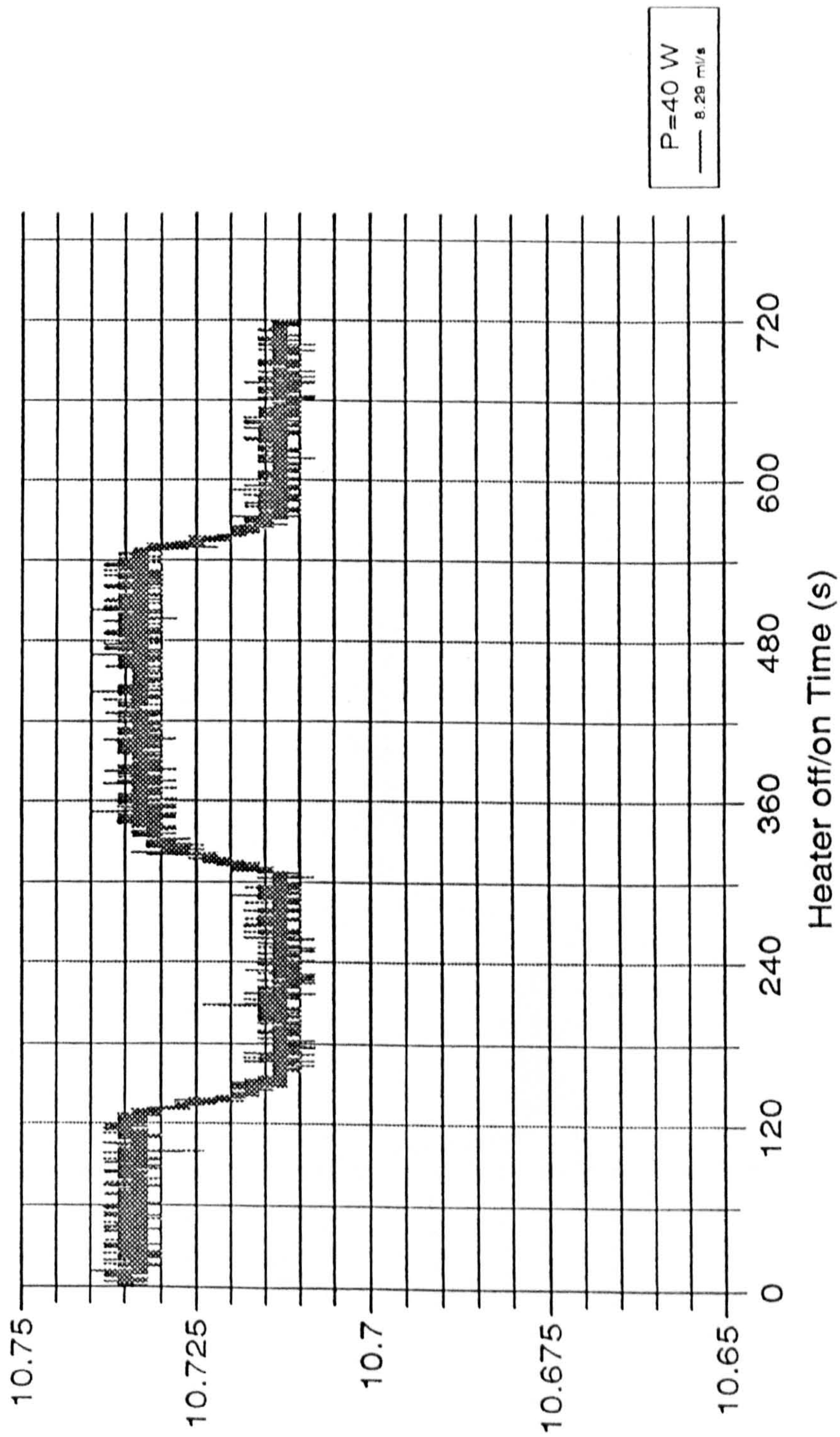

Fig. 8.6.1c Typical Tra

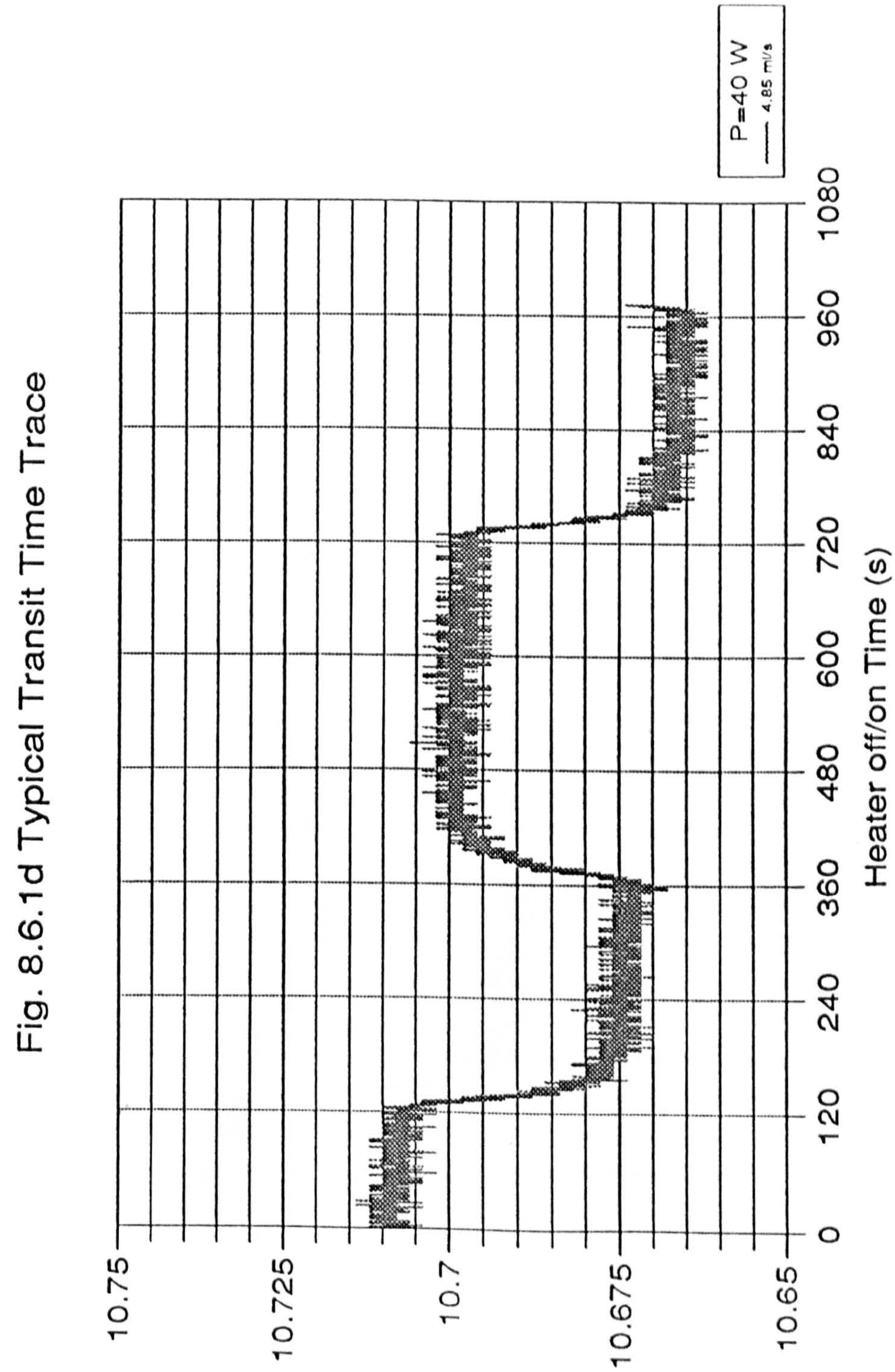

Fig. 8.6.1d Typical T

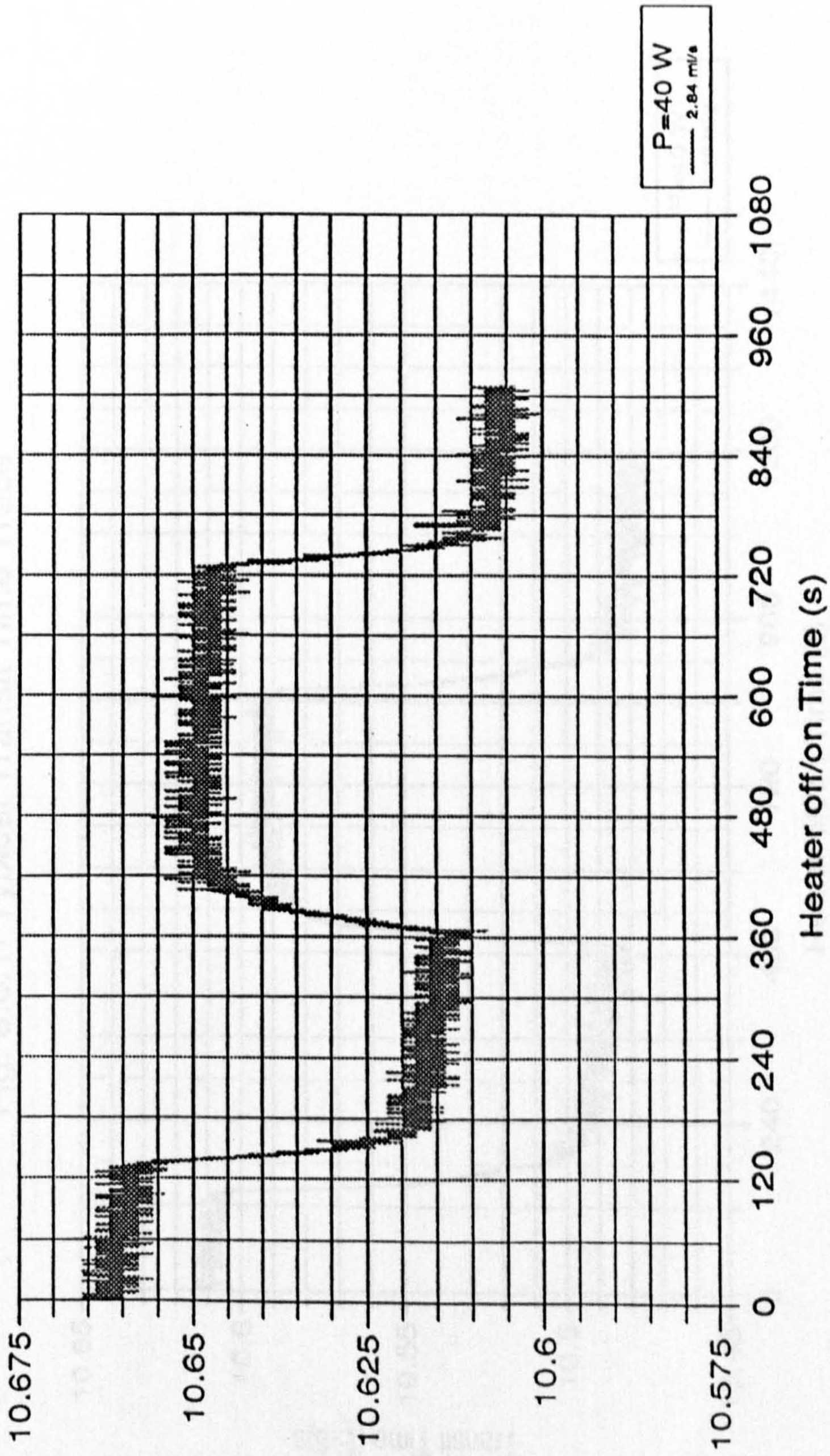

Fig. 8.6.1e Typical Transit Time Trace

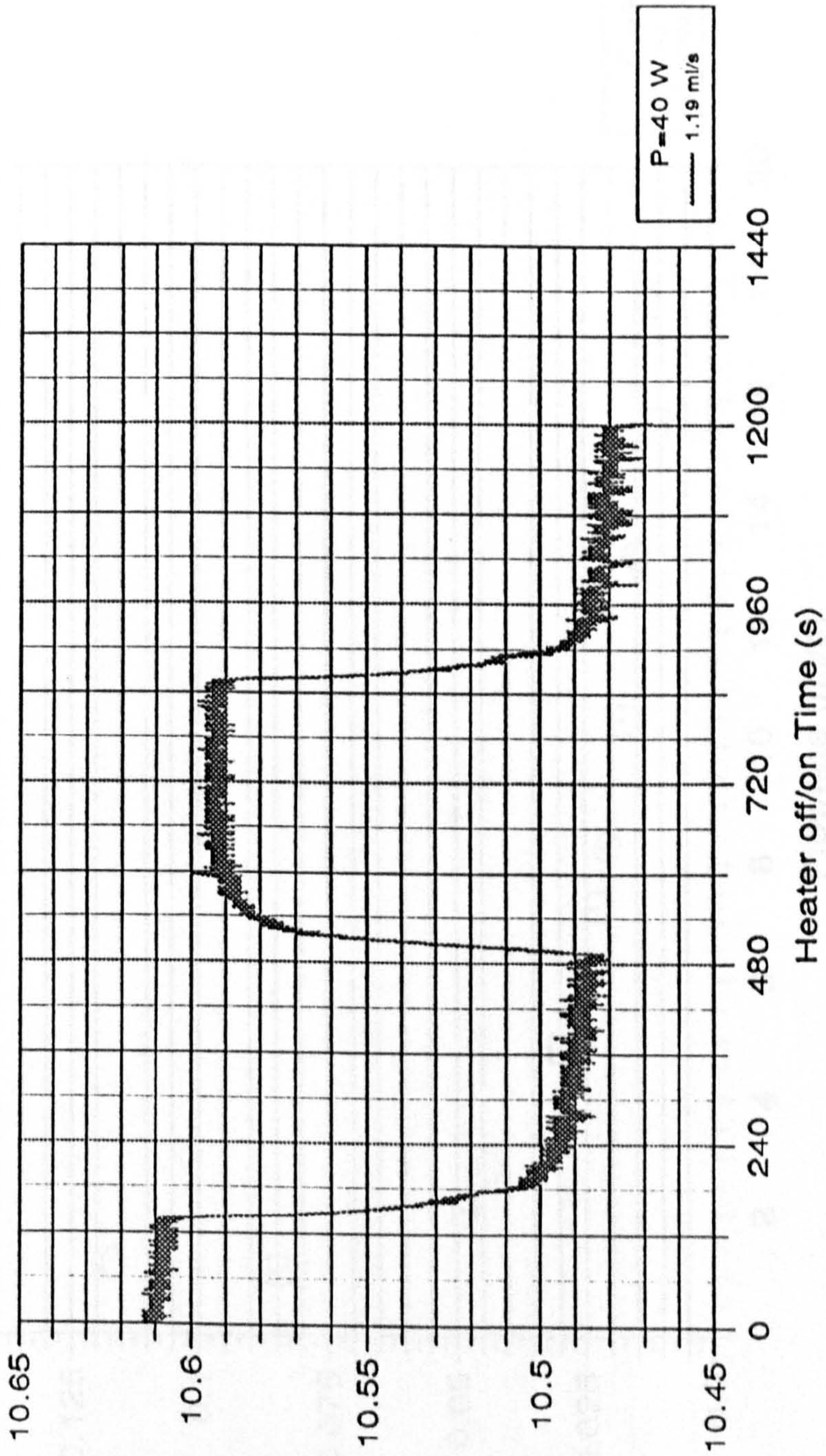

Fig. 8.6.1f Typical Tra

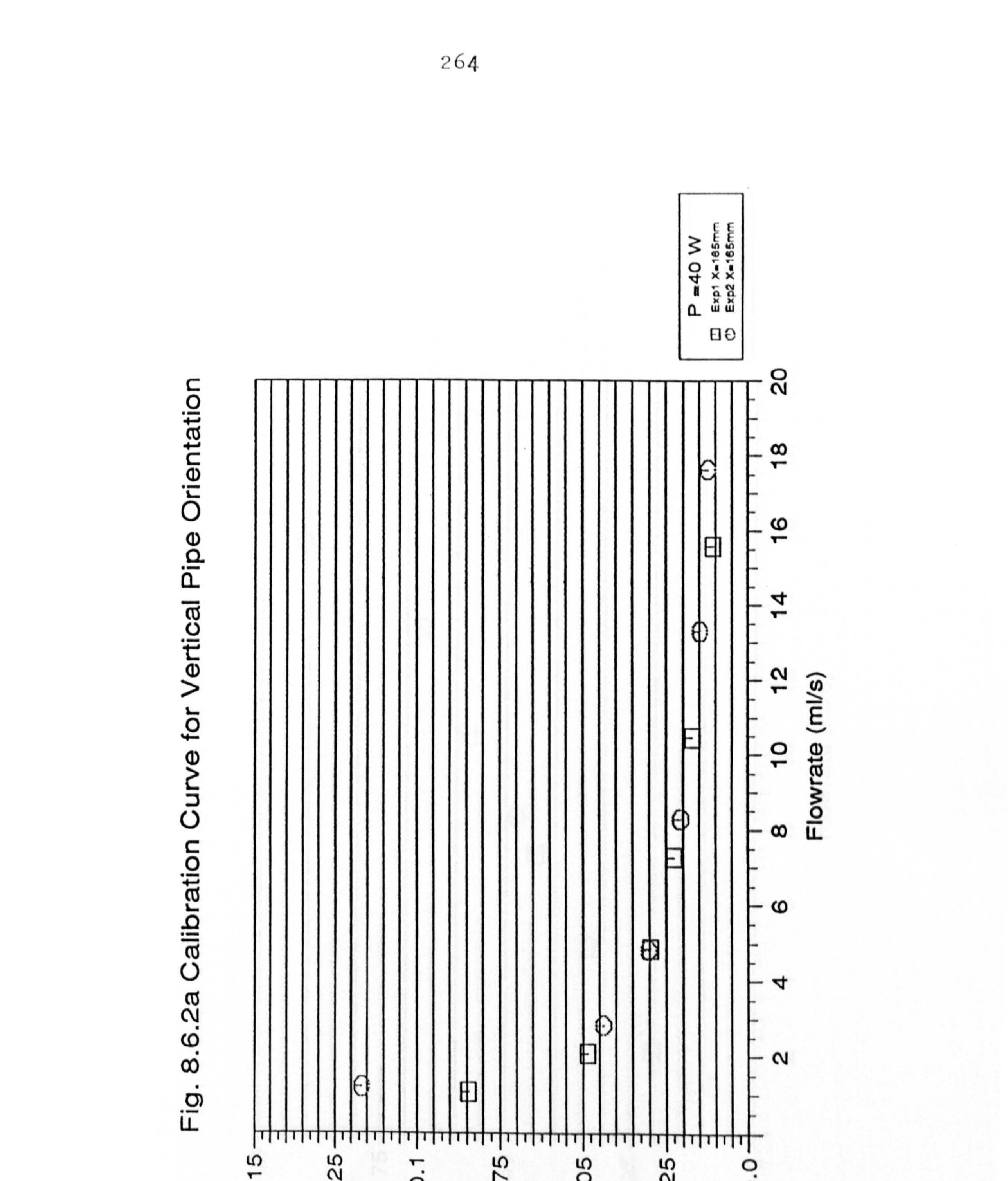

Fig. 8.6.2a Calibration Curve for Vertical Pipe Orientation

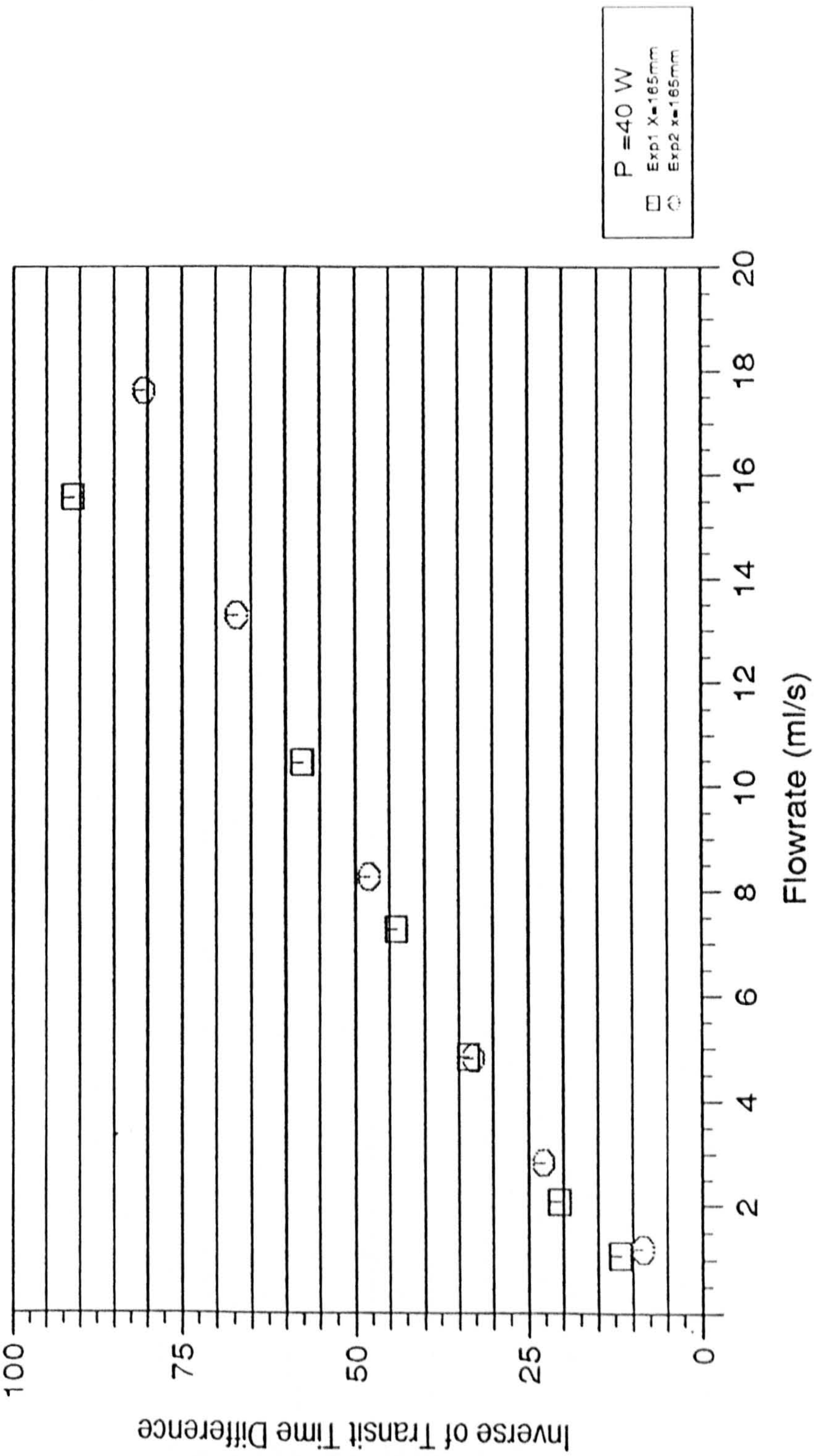

Fig. 8.6.2b Calibration Curve for Vertical Pipe Orientation

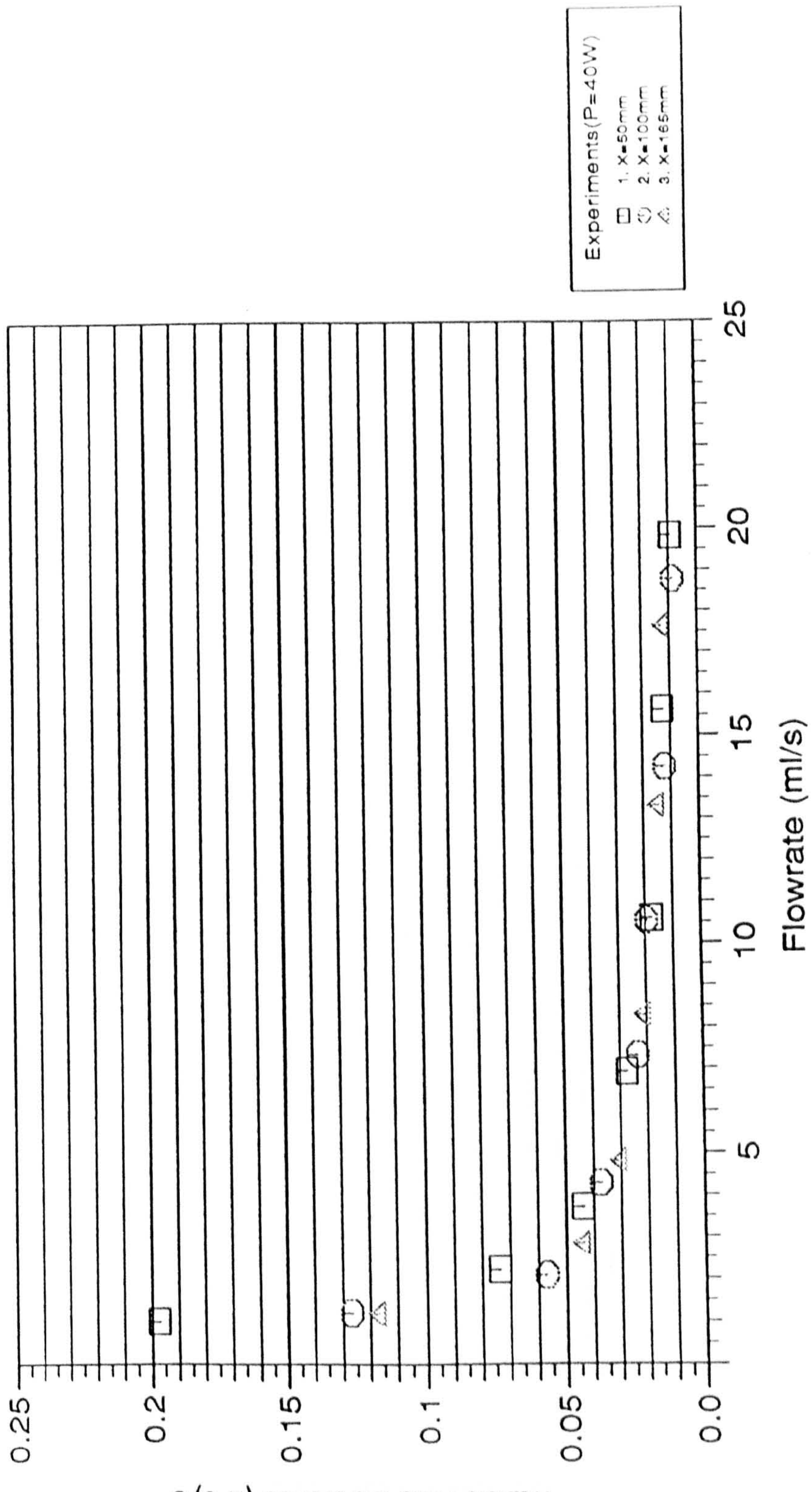

Fig. 8.6.3a Heater - Transducers Separations(Vertical Pipe Orientation)

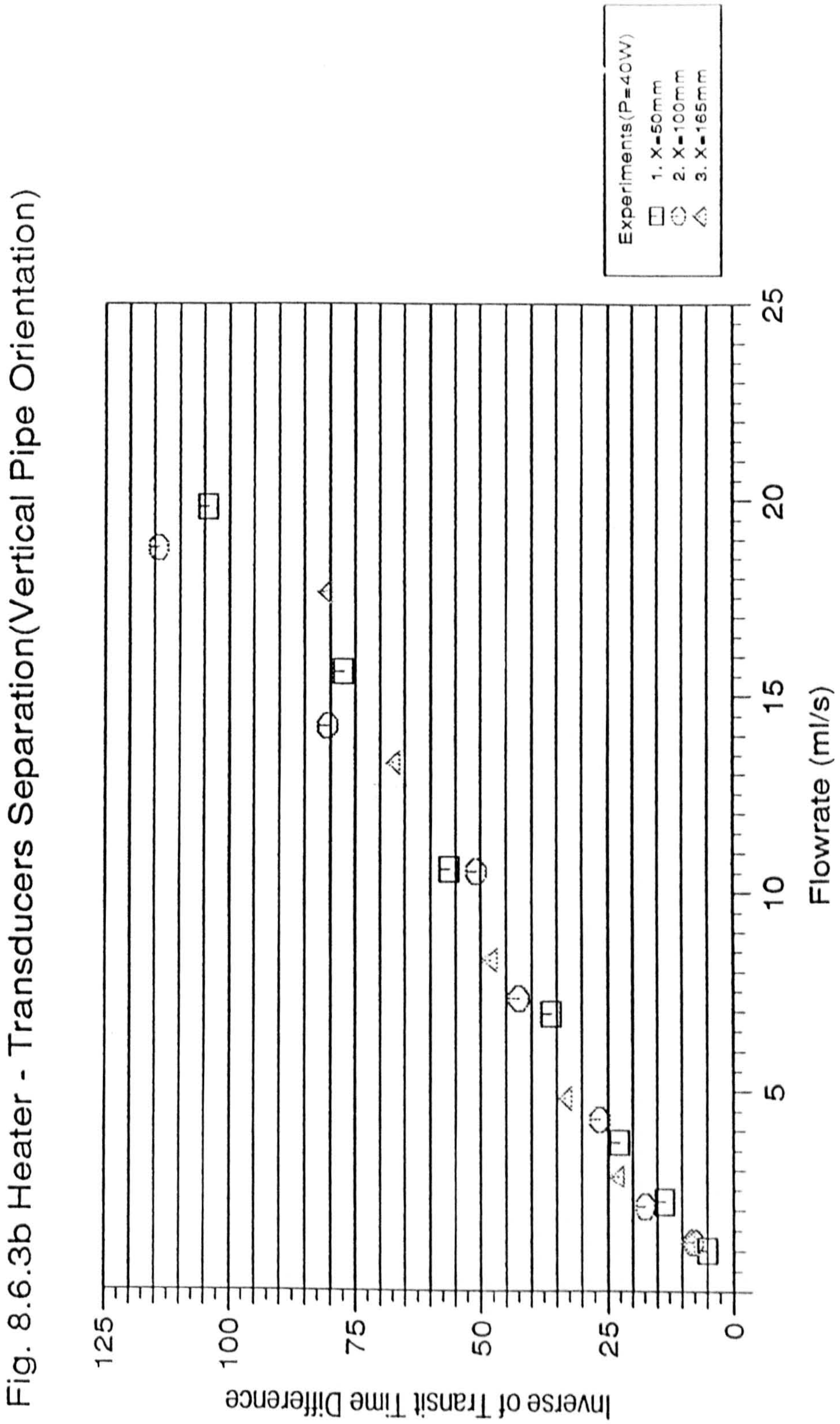

Fig. 8.6.3b Heater - Transducers Separation(Vertical Pipe Orientation)

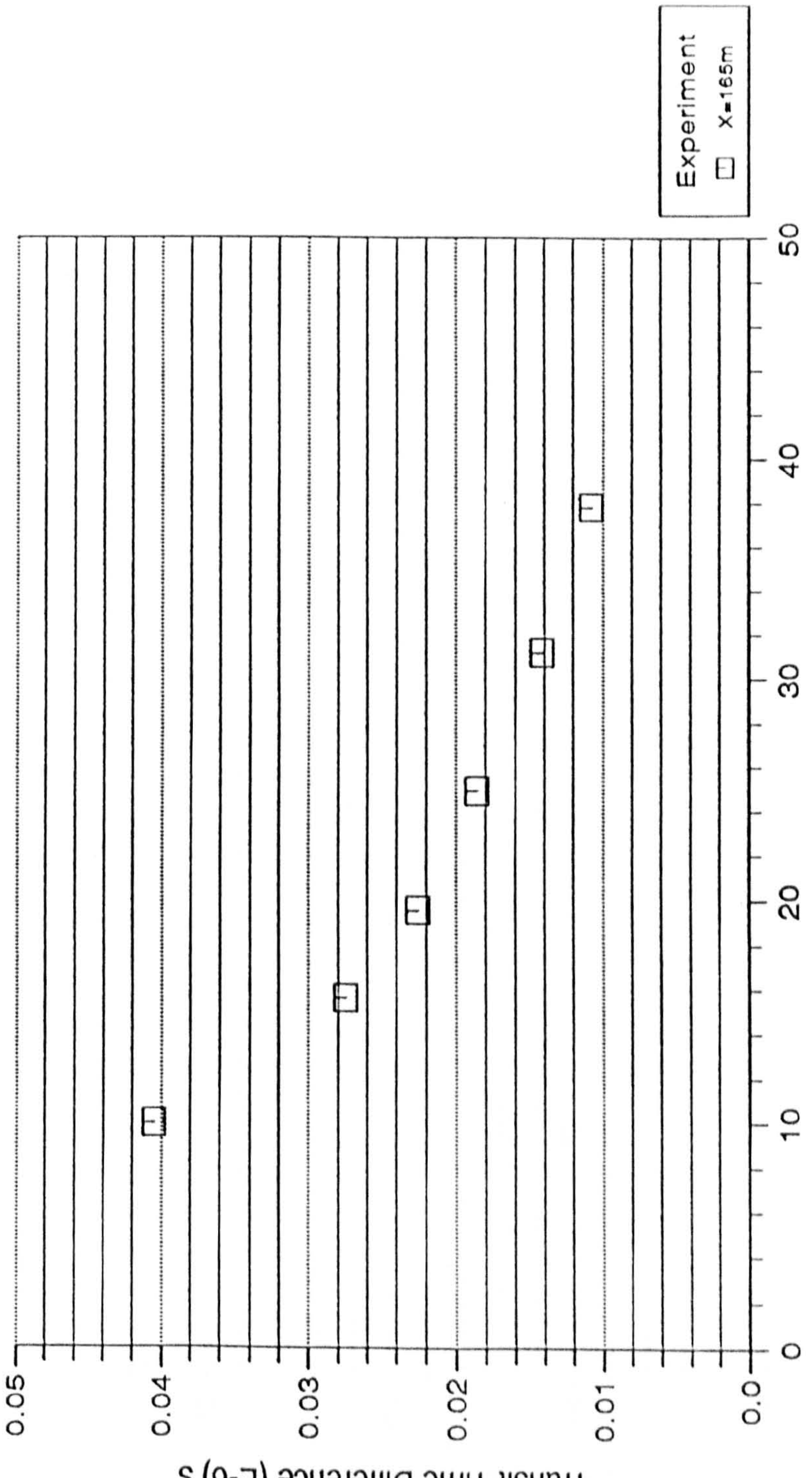

Fig.8.6.4a Calibration Curve for Vertical Pipe (P=100W)

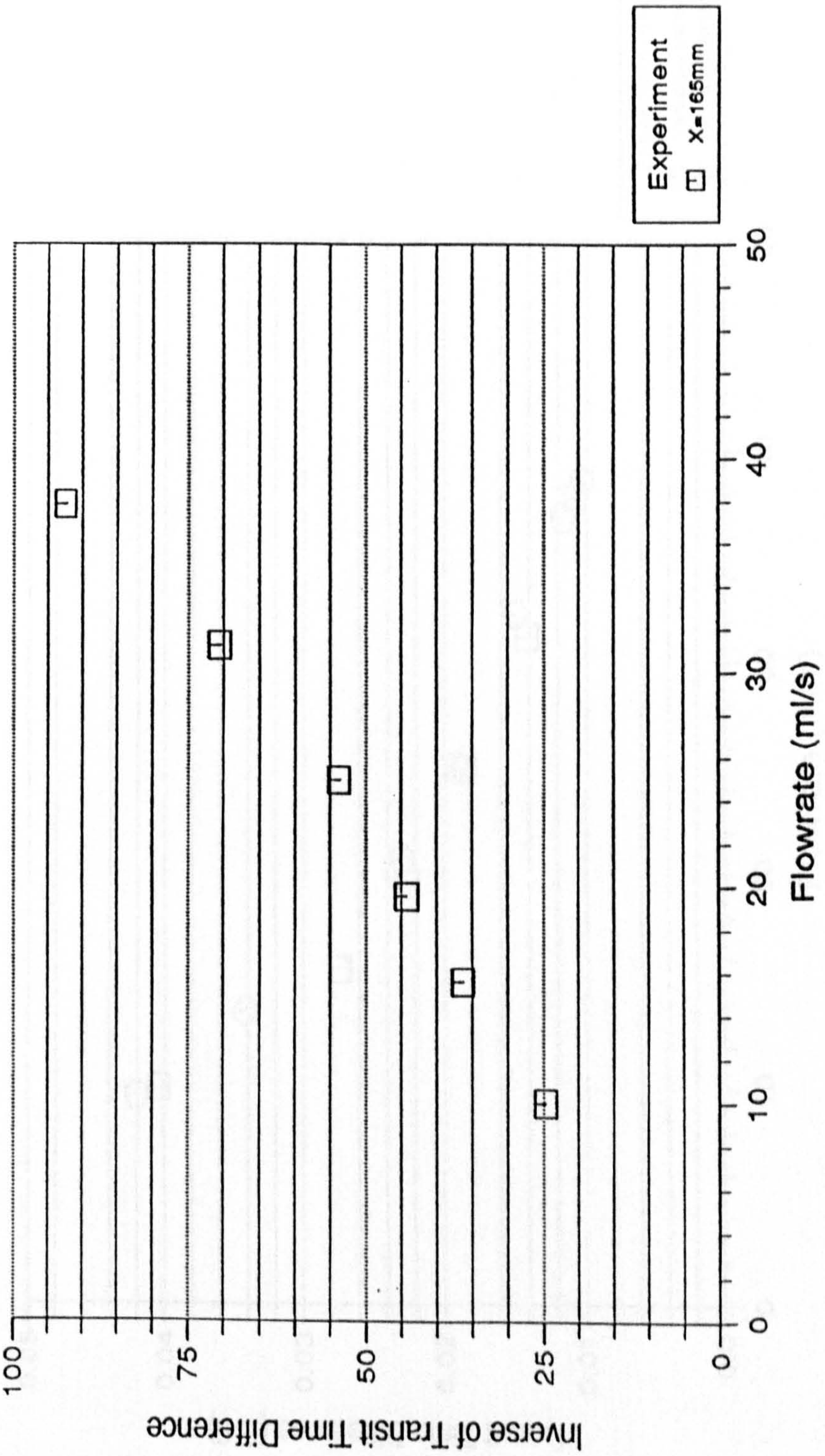

Fig. 8.6.4b Calibration Curve for Vertical Pipe (P=100W)

Fig. 8.6.5a Repeatability of The Flowmeter

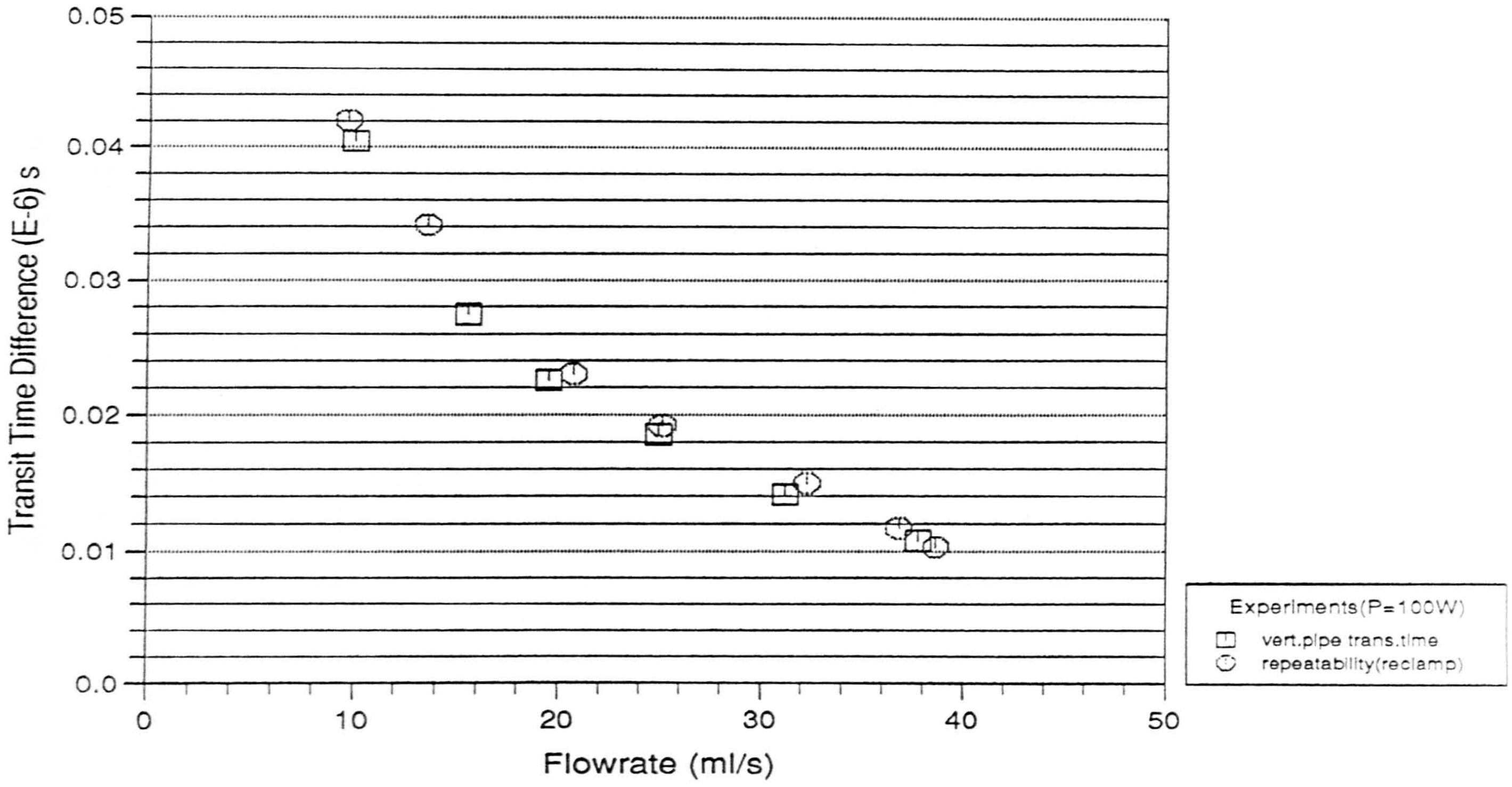

Fig. 8.6.5b Repeatability of The Flowmeter

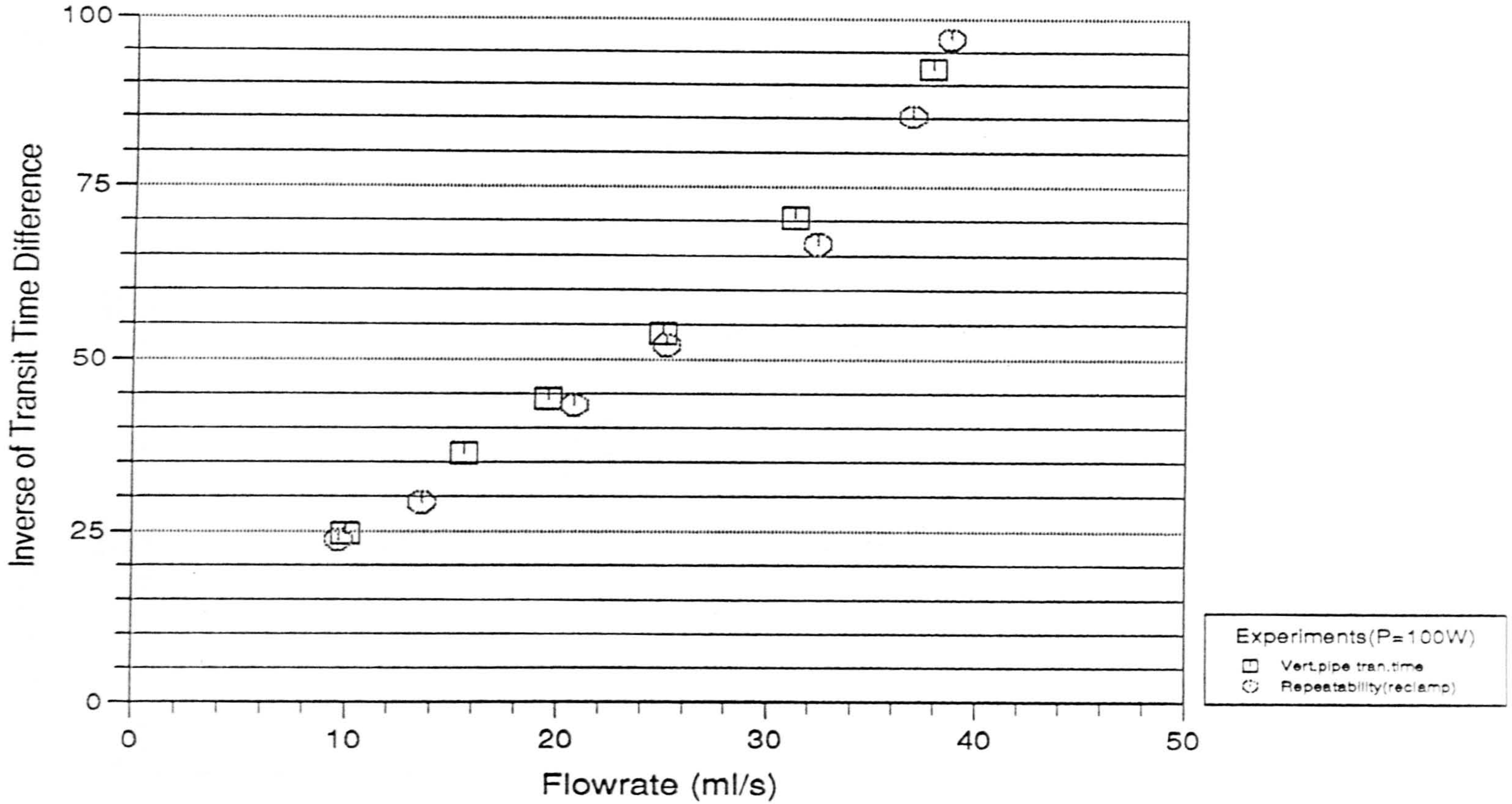

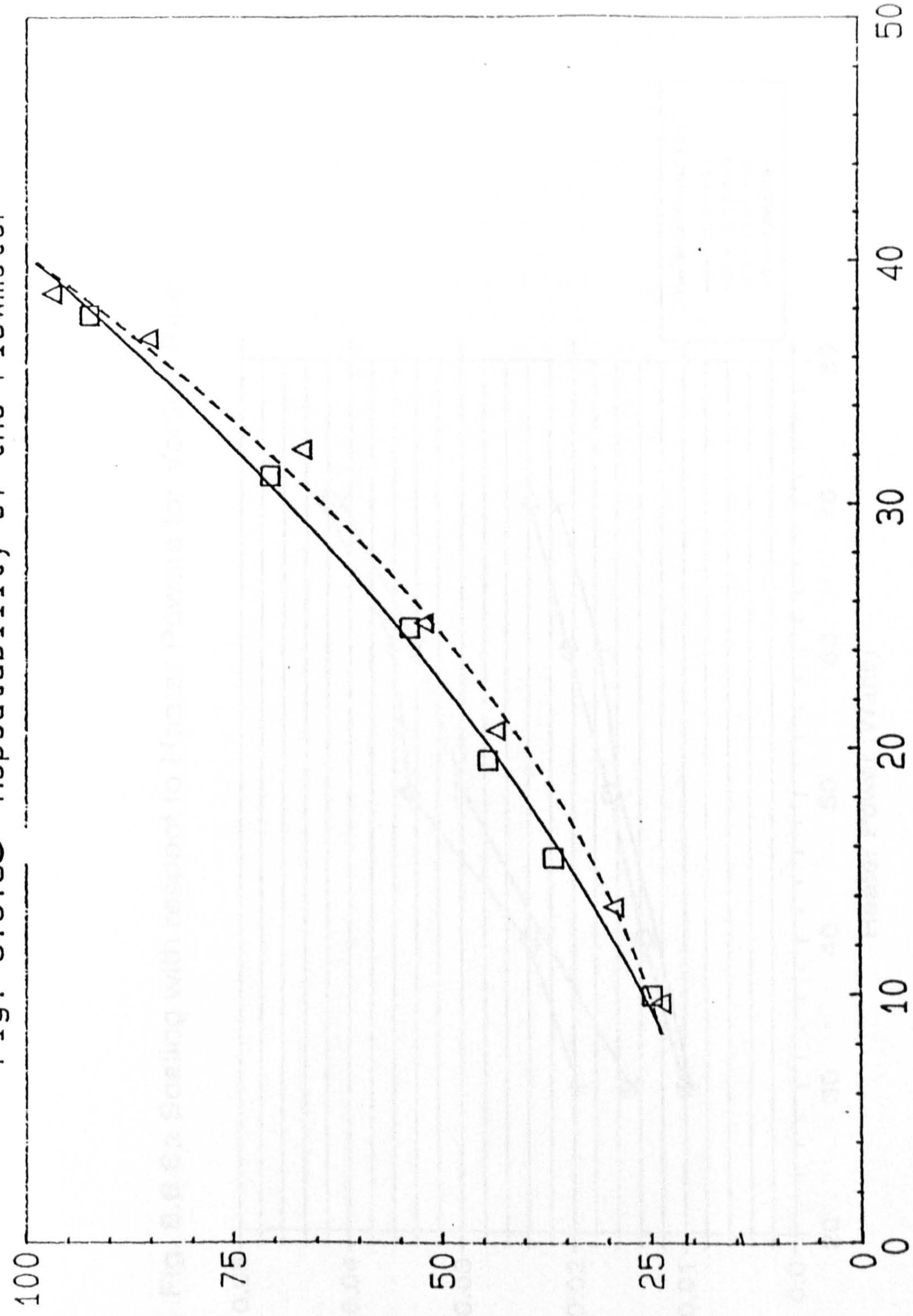
Repeatability of the Flowmeter
0
5
0
5
0
10
20
30
40
50
Flowrate (ml/s)
Inverse of Transit Time Difference
10
7
5
2

Fig. 8.6.5c

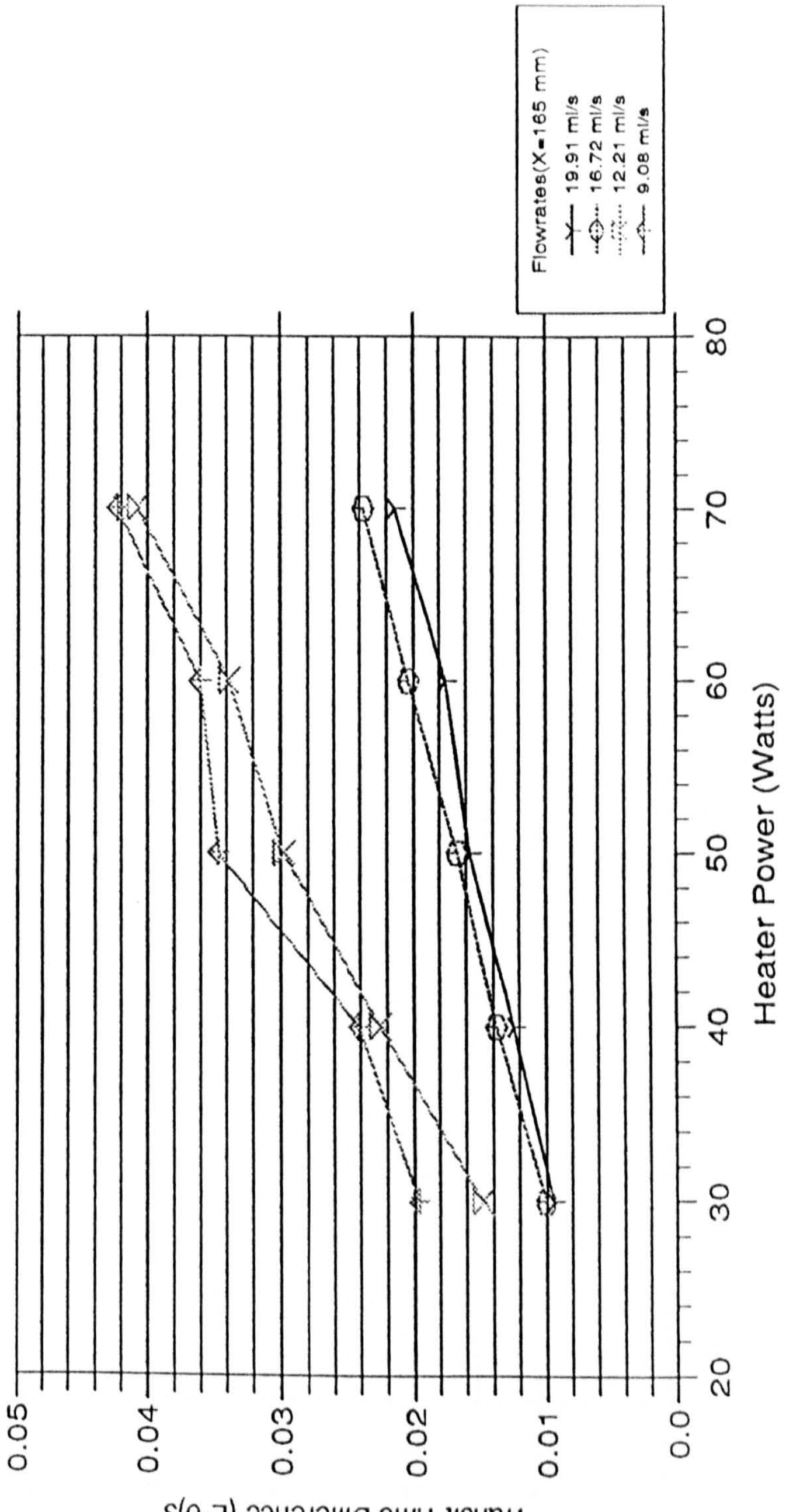

Fig. 8.6.6a Scaling with respect to Heater Powers for Vertical Pipe

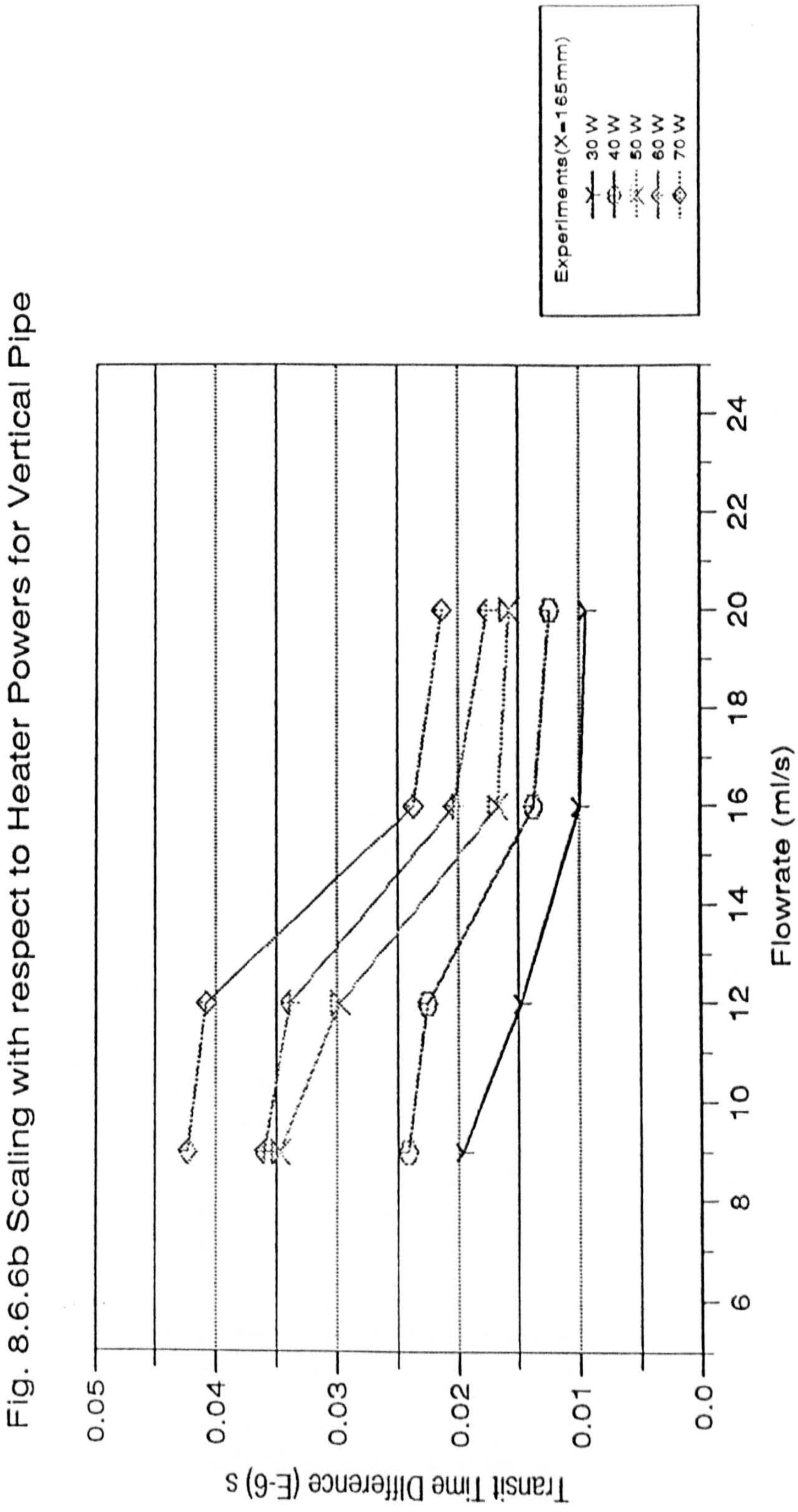

Fig. 8.6.6b Scaling with respect to Heater Powers for Vertical Pipe

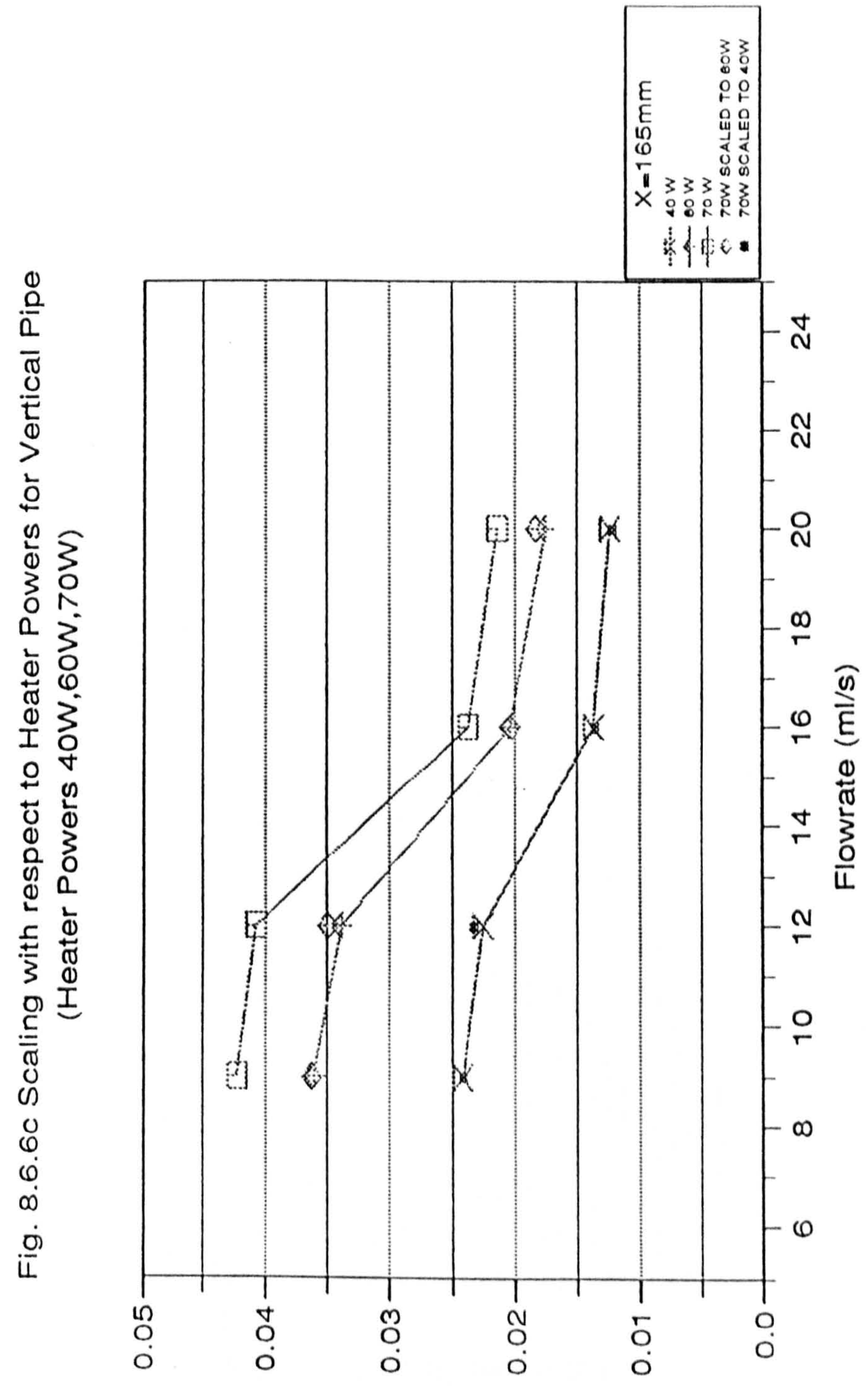

Fig. 8.6.6c Scaling with respect to Heater Powers for Vertical Pipe
(Heater Powers 40W,60W,70W)

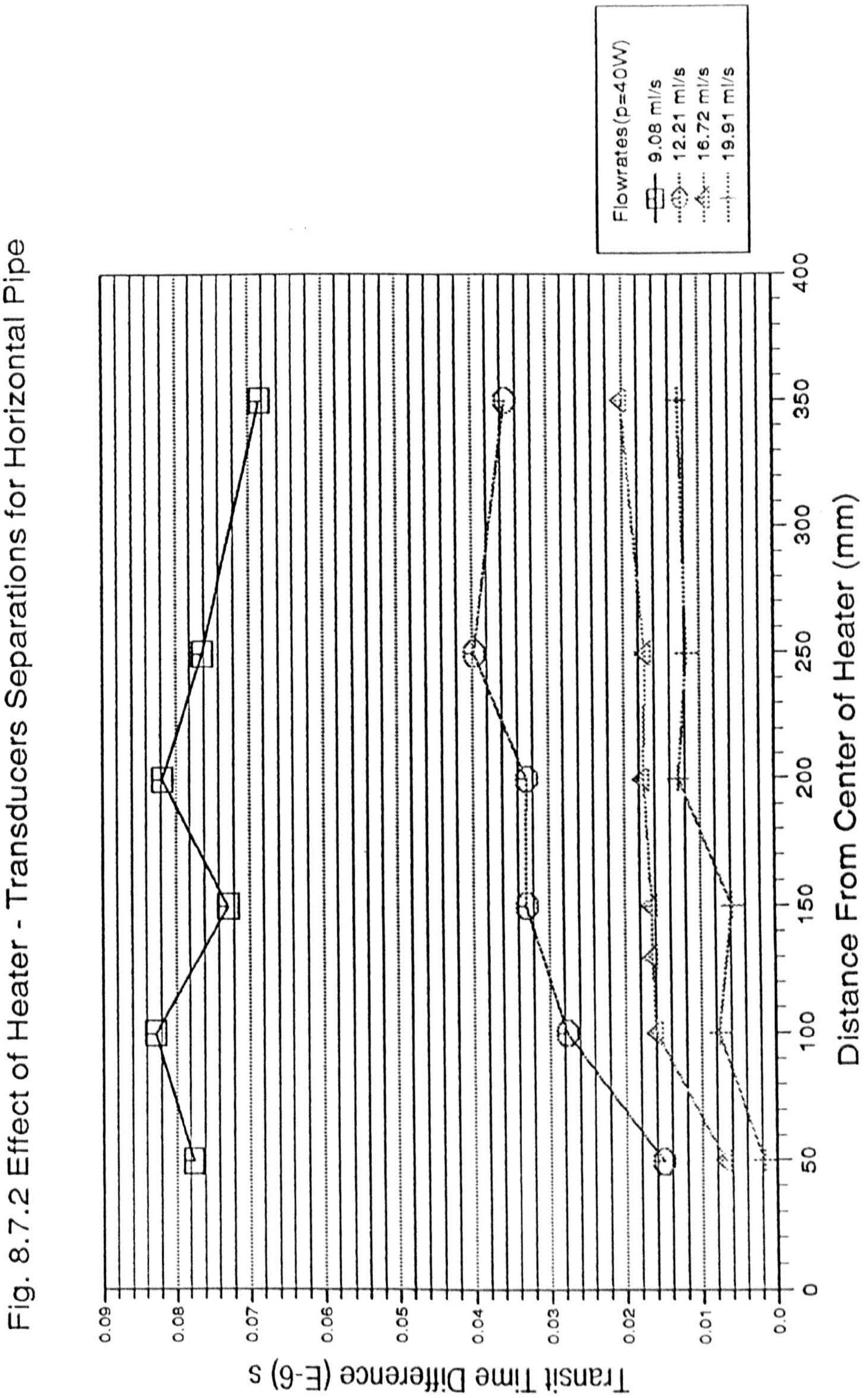

Fig. 8.7.2 Effect of Heater - Transducers Separations for Horizontal Pipe

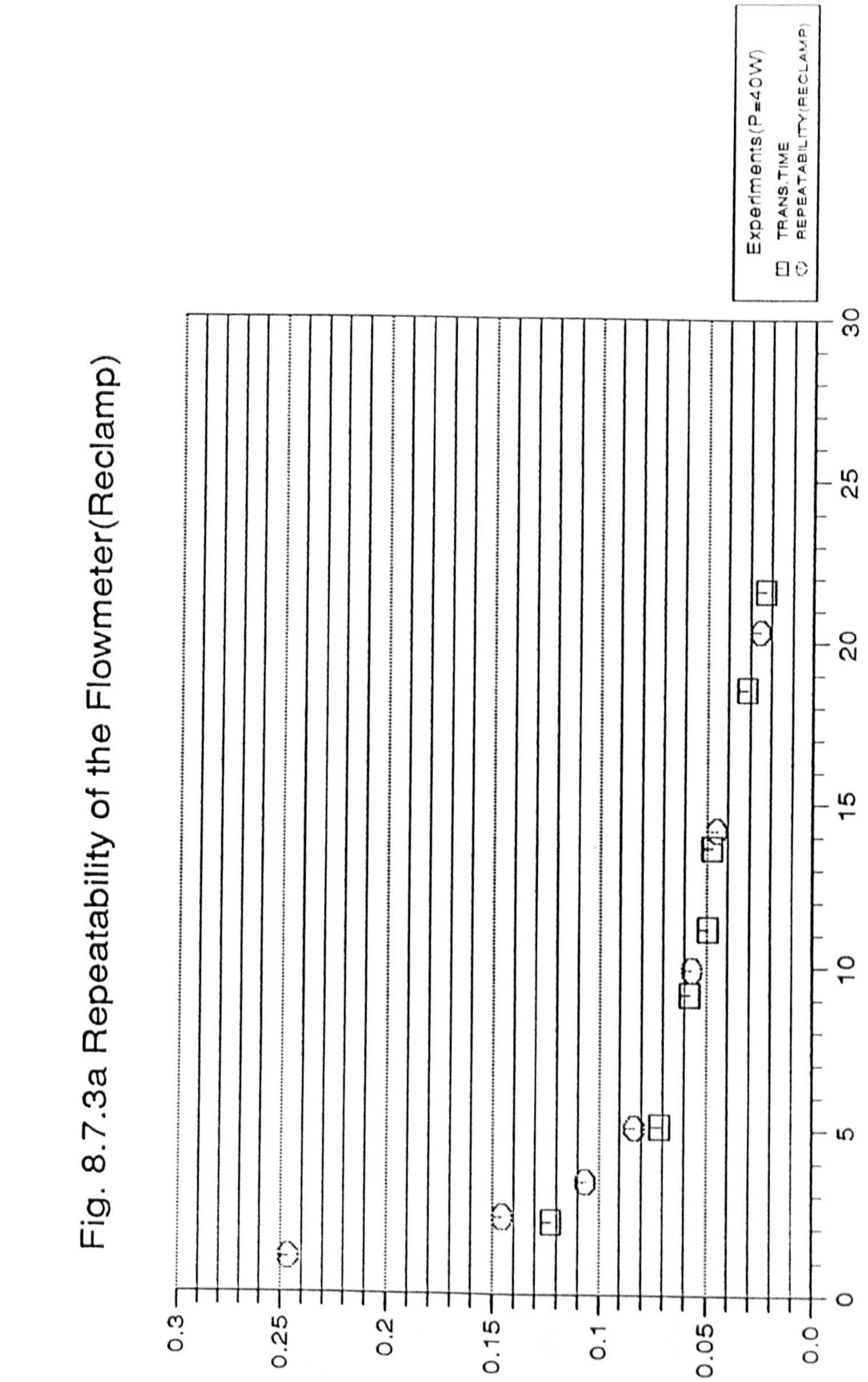

Fig. 8.7.3a Repeatability of the Flowmeter(Reclamp)

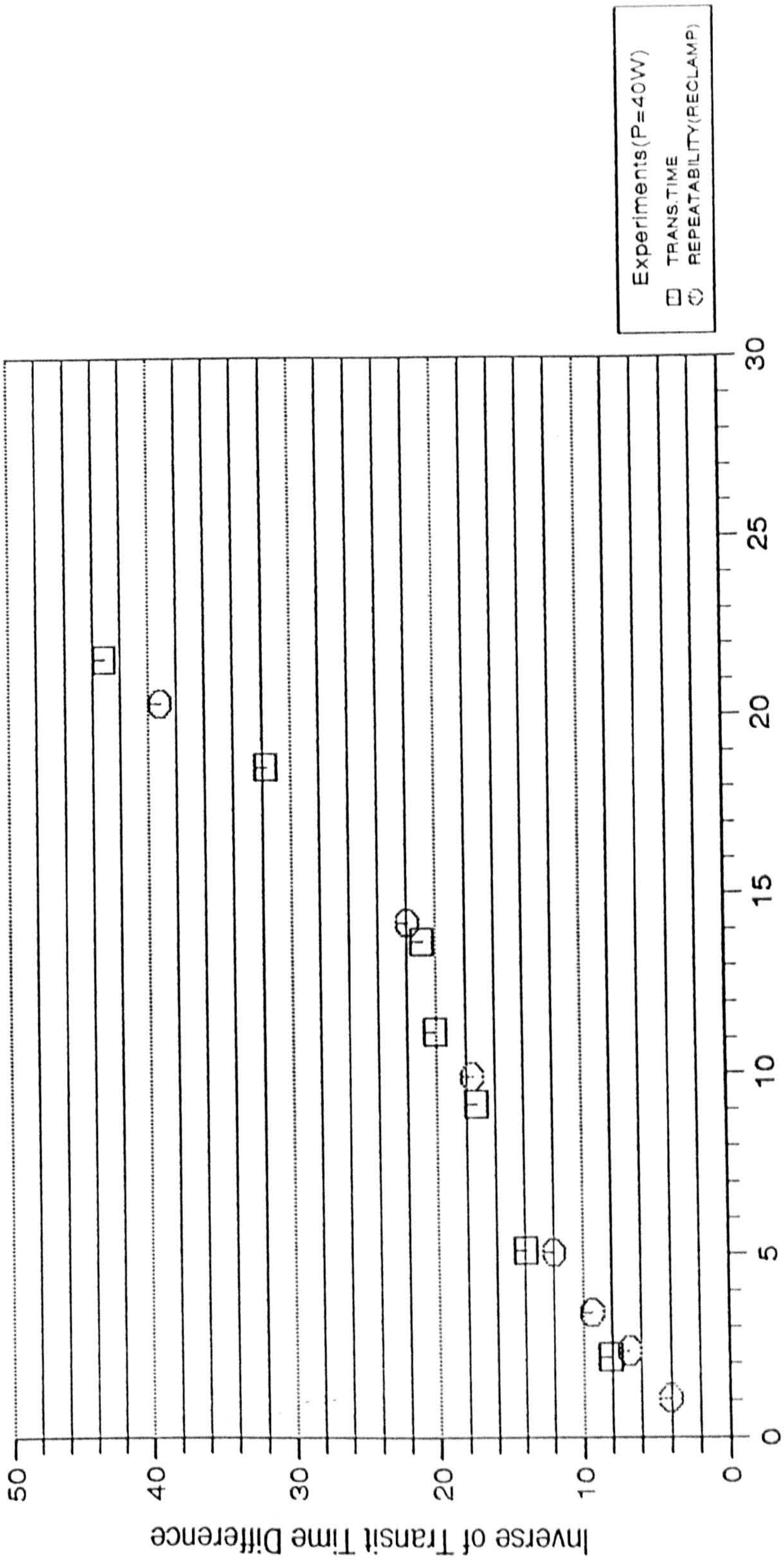

Fig. 8.7.3b Repeatability of the Flowmeter(Reclamp)

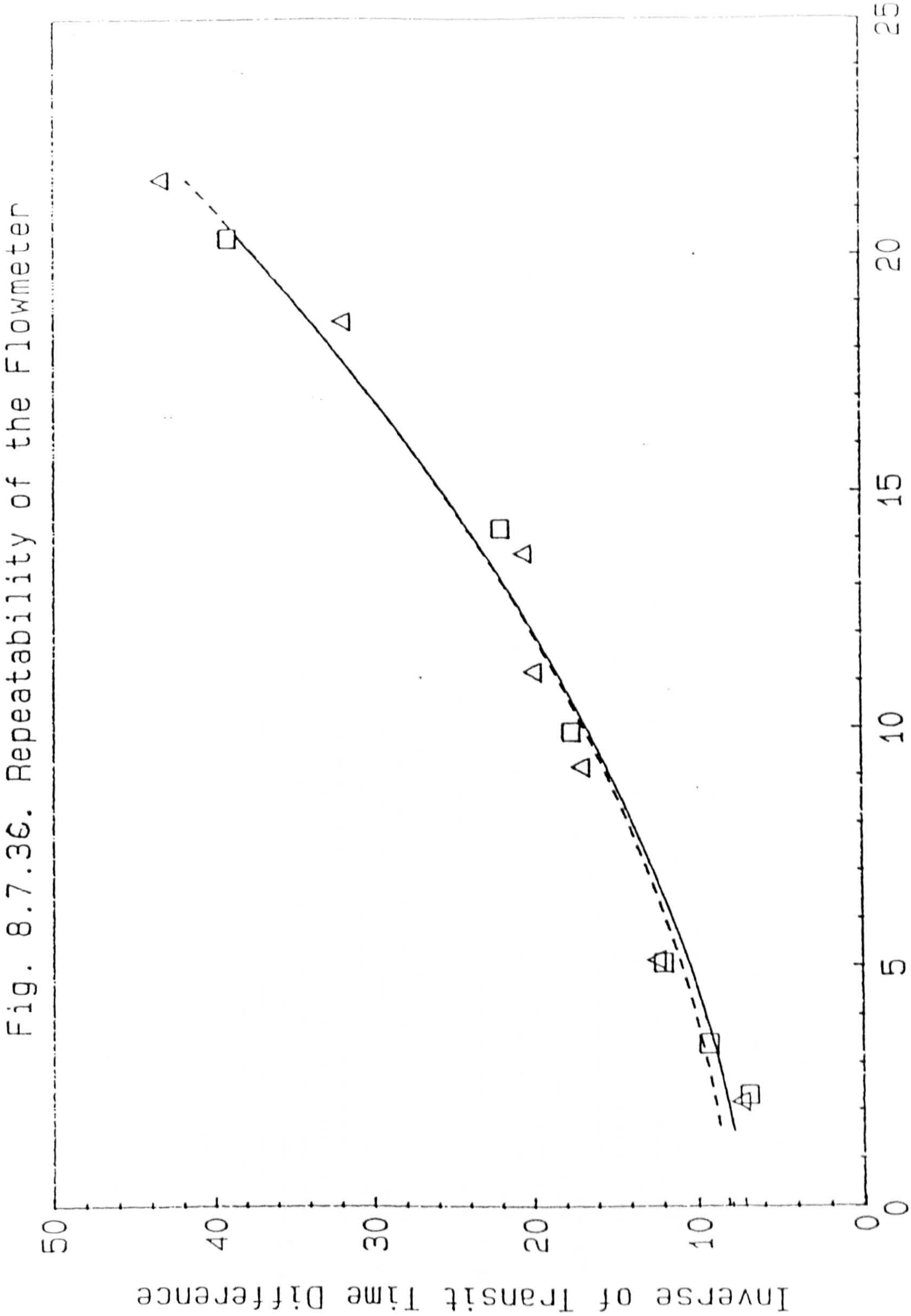

Fig. 8.7.36. Repeatability of the Flowmeter

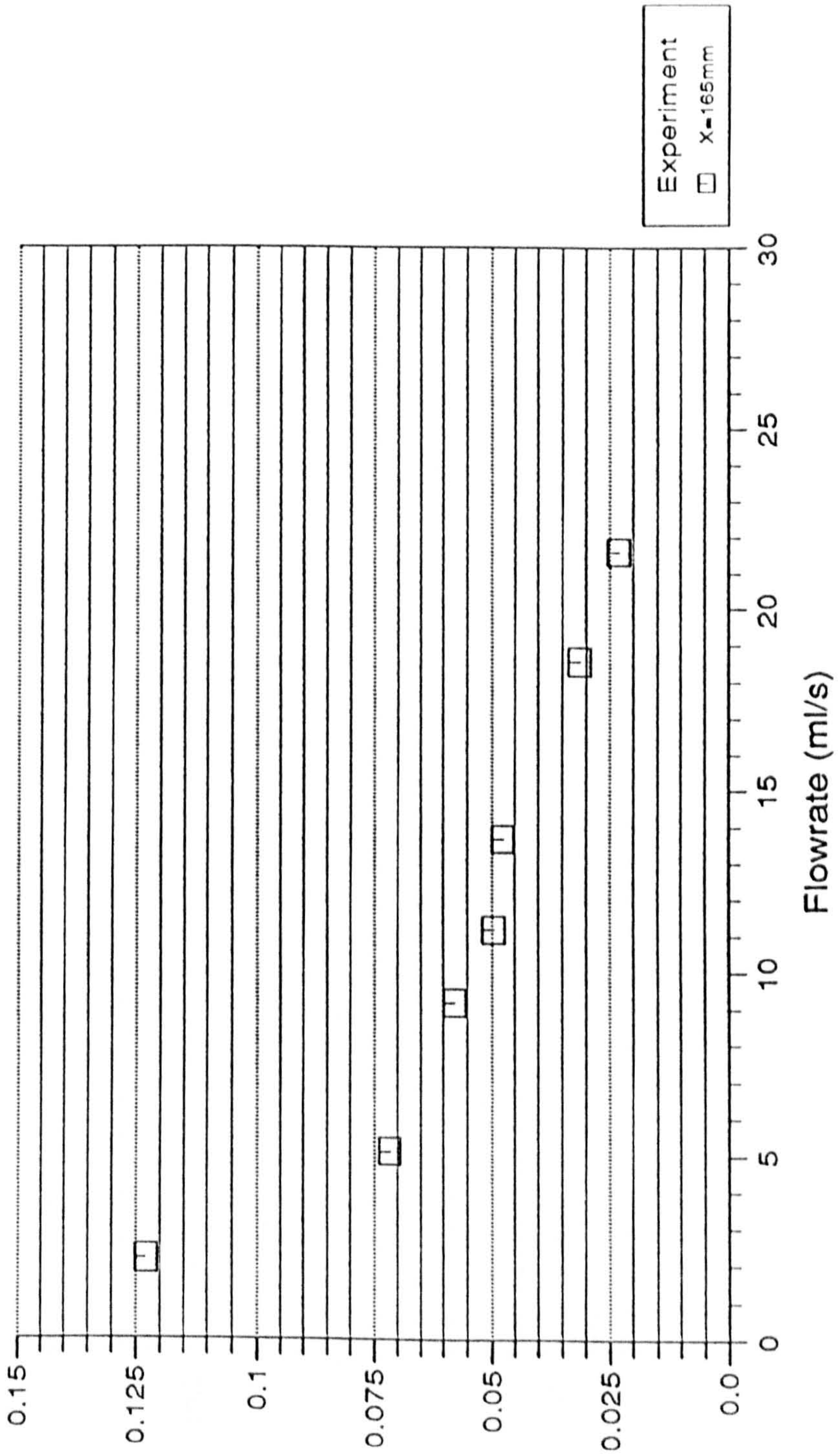
Experiment
X=165mm
Fig. 8.7.4a Calibration Curve for Horizontal Pipe (P=40W)
Transit Time Difference (E-6) s
Flowrate (ml/s)
0.15
0.125
0.1
0.075
0.05
0.025
0.0
0
5
10
15
20
25
30

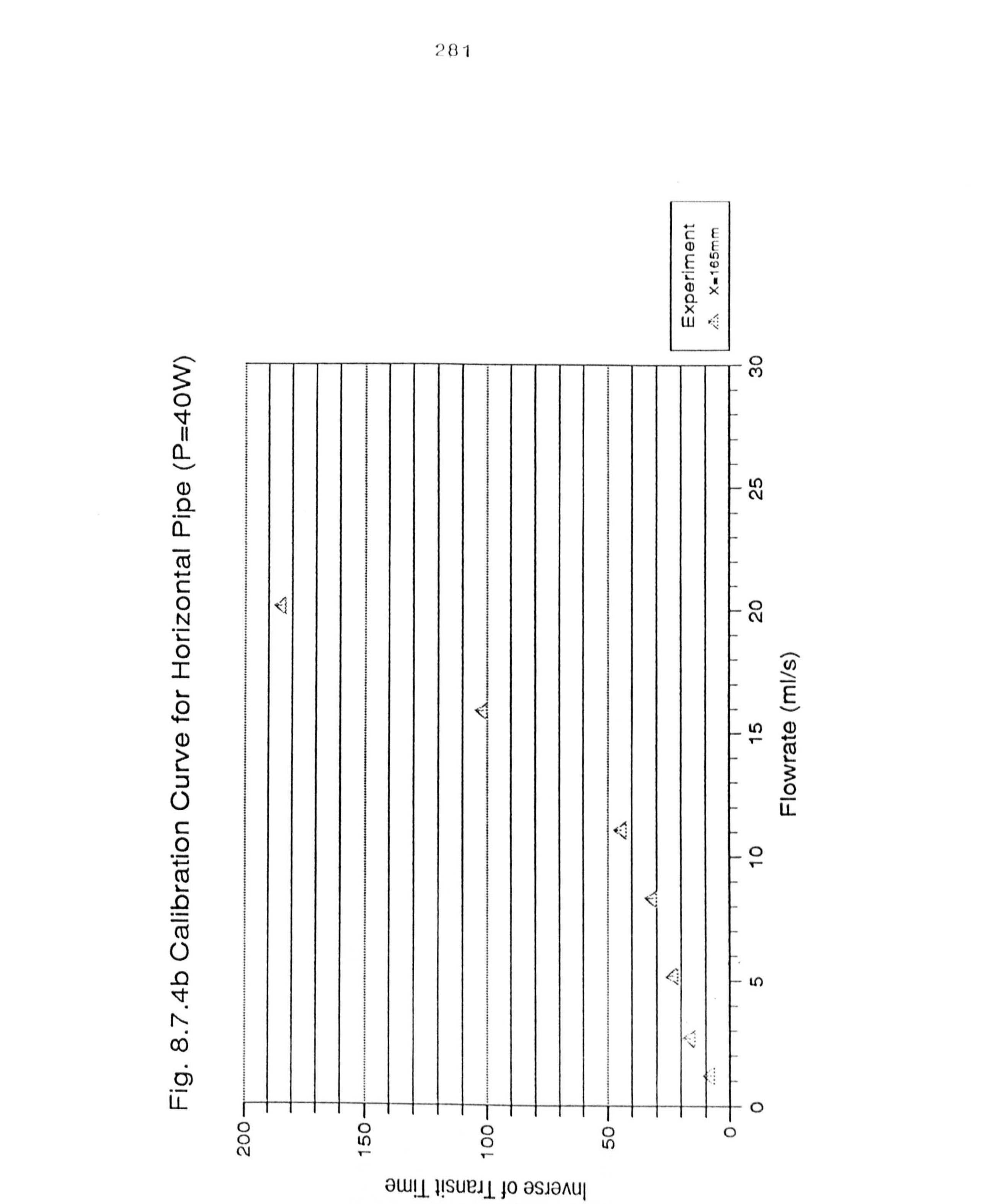

Fig. 8.7.4b Calibration Curve for Horizontal Pipe (P=40W)

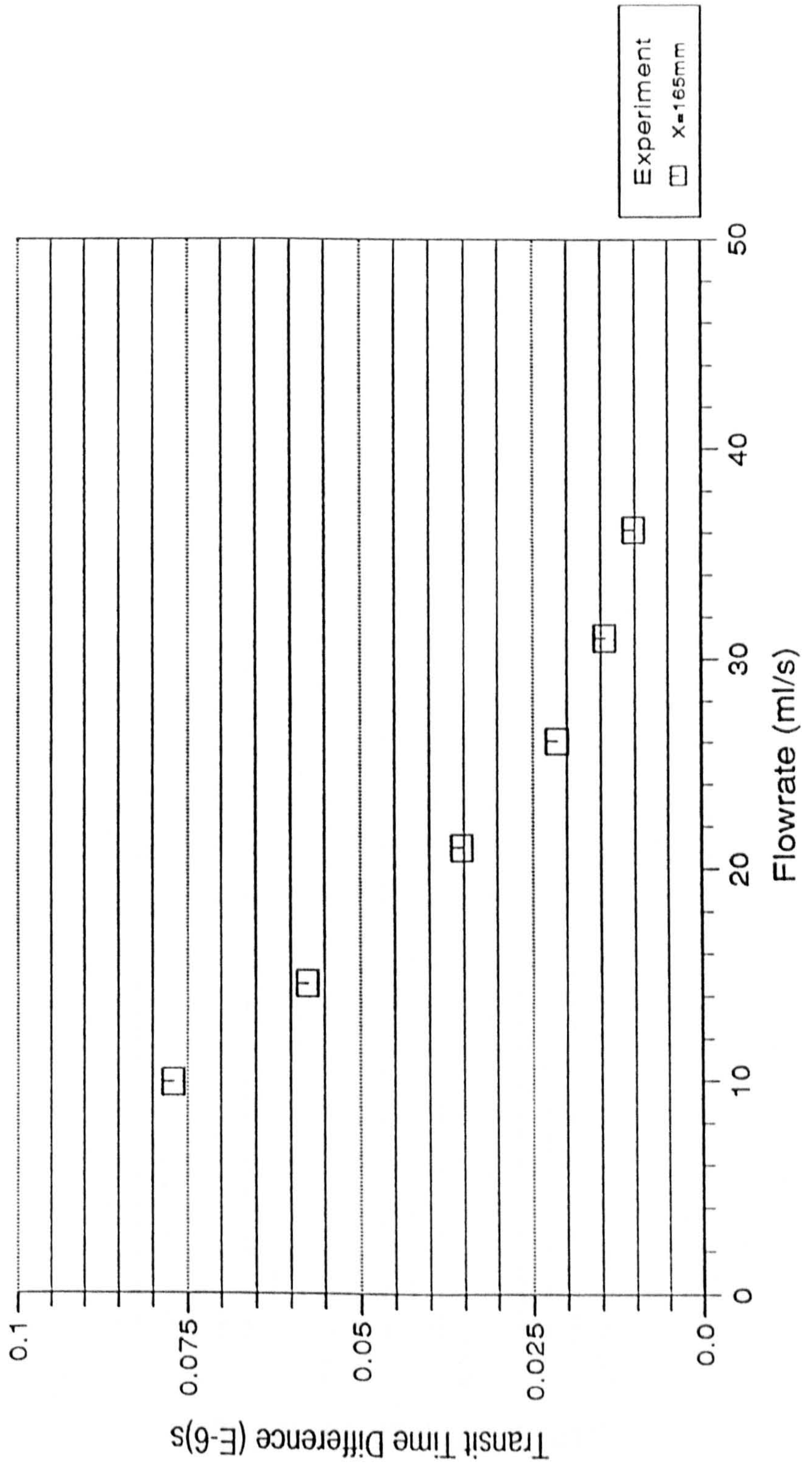

Fig. 8.7.5a Calibration Curve for Horizontal Pipe (P=100W)

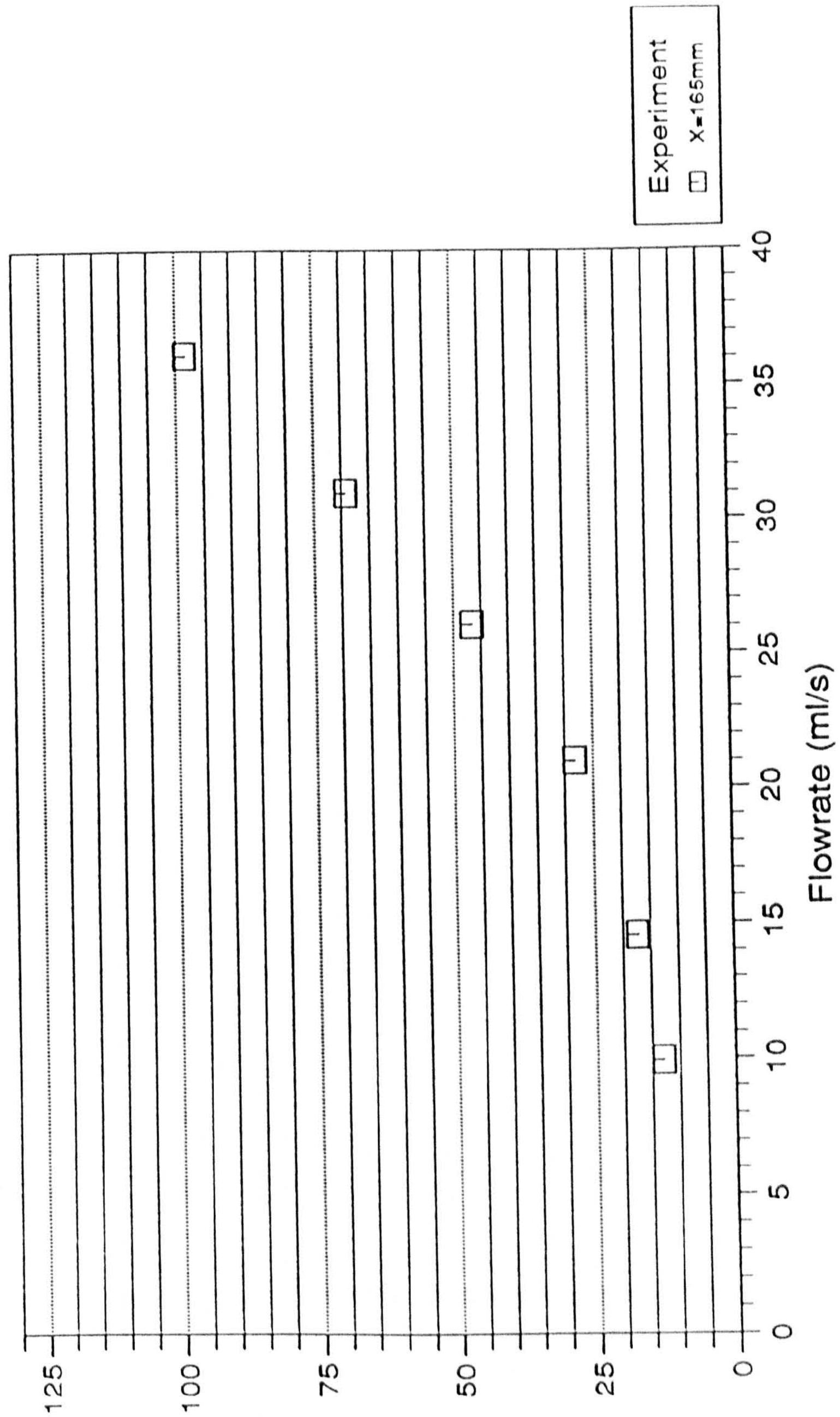

Fig. 8.7.5b Calibration Curve for Horizontal Pipe (P=100W)

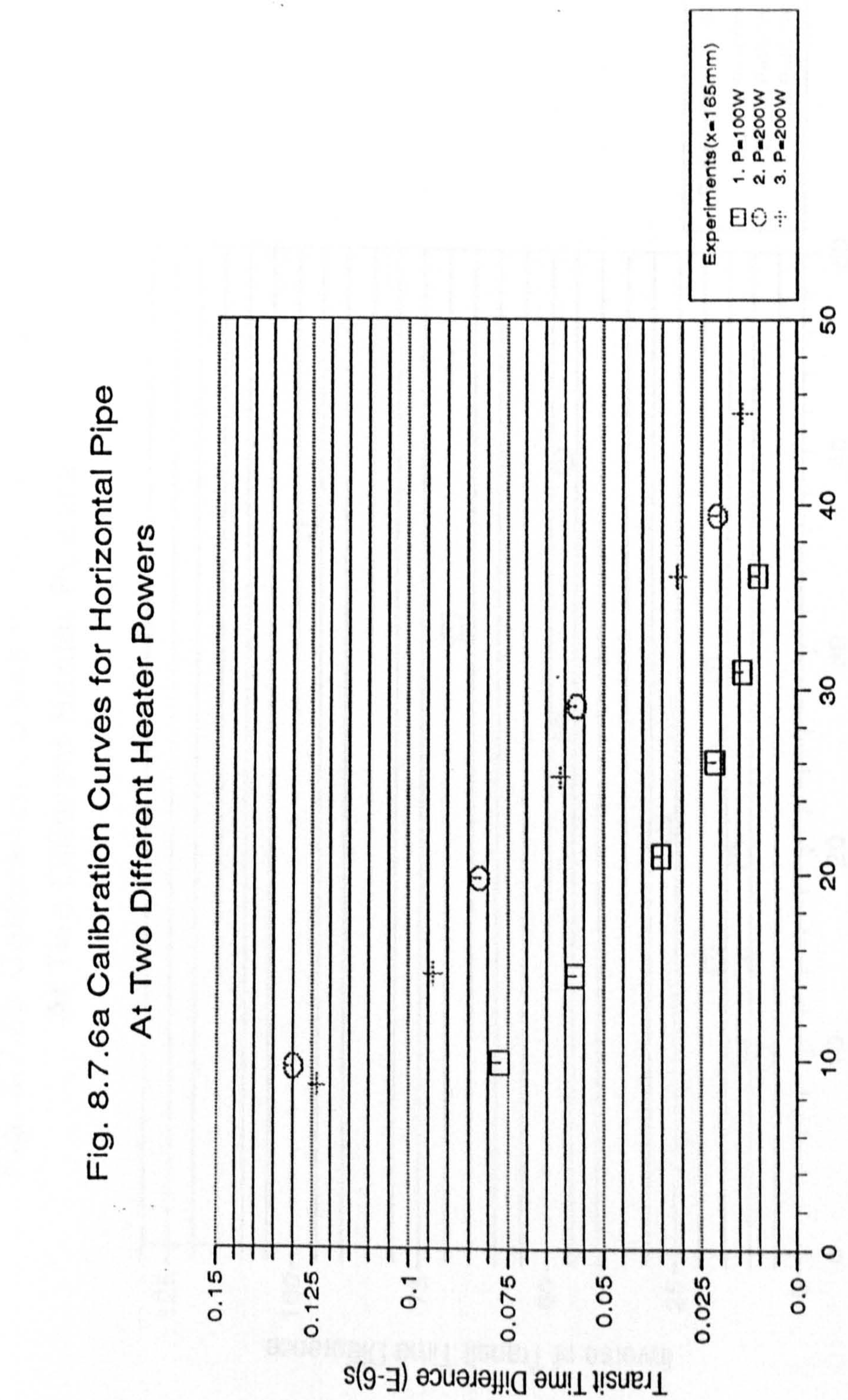

Fig. 8.7.6a Calibration Curves for Horizontal Pipe
At Two Different Heater Powers

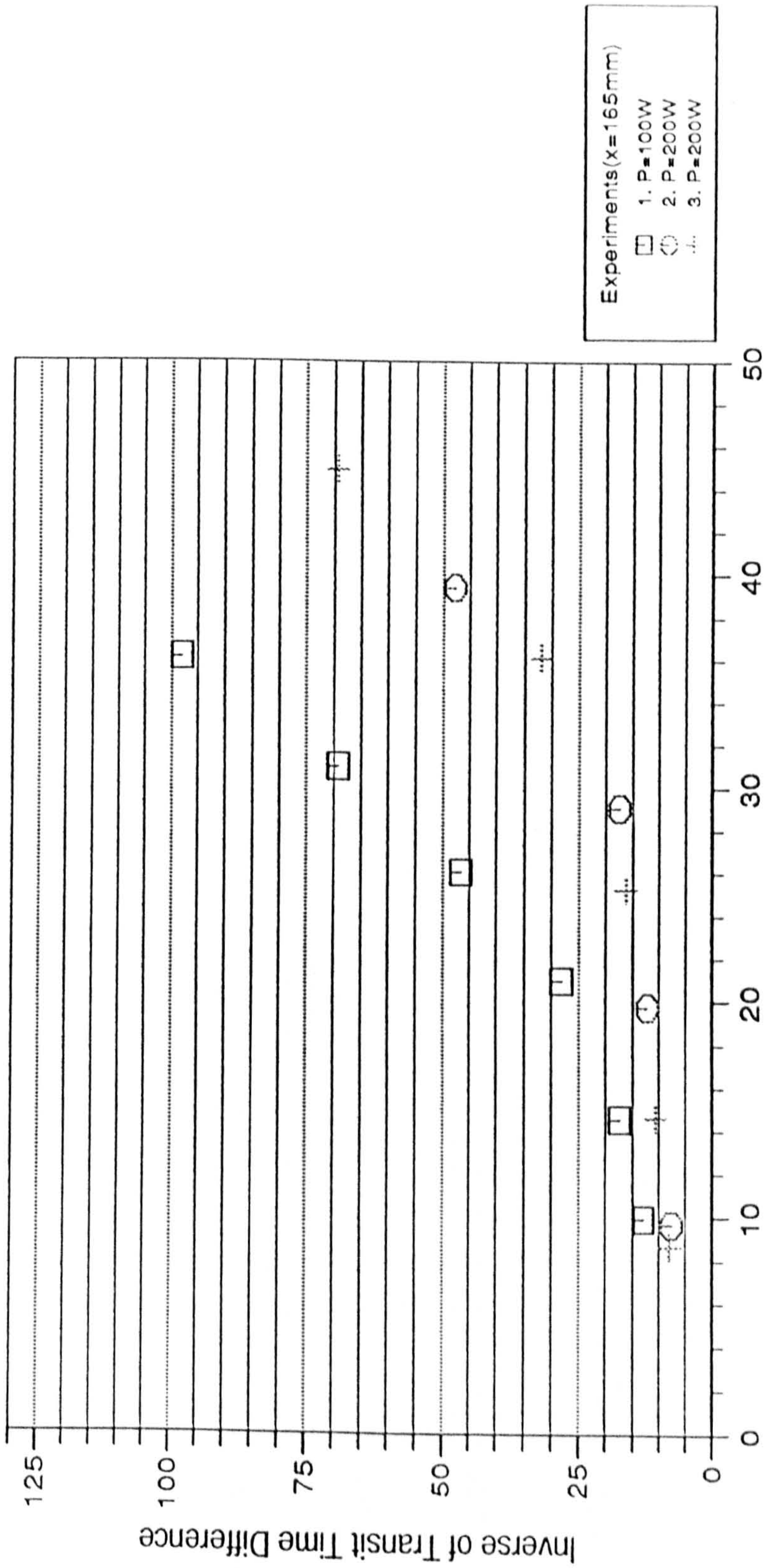

Fig. 8.7.6b Calilbration Curves for Horizontal Pipe
At Two Different Heater Powers

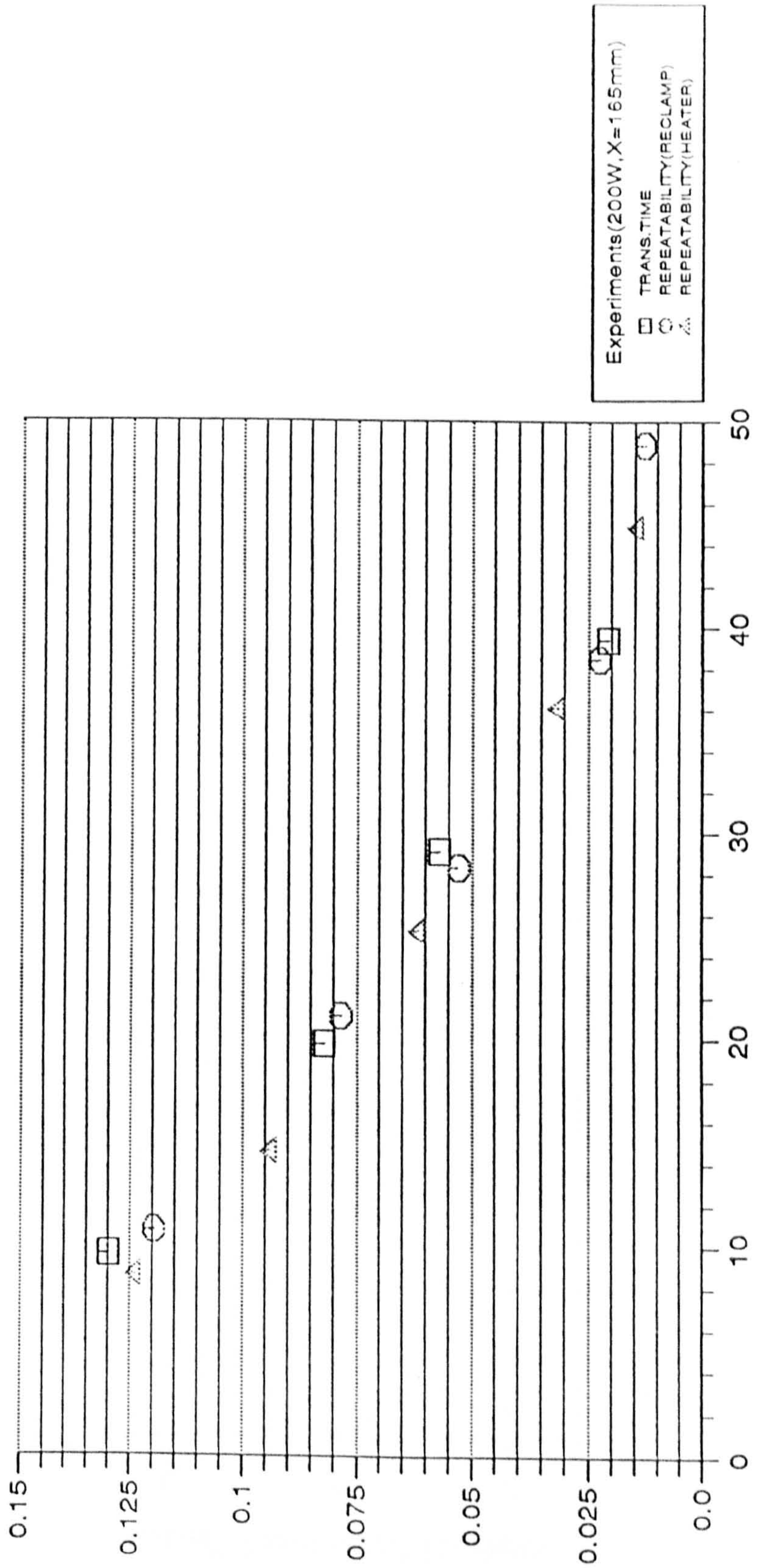

Fig. 8.7.7a Repeatability of the Flowmeter

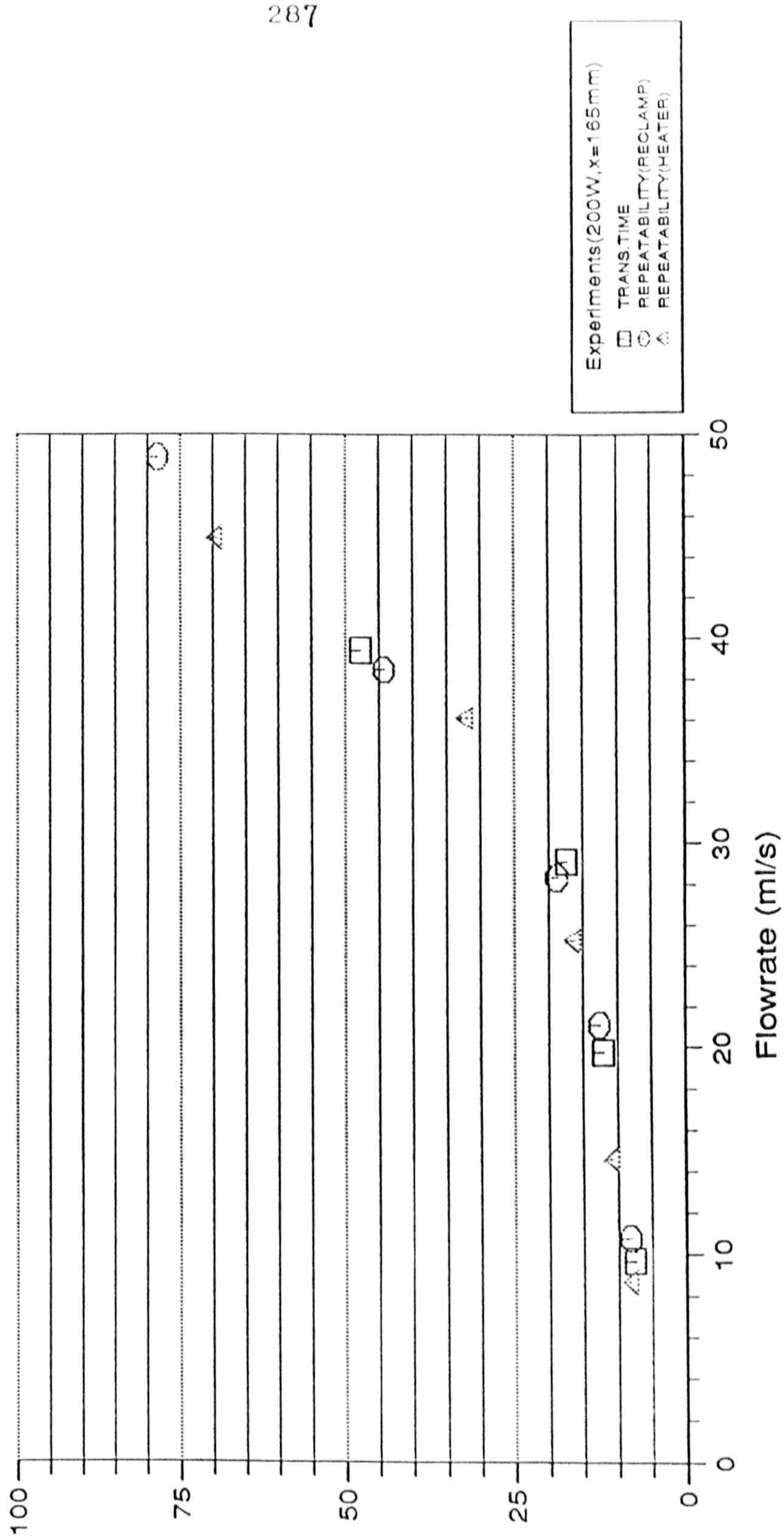

Fig. 8.7.7b Repeatability of the Flowmeter

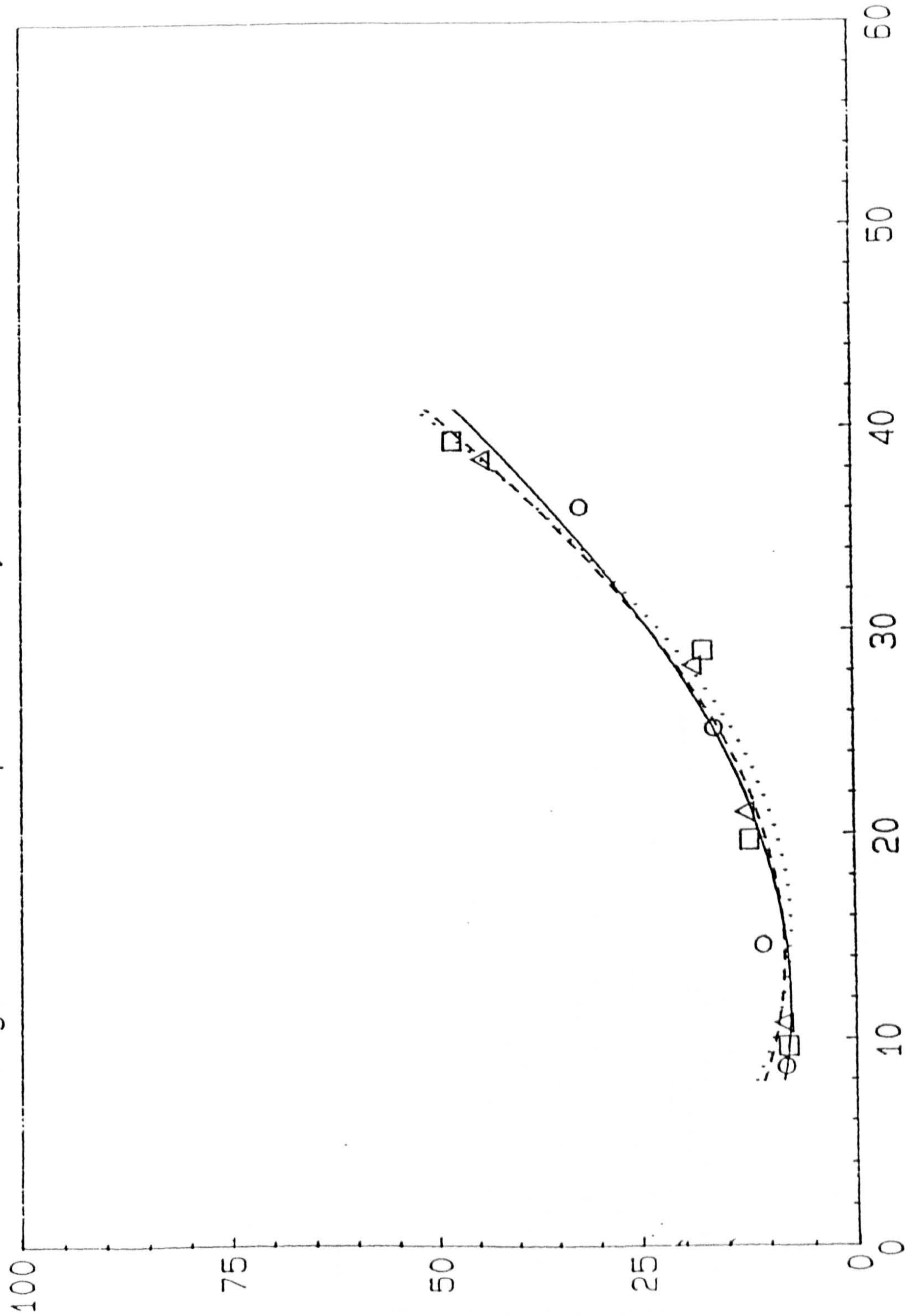
Fig. 8.7.7C.. Repeatability of the Flowmeter
Flowrate (ml/s)
Inverse of Transit Time Difference
0
10
20
30
40
50
60
0
25
50
75
100

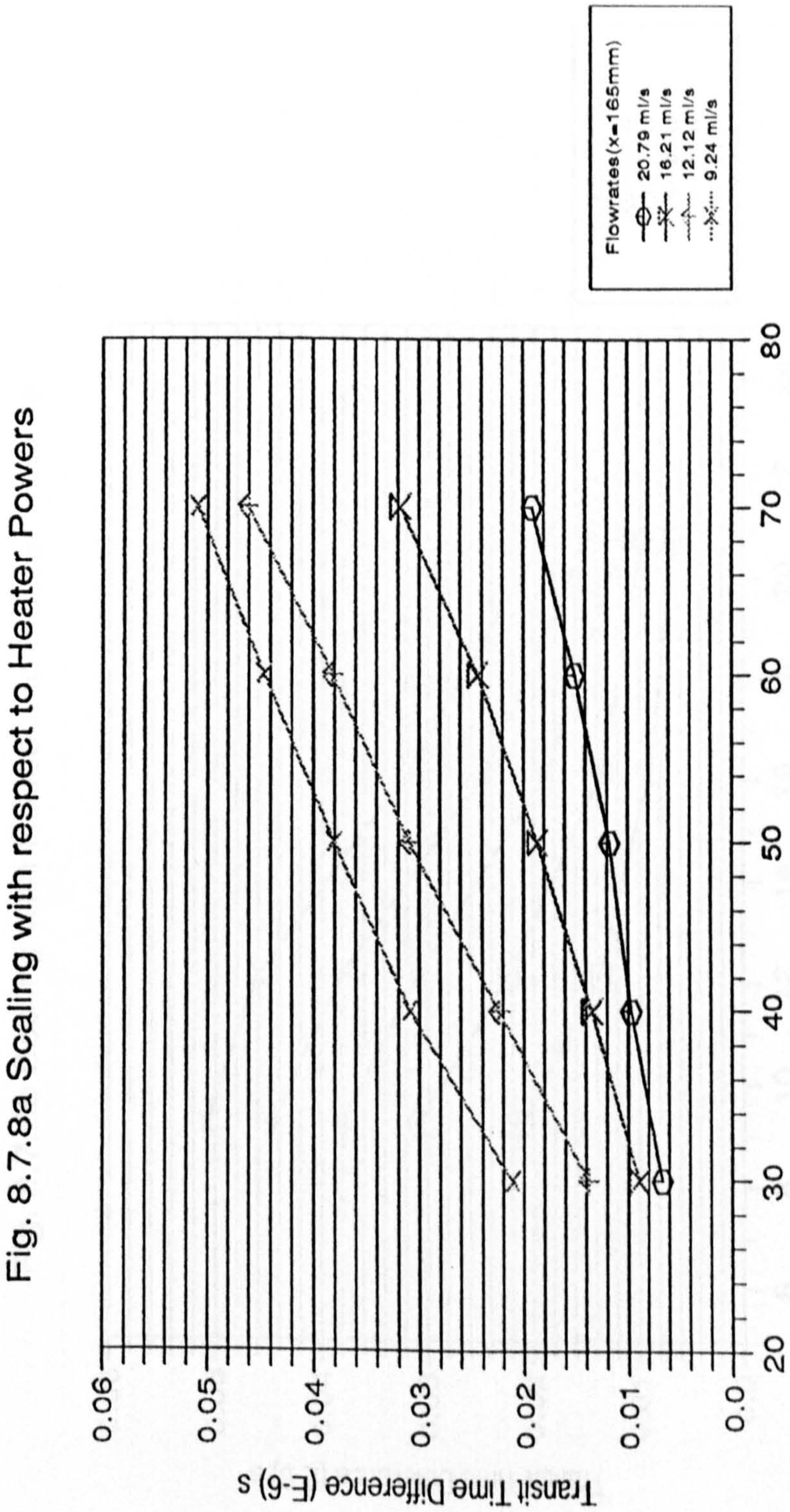

Fig. 8.7.8a Scaling with respect to Heater Powers

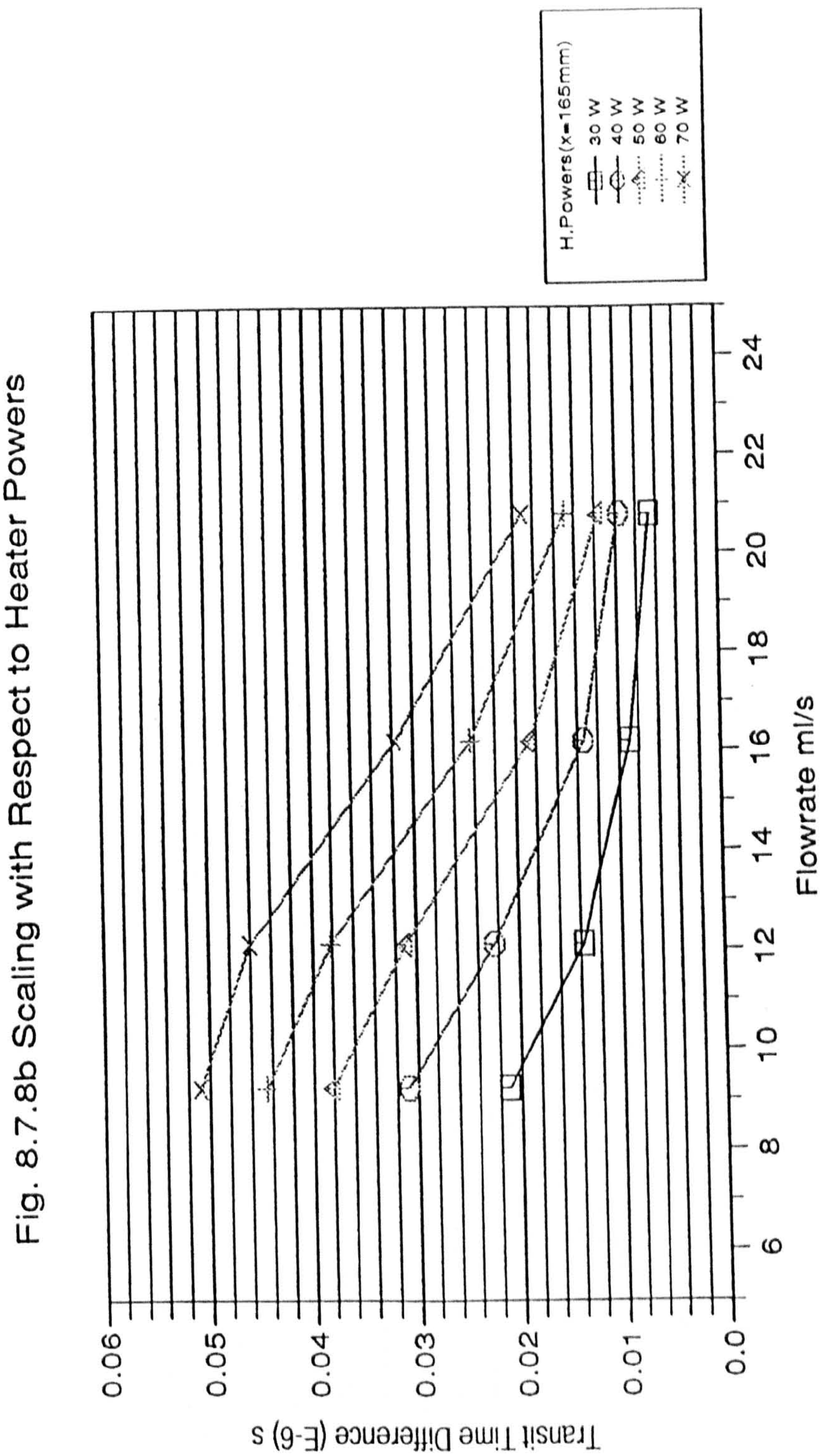

Fig. 8.7.8b Scaling with Respect to Heater Powers

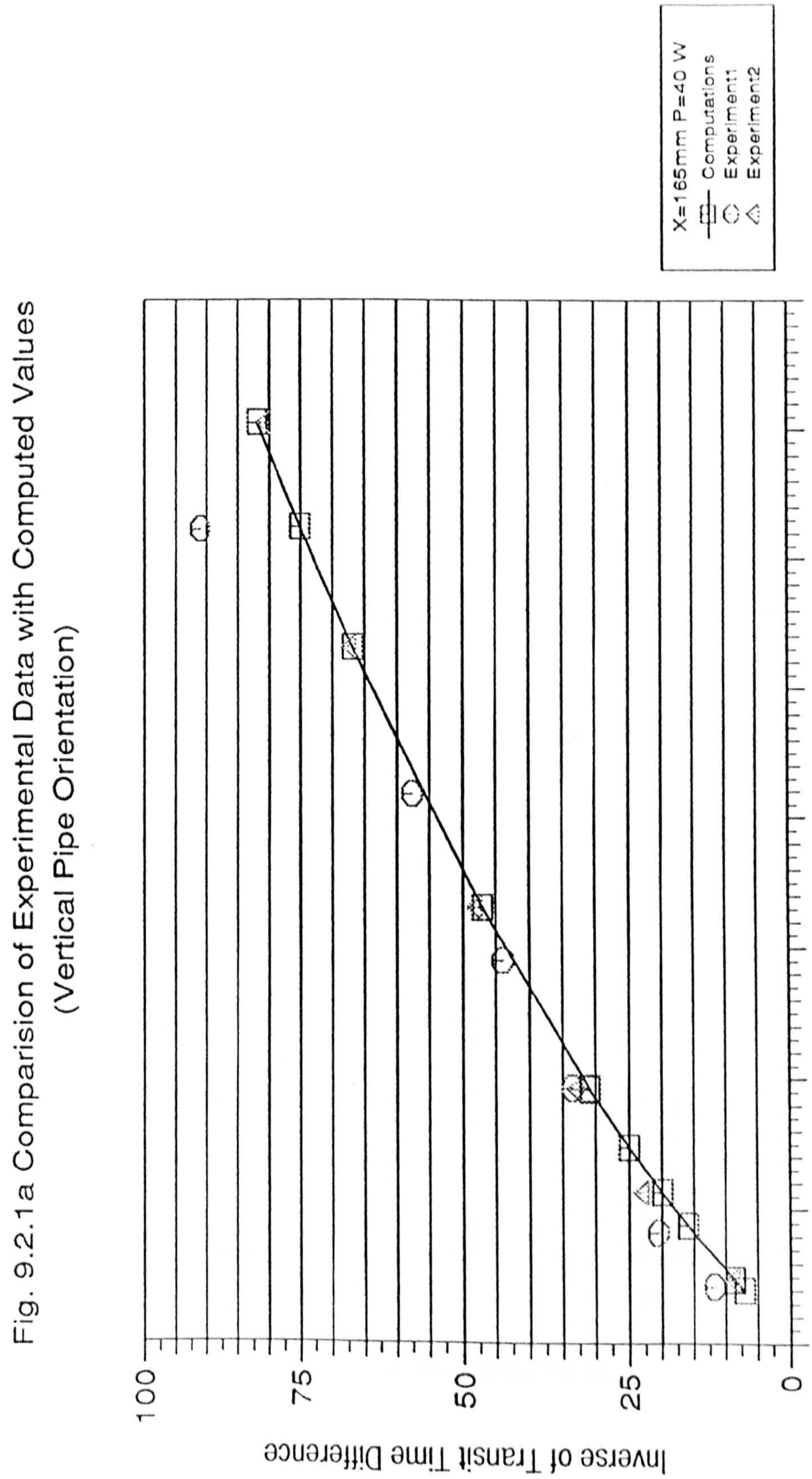

Fig. 9.2.1a Comparision of Experimental Data with Computed Values
(Vertical Pipe Orientation)

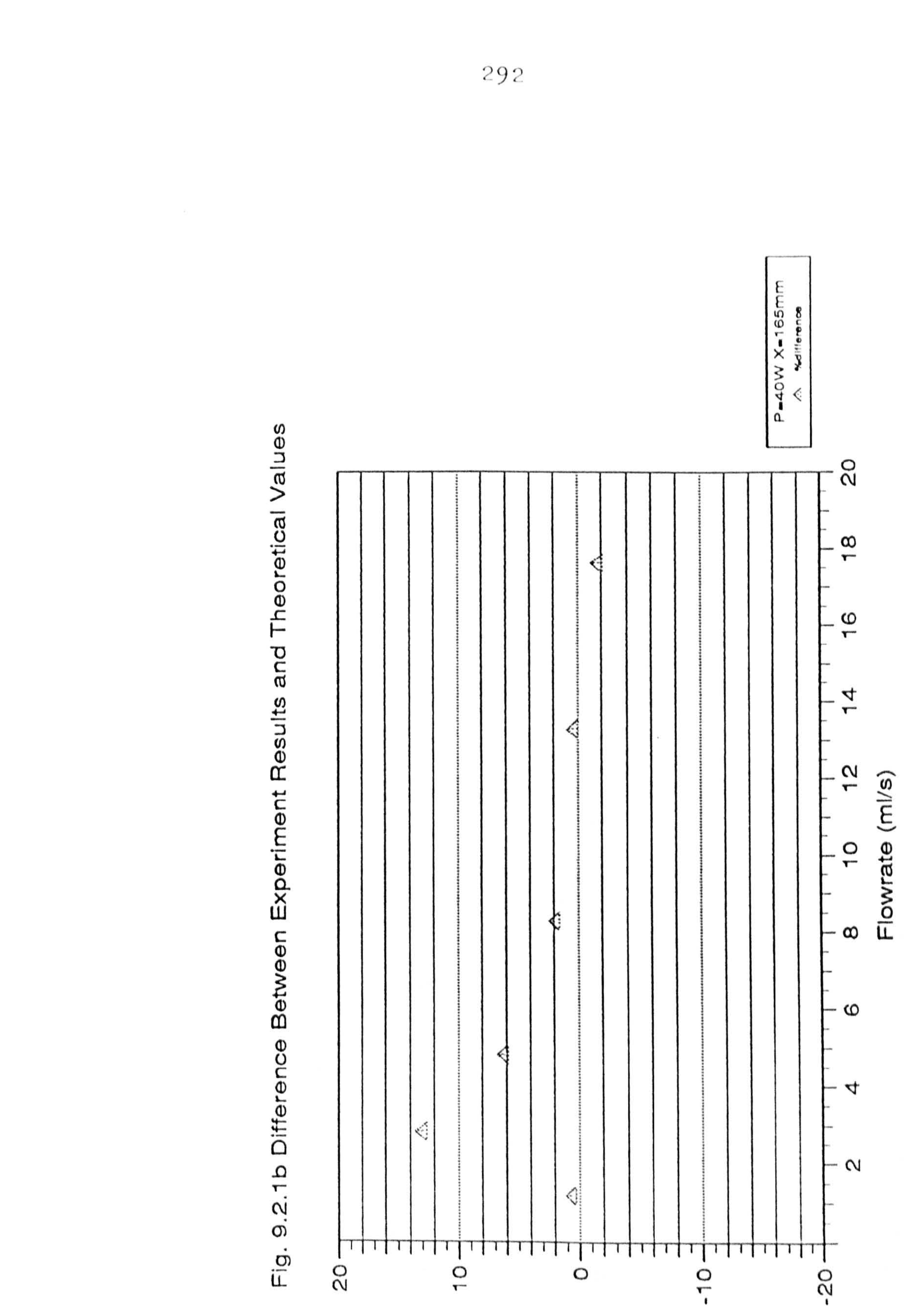

Fig. 9.2.1b Difference Between Experiment Results and Theoretical Values

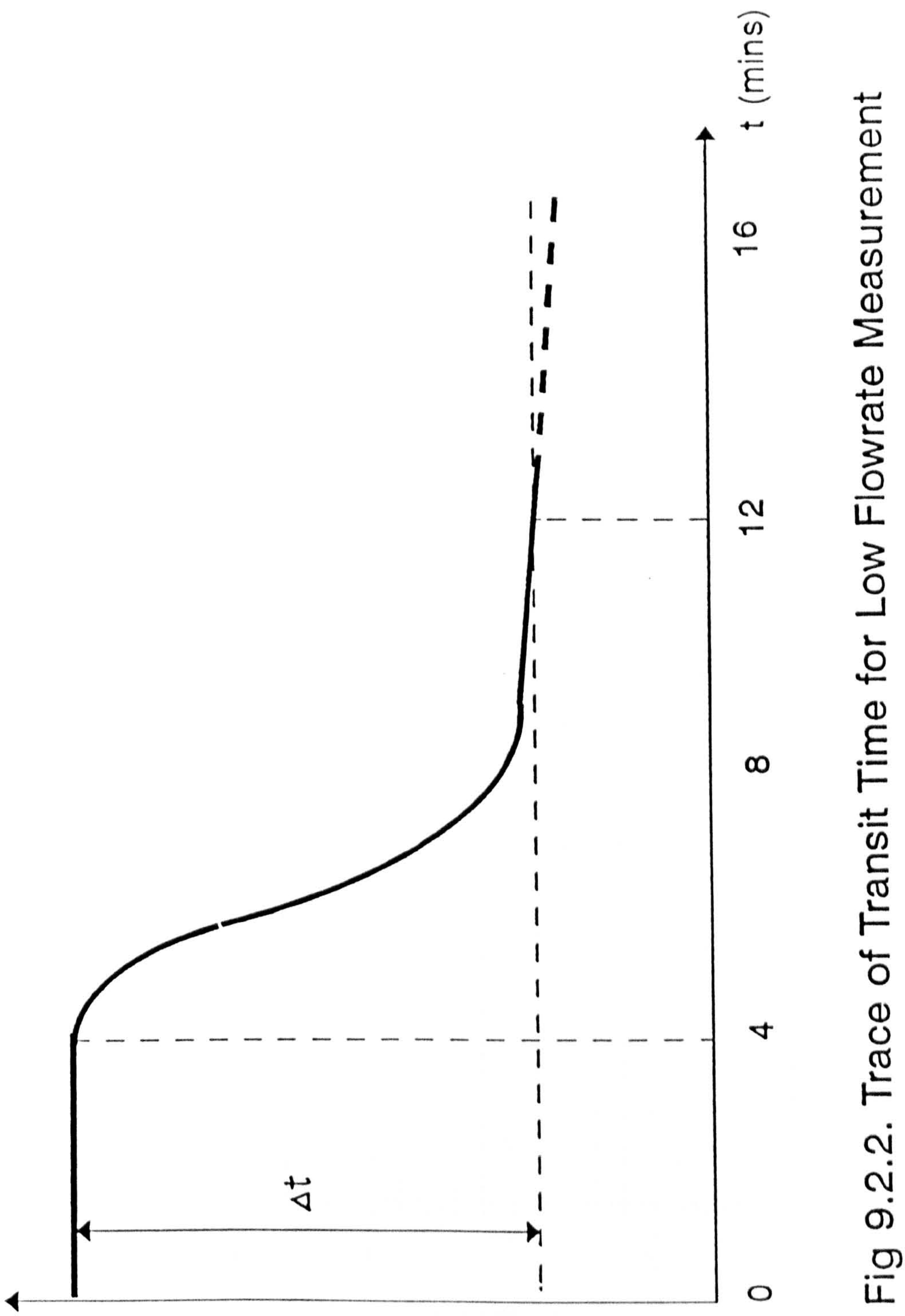

Fig 9.2.2. Trace of Transit Time for Low Flowrate Measurement

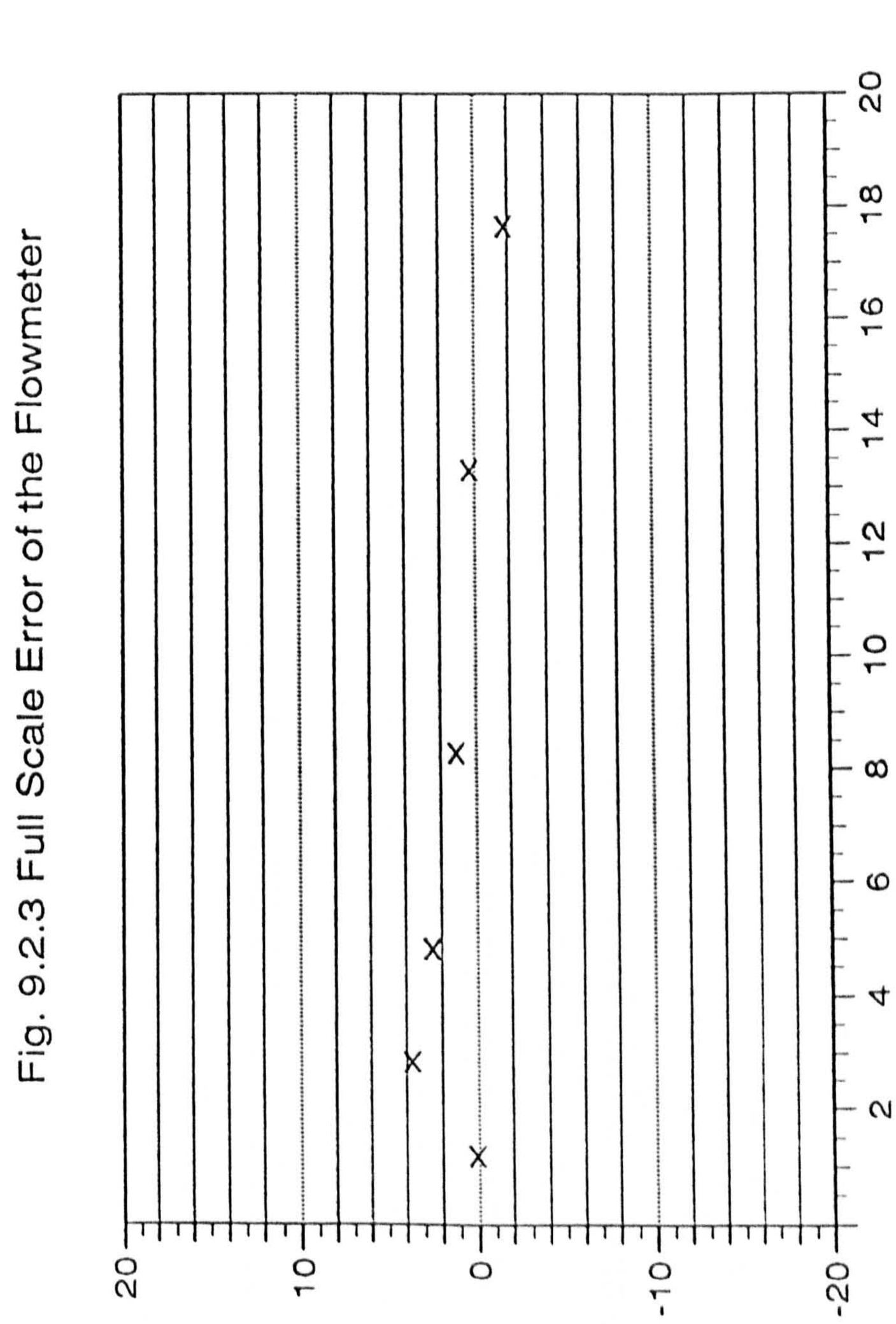

Fig. 9.2.3 Full Scale Error of the Flowmeter

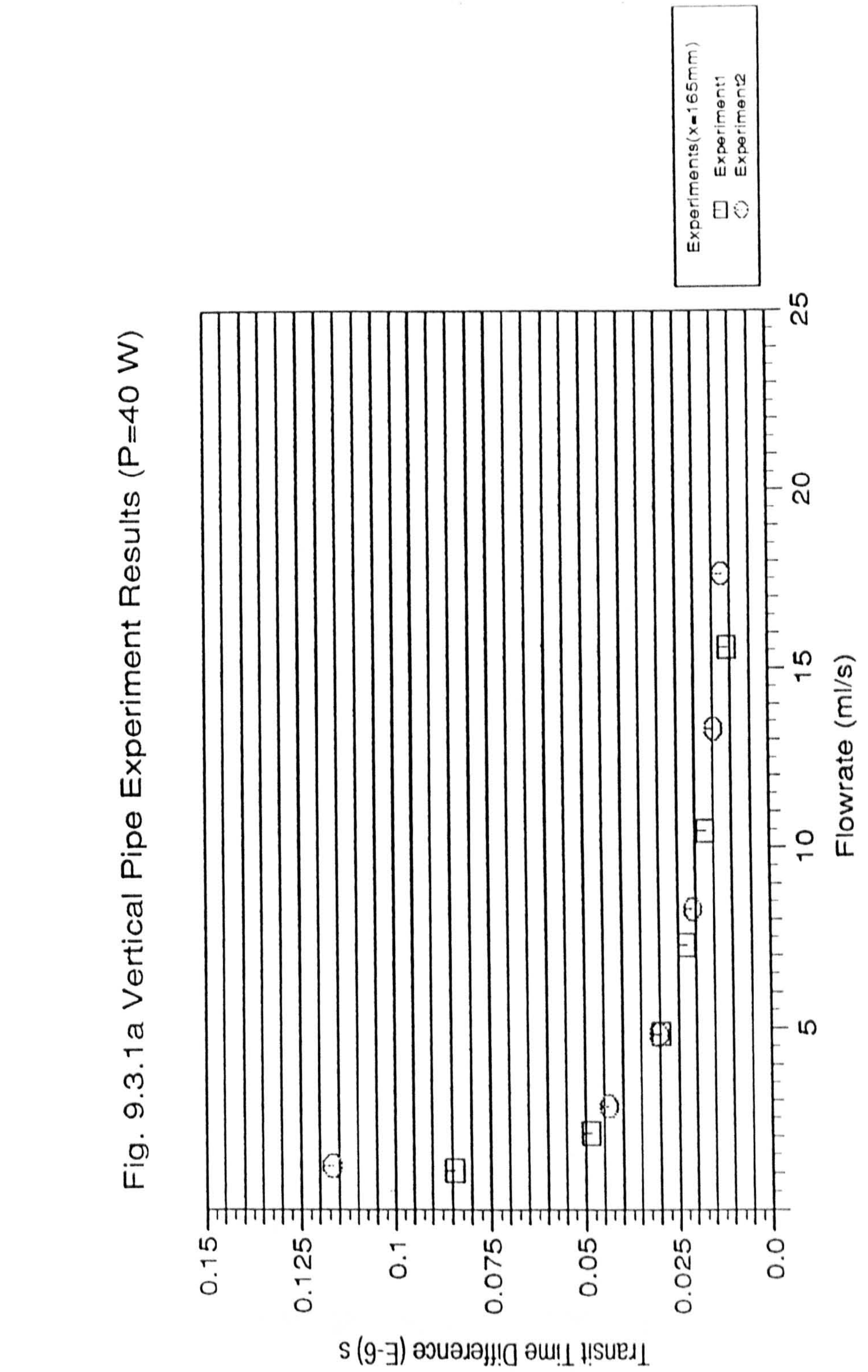

Fig. 9.3.1a Vertical Pipe Experiment Results (P=40 W)

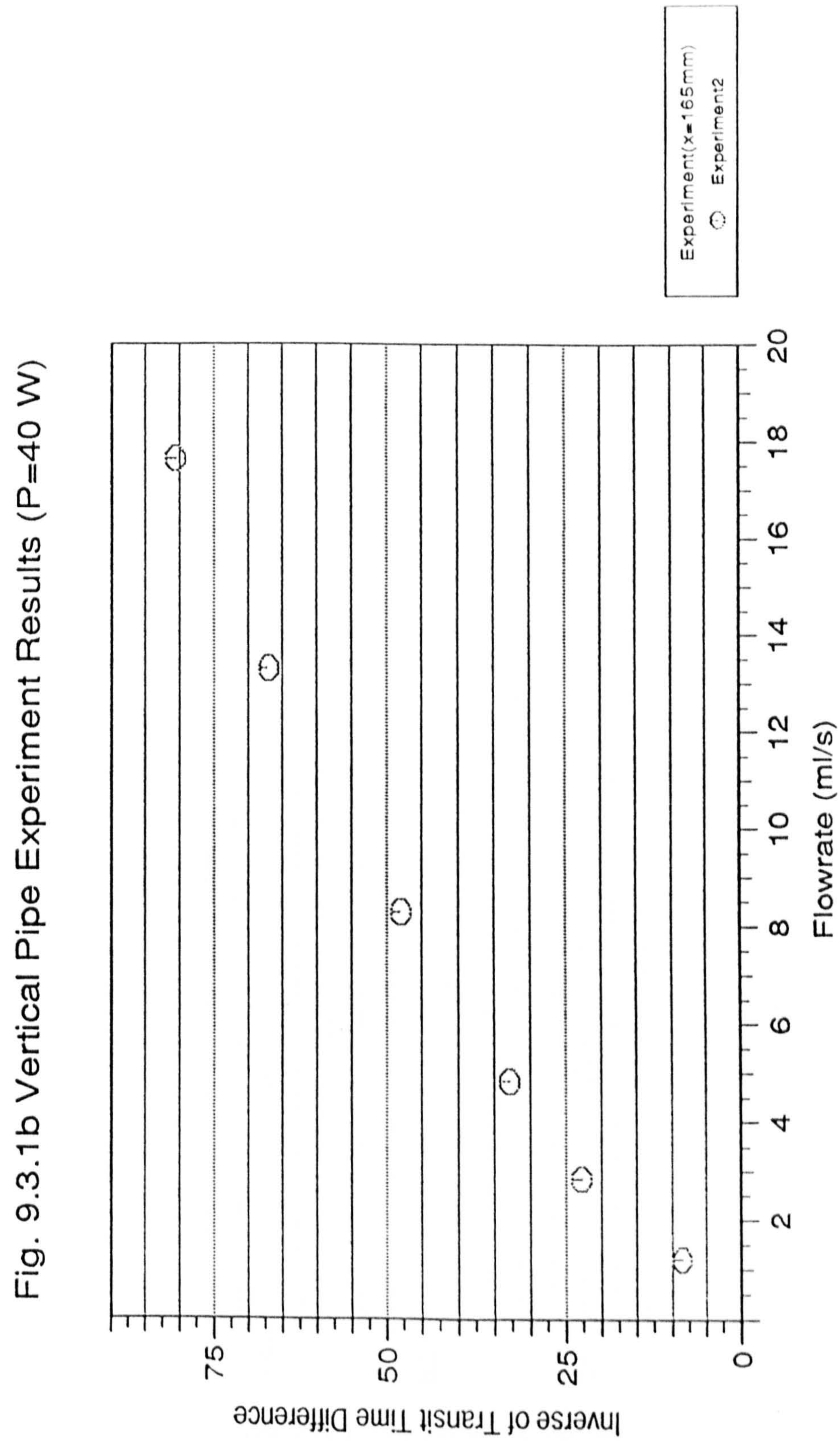

Fig. 9.3.1b Vertical Pipe Experiment Results (P=40 W)

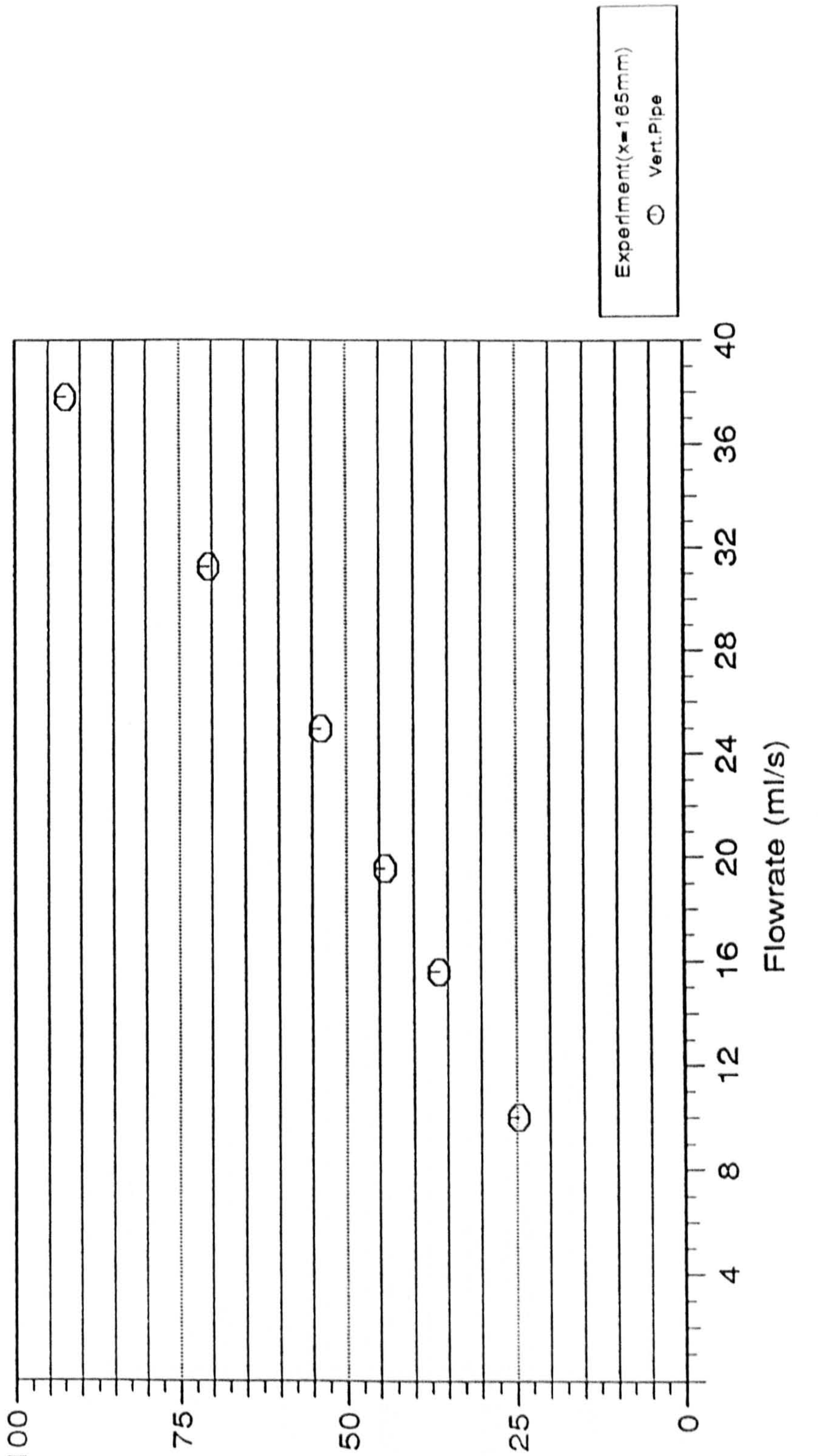

Fig. 9.3.2 Vertical Pipe Experiment Results (P=100 W)

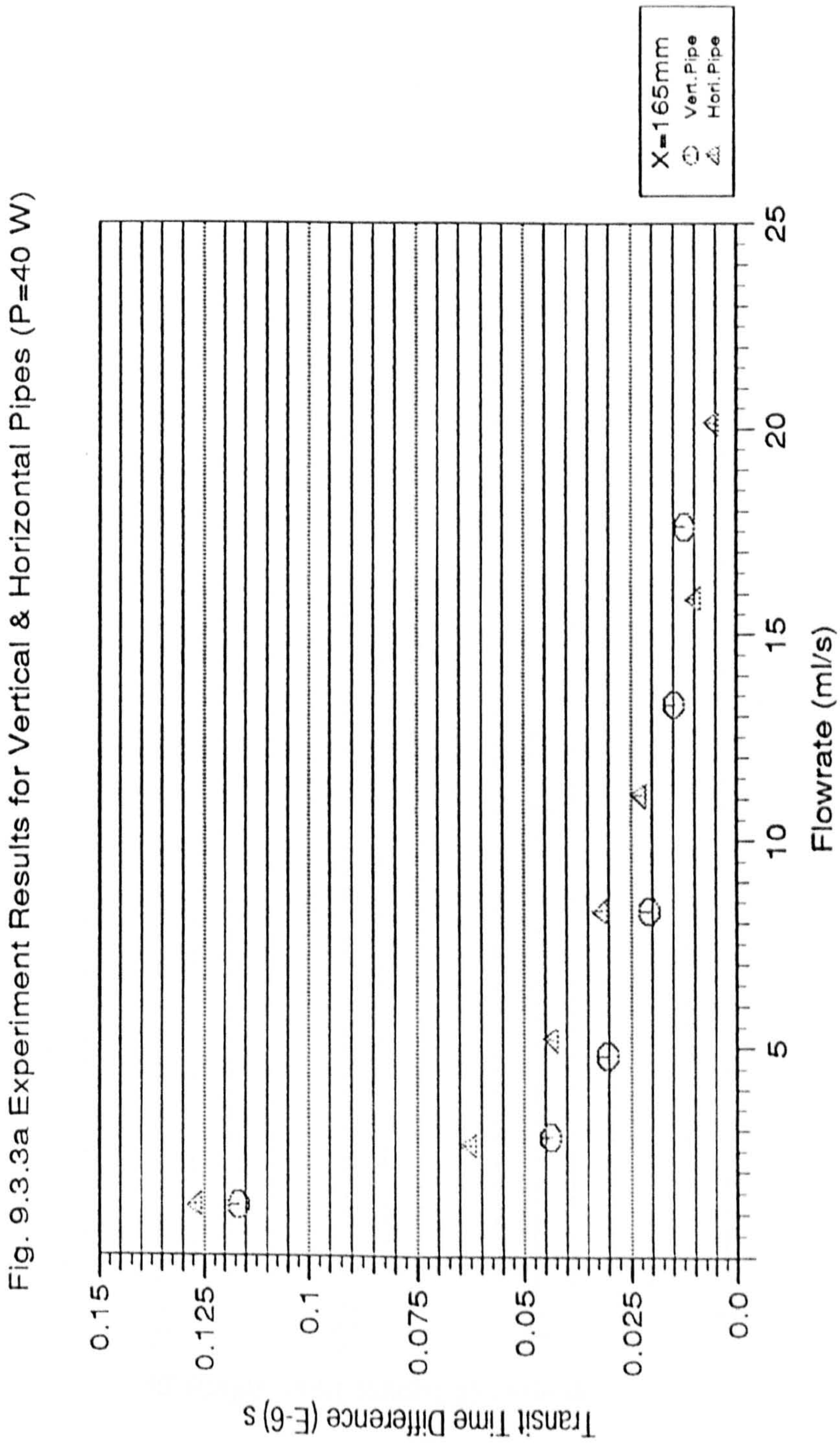

Fig. 9.3.3a Experiment Results for Vertical & Horizontal Pipes (P=40 W

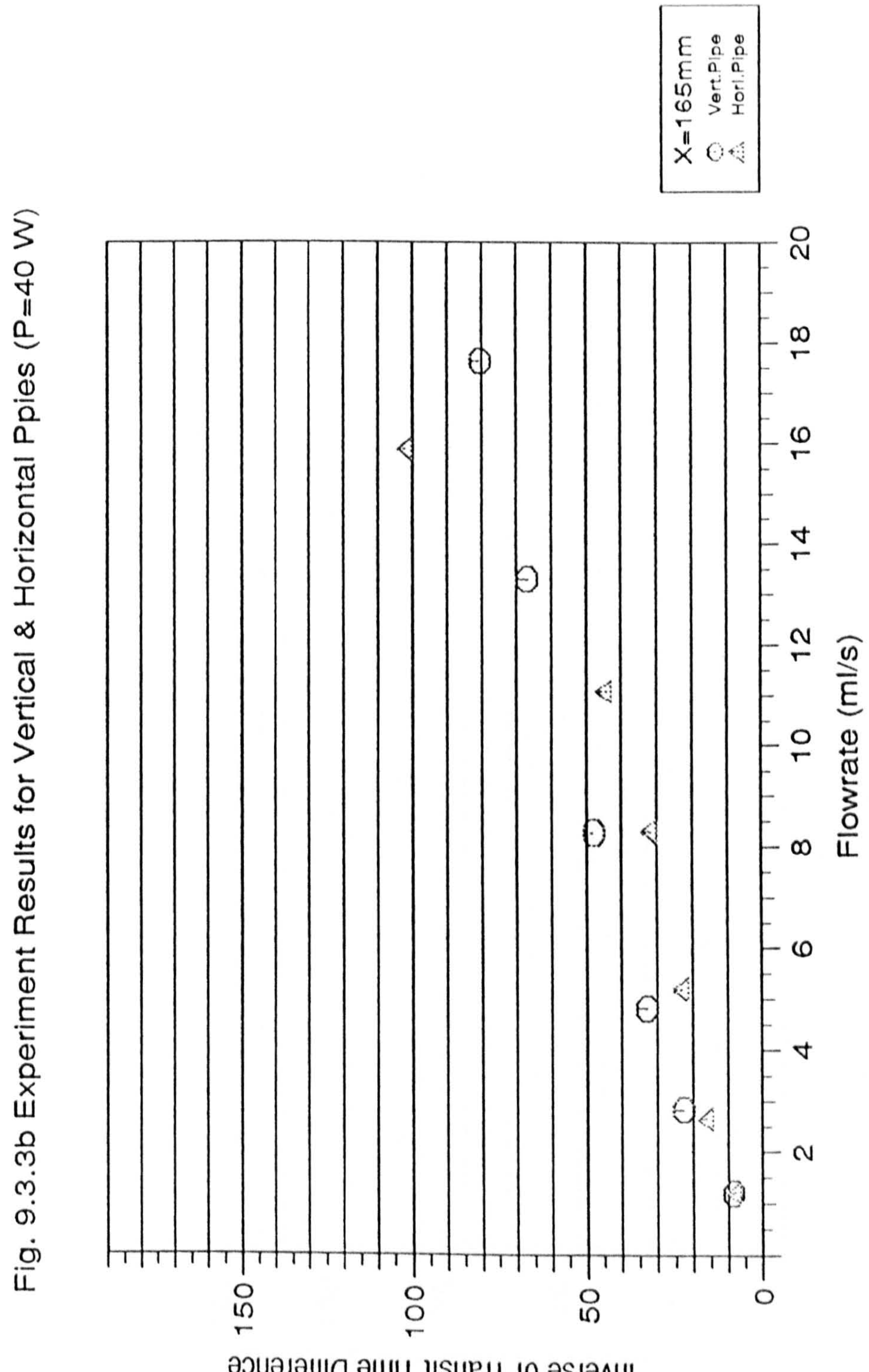
X=165mm
Vert.Pipe
Horl.Pipe
Fig. 9.3.3b Experiment Results for Vertical & Horizontal Ppies (P=40 W
Inverse of Transit Time Difference
0
50
00
50
2
4
6
8
10
12
14
16
18
20
Flowrate (ml/s)

Fig. 9.3.4 Experiment Results for Vertical & Horizontal Pipes (P=100W)

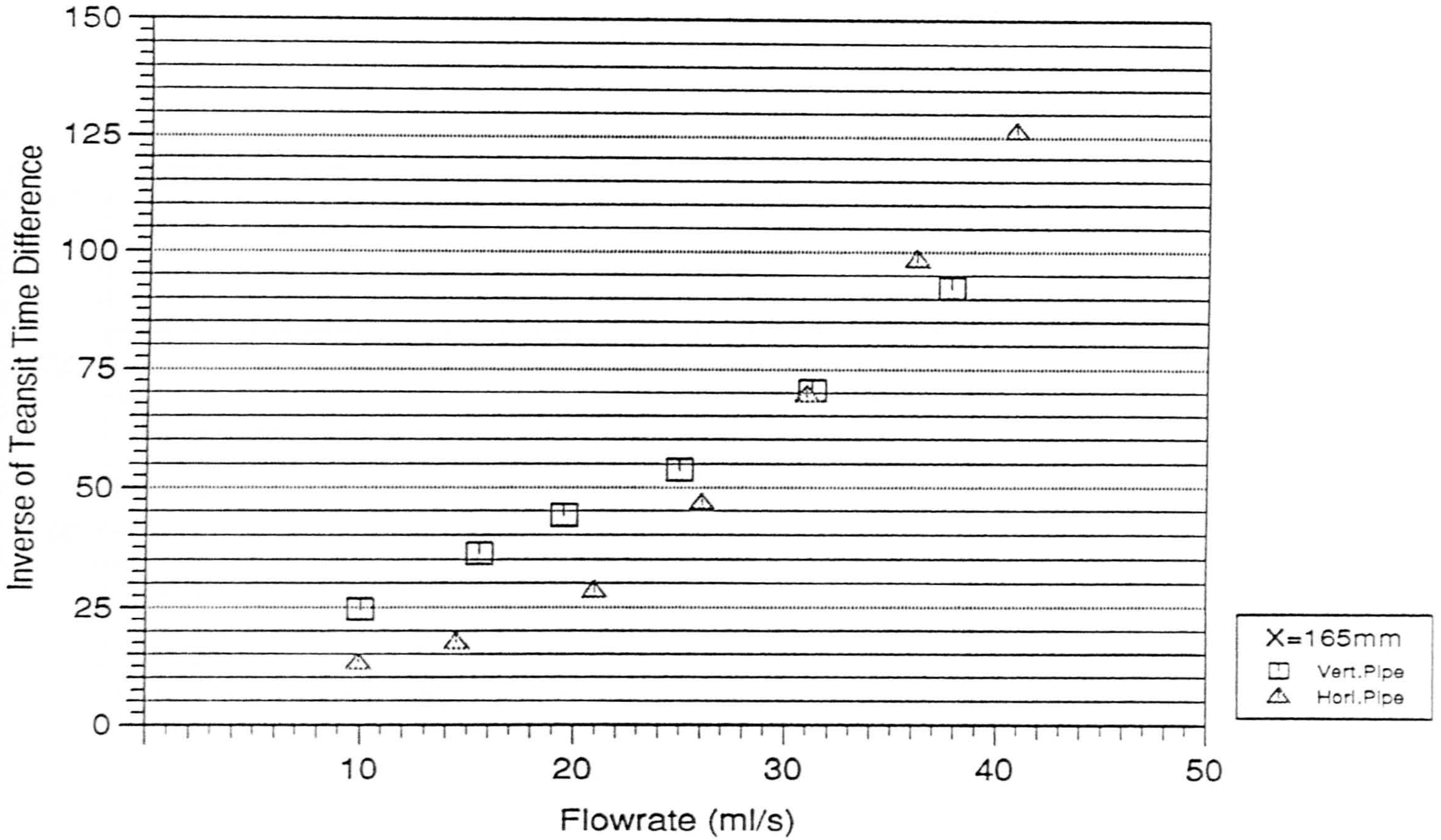

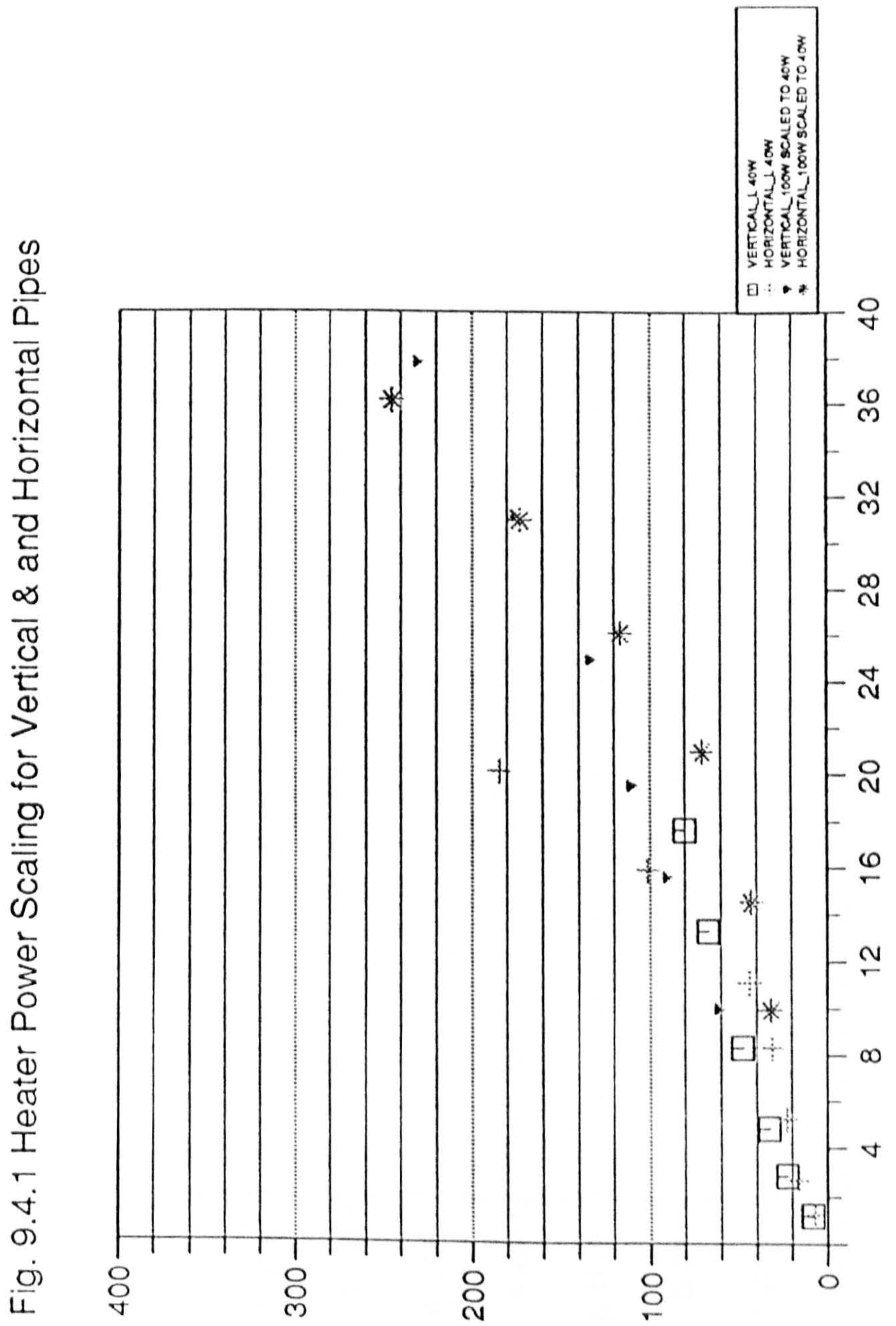

Fig. 9.4.1 Heater Power Scaling for Vertical & and Horizontal Pipes

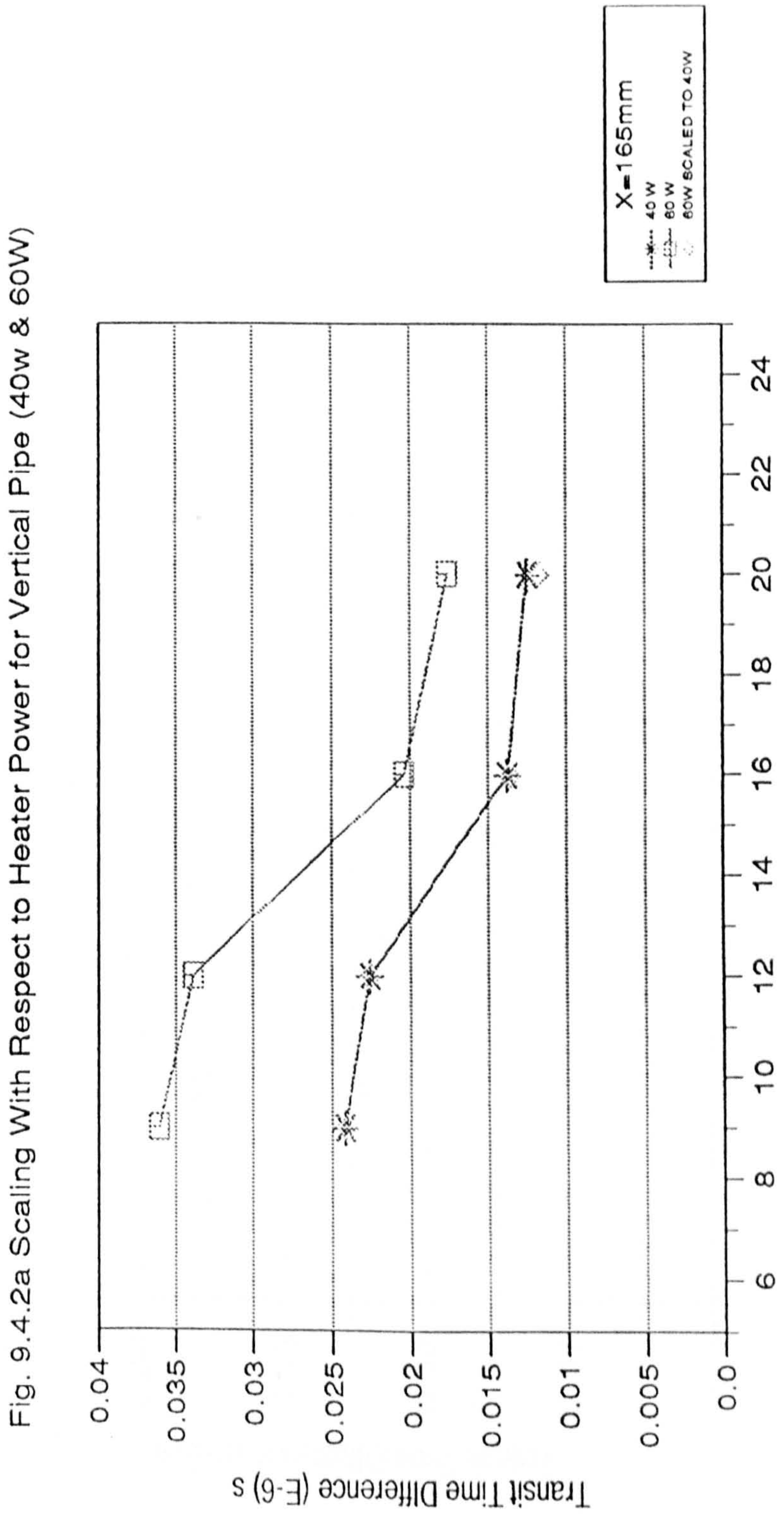

Fig. 9.4.2a Scaling With Respect to Heater Power for Vertical Pipe (40w & 60w)

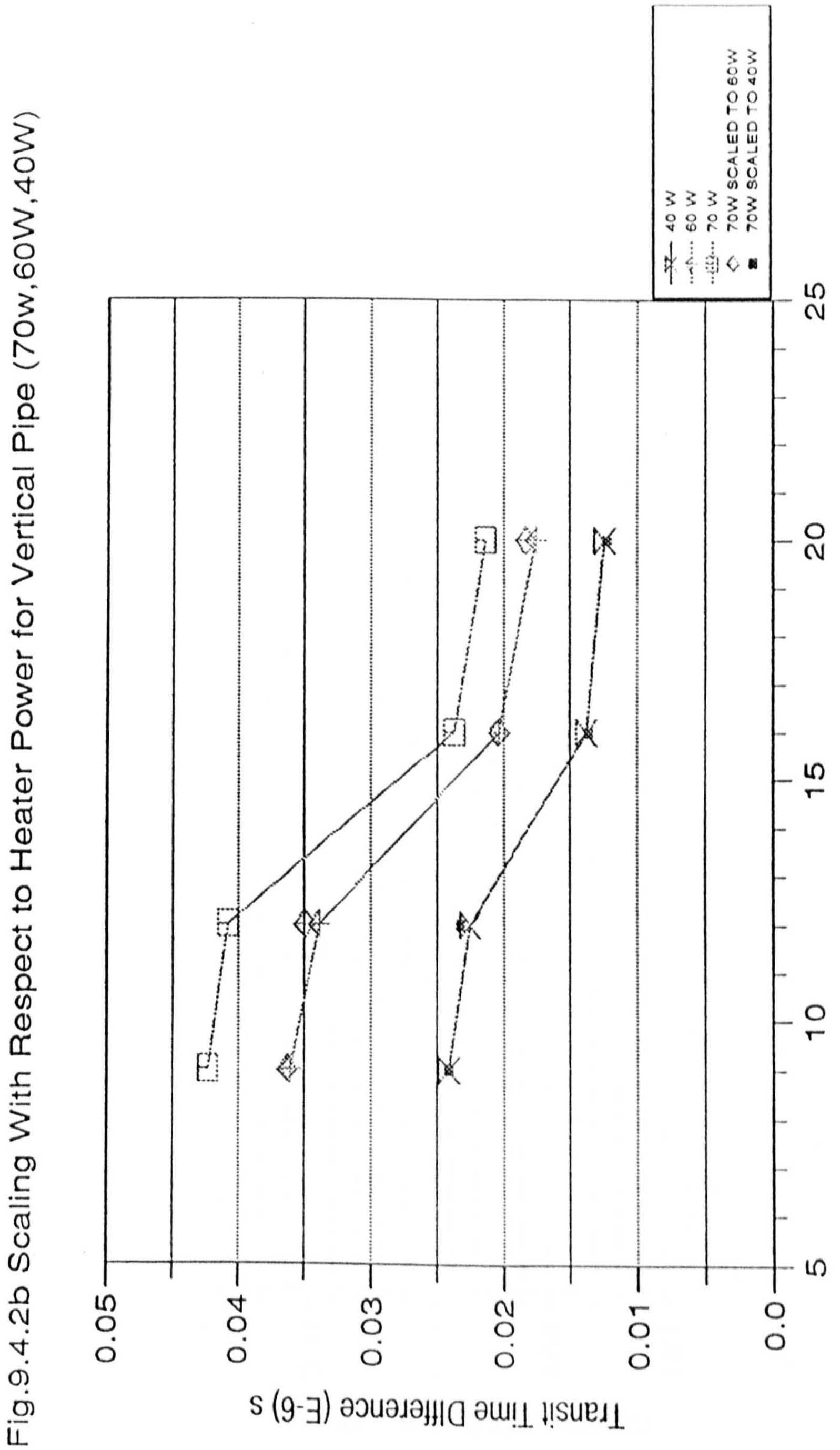

Fig. 9.4.2b Scaling With Respect to Heater Power for Vertical Pipe (70w,60W,40W)

Fig. 9.4.3 Scaling with respect to Heater Power for Horizontal Pipe

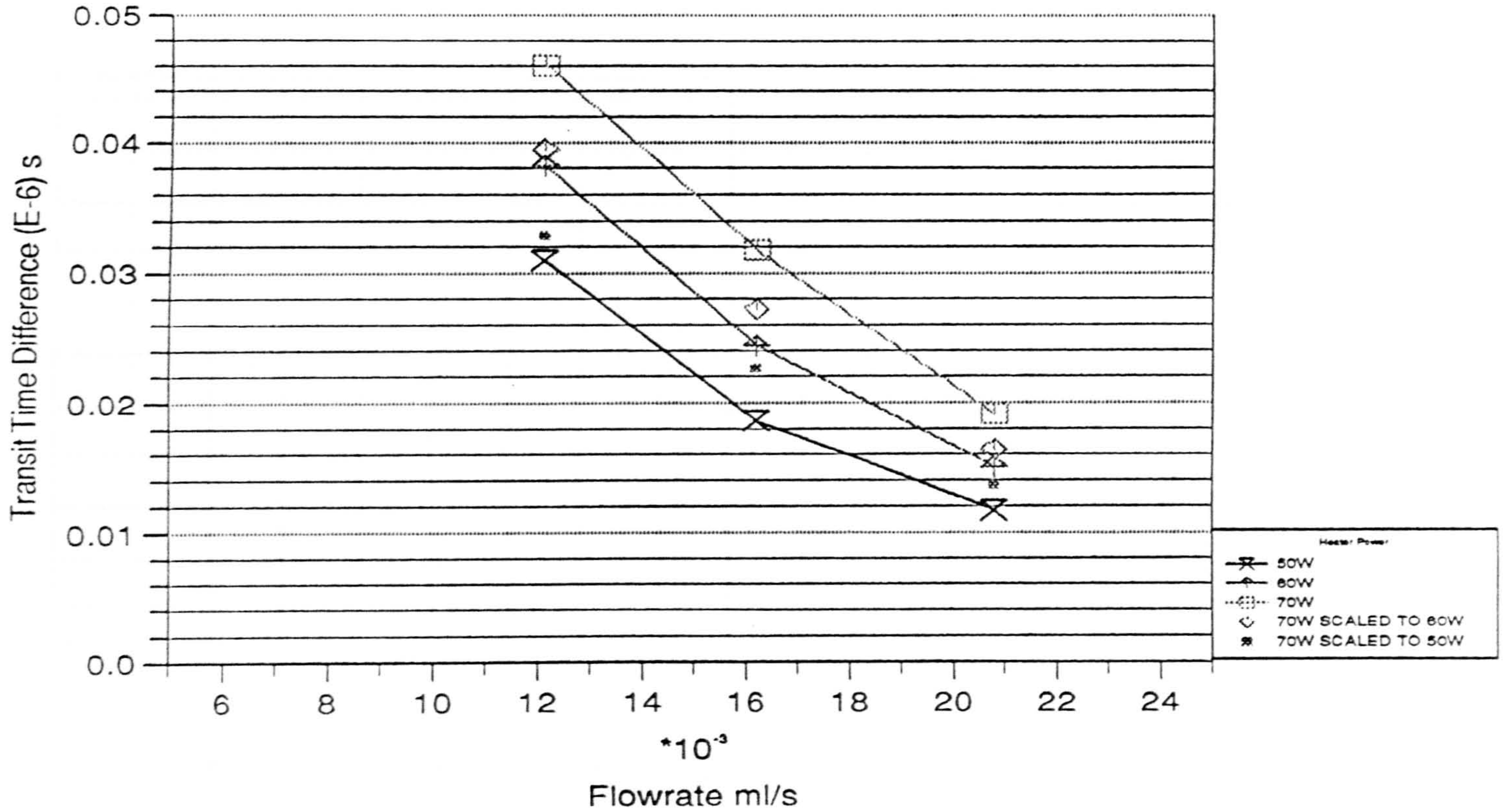

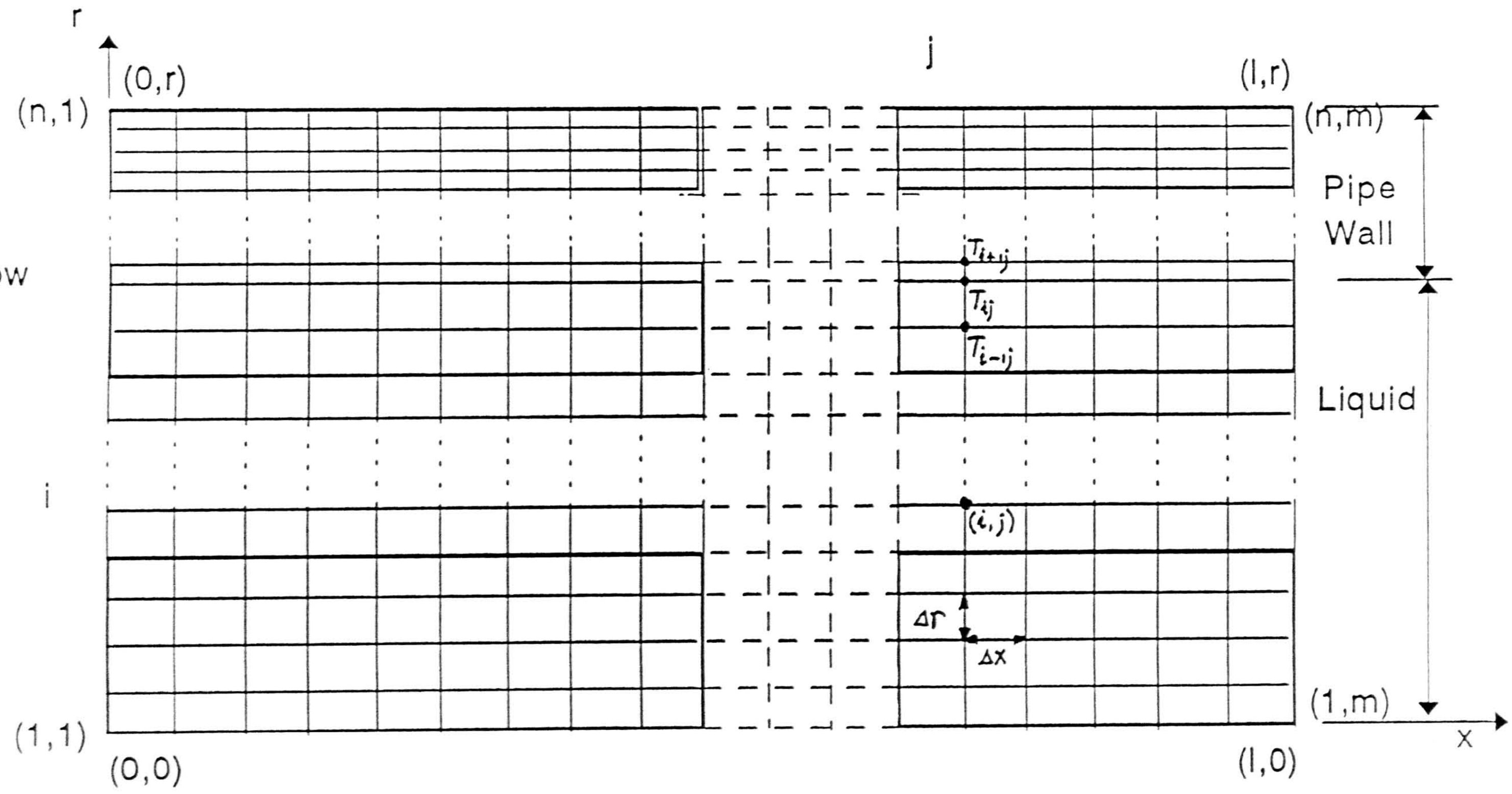

Fig A.1.1. Finite Difference Mesh for ADI Method

Fig. A.3.1. Flowchart for the Finite Difference Technique

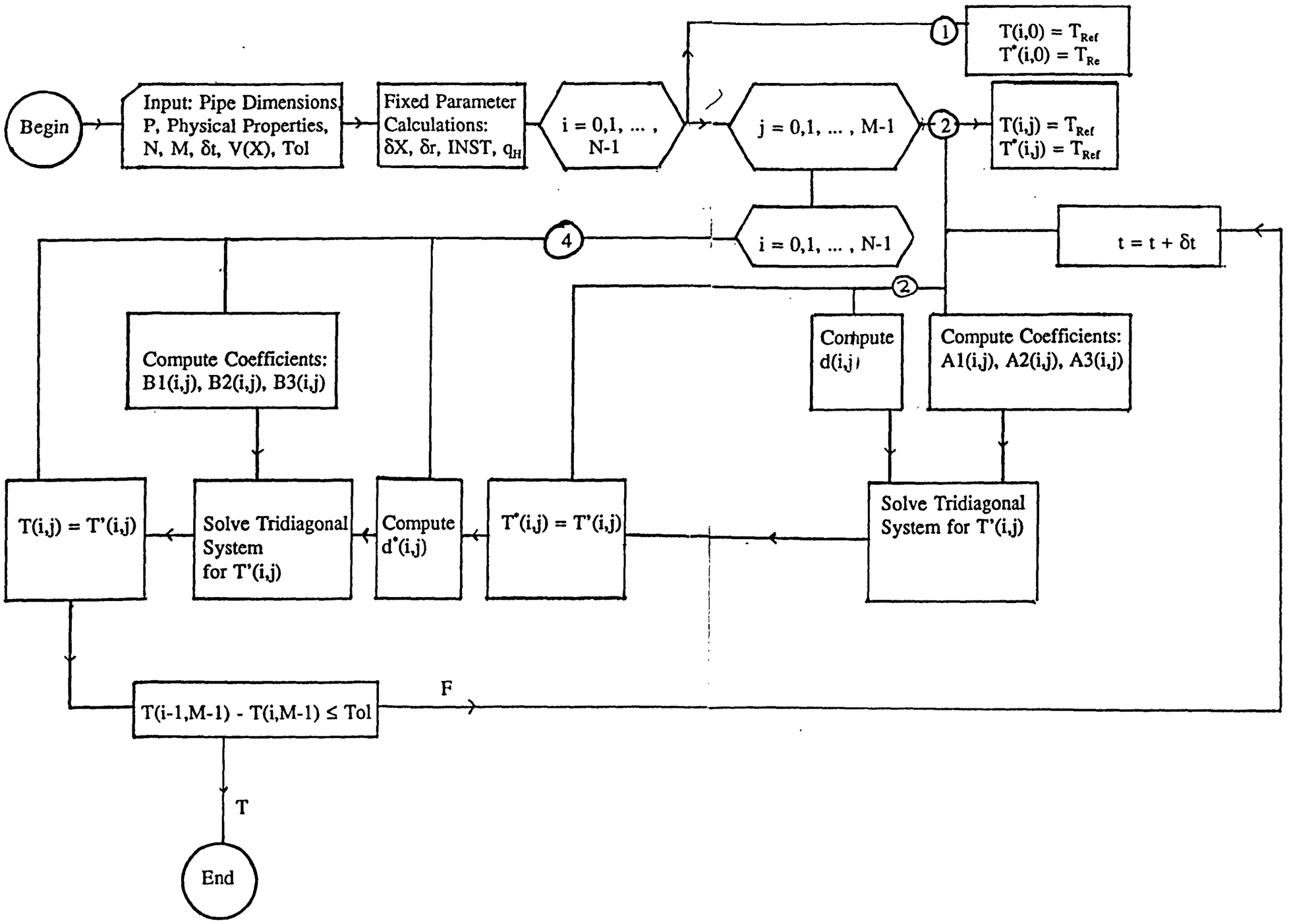

306.

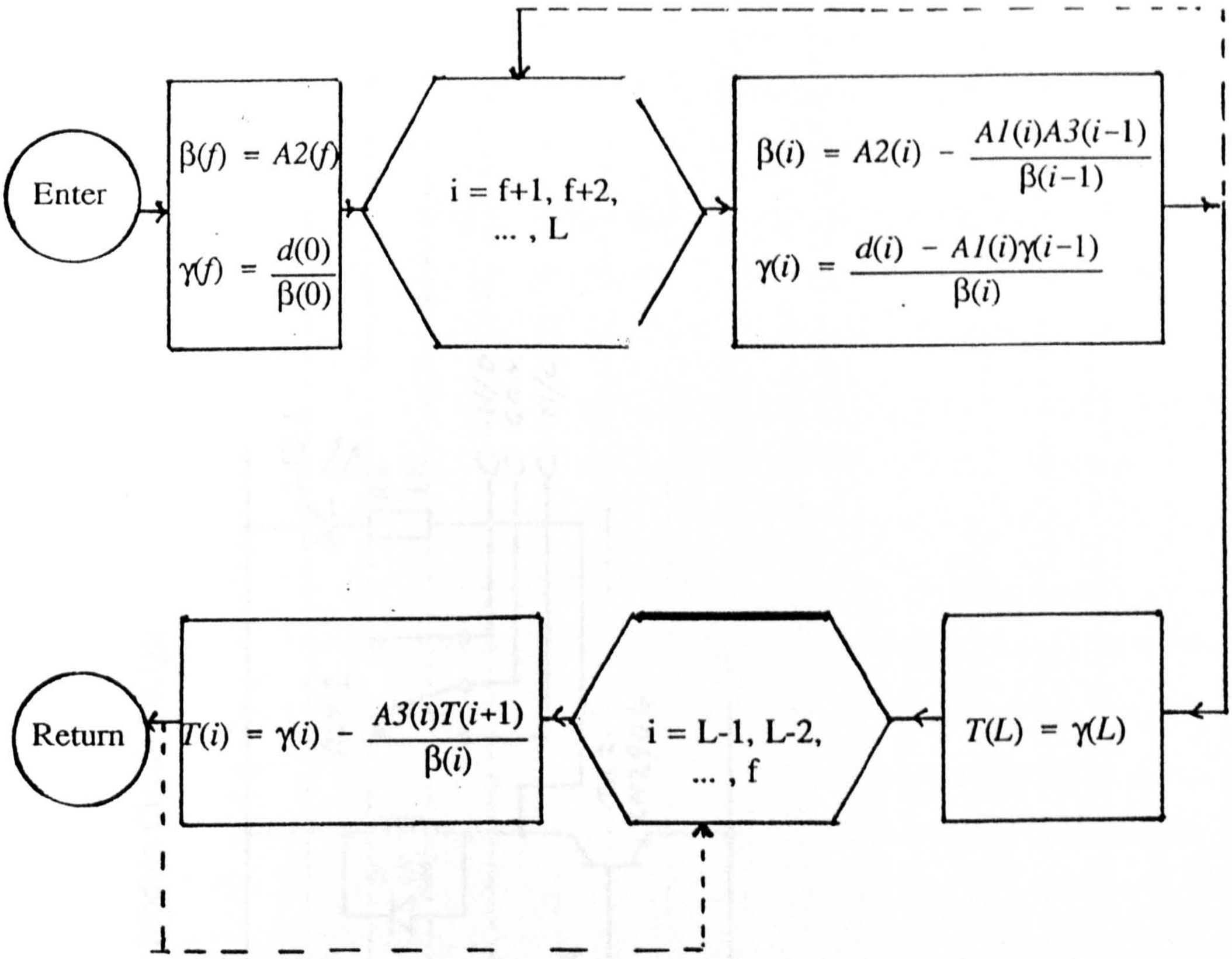

Fig. A.3.2. Subroutine for Solving Tridiagonal Matrix System

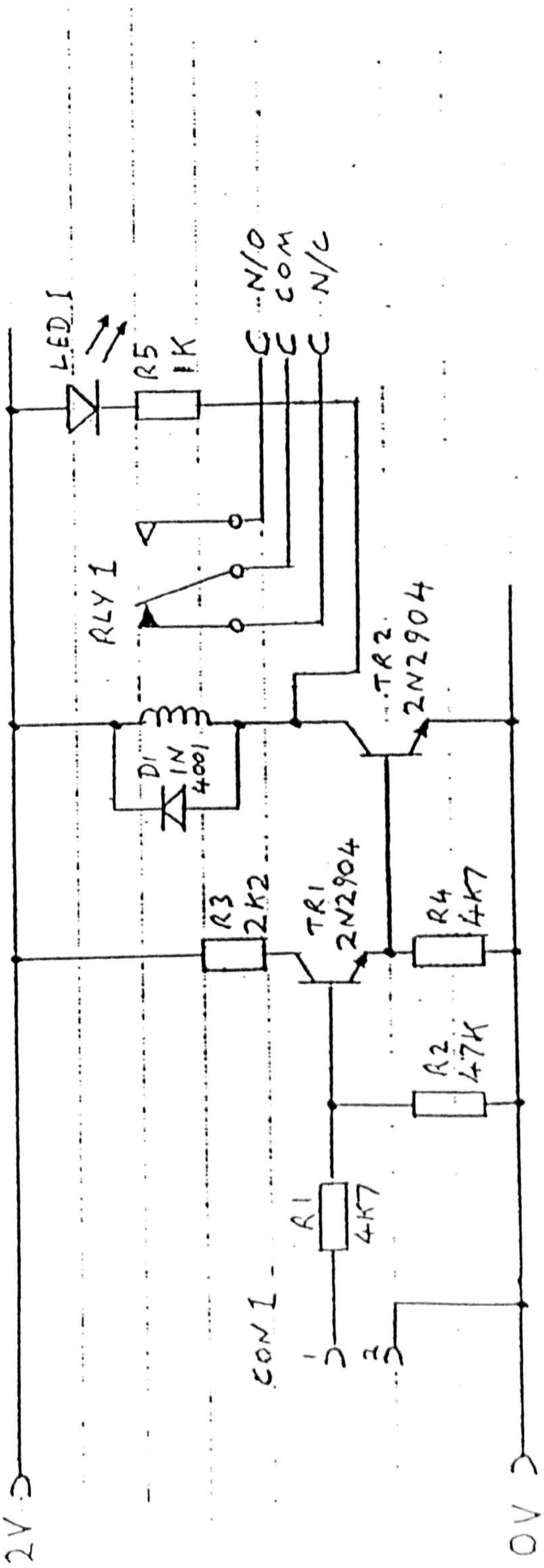

Fig. B.2.1. Computer Controlled Switch Relay Module Circuit Design

Fig. B.3.1. Wavetek Gate Mode Burst Controller Circuit Design

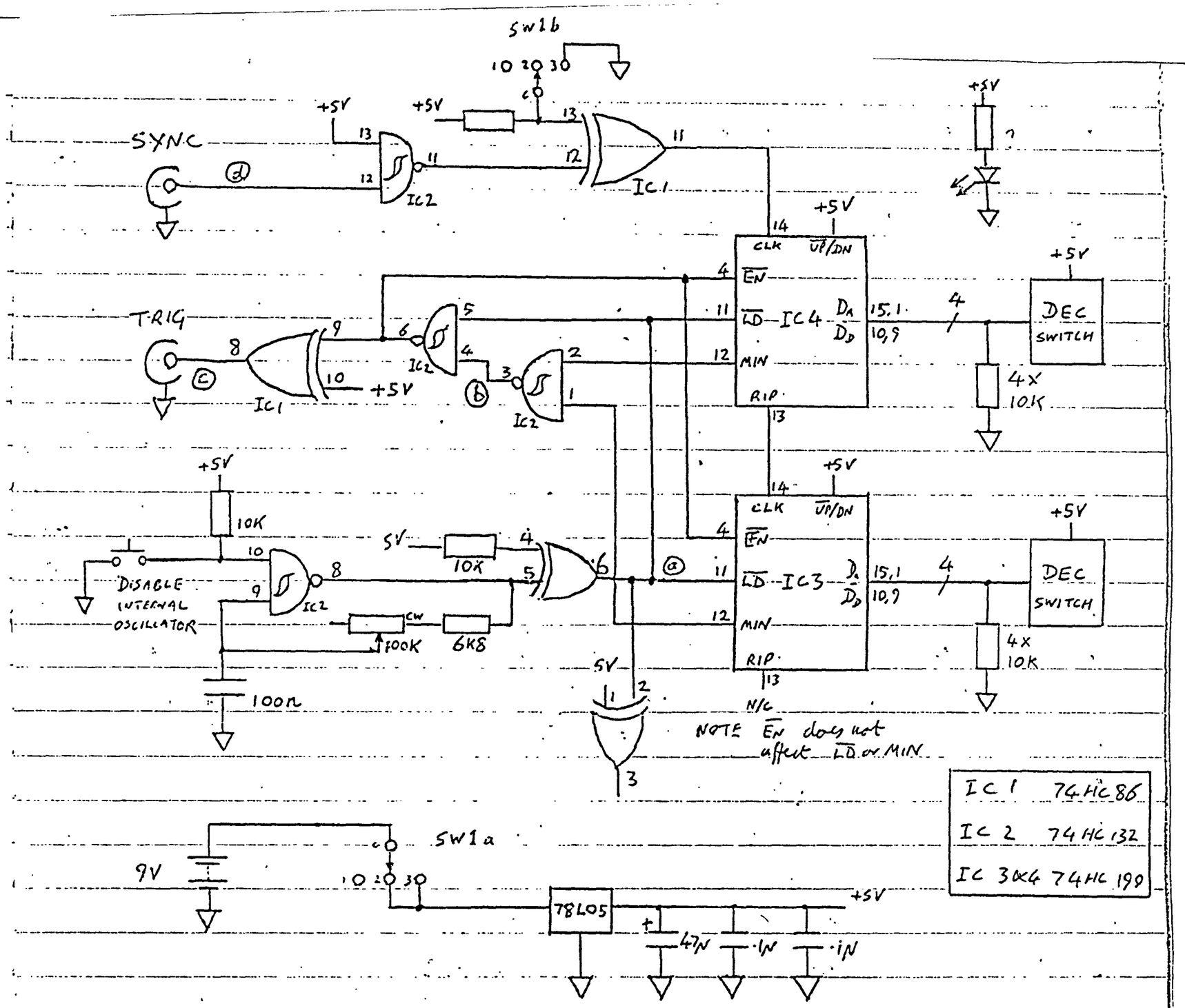

Fig. B.3.2. Input/Output Signals

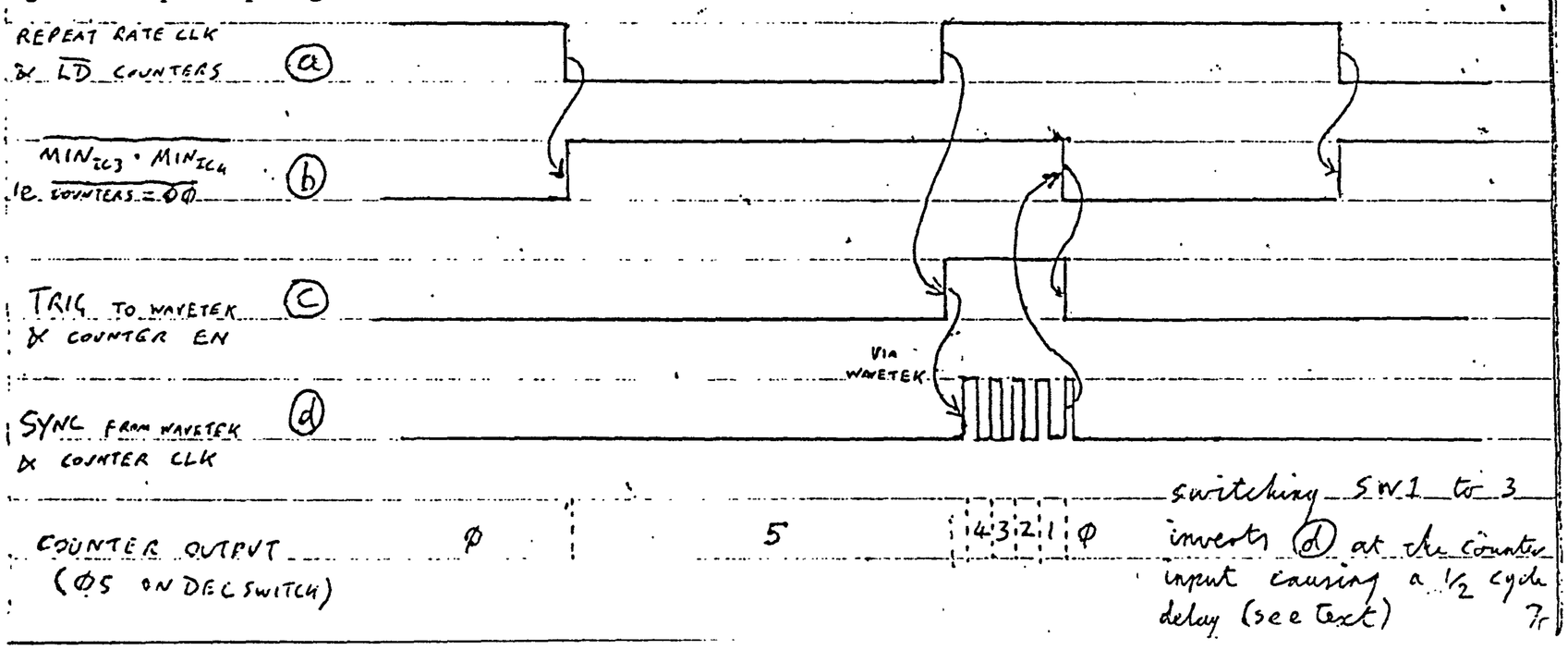

Fig. B.4.1a. Ultrasonic Timing Interface

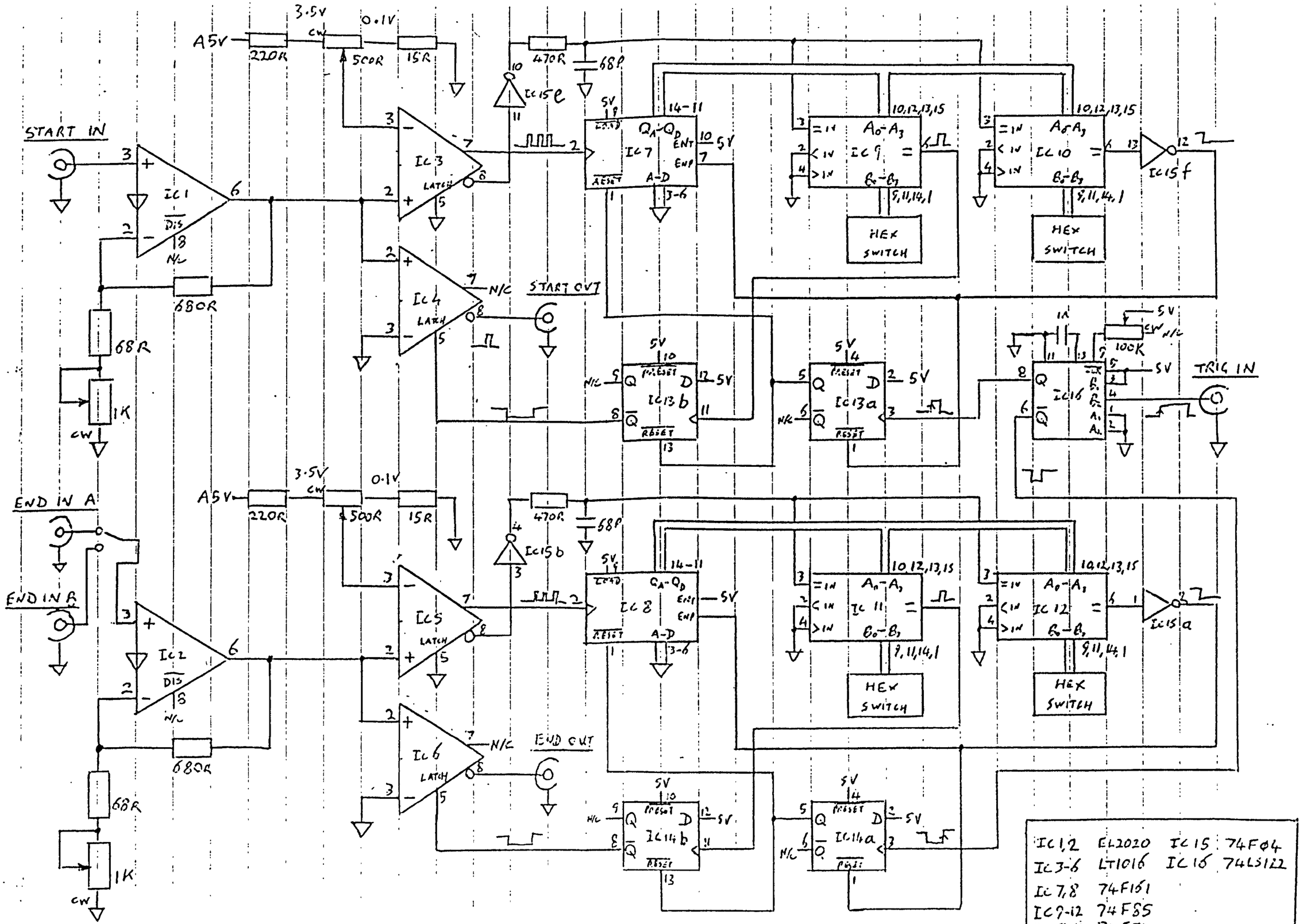

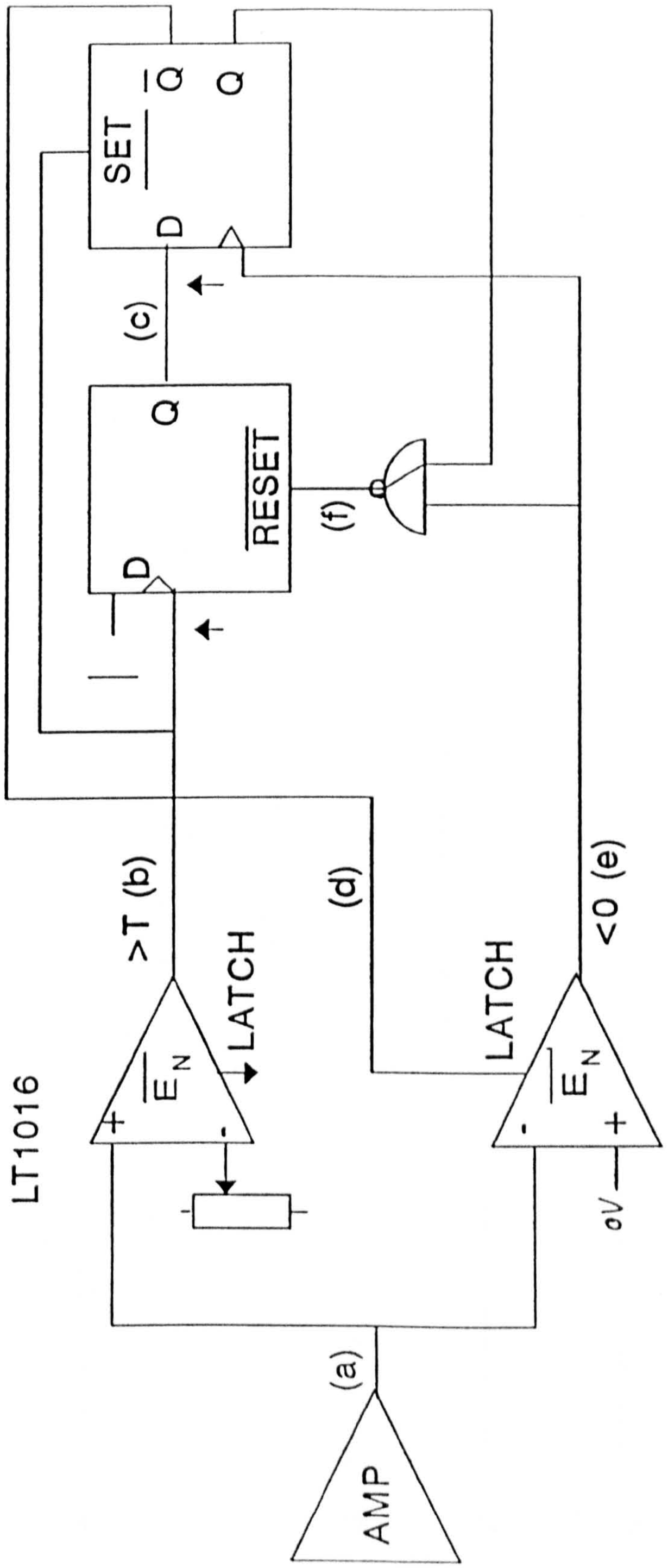

Fig. B.4.1b. Logic Diagram for Ultrasonic Timing Interface Electronics

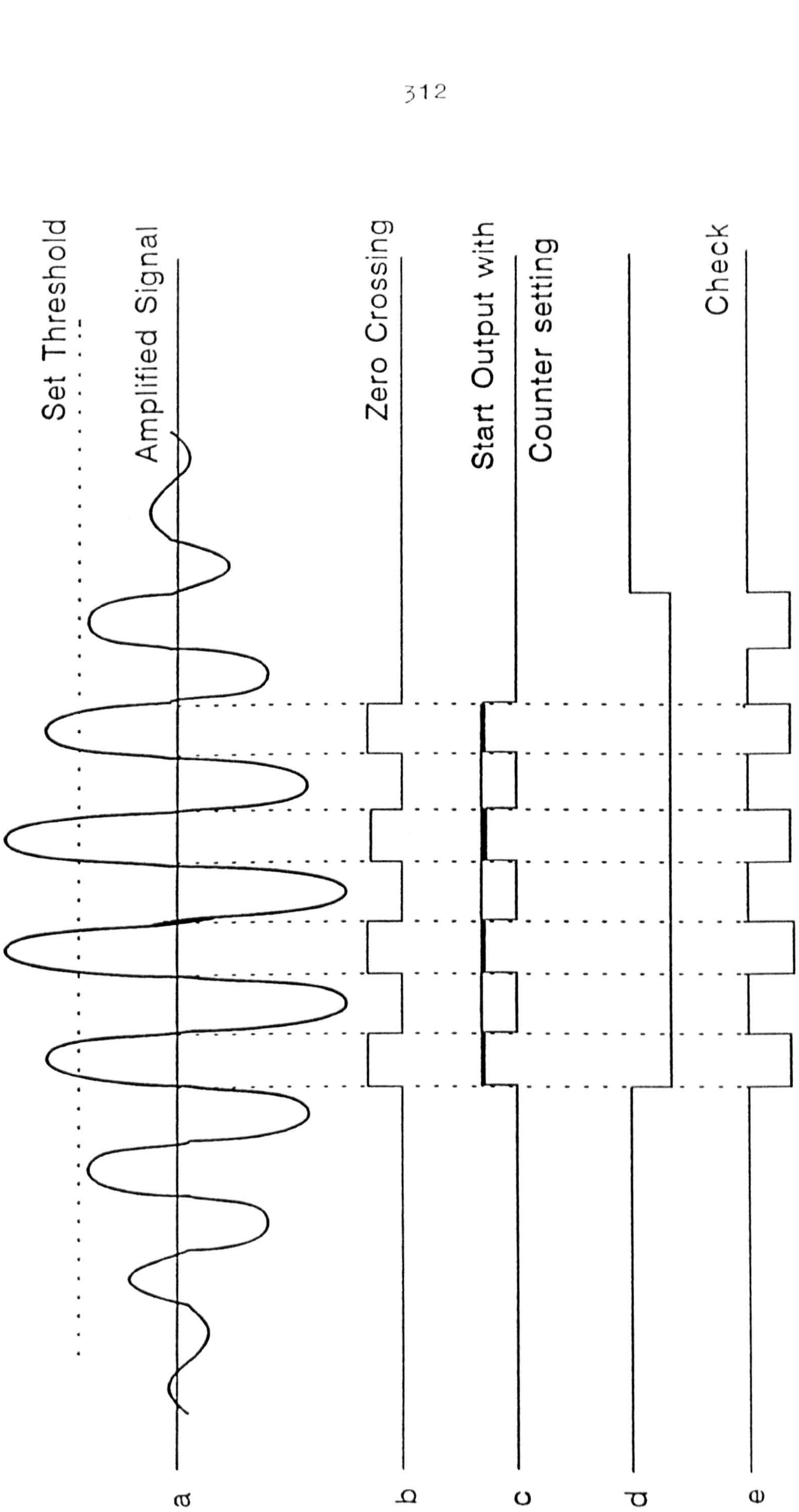
Set Threshold
Amplified Signal
Zero Crossing
Start Output with
Counter setting
Check
Step by Step Output
a
b
c
d
e

Fig B.4.2

TABLES

Table 1.2.1. Commercially Available Flowmeters

1	2	3	4	5	6	7	8	9	10	11	
Flowmeter type	*Liquid or gas*	*Slurry*	*Other two-phase*	*Precision*	*Diameter range[3] (mm)*	*Temperature range (°C)[4]*	*Flow range[4] (m^3/hr (kg/hr))*	*Pressure loss*	*Sensitivity to installation[5]*	*Initial cost*	*Notes*
Momentum[1]		†	†	†				‡	‡	‡	
Orifice	L G	x	?	••	50–1000	up to +540	$1–3 \times 10^6$ (L) $10–4 \times 10^6$ (G)	H	H	L/M	Concentric ISO orifice with differential pressure cell assumed. Eccentric used for two-phase flow.
Venturi	L G	•	•	••	50–1200	−180 to +540	30–7000 (L) 400–10^5 (G)	M	M/L	M/H	
Target	L G	?[2]	•	•	12–100	−45 to +540	$1–5 \times 10^4$(L) 0·5– (G)	H	H	M	
Variable area	L G	x	x		15–150	−200 to +350	10^{-3}–1000 (L) 10^{-4}–2000 (G)	M	L	L	Glass/plastic assumed; higher ratings for steel.
Volume											
Positive displacement	L G	x	?[2]	•••	4–1000	−50 to +315 (L) −50– +120 (G)	0·01–2000 (L) 0·01–3000 (G)	H/M	L	H	
Turbine	L G	x	x	•••	5–600	−200 to +260	0·01–10 000 (L) 0·01–10^5 (G)	M	H	L/M	Assumes high precision instruments rather than robust water meters, etc. Pelton wheel for very low flows.
Vortex	L G	x	x	••	12–200	−40 to +200	3–2000 (L) 50–10^5 (G)	H/M	H	L/M	Fluidic flowmeter suitable for very low flows.
Electromagnetic	L	••	••	••	2–3000	−50 to +190	10^{-2}–3×10^5	L	M	M	Only available commercially for electrically conducting liquids
Ultrasonic transit time	L G	?[2]	?[2]	•	3–3000 (L) 20–2000 (G)	−40 to +200	$3–3 \times 10^5$ (L) $3–10^6$ (G)	L	M/H	M/H	Single beam design are more sensitive to installation. Correlation and Doppler for two-phase flows.
Mass											
Thermal	G	x	x	•	3–6	0 to +65	3×10^{-4}–0·03	M	L	M	Available as a by-pass flowmeter for higher flows (up to 400 m^3/h) Low flow liquid versions available.
Wheatstone Bridge	L	x	x	••	6–60	−50 to +150	(0·05–$2·5 \times 10^4$)	n/a	L	H	Specialist instrument more suitable for R & D laboratory
Angular momentum	L	x	x	••	20–30	−40 to +150	(100–5×10^3)	M	M	M	Particularly suitable for aircraft fuel flow.
Coriolis	L	•	x	••	1–150	−75 to +245	(5–5×10^5)	M	M/L	H	

† ••• Very high, •• more suitable/high, • Suitable/medium; ?/blank Uncertain/lower; x Unsuitable.
‡ L = Low, M = Medium; H = High.

Notes
[1] Some proprietary devices offer special features: higher differential pressure, linear characteristic, suitabl for pulsating flows, etc.
[2] Observe specific constraints for each type of meter: installed life, solids limits, material compatibility, etc
[3] Larger or smaller sizes may be available.
[4] Other ranges may be available.
[5] Flow conditioning may be used in some applications to reduce this effect.

Table 2.3.1 Trial site location descriptions (April 1990)

TRIAL AREA	NO. PROPERTIES	LOCATION DESCRIPTION	ACORN GROUP
Isle of Wight (Southern Water)	53,500	South Coast	C/K
Bristol Water Co. (Hotwells)	839	Central Bristol	I/F
East Worcs. Water Co. (Marlbrook)	1,100	North East Bromsgrove	J/C
Lee Valley Water Co. (Brookmans Park)	1,148	3km North of Potters Bar	J
Mid-Southern Water Co. (Camberley)	1,184	East Camberley, Surrey	B/J
Northumbrian Water (Hutton Rudby)	797	10km South of Teeside	J
Rickmansworth Water Co. (Chorleywood)	748	SW Hertfordshire	J
Southern Water (Chandlers Ford)	602	5km South of Winchester	J
Thames Water (Haling Park)	754	5km South of Croydon	J/I
Wessex Water (Broadstone)	358	NW Poole, Dorset	J/K
Wessex Water (Turlin Moor)	320	West Poole, Dorset	E/F
Yorkshire Water (South Normanton)	720	5km East of Wakefield	E/F
TOTAL PROPERTIES (as of April 1990)	**62,070**		

Table 2.3.2 **Performance Summary of Metering Equipment on the Isle of Wight following Installation**

EQUIPMENT	FAULTS/PROBLEMS	COST TO SOUTHERN WATER
External Manifold Meters	187 meters with condensation on dials – unreadable 162 meters stopped recording	£30 per meter
Internal Meters	47 meters stopped recording	£35 per meter
Outreaders	8 recording unacceptable variance betwen readings on meter and outreader	Not yet repaired
Meter Boxes	134 screw type lids proved hard to remove. Cross threading has occured.	£60 per lid, dug out and replaced

Table 2.3.3 **Performance Summary of Metering Equipment at the Small Scale Sites following Installation**

AREA	FAULTS/PROBLEMS		COST PER UNDERTAKING
Bristol	2	sticking box lids	not available
	3	external meters leaking	
	3	external in-line meters leaking	
		Some misting of displays	
East Worcester	27	external in-line meters replaced	£ 925.29
	1	internal meter replaced	£ 34.27
	573	outreader leads and batteries replaced	£3,496.30
Lee Valley	24	external manifold meters - condensation inside meter head	not available
	20	outreaders with a blank display	
	225	installations with a difference between water meter and outreader total	
	8	installations recording "No Flow" condition	
	4	installations recording "Cable OC" condition	
	2	installations recording "Cable SC" condition	
	1	installation recording "Error" condition	
	88	installations showing a difference between outreaders total and total of individual stores	
	16	outreaders failing to "debrief"	
	9	outreaders showing "no data"	
	37	outreaders showing "corrup. data"	
Mid-Southern	2	external manifold meters misted up	not available
	2	faulty outreaders - cable connections	
Northumbrian	20	watertight box lids sticking	£ 180.00
	6	external manifold meters replaced (due to sheared register drive pin)	
Rickmansworth	30	leaking in-line external meters replaced - O-ring too tight	£ 600.00
Southern	1	stopped external manifold meter replaced	£ 35.00
Thames	9	external manifolds replaced (leaking, malfunction)	£ 90.00
	96	external manifolds with condensation on display	
	1	internal replaced (condensation)	£ 10.00
	2	internals replaced (leaking)	£ 20.00
	6	outreaders replaced (wiing fault)	£ 80.00
	6	boxes replaced	£ 780.00
	695	watertight box lids to be replaced - too tight	£ 180.00
Broadstone	14	internal meters - pulse/meter stopped	£1,190.00
	26	faulty outreader displays - no material cost as replaced under guarantee. Cost for reinstallation only	£ 30.00
Turlin Moor	12	manifold meters replaced - meter stopped	£ 420.00
	8	damaged watertight boxes - unable to remove lid - complete box replaced	£ 960.00

TABLE 4.2.5. Typical calibration curve for vertical pipe (X = 165 mm)

Flowrate ($ml\ s^{-1}$)	Transit Time Difference (μs)	Inverse Transit Time Difference
1.003	0.141	7.055
1.193	0.117	8.508
2.211	0.0630	15.864
2.837	0.0503	19.872
3.709	0.0400	24.959
4.825	0.0323	30.920
4.848	0.0322	31.038
8.288	0.0212	47.076
13.298	0.0149	66.892
15.619	0.0133	75.172
17.635	0.0121	82.023

TABLE 4.4.1. Computer prediction for distance X_M and transit time t_M

Number of Reflections N	Distance between Transmitter & Receiver (mm)	Transit Time (μs)
1	4.98	17.683
2	8.30	27.106
3	11.62	36.530
4	14.93	45.953
5	18.25	55.376
6	21.57	64.800
7	24.89	74.223
8	28.22	83.646

Table 6.3.1. Selection of Resistance Wire

Name of Wire	Physical Properties					
	ϱ	K_m	β_M	Max Temp	ρ	Strength
	$\mu\Omega cm$	$Wm^{-1}K^{-1}$	$10^{-3}K^{-1}$	°C	gcm^{-3}	m Pa
Aluchrom O[R] R.A.*	135-145	12.5	0.02	1250	7.1	650-1000
Alumel[R] T.A.**	29-33	30-32	1.9	1100	8.5-8.7	550-780
Chromel[R] T.A.	70.6	19	0.32	1100	8.5	620-780
Constantan R.A.	52	19.5	0.02	900	8.9	400-590
Copper	1.69	410	4.3	1083	8.96	314
Inconel600[R] Heat R.A.	103	12.5 x 10^{-6}		1400	8.42	600-1200
Manganin[R] R.A.	43-48	22	1E(-5)	300	8.4	300-600
Nickel	6.9	90	6.8	1459	8.9	400
Platinum	10.5	71.6	3.92	1772	21.4	200-300
Pt/Iridium T.A.	25	31	1.3	1800	21.56	380-620
Pt/Rhodium T.A.	18.4-19.2	38	1.7	1840	19.97	320-620
Silver	1.63	429	4.1	962	10.5	172
Tungsten	54	173	4.8	3410	19.3	550-620

* T.A.: Thermocouple Alloy.
** R.A.: Resistance Alloy.

Table 6.3.2. Selection of Resistance Wire Support Material

Name of Product	Operating Temperature (°C)	Bonding Strength to Metal	Other Comments
Silicon Rubber non-corrosive	-70 to 200	Excellent	
Two Part RTV	-40 to 250	Good	Mixing is required
Mechanical Grade Pasta	-50 to 250		
Adhesive Tapes			Not easy to fix the tape onto the heater frame
Polyamide	310	One side only	
Polyester	- 5 to 180		
Glass Cloth	- 7 to 150		

Table 6.3.3. Electrical Insulating Material used between the Resistance Wire and the Pipe

Name of Product	Temp (°C)	Dimensions (mm)	Thermal Conductivity	Comments
foam seal strip (p.t.f.e)	-260 to 260		0.33	easy to use
thread seal tape	-200 to 260	12000 x 12	0.33	easy to use
silicon insulating sheet	-60 to 180	300 x 300 x 0.177	0.83	wide but too thick
heat sink compound paste	-100 to 200		0.90	mixing & moulding required
heat sink bonder	150		0.82	required to mould in right form

Table 6.4.1. Preliminary Ultrasonic/Thermal Experimental Results

Flowrate (cm s^{-1} ml s^{-1})		Transit Time (μs)		Transit Time Difference (μs)
		Δt_0 (Heater off)	Δt_1 (Heater on for 60 s)	
1.07	1.53	12.50	12.32	0.18
1.72	2.46	12.50	12.40	0.10
2.37	3.39	12.50	12.41	0.09
2.75	3.93	12.50	12.42	0.08
3.30	4.72	12.50	12.40	0.10
3.36	4.81	12.50	12.43	0.07
4.40	6.29	12.50	12.40	0.10
5.20	7.44	12.50	12.46	0.04

TABLE 6.4.4a. Comparison of experimental dat with computation results

Flow Velocity ($cm\ s^{-1}$)	Transit Time (μs)
Computation	
1.00	9.206
1.40	9.250
1.80	9.271
2.20	9.288
2.60	9.301
5.00	9.347
Experimental Results	
1.070	9.341
1.720	9.421
2.370	9.431
2.750	9.441
3.300	9.446
3.360	9.451
4.440	9.461
5.200	9.481

TABLE 6.4.4b. Evaluation of the error associated with the instruments

Flow Velocity (cm s^{-1})	$\frac{1}{\Delta t_0 - \Delta t_1}$	- Difference	+ Difference
1.070	5.555	5.405	5.7142
1.720	9.999	9.523	10.526
2.370	11.111	10.520	11.764
2.750	12.500	11.764	13.333
3.300	13.333	12.500	14.285
3.360	14.285	13.333	15.384
4.440	16.666	15.384	18.181
5.200	25.000	22.222	28.571

Table 6.5.1 Investigation of Multiple Ultrasonic Reflections (Full pipe, 0.75 ml s^{-1})

Number of Crossings	Distance (mm)	Transit Time (μs)		Error (%)
		Theoretical	Experimental	
1	4.92	17.75	17.80	0.56
3	11.62	36.50	36.60	0.27
5	18.25	55.30	56.60	2.30

TABLE 8.5.1a. Preliminary experiment for vertical pipe (40W, Δt vs Q)

Flowrate (ml s^{-1})	Transit Time Difference (μs)
1.069	0.0845
2.077	0.0486
4.848	0.0297
7.275	0.0227
10.466	0.0173
15.579	0.0109

TABLE 8.5.1b. Preliminary experiment for vertical pipe (40W, inverse Δt vs Q)

Flowrate (ml s^{-1})	Inverse of Transit Time Difference
1.069	11.828
2.077	20.564
4.848	33.628
7.275	44.047
10.466	57.692
15.579	91.104

TABLE 8.5.2a. Preliminary experiment for horizontal pipe (P = 200W, Δt vs Q)

Flowrate (ml s^{-1})	Transit Time Difference (μs)
11.625	0.181
20.579	0.104
29.395	0.0476
38.470	0.0307
48.876	0.0175
59.310	0.0113
70.335	0.00796

TABLE 8.5.2b. Preliminary experiment for horizontal pipe

(P = 200W, inverse Δt vs Q)

Flowrate (ml s^{-1})	Inverse of Transit Time Difference
11.625	5.506
20.579	9.528
29.395	20.999
38.470	32.512
48.876	56.910
59.310	88.081
70.335	125.519

TABLE 8.6.2a. Calibration curve for vertical pipe orientation (40W, Δt vs Q)

	Flowrate (ml s^{-1})	Transit Time Difference (μs)
Expt.1.	1.069	0.0845
	2.077	0.0486
	4.848	0.0297
	7.275	0.0227
	10.466	0.0173
	15.579	0.0109
Expt. 2	1.193	0.116
	2.837	0.0437
	4.825	0.0303
	8.288	0.0208
	13.298	0.0149
	17.635	0.0124

TABLE 8.6.2b. Calibration curve for vertical pipe orientation

(40W, inverse Δt vs Q)

	Flowrate ($ml\ s^{-1}$)	Inverse of Transit Time Difference
Expt. 1	1.069	11.828
	2.077	20.564
	4.848	33.628
	7.275	44.047
	10.466	57.692
	15.579	91.104
Expt. 2	1.193	8.560
	2.837	22.832
	4.825	32.954
	8.288	47.982
	13.298	67.103
	17.635	80.610

TABLE 8.6.3a. Heater-transducer separations for vertical pipe (40W, Δt vs Q)

	Flowrate (ml s^{-1})	Transit Time Difference (μs)
X = 50 mm	1.003	0.197
	2.211	0.0738
	3.709	0.0439
	6.927	0.0275
	10.591	0.0177
	15.619	0.0128
	19.819	0.00959
X = 100 mm	1.204	0.126
	2.083	0.0571
	4.289	0.0374
	7.314	0.0234
	10.540	0.0196
	14.238	0.0124
	18.764	0.00875
X = 165 mm	1.193	0.116
	2.837	0.0437
	4.825	0.0303
	8.288	0.0208
	13.298	0.0149
	17.635	0.0124

TABLE 8.6.3b. Heater-transducer separations for vertical pipe

(40W, inverse Δt vs Q)

	Flowrate (ml s^{-1})	Inverse of Transit Time Difference
X = 50 mm	1.003	5.069
	2.211	13.545
	3.709	22.744
	6.927	36.234
	10.591	56.329
	15.619	77.594
	19.819	104.270
X = 100 mm	1.204	7.889
	2.083	17.510
	4.289	26.666
	7.314	42.589
	10.540	50.945
	14.238	80.615
	18.764	114.248
X = 155	1.193	8.560
	2.837	22.832
	4.825	32.954
	8.288	47.982
	13.298	67.103
	17.635	80.610

TABLE 8.6.4a. Calibration curve for vertical pipe (P = 100W, Δt vs Q)

Flowrate (ml s^{-1})	Transit Time Difference (μs)
10.018	0.0404
15.603	0.0274
19.572	0.0225
24.973	0.0185
31.231	0.0141
37.818	0.0108

TABLE 8.6.4b. Calibration curve for vertical pipe (P = 100W, inverse Δt vs Q)

Flowrate (ml s^{-1})	Inverse of Transit Time Difference
10.018	24.694
15.603	36.368
19.572	44.297
24.973	53.776
31.231	70.524
37.818	92.435

TABLE 8.6.5a. Repeatability of the flowmeter (Δt vs Q)

	Flowrate ($ml\ s^{-1}$)	Transit Time Difference (μs)
Expt. 1	10.018	0.0404
	15.603	0.0274
	19.572	0.0225
	24.973	0.0185
	31.231	0.0141
	37.818	0.0108
Expt. 2	9.699	0.0420
	13.592	0.0341
	20.781	0.0230
	25.153	0.0192
	32.298	0.0149
	36.855	0.0117
	38.694	0.0103

TABLE 8.6.5b. Repeatability of the flowmeter (inverse Δt vs Q)

	Flowrate ($ml\ s^{-1}$)	Inverse of Transit Time Difference
Expt. 1	10.018	24.694
	15.603	36.368
	19.572	44.297
	24.973	53.776
	31.231	70.524
	37.818	92.435
Expt. 2	9.699	23.783
	13.592	29.246
	20.781	43.356
	25.153	52.039
	32.298	66.755
	36.855	85.352
	38.694	96.972

TABLE 8.6.6. Scaling with respect to heater power for Vertical pipe

Flowrate	Heater Input Power				
	70W	60W	50W	40W	30W
19.91 ml s^{-1}	0.0213	0.0175	0.0157	0.0124	0.00942
16.72 ml s^{-1}	0.0237	0.0203	0.0166	0.0137	0.00997
12.21 ml s^{-1}	0.0407	0.0338	0.0297	0.0225	0.0148
9.08 ml s^{-1}	0.0422	0.0360	0.0346	0.0241	0.0196

TABLE 8.7.2. Effect of Heater-transducer separation (Δt vs distance X)

	Separation Distance (mm)	Transit Time Difference (μs)
19.91 ml s^{-1}	50.0	0.00694
	100.0	0.0160
	150.0	0.0164
	200.0	0.0174
	250.0	0.0172
	350.0	0.0201
16.71 ml s^{-1}	50.0	0.00171
	100.0	0.00767
	150.0	0.00586
	200.0	0.0128
	250.0	0.0117
	350.0	0.0126
12.21 ml s^{-1}	50.0	0.0151
	100.0	0.0276
	150.0	0.0329
	200.0	0.0328
	250.0	0.0396
	350.0	0.0354
9.08 ml s^{-1}	50.0	0.0775
	100.0	0.0828
	150.0	0.0728
	200.0	0.0818
	250.0	0.0762
	350.0	0.0684

TABLE 8.7.3a. Repeatability of the flowmeter (Δt vs Q)

	Flowrate ($ml\ s^{-1}$)	Transit Time Difference (μs)
Expt. 1	2.170	0.133
	5.129	0.0804
	9.176	0.0587
	11.186	0.0500
	13.674	0.0485
	18.577	0.0313
	21.599	0.0230
Expt. 2	1.049	0.246
	2.333	0.145
	3.409	0.106
	5.089	0.0833
	9.938	0.0569
	14.220	0.0454
	20.357	0.0255

TABLE 8.7.3b. Repeatability of the flowmeter (inverse Δt vs Q)

	Flowrate (ml s^{-1})	Inverse of Transit Time Difference
Expt. 1	2.170	7.471
	5.129	12.433
	9.176	17.032
	11.186	19.993
	13.674	20.602
	18.577	31.929
	21.599	43.464
Expt. 2	1.049	4.055
	2.333	6.858
	3.409	9.362
	5.089	12.003
	9.938	17.566
	14.220	21.981
	20.357	39.152

TABLE 8.7.4a. Calibration curve for horizontal pipe (P = 40W, Δt vs Q)

Flowrate (ml s^{-1})	Transit Time Difference (μs)
1.204	0.126
2.656	0.0624
5.202	0.0433
8.308	0.0316
11.090	0.0226
15.887	0.00983
20.146	0.00542

TABLE 8.7.4b. Calibration curve for horizontal pipe (P = 40W, inverse Δt vs Q)

Flowrate (ml s^{-1})	Inverse of Transit Time Difference
1.204	7.889
2.656	16.024
5.202	23.058
8.308	31.568
11.090	44.224
15.887	101.636
20.146	184.480

TABLE 8.7.5a. Calibration curve for horizontal pipe (P = 100W, Δt vs Q)

Flowrate (ml s^{-1})	Transit Time Difference (μs)
9.930	0.0770
14.546	0.0575
21.008	0.0353
26.077	0.0214
30.985	0.0144
36.133	0.0101

TABLE 8.7.5b. Calibration curve for horizontal pipe

(P = 100W, inverse Δt vs Q)

Flowrate (ml s^{-1})	Inverse of Transit Time Difference
9.930	12.975
14.546	17.378
21.008	28.248
26.077	46.635
30.985	69.295
36.133	98.188

TABLE 8.7.6a. Transit time measured at different heater power

(horizontal pipe, Δt vs Q)

	Flowrate ($ml\ s^{-1}$)	Transit Time Difference (μs)
Expt. 1	9.930	0.0770
	14.546	0.0575
	21.008	0.0353
	26.077	0.0214
	30.985	0.0144
	36.133	0.0101
	40.873	0.00792
Expt. 2	9.664	0.129
	19.784	0.0821
	29.100	0.0571
	39.421	0.0209
	50.406	0.0135
	58.731	0.0100
	70.908	0.00952
	78.584	0.0114
Expt.3	8.665	0.123
	14.611	0.0938
	25.257	0.0613
	36.114	0.0313
	44.934	0.0144

TABLE 8.7.6b. Transit time measured at different heater power

(horizontal pipe, inverse Δt vs Q)

	Flowrate (ml s^{-1})	Inverse of Transit Time Difference
Expt. 1	9.930	12.975
	14.546	17.378
	21.008	28.248
	26.077	46.635
	30.985	69.295
	36.133	98.188
	40.873	126.109
Expt. 2	9.664	7.697
	19.784	12.168
	29.100	17.492
	39.421	47.826
	50.406	74.050
	58.731	99.336
	70.908	104.959
	78.584	87.242
Expt. 3	8.665	8.073
	14.611	10.652
	25.257	16.296
	36.114	31.937
	44.934	69.350

TABLE 8.7.7a. Repeatability of the flowmeter (Δt vs Q)

	Flowrate ($ml\ s^{-1}$)	Transit Time Difference (μs)
Expt. 1	9.664	0.129
	19.784	0.0821
	29.100	0.0571
	39.421	0.0209
	50.406	0.0135
	58.731	0.0100
	70.908	0.00952
	78.584	0.0114
Expt. 2	10.781	0.119
	21.118	0.0784
	28.350	0.0530
	38.485	0.0225
	48.861	0.0127
	58.979	0.00802
	69.313	0.0104
	79.854	0.0119
Expt. 3	8.665	0.123
	14.611	0.0938
	25.257	0.0613
	36.114	0.0313
	44.934	0.0144

TABLE 8.7.7b. Repeatability of the flowmeter (inverse Δt vs Q)

	Flowrate (ml s^{-1})	Inverse of Transit Time Difference
Expt. 1	9.664	7.697
	19.784	12.168
	29.100	17.492
	39.421	47.826
	50.406	74.050
	58.731	99.336
	70.908	104.959
	78.584	87.242
Expt. 2	10.781	8.349
	21.118	12.749
	28.350	18.862
	38.485	44.297
	48.861	78.498
	58.979	124.592
	69.313	95.958
	79.854	84.003
Expt. 3	8.665	8.073
	14.611	10.652
	25.257	16.296
	36.114	31.937
	44.934	69.350

TABLE 8.7.8. Scaling with respect to heater power for horizontal pipe

Flowrate	Heater Input Power				
	70W	60W	50W	40W	30W
20.79 ml s^{-1}	0.0191	0.0150	0.0117	0.00970	0.00668
16.21 ml s^{-1}	0.0317	0.0244	0.0186	0.0134	0.00892
12.12 ml s^{-1}	0.0460	0.0382	0.0309	0.0224	0.0137
9.24 ml s^{-1}	0.0509	0.0445	0.0380	0.0309	0.0211

Table 9.2.1a. Comparison of experimental data with computed values (inverse Δt vs Q)

Flowrate (ml s^{-1})	Inverse of Transit Time Difference
Computation	
1.003	7.055
1.193	8.508
2.211	15.864
2.837	19.872
3.709	24.959
4.825	30.920
4.848	31.038
8.288	47.076
13.298	66.892
15.619	75.172
17.635	82.023
Experiment 1	
1.204	7.889
2.083	17.510
4.289	26.666
7.314	42.589
10.540	50.945
14.238	80.615
18.764	114.248
Experiment 2	
1.193	8.560
2.837	22.832
4.825	32.954
8.288	47.982
13.298	67.103
17.635	80.610

Table 9.2.1b. Percentage difference between experimental data and computed values (percentage difference vs Q)

Flowrate	Inverse Transit Time Difference		Difference	
ml s^{-1}	Computation	Experiment	%	Full Scale %
1.193	8.508	8.560	0.61	0.065
2.837	19.872	22.832	12.96	3.67
4.825	30.920	32.954	6.17	2.52
8.288	47.076	47.982	1.88	1.12
13.298	66.892	67.103	0.31	0.26
17.635	82.023	80.610	-1.75	-1.75

Table 9.3.1a. Experiment results for vertical pipe (Δt vs Q)

Flowrate ($ml\ s^{-1}$)	Transit Time Difference (μs)
Experiment 1	
1.204	0.126
2.083	0.0571
4.289	0.0374
7.314	0.0234
10.540	0.0196
14.238	0.0124
18.764	0.00875
Experiment 2	
1.193	0.116
2.837	0.0437
4.825	0.0303
8.288	0.0208
13.298	0.0149
17.635	0.0124

Table 9.3.1b. Experiment results for vertical pipe (inverse Δt vs Q)

Flowrate ($ml\ s^{-1}$)	Inverse of Transit Time Difference
1.193	8.560
2.837	22.832
4.825	32.954
8.288	47.982
13.298	67.103
17.635	80.610

Table 9.3.2. Vertical pipe experimental results

Flowrate ($ml\ s^{-1}$)	Inverse of Transit Time Difference
10.018	24.694
15.603	36.368
19.572	44.297
24.973	53.776
31.231	70.524
37.818	92.435

Table 9.3.3a. Experiment results for horizontal and vertical pipe (Δt vs Q)

	Flowrate ($ml\ s^{-1}$)	Transit Time Difference (μs)
Vertical	1.193	0.116
	2.837	0.0437
	4.825	0.0303
	8.288	0.0208
	13.298	0.0149
	17.635	0.0124
Horizontal	1.204	0.126
	2.656	0.0624
	5.202	0.0433
	8.308	0.0316
	11.090	0.0226
	15.887	0.00983
	20.146	0.00542

Table 9.3.3b. Experiment results for horizontal and vertical pipe (inverse Δt vs Q)

	Flowrate ($ml\ s^{-1}$)	Inverse of Transit Time Difference
Vertical	1.193	8.560
	2.837	22.832
	4.825	32.954
	8.288	47.982
	13.298	67.103
	17.635	80.610
Horizontal	1.204	7.889
	2.656	16.024
	5.202	23.058
	8.308	31.568
	11.090	44.224
	15.887	101.636
	20.146	184.480

Table 9.3.4. Horizontal and vertical pipe experimental results

Flowrate (ml s^{-1})	Inverse of Transit Time Difference
Vertical	
10.018	24.694
15.603	36.368
19.572	44.297
24.973	53.776
31.231	70.524
37.818	92.435
Horizontal	
9.930	12.975
14.546	17.378
21.008	28.248
26.077	46.635
30.985	69.295
36.133	98.188
40.874	126.11

Table 9.4.1. Heater power scaling for vertical and horizontal pipes

Flowrate (ml s^{-1})	Inverse of Transit Time Difference
Vertical (40 W)	
1.193	8.560
2.837	22.832
4.825	32.954
8.288	47.982
13.298	67.103
17.635	80.610
Horizontal (40 W)	
1.204	7.889
2.656	16.024
5.202	23.058
8.308	31.568
11.090	44.224
15.887	101.636
20.146	184.480
Vertical (100 W Scaled to 40 W)	
10.018	9.878 (24.694/2.5)
15.603	14.547 (36.368/2.5)
19.572	17.719 (44.297/2.5)
24.973	21.510 (53.776/2.5)
31.231	28.210 (70.524/2.5)
37.818	36.974 (92.435/2.5)
Horizontal (100 W Scaled to 40 W)	
9.930	5.17 (12.975/2.5)
14.546	6.931 (17.378/2.5)
21.008	11.299 (28.248/2.5)
26.077	18.654 (46.635/2.5)
30.985	27.718 (69.295/2.5)
36.133	39.275 (98.188/2.5)
40.874	50.444 (126.11/2.5)

Table 9.4.2a. Heater power scaling for vertical pipe (40 W and 60 W)

	Flowrate (ml s^{-1})	Transit Time Difference (μs)	
P = 40 W			
	19.912	0.0124	
	16.726	0.0137	
	12.213	0.0225	
	9.080	0.0241	
P = 60 W			
	19.912	0.0175	
	16.726	0.0203	
	12.213	0.0338	
	9.080	0.0360	
60 W Scaled to 40 W			
	19.912	0.0117	(0.0175/1.5)
	16.726	0.0135	(0.0203/1.5)
	12.213	0.0225	(0.0338/1.5)
	9.080	0.024	(0.0360/1.5)

Table 9.4.2b. Scaling with respect to heater power for vertical pipe (70 W, 60 W and 40 W)

	Flowrate ($ml\ s^{-1}$)	Transit Time Difference (μs)
P = 40 W		
	19.912	0.0124
	16.726	0.0137
	12.213	0.0225
	9.080	0.0241
P = 60 W		
	19.912	0.0175
	16.726	0.0203
	12.213	0.0338
	9.080	0.0360
P = 70 W		
	19.912	0.0213
	16.726	0.0237
	12.213	0.0407
	9.080	0.0422
70 W Scaled to 40 W		
	19.912	0.0122 (0.0213/1.75)
	16.726	0.0135 (0.0237/1.75)
	12.213	0.0233 (0.0407/1.75)
	9.080	0.0241 (0.0422/1.75)
70 W Scaled to 60 W		
	19.912	0.0183 (0.0213/1.167)
	16.726	0.0203 (0.0237/1.167)
	12.213	0.0348 (0.0407/1.167)
	9.080	0.0362 (0.0422/1.167)

Table 9.4.3. Heater power scaling for horizontal pipe

	Flowrate ($ml\ s^{-1}$)	Transit Time Difference (μs)
P = 50 W		
	20.791	0.0117
	16.207	0.0186
	12.128	0.0309
P = 60 W		
	20.791	0.0150
	16.207	0.0244
	12.128	0.0382
P = 70 W		
	20.791	0.0191
	16.207	0.0317
	12.128	0.0460
70 W Scaled to 50 W		
	20.791	0.0136 (0.0191/1.4)
	16.207	0.0226 (0.0317/1.4)
	12.128	0.0329 (0.0460/1.4)
70 W Scaled to 60 W		
	20.791	0.0163 (0.0191/1.167)
	16.207	0.0272 (0.0317/1.167)
	12.128	0.0394 (0.0460/1.167)

REFERENCE

[Anon, 1983]
Anon, "Colloquium on non-invasive on-line measurement in industry", IEE Colloq Dig n 1983/36, Colloq on non-invasive on-line meas in ind, Manchester, England, Apr 13 1983

[Anon, 1985]
Anon, "Measurement of liquid flow in closed circuits using transit-time ultrasonic flowmeters", ANSI STAND MFC-5M, July 15 1985

[Anon, 1986]
Anon, "Evaluation of non-intrusive flow meters", Res Rep Can Electr Assoc 216-G-400, Mar 1986

[Antonov, Klimachev, Reshatnikov and Safin, 1980]
Antonov, N.N.; Klimachev, A.F.; Reshatnikov, V.A. & Safin, A.E., "Recalculation of characteristics for ultrasonic flowmeter", MEASUREMENT TECHNIQUE (U.S.A.), vol. 22, no.10, 1214-1215, March, 1980

[Antonov, Borisevich, Dmitriev, Reshatnikov and Safin, 1980]
Antonov, N,N.; Borisevich, E.A.; Dmitriev, E.V.; Reshatnikov, V.A. & Safin, A.E., "Multichannel ultrasonic flowmeter", MEASUREMENT TECHNIQUE (U.S.A.), vol. 22, no.10, 1221-1223, March, 1980

[Aprilesi, Dondi, Taroni and Giannelli, 1984]
Aprilesi, G. C.; Dondi, M.; Taroni A. and Giannelli, L., "Ultrasonic instrumentation; a microprocessor-based US flowmeter", IEEE 1984 Ultrasonics Symposium Proceedings, Vol. 1, 484-487, Dallas, TX, USA, 14-16 Nov., 1984

[Audunson and McClimans, 1975]
Audunson, T. and McClimans, T. A., "Some observations of velocity fluctuations in a strongly stratified estuary using an ultrasonic transit-time difference current meter", Proceeding of the International Seminar and Exposition on Water Resources Instrumentation, Vol. 1, 90-108, Chicago, IL, USA, 4-6 June 1975

[Aung, Fletcher and Sernas, 1972]

Aung, W.; Fletcher, L. S. and Sernas, V., "Developing laminar free convection between vertical flat plate with asymmetric heating", INT. J.H.M.T., vol. 15, 2293-2308, 1972

[Baily, 1990]

Baily, M., "Mid Southern Water Co. Camberley metering trail", Mid Southern Water Co. Camberley

[Baird, 1983]

Baird, J.D., "Application of ultrasonic flowmeters to hazardous wastewater", Haz Mat 83, Proc. First annual Hazardous Materials management Conf., Philadelphia, USA, July 12-14, 1983

[Baird, 1983]

Baird, J.D., "Noninvasive ultrasonic phase-shift flowmeter", ADVANCES IN INSTRUMENTATION, vol. 38, no.1, 1983, p.13-21

[Baker, 1989]

Baker, R. C., "An Introductory Guide to Flow Measurement", Mechanical Engineering Publications Limited, London.

[Baker and Thompson, 1975]

Baker, R.C. & Thompson, "A two beam ultrasonic phase-shift flowmeter", Conf. on fluid flow measurement in the mid 70's, April 1975, NEL Scotland

[Banard, Mollot, Beslot and Malmasson, 1985]

Banard, D.; Mollot, C.; Beslot, M. and Malmasson, J., "Water flow measurement using ultrasonic signal cross correlation applications to hydraulic circuits of nuclear reactors", PROGRESS IN NUCLEAR ENERGY, V. 15, 745-751, 1985

[Barakat and Clark, 1966]

Barakat, H. Z. and Clark, J. A., "On the solution of the diffusion equation by numerical methods", J. OF HEAT TRANSFER, TRANS. A.S.M.E., SERIES C, 88, 421-427, 1966

[Bates, 1990]

Bates, D., "Southern Water Chandlers Ford metering trail", Southern Water Chandlers Ford

[Bau and Kelley, 1985]

Bau, H.H. & Kelley, J.P., "Ultrasonic flow rate measurement of low speed non-isothermal flows", INT. COMMUN. HEAT & MASS. TRANSFER, vol., no. 4, July-August, 1985, p. 381-392

[Baumoel, 1983]

Baumoel, J., U.S. Patent no. 4,373,401, February 1983

[Bazerghi and Serdula, 1977]

Bazerghi, H. and Serdula, K. J., "Evaluation of the performance of an ultrasonic cross-correlation flowmeter", Canadian Nuclear Association Conference, Montreal, Quebec, Canada, 5 June 1977

[Bazerghi and Serdula, 1977]

Bazerghi, H. and Serdula, K. J., "Estimation and reduction of errors in flow measurements which use cross-correlation techniques", Progress in Nuclear Energy, New Series, Vol. 1, no. 2-4, 629-648, 1977

[Beck, 1987]

Beck, M.S., "Cross-correlation flowmeters", BULL. NAT. RES. DEV. CORP., no. 52, 26-28, 30 and 31, Summer 1980,

[Beck, Green and Thorn, 1987]

Beck, M.S.; Green, R.G. & Thorn, R., "Non-intrusive measurement of solids mass flow in pneumatic conveying", J. PHYS. E. v 20, no. 7, July 1987 p 835-840

[Benard, 1988]

Benard, C.J., "Ultrasonic flowmeters handbook of fluid flowmetering", Morden, U.K., Trade & Tech. Press Ltd. Section 2, P.73-89

[Birkhoff and Varga, 1959]

Birkhoff, G and Varga, R.S., "Implicit alternating direction methods", TRANS.

AMER. MATH. SOC., 92, 13-24, 1959

[Bobrovnikov and Novozhilov, 1979]

Bobrovnikov, G.N & Novozhilov, B.M., "Calibration characteristics of a contactless thermal flowmeter", TEKHNIKA, No. 10, p34-35, Oct., 1979

[Bobrovnikov and Novozhilov, 1989]

Bobrovnikov, G.N & Novozhilov, B.M., "Calibration characteristics of a contaction flowmeter", MEASUREMENT TECHNIQUE (U.S.A.), vol. 22, no. 10, March, 1980, p. 1207-1208

[Bradman,1992]

Bradman, R., "Management of innovation & R & D", Management Short Course Lecture Notes, School of Management, Cranfield University, 8 Jan. 1992

[Bradman,1992]

Bradman, R., "An innovation case study: general transport plc", Management Short Course Lecture Notes, School of Management, Cranfield University, 8 Jan. 1992

[Bruner, 1977]

Bruner, R.F., "Theoretical and experimental assessment of uncertainties in non-intrusive, ultrasonic flow measurement", Proc. Symp. on flow measurement in open channels and closed conduits, Gaithersburg, USA, Feb. 23-25, 1977

[Byrne, Coulthard and Yong Yan, 1990]

Byrne, B.; Coulthard, J. & Yong Yan, "Cross-correlation flow measurements of liquid-solid mixture", TRANSDUCER TECHNOL., vol. 13, no. 10, p.4-5

[Cebeci and Bradshaw, 1984]

Cebeci, T and Bradshaw, P. "Physical and computational aspects of convection heat transfer", 187-188, Springer, New York, 1984

[Chappell, 1978]

Chappell, G.A., "Ultrasonics and flow - a different approach", INSTRUM PULP PAP IND, vol. 17, Proc of the ISA Pac Northwest Instrum' 78 Symp, Portland,

Oreg, apr 25 - 27 1978, p. 103-104

[Cheesewright, 1968]
Cheeseright, R., "Turbulent convection from a vertical plate surface", J. HEAT TRANSFER 90, 1-8, 1968

[Christopher and McDonald, 1986]
Christopher, M., and McDonald, M., "Effective marketting management", Printed by Newnorth-Burt Ltd, Kempston, Beford

[Churchill, 1982]
Churchill, J.L.W., "Capacitance probes for liquid level measurement", in "Innovation in industrial level measurement", London Conf. Transcript (Oct. 1982), Oyez Sci & Tech. Serv. Ltd, 1982, 8-21

[Codassi, Mioque and etc., 1987]
Codassi, D.; Mioque, J.L. and etc., "High pressure universal volume flowmeter for cementing, stimulation, drilling and production", 1987 SPE Annual Tech. Conf. & Exhib. , II, Production operations & engineering Soc. Pet Engrs. Dallas, USA, Sept. 27-30, 1987

[Coulthard, 1973]
Coulthard, J. "Ultrasonic cross-correlation flowmeters", ULTRASONICS, Vol. 11, no. 2, 83-88, 1973

[Coulthard, 1975]
Coulthard, J. "The principle of ultrasonic cross-correlation flowmetering", MEASUREMENT AND CONTROL, Vol. 8, no. 2, 65-70, 1975

[Coulthard and Olszowski, 1974]
Coulthard, J. and Olszowski, S. T., "Ultrasonics in cross-correlation flow measurement", Inst. Elect. Engrs. Colloquium on Advances in Flow measurement, QUEST Accession Number: 77010127

[Coulthard and Bradley, 1977]
Coulthard, J. and Bradley, D., "Ultrasonic correlation flow metering applied to

single phase liquids and gases", Flow-Con'77, Procs. Symp. on the application of Flow Measuring Techniques, Brighton, U.K., April 26-28, 1977, INST. MEAS. & CONTROL, Gatton & Kent Section, 433-450, 1977

[Crank and Nicolson, 1947]

Crank, J. and Nicolson, P., "A practical method for numerical evaluation of solutions of partial differential equations of the heat conduction type", PROC. CAMB. PHIL. SOC., 43, 50-57, 1947

[Dalke and Welkowitz, 1960]

Dalke, H.E. and Welkowitz, W., "A new ultrasonic flowmeter for industry", ISA JOURNAL, Vol 7, No 10, 60-63

[Dallman, 1981]

Dallman, J. C., "Application of ultrasonics to the measurement of thin flowing liquid films", TRANSACTION OF THE AMERICAN NUCLEAR SOCIETY, Vol. 39, 1039-1041, Nov.-Dec., 1981

[Douglas, 1955]

Douglas, J. Jr., "On the numerical integration of $\partial^2 u/\partial x^2 + \partial^2/\partial y^2 = \partial u/\partial t$ by implicit methods", J. SOC. INDUST. APPL. MATH., 3, 42-65, 1955

[Douglas, 1956]

Douglas, J. Jr., "On the relation between stability and convergence in the numerical solution of linear parabolic and hyperbolic differential equations". J. SOC. INDUST. APPL. MATH., 41, 20-37, 1956

[Douglas, 1962]

Douglas, J., "Alternation direction methods for three space variables", NUMERISCHE MATHEMATIK, 4, 41-63, 1962

[Douglas and Gunn, 1964]

Douglas, J. and Gunn, J. E., "A general formulation of alternating direction methods, Part I, Parabolic and hyperbolic problems", NUMERISCHE MATHEMATIK, 6, 428-453, 1964

[Douglas and Rachford, 1956]

Douglas, J. Jr. and Rachford, H. H. Jr., "On the numerical solution of heat conduction problems in two and three space variables", TRANS. AMER. MATH. SOC., 82, 421-439, 1956

[Drenthem, Builtjes and Vermeulen, 1981]

Drenthem, J. G.; Builtjes, P. J. H. and Vermeulen, P. E. J., "The accuracy of the total discharge determined by acoustical velocity measurement", Proc. Second Symp. on Flow: Its Measurement and Control in Science and Industry, St. Louis, USA, March 23-26, 1981

[Drost, 1978]

Drost, C.J., "Vessel diameter-independent volume'flow measurements using ultrasound", Proc. San Diego Bio. Med. Symp. 17th, Feb. 1978, San Diego

[DuFort and Frankel, 1953]

DuFort, E. C. and Frankel, S. P., "Stability conditions in the numerical treatment of parabolic differential equations", MATH. TABLES AIDS COMPUT., 7, 135-152, 1953

[Dymling, Persson and Hertz, 1991]

Dymling, S.O., Persson, H.W. and Hertz, C.H., "Measurement of blood perfusion in tissue using doppler ultrasound", ULTRASOUND IN MED. & BIOL., Vol 17, No 5, 1991, 433-444

[Eckert and Diaguila, 1955]

Eckert, E. R. G. and Diaguila, A. J., "Experimental investigation of free-convection heat transfer in vertical tube at large Grashof numbers", NACA report 1211, 1955

[Eilon,Hall, King, 1966]

Eilon, S., Hall, R. I., King, J. R., " Exercises in industrial management", William Clowes and Sons, Limited, London and Beccles

[Erickson and Graber, 1983]

Erickson, G.P. & Graber, J.C., "Ultrasonic flowmeters" measurement and control October, 1983

[Erdogan, 1963]
Erdogan, F., "On the approximate solutions of heat-conduction problems", J. OF HEAT TRANSFER, August, 1963, 203-207

[FIDAP, 1991]
FIDAP, "Fluid dynamics international", Inc. 500 Davis St. Suit 600 Evanston, Illinois 60201 (USA)

[Fischbacher, 1962]
Fischbacher, R.E., "Ultrasonic flowmeter design", CONTROL, vol. 5, part 43, 1962

[Flemons, 1977]
Flemons, R.S., "A new non-intrusive flowmeter", Proc. Symp. on flow measurement in open channels and closed conduits, Gaithersburg, USA, Feb. 23-25, 1977

[Flowmeter, 1982]
Ultrasonic instrumentation, "Measure flow outside of pipe", CHEM. PROCESSING (Chicago) Vol. 45, Issue 11, 60, Oct. 1982

[Flowmeter, 1982/2]
Ultrasonic instrumentation, "An ultrasonic meter for mainly clean liquids", CONTROL INSTRUM. Dec. 1982, p. 33, 35

[Flowmeter, 1983]
Ultrasonic instrumentation, "Clamp-on flow measurement for liquids of all types", CONTROL INSTRUM. Vol. 15, Issue 1, 11, 1983

[Flowmeter, 1985]
Ultrasonic instrumentation, "Multi-path flowmeters give sound readings", CONTROL INSTRUM. Dec. 1985, p. 29, 31, 33

[Flowmeter, 1986]
Ultrasonic instrumentation, "Flow measurement critical in compound structures", WATER & WASTEWATER INT., Vol. 1, no. 3, 15-16, June 1986

[Flowmeter, 1986/2]

Ultrasonic instrumentation, "Portable clamp-on flowmeter", PROCESS BIOCHEM., Vol. 21, issue 1, page: Pro Bio Tech ix, 1986

[Flowswitches, 1984]

Instrumentation, "Flow switches", CONTROL INSTRUM. April 1984, 37, 39-40

[Forsythe and Wasow, 1960]

Forsythe, G. E. and Wasow, W. R., "Finite-difference methods for partial differential equations", Wiley, New York, 1960

[Fromm, 1964]

Fromm, J., "The time dependent flow of an incompressible viscous fluid", METHODS IN COMPUTATIONAL PHYSICS, Vol. 3, 345-382, Academic Press, New York, 1964

[Geankoplis, 1978]

Geankoplis, J. C., "Transport processes & unit operations", Boston; Allyn and bacon, 1978.

[Genthe and Yamamoto, 1974]

Genthe, W.K. and Yamamoto, K., "A new ultrasonic flowmeterr for flow in large conduits and open channels" in Flow - Its Measurement and Control in Science and Industry, ISA, Pittsburg, Pennsylvania, 947-955, 1974

[Gentry, Martin and Daly, 1966]

Gentry, R.A.; Martin, R.E. and Daly, B.J., "An eulerian differencing method for unsteady compressible flow problems", J. OF COMPUTATIONAL PHYSICS, 1, 1966, 87-118

[Gerrard, 1985]

Gerrard, D., "Multi-path flowmeters give sound readings", CONTROL & INSTRUMENTATION, Vol. 17, no. 12, 29-31, 1985

[Gleed, 1990]

Gleed, I., "Bristol Water Company Hotwells metering trails", Bristol Water Company, Hotwells, 1990

[Godber, 1990]

Godber, E., "Worcestershire Waterworks co. Bromsgrove metering trail" Worcestershire Waterworks co. Bromsgrove, 1990

[Godber, 1990]

Godber, E., "Lee Varlley Water Co. Brookmans Park metering trails" Lee Varlley Water Co. Brookmans Park

[Goodman, 1962]

Goodman, T.R., "Effect of arbitrary nonsteady wall temperature on incompressible heat transfer", J. OF HEAT TRANSFER, Nov. 1962, 347-351

[Goodyer, 1980]

Goodyer, E.N., "A microprocessor based gas flow meter", INST. MEAS. & CONTROL, section 2, 1980, p. 57-66

[GPAD, Version 1]

Graphic package, "GPAD", Version 1, I.S.I. Software

[Graham-Leigh, 1990]

Graham-Leigh, J., "Thames Water Haling Park metering trail", Thames Water Haling Park

[Gray, 1945]

Gray, J.W., US Patent 2,534,712, filed Nov. 30, 1945 - granted Dec. 19, 1950

[Green, Foo, and Mitchell, 1980]

Green, R.G.; Foo, S.H. & Mitchell, S., "Application of a PET microcomputer to the measurement of mass flow rate of pneurratially conveyed solids", INST. MEAS. & CONTROL, section 2, 1980, p.53-56,

[Grosso and Spurlock, 1957]

Del Grosso, V.A. & Spurlook, E.M., "The feasibility of using wholly external

ultrasonics to measure fluid flow within thick walled metal pipes", Naval Research Laboratory report no. 4967, November, 1957 (USA)

[Guilbert and Law, 1992]

Guilbert, A. & Law, M., "Low flow calibration of the controlotron uniflow model 990 clamp-on ultrsonic flowmeters", Dept. of Fluid Engineering & Intrumentaion, Cranfield University. Report, Jan., 1992

[Guilbert and Law and Sanderson, 1993]

Guilbert, A., Law, M., and Sanderson, M. L., "Developement of a novel clamp-on ultrasonic/thermal flowmeter", Proc. of FLOWMEKO Int. Conf., Seoul, Korea, 25-29, 1993. (Acepted in July 1992)

[Hampton, 1991]

Hampton, B., "SOCAM mechanical meter calibration", Dept. of Fluid Engineering & Intrumentaion, Cranfield University.

[Harrison, 1981]

Harrison, A., "A non-invasive flow monitor for metal pipelines", J. PHYS. -E, vol. 14, no. 11, Nov. 1981, p.1266-1269

[Hellums and Churchill, 1962]

Hellums, J. D. and Churchill, S. W., "Transient and steady state, free and natural convection, numerical solutions: Part 1, The isothermal, vertical plate", A.I.CH.E. Journal, 8, 690-692, 1962

[Hemp, 1982]

Hemp, J., "Theory of Transit Time Ultrasonic Flowmeters", J. OF SOUND & VIBRATION, Vol 84, No 1, 133-147, 1982

[Hemp, 1988]

Hemp, J., Fluid Engineering & Intrumentation Short Course Lecture Notes, Cranfield University 6-9 Dec. 1988

[Hemp, 1993]

Hemp, J., "A theory of thermal diffusion flowmeters", Proc. of FLOWMEKO Int. Conf., Seoul, Korea, 25-29, 1993.

[Hess, Swengel and Waldorf, 1950]
Hess, W.B.; Swengel, R.C. and Waldorf, S.K., Elect. Eng. 69:983, 1950

[Hoene, 1978]
Hoene, E., "Ultrasonic Flowmeter - Frequency Difference Method" in "Flow Measurement of Fluids", H.H. Dijstelbergen and E.A. Spencer eds., North-Holland Publishing Co. Amsterdam, 147-151, 1978

[Hojholt, 1986]
Hojholt, P., "Installation effects on single and dual beam ultrasonic flowmeters" in Proc. Int. Conf. on Flow Measurement in Mid 80's, NEL, East Kilbride, Glasgow, 11.1 1-17, 1986

[Homans, 1982]
Homans, K., "Through the liquid ultrasonics" in "Innovation in industrial level measurement", London Conf. Transcript (Oct. 1982), Oyez Sci & Tech. Serv. Ltd, 1982, 83-88

[Holmes, Carraway, Holmes and Moore, 1987]
Holmes, B. J.; Carraway, D. L.; Holmes, H. K. and Moore, T. C., "Crossflow vorticity sensor", patent application, QUEST Accession Number: 87N23587, 1987

[Hummel, Ohlmer and Chenneaux, 1991]
Hummel, R.; Ohlmer, E. & Chenneaux, F., "A flow velocity measurement system based on temperature noise correlation", International Conf. on flow measurement industry & Science. London, 14/5. May 1991

[Ikenaga, Matsumoto, Takahashi and etc., 1983]
Ikenaga, Y.; Matsumoto, H.; Takahashi, S.; Ozaki, Y.; Oda, M.; Tomoda, T. and Tanaka, M., "Development of an ultrasonic flowmeter for PWRs", TRANSACTIONS OF THE AMERICAN NUCLEAR SOCIETY, Vol. 45, 557-558, 1983

[Irons,1987]

Irons, B., Shrive, N.G., "Numerical methods in engineering and applied science", Chichester; E llis Horwood, 1987, (Ellis Horwood series in Mathematics and its applications)

[Jacobson, Korba, Lynnworth, etc., 1987]

Jacobson, S. A.; Korba, J. M. and Lynnworth, L. C.; etc., "Low-gravity sensing of liquid/vapour interface and transient liquid flow", IEEE Transactions on ultrasonics, Ferroelectric and Frequency Control, Vol. UFFC-34, no. 2, 212-224, 1987

[Kalmus, 1952]

Kalmus, H.P., US Patent 2,724,269, filed Dec. 30, 1952, accepted Nov. 22, 1955

[Kalinoski and Vignos, 1980]

Kalinoski, R.W. & Vignos, J.H., U.S. patent no. 4,195,517, April 1980

[Karras, Tornberg, and Harkonen, 1985]

Karras, Tornberg, and Harkonen, 1985, "The ultrasonic inferential mass flowmeter for solids carried by the pulp suspension", FLOMEKO'85, Int. Conf. on Flow Measurement, 177-179, Melbourne, Australia, 20-23 August, 1985

[Kaye and Laby, 1973]

Kaye, G. W. S., and Laby, T. H., "Table of physical and chemical constants", Longman group limited, 1973

[Kelley and Bau, 1985]

Kelley, J. P. and Bau, H. H., "Ultrasonic flow rate measurement of low speed non-isothermal flows", INT. COMMUN. HEAT MASS TRANSFER, Vol. 12, no. 4, 381-392, Jul-Aug 1985

[Keech and Coulthard, 1985]

Keech, R. P. and Coulthard, J., "Advances in cross-correlation flow measurement and its application", FLOMEKO'85, Int. Conf. on Flow Measurement, Paper H2, 195-202, Melbourne, Australia, 20-23 August, 1985

[Komiya, Higuchi and Ohtani, 1988]

Komiya, K.; Higuchi, F. and Ohtani, K., "Characteristics of a thermal gas flowmeter", REV. SCI. INSTRUM., 59(3), March 1988, 477-479

[Kou, 1984]

Kou, A.H., "A pulsed phase measurement ultrasonic flowmeter for medical gases", ANNUAL OF BIOMEDICAL ENGINEERING, Vol 12, 1984, 263-280

[Krigman, 1982]

Krigman, A., "Guide to selecting non-intrusive flowmeters for closed pipe measurements", INTECH, vol. 29, no, 12, Dec. 1982, p.29-35

[Krishan, 1982]

Krishan, B., "On conjugated heat transfer in fully developed flow", INT. J. HEAT MASS TRANSFER, Vol 25, No 2, 1982, 288-289

[Kritz, 1955]

Kritz, J., Insor. & Automation, 28:1012, 1955

[Kuchnir, Gonczy and Tague, 1985]

Kuchnir, M.; Gonczy, J.D. and Tague, J.L., "Measuring heat leak with a heatmeter", Proceeding of cryogenic engineering conference and international cryogenic materials conference, Boston, MA, USA, 12 Aug 1985

[Lauber, 1982]

Lauber, A., "The influence of flow distortion on the accuracy of non-intrusive flowmeters", 9th IMEKO World Congress 1982 on Technological & Methodological advances in Measurement, Berlin, Fed. Rep. Germany, May 24-28, 1982

[Lechner, 1981]

Lechner, H., "Vibration patterns of fully and partially electroded piezoceramic disks with one face acoustically coupled to water", LANDIS & GYR REVIEW, Vol. 28, no. 2, 19-20, 1981

[Leitner, 1980]

Leitner, J., "A microprocessor-based cross-correlation flowmeter", Application of

Microprocessors in Devices for Instrumentation & Automatic Control, Collected Papers of Symp., (London, U.K.:Nov. 18-20, 1980), London, U.K., Inst. Meas. & Control, 1980, Session 2, P. 67-76

[Lewis and Jones, 1982]
Lewis, H.; & Jones, B., "Ultrasonic measurement", Innovations in Industrial Level Measurement Conf., (London, U.K.: Oct. 1982), London, U.K., Oyez Sci. & Tech. Serv. Ltd., 1982, p.24-35

[Lilly, 1965]
Lilly, D.K., "On the computational stability of numerical solutions of time-dependent non-linear geophysical fluid dynamics problems", MONTHLY WEATHER REVIEW, Vol 93, No 1, 1965, 11-26

[Lynnworth, 1975]
Lynnworth, L., U.S. patent no. 3,906,791, September 1975

[Lynnworth, 1975]
Lynnworth, L., "Clamp-on ultrasonic flowmeters, limitation and remedies", INST. TECHNOLOGY, September 1975

[Lynnworth, 1979]
Lynnworth, L., "Ultrasonic flowmeters" in Physical Acoustics Vol 14, W. C. Mason and R. N. Thurston, eds., Academic Press, New York, 407-525

[Lynnworth, 1981]
Lynnworth, L., "Ultrasonic flowmeters. Part 1: eight types of ultrasonic flowmeters", TRANS. INST. MEAS. & CONTROL, Vol. 3, no. 4, Oct. - Dec., 217-223, 1981

[Lynnworth, 1982]
Lynnworth, L., "Generation and propagation of pulses in single path contrapropagating flowmeters", TRANS. INST. MC, vol. 4, no. 1, March, 1982

[Lynnworth, 1986]
Lynnworth, L., "Engineering aspects of ultrasonic process control - flow,

temperature and liquid level applications", Trans. ASME J. Vib. Acoust. Stress & Reliab. Des., Vol. 108, no. 1, 69-81, 1986

[Lynnworth, 1981]

Lynnworth, L. C., "Ultrasonic flowmeters", Trans Inst M C Vol 3, No 4, Oct-Dec 217-223, 1881

[Macleod and Law, 1992]

Macleods, D., Law, M., "Ultrasonic Timing Interface Electronics", Dept. of Fluid Engineering & Intrumentaion, Cranfield University.

[Markato and Pericleous, 1984]

Markato, N. C. and Pericleous, K. A., "Laminar and turbulent natural convection in an enclosed cavity", INT. J. HEAT MASS TRANSFER, 27, 755-772, 1984

[Massen, 1982]

Massen, R., "Some remarks of the selection of sensors for correlation velocity measurement systems", SENSORS AND ACTUATORS, 3 (1982/83) 221-231

[McCarthy, 1990]

McCarthy, T., "Rickmansworth Water Co. Chorleywood metering trail", Rickmansworth Water Co. Chorleywood

[Mcknight and Clare, 1990]

Mcknight, J. A. and Clare, A., "Using ultrasonics to measure process variables", MEASUREMENT & CONTROL, 23, 7, 208-210, Sept. 1990

[McShane, 1974]

McShane, J.L., "Ultrasonic Flowmeters in flow, Its measurement and control in science and industry", ISA, Pittsburg, Pennsylvania, 897-915, 1974

[Mills, 1990]

Mills, P., "Wessex Water Broadstone metering trail", Wessex Water Broadston

[Mills, 1990]

Mills, P., "Wessex Water Turlin Moor metering trail", Wessex Water Turlin Moor

[Miyamoto, Katoh, Kurima and Sasaki, 1986]

Miyamoto, M.; Katoh, Y.; Kurima J. and Sasaki, H., "Turbulent free convection heat transfer from vertical parallel plates", PROC. 8th INT. HEAT TRANSFER CONF. San Francisco, Vol. 4, 1593-1598, 1986

[Moncharmont and Montaron, 1987]

Moncharmont, J.A.; & Montaron, B., "Cementing, stimulation, drilling and production", 1987 SPE Annual Tech. Conf. & Exhib., II, Production operations & Engineering, Dallas, USA, Soc. Pet. Engs., 1987, Paper SPE 16650, p. 577-582

[Nelkon and Parker, 1977]

Nelkon, M., and Parker, P., "Advanced Level Physical", Heinemann Education Books, Fourth Edition 1977.

[Numoto, Hara, Sakai, Kadowaki, and Takeuchi, 1984]

Numoto, M.; Hara, M.; Sakai, T.; Kadowaki, C. & Takeuchi, K.: "Non-invasive CSF flowmeter", J. MED ENG TECHNOL, vol. 8, no. 5, Sep-Oct, 1984, p. 218-220

[O'Brien, Hyman and Kaplan, 1951]

O'Brien, G, Hyman, M. and Kaplan, S., "A study of the numerical solution of partial differential equations", J. MATH. PHYS., 29, 233-251, 1951

[Olcer, 1969]

Olcer, N.Y., "Unsteady temperature distribution in a sphere subjected to time-dependent surface heat flux and internal heat source", J. OF HEAT TRANSFER, Feb. 1969, 45-50

[Oosthuizen and Champlain, 1989]

Oosthuizen, P. and Champlain, A., "Mixed convective heat transfer in an inclined cavity with multiple heated elements on one wall", AIAA 89-1687, AIAA 24th thermophysics conference, Buffalo, New York, June 12-14 1989

[Oosthuizen and Paul, 1989]

Oosthuizen, P. and Paul, J.T., "Laminar forced convective heat transfer downstream of a rearward facing step", AIAA 90-1726, AIAA 5th Joint Thermophysics and heat Transfer Conference, Seattle, WA, June 18-20, 1990

[O'Malley, 1982]

O'Malley, M.: "An ultrasonic meter for mainly clean liquids", CONTROL & INSTRUM., vol. 14, no. 12, Dec. 1982, p. 33,35

[Patankar, 1980]

Patankar, S. V., "Numerical heat transfer and fluid flow", Chap. 4. Hemisphere/McGraw-Hill, New York, 1980

[Peaceman and Rachford, 1955]

Peaceman, D. W. and Rachford, Jr., H.H., "The numerical solution of parabolic and elliptic differential equations", J. SOC. INDUST. APPL. MATH., 3, 28-41, 1955

[Pedersen and Lynnworth, 1973]

Pedersen, N.E. & Lynnworth, L.: "Non-intrusive dynamic flowmeter", IEEE Ultras. Symp. Proc. November 1973

[Petermann, 1957]

Petermann, L., U.S. Patent no. 2574568. 1957

[Peters, 1984]

Peters, M.: "Elementary Chemical Engineering", McGraw-Hill, London, 1984, p 145-147

[Piarrat and Multon, 1991]

Piarrat, O. and Multon, F. "Multipath digital ultrasonic flowmeter for important water networks", L'EAU L'INDUSTRIA LES NUISANCES, 150, 62-63, 1991

[Redding, 1982]

Redding, R.J., "Moving towards non intrusive measurement", in "Innovation in industrial level measurement", London Conf. Transcript (Oct. 1982), Oyez Sci & Tech. Serv. Ltd, 1982, 3-6

[Ritchie, 1992]

Ritchie, G. J., "Project management: charateristics, advantages and phases", Management Short Course Lecture Notes, School of Management, Cranfield University, 8 Jan. 1992

[Ritchie, 1992]

Ritchie, G. J., "Project control overview", Management Short Course Lecture Notes, School of Management, Cranfield University, 8 Jan. 1992

[Rotem, 1967]

Rotem, Z., "The effect of thermal conduction of the wall upon convection from a surface in a laminar boundary layer", INT. J. HEAT MASS TRANSFER, Vol 10, 1967, 461-466

[Rutten, 1928]

Rutten, O., German Patent no. 520484, September, 1928. March 23, 1931

[Sadhal, 1981]

Sadhal, S.S., "Unsteady heat flow between solids with partially contacting interface", TRANSACTION OF THE ASME: J. OF HEAT TRANSFER, Vol 103, 1981, 32-35

[Sanderson, 1984]

Sanderson, M.L., "Other flow measuring devices", Chap. 3 in, Measurement and Instrumentation for Control", Mylroi, M.G.; Calvert, G. (eds.) London, U.K., Peter Peregrinus Ltd., 1984, p. 38-60

[Sanderson, 1990]

Sanderson, M. L., Fluid Engineering & Intrumentation Short Course Lecture Notes, Cranfield 22-25 Jan. 1990

[Sanderson, and Hemp, 1981]

Sanderson, M.L. & Hemp, J., "Ultrasonic flowmeters - A review of the state of the art", Int. Conf. on Advances in Flow Measurement Techniques, BHRA publishers, September 1981

[Sanderson and Torley, 1985]

Sanderson, M.L. and Torley, B., "A self calibrating clamp-on transit time ultrasonic flowmeter", FLOMEKO'85, Int. Conf. on Flow Measurement, University of Melbourne, Australia, 20-23 August 1985

[Schmidt, 1981]

Schmidt, T.R., "What you should know about clamp-on ultrasonic flowmeters", INTECH, May 1981, 59-62

[Schwab, Greiner and Winter, 1990]

Schwab, A.; Greiner, M. and Winter, E.R.F., "Highly accurate pipe flow enthalpy difference meter", EXPERIMENTAL HEAT TRANSFER, Vol 3, 1990, 1-7

[Seclacek and Asenbaum, 1977]

Seclacek, M. and Asenbaum, A., "Simultaneous measurement of sound velocity and sound attenuation in liquids by a correlation method", J. ACOUST. SOC. AM., Vol 62, No 6, Dec. 1977, 1420-1423

[Sellers, Tribus and Klein, 1956]

Sellers, J.R.; Tribus, M. and Klein, J.S., "Heat transfer to laminar flow - problem extended", TRANSACTIONS OF THE ASME, Feb. 1956, 441-448

[Sheen and Raptis, 1983]

Sheen, S. H. and Raptis, A. C., "Active acoustic cross-correlation technique applied to flow velocity measurement in coal/liquid slurry", 1983 Ultrasonics Symposium Proceedings, Vol. 1, 591-594, Atlanta, GA, USA, 31 Oct. - 2 Nov., 1983

[Sheen, Raptis, Bobis, lee and Simpson, 1985]

Sheen, S. H.; Raptis, A. C.; Bobis, J. P.; Lee, S. and Simpson, T., "Evaluation of active ultrasonic cross-correlation technique in coal/liquid pipe flow measurements", QUEST Accession Number: 86018159

[Sheen, Karvelas and Raptis, 1987]

Sheen, S. H.; Karvelas, D. E. and Raptis, A. C., "Nonintrusive ultrasonic flow measurement techniques and their applications to Btu metering", International

District Heating and Cooling Association conference, Baltimore, MD, USA, 21 June 1987

[Sheen, Bobis, Raptis and Turgeon, 1987]

Sheen, S. H.; Bobis, J. P.; Raptis, A. C. and Turgeon, M., "Development, evaluation and testing of an active ultrasonic cross-correlation coal-slurry flowmeter", INSTRUMENTATION IN THE AEROSPACE INDUSTRY, V. 33, 359-382, 1987

[Shelaputin, 1983]

Shelaputin, I.D., "Method of analysis and optimization of acoustic ultrasonic level gauge and flowmeter systems", IZMERITEL 'NAYA TEKHNIKA, No. 11, Nov. 1983, 34-36

[Siegel and Sparrow, 1959]

Siegel, R. and Sparrow, E.M., "Transient heat transfer for laminar forced convection in the thermal entrance region of flat ducts", TRANSACTIONS OF THE ASME: J. OF HEAT TRANSFER, Feb. 1959, 29-36

[Siegel 1960]

Siegel, R., "heat transfer for laminar flow in ducts with arbitrary time variations in wall temperature", TRANSACTIONS OF THE ASME: J. OF APPLIED MECHANICS, June 1960, 241-249

[Siegel and Perlmutter 1963]

Siegel, R., "Laminar heat transfer in a channel with unsteady flow and wall heating varying with position and time", TRANSACTIONS OF THE ASME: J. OF HEAT TRANSFER, Nov. 1963, 359-365

[Sparrow and Azevedo, 1985]

Sparrow, E. M. and Azevedo, L. F. A., "Vertical-channel natural convection spanning between the fully-developed limit and the single-plate boundary-layer limit", INT. J. HEAT MASS TRANSFER, 28, 1847-1857, 1985

[Spendal, 1987]

Spendal, K., "Non-invasive ultrasonic flowmeters", Dept. of Fluid Engineering & Intrumentation, Cranfield University 1987

[Sproule, 1949]
Donald Orr Sproule, British Patent 623,022 applied June 3, 1946; accepted May 11, 1949

[Stockton, 1990]
Stockton, J., "Northumbrian Water Hutton Rudby metering trail", Northumbrian Water Hutton Rudby

[Stull, 1955]
Stull, K.S., Jr., Electronics, 28:128, 1955

[Sweetland, 1989]
Sweetland, D., "Calibration of Turbine flowmeter", Dept. of Fluid Engineering & Intrumentaion, Cranfield University.

[Swengel, Hess and Waldorf, 1954]
Swengel, R.C., Hess, W.B. and Waldorf, S.K, Elec. Eng. 73:1082, 1954

[Szebeszczyk and Pietraszek, 1991]
Szebeszczyk, J. and Pietraszek, S., "Clamp-on ultrasonic flowmeter for homogeneous liquids", MSR (MESSEN STEUERN TEGILN), Vol. 34, no. 5, 208-211, May 1991

[Tahkola and Karras, 1984]
Tahkola, E. and Karras, M., "The flowmeter for water using the phase modulation of ultrasonic beams analyzed by cross-correlation", IEEE 1984 ultrasonics Symposium Proceedings, V. 1, 488-492, Dallas, TX, USA, 14-16 Nov., 1984

[Tanguy, Philippe, 1982]
Tanguy, Philippe: "Toward a non-traumatic determination of the rheological properties of the vascular wall", J. BIOMECH. vol 15, no. 9, 1982, p. 661-667

[To and Humphrey, 1986]
To, W. M. and Humphrey, A. C., "Numerical simulation of buoyant, turbulent flow-I. Free convection along a heated, vertical, flat plate, INT. J. HEAT MASS

TRANSFER, 29, 573-592, 1986

[Van Oudheusden, 1989]

Van Oudheusden, B.W., "The behaviour of a thermal-gradient sensor in laminar and turbulent shear flow", J. PHYS. E: SCI. INSTRUM. 22 (1989) 490-498

[Van Oudheusden, Bruijn and etc, 1989]

Van Oudheusden, B.W.; De Bruijn, J.M. and etc., "Integrated sensor for non-invasive monitoring of flow in pipes", SENSORS AND ACTUATORS, 18 (1989) 259-267

[Van Oudheusden and Bruijn, and et al., 1989]

Oudheusden and Bruijn, and et al., "Direct-sensitive thermal IC flow sensors", SENSORS AND ACTUATORS, 18, (1989), 259-267.

[Trivedi, 1977]

Trivedi, A.S.: "A non-contacting ultrasonic cross correlation flowmeter for liquids", Bradford, U.K., Bradford Univ., Dec. 1977, 400p. (Thesis).

[Waller, 1982]

Waller, J.: "Doppler flowmeters: common questions about uncommon instruments", InTech. Vol. 29, no. 12, 43-45, 1982

[Waller, 1984]

Waller, J.: "Doppler flowmeters - proper practices", Instrumentation in the Aerospace Industry, vol. 30, Advances in Test Measurement, vol. 21, 30th Int. Instrumentation Symp., (Denver, U.S.A.: May 7 - 10, 1984), Research Triangle Park, U.S.A., Instrum. Soc. Am., 1984, p. 209-217

[Ward, 1992]

Ward, G. G. F., "Work BreakDown structures", School of Management, Cranfield University, 8 Jan. 1992

[Watson, 1978]

Watson, C. A., "Ultrasonic Flowmeters" in "Flow Measurement of Fluids", H.H. Dijstelbergen and E.A. Spencer eds., North-Holland Publishing Co. Amsterdam,

571-577, 1978

[Westinghouse, 1976]

Westinghouse: U.S. Patent no. 3,940,985, March 1976

[Whatley and Morton, 1990]

Whatley, P., and Morton, G., "Metering trail second interim report: data relaing to the Isle of Wight metering trail", Isle of Wight, Southern Water, 1990

[Yan and Lin, 1989]

Yan, W. M. and Lin, T. F., "Buoyancy effects on low Reynolds number turbulent forced convection in vertical plate channels with symmetric or asymmetric wall temperature", J. CHIN. SOC. MECH. ENGRS, 8, 321-330, 1987

[Yan and Lin, 1989]

Yan, W. M. and Lin, T. F., "Heat transfer in buoyancy-driven flows with the simultaneous presence of laminar, transitional and turbulent flow regimes", WARME- UND STOFFUBERTR, 24, 125-132, 1989

[Yan and Lin, 1991]

Yan, W. M. and Lin, T. F., "Theoretical and experimental study of nature convection pipe flows at high Rayleigh numbers", INT. J. HEAT MASS TRANSFER, Vol 34, 291-303, 1991.

[Yada, 1981]

Yada, H., et al, "A clamp-on ultrasonic flowmeter for high temperature fluids in small conduits" in "Flow - Its Measurements and Control in Science and Industry", Vol 2, ISA, 549-553, 1981

[Yuen and Wessel, 1981]

Yuen, W.W. and Wessel, R.A., "Application of the integral method to two-dimensional transient heat conduction problems", TRANSACTION OF THE ASME: J. OF HEAT TRANSFER, May 1981, Vol 103, 397-399

APPENDIX A. FINITE DIFFERENCE NUMERICAL APPROACH

A.1. Additional Equations (Central Line & Interface Between Two Media)

The two energy equations (3.2.14) & (3.2.15) obtained in Section 3.2 are valid only for the energy transfer in the fluid and pipe wall respectively. Equations governing heat transfer at the centre of the pipe and at the interface between the two media were needed in order to find the temperature profile of the whole region.

For case r = 0, i.e., at the centre of the pipe, equation (3.2.14) is indeterminate. A special treatment for this singular point was needed in order to obtain the temperature distribution on the centre line. The problem could be dealt with by finding an approximation to Equation (3.2.14) as follows:

By Taylor's expansion

$$\frac{\partial T}{\partial r} = \frac{\partial T}{\partial r}\Big|_{r=0} + \frac{r(0)}{1!}\frac{\partial^2 T}{\partial r^2}\Big|_{r=0} + \frac{r^2(0)}{2!}\frac{\partial^3 T}{\partial r^3}\Big|_{r=0} + \cdots \qquad \text{(A.1a)}$$

Due to symmetry, at the centre line $\frac{\partial T}{\partial r} = 0$, and if the third and higher derivatives are ignored then the limiting value of $(\frac{1}{r}\frac{\partial T}{\partial r})$ as r tends to zero is the value of $(\frac{\partial^2 T}{\partial r^2})$, hence the PDE governing heat transfer at the centre of the pipe is given by

$$\frac{\partial T}{\partial t} = \alpha_L(2\frac{\partial^2 T}{\partial r^2} + \frac{\partial^2 T}{\partial x^2}) - V_x\frac{\partial T}{\partial x} \qquad \text{(A.1b)}$$

The equations obtained so far were not suitable for deriving a solution for the points on the interface between the liquid and the pipe wall. An additional equation was therefore required.

The PDE for the interface was obtained by approximating T_{ij} by the points T_{i-1j} and T_{i+1j} (see Fig A.1.1), using Taylor's expansion and the assumption of continuity of heat flux between two medium.

$$-K_L\frac{\partial T}{\partial r} = -K_w\frac{\partial T}{\partial r} \qquad \text{(A.2)}$$

The mathematics involved to obtain the PDE for the interface is summarized as follows: let T_{ij} represent the temperature of the interface row (row = i, column = j {j = 1 to m}).

The Taylor expansion for T_{i-1j} w.r.t r (in the liquid) is

$$T_{i-1j} = T_{ij} - \Delta r\frac{\partial T}{\partial r} + \frac{(\Delta r)^2}{2}\frac{\partial^2 T}{\partial r^2} + \cdots$$

With the assumption Δr is small, the higher order terms of Δr can be ignored and approximating the derivatives by T_{i-1j}, T_{ij} and lower order derivatives, then

$$\frac{\partial^2 T}{\partial r^2} = \frac{2}{(\Delta r)^2}(T_{i-1j} - T_{ij} + \Delta r\frac{\partial T}{\partial r}) \qquad \text{(A.3)}$$

and

$$\frac{\partial T}{\partial r} = \frac{1}{\Delta r}(T_{ij} - T_{i-1j}) \qquad \text{(A.4)}$$

Substituting (A.3) and (A.4) into equation (3.2.14), gives

$$\frac{\partial T}{\partial t} = \frac{2\alpha_L}{(\Delta r)^2}\left[(T_{i-1j} - T_{ij}) + \Delta r\frac{\partial T}{\partial r}\right] +$$

$$\frac{\alpha_L}{i(\Delta r)^2}(T_{ij} - T_{i-1j}) + \alpha_L\frac{\partial^2 T}{\partial x^2} - V_x\frac{\partial T}{\partial x}$$

Multiplying through by K_L and rearranging the above expression

$$K_L\Delta r\frac{\partial T}{\partial r} = \frac{K_L(\Delta r)^2}{\partial\alpha_L}\frac{\partial T}{\partial t} - K_L(T_{i-1j} - T_{ij}) - \frac{K_L}{2i}(T_{ij} - T_{i-1j}) -$$

$$K_L\frac{(\Delta r)^2}{2}\frac{\partial^2 T}{\partial x^2} + K_L\frac{(\Delta r)^2}{2\alpha_L}V_x\frac{\partial T}{\partial x} \qquad \text{(A.5)}$$

Using the same procedure for T_{i+1j} (these are the points for the pipe wall region),

$$T_{i+1j} = T_{ij} + \Delta r\frac{\partial T}{\partial r} + \frac{(\Delta r)^2}{2}\frac{\partial^2 T}{\partial r^2} + \cdots$$

leads to

$$K_W \Delta r \frac{\partial T}{\partial r} = - K_W \frac{(\Delta r)^2}{2\alpha_W} \frac{\partial T}{\partial t} + K_W (T_{i+1j} - T_{ij}) +$$

$$\frac{K_W}{2i}(T_{i+1j} - T_{ij}) + K_W \frac{(\Delta r)^2}{2} \frac{\partial^2 T}{\partial x^2} \qquad (A.6)$$

Applying the continuity of heat flux specified by Expression (A.2), rearranging and collecting the terms T_{i-1j}, T_{ij} and T_{i+1j} in (A.5) and (A.6) leads at the pipe wall to

$$\frac{(\Delta r)^2}{2}\left(\frac{K_L}{\alpha_L} + \frac{K_W}{\alpha_W}\right)\frac{\partial T}{\partial t} =$$

$$K_L\left(1 - \frac{1}{2i}\right)T_{i-1j} - \left[K_L\left(1 - \frac{1}{2i}\right) + K_W\left(1 + \frac{1}{2i}\right)\right]T_{ij} +$$

$$K_W\left(1 + \frac{1}{2i}\right)T_{i+1j} + \frac{(\Delta r)^2}{2}(K_L + K_W)\frac{\partial^2 T}{\partial x^2} - \frac{(\Delta r)^2}{2\alpha_L} K_L V_x \frac{\partial T}{\partial x} \qquad (A.7a)$$

or

$$\frac{\partial T}{\partial t} = \frac{2}{(\Delta r)^2 (C)}\left[K_L\left(1 - \frac{1}{2i}\right)T_{i-1j} - \left[K_L\left(1 - \frac{1}{2i}\right) + K_W\left(1 + \frac{1}{2i}\right)\right]T_{ij} + K_W\left(1 + \frac{1}{2i}\right)T_{i+1j}\right] + \frac{(K_L + K_W)}{(C)}\frac{\partial^2 T}{\partial x^2} - \frac{K_L}{\alpha_L (C)} V_x \frac{\partial T}{\partial x} \qquad (A.7b)$$

where $$(C) = \frac{K_L}{\alpha_L} + \frac{K_W}{\alpha_W}$$

In next section, finite difference numerical technique for solving the coupled heat transfer in pipe flow will be discussed.

A.2. Finite Difference Approach

The temperature profile for the fluid and the pipe wall regions at any given time could be found by solving the coupled heat transfer differential Equations (A.1b), (3.2.14), (A.7b) and (3.2.15) numerically in conjunction with the boundary conditions specified in Fig 3.3.1. Which are

a. $T = T_{Ref}$ $x = 0,$ $0 \le r_i \le r$

(the up stream temperature condition)

b. $\frac{\partial T}{\partial r} = 0$ $0 \le x \le l_1,$ $r_i = r$

$\frac{\partial T}{\partial r} = 0$ $l_2 \le x \le l,$ $r_i = r$

(assuming no heat loss from pipe wall into air)

c. $\frac{\partial T}{\partial r} = \frac{Q}{A}$ $l_1 \le x \le l_2,$ $r_i = r$

(heat flux at the heated section of the pipe)

d. $\frac{\partial T}{\partial x} = 0$ $0 \leq x \leq l,$ $r_i = 0$

(the symmetry heat transfer condition at centre of the pipe)

e. $\frac{\partial T}{\partial r} = 0$ $x = l,$ $0 \leq r_i \leq r$

(assuming the steady state down stream temperature reached)

f. $T_{i,m+1} = T_{i,m} + \delta T_{i,m-1}$ $x = l,$ $0 \leq r_i \leq r$

(the fixed temperature gradient at down stream).

The numerical method chosen to solve these equations is the finite difference approximation IAD (Implicit Alternative Direction) method. Detail of the discretized equations are given in Appendix A.3. The solution procedure can be outlined as follows:

A. Compute velocity V_x $[V_x = 2V_m(1 - (\frac{r_i}{r})^2)]$.

B. For each time step solve:

a. Equation (3.2.15) for wall temperature

b. Equation (A.7b) for interface temperature between two media

c. Equation (3.2.14) for liquid temperature

d. Equation (A.1b) for central line temperature

e. output solution at time interval t.

In next section, a class of Numerical technique for solving the coupled heat transfer equation is discussed.

A.3. Finite Difference Procedures & the IAD Technique

Solutions of the problem defined by Equations (3.2.14) and (3.2.15) together with the equations for the central line of the pipe and equation governing heat transfer at the interface between the solid and the fluid were attempted numerically using a finite difference scheme.

The numerical technique chosen for solving the problem was the IAD method. In this class of technique, one has to divide the time step $(n + 1)\Delta t$ into sub time steps

$(n + \frac{1}{2})\Delta t$ and $(n + 1)\Delta t$ (or divide into 3 steps for 3-D problems). At each time

step, unknowns for either the r or x direction (or z direction) are determined. Although for each time step, simulation of 2 (or 3) sets of equations is required the matrix involved is always in tridiagonal form.

The numerical procedure is started by expressing the PDEs in finite difference form at time steps

$(n + \frac{1}{2})\Delta t$ and $(n + 1)\Delta t$ (n = 1 to k).

The discretized Equation (A.1b) for the centre of the pipe at the beginning of a half time step $(n + \frac{1}{2})\Delta t$ and the end of a half time step $(n + 1)\Delta t$ respectively are

$$\frac{T_{ij}^{*} - T_{ij}^{n}}{\frac{\Delta t}{2}} = 2\alpha_L\left(\frac{T_{i-1j}^{*} - 2T_{ij}^{*} + T_{i+1j}^{*}}{(\Delta r)^2}\right) + \alpha_L\left(\frac{T_{ij-1}^{n} - 2T_{ij}^{n} + T_{ij+1}^{n}}{(\Delta x)^2}\right) -$$

$$V(r)\left(\frac{T_{ij}^{n} - T_{ij-1}^{n}}{\Delta x}\right) \qquad \text{(A.8a)}$$

$$\frac{T_{ij}^{n+1} - T_{ij}^{*}}{\frac{\Delta t}{2}} = 2\alpha_L\left(\frac{T_{i-1j}^{*} - 2T_{ij}^{*} + T_{i+1j}^{*}}{(\Delta r)^2}\right) + \alpha_L\left(\frac{T_{ij-1}^{n+1} - 2T_{ij}^{n+1} + T_{ij+1}^{n+1}}{(\Delta x)^2}\right) -$$

$$V(r)\left(\frac{T_{ij}^{n+1} - T_{ij-1}^{n+1}}{\Delta x}\right) \qquad \text{(A.8b)}$$

Where T_{ij}^{*} denotes the temperature at time step $(n + \frac{1}{2})\Delta t$ and T_{ij}^{n+1} denotes the temperature at time step $(n + 1)\Delta t$. For the liquid region, discretizing Equation (3.2.14) by the same procedure, gives,

$$\frac{T_{ij}^{*} - T_{ij}^{n}}{\frac{\Delta t}{2}} = \alpha_L\left(\frac{T_{i-1j}^{*} - 2T_{ij}^{*} + T_{i+1j}^{*}}{(\Delta r)^2} + \frac{1}{i\Delta r}\frac{T_{i+1j}^{*} - T_{i+1j}^{*}}{2\Delta r}\right) +$$

$$\alpha_L\left(\frac{T_{ij-1}^{n} - 2T_{ij}^{n} + T_{ij+1}^{n}}{(\Delta x)^2}\right) - V_x\left(\frac{T_{ij} - T_{ij-1}}{\Delta x}\right) \qquad \text{(A.9a)}$$

$$\frac{T_{ij}^{n+1} - T_{ij}^{*}}{\frac{\Delta t}{2}} = \alpha_L\left(\frac{T_{i-1j}^{*} - 2T_{ij}^{*} + T_{i+1j}^{*}}{(\Delta r)^2} + \frac{1}{i\Delta r}\frac{T_{i+1j}^{*} - T_{i-1j}^{*}}{2\Delta r}\right) +$$

$$\alpha_L\left(\frac{T_{ij-1}^{n+1} - 2T_{ij}^{n+1} + T_{ij+1}^{n+1}}{(\Delta x)^2}\right) - V_x\left(\frac{T_{ij}^{n+1} - T_{ij-1}^{n+1}}{\Delta x}\right) \qquad \text{(A.9b)}$$

The finite difference equations for the interface between the liquid and the pipe wall are obtained by discretizing Equation (A.7b). The two equations are

$$\frac{T_{ij}^{*} - T_{ij}^{n}}{\frac{\Delta t}{2}} =$$

$$\frac{2}{(\Delta r)^2(C)}[K_L(1 - \frac{1}{2i})T_{i-1j}^{*} - [K_L(1 - \frac{1}{2i}) + K_W(1 + \frac{1}{2i})]T_{ij}^{*} + K_W(1 + \frac{1}{2i})T_{i+1j}^{*}] +$$

$$\frac{(K_L + K_W)}{(C)}(\frac{T_{ij-1}^{n} - 2T_{ij}^{n} + T_{ij+1}^{n}}{(\Delta x)^2}) - \frac{K_L V_X}{\alpha_L(C)}(\frac{T_{ij}^{n} - T_{ij-1}^{n}}{\Delta x}) \qquad \text{(A.10a)}$$

$$\frac{T_{ij}^{n+1} - T_{ij}^{*}}{\frac{\Delta t}{2}} =$$

$$\frac{2}{(\Delta r)^2(C)}[K_L(1 - \frac{1}{2i})T_{i-1j}^{*} - [K_L(1 - \frac{1}{2i}) + K_W(1 + \frac{1}{2i})]T_{ij}^{*} + K_W(1 + \frac{1}{2i})T_{i+1j}^{*}] +$$

$$\frac{(K_L + K_W)}{(C)}(\frac{T_{ij-1}^{n+1} - 2T_{ij}^{n+1} + T_{ij+1}^{n+1}}{(\Delta x)^2}) - \frac{K_L V_X}{\alpha_L(C)}(\frac{T_{ij}^{n+1} - T_{ij-1}^{n+1}}{\Delta x}) \qquad \text{(A.10b)}$$

where $$(C) = \frac{K_L}{\alpha_L} + \frac{K_W}{\alpha_W}$$

Finite difference forms for the equations governing heat transfer in the pipe wall are obtained by replacing the convective term in Equations (A.9a) and (A.9b) by zero (in solid region, velocity equals to zero). The two discretized equations are

$$\frac{T_{ij}^{*} - T_{ij}^{n}}{\frac{\Delta t}{2}} = \alpha_W\left(\frac{T_{i-1j}^{*} - 2T_{ij}^{*} + T_{i+1j}^{*}}{(\Delta r)^2} + \frac{1}{i\Delta r}\frac{T_{i+1j}^{*} - T_{i+1j}^{*}}{2\Delta r}\right) +$$

$$\alpha_W\left(\frac{T_{ij-1}^{n} - 2T_{ij}^{n} + T_{ij+1}^{n}}{(\Delta x)^2}\right) \qquad \text{(A.11a)}$$

$$\frac{T_{ij}^{n+1} - T_{ij}^{*}}{\frac{\Delta t}{2}} = \alpha_W\left(\frac{T_{i-1j}^{*} - 2T_{ij}^{*} + T_{i+1j}^{*}}{(\Delta r)^2} + \frac{1}{i\Delta r}\frac{T_{i+1j}^{*} - T_{i-1j}^{*}}{2\Delta r}\right) +$$

$$\alpha_W\left(\frac{T_{ij-1}^{n+1} - 2T_{ij}^{n+1} + T_{ij+1}^{n+1}}{(\Delta x)^2}\right) \qquad \text{(A.11b)}$$

After rearranging the terms in Equations (A.8a), (A.9a), (A.10a) and (A.11a), and applying the boundary conditions, the set of equations governing the heat transfer at the beginning of a half time step can be summarized as follows (refer to Fig A.1.1 for the mesh and index i,j):

$$(2 + 4\alpha_L\frac{\Delta t}{(\Delta r)^2})T_{ij}^{*} - 4\alpha_L\frac{\Delta t}{(\Delta r)^2}T_{i+1j}^{*} = d_{0j}$$

$$- \alpha_L\frac{\Delta t}{(\Delta r)^2}(1 - \frac{1}{2i})T_{i-1j}^{*} + (2 + 2\alpha_L\frac{\Delta t}{(\Delta r)^2})T_{ij}^{*} - \alpha_L\frac{\Delta t}{(\Delta r)^2}(1 + \frac{1}{2i})T_{i+1j}^{*}$$

$$= d_{ij}$$

$$- [\frac{2K_L}{(C)}\frac{\Delta t}{(\Delta r)^2}(1 - \frac{1}{2i})]T^*_{i-ij} + [2 + \frac{2}{(C)}\frac{\Delta t}{(\Delta r)^2}[K_L(1 - \frac{1}{2i}) + K_W(1 + \frac{1}{2i})]\ ]T^*_{ij} -$$

$$[\frac{2K_W}{(C)}\frac{\Delta t}{(\Delta r)^2}(1 + \frac{1}{2i})]T^*_{i+1j} \qquad = d_{ij}$$

$$[- \alpha_W\frac{\Delta t}{(\Delta r)^2}(1 - \frac{1}{2i})]T^*_{i-ij} + [2 + 2\alpha_W\frac{\Delta t}{(\Delta r)^2}]T^*_{ij} - [\alpha_W\frac{\Delta t}{(\Delta r)^2}(1 + \frac{1}{2i})]T^*_{i+1j}$$

$$= d_{ij}$$

$$[- \alpha_W\frac{\Delta t}{(\Delta r)^2}(1 - \frac{1}{2i}) - \alpha_W\frac{\Delta t}{(\Delta r)^2}(1 + \frac{1}{2i})]T^*_{i-1j} + \quad [2 + 2\alpha_W\frac{\Delta t}{(\Delta r)^2}]T^*_{ij}$$

$$= d_{ij} + \alpha_W\frac{\Delta t}{(\Delta r)^2}(1 + \frac{1}{2i})\frac{2\Delta rQ}{K_W A} \qquad \text{(A.12a)}$$

This can then be written in the matrix form

$$[A]\ \underline{T}^* = \underline{d}^n$$

where d_{ij} is computed according to following expressions

$$d_{ij} = [\alpha_L\frac{\Delta t}{(\Delta x)^2} + V_X\frac{\Delta t}{\Delta x}]T^n_{ij-1} + [2 - (2\alpha_L\frac{\Delta t}{(\Delta x)^2} + V_X\frac{\Delta t}{\Delta x})]T^n_{ij} + [\alpha_L\frac{\Delta t}{(\Delta x)^2}]T^n_{ij+1}$$

(I < interface row)

$$d_{ij} = [\frac{(K_L + K_W)}{(C)}\frac{\Delta t}{(\Delta x)^2} + \frac{K_L V_X}{\alpha_L (C)}\frac{\Delta t}{\Delta x}]T_{ij-1}^{n} +$$

$$[2 - (2\frac{K_L + K_W}{(C)}\frac{\Delta t}{(\Delta x)^2} + \frac{K_L V_X}{\alpha_L (C)}\frac{\Delta t}{\Delta x})]T_{ij}^{n} +$$

$$[\frac{(K_L + K_W)}{(C)}\frac{\Delta t}{(\Delta x)^2}]T_{ij+1}^{n}$$

(I = interface row)

$$d_{ij} = [\alpha_W \frac{\Delta t}{(\Delta x)^2}]T_{ij-1}^{n} + [2 - (2\alpha_W \frac{\Delta t}{(\Delta x)^2})]T_{ij}^{n} + [\alpha_W \frac{\Delta t}{(\Delta x)^2}]T_{ij+1}^{n}$$

(interface row < I < n)

$$d_{ij} = [\alpha_W \frac{\Delta t}{(\Delta x)^2}]T_{ij-1}^{n} + [2 - (2\alpha_W \frac{\Delta t}{(\Delta x)^2})]T_{ij}^{n} + [\alpha_W \frac{\Delta t}{(\Delta x)^2}]T_{ij+1}^{n} + \alpha_W \frac{\Delta t}{(\Delta x)^2}\frac{2\Delta r Q_i}{K_W A}$$

(I = n)

Refer to Fig 3.3.1 for the specified boundary conditions.

The temperature profile at beginning of a half time step $(n + \frac{1}{2})\Delta t$ is obtained by solving (A.12a) for each point, i = 0,1,2, ··· n in the jth column (j = 1,2, ··· m). i.e. by solving the system of equations

$$[A]\ \underline{T}^{*} = \underline{d}^{n}$$

for the unknown $\underline{T}^{*}$.

At the end of a half time step, Equations (A.8b), (A.9b), (A.10b) and (A.11b) are solved for each point for the jth column (j = 1, 2, 3, ··· m) in the ith row (i = 0, 1, 2, ··· n), using the same procedure as above to obtain the required system of equations below:

$$[2 + (2\alpha_L\frac{\Delta t}{(\Delta x)^2} + V_X\frac{\Delta t}{\Delta x})]T_{ij}^{n+1} - [\alpha_L\frac{\Delta t}{(\Delta x)^2}]T_{ij+1}^{n+1}$$

$$= d_{i0} + T_0$$

(for j = 0, i < Irow)

$$- [\alpha_L\frac{\Delta t}{(\Delta x)^2} + V_X\frac{\Delta t}{\Delta x}]T_{ij-1}^{n+1} + [2 + (2\alpha_L\frac{\Delta t}{(\Delta x)^2} + V_X\frac{\Delta t}{\Delta x})]T_{ij}^{n+1} - [\alpha_L\frac{\Delta t}{(\Delta x)^2}]T_{ij+1}^{n+1}$$

$$= d_{ij}$$

(i < Irow)

$$- [\frac{(K_L + K_W)}{(C)}\frac{\Delta t}{(\Delta x)^2} + \frac{K_L V_X}{\alpha_L(C)}\frac{\Delta t}{\Delta x}]T_{ij-1}^{n+1} +$$

$$[2 + (2\frac{K_L + K_W}{(C)}\frac{\Delta t}{(\Delta x)^2} + \frac{K_L V_X}{\alpha_L(C)}\frac{\Delta t}{\Delta x})]T_{ij}^{n+1} -$$

$$[\frac{(K_L + K_W)}{(C)}\frac{\Delta t}{(\Delta x)^2}]T_{ij+1}^{n+1} \qquad = d_{ij}$$

(i = Irow)

$$- [\alpha_W\frac{\Delta t}{(\Delta x)^2}]T_{ij-1}^{n+1} + [2 + (2\alpha_W\frac{\Delta t}{(\Delta x)^2})]T_{ij}^{n+1} - [\alpha_W\frac{\Delta t}{(\Delta x)^2}]T_{ij+1}^{n+1}$$

$$= d_{ij}$$

(j = m, i > Irow)

(A.12b)

where

$$d_{0j} = (2 + 4\alpha_L \frac{\Delta t}{(\Delta r)^2})T_{ij}^{*} + 4\alpha_L \frac{\Delta t}{(\Delta r)^2} T_{i+1j}^{*}$$

$$d_{ij} = + \alpha_L \frac{\Delta t}{(\Delta r)^2}(1 - \frac{1}{2i})T_{i-ij}^{*} + (2 - 2\alpha_L \frac{\Delta t}{(\Delta r)^2})T_{ij}^{*} + \alpha_L \frac{\Delta t}{(\Delta r)^2}(1 + \frac{1}{2i})T_{i+1j}^{*}$$

(i < Irow)

$$d_{ij} = [\frac{2K_L}{(C)} \frac{\Delta t}{(\Delta r)^2}(1 - \frac{1}{2i})]T_{i-ij}^{*} + [2 - \frac{2}{(C)} \frac{\Delta t}{(\Delta r)^2}[K_L(1 - \frac{1}{2i}) + K_W(1 + \frac{1}{2i})]]T_{ij}^{*} +$$

$$[\frac{2K_W}{(C)} \frac{\Delta t}{(\Delta r)^2}(1 + \frac{1}{2i})]T_{i+1j}^{*}$$

(i = Irow)

$$d_{ij} = \alpha_W \frac{\Delta t}{(\Delta r)^2}(1 - \frac{1}{2i})T_{i-ij}^{*} + (2 - 2\alpha_W \frac{\Delta t}{(\Delta r)^2})T_{ij}^{*} + \alpha_W \frac{\Delta t}{(\Delta r)^2}(1 + \frac{1}{2i})T_{i+1j}^{*}$$

(Irow < i =< n)

Refer to Fig 3.3.1 for specified boundary conditions. The temperature profile at the end of a half time step $(n + 1)\Delta t$ is obtained by solving Equation (A.12b) for each point

j = 1,2,3, ... m

in the ith row

$$i = 1, 2, 3, \ldots n$$

i.e. by solving the tridiagonal system of Equations

$$[B]\ \underline{T}^{n+1} = \underline{d}^{*}$$

A flow chart for solving this heat transfer model is given in Fig A.3.1 and Fig A.3.2.

A computer program (written in FORTRAN 77) has been developed for the numerical simulation.

A.4. FIDAP INTERFACE INPUT FILES

A.4.1. 2-D Symmetry Heat Transfer Simulation

```
 *TITLE
VERTICAL PIPE LAMINAR HEAT TRANSFER
*FIMESH(2-D,IMAX=11,JMAX=15)
/DEFINE INDEX I,J FOR THE MESH
EXPI
/1 2 3 4 5 6 7 8 9
1 0 31 0 51 0 71 0 91
EXPJ
/1 2 3 4 5 6 7 8 9 10 11 12 13 14 15
1 0 21 0 31 0 41 0 51 0 61 0 71 0 91
/
PARAMETER
/CONSTANTS
ICE 1
IFL 3
IWA 5
ITH 7
IWE 9
/Change for pipe of different diameters
CE 0
FL 6.75
WA 7.5
TH 8.1
WE 9.2
/
JFI 1
JW1 3
JE1 5
```

```
JHB 7
JHE 9
JE2 11
JW2 13
JFO 15
/Change for pipe of different length
FI 0
W1 20
E1 21
HB 23
HE 27
E2 29
W2 30
FO 50
/
KK 1
/HEAT FLUX
HS 1.0
/INPUT FLOW VELOCITY
VEL 1.511186
/INITIAL TEMPERATURE
T0 0.
/
/DEFINE POINTS FOR THE MESH
POINT
/ I   J  K  Z  R
/INFLOW
1 ICE JFI KK FI 0
2 IFL JFI KK FI FL
3 IWA JFI KK FI WA
41 ITH JFI KK FI TH
51 IWE JFI KK FI WE
/TRANSDUCER SHOES
```

```
15 ICE JW1 KK W1 0
16 IFL JW1 KK W1 FL
17 IWA JW1 KK W1 WA
43 ITH JW1 KK W1 TH
18 IWE JW1 KK W1 WE
/
20 ICE JE1 KK E1 0
21 IFL JE1 KK E1 FL
22 IWA JE1 KK E1 WA
45 ITH JE1 KK E1 TH
19 IWE JE1 KK E1 WE
/HEATER REGION.
4 ICE JHB KK HB 0
5 IFL JHB KK HB FL
6 IWA JHB KK HB WA
13 ITH JHB KK HB TH
37 IWE JHB KK HB WE
/
7 ICE JHE KK HE 0
8 IFL JHE KK HE FL
9 IWA JHE KK HE WA
14 ITH JHE KK HE TH
39 IWE JHE KK HE WE
/TRANSDUCER SHOES
23 ICE JE2 KK E2 0
24 IFL JE2 KK E2 FL
25 IWA JE2 KK E2 WA
47 ITH JE2 KK E2 TH
27 IWE JE2 KK E2 WE
/
35 ICE JW2 KK W2 0
33 IFL JW2 KK W2 FL
31 IWA JW2 KK W2 WA
```

```
49 ITH JW2 KK W2 TH
29 IWE JW2 KK W2 WE
/OUT FLOW
10 ICE JFO KK FO 0
11 IFL JFO KK FO FL
12 IWA JFO KK FO WA
50 ITH JFO KK FO TH
53 IWE JFO KK FO WE
/
/DEFINE LINES FOR THE MESH
LINE
/
/HORIZONTAL LINES
/CENTER OF THE PIPE
1 15
15 20
20 4
4 7
7 23
23 35
35 10
/INTER FACE BETWEEN THE LIQUID AND THE PIPE WALL
2 16
16 21
21 5
5 8
8 24
24 33
33 11
/PIPE WALL
3 17
17 22
22 6
```

6 9

9 25

25 31

31 12

/HEATER INSULATING LAYER

41 43

43 45

45 13

13 14

14 47

47 49

49 50

/TRANSDUCER SHOES

51 18

18 19

19 37

37 39

39 27

27 29

29 53

/VERTICAL LINES

/FLUID REGIONS.

1 2

15 16

20 21

4 5

7 8

23 24

35 33

10 11

/WALL

2 3

16 17

```
21 22
5 6
8 9
24 25
33 31
11 12
/HEATER INSULATING LAYER
3 41
17 43
22 45
6 13
9 14
25 47
31 49
12 50
/TRANSDUCER SHOES
41 51
43 18
45 19
13 37
14 39
47 27
49 29
50 53
/
/DELETE THE UNWANTED REGIONS.
DELETE
3 18 0
22 37 0
9 27 0
31 53 0
/DEFINE SURFACE
SURFACE
```

```
1 11
2 12
17 19
6 14
13 39
25 29
/
/DEFINE BOUNDARY CONDITIONS
BCNODE(UZC)
2 11 0.
BCNODE(URC)
1 2 0.
2 11 0.
1 10 0.
BCNODE(UZC,FREE)
1 10
10 11
BCNODE(URC,FREE)
10 11
BCNODE(UZC,PARABOLIC=1)
1 2 VEL
BCNODE(TEMPERATURE)
1 2 T0
2 3 T0
3 41 T0
41 51 T0
BCFLUX(HEAT,NODES=2)
13 14 HS
/
/
/DEFINE ELEMENT GROUPS FOR THE SOLVER
/FLUID ELEMENTS
ELEMENTS(QUADRILATERALS,NODES=4)
```

```
1 11
/SOLID ELEMENTS
ELEMENTS(QUADRILATERALS,NODES=4)
2 12
17 19
6 14
13 39
25 29
/RENUMBER
NUMBER
0
END
/
/FIPREP COMMANDS
*FIPREP
/STEADY STATE
PROBLEM(AXI-SYMMETRIC,NONLINEAR,STRONGLY)
/PROBLEM(AXI-SYMMETRIC,NONLINEAR)
/
/TRANSIENT STATE
/PROBLEM(AXI-SYMMETRIC,TRANSIENT,NONLINEAR)
/PROBLEM(AXI-SYMMETRIC,TRANSIENT,NONLINEAR,STRONGLY)
/
EXECUTION(NEWJOB)
/EXECUTION(RESTART)
SOLUTION(S.S.=100,VELC=.01,RESC=.01,ACCF=0.4)
/
PRESSURE(PENALTY)
/PRESSURE(MIXED,DISCONTINUOUS)
/
ICNODE(TEMPERATURE,CONSTANT=0)
ICNODE(VELOCITY,STOKES)
/RESTART JOB
```

```
/ICNODE(TEMPERATURE,READ)
/ICNODE(VELOCITY,READ)
/
/TIME STEP FOR TRANSIENT STATE PROCESSING

/TIME(NSTEPS=501,DT=.01,TRAPEZOIDAL,FIXED)
/POSTPROCESS(NBLOCKS=1)
/1 171 50
/
/PHYSICAL VALUES
/set1 :water,set2:COPPER
DENSITY (SET=1,CONSTANT=1)
DENSITY (SET=2,CONSTANT=8933.5)
/
SPECIFICHEAT (SET=1,CONSTANT=2615.820)

SPECIFICHEAT (SET=2,CONSTANT=379)
/
CONDUCTIVITY (SET=1,CONSTANT=1)
CONDUCTIVITY (SET=2,CONSTANT=403)
/
VISCOSITY(CONSTANT=2.8549344E-03)
/VISCOSITY(CURVE=31)
/(FOR VARIABLE VISCOSITY MODELS,VISCOSITY VALUES FOR A RANGE OF
TEMPERATURE
/TEMPERATURE MUST BE INSERT )
/
/DIRECTION OF FLOW
/FLOW UPWARD
VOLUMEXPANSION(CONSTANT=1,GRAVITY=-1,THETA=90.,REFTEMP=0)
BODYFORCE(CONSTANT,REFERENCE)
-1.0 0
/FLOW IN DIRECTION OF GRAVITY(DOWNWARD FLOW)
```

```
/VOLUMEXPANSION(CONSTANT=1,GRAVITY=1,THETA=90.,REFTEMP=0)
/BODYFORCE(CONSTANT,REFERENCE)
/1.0 0
/DEFINE ELEMENTS FOR SOLVING
NODES(FIMESH)
/FLUID ELEMENT
ELEMENTS(QUADRILATERAL,NODES=4,FLUID,FIMESH,MCOND=1)
/PIPE
ELEMENTS(QUADRILATERAL,NODES=4,SOLID,FIMESH,MCOND=2)
/OUTPUT CONTROLS
DATAPRINT(CONTROL)
PRINTOUT(NONE)
RENUMBER
END
*END
```

A.4.2. Complex 3-D Mesh Generation

```
*TITLE
HORIZONTAL PIPE LAMINAR HEAT TRANSFER
*FIMESH(3-D, IMAX=19, JMAX=11, KMAX=15,MXPOIT=9999)
/DEFINE INDEX I,J,K FOR THE MESH
EXPI
1 0 5 0 9 0 13 0 17 0 21 0 25 0 29 0 33 0 37
EXPJ
1 0 5 0 9 0 13 0 17 0 21
EXPK
1 0 5 0 9 0 13 0 17 0 21 0 25 0 29
/
PARAMETER
/I,J,K INDEX
IWER 1
```

```
IINR 3
IWAR 5
ILIR 7
ISQR 9
ISQL 11
ILIL 13
IWAL 15
IINL 17
IWEL 19
/
J1 1
J3 3
J5 5
J7 7
J9 9
J11 11
/
KBOT 1
KWE1 3
KEX1 5
KHB1 7
KHE2 9
KEX2 11
KWE2 13
KTOP 15
/
/RADIUS
RADD1
RADD3 6.75
RADD5 7.5
RADD7 8.1
RADD9 9.2
SP .14144214
```

```
/
/ANGLE OF CYLIN.
CEN        100
PI         180
RIG         45
LEF         135
ZZ          0
/VALUES ON K DIRECTION
BOT 0
WE1 20
EX1 21
HB1 23
HE2 27
EX2 29
WE2 30
TOP 50
/
/HEAT FLUX
HS 1.0
/FLOW VELOCITY
VEL 1.511186
/INITIAL TEMPERATURE
T0 0
/
/DEFINE POINTS FOR THE MESH
/SQUARE REGION.
POINT(CARTESIAN)
/TOP FACE
/ #  I,J,  K    X  Y  Z
9  ISQR J1 KTOP SP ZZ TOP
11 ISQL J1 KTOP -SP ZZ TOP
93 ISQR J3 KTOP SP sp TOP
113 ISQL J3 KTOP -SP sp TOP
```

```
/OUT FLOW PLATE
293 ISQR J3 KBOT SP sp BOT
2113 ISQL J3 KBOT -SP SP BOT
/CEN POINT
100 0,0,0 ZZ ZZ TOP
/CDRIVE LINE ON Z DIRECTION 93-293
4 ISQR J3 KWE1 SP sp WE1
6 ISQR J3 KEX1 SP sp EX1
8 ISQR J3 KHB1 SP sp HB1
10 ISQR J3 KHE2 SP sp HE2
12 ISQR J3 KEX2 SP sp EX2
14 ISQR J3 KWE2 SP sp WE2
/
POINT(CYLINDRICAL)
/ I   J   K   RADD  ^   Z
/INFLOW PLATE
/CENTER LINE
1 IWER J1 KTOP RADD1 ZZ TOP
3 IINR J1 KTOP RADD3 ZZ TOP
5 IWAR J1 KTOP RADD5 ZZ TOP
7 ILIR J1 KTOP RADD7 ZZ TOP
/
13 ILIL J1 KTOP RADD7 PI TOP
15 IWAL J1 KTOP RADD5 PI TOP
17 IINL J1 KTOP RADD3 PI TOP
19 IWEL J1 KTOP RADD1 PI TOP
/POINT ON LINE J3
103 IWER J3 KTOP RADD1 RIG TOP
33 IINR J3 KTOP RADD3 RIG TOP
53 IWAR J3 KTOP RADD5 RIG TOP
73 ILIR J3 KTOP RADD7 RIG TOP
/POINT ON LINE J9
139 ILIL J3 KTOP RADD7 LEF TOP
```

159 IWAL J3 KTOP RADD5 LEF TOP

179 IINL J3 KTOP RADD3 LEF TOP

199 IWEL J3 KTOP RADD1 LEF TOP

/POINT ON LINE J5

95 ISQR J5 KTOP RADD7 RIG TOP

97 ISQR J7 KTOP RADD5 RIG TOP

99 ISQR J9 KTOP RADD3 RIG TOP

911 ISQR J11 KTOP RADD1 RIG TOP

/POINT ON LINE J7

115 ISQL J5 KTOP RADD7 LEF TOP

117 ISQL J7 KTOP RADD5 LEF TOP

119 ISQL J9 KTOP RADD3 LEF TOP

111 ISQL J11 KTOP RADD1 LEF TOP

/

/OUTFLOW PLATE

/CENTER LINE

21 IWER J1 KBOT RADD1 ZZ BOT

23 IINR J1 KBOT RADD3 ZZ BOT

25 IWAR J1 KBOT RADD5 ZZ BOT

27 ILIR J1 KBOT RADD7 ZZ BOT

/

213 ILIL J1 KBOT RADD7 PI BOT

215 IWAL J1 KBOT RADD5 PI BOT

217 IINL J1 KBOT RADD3 PI BOT

219 IWEL J1 KBOT RADD1 PI BOT

/POINT ON LINE J3

2103 IWER J3 KBOT RADD1 RIG BOT

233 IINR J3 KBOT RADD3 RIG BOT

253 IWAR J3 KBOT RADD5 RIG BOT

273 ILIR J3 KBOT RADD7 RIG BOT

/POINT ON LINE J9

2139 ILIL J3 KBOT RADD7 LEF BOT

2159 IWAL J3 KBOT RADD5 LEF BOT

2179 IINL J3 KBOT RADD3 LEF BOT

2199 IWEL J3 KBOT RADD1 LEF BOT

/POINT ON LINE J5

295 ISQR J5 KBOT RADD7 RIG BOT

297 ISQR J7 KBOT RADD5 RIG BOT

299 ISQR J9 KBOT RADD3 RIG BOT

2911 ISQR J11 KBOT RADD1 RIG BOT

/POINT ON LINE J7

2115 ISQL J5 KBOT RADD7 LEF BOT

2117 ISQL J7 KBOT RADD5 LEF BOT

2119 ISQL J9 KBOT RADD3 LEF BOT

2111 ISQL J11 KBOT RADD1 LEF BOT

/TRANSDUCER SHOES

/CENTER LINE

31 IWER J1 KWE1 RADD1 ZZ WE1

333 IINR J1 KWE1 RADD3 ZZ WE1

35 IWAR J1 KWE1 RADD5 ZZ WE1

37 ILIR J1 KWE1 RADD7 ZZ WE1

/

313 ILIL J1 KWE1 RADD7 PI WE1

315 IWAL J1 KWE1 RADD5 PI WE1

317 IINL J1 KWE1 RADD3 PI WE1

319 IWEL J1 KWE1 RADD1 PI WE1

/POINT ON LINE J3

3103 IWER J3 KWE1 RADD1 RIG WE1

3133 IINR J3 KWE1 RADD3 RIG WE1

353 IWAR J3 KWE1 RADD5 RIG WE1

373 ILIR J3 KWE1 RADD7 RIG WE1

/POINT ON LINE J9

3139 ILIL J3 KWE1 RADD7 LEF WE1

3159 IWAL J3 KWE1 RADD5 LEF WE1

3179 IINL J3 KWE1 RADD3 LEF WE1

3199 IWEL J3 KWE1 RADD1 LEF WE1

```
/POINT ON LINE J5
395 ISQR J5 KWE1 RADD7 RIG WE1
397 ISQR J7 KWE1 RADD5 RIG WE1
399 ISQR J9 KWE1 RADD3 RIG WE1
3911 ISQR J11 KWE1 RADD1 RIG WE1
/POINT ON LINE J7
3115 ISQL J5 KWE1 RADD7 LEF WE1
3117 ISQL J7 KWE1 RADD5 LEF WE1
3119 ISQL J9 KWE1 RADD3 LEF WE1
3111 ISQL J11 KWE1 RADD1 LEF WE1
/
/CENTER LINE
41 IWER J1 KEX1 RADD1 ZZ EX1
43 IINR J1 KEX1 RADD3 ZZ EX1
45 IWAR J1 KEX1 RADD5 ZZ EX1
47 ILIR J1 KEX1 RADD7 ZZ EX1
/
413 ILIL J1 KEX1 RADD7 PI EX1
415 IWAL J1 KEX1 RADD5 PI EX1
417 IINL J1 KEX1 RADD3 PI EX1
419 IWEL J1 KEX1 RADD1 PI EX1
/POINT ON LINE J3
4103 IWER J3 KEX1 RADD1 RIG EX1
433 IINR J3 KEX1 RADD3 RIG EX1
453 IWAR J3 KEX1 RADD5 RIG EX1
473 ILIR J3 KEX1 RADD7 RIG EX1
/POINT ON LINE J9
4139 ILIL J3 KEX1 RADD7 LEF EX1
4159 IWAL J3 KEX1 RADD5 LEF EX1
4179 IINL J3 KEX1 RADD3 LEF EX1
4199 IWEL J3 KEX1 RADD1 LEF EX1
/POINT ON LINE J5
495 ISQR J5 KEX1 RADD7 RIG EX1
```

```
497 ISQR J7 KEX1 RADD5 RIG EX1
499 ISQR J9 KEX1 RADD3 RIG EX1
4911 ISQR J11 KEX1 RADD1 RIG EX1
/POINT ON LINE J7
4115 ISQL J5 KEX1 RADD7 LEF EX1
4117 ISQL J7 KEX1 RADD5 LEF EX1
4119 ISQL J9 KEX1 RADD3 LEF EX1
4111 ISQL J11 KEX1 RADD1 LEF EX1
/HEATER PLATE1.
/CENTER LINE
51 IWER J1 KHB1 RADD1 ZZ HB1
5203 IINR J1 KHB1 RADD3 ZZ HB1
55 IWAR J1 KHB1 RADD5 ZZ HB1
57 ILIR J1 KHB1 RADD7 ZZ HB1
/
513 ILIL J1 KHB1 RADD7 PI HB1
515 IWAL J1 KHB1 RADD5 PI HB1
517 IINL J1 KHB1 RADD3 PI HB1
519 IWEL J1 KHB1 RADD1 PI HB1
/POINT ON LINE J3
5103 IWER J3 KHB1 RADD1 RIG HB1
533 IINR J3 KHB1 RADD3 RIG HB1
553 IWAR J3 KHB1 RADD5 RIG HB1
573 ILIR J3 KHB1 RADD7 RIG HB1
/POINT ON LINE J9
5139 ILIL J3 KHB1 RADD7 LEF HB1
5159 IWAL J3 KHB1 RADD5 LEF HB1
5179 IINL J3 KHB1 RADD3 LEF HB1
5199 IWEL J3 KHB1 RADD1 LEF HB1
/POINT ON LINE J5
595 ISQR J5 KHB1 RADD7 RIG HB1
597 ISQR J7 KHB1 RADD5 RIG HB1
599 ISQR J9 KHB1 RADD3 RIG HB1
```

5911 ISQR J11 KHB1 RADD1 RIG HB1

/POINT ON LINE J7

5115 ISQL J5 KHB1 RADD7 LEF HB1

5117 ISQL J7 KHB1 RADD5 LEF HB1

5119 ISQL J9 KHB1 RADD3 LEF HB1

5111 ISQL J11 KHB1 RADD1 LEF HB1

/HEATER PLATE2

/CENTER LINE

61 IWER J1 KHE2 RADD1 ZZ HE2

63 IINR J1 KHE2 RADD3 ZZ HE2

65 IWAR J1 KHE2 RADD5 ZZ HE2

67 ILIR J1 KHE2 RADD7 ZZ HE2

/

613 ILIL J1 KHE2 RADD7 PI HE2

615 IWAL J1 KHE2 RADD5 PI HE2

617 IINL J1 KHE2 RADD3 PI HE2

619 IWEL J1 KHE2 RADD1 PI HE2

/POINT ON LINE J3

6103 IWER J3 KHE2 RADD1 RIG HE2

633 IINR J3 KHE2 RADD3 RIG HE2

653 IWAR J3 KHE2 RADD5 RIG HE2

673 ILIR J3 KHE2 RADD7 RIG HE2

/POINT ON LINE J9

6139 ILIL J3 KHE2 RADD7 LEF HE2

6159 IWAL J3 KHE2 RADD5 LEF HE2

6179 IINL J3 KHE2 RADD3 LEF HE2

6199 IWEL J3 KHE2 RADD1 LEF HE2

/POINT ON LINE J5

695 ISQR J5 KHE2 RADD7 RIG HE2

697 ISQR J7 KHE2 RADD5 RIG HE2

699 ISQR J9 KHE2 RADD3 RIG HE2

6911 ISQR J11 KHE2 RADD1 RIG HE2

/POINT ON LINE J7

6115 ISQL J5 KHE2 RADD7 LEF HE2

6117 ISQL J7 KHE2 RADD5 LEF HE2

6119 ISQL J9 KHE2 RADD3 LEF HE2

6111 ISQL J11 KHE2 RADD1 LEF HE2

/

/TRANSDUCER SHOES

/CENTER LINE

71 IWER J1 KEX2 RADD1 ZZ EX2

723 IINR J1 KEX2 RADD3 ZZ EX2

75 IWAR J1 KEX2 RADD5 ZZ EX2

77 ILIR J1 KEX2 RADD7 ZZ EX2

713 ILIL J1 KEX2 RADD7 PI EX2

715 IWAL J1 KEX2 RADD5 PI EX2

717 IINL J1 KEX2 RADD3 PI EX2

719 IWEL J1 KEX2 RADD1 PI EX2

/POINT ON LINE J3

7103 IWER J3 KEX2 RADD1 RIG EX2

733 IINR J3 KEX2 RADD3 RIG EX2

753 IWAR J3 KEX2 RADD5 RIG EX2

773 ILIR J3 KEX2 RADD7 RIG EX2

/POINT ON LINE J9

7139 ILIL J3 KEX2 RADD7 LEF EX2

7159 IWAL J3 KEX2 RADD5 LEF EX2

7179 IINL J3 KEX2 RADD3 LEF EX2

7199 IWEL J3 KEX2 RADD1 LEF EX2

/POINT ON LINE J5

795 ISQR J5 KEX2 RADD7 RIG EX2

797 ISQR J7 KEX2 RADD5 RIG EX2

799 ISQR J9 KEX2 RADD3 RIG EX2

7911 ISQR J11 KEX2 RADD1 RIG EX2

/POINT ON LINE J7

7115 ISQL J5 KEX2 RADD7 LEF EX2

7117 ISQL J7 KEX2 RADD5 LEF EX2

```
7119 ISQL J9 KEX2 RADD3 LEF EX2
7111 ISQL J11 KEX2 RADD1 LEF EX2
/
/CENTER LINE
81 IWER J1 KWE2 RADD1 ZZ WE2
83 IINR J1 KWE2 RADD3 ZZ WE2
85 IWAR J1 KWE2 RADD5 ZZ WE2
87 ILIR J1 KWE2 RADD7 ZZ WE2
/
813 ILIL J1 KWE2 RADD7 PI WE2
815 IWAL J1 KWE2 RADD5 PI WE2
817 IINL J1 KWE2 RADD3 PI WE2
819 IWEL J1 KWE2 RADD1 PI WE2
/POINT ON LINE J3
8103 IWER J3 KWE2 RADD1 RIG WE2
833 IINR J3 KWE2 RADD3 RIG WE2
853 IWAR J3 KWE2 RADD5 RIG WE2
873 ILIR J3 KWE2 RADD7 RIG WE2
/POINT ON LINE J9
8139 ILIL J3 KWE2 RADD7 LEF WE2
8159 IWAL J3 KWE2 RADD5 LEF WE2
8179 IINL J3 KWE2 RADD3 LEF WE2
8199 IWEL J3 KWE2 RADD1 LEF WE2
/POINT ON LINE J5
895 ISQR J5 KWE2 RADD7 RIG WE2
897 ISQR J7 KWE2 RADD5 RIG WE2
899 ISQR J9 KWE2 RADD3 RIG WE2
8911 ISQR J11 KWE2 RADD1 RIG WE2
/POINT ON LINE J7
8115 ISQL J5 KWE2 RADD7 LEF WE2
8117 ISQL J7 KWE2 RADD5 LEF WE2
8119 ISQL J9 KWE2 RADD3 LEF WE2
8111 ISQL J11 KWE2 RADD1 LEF WE2
```

```
/
/DEFINE LINES,ARC AND SURFACE FOR THE MESH
LINE
/CENTER LINE
1 3
3 5
5 7
7 9
9 11
11 13
13 15
15 17
17 19
/J3
103 33
33 53
53 73
73 93
/J5
9 93
93 95
95 97
97 99
99 911
/SQ
93 113
/J7
11 113
113 115
115 117
117 119
119 111
/J9
```

```
113 139
139 159
159 179
179 199
/AXIAL DIRECTION(Z)
93 4
4 6
6 8
8 10
10 12
12 14
14 293
93 293
/
ARC
1 103 100
3 33 100
5 53 100
7 73 100
95 115 100
97 117 100
99 119 100
911 111 100
13 139 100
15 159 100
17 179 100
19 199 100
/
SURFACE
1 199
93 111
CDRIVE
1 199 93 293
```

```
93 111 93 293
/
MERGE
103 293 911 293
111 2113 199 2113
/
/DEFINE ELEMENT GROUPS FOR THE SOLVER
ELEMENTS(BRICK, NODES=8)
/
35 4103
397 4111
315 4199
/
55 633
597 6119
515 6199
/
75 8103
797 8111
715 8199
/
/SOLID WALL
5 273
95 2117
13 2159
/LIQUID
7 2139
93 2115
/
END
*END
```

A.4.3. 3-D Heat Transfer FIDAP Interface Input File

```
*TITLE
HORIZONTAL PIPE LAMINAR HEAT TRANSFER
*FIMESH(3-D, IMAX=11, JMAX=7, KMAX=11, MXPOINT=999)
/DEFINE INDEX I,J,K FOR THE MESH
EXPI
1 0 5 0 9 0 13 0 17 0 21
EXPJ
1 0 5 0 9 0 13
EXPK
1 0 5 0 9 0 13 0 17 0 21
/
PARAMETER
RADIUS1      1.0
RADIUS3      0.9
RADIUS5      0.2
SP           0.14144214
/
CENTER       100
PI           180
RIGHT         45
LEFT         135
ZERO          0
/
LENGTH 26.66667
EX1 10.66667
HB 12
HE 14.66667
EX2 16
/
BTM 1
KK1 3
```

```
K1 5
K2 7
KK2 9
TOP 11
/
/HEAT FLUX
HS 1.0
/FLOW VELOCITY
VEL 1.511186
/INITIAL TEMPERATURE
T0 0
/
/DEFINE POINTS FOR THE MESH
POINT(CARTESIAN)
/ #  I,J,  K          X        Y        Z
  5  5,1,TOP       SP       ZERO     LENGTH
  7  7,1,TOP      -SP       ZERO     LENGTH
 53  5,3,TOP       SP       SP       LENGTH
 73  7,3,TOP      -SP       SP       LENGTH
/
835 5,3,kK1        SP       SP       EX1
535 5,3,K1         SP       SP       HB
537 5,3,K2         SP       SP       HE
837 5,3,KK2        SP       SP       EX2
/CENTER POINT
 100 0,0,0         ZERO     ZERO     LENGTH
/CDRIVE LINE 53-533
533 5,3,BTM        SP       SP       ZERO
733 7,3,BTM       -SP       SP       ZERO
535 5,3,K1         SP       SP       HB
537 5,3,K2         SP       SP       HE
POINT(CYLINDRICAL)
/ #  I,J,  K       RADIUS     ANGLE          Z
```

```
  1  1,1,TOP     RADIUS1      ZERO     LENGTH
  3  3,1,TOP     RADIUS3      ZERO     LENGTH
  9  9,1,TOP     RADIUS3        PI     LENGTH
 11 11,1,TOP     RADIUS1        PI     LENGTH
/
 13  1,3,TOP     RADIUS1     RIGHT     LENGTH
 33  3,3,TOP     RADIUS3     RIGHT     LENGTH
/
 93  9,3,TOP     RADIUS3      LEFT     LENGTH
 41 11,3,TOP     RADIUS1      LEFT     LENGTH
/
 55  5,5,TOP     RADIUS3     RIGHT     LENGTH
 57  5,7,TOP     RADIUS1     RIGHT     LENGTH
/
 75  7,5,TOP     RADIUS3      LEFT     LENGTH
 77  7,7,TOP     RADIUS1      LEFT     LENGTH
REFPOINTS
 113  1,1,BTM
 313  3,1,BTM
 773  7,7,BTM
 753  7 5 BTM
 933  9,3,BTM
 413 11,3,BTM
/HEATER REF. POINT
 813 1 1 KK1
 873 7 7 Kk1
 814 11 3 KK1
 613 1 1 K1
 673 7 7 k1
 614 11 3 K1
 513 1 3 k2
 557 5 7 k2
 511 11 1 k2
```

```
913 1 3 Kk2
957 5 7 Kk2
911 11 1 Kk2
/
/DEFINE LINES,ARC AND SURFACE FOR THE MESH
LINE
  1   3
  3   5
  5   7
  7   9
  9  11
  5  53
  7  73
 13  33
 33  53
 53  73
 73  93
 93  41
 53  55
 55  57
 73  75
 75  77
/
53 837
837 537
537 535
535 835
835 533
/
ARC
  1  13 100
  3  33 100
  9  93 100
```

```
 11  41 100
 55  75 100
 57  77 100
SURFACE
  1  41
 53  77
CDRIVE
  1  41  53 533
 53  77  53 533
MERGE
 13 533  57 533
 77 733  41 733
/
/DEFINE ELEMENT GROUPS FOR THE SOLVER
ELEMENTS(BRICK, NODES=8)
/SOLID REGION
  9 413
 55 773
 33 113
/FLUID REGION
 93 313
 75 533
/
/DEFINE BOUNDARY CONDITIONS
BCNODE(UT1)
  3  93
 53  75
313 933
533 753
33 313
9 933
55 753
BCNODE(UT2)
```

```
  3  93
 53  75
313 933
533 753
9 313
33 313
9 933
55 753
BCNODE(UN3)
33 313
9 933
55 753
BCNODE(UN3,FREE)
313 933
533 753
9 313
/
POINT
100 0,0,0 ZERO ZERO LENGTH
BCNODE(COORDINATE)
3 93 2
53 75 2
COORDINATE(SYSTEM=2,ROTAT,CYLIND)
100 1 -45
BCNODE(UN3,POLY,SYST=2)
3 93  -VEL,0 0 0 1 VEL1,2 0 0
53 75 -VEL,0 0 0 1 VEL1,2 0 0
/
BCNODE(TEMP)
1 41 T0
53 77 T0
/
BCFLUX(HEAT,FACE)
```

```
513 613 HS
511 614 HS
557 673 HS
/
NUMBER
2,3,1
END
/FIPREP COMMANDS
*FIPREP
/STEADY STATE
PROBLEM(NONLINEAR,3-D,STRONGLY)
/PROBLEM(NONLINEAR,3-D)
/TRANSIENT STATE
/PROBLEM(3-D,TRANSIENT,NONLINEAR,STRONGLY)
/PROBLEM(3-D,TRANSIENT,NONLINEAR
/
EXECUTION(NEWJOB)
/RESTART RUN
/EXECUTION(RESTART)
SOLUTION(S.S.=100,VELC=.01,RESC=.01,ACCF=0.4)
/
PRESSURE(PENALTY)
/PRESSURE(MIXED,DISCONTINUOUS)
/
ICNODE(TEMPERATURE,CONSTANT=0)
ICNODE(VELOCITY,STOKES)
/RESTAR
/EXECUTION(RESTART)
/ICNODE(VELOCITY,READ)
/ICNODE(TEMPERATURE,READ)
/
/TIME STEP FOR TRANSIENT STATE PROCESSING
        /TIME(NSTEPS=101,DT=.01,TRAPEZOIDAL,FIXED)
```

```
/POSTPROCESS(NBLOCKS=1)
/1 101 10
/
/PHYSICAL VALUES
/set1 :water,set2:COPPER
DENSITY (SET=1,CONSTANT=1)
DENSITY (SET=2,CONSTANT=8933)
/
SPECIFICHEAT (SET=1,CONSTANT=1849.664)
SPECIFICHEAT (SET=2,CONSTANT=379)
/
CONDUCTIVITY (SET=1,CONSTANT=1)
CONDUCTIVITY (SET=2,CONSTANT=403)
/
/VISCOSITY(CONSTANT=4.0374869E-3)
VISCOSITY(CURVE=31)
/Insert a range of viscosity values
/
/DEFINE ANGLE OF GRAVITY
VOLUMEXPANSION(CONSTANT=1,GRAVITY=1,THETA=0,PHI=90,REFTEMP=0)
BODYFORCE(CONSTANT,REFERENCE)
0 0 1
/DEFINE ELEMENTS FOR SOLVING
NODES(FIMESH)
/SOLID REGION
ELEMENT(BRICK, NODE=8, FIMESH, MCOND=2, SOLID)
ELEMENT(BRICK, NODE=8, FIMESH, MCOND=2, SOLID)
ELEMENT(BRICK, NODE=8, FIMESH, MCOND=2, SOLID)
/ FLUID REGION
ELEMENT(BRICK, NODE=8, FIMESH, MCOND=1, FLUID)
ELEMENT(BRICK, NODE=8, FIMESH, MCOND=1, FLUID)
/OUTPUT CONTROLS
DATAPRINT(CONTROL)
```

```
PRINTOUT(NONE)
RENUMBER
END
*END
```

APPENDIX B. ASSOCIATED ELECTRONICS

B.1. Introduction

Design and description of various electronic instruments mentioned in Section 7.4 will be discussed in detail. The instruments to be discussed are: Computer Controlled Relay Switch Module; the Wavetek Gate Mode Controller and Ultrasonic Timing Interface

B.2. Computer Controlled Relay Switch Module

The designed circuit for the computer controlled relay switch model is shown in Fig B.2.1. This module allows a direct current of up to 16 A to be switched by a relay under computer control. The input control voltage (con. 1, pin 1) can be driven by a TTL logic level; a high level energizing the relay and a low level turning it off. The input threshold is set at 1.6 V though any voltage between 1.6 V and 35 V may be used to energize the relay. The N/C contact is connected to COM and the N/O contact is open circuit when the relay is off. When it is on the N/C contact is open circuit and the N/O contact is connected to COM. An LED indicates when the relay is energized.

B.3. The Wavetek Gate Mode Burst Controller

Fig B.3.1 shows the circuit design for the Wavetek gate mode burst controller. Fig B.3.2 shows the input/output signals of the Wavetek used in conjunction with the Wavetek gate mode burst controller.

The Wavetek gate mode controller is designed to be used with the Wavetek Model 22 signal generator to produce between 1 to 99 complete output cycles at a set repetition rate. The repetition rate is between 120 Hz to 2 KHz, and is set by the 100K pot, accessible at the back of the box. The controller is powered by an internal 9 V PP3 battery and is turned on by a three way switch at the side of the box. The three

positions are OFF (1) (nearest the front), ON (2) (middle) and ON with SYNC invert (3) (back). The LED indicates power ON. The On switch in position (3) is used at high frequencies where the propagation delay around the system is long enough to give spurious extra cycles intermittently. The extra 1/2 cycle delay adds an extra cycle and removes the intermittent response. It should be noted that at high frequencies (2 to 3 MHz), the propagation delay may be long enough to give an extra cycle(s). This is mainly due to internal Wavetek propagation delays and the exact number of cycles generated should be checked on an oscilloscope, setting the ON/OFF switch to (2) or (3) for reliable operation.

TRIG IN and SYNC OUT on the Wavetek should be connected to TRIG, and SYNC IN on the controller. The desired burst frequency should be set in CONT mode on the Wavetek, the number of cycles keyed in and the repeat rate set. GATE mode should be selected on the Wavetek and correct operation checked on the oscilloscope bearing in mind the above notes on high frequency.

B.4. Ultrasonic Timing Interface

The circuit design for the ultrasonic timing interface is shown in Fig B.4.1a. Fig B.4.1b is a simplified logic diagram of Fig B.4.1a. From this diagram, the step by step performance of the circuit can be summarized as the signals shown in Fig B.4.2. The ultrasonic timing interface was used with the Philips 6654 counter-timer to measure the time of an ultrasonic sine wave burst sent across a pipe.

The circuit in primed with a rising TTL edge at TRIG IN. Monostable IC 16 immediately enables the start circuitry and enables the end circuitry after an adjustable hold-off time of up to 40 μs. The start and end circuitry are identical, each producing a TTL level pulse on detection of a signal which is output to the Philips 6654 counter-timer. IC1 is a fast current feedback OP-AMP with an adjustable voltage gain of between 1.6 and 11 volts with a 30 MHz bandwidth. The output from this gain stage is fed to the two high-speed comparators, IC3 and IC4. IC3 has a threshold between 0.1 V and 3.5 V. When this is exceeded, pin 7 of IC3 goes high and these excursions are

counted by binary counter, IC7. When the output of the binary counter, Q_A - Q_D, is equal to the setting on the 4 bit comparator, IC9's hex switch, flip-flop IC13b is set, enabling the zero-crossing comparator, IC4. IC4 is disabled when 4 bit comparator IC10's hex switch is equal to counter IC7's output, and flip-flops IC13 a and b are reset, resetting the counter. In this application, IC10's hex switch was set to one more than IC9's hex switch, giving a single pulse output. The Philips counter-timer measures the time between start pulse and end pulse to a resolution of 2ns.